Dissecting the Telomere-Independent Pathways Underlying Human Cellular Senescence

By

Louise Victoria Mansfield

A thesis submitted to the University of London
for the degree of Doctor of Philosophy

Ludwig Institute for Cancer Research
University College Branch
91 Riding House Street
London W1W 7BS

Department of Biochemistry and Molecular Biology
University College London
Gower Street
London WC1E 6BT

2006

ProQuest LLC
789 East Eisenhower Parkway
P.O. Box 1346
Ann Arbor, MI 48106-1346

Abstract

Replicative senescence describes the irreversible growth arrest that primary human fibroblasts undergo when cultivated *in vitro* and represents one example of a biological process known as cellular senescence. Cellular senescence is associated with organismal ageing and functions an important tumour suppressive mechanism.

A conditionally immortalised human mammary fibroblast cell line, HMF3A, has been developed with the aim of determining the precise molecular basis of telomere-independent cellular senescence. HMF3A cells constitutively express hTERT, the catalytic component of human telomerase, and a temperature sensitive non-DNA-binding mutant of Simian Virus 40 large T (LT) antigen. At the permissive temperature, 33.5℃, HMF3A cells grow normally but at the non-permissive temperature, 39.5℃, LT antigen is inactivated and the cells undergo a rapid and synchronous irreversible growth arrest.

The stringency of HMF3A growth complementation has enabled me to functionally analyse the pathways implicated in the induction of senescence in these cells. It was concluded that inactivation of the p53 pathway was sufficient to overcome the conditional HMF3A growth arrest. However, expression of a $p16^{INK4a}$-insensitive cyclin D1-$CDK4^{R24C}$ fusion construct indicated that the pRb pathway was not critical for the induction of this process.

I subsequently identified three novel markers of telomere-independent cellular senescence by cDNA microarray analysis (namely, *AKR1B1*, *CDH13* and *UBE2C*), and three potential regulators of senescence by an RNA interference screen (namely, *NEUROD2*, *TARBP1* and *RRM2*).

Finally, I detected a novel functional activity of the Adenovirus E1A 13S splice variant that is not shared with the E1A 12S splice variant. This activity enabled 13S E1A, but not 12S E1A, to bypass the conditional HMF3A growth arrest.

The genes identified using these independent experimental approaches constitute novel markers of senescence and, upon validation of these findings, may provide prognostic and/or diagnostic value in the context of tumorigenesis.

Table of Contents

List of Figures

List of Tables

Abbreviations

2D-DIGE	two-dimensional difference gel electrophoresis
3D	three-dimensional
6-FAM	6-carboxyfluorescein
aa	amino acid
AEBSF	4-(2-aminoethyl)benzenesulphonyl fluoride
Ago	Argonaute
ALT	alternate lengthening of telomeres
amp^R	ampicillin resistance gene
APC	anaphase-promoting complex
APS	ammonium persulphate
ARF	alternate reading frame
ATP	adenosine triphosphate
bHLH	basic helix-loop-helix
BLAST	Basic Local Alignment Search Tool
blast^R	blasticidin resistance gene
bp	base pair
BrdU	bromo-deoxyuridine
BSA	bovine serum albumin
$CaCl_2$	calcium chloride
CDK	cyclin-dependent kinase
CDKI	cyclin-dependent kinase inhibitor
cDNA	complementary deoxyribonucleic acid
Cfu	colony forming units
ChIP	chromatin immunoprecipitation
CIP	calf intestinal alkaline phosphatase
CR	conserved region
C-terminal	carboxy-terminal
DAPI	4'-6-diamidino-2-phenylindole

dd	double-distilled
DEPC	diethyl pyrocarbonate
DK	cyclin D1-CDK4^{R24C} fusion construct
DMEM	Dulbecco's modified Eagle medium
DMSO	dimethyl sulphoxide
DNA	deoxyribonucleic acid
dNTP	deoxyribonucleotide triphosphate
dsRNA	double-stranded ribonucleic acid
DTT	dithiothreitol
EBV	Epstein Barr Virus
ECL	enhanced chemiluminescence
Eco^{R}	murine ecotropic receptor
EDTA	ethylenediaminetetraacetic acid
ES	embryonic stem
FCS	foetal calf serum
FDR	false-discovery rate
G_0	quiescence
G_1	first gap phase
G_2	second gap phase
GFP	green fluorescent protein
GPI	glycosylphosphatidylinositol
GSE	genetic suppressor element
GTP	guanine triphosphate
HAT	histone acetylase
HCl	hydrochloric acid
hCMV	human cytomegalovirus
HDAC	histone deacetylase
HDF	human diploid fibroblast
HEPES	4-(2-hydroxyethyl)-1-piperazineethanesulphonic acid
HGPS	Hutchinson-Gilford Progeria Syndrome
HPV	Human Papilloma Virus

hr	hour
HRP	horseradish peroxidase
hTERT	catalytic component of human telomerase
IE	immediate early promoter
IPTG	isopropyl-β-D-thiogalactopyranoside
IR	ionizing radiation
IRES	internal ribosomal entry site
kb	kilobase
KCl	potassium chloride
kDa	kilodalton
LB	luria broth base
Liquid N_2	liquid nitrogen
LOWESS	locally weighted linear regression
LT	SV40 large T antigen
LTR	long terminal repeat
M	molar
M1	mortality stage I
M2	mortality stage II
mM	millimolar
M phase	mitosis phase
MCS	multiple cloning site
MEF	mouse embryo fibroblast
$MgCl_2$	magnesium chloride
$MgSO_4$	magnesium sulphate
min	minute
miRNA	micro ribonucleic acid
MoMuLV	Moloney Murine Leukaemia Virus
MoMuSV	Moloney Murine Sarcoma Virus
MOPS	3 – [N-morpholino] propanesulphonic acid
MPF	maturation promoting factor
mRNA	messenger ribonucleic acid

N	ploidy
NaCl	sodium chloride
NaOH	sodium hydroxide
NES	nuclear export signal
$(NH_4)_2SO_4$	ammonium sulphate
NHEJ	non-homologous end-joining
NLS	nuclear localisation signal
nt	nucleotide
N-terminus	amino-terminus
OD	optical density
ORF	open reading frame
P	phosphorylation
PAGE	polyacrylamide gel electrophoresis
PBS	phosphate buffered saline
PcG	polycomb group
PCR	polymerase chain reaction
PD	population doubling
PMT	photomultiplier tube
PNK	polynucleotide kinase
PTGS	post-translational gene silencing
puro^R	puromycin resistance gene
R	restriction point
REF	rat embryo fibroblast
RIPA	radioimmunoprecipitation
RISC	ribonucleic acid -induced silencing complex
RITS	ribonucleic acid -induced transcriptional silencing
RNA	ribonucleic acid
RNAse	ribonuclease
RNAi	ribonucleic acid interference
ROS	reactive oxygen species
rpm	revolutions per minute

RT	reverse transcription
RT-PCR	reverse transcription-polymerase chain reaction
S phase	deoxyribonucleic acid synthesis phase
SA	senescence-associated
SAHF	senescence-associated heterochromatic foci
SAM	significance analysis of microarrays
SCF	Skp1/Cullin/F-box protein
SDS	sodium dodecyl sulphate
sec	second
shRNA	short hairpin ribonucleic acid
SIPS	stress-induced premature senescence
siRNA	short-interfering ribonucleic acid
SNP	single nucleotide polymorphism
STASIS	stress or aberrant signalling-induced senescence
SV40	Simian Virus 40
TEMED	N,N,N',N' tetraethylenemethyldiamine
TERC	catalytic ribonucleic component of human telomerase
TKO	triple knockout
T-OLA	telomere oligonucleotide ligation assay
ts	temperature sensitive
Ub	ubiquitination
UNG	uracil-N-glycosylase
UTR	untranslated region
UV	ultraviolet radiation
UVP	dual intensity ultraviolet trans-illuminator
V	Volt
v/v	volume per volume
w/v	weight per volume
WS	Werner Syndrome
wt	wildtype
X-gal	5-bromo-4-chloro-3-indolyl-β-D-galactopyranoside

Enclosed Unbound Material

Publication:

Hardy K., Mansfield L.V., *et al* (2005). Transcriptional networks and cellular senescence in human mammary fibroblasts. *Mol Biol Cell* **16**(2), 943-953.

Statement Concerning Collaborations

The work presented in this thesis is the work of the author unless otherwise indicated.

Acknowledgements

My thanks go, of course, to Parmjit for being an excellent PhD supervisor who has been a great teacher and has always been willing to discuss my work with me as well as suggest new ideas. I am greatly indebted to him for his guidance.

I would also like to thank the past and present members of the Jat laborartory, namely Nunu Aurora, Kristine Hardy, Maria Leao, Rowena Martin, Athena Nikatopolou, Kate Relph, Tim Szeto and Marina Tarunina. They have all helped to make these past three years a very enjoyable time for me. Particular thanks are due to Kristine Hardy for getting me started with this project, providing excellent advice and teaching me how to do the microarrays.

I am also grateful to Mike O'Hare, Nicola Brookman-Amissah, Anita Grigoradis and Alan Mackay for their helpful discussions and practical advice.

I would also like to extend my thanks to the UCL branch of the Ludwig Institute for Cancer Research for providing me with the opportunity to carry out this work.

For provision of reagents, I would like to thank Reuven Agami, Alan Ashworth, Arnold Berk, Anthony Capobianco, Julian Downward, Ole Gjoerup, Gregory Hannon, Ed Harlow, Francesco Hoffmann, Elizabeth Irons, Tony Kouzarides, Scott Lowe, Xin Lu, Antoine Martinez, Karl Munger, Gordon Peters, Rob Ricciardi, Felicity Savage, John Sedivy and Martin von Lohuizen.

Finally, this project would not have been completed without the invaluable support of both family and friends. Needless to say, there are too many people to mention and so I won't list them for fear of omitting someone. However, I would specifically like to thank my parents, David and Gillian, for their constant support. I dedicate this work to them.

This research was supported by the Ludwig Institute for Cancer Research.

1. Introduction

Replicative senescence describes the irreversible growth arrest that primary HDFs undergo when cultivated in vitro [Hayflick and Moorhead, 1961]. Since this discovery more than 40 years ago, replicative senescence has been described in many different species and cell types and is thought to represent one example of a general biological process termed cellular senescence. This irreversible growth arrest is induced in response to a variety of intrinsic and extrinsic stimuli including alteration in telomere length and structure, deoxyribonucleic acid (DNA) damage, physiological stresses and activation of certain oncogenes. The induction of senescence in vivo is associated with organismal ageing; for example, senescent cells may compromise homeostatic tissue renewal processes and wound healing. Senescence also represents a mechanism by which defective and potentially cancerous cells can be removed from the proliferating pool thereby preventing neoplastic transformation and tumour development. Therefore, it has also been proposed that senescence represents an important tumour suppressive mechanism that limits finite proliferative potential. Overcoming finite proliferative potential is one of the six hallmarks of cancer that are required in the Hanahan and Weinberg model of tumorigenesis [Hanahan and Weinberg, 2000]. However, the underlying mechanism that controls cellular senescence and the signal transduction pathways involved are poorly understood.

This first chapter will introduce the concept of human cellular senescence. Firstly, the cell cycle will discussed since the signalling pathways that are involved in this process are also associated with the induction of cellular senescence. However, due to the extensive number of publications in the literature relating to the cell cycle, discussion will focus specifically upon its role in the context of cellular senescence. Secondly, senescence will be discussed in terms of the stimuli that induce it, the mechanisms by which it is

induced and theories of its evolution. Finally, two experimental techniques that can be used to study this process, namely microarray analysis and ribonucleic acid (RNA) interference, will be described.

1.1 THE CELL CYCLE

In complex, multicellular organisms, the ability of cells to divide is critical for both development and viability. This activity is carefully regulated by the cell cycle; a process that ensures the DNA of a cell is accurately replicated to maintain genomic stability in the daughter cells (**Figure 1.1**). In eukaryotes, the cell cycle operates in a series of defined and unidirectional stages involving DNA replication, spindle assembly, nuclear division and mitosis. Mitosis is also comprised of a series of stages that results in the physical division of the cell into two daughter cells; namely prophase, prometaphase, metaphase, anaphase, telophase and cytokinesis.

A cell becomes committed to enter mitosis, rather than remain in interphase, at the Restriction Point (R; [Pardee, 1974]) that occurs two thirds of the way through the first gap phase (G_1). At R, environmental conditions such as the presence of mitogens determine whether the cell will become committed to complete the cell cycle. At this point, the cell may also withdraw from the cell cycle and become terminally differentiated, or enter a reversible non-diving state known as quiescence or G_0. Cells that are committed to completing the cell cycle become irresponsive to mitogenic signals and proceed to DNA synthesis phase (S phase), where the genome is replicated. S phase is followed by a second gap phase (G_2) that occurs prior to mitosis phase (M phase).

Surveillance mechanisms known as checkpoints operate during all stages to ensure that cell cycle progression does not continue until everything has been satisfactorly completed and any errors have been corrected (reviewed in [Elledge, 1996; Hartwell and Kastan, 1994; Hartwell and Weinert, 1989; Nurse, 1994, 1997; Paulovich *et al*, 1997; Zhou and Elledge, 2000]).

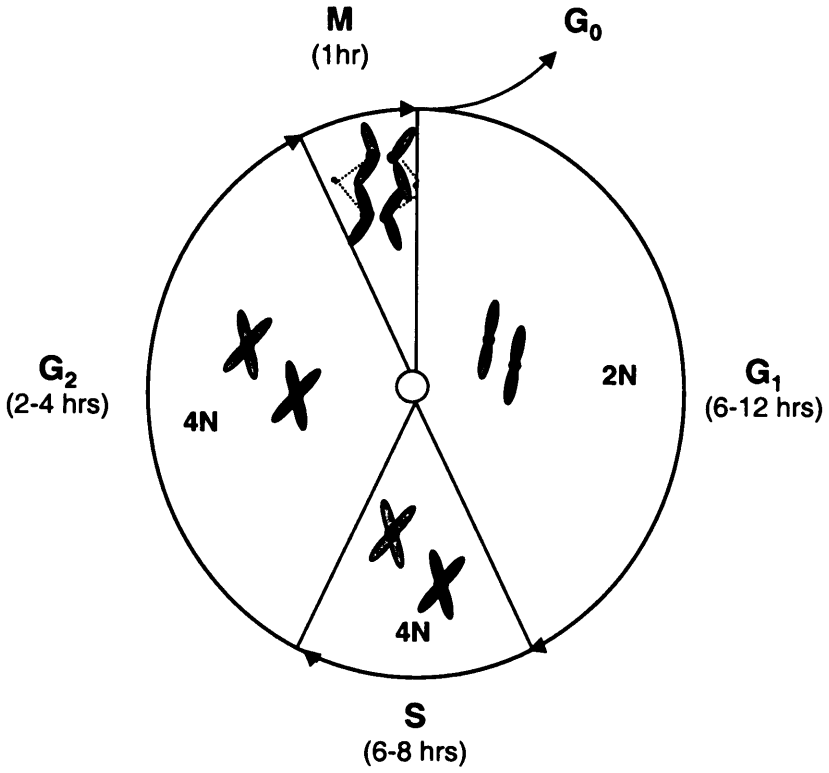

Figure 1.1: The Mammalian Cell Cycle

Schematic diagram of the mammalian cell cycle. For simplicity, one pair of homologous chromosomes are depicted; G_0: Quiescence; G_1: First Gap Phase; S: DNA synthesis phase; G_2: Second Gap Phase; M: Mitosis phase; N: Ploidy.

1.1.1 Cyclins and Cyclin-Dependent Kinases

Cyclins were the first regulators of the cell cycle to be discovered and were so called because of their ability to oscillate during early embryogenesis and drive the cell cycle in a cell autonomous process; cyclin levels were shown to rise prior to mitosis before they were degraded during cytokinesis ([Evans *et al*, 1983]; reviewed in [Murray, 2004]). Since this discovery, many different cyclins have been described and these can be grouped by the timing of their activity during the cell cycle; for example, D-type cyclins are active during G_1, cyclins A and E are active during S phase, and cyclins A and B are active during M phase. Differences in the timing of cyclin expression, sub cellular localisation and biochemical activity ensures that the cell cycle occurs precisely (reviewed in [Murray, 2004; Roberts, 1999]).

Cyclins function by binding to their cognate partners, cyclin-dependent kinases (CDKs), and activating the CDK component of these complexes. CDKs are a family of serine-threonine kinases that, unlike cyclins, remain at relatively constant levels throughout the cell cycle. The ability of cyclins to regulate the timing of CDK activity ensures that CDKs phosphorylate their target proteins in a cell cycle stage-specific manner (reviewed in [Tessema *et al*, 2004]). The fact that these processes occur by the regulation of post-translational modifications also ensures that these regulatory events occur rapidly.

1.1.2 CDK Inhibitors

Cyclin-CDK activity is also regulated by the activity of CDK inhibitors (CDKIs). CDKIs function by phosphorylating specific serine, threonine or tyrosine residues in cyclin-CDK complexes. CDKIs can be classified into two sub-groups, namely the INK4A family and the Cip/Kip family. The INK4A family consists of $p16^{INK4a}$, $p15^{INK4b}$, $p18^{INK4c}$ and $p19^{INK4d}$ and all proteins contain four or more highly conserved ankyrin repeats. INK4A family

members function by abrogating the kinase activity of CDK4 and CDK6 [Serrano *et al*, 1993]. Functional differences are likely to occur as a result of different patterns of gene expression; for example in mammals, *p18*^{INK4c} and *p19*^{INK4d} are highly expressed during development [Zindy *et al*, 1997], whereas p15^{INK4b} and p16^{INK4a} are associated with tumour suppression. P18 may have a role in tumorigenesis, since mice lacking p18^{INK4c} are tumour prone and sensitive to carcinogens [Franklin *et al*, 2000; Luedde *et al*, 2003], however, a link between p18^{INK4c} and human cancer has not been firmly established.

The Cip/Kip family consists of family members p21, p27 and p57 (reviewed in [Sherr and Roberts, 1999]). These family members share a common function in binding to and inactivating CDK2-containing complexes. However, the mechanism by which they inactivate CDK complexes varies between family members. The Cip/Kip family also regulates the activity of CDK4/6 complexes, yet in this context, they function as both positive and negative regulators of CDK4/6 complexes. The ability to function as either a positive or negative regulator is concentration-dependent; for example, p21 functions as an assembly factor for CDK4/6 complexs at low levels, yet as an inactivator of these complexes at high levels.

1.1.3 Cyclin-CDK Activity in the Cell Cycle

During G_0 and early G_1, a combination of low cyclin levels and high CDKI activity ensures pRb remains bound to the E2F transcription factor. This impairs the ability of E2F to transcriptionally activate genes that are required for S phase (described in **Sections 1.15** and **1.16**). In response to extracellular signals, D-type cyclins (D1-3) accumulate and increase the level of cyclin D-CDK4/6 activity. This results in the phosphorylation of pRb and subsequent release of E2F such that E2F is free to transcriptionally activate E2F-responsive genes (reviewed in [Bartek *et al*, 1996; Weinberg, 1995]). During late G_1, cyclin E-CDK2 activity increases (reviewed in [Morgan,

1997]), before peaking at the G_1/S phase boundary [Dulic *et al*, 1992; Koff *et al*, 1992]. The abilty of cyclin E-CDK2 to increase the phosphorylation status of pRb results in the complete inactivation of pRb at this stage of the cell cycle. During S phase, cyclin A-CDK2 becomes the predominant, active cyclin-CDK complex. Cyclin A-CDK2 promotes the phosphorylation of components of the DNA replication machinery; for example Cdc45 becomes activated and the replication origins are fired. CDK2 activity also inhibits E2F, thereby forming a negative feedback loop to ensure that the cell cycle progresses beyond S phase. Cyclin A-CDK2 remains active until the G_2/M phase boundary. During this transition, cyclin B-CDK1, also known as Maturation Promoting Factor (MPF), also becomes active by dephosphorylation events mediated by at least two phosphatases, namely Cdc25b and Cdc25c (reviewed in [Nilsson and Hoffmann, 2000]). This enables MPF to phosphorylate many substrates, including motor and microtubule-binding proteins important for chromosome condensation, nuclear envelope breakdown, spindle assembly and centrosome separation (reviewed in [Nigg, 2001]). Degradation of cyclin B is required for exit from M phase and the start of the next cell cycle.

1.1.4 Rb Family of Proteins

One of the major targets of cyclin-CDK regulation is the Rb family of proteins. The Rb family is defined by the possession of a bipartite pocket region and is comprised of three members, pRb, p107 and p130. The pocket region consists of two conserved domains that are separated by a spacer region. In the case of pRb, this region encompasses amino acid residues 379-928 ([Hannon *et al*, 1993; Lee *et al*, 1987; Mayol *et al*, 1993; Zhu *et al*, 1993]; reviewed in [Stiegler *et al*, 1998]). Specific residues within the pocket region enable family members to directly interact with proteins possessing an LXCXE motif such as HDAC1 and 2 [Lee *et al*, 1998; Whitaker *et al*, 1998]. The fact that Rb family members exhibit a high level of sequence homology

results in some level of functional redundancy; for example, Rb family members share common activities in the regulation of cell proliferation, differentiation and apoptosis [Claudio *et al*, 1996]. However, functional specificity of individual family members has also been described; for example, p107 is the predominant family member that remains bound to E2F-responsive promoters during G_0, p130 is the predominant family member that remains bound during G_1 phase [Rayman *et al*, 2002; Takahashi *et al*, 2000], whereas pRb is commonly expressed in both proliferating and non-proliferating cells.

1.1.5 PRb

The *RB1* gene encodes pRb, a ubiquitously expressed 105 kilodalton (kDa) protein. The fact that pRb is ubiquitously expressed and regulated in a cell cycle-dependent manner is consistent with it functioning as a general regulator of the cell cycle ([Buchkovich *et al*, 1989; DeCaprio *et al*, 1989; Lee *et al*, 1987]; reviewed in [Cobrinik *et al*, 1992]). Its primarily function is to inactivate the E2F family of transcription factors during G_1/S phase transition of the cell cycle, yet over 100 other pRb-binding proteins have been described (reviewed in [Morris and Dyson, 2001]). These include cell cycle regulated proteins such as Mdm2 [Xiao *et al*, 1995] and PML [Alcalay *et al*, 1998].

RB1 was the first tumour suppressor gene to be cloned in humans and originally formed the basis of Knudson's two-hit hypothesis [Knudson, 1971], a hypothesis that was supported by evidence derived from analysis of patients with hereditary and non-hereditary forms of retinoblastoma, a rare tumour of the eye; Knudson showed that individuals with the hereditary form of retinoblastoma often developed bilateral tumours whereas individuals with the non-hereditary form usually developed unilateral tumours. This led Knudson to hypothesize that two mutational events were required to inactivate the gene responsible for retinoblastoma, but, in individuals that inherited a mutation in the retinoblastoma gene, only one mutational event was required to inactivate

the remaining functional allele. *RB1* was subsequently identified as the gene that was causal to this process and it has since been shown that most human cancers harbor mutations that directly or indirectly compromise pRb function (reviewed in [Sellers and Kaelin, 1997]); for example, inactivating mutations frequently occur in *RB1* itself, in addition to the mutation of upstream regulators of pRb, such as the homozygous deletion of $p16^{INK4a}$ or amplification of the *CDK4* locus. Significantly, most tumour-associated *RB1* mutations occur in the pocket protein domain ([Hu *et al*, 1990; Huang *et al*, 1990]; reviewed in [Classon and Dyson, 2001]).

During G_0 and early G_1, the carboxy-terminal (C-terminal) domain of pRb is hypophosphorylated [Bonetto *et al*, 1999; Knudsen and Wang, 1996]. This enables pRb to bind directly to E2F (**Figure 1.2**) and inactivate E2F in two ways; firstly, by binding to an 18 amino acid (aa) motif within the E2F transactivation domain, pRb directly blocks the ability of E2F to form a transcriptional activational complex [Flemington *et al*, 1993; Helin *et al*, 1993]. Secondly, pRb recruits repressive complexes such as histone deacetylase (HDAC) complexes and histone methyltransferases to the promoter regions of these genes to actively repress E2F transcription ([Brehm *et al*, 1998; Chen and Wang, 2000; Dahiya *et al*, 2000; He *et al*, 2000; Lai *et al*, 2001; Luo *et al*, 1998; Zhang *et al*, 1999]; reviewed in [Frolov and Dyson, 2004]). PRb also binds to a heterochromatic protein, HP1, via its LXCXE motif to promote the binding of HP1 to modified histones. HP1 uses its chromodomain to directly bind to modified histones, in addition to adjacent histone tails, thereby spreading the transcriptional silencing signal to nearby nucleosomes [Bannister *et al*, 2001; Lachner *et al*, 2001; Nielsen *et al*, 2001]. This activity leads to the formation of a compact DNA structure that is inaccessible to transcription factors.

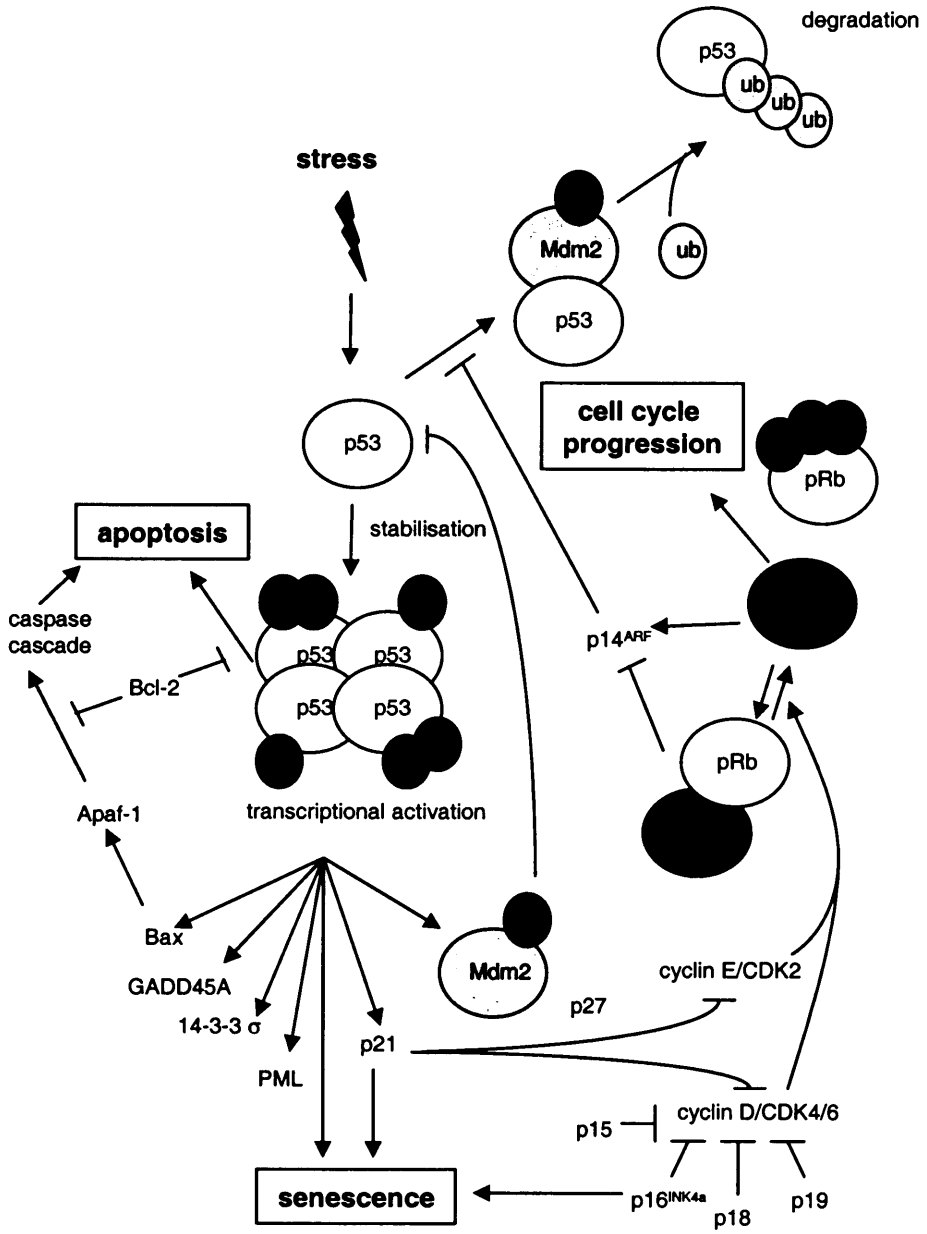

Figure 1.2: The PRb and P53 Signalling Pathways

Schematic diagram of the p53 and pRb signalling pathways that are involved in regulating progression through the cell cycle in response to genotoxic stress or oncogenic signals. Ub: ubiquitin; P: phosphorylation.

Evidence to support the role of pRb in transcriptional silencing is shown by the fact that, during G_1 phase, pocket proteins can be detected in peri-nucleolar foci that also contain E2Fs and histone deacetylase proteins [Kennedy *et al*, 2000].

During mid G_1 phase, pRb is phosphorylated by the activity of cyclin D1-CDK4/6. At R and late G_1 phase, pRb is further phosphorylated by the activity of cyclin E-CDK2 (reviewed in [Adams, 2001]). Hyperphosphorylation of pRb in the C-terminal domain peaks during late G_1 phase and causes pRb to dissociate from E2F ([Bonetto *et al*, 1999; Knudsen and Wang, 1996]; reviewed in [Weinberg, 1995]). This is supported by evidence that loss of Rb family repressor complexes at E2F-responsive promoters enables E2F to induce expression of S phase genes required for DNA synthesis [Rayman *et al*, 2002; Takahashi *et al*, 2000; Taubert *et al*, 2004]. PRb is maintained in its hyperphosphorylated form until emergence from M phase (reviewed in [Weinberg, 1995]), where upon it is dephosphorylated by PP1, a type 1 serine/threonine phosphatase [Nelson *et al*, 1997].

In addition to regulating cell cycle progression, pRb also plays a role in senescence, differentiation and apoptosis. During senescence, pRb interacts with HP1 and histone methyltransferases such as SUV39H1 to specifically repress E2F-responsive promoters and maintain the senescent state. However, experimental data is limiting due to the difficulty of obtaining good immunofluorescence data from compact chromatin [Narita *et al*, 2003]. In contrast, differentiation requires the direct interaction of pRb with tissue specific transcription factors to induce the differentiation of many different cell lineages, including adipogenesis, myogenesis and haematopoiesis [Condorelli and Giordano, 1997; Condorelli *et al*, 1995; Dunaief *et al*, 1994; Gu *et al*, 1993]. PRb activity is essential for this process [Lee *et al*, 1992], and this is shown by the inability of cells from mice deficient in pRb activity to differentiate both *in vitro* and *in vivo* ([de Bruin *et al*, 2003; Maione *et al*, 1994; Slack *et al*, 1995; Thomas *et al*, 2001]; reviewed in [Classon and

Harlow, 2002; Lipinski and Jacks, 1999]). There is also some evidence to indicate that pRb can inhibit apoptosis; for example, reconstitution of pRb in Saos-2 cells (a p53- and pRb- null osteosarcoma cell line) is sufficient to bypass apoptosis induced by exposure to ionizing radiation (IR) [Haas-Kogan *et al*, 1995]. Moreover, functional pRb activity is sufficient to inhibit IFN γ-induced apoptosis [Berry *et al*, 1996].

1.1.6 E2F

The predominant function of Rb family members is to negatively regulate E2F activity (**Figure 1.2**). Consequently, E2F plays a critical role in cycle regulation and this is shown by the fact that E2F activity is commonly abrogated during tumorigenesis; for example, deregulation of the E2F family occurs in almost all cancers (reviewed in [Phillips and Vousden, 2001]), whereas over-expression of E2F induces senescence in primary HDFs [Dimri *et al*, 2000].

E2F functions as a transcriptional regulator by forming a heterodimer with its cognate partner DP. Two DP proteins have been identified, namely DP1 and DP2, and heterodimerisation enhances both E2F transactivational activity, and the ability of Rb family members to bind to and negatively regulate E2F. Seven E2F family members have been described to date and these can be sub-divided into transcriptional activators (E2Fs 1-3a) and transcriptional repressors (E2Fs 3b-7; **Figure 1.3A**). The lack of transactivation and pocket protein-binding domains in E2F6 [Cartwright *et al*, 1998; Gaubatz *et al*, 1998; Trimarchi *et al*, 1998] is thought to render this particular E2F as a repressor as it prevents activator E2Fs from binding to the DNA and/or recruits polycomb group (PcG) proteins to target genes [Trimarchi *et al*, 2001]. E2F7 represents a recently identified E2F family member that is likely to function as a transcriptional repressor, as determined by sequence analysis [de Bruin *et al*, 2003].

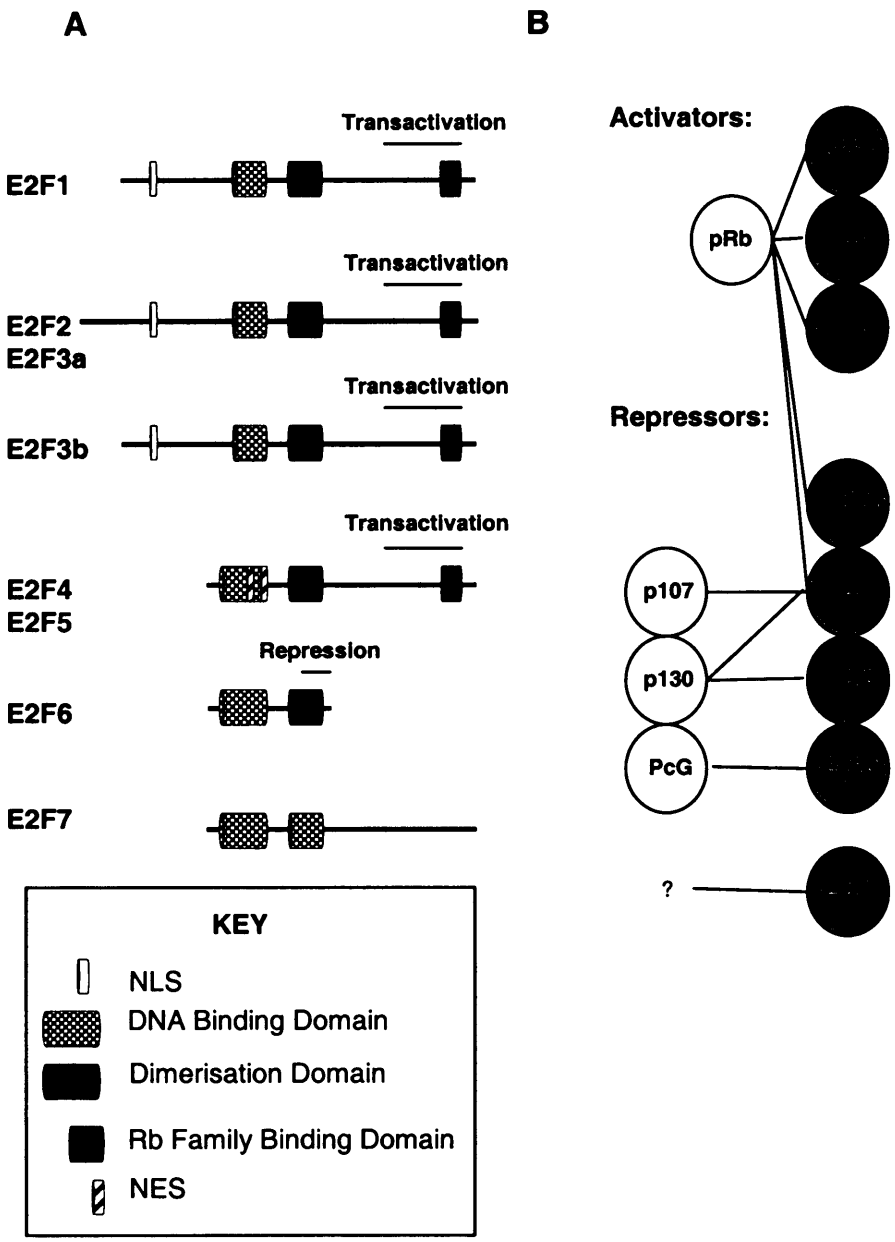

Figure 1.3: The Rb and E2F Protein Families

A: Schematic diagram of E2F family members. E2F proteins can be grouped with respect to their protein structure; NLS: Nuclear Localisation Signal; NES: Nuclear Export Signal; PcG: Polycomb group protein; **B:** Known interactions of the Rb and E2F family members (adapted from [Dimova and Dyson, 2005]). It should be noted that no binding partner of E2F7 has been identified, to date.

E2F does not contain the canonical LXCXE motif, however, E2F interaction with Rb family members occurs via the pocket protein domain and a C-terminal domain [Hiebert, 1993; Qin *et al*, 1992]. Specific combinations of Rb family–E2F interactions have been described; for example p107 and p130 preferentially bind to the repressive E2Fs (4-6) whereas pRb binds to E2Fs 1-4 (**Figure 1.3B**). However, the ability of the three pocket proteins to associate with six different E2Fs and two associated heterodimeric partners DPs (DP1-2; reviewed in [Cobrinik, 1996; Dimova and Dyson, 2005; Dyson, 1998; Nevins, 1998]), coupled with their distinct expression, sub cellular localisation and promoter-binding patters (reviewed in [Bracken *et al*, 2004; Cam and Dynlacht, 2003; Stevaux and Dyson, 2002; Trimarchi and Lees, 2002]), generates a complex pattern of finely-tuned transcription regulation. This is also indicated by evidence derived from gene expression profiling experiments; many genes appear to be regulated by E2F and these include genes involved DNA synthesis, DNA repair, recombination, apoptosis, differentiation and development ([Muller *et al*, 2001; Polager *et al*, 2002; Ren *et al*, 2002; Weinmann *et al*, 2002]; reviewed in [Cam and Dynlacht, 2003; DeGregori, 2002; Dimova *et al*, 2003; Stevaux and Dyson, 2002]). Moreover, recent evidence suggests that micro RNAs (miRNAs) may also be involved in regulating E2F activity [O'Donnell *et al*, 2005]. During late G_1 phase, pRb inactivation permits the releases of activating E2Fs 1-3 such that they become free to bind to their transcriptional targets. The interaction of E2Fs 1-3 with histone acetyltransferases (HATs) promotes localised histone acetylation at E2F-responsive promoters such that E2F can bind to DNA and activate transcription [Rayman *et al*, 2002; Takahashi *et al*, 2000; Taubert *et al*, 2004]. The transactivational activity of E2F is critical for cell cycle progression since the combined inactivation of E2Fs1-3 is sufficient to induce cell cycle arrest [Wu *et al*, 2001]. The transcriptional targets of the activating E2Fs include growth promoting and growth responsive genes such as *MYC* and *MYB*, genes necessary for DNA synthesis such as *DHFR*, *TK1*, *TYMS*, *POLA*, and cell cycle regulators such as *RB1*, *RBL1*, *CCNA*, *CCND1*, *CDC25A* and *E2F1*

itself, in addition to components of the DNA-replication machinery such as *CDC6*. The ability of E2F to transcriptionally activate *CCNE1* and *CDK2* also ensures that progression through to the next phase of the cell cycle occurs by forming a positive feedback loop.

In contrast, the repressive E2Fs (4 and 5) function in an antagonistic manner to the activating E2Fs; chromatin-immunoprecipitation (ChIP) analysis indicates that during G_0 and early G_1 phase, E2F 4- and 5-containing Rb family member complexes bind to and negatively regulate transcription from E2F-responsive promoters [Takahashi *et al*, 2000]. Evidence to support this is shown by the fact that inactivation of both E2F 4 and 5 do not inhibit cell proliferation, but does impair $p16^{INK4a}$-induced growth arrest [Gaubatz *et al*, 2000]. This indicates that negative E2F regulation is compromised during G_1 phase by replacement with transactional E2Fs that are activated during this phase of the cell cycle [Rayman *et al*, 2002; Takahashi *et al*, 2000; Taubert *et al*, 2004]. Therefore, it is proposed that the multiplicity of E2F factors provides a spectrum of transcriptional regulation, ranging from active transcriptional repression to active transcriptional activation. Furthermore, it has been suggested that the total level of E2F activity is not important for cell cycle regulation; rather, the balance between activating and repressive E2F is important. In support of this model, over-expression of E2F or DP has been shown to abolish a variety of growth arrest pathways, such as TGFβ-induced growth arrest, $p16^{INK4a}$-induced cell cycle arrest or contact inhibition [Bargou *et al*, 1996; Zhang *et al*, 1999]. Moreover, activating E2F mutants that escapes recognition by pRb can bypass a pRb-induced cell cycle block [Qin *et al*, 1995; Shan *et al*, 1996].

However, the precise role of E2F in the cell cycle remains contentious as there is some controversy regarding the interpretation of E2F experimental data; for example, it has been argued that, in many E2F studies, E2F activity is not sufficiently impaired [Maehara *et al*, 2005], and much of the experimental data is based upon *in vitro* analysis of classic E2F responsive genes by over-expression studies or by ChIP analysis. Significantly,

endogenous pRb has not been found on any human E2F target promoter during normal cell cycle regulation, it has rarely been detected on mouse promoters, and there is some discrepancy as to the complexes that are bound to promoter regions *in vitro* and *in vivo* [Narita *et al*, 2003; Takahashi *et al*, 2000; Wells *et al*, 2000]. Moreover, many of the cell cycle regulated E2F genes exhibit depression in p107- and p130- double-null cells but show little or no change in pRb-null cells [Herrera *et al*, 1996; Hurford *et al*, 1997; Mulligan *et al*, 1998].

1.1.7 P53 Pathway

The p53 family of proteins is comprised of three family members, p53, p63 and p73. All family members share structural and functional similarities (reviewed in [Levrero *et al*, 2000]); for example they exhibit a high level of amino acid sequence conservation within the DNA-binding region and this suggests a common role in transcriptional regulation. Indeed, all family members can form homo-oligomers, bind DNA and activate transcription from p53-responsive promoters ([Osada *et al*, 1998; Yang *et al*, 1998]; reviewed in [Irwin and Kaelin, 2001]). Moreover, over-expression of p63 and p73 is sufficient to activate p53 transcriptional targets and apoptosis ([Jost *et al*, 1997]; reviewed in [Urist and Prives, 2002; Yang *et al*, 2002]), whereas abrogation of p63 or p73 activity, like p53 inactivation alone, leads to the abrogation of apoptosis [Flores *et al*, 2002]. However, p53 possesses additional tumour suppressive activity that is not shared with p63 or p73; for example, p53-null mice are prone to both spontaneous and induced tumours [Donehower *et al*, 1992], unlike p63- or p73- null mice [Donehower *et al*, 1992; Mills *et al*, 1999; Yang *et al*, 1999; Yang *et al*, 2000].

1.1.8 P53

P53 was first identified as a cellular protein that co-immunoprecipitated with Simian Virus 40 (SV40) large T antigen (LT; [Lane and Crawford, 1979; Linzer and Levine, 1979]), and has since been shown to induce cell cycle arrest and DNA repair or apoptosis in response to DNA damage (**Figure 1.2**; reviewed in [Jin and Levine, 2001; Vogelstein *et al*, 2000]) to ensure that DNA replication, chromosome segregation and cell division occurs accurately [Vogelstein *et al*, 2000]. The vast number of cellular proteins that associate with the p53 pathway emphasises the critical role that p53 plays in controlling and integrating signals for cell cycle regulation and this has led to the labelling of p53 as the 'guardian of the genome' [Lane, 1992]. Moreover, *p53* has been shown to be one of the most commonly mutated genes in cancer; approximately half of all human cancers carry a mutation in *p53* and normal p53 function is lost in almost all human cancers [Hollstein *et al*, 1994]. It has also been shown that p53 inactivation predisposes organisms to develop cancers at a younger age [Malkin *et al*, 1990].

There is also much evidence to link the activity p53 to replicative senescence; for example, the introduction of wildtype (wt) p53 into p53-null cells is sufficient to induce senescence in these cells [Sugrue *et al*, 1997]. Moreover, p53 co-localizes with DNA damage signalling components at telomeres that have reached replicative senescence [d'Adda di Fagagna *et al*, 2003; Gire *et al*, 2004; Sugrue *et al*, 1997]. P53 also appears to be important in the maintenance of the senescent state, since, under these conditions, p53 is active [Atadja *et al*, 1995; Bond *et al*, 1996; Kulju and Lehman, 1995], and ablation of p53 function by microinjection of p53 antibodies in primary HDFs is sufficient to permit temporary reversal of senescence and re-entry in the cell cycle [Gire and Wynford-Thomas, 1998].

P53 is ubiquitously expressed, however, stabilisation and activation only occurs in response to genotoxic stress signals such as DNA damage, hypoxia, deregulation of microtubule assembly, low cell density or

deregulated growth signalling (reviewed in [Enoch and Norbury, 1995; Levine, 1997]). P53 activation occurs by a series of post-translational modifications that include phosphorylation, sumoylation, methylation and acetylation. These modifications promote changes in p53 conformation, stabilisation, interaction with binding partners and sub-localisation (reviewed in [Woods and Vousden, 2001]).

In response to IR, p53 is directly phosphorylated at serine 15 by ATM activity. Phosphorylation of serine 20 may also occur indirectly via Chk2 activity [Turenne *et al*, 2001]. It is also directly phosphorylated in response to ultraviolet radiation (UV) DNA damage by an ATM-related protein, ATR ([Hirao *et al*, 2000]; reviewed in [Appella and Anderson, 2001]). Serine residues, 33 and 37, are also phosphorylated in response to DNA damage [Tibbetts *et al*, 1999]. These modifications are critical for promoting the interaction of p300 and PCAF with p53, such that specific C-terminal residues in p53 are acetylated. These modifications localise p53 to the nucleus and enable it to overcome negative auto-regulation of its transactivational domain ([Dumaz and Meek, 1999; Lambert *et al*, 1998; Lill *et al*, 1997; Sakaguchi *et al*, 1998]; reviewed in [Appella and Anderson, 2001]).

P53 is also stabilised by phosphorylation of threonine residue 18 or serine residue 20 in the amino-terminus (N-terminus) of the protein. Phosphorylation of these residues blocks the negative regulatory activity of Mdm2 [Kussie *et al*, 1996], a ubiquitin E3 ligase that directly binds to the transactivational domain of p53 to directly block p53 transcriptional activity, and also promotes p53 ubiquitination [Haupt *et al*, 1997; Kubbutat *et al*, 1997]. Moreover, Mdm2 exports p53 to the cytoplasm where it is targetted for degradation by ubiquitin-mediated proteolysis [Momand *et al*, 2000]. Additional E3 ubiquitin ligases that negatively regulate p53 have been described; these include hPirh2 and COP1 (reviewed in [Lu, 2005]). Dissociation of p53 from Mdm2 results in the retention of p53 in the nucleus where its half-life is increased from 6-20 minutes (mins) to hours, thereby leading to a 3-10 fold increase in the concentration of p53 in the nucleus

(reviewed in [Harris and Levine, 2005]). Positive regulators that also stabilize p53 by inducing post-translational modifications include $p14^{ARF}$, PML, PTEN, NPM and p33ING1 [Bernardi *et al*, 2004; Freeman *et al*, 2003; Kurki *et al*, 2004; Leung *et al*, 2002; Weber *et al*, 1999].

Upon stabilisation, p53 forms a tetramer that binds to DNA in a sequence-specific manner. Tetrameric p53 binds to two repeats of an inverted consensus sequence separated by a spacer region of variable length ([el-Deiry *et al*, 1992]; reviewed in [Levine, 1997]). This p53-responsive element has been identified in the promoters and introns of many genes [Hoh *et al*, 2002] and the degenerate nature of the DNA-binding consensus sequence has been suggested to allow diversity and flexibility in the timing of the transcriptional response. Direct transcriptional targets of p53 include *p21*, *MDM2*, *BAX*, and *CCND1*, and the ability to transcriptionally activate *MDM2* leads to a negative feedback loop [Momand *et al*, 2000]. Furthermore, p53 associates with transcriptional co-regulators, such as acetyltransferases p300/CBP, to enhance transcriptional activation activity.

P53 activation leads to a block in G_1 phase such that DNA damage can be repaired. In this response, *p21* is transcriptionally activated and inhibits CDK activity [Brugarolas *et al*, 1995; Deng *et al*, 1995; el-Deiry *et al*, 1993; Harper *et al*, 1993; Pines, 1994; Waldman *et al*, 1995; Xiong *et al*, 1993]. The importance of this activity is shown by mice knock-ins that express a mutant form of p53 and are compromised for their ability to induce apoptosis but not arrest in G1 phase; the mutant mice retain the ability to delay the onset of tumorigenesis, unlike p53-null mice [Liu *et al*, 2004].

There is also evidence that a p53-dependent G_2/M phase boundary block occurs following DNA damage. This p53-mediated response again involves p21 and also involves 14-3-3σ (also known as Stratifin; [Aloni-Grinstein *et al*, 1995; Goi *et al*, 1997; Stewart *et al*, 1995]; reviewed in [Agarwal *et al*, 1995; North and Hainaut, 2000; Taylor and Stark, 2001]). Transcriptional activation of 14-3-3σ leads to the sequestration of Cdc25B

and cyclin B1-CDK1 in the cytoplasm [Hermeking *et al*, 1997]. A p53-mediated halt in DNA replication during S phase has also been described.

In addition to its role as a potent transcriptional activator, p53 transcriptional repression activity has also been described; for example, repression of *BCL2*, *RB1*, *FOS*, *JUN*, *MYC* and *PCNA* [Ginsberg *et al*, 1991; Mercer *et al*, 1991; Miyashita *et al*, 1994; Moberg *et al*, 1992; Shiio *et al*, 1992]. P53-mediated transcriptional repression may involve indirect interactions with other promoter-bound transcription factors [Horikoshi *et al*, 1995; Ragimov *et al*, 1993] and Sin3A, a co-repressor that recruits HDACs ([Murphy *et al*, 1999].

In addition to growth arrest, a second potent tumour suppressive mechanism mediated by p53 is the induction of apoptosis, a form of programmed cell death. Apoptosis occurs when damage is too extensive to be repaired and is induced by p53 in response to a number of stress stimuli, such as DNA damage, hypoxia and growth factor deprivation [Soengas *et al*, 1999]. Several p53-regulated genes have been identified, such as *BAX*, *NOXA* and *PUMA*, that each function to enhance the secretion of cytochrome *c* from mitochondria into the cytoplasm. In addition, genes that are involved in a second, extrinsic apoptotic pathway are also p53-regulated; for example, *FAS* and *DR5* [Owen-Schaub *et al*, 1995; Wu *et al*, 1997]. One hypothesis is that the ability of p53 to activate apoptosis by multiple pathways is important in its role as a tumour suppressor gene as there is immense selective pressure to lose pro-apoptotic activity during tumorigenesis. There is also evidence that p53 can negatively regulate the induction of apoptosis. Therefore, it is likely that the p53-induced response is dependent upon multiple factors involving both the cellular context and microenvironment.

1.1.9 P21$^{Waf1/Cip1/Sdi1}$

P21$^{Waf1/Cip1/Sdi1}$, or p21, is a 21 kDa protein that is a direct transcriptional target of p53 [el-Deiry *et al*, 1993] and was the first CDK

inhibitor to be identified [Harper *et al*, 1993]. P21 exhibits multifunctional activity and this is shown by the different functional assays that independently identified this protein; p21 was identified as an interacting partner of CDK in a yeast two-hybrid screen [Harper *et al*, 1993], co-purified with cyclin-CDK2 complexes [Gu *et al*, 1993] and co-precipitated with cyclin D [Xiong *et al*, 1993]. Independently, *p21* was also identified as a gene that was induced by over-expression of p53 in a subtractive hybridisation experiment [el-Deiry *et al*, 1993], and was also cloned from both senescent HDFs, where its over-expression was sufficient to inhibit DNA synthesis of cycling cells, and from differentiating melanocytes in a subtractive hybridisation experiment [Jiang *et al*, 1995]. Consequently, p21 has been labelled as Cip1 (CDK-Interacting Protein), Cap20 (CDK2-Associated Protein-20, Waf1 (wt p53 Activated-Fragment 1) and Sdi1 (Senescent Cell-Derived Inhibitor 1) and Mda6 (Melanoma Differentiation Antigen 6). This indicates that p21 induced upon G_1 phase growth arrest, senescence and differentiation ([Harvat *et al*, 1998; Martinez *et al*, 1999; Missero *et al*, 1995; Stein and Dulic, 1998; Todd and Reynolds, 1998]; reviewed in [Weinberg, 1995]).

As a direct target of p53, p21 mediates the growth suppressive activity of p53, but not apoptosis [Attardi *et al*, 1996; Cox, 1997; Deng *et al*, 1995]. Indeed, the C-terminus of p21 contains a caspase cleavage site that is cleaved during apoptosis, such that p21 cannot induce growth arrest [Poon and Hunter, 1998; Zhang *et al*, 1999]. P21 can also induce a growth arrest by p53–independent mechanisms [Gartel and Tyner, 1998].

Abrogation of p21 activity is associated with tumorigenesis; for example, p21 can block tumour cell growth both *in vitro* and *in* vivo [Cardinali *et al*, 1998; el-Deiry *et al*, 1993] and p21-null mice are susceptible to tumour development ([Martin-Caballero *et al*, 2001]; reviewed in [Lozano and Zambetti, 2005]). Moreover, mice that express a p53 mutant that retains the ability to activate *p21* develop tumours later than mice that express a p53 mutant that is unable to activate *p21*. However, it is important to note that p21 expression is rarely altered in human tumour samples. This observation

may be explained by the fact that p21 may exhibit functional redundancy with other p53 targets. Alternatively, factors that regulate the stability of p21 may be abrogated.

P21 is also transcriptionally activated upon the induction of senesce in primary HDFs, whereas inactivation of p21 permits a limited lifespan extension [Brown *et al*, 1997]. However, it is unknown how the activity of p21 in the induction of an irreversible growth arrest differs from its role in inducing a reversible growth arrest. Interestingly, p21 accumulation upon senescence is transient as it falls after the onset of senescence [Stein and Dulic, 1998] and this activity is unlike that of $p16^{INK4a}$, which is maintained at high levels in senescent cells [Stein *et al*, 1999].

In G_1 phase growth arrest, p21 functions by negatively regulating cyclin E-CDK2 activity (**Figure 1.2**). At high levels, it also represses cyclin D-CDK4/6 complexes. This activity maintains Rb family members in their hypophosphorylated, and therefore active, forms. The N-terminal region of p21 is critical for this activity since this region alone can inhibit the growth of tumour cells [Chen *et al*, 1995; Zakut and Givol, 1995]. However, p21 activity in mediating G_1 phase growth arrest is complicated by the fact that p21 can stabilize interaction between cyclin D-CDK4/6 complexes at low levels, promote the formation of active complexes [LaBaer *et al*, 1997] and thereby function as a positive regulator of cell cycle progression. P21 also promotes DNA repair by competing for binding to PCNA [Cox, 1997; Warbrick, 1998]; PCNA is a component of the DNA replication machinery that is required for both DNA replication and repair. Therefore, the interaction of p21 with the C-terminus of PCNA impairs the ability of PCNA to promote DNA replication. However, this does not affect PCNA-dependent nucleotide excision repair activity [Flores-Rozas *et al*, 1994; Li *et al*, 1994; Waga *et al*, 1994]. Upon repair, a negative feedback loop operates since p53 levels are reduced, the transcriptional activation of *p21* is reduced and CDKs become active.

1.1.10 INK4A Locus

The *INK4A* locus situated on human chromosome 9p21 is amongst the most frequent sites of genetic loss in human cancer and constitutes a unique feature in eukaryotes in that it transcribes two splice variants that both encode tumour suppressive proteins, namely $p16^{INK4a}$ and $p14^{ARF}$ (**Figure 1.4**). These CDKIs share no sequence homology at the protein level and differ in their functional activity, yet both function to negatively regulate distinct pathways that are critical for cell cycle progression; $p16^{INK4a}$ regulates the pRb pathway whereas $p14^{ARF}$ regulates the p53 pathway (**Figure 1.2**). Both $p16^{INK4a}$ and $p14^{ARF}$ share common regulatory mechanisms since they are both induced in response to aberrant growth or oncogenic stress, and both can be induced upon senescence. Yet, whilst there is substantial evidence to associate functional inactivation of $p16^{INK4a}$ with tumorigenesis, evidence to link $p14^{ARF}$ inactivation to tumorigenesis is less clear. This is due to the fact that $p14^{ARF}$ promoter methylation and missense mutations specific to $p14^{ARF}$ are rare and $p14^{ARF}$ has not been as extensively analysed as $p16^{INK4a}$ in the context of human cancer. Moreover, $p14^{ARF}$ activity is often lost concomitantly with $p16^{INK4a}$ and/or $p15^{INK4b}$; for example, $p15^{INK4b}$ is located only 10 Kilobases (kb) from the first exon of $p14^{ARF}$, therefore, co-deletion of $p14^{ARF}$ with $p15^{INK4b}$ frequently occurs. It is likely that $p16^{INK4a}$ and $p14^{ARF}$ evolved by selection of a common function and this hypothesis is supported by their common ability to function as tumour suppressive proteins, their ability to be expressed under similar conditions and to be co-regulated by molecules such as Bmi-1, CBX7 and TBX2 [Gil *et al*, 2004; Jacobs *et al*, 2000; Jacobs *et al*, 1999].

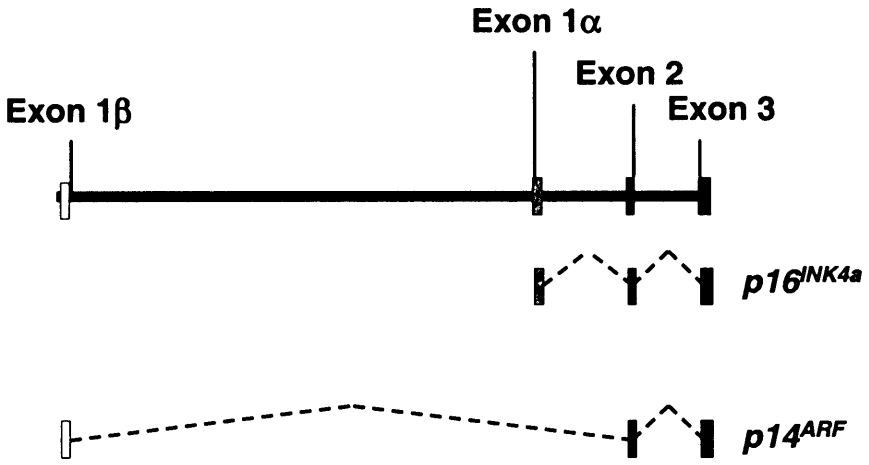

Figure 1.4: The *INK4A* Locus

Genomic organization of the *INK4A* locus. The two splice variants that are encoded by the *INK4A* locus are depicted.

1.1.11 P16^{INK4a}

The role of p16^{INK4a} as a tumour suppressor was first indicated by studies of familial melanoma that showed that incidences of melanoma segregated with missense mutations in *p16^{INK4a}* [Holland *et al*, 1995; Hussussian *et al*, 1994; Liu *et al*, 1995; Zuo *et al*, 1996]. It has since been shown that *p16^{INK4a}* is inactivated by deletion, point mutation and promoter methylation in many primary tumours and derived cell lines. However, the fact that humans homozygous for a severely truncated form of *p16^{INK4a}* may remain tumour free for several decades indicates that loss of p16^{INK4a} activity is not sufficient to induce tumorigenesis. More likely, p16^{INK4a} cooperates with other events to induce this [Gruis *et al*, 1995; Pavel *et al*, 2003].

P16^{INK4a} functions by specifically inactivating cyclin D-containing CDK complexes; p16^{INK4a} binds to and induces a conformational change in CDK4/CDK6 that results in the inhibition of adenosine triphosphate (ATP) - binding and thereby disrupts the interaction with D-type cyclins. This activity prevents CDK4/6 from phosphorylating pRb [Alcorta *et al*, 1996; Hara *et al*, 1996; Kiyono *et al*, 1998; Ohtani *et al*, 2001; Schmitt *et al*, 2002; Serrano *et al*, 1997; Zhu *et al*, 1998]. Evidence to support this includes the fact that loss of pRb and p16^{INK4a} activity generally occurs as mutually exclusive events in non-small cell lung cancer [Otterson *et al*, 1994; Shapiro *et al*, 1995]. Moreover, *p16^{INK4a}* expression cannot efficiently arrest pRb-deficient cell lines [Lukas *et al*, 1995].

P16^{INK4a} is positively regulated at the transcriptional level by Ets-1, a transcriptional activator that is activated by phosphorylation via ERK and p38 in response to Ras signalling. This pathway is subject to negative regulation; for example Wip-1 phosphatase negatively regulates p38 [Bulavin *et al*, 2004] and other negative regulators of p16^{INK4a} include Bmi-1 (B lymphoma Moloney Murine Leukaemia Virus [MoMuLV] insertion region 1; [Itahana *et al*, 2003;Park *et al*, 2004]), and Id1 (Inhibitor of DNA-binding 1; [Zheng *et al*, 2004]).

P16^{INK4a} also represents one of the few genes up-regulated upon replicative senescence and maintained in senescent cells. This up-regulation correlates with the constitutive hypophosphorylation of pRb in senescent cells [Alcorta *et al*, 1996; Hara *et al*, 1996; Stein *et al*, 1999; Zindy *et al*, 1997]. In contrast, inactivation of p16^{INK4a} is sufficient to enable some human cell types to become immortalised in conjuction with reconstitution of telomerase activity; for example, human mammary epithelial cells and keratinocytes [Kiyono *et al*, 1998; Rheinwald *et al*, 2002].

1.1.12 P14^{ARF}

P14^{ARF} was originally identified as a splice variant of the *INK4A* locus and is also known as ARF (Alternate Reading Frame), p14^{ARF} in humans, or p19^{ARF} in mice. *P14*^{ARF} has its own promoter and differs to *p16*^{INK4a} by the inclusion of an alternative first exon [Quelle *et al*, 1995]. This results in the translation of *p14*^{ARF} in an alternate reading frame to *p16*^{INK4a}, such that it exhibits no amino acid homology to p16^{INK4a}.

The first indication that p14^{ARF} functioned as a tumour suppressor came from the observation that mice lacking the first exon of *p14*^{ARF} were highly prone to spontaneous and carcinogen-induced tumours [Serrano *et al*, 1996]. Loss of p14^{ARF} activity was subsequently shown to render p53 inactivation surplus for immortalisation of mouse embryo fibroblasts (MEFs), both *in vitro* [Kamijo *et al*, 1997] and in tumours *in* vivo [Chin *et al*, 1997], and could inhibit transformation of MEFs by Mdm2. Yet, this activity did not occur in cells lacking *p53* [Pomerantz *et al*, 1998]. This indicated that p14^{ARF} functioned upstream of p53 in a linear pathway. *P14*^{ARF} specific mutations have since been reported in incidences of familial melanoma and astocytoma [Randerson-Moor *et al*, 2001; Rizos *et al*, 2001]. Moreover, promoter methylation of *p14*^{ARF}, but not *p16*^{INK4a} has been implicated in some incidences of colon cancer [Esteller *et al*, 2001; Esteller *et al*, 2000; Sato *et al*, 2002], and the finding that TBX2 and Pokemon, two transcriptional repressors

of $p14^{ARF}$ [Jacobs *et al*, 2000; Maeda *et al*, 2005], are both aberrantly over-expressed in a subset of human breast cancers and lymphomas indirectly links $p14^{ARF}$ to human cancer.

$P14^{ARF}$ functions by sequestering Mdm2 to the nucleolus, thereby impairing the ability of Mdm2 activity to promote the degradation of p53 by ubiquitin-mediated proteolysis ([Pomerantz *et al*, 1998; Zhang *et al*, 1998]; reviewed in [Sherr and Weber, 2000]). This activity enables $p14^{ARF}$ to indirectly stabilise p53 ([Pomerantz *et al*, 1998; Weber *et al*, 1999]; reviewed in [Lowe and Sherr, 2003; Sherr and Weber, 2000]). The N-terminal 25 aa are critical for $p14^{ARF}$ functional activity, and this region is encoded entirely by exon 1β [Quelle *et al*, 1995]. It has also been shown that $p14^{ARF}$ can inhibit cell proliferation by p53-independent pathways (reviewed in [Cleveland and Sherr, 2004]).

$P14^{ARF}$ expression is repressed under normal cellular conditions but is activated in response to aberrant signalling; for example, in response to oncogenic signals such as c-Myc, E2F-1, oncogenic Ras, v-abl, DMP1 and β-Catenin ([Inoue *et al*, 2000; Inoue *et al*, 2001]; reviewed in [DeGregori *et al*, 1997; Dimri *et al*, 2000; Sherr, 2001]). These data, in addition to the development of a $p19^{ARF}$-Green fluorescent protein (GFP) knock-in mouse, has provided *in vivo* evidence that the $p14^{ARF}$ promoter primarily functions as a sensor of oncogenic signalling [Zindy *et al*, 2003]. Furthermore, it has been suggested that a repressive E2F, E2F3b, binds to the $p14^{ARF}$ promoter throughout the cell cycle and only becomes displaced in response to aberrant E2F1 activation [Aslanian *et al*, 2004].

The $p19^{ARF}$-p53 pathway is the major pathway that induces senescence in mice (reviewed in [Lowe and Sherr, 2003; Sharpless, 2005]) since $p19^{ARF}$ expression correlates with the onset of senescence in MEFs and cells that lack $p19^{ARF}$ do not senesce in culture [Kamijo *et al*, 1997; Zindy *et al*, 1997]. Moreover, $p19^{ARF}$-null mice are prone to develop spontaneous tumours [Kamijo *et al*, 1999; Kamijo *et al*, 1997]. There is also evidence to suggest that over-expression of *E2F1* induces $p14^{ARF}$, thereby negatively regulating

Mdm2 activity and stabilising p53 (reviewed in [DeGregori *et al*, 1997; Prives, 1998; Sherr and DePinho, 2000]). This activity indirectly links the pRb and p53 pathway, and also links E2F activity to the induction of senescence [Zhu *et al*, 1998]. However, the significance of this pathway in humans is unclear; for example, despite the fact that $p14^{ARF}$ over-expression can induce cell cycle arrest or senescence [Dimri *et al*, 2000; Kamijo *et al*, 1997; Quelle *et al*, 1995; Wei *et al*, 2001], it has been argued that $p14^{ARF}$ activity is not critical for these processes ([Wei *et al*, 2001]; reviewed in [Munro *et al*, 1999; Rheinwald *et al*, 2002; Sharpless, 2005]). Moreover, $p14^{ARF}$ expression levels rise only in some HDF strains upon replicative senescence [Dimri *et al*, 2000].

1.1.13 Bmi-1

The transcriptional activation of both $p16^{INK4a}$ and $p14^{ARF}$ [Jacobs *et al*, 1999] are negatively regulated by Bmi-1. Bmi-1 is a transcriptional repressor of the PcG family that was originally identified as a c-Myc co-operating oncoprotein in murine B- and T-cell lymphomagenesis [Haupt *et al*, 1997; van Lohuizen *et al*, 1991]. PcG group proteins primarily function as transcriptional repressors that promote stable, epigenetic gene silencing though chromatin modifications mediated by histone methylation [van der Lugt *et al*, 1994]. They play a critical role during development where they function with Trithorax group of proteins to maintain proper gene expression patterns (reviewed in [Pirrotta, 1998]). Bmi-1 utilises its chromatin modification activity to interact with histone methyltransferases and histones to counteract SWI/SNF-chromatin re-modelling complexes [Breiling *et al*, 2004; Levine *et al*, 2002; Ogawa *et al*, 2002; Sewalt *et al*, 2002].

BMI1 is over-expressed in several different types of human cancer [Bea *et al*, 2001; Kim *et al*, 2004; Kim *et al*, 2004; Vonlanthen *et al*, 2001] and has been shown to be significantly down-regulated upon replicative senescence in primary HDFs, but not during quiescence. In contrast, *BMI1* over-expression

is sufficient to extend the replicative lifespan of some HDF strains [Itahana *et al*, 2003; Jacobs *et al*, 1999]. Bmi-1 also has a role in the self-renewal capacity of stem cells; for example, Bmi-1-null mice exhibit progressive loss of hematopoietic cells and cerebellar neurons [van der Lugt *et al*, 1994], concomitant with the up-regulation of both $p16^{INK4a}$ and $p19^{ARF}$. In contrast, mice deficient in Bmi-1, $p16^{INK4a}$ and $p19^{ARF}$ activity do not exhibit this loss; lymphocyte counts are restored and the cerebellar exhibits a normal size [Jacobs *et al*, 1999].

1.2 DNA TUMOUR VIRUSES

SV40, Adenovirus, and Human Papilloma Virus (HPV) are three examples of DNA tumour viruses. The natural hosts of DNA tumour viruses are differentiated cells, therefore, these viruses have evolved mechanisms to enable them to replicate in a non-proliferative cellular environment. These mitogenic properties include the ability to alter the cellular transcription machinery to promote the expression of proteins that are required for viral replication, to overcome the finite proliferative potential and to block cellular defenses against viral intrusion. Consequently, some of the viral proteins encoded by the DNA tumour viruses are able to inactivate the major control pathways regulating the cell cycle and are therefore implicated in the induction of tumorigenesis; for example, SV40 LT, HPV Type 16 E6 and E7 and Adenovirus Type 5 E1A and E1B all function as potent viral oncoproteins to induce immortalisation and transformation of many cell types [Braithwaite *et al*, 1983; Caporossi and Bacchetti, 1990; Chang *et al*, 1997; Duensing and Munger, 2002]. This has led to the extensive use of these viruses as molecular tools to delineate many signalling pathways in mammals. Importantly, these viral oncoproteins were the first to reveal the critical roles of p53 and pRb in the regulation of the cell cycle.

1.2.1 SV40

SV40 is a member of the papovavirus family of small icosahedral DNA viruses. SV40 was first linked to tumorigenesis by its ability to stably transform a proportion of hamster and rodent cell lines infected with this virus. Moreover, infection of newborn hamsters with SV40 induced the formation of tumours (reviewed in [Hilleman, 1998]). Unlike the natural lytic lifecycle of SV40 in its natural hosts (rhesus monkey or African green monkey cells), human or hamster cells are semi-permissive to infection with SV40; infection of these cells is sufficient for early SV40 genes to be expressed in a transient manner and survive infection. Moreover, a small proportion of infected cells permit viral replication. In contrast, mouse cells can be infected with SV40 but are non-permissive for viral replication and do not produce progeny virus particles.

1.2.1.1 LT

Three antigens are expressed from the SV40 early region by differential splicing of the same messenger RNA (mRNA) transcript; namely, LT, small t antigen and 17 kT antigen. The 708 aa LT protein alone is responsible for many of the functions of SV40 that are required for it to complete its lifecycle. LT is also involved in promoting the immortalisation of many cell types; for example, LT activity is sufficient to bypass replicative senescence in rat embryo fibroblasts (REFs; [Jat and Sharp, 1989]). Moreover, LT activity is required to maintain these cells in an immortalised state since inactivation of LT results in a rapid and irreversible arrest in either G_1 or G_2 phase [Jat and Sharp, 1989]. This indicates that the endogenous senescence machinery remains intact during this process. In accordance with this finding, MEFs become dependent upon LT for maintaining growth only when their normal mitotic lifespan has elapsed [Ikram *et al*, 1994].

LT possesses multifunctional activity (**Figure 1.5A**); for example, it possesses both DNA and RNA helicase activity [Scheffner *et al*, 1989], ATPase activity [Tjian and Robbins, 1979], RNA-binding activity [Carroll *et al*, 1988], DNA-binding activity [Carroll *et al*, 1974] and transcriptional regulation activity [Alwine *et al*, 1977; Gilinger and Alwine, 1993; Gruda *et al*, 1993; Hansen *et al*, 1981; Mitchell *et al*, 1987; Rice and Cole, 1993; Rushton *et al*, 1997; Saffer *et al*, 1990; Zhu *et al*, 1991]. LT can also impair the activities of many host cell proteins such as p53 [Lane and Crawford, 1979; Linzer and Levine, 1979], pRb [DeCaprio *et al*, 1988], p107 [Dyson *et al*, 1989; Ewen *et al*, 1989], p130 [Hannon *et al*, 1993], CBP, p300 [Avantaggiati *et al*, 1996; Eckner *et al*, 1996] and TBP [Martin *et al*, 1993]. Nuclear localisation is mediated the N-terminal region of LT [Kalderon *et al*, 1984; Soule and Butel, 1979].

LT shares significant sequence homology to the conserved region 2 (CR2) domain of E1A and E7 protein between amino acid residues 103-107. This region contains the canonical LXCXE-binding motif that mediates stable Rb family binding [DeCaprio *et al*, 1988; Moran, 1988; Munger *et al*, 1989]. LT only binds to the hypophosphorylated and therefore active form of Rb family members [Ludlow *et al*, 1989; Ludlow *et al*, 1990]. Consequently, LT promotes the release of E2F, enabling it to activate transcription from E2F-responsive promoters. This activity is critical for immortalisation as mutants defective for pRb-binding exhibit a reduced ability to immortalise rodent cells [DeCaprio *et al*, 1988; Powell *et al*, 1999]. Moreover, there is evidence to suggest that pRb-binding is important for the ability of LT to transform cells since some pRb-binding LT mutants are defective for transformation (reviewed in [Ali and DeCaprio, 2001]).

The N-terminal 82 aa constitute a functional dnaJ domain [Kelley and Georgopoulos, 1997] that includes a conserved hexapeptide sequence, HPDKGG, which can be found in nearly all papoviruses.

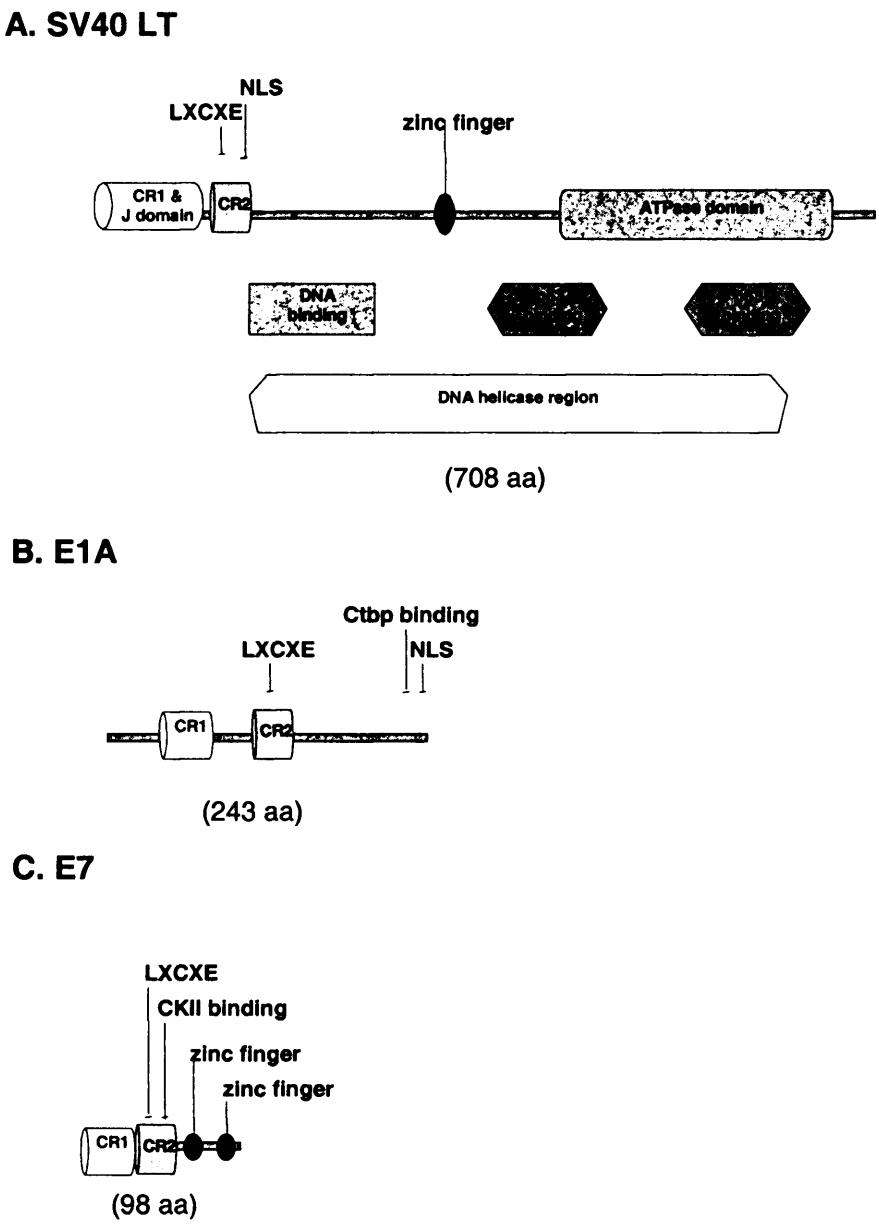

Figure 1.5: Conserved Regions of the DNA Tumour Viruses

Diagram of: **A:** SV40 LT; **B:** Adenovirus type 5 12S E1A; and **C:** HPV type 16 E7. NLS: Nuclear Localisation Signal; CR1: Conserved Region 1; CR2: Conserved Region 2; LXCXE: Rb family binding motif.

Cellular proteins, such as the dnaJ partner Hsc70 chaperone, are thought to be recruited to the J domain, transferred to complexes such as pRb-E2F located *in cis*, and undergo an ATP-dependent conformational change to promote the productive interaction of LT with pRb [Zalvide *et al*, 1998].

P53 was originally identified as an LT-binding protein [Lane and Crawford, 1979; Linzer and Levine, 1979] and binding to p53 is mediated by a bipartite region located towards the C-terminus of the protein between amino acid residues 351-450 and 533-626. LT interaction with p53 occurs via direct binding of LT to the sequence-specific DNA-binding domain of p53, as mutants of p53 that are impaired in sequence-specific DNA-binding activity are unable to bind to LT. The interaction of LT with p53 leads to abrogation of p53 activity since p53 is unable to transcriptionally regulate its target genes. Furthermore, this interaction stabilises p53 as both the half-life and steady-state levels of p53 are increased [Deppert *et al*, 1987; Oren *et al*, 1981]. It has also been suggested that the association of p300 and Mdm2 with p53 in a LT-binding complex contributes to this activity [Brown *et al*, 1993; Grossman *et al*, 1998; Henning *et al*, 1997]. The ability of LT to impair p53 activity appears to be critical for the immortalisation of MEFs [Conzen and Cole, 1995]. This is in contrast to data derived from rats since LT mutants that lack the C-terminal p53 bipartite binding domain are able to immortalise REFs [Powell *et al*, 1999]. This indicates that additional activities of LT may be able to inactivate downstream effectors of p53, and this may be mediated via Rb family binding [Quartin *et al*, 1994; Rushton *et al*, 1997].

P300 and CBP binding sites are also present in both the N-terminal and C-terminal domains of LT [Eckner *et al*, 1996; Lill *et al*, 1997], although their interactions may occur indirectly via p53-binding.

1.2.2 Adenovirus Type 5

Adenoviridae are double-stranded DNA viruses, 51 different serotypes of which have been identified. They primarily infect host epithelial tissues in the lung or enteric system and have been associated with the development of acute respiratory diseases. Adenovirus type 12 was the first serotype to be identified as being associated with tumorigenesis in rodents [Trentin *et al*, 1962], however, there is no evidence to indicate that adenovirus can induce tumorigenesis in humans. Transcription of the adenovirus genome is regulated by virus-encoded regulatory factors and two of the genes to be transcribed are E1A and E1B.

1.2.2.1 E1A

E1A represents a major regulatory protein expressed very early during adenovirus infection that is capable of activating transcription from a variety of viral and cellular promoters. Like LT, E1A exhibits multifunctional activity and can directly bind to multiple cellular proteins required for cell proliferation to mediate this activity (**Figure 1.5B**). Indeed, Rb family members, cyclin A, p300 and others were originally identified by their interaction with E1A [Whyte *et al*, 1988]. E1A is synthesised almost immediately after infection and two of the most abundant products are the 13S and 12S E1A splice variants [Perricaudet *et al*, 1980].

The conserved CR2 motif defines the region in E1A where Rb family members bind [Harlow *et al*, 1986; Whyte *et al*, 1988; Whyte *et al*, 1989]. However, residues in conserved region 1 (CR1) of E1A are also involved in this process [Whyte *et al*, 1989]. This interaction disrupts pRb-E2F complexes and enables E2F to promote entry into S phase (**Figure 1.5B**; reviewed in [Sherr, 1996]). E1A is localised to the nucleus by virtue of a highly basic pentapeptide signal sequence located at the extreme C-terminus. E1A, like LT, can also bind to p300 [Dorsman *et al*, 1995; Goodman and

Smolik, 2000; Wang *et al*, 1995], and this promotes the formation of a pRb/p300/E1A complex that may both stabilise the E1A-pRb interaction [Barbeau *et al*, 1994] and promote acetylation of pRb at the C-terminus [Chan *et al*, 2001]. This activity is important for E1A-induced cell cycle progression and transformation [Egan *et al*, 1989; Whyte *et al*, 1989]. CtBP, a putative HDAC recruitment protein, binds to a region in the C-terminus [Goodman and Smolik, 2000]. Other known cellular binding partners include cyclin A, p400, CDK2, BS69, TBP and various components of the TFIID complex.

1.2.2.2 E1B

E1A can induce apoptosis through the stabilisation of the p53 tumour suppressor protein during oncogenic transformation [Lowe and Ruley, 1993; White *et al*, 1994; White *et al*, 1992], therefore, additional factor(s) are required to abrogate p53 and prevent the induction of apoptosis. In adenovirus, this activity is performed by E1B. The ability of adenovirus to segregate pRb and p53-abrogation activities between two different viral oncoproteins is in contrast to the combined functional activity of LT. Moreover, multiple proteins are transcribed by adenovirus to inhibit p53-dependent apoptosis; E1B-55kDa and E4orf directly bind to and inactivate p53 [Nevels *et al*, 1997; Yew *et al*, 1994], whereas E1B-19kDa blocks apoptosis by mimicking the anti-apoptotic activity of Bcl2 [Rao *et al*, 1992].

The E1B-55kDa protein binds to the N-terminal transactivation domain of p53 [Kao *et al*, 1990] and blocks the ability of p53 to activate transcription from p53-responsive promoters [Yew *et al*, 1994]. Moreover, mutational analysis indicates that inhibition of p53-mediated transactivation correlates with the transformation potential of E1B-55kDa [Yew and Berk, 1992]. E1B-55kDa can also associate with E4orf6 to down-regulate p53 by ubiquitin-mediated proteolysis [Querido *et al*, 1997; Steegenga *et al*, 1998].

E1B-19kDa protein impairs p53 activity by a different process to E1B-55kDa; E1B-19kDa blocks apoptosis induced by p53 [Debbas and White,

1993], TNF-α, and Fas antigen [Sabbatini *et al*, 1995; White *et al*, 1992] in a process that mimics endogenous Bcl2 anti-apoptotic activity. Indeed, E1B-19kDa has been shown to share both functional and structural homologies with the Bcl2 protein [Rao *et al*, 1992]. It has also been shown that E1B-19kDa can overcome p53-induced apoptosis by alleviating p53-mediated transcriptional repression [Sabbatini *et al*, 1995; Shen and Shenk, 1994] and by binding to the p53-inducible death-promoting protein Bax [Han *et al*, 1996].

1.2.3 HPV Type 16

HPV type 16 is a member of the small double-stranded DNA tumour virus family that specifically infects squamous epithelial cells. The lifecycle of HPVs are linked to the differentiation program of the host epithelial cells since HPVs infect undifferentiated, basal keratinocytes, but most of the viral lifecycle occurs in the differentiated upper epithelial strata where virus particles are shed. Papilloma viruses can be divided into mucosal or cutaneous growth tropism groups and further subdivided in respect to their propensity for malignant progression, namely high or low risk. HPV type 16 represents the most prevalent mucosal high risk HPV type and two proteins encoded by HPV function in an analogous manner to both LT and E1A and E1B, namely E6 and E7. E6 and E7 are stably expressed in HPV-positive cervical cancers and cancer-derived cell lines [Schwarz *et al*, 1985], and they are essential to maintain the transformed state of HPV-positive cells [Alvarez-Salas *et al*, 1998]

1.2.3.1 E7

E7 has been identified in approximately 90% of all human cervical cancers [zur Hausen, 2001] and 20% of oral cancers [Gillison *et al*, 2000]. E7 is a small multifunctional protein of 98 aa encoded by the early region of HPV and is responsible for the ability of this virus in overcoming G_1 phase arrest induced by loss of cell adhesion, growth factor withdrawl, DNA damage and differentiation signals (**Figure 1.5C**). Similar to LT and E1A, E7 possesses the canonical LXCXE motif of Rb family binding in CR2 that facilitates the targetted binding of hypophosphorylated pRb [Gage *et al*, 1990] and other members of the Rb family [Davies *et al*, 1993; Dyson *et al*, 1992]. In addition to the LXCXE motif, E7 also shares sequence homology with LT and E1A in a small region of CR1. E7 exhibits a high turnover rate of approximately 2 hours (hrs), mediated by ubiquitin-mediated proteolysis. Therefore, efficient pRb-inactivation is achieved by targetting E2F for ubiquitin-dependent proteolysis [Alani and Munger, 1998; Boyer *et al*, 1996] and this activity distinguishes E7 from LT and E1A. Indeed, it has been suggested that elimination of pocket proteins in this manner enables E7 to subvert many cellular activities that are specific to the pocket proteins, independently of E2F.

E7 contains two copies of a zinc-binding CysXXCys sequence in the C-terminus that promotes E7 oligomerisation. Despite the lack of a characterised nuclear localisation signal, E7 is predominantly nuclear [Greenfield *et al*, 1991]. However, the low steady-state levels of E7 render analysis of this protein difficult. E7 may undergo phosphorylation at a CKII phosphorylation site in the N-terminus [Barbosa *et al*, 1990] and at another site in the C-terminus [Massimi and Banks, 2000], yet the significance of these post-translational modifications is not properly understood. E7 expression is also known to induce primary centrosome and centriole duplication errors in normal diploid cells [Duensing *et al*, 2001]. This activity may occur independently of Rb family abrogation due to similar effects seen

in MEFs lacking expression of Rb family members [Duensing and Munger, 2003].

A number of additional E7-interacting proteins have been described; for example, E7 can bind to two CDKIs, namely p21 and $p27^{kip1}$. Moreover, it has been suggested that p21 inactivation is critical for the ability of E7 to promote viral DNA replication during keratinocyte differentiation, in addition to overriding the cytostatic effect of TNF-α in these cells. E7 has also been shown to associate indirectly with cell cycle regulators such as cyclin A, cyclin E and CDK2 via p107 to promote their aberrant expression and activity. There is also evidence that E7 can inhibit p53 transcriptional activity [Massimi and Banks, 2000]; in this model, CKII activity may be required to phosphorylate E7 and stimulate the ability of E7 to complex with TBP and form a tripartite complex with p53. This activity is similar to the tripartite complex proposed for E1A, p53 and TBP.

1.2.3.2 E6

Like adenovirus, the activity of a second viral oncoprotein is required to directly bind to and inactivate p53 to inhibit the induction of apoptosis. In HPV-16, E6, a small protein of 151 aa mediates this activity [Scheffner *et al*, 1992]. Unlike LT and E1B however, E6 destabilises p53 by association with the ubiquitin ligase E6ap to promote p53 degradation by the ubiquitination pathway [Huibregtse *et al*, 1991; Rapp and Chen, 1998; Scheffner *et al*, 1993]. This activity impairs the ability of p53 to induce apoptosis or growth arrest; for example, the majority of human cervical cancers exhibit wt p53 activity, yet its activity is functionally neutralised by the activity of E6 [Thomas *et al*, 1999]. The oncogenic activity of E6 has also been demonstrated by its ability to transform established MEFs and to confer resistance to terminal differentiation of human keratinocytes (reviewed in [Mantovani and Banks, 2001]). Moreover, its ability to transcriptionally activate the catalytic component of human telomerase (hTERT) in some cell

types [Gewin and Galloway, 2001; Oh *et al*, 2001; Veldman *et al*, 2001] is important for it to function as an oncoprotein.

E6 contains four copies of a zinc-binding CysXXCys sequence [Barbosa *et al*, 1989; Grossman *et al*, 1989; Kanda *et al*, 1991] and has been implicated in transcriptional activation, immortalisation and transformation [Dalal *et al*, 1996; Foster *et al*, 1994; Kanda *et al*, 1991; Lamberti *et al*, 1990; Ned *et al*, 1997; Vousden *et al*, 1989]. E6 is localised to the nuclear, cytoplasmic and non-nuclear membrane (including Golgi membrane) fractions in a variety of cells [Androphy *et al*, 1987; Guccione *et al*, 2002]. Furthermore, E6 exhibits both non-specific double-stranded [Kanda *et al*, 1991; Mallon *et al*, 1987] and sequence-specific DNA-binding activity [Kammer *et al*, 2000]. However, the low steady-state levels of E6 in cells, like E7, render E6 activity difficult to analyse.

In addition to inactivating p53, E6 can impair the activity of many other cellular proteins; for example, E6 down-regulates p21 in many normal cell types [Burkhart *et al*, 1999] and interacts with the pro-apoptotic Bak, TNFR-1, and DNA repair proteins MGMT and XRCC1 [Filippova *et al*, 2002; Jackson *et al*, 2000; Mantovani and Banks, 2001], amongst others. The fact that both pro- and anti-apoptotic activities for E6 have been described is difficult to reconcile but may be cell context-dependent; for example, in HDFs, E6 expression inhibits oxidant-induced apoptosis within 24 hrs but sensitises cells to apoptosis after prolonged incubation [Chen *et al*, 2000].

1.3 HUMAN CELLULAR SENESCENCE

Replicative senescence is a biological process that was first described by Leonard Hayflick and Paul Moorhead [Hayflick and Moorhead, 1961]. It was observed that serially passaged primary HDFs derived from embryonic tissues exhibited a finite proliferative potential of approximately 50 population doublings (PDs) before entering into an irreversible state of growth arrest (**Figure 1.6**; [Hayflick and Moorhead, 1961]). Replicative senescence

has since been described in many different cell types and different species, including adult stem cells [Allsopp *et al*, 2003; Allsopp and Weissman, 2002; Ramirez *et al*, 1997; Yui *et al*, 1998], with the notable exception of embryonic stem (ES) cells and most cell lines [Hayflick, 1974]. A variety of intrinsic and extrinsic stimuli have also been shown to induce this process, therefore, replicative senescence represents just one example of a general biological process known as cellular senescence.

1.3.1 Senescence is a Genetically Determined Process

Somatic cell hybridisation studies provided the first experimental evidence that cellular senescence is a dominant genetically determined process; the fusion of immortal cells with pre-senescent fibroblasts was not sufficient to overcome a finite proliferative lifespan, as the resultant hybrid cells eventually became senescence [Bunn and Tarrant, 1980; Muggleton-Harris and DeSimone, 1980; Pereira-Smith and Smith, 1983]. It was subsequently shown that the fusion of senescent cells to a number of immortalised cell lines was also not sufficient to bypass the induction of senescence in the resultant hybrid cells, despite the fact that mitogen-responsible genes remained responsive [Pereira-Smith and Smith, 1988]. These findings indicated that senescence can be induced in pre-senescent cells and that immortal cells exhibit a recessive phenotype.

It has since been shown that transcriptional activation events can induce senescence; for example, treatment of HDFs with inhibitors of protein synthesis prior to fusion is sufficient to impair the induction of senescence. Moreover, microinjection of poly $(A)^+$ RNA prepared from senescent HDFs into proliferating cells is sufficient to inhibit DNA synthesis in these cells, whereas poly (A)+ RNA derived from young cells made quiescent by serum starvation only has a minor effect [Lumpkin *et al*, 1986].

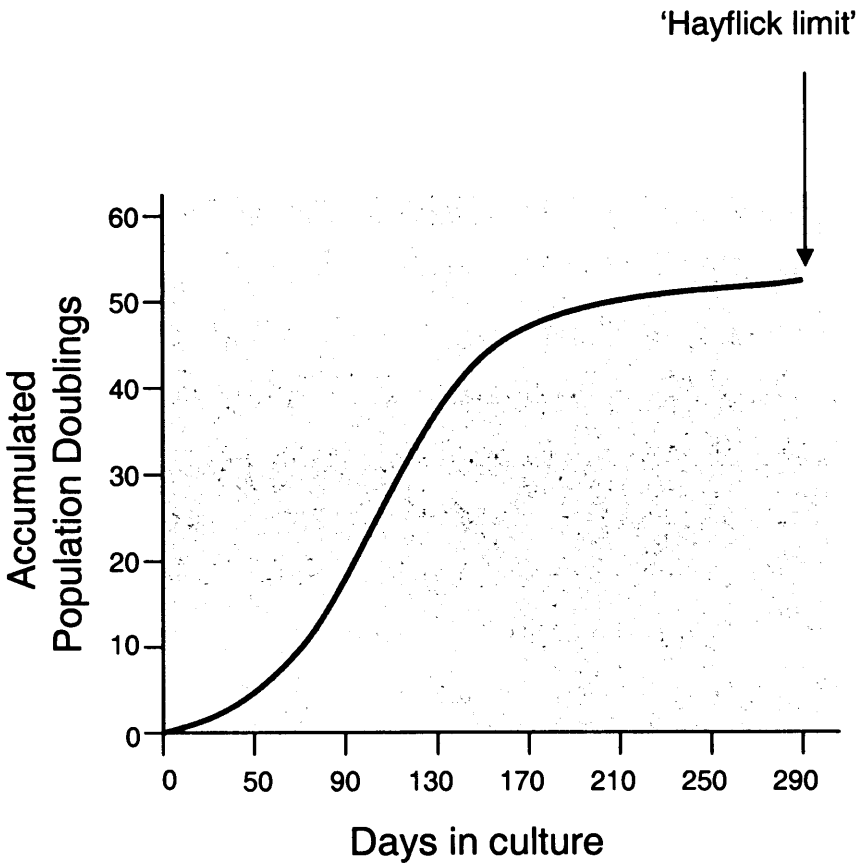

Figure 1.6: Replicative Senescence

Hayflick and Moorhead [Hayflick and Moorhead, 1961] analysed primary HDFs sub-cultivated in vitro and demonstrated that these cells exhibited a finite proliferative potential; after approximately 50 PDs, at a point termed the 'Hayflick limit', the cultures failed to expand, and the cells were considered senescent.

To further delineate this process, Pereira-Smith and Smith [Pereira-Smith and Smith, 1988] fused 40 different immortal human cell lines with each other and classified immortal hybrids into the same complementation group whereas senescent hybrids were classified into different complementation groups. Four different complementation groups were identified in this process. This indicated that multiple genes were involved in inducing senescence. Furthermore, the ability to assign immortal cell lines to different groupings provided an opportunity to determine the identity of the genes involved in this process; for example, microcell transfer of human chromosome 1 into an immortal Syrian hamster cell line was sufficient to induce a senescent phenotype [Sugawara *et al*, 1990]. This indicated that human chromosome 1 contains senescence promoting activities, and, in accordance with this finding, it has since been shown that this chromosome contains two senescence-inducing loci [Vojta *et al*, 1996].

1.3.2 Senescence Phenotype

The irreversible growth arrest typified by senescent cells usually occurs in G_1 phase of the cell cycle, although it may also occur during G_2 phase. Phenotypically, senescent cells are characterised by their enlarged, flattened morphology and their ability to be maintained in culture for long period of time. They are resistant to apoptosis and remain metabolically active, as shown by their ability to synthesise mRNAs and proteins [Lumpkin *et al*, 1986]. However, unlike quiescence cells, the growth arrest exhibited by senescent cells is irreversible [Cristofalo *et al*, 1989]; for example, serum growth factors can induce many early response genes such as *MYC*, but the cells do not enter the cell cycle [Matsumura *et al*, 1979].

Transcriptional up-regulation of markers such as senescence-associated acid-β-galactosidase (SA-β-galactosidase; [Dimri *et al*, 1995]), PAI-1, fibronectin [Kumazaki *et al*, 1991], collagenase I [Millis *et al*, 1992], $p14^{ARF}$, p53 [Kulju and Lehman, 1995], p21 and $p16^{INK4a}$ [Alcorta *et al*, 1996; Hara *et*

al, 1996; Tahara *et al*, 1995] have all been described. In contrast, positive regulators of the cell cycle, such as CDK2 [Afshari *et al*, 1993], cyclin A, cyclin B [Stein *et al*, 1991], cyclin E and cyclin D1 [Dulic *et al*, 1993] in addition to enzymes required for DNA replication, such as TK1 and DHFR [Drayton and Peters, 2002; Seshadri and Campisi, 1990; Sherr and DePinho, 2000], are all down-regulated upon senescence. However, it is not known if these changes are causal or consequential to the induction of this process.

1.3.3 Senescence Biomarkers

Only a few *bona fide* biomarkers of senescence have been identified to date. These include SA acid-β-galactosidase activity [Dimri *et al*, 1995] and senescence-associated heterochromatic foci (SAHF; [Narita *et al*, 2003]).

Currently, SA acid-β-galactosidase activity represents the most commonly utilised biomarker. This biomarker exploits the property of senescent HDFs to exhibit lysosomal hydrolase β-galactosidase activity at pH4.0, unlike pre-senescent, quiescent and immortal HDFs that only exhibit lysosomal hydrolase β-galactosidase activity at pH6.0 [Dimri *et al*, 1995]. The physiological relevance of this activity is not understood, however, one hypothesis suggests that it represents a bystander effect caused by an alteration in the lysosomal pH optimum [Dimri *et al*, 1995], or a general increase in lysosomal activity [Gary and Kindell, 2005; Kurz *et al*, 2000]. Accordingly, the use of this biomarker remains contentious; for example, positive SA acid-β-galactosidase activity may also occur under senescence-independent conditions such as stressful culture conditions [Iwasa *et al*, 2003] or confluency [Gary and Kindell, 2005]. Moreover, the method used to detect SA acid-β-galactosidase activity is technically difficult; for example, it is tedious, subjective, and semi-quantitative and varies considerably even within an apparently homogeneous population of cultured cells [Severino *et al*, 2000]. An improvement to the detection mechanism, by development of a quantitative assay of SA acid-β-galactosidase activity that rapidly measures

accumulation of a fluorogenic galactose analog from cell lysates has, to some extent, addressed these issues [Gary and Kindell, 2005]. Yet, these findings illustrate the need to identify novel markers of senescence.

The fact that that permanent, epigenetic changes are likely to be induced upon senescence to mediate stable transcriptional repression [Zhang *et al*, 2005], as indicated by micrococcal nuclease digestion and 4'-6-diamidino-2-phenylindole (DAPI) staining of senescent cells, has also revealed that senescent cells contain many heterochromatic rich regions of DNA, also known SAHF [Narita *et al*, 2003].

SAHF is dependent upon hypophosphorylation of both pRb and $p16^{INK4a}$ and has been shown to inhibit expression of E2F target genes [Narita *et al*, 2003]; for example, the promoters of several E2F targets have been shown to contain markers of heterochromatin, such as hypoacetylated histones, histone H3 methylation on lysine 9 ($Me\text{-}K^9\text{-}H3$) and heterochromatic proteins HP1 α, β and γ [Narita *et al*, 2003]. Other factors that are known to modulate changes in the formation of heterochromatin have also been associated with the formation of SAHF; for example, a transcriptionally repressive variant of histone H2A, namely MacroH2A, that is a member of a protein family associated with inactive X chromosomes in female mammals [Zhang *et al*, 2005], and a histone methylation promoting enzyme, SUV39H1, that has been shown to be associated with Ras-induced senescence (discussed in **Section 1.3.7**) in lymphocytes [Braig *et al*, 2005].

1.3.4 Senescence and Terminal Differentiation

Senescence exhibits similarities with terminal differentiation as, in both cases, cells undergo an irreversible growth arrest that is resistant to mitogenic signalling, yet remain viable [Peacocke and Campisi, 1991]. In addition, both senescent and terminally differentiated cells exhibit significant changes in cell morphology [Dimri *et al*, 1996] and common changes in gene transcription, such as the induction of interleukins (such as *IL1*), cell cycle regulatory genes

(such as *p21*) and DNA damage-inducible genes (such as *GADD153* and *GADD34*; [Huang *et al*, 1999; Ikeyama *et al*, 2003]). Similar to premature senescence, terminal differentiation can also be induced in a variety of cell types by non-specific chemical reagents; for example, ionising radiation can induce premature terminal differentiation in HDFs [Rodemann *et al*, 1991]. However, there is conflicting evidence that indicates that senescence and terminal differentiation are distinct; for example, only differentiated melanocytes display elevated levels of *p21* and the melanocyte-specific transcription factor *MITF* [Medrano *et al*, 1994; Smith and Pereira-Smith, 1996].

These observations can be reconciled by the hypothesis that senescence represents an example of terminal differentiation; for example, senescent fibroblasts may represent a form of terminally differentiated fibroblasts, also known as fibrocytes, which remain functional in connective tissues. This hypothesis predicts that the signalling processes that occur in terminal differentiation and senescence will exhibit significant similarities and overlaps and this is indeed observed; for example pRb is known to have a critical role in the induction of senescence and also has a critical role in the switch between proliferation and differentiation through association with various tissue specific transcription factors [Benevolenskaya *et al*, 2005]. Many different cell lineages depend upon the activity of pRb to lead to the differentiation of neuronal, myogenic, adipocyte, ostreogeneic, hematopoietic, and lens cells. In agreement with these data, it has also been demonstrated that inactivation of pRb impairs differentiation both *in vitro* and *in vivo* ([de Bruin *et al*, 2003; Lipinski and Jacks, 1999; Maione *et al*, 1994; Slack *et al*, 1995; Thomas *et al*, 2001]; reviewed in [Classon and Harlow, 2002]).

1.3.5 Senescence as an Artefact of in vitro Manipulation

The possibility that senescence represents an artefactual *in vitro* response that occurs in response to technical manipulation should be considered (reviewed in [Gershon and Gershon, 2000; Wright and Shay, 2000]); for example, the expression of oncogenic *RAS* is sufficient to induce premature senescence in primary cells *in vitro*. However, this does not occur when oncogenic *RAS* is expressed from its endogenous locus [Benanti and Galloway, 2004; Guerra *et al*, 2003; Tuveson *et al*, 2004].

Cells sub-cultivated *in vitro* are subject to considerable stress and architectural differences that are not present *in vivo* and this has a profound consequence upon the activity of the cell. Firstly, culture conditions are subject to elevated oxygen levels when compared to normal physiological conditions and increased oxidative stress can affect the proliferative capacity of cells; for example, an inverse correlation between population doublings and oxygen gas conditions has been shown in HDFs [Saito *et al*, 1995]. Moreover, data derived from MEFs indicates that murine cells are particularly susceptible to culture stress conditions, as they do not undergo senescence when they are sub-cultivated in low (3%) oxygen conditions [Parrinello *et al*, 2003]. However, it should be noted that not all cell types exhibit sensitivity to hyperoxia; for example human epithelial cells, unlike HDFs, exhibit only a modest reduction in their proliferative capacity in 40% oxygen conditions [Honda *et al*, 2001].

The processes that are used to manipulate cells *in vitro* may also affect cellular function; for example, trypsin may degrade receptors and other extracellular domain molecules and may be toxic at 37°C [Huggins *et al*, 1976; McKeehan, 1977; Reiners *et al*, 2000]. The cellular microenvironment similarly plays an integral role to the appropriate function of a cell within a tissue. Therefore, the monolayers that cells typically form when cultured *in vitro* will differ dramatically from the three-dimensional (3D) tissue

architecture exhibited *in* vivo and this may have an affect upon the regulation of cellular processes such as proliferation, differentiation and apoptosis.

1.3.6 Telomere-Dependent Cellular Senescence

In MEFs, spontaneous immortalisation occurs at a relatively frequent rate. In comparison, spontaneous immortalisation in REFs is rare but may be induced by treatment with chemical carcinogens [Newbold *et al*, 1982]. However, in HDFs, spontaneous immortalisation occurs rarely, if at all. These findings indicate that additional regulatory mechanisms have evolved in human cells to ensure more stringent regulation of this process (reviewed in [Reddel, 2000]).

One hypothesis proposes that in long-lived species such as *Homo sapiens*, a potent selection pressure must have driven the evolution of somatic cell repair process such that they are more precise than those of short-lived species. This is supported by evidence that the *in vitro* replicative lifespan of cells from various species correlates with the maximum lifespan of members of those species [Rohme, 1981]. However, as it is unlikely that natural selection could act to produce a programmed cellular response that operates at the end of life (ie after organismal reproduction has ceased), it has been suggested that cellular senescence must have evolved as a process that benefited the organism prior to the end of reproductive age. Accordingly, it has been suggested that senescence represents a mechanism by which cells within an organism can retain their biochemical function, but are prevented from replicating and propagating genetic damage that it has accumulated.

It is very likely that senescence occurs *in vivo* to limit tumorigenesis since the induction of this process increases the chance of cancer-free pre-reproductive survival. This is particularly important in a long-lived species such as *Homo sapiens* where reproduction occurs relatively late. Therefore, has been suggested that the detrimental effects that occur in tissue function and promote organismal ageing are merely bystander effects. Accordingly,

the link between senescence and ageing may represent an example of antagonistic pleiotropy; an evolutionary model to explain the deleterious effects of a biological process that is exhibited in later life [Williams, 1957]. For example, p53-null mice spontaneously develop tumours and consequently exhibit short lifespan [Jacks, 1996], whereas mice that constitutively express p53 exhibit a decrease in the incidence of spontaneous tumours concomitant with an increased rate of induction of premature ageing [Tyner *et al*, 2002]. However, the development of a novel transgenic mice, named 'super-53', that expresses wt endogenous p53 in addition to 1-2 extra copies of wt *p53* inserted as a transgene expressed from its own promoter [Garcia-Cao *et al*, 2002], has questioned these findings since these mice exhibit a reduced rate of tumorigenesis but not premature ageing; the authors concluded that, unlike in the mutant mice generated by Tyner and colleagues, *p53* was induced only under physiologically appropriate conditions in the mutant mice generated by Garcia-Cao and colleagues.

As below, there is much evidence to suggest that telomere shortening represents the extra control mechanism in humans, since repression of telomerase activity in normal human cells confers a limited replicative potential *in vitro* and primary human cells undergo an intrinsically programmed number of PDs before entering into an irreversible state of growth arrest known as replicative senescence. This limit is often referred to as the 'Hayflick limit' (**Figure 1.6**) and, as such, telomere shortening is often referred to as functioning as a 'mitotic clock'.

1.3.6.1 Telomeres

Telomeres are nucleoprotein structures located at the ends of the chromosomes. The primary function of these structures is to protect the end of chromosomes from being recognised as double-strand DNA breaks, followed by degradation and end-to-end fusion with other chromosomes; for example recombination may occur by non-homologous DNA end-joining

(NHEJ; [Chan and Blackburn, 2002; Lundblad, 2000]). The consequences of telomeric fusions are significant since the formation of dicentric chromosomes may result in chromosomal DNA breakages, fusions and genomic rearrangements during mitosis (reviewed in [Gisselsson, 2003]). Consequently, telomeres perform an important role in maintaining genomic integrity and stability by preventing checkpoint activation.

In human germ cells, telomeres consist of a long double-strand DNA region that is tightly compacted into a heterochromatic structure by virtue of dense nucleosome packing [Tommerup *et al*, 1994]. Telomeric DNA consists of TTAGGG repeats of between 10-15 kb in length followed by a single-stranded DNA sequence at the 3' end consisting of a few hundred bases (**Figure 1.7A**; [Lingner and Cech, 1998; McEachern *et al*, 2000]), yet the overall length is heterogeneous and varies considerably within individual cells, in a population of dividing cells and between vertebrate species [Baird *et al*, 2003; Martin-Ruiz *et al*, 2004].

1.3.6.2 The End Replication Problem

The inherent nature of bi-directional replication of DNA means that linear chromosomes experience the 'end-replication problem' [Harley, 1991]. Understanding the mechanism of DNA replication in eukaryotes reveals this problem; DNA replication can only occur in a 5' to 3' direction by linking the terminal phosphate group of the 5' carbon of a deoxyribose nucleotide to the hydroxyl group of the 3' carbon of an adjacent nucleotide. Consequently, DNA replication requires a template sequence from which it can extend. Therefore, DNA synthesis can occur in a continuous process in the leading strand, however, replication of the second parental DNA strand (also known as the lagging strand) is complicated by the fact that it can only occur in a discontinuous process.

To start this process, RNA primers are synthesised by the activity of primase, an RNA polymerase complex that does not require a template for

RNA polymerisation. Primase activity occurs on the DNA strand opposite to the lagging strand and upon generation of the RNA primer, DNA polymerase activity replaces primase and catalyses the polymerisation of DNA nucleotides to the RNA primer. DNA synthesis then continues until it reaches an adjacent RNA primer where upon 5' to 3' exonuclease activity is used to replace the RNA primer with deoxyribonucleotide triphosphate molecules (dNTPs). This activity results in the formation of short DNA fragments of approximately 100 nucleotides, also known as Okazaki fragments. The Okazaki fragments are then covalently linked by DNA ligase activity to complete DNA synthesis of the lagging strand. Consequently, the end replication occurs as a result of the inability to replace the RNA primer sequence at the very 3' end of the linear chromosome, as this is removed during Okazaki fragment processing [Olovnikov, 1973]. This means that DNA is lost from the ends of chromosomes each time a cell divides. Therefore, without a mechanism to maintain the ends of chromosomes, telomeres become critically shortened and eventually undergo senescence. To support this model, the average length of telomeres has been shown to shorten during the serial sub-cultivation of human cells *in vitro* [Harley *et al*, 1990].

1.3.6.3 Telomerase

Telomerase is a ribonucleoprotein complex that functions to lengthen telomeres to maintain genomic integrity. It is composed of telomeric reverse transcriptase, hTERT, that has seven protein domains in common with retroviral and retrotransposon reverse transcriptases, a catalytic RNA component (TERC) and a number of associated factors that regulate its catalytic activity. Telomerase functions by directly adding telomeric repeat sequences to the 3' single-stranded telomeric overhang, using its TERC RNA template (**Figure 1.7A**; reviewed in [Blackburn, 2001]). The gene that encodes the catalytic component in humans, *TERT*, is expressed at almost undetectable levels in somatic cells and slows, but does not prevent, telomere

shortening. Consequently, telomerase activity is limited to the germ cells, activated lymphocytes and stem cells.

1.3.6.4 Telomerase Structure

The secondary and tertiary conformations adopted by the telomere are critical for its activity and the current model for telomeric structure is one that switches between two conformations, namely, open or closed. In support of this hypothesis, the closed conformation has been detected by electron microscopy [Griffith *et al*, 1999], and is referred to as a 'T-loop' or 'lariat structure' (**Figure 1.7B**).

It has been suggested that the primary function of the T-loop is to protect the end of the chromosome from degradation, such that the 3' single-stranded DNA overhang invades the double-stranded telomeric region, to form a displacement or 'D-loop' [Griffith *et al*, 1997; Stansel *et al*, 2001] that may be similar in structure to stalled replication forks or homologous DNA recombination intermediates [de Lange and Petrini, 2000; Griffith *et al*, 1999]. A number of telomeric-binding proteins associate with the telomere and regulate the conformation of the T-loop; for example, two factors known to bind directly to the double stranded telomeric region as homodimers are TRF1 and TRF2, whereas another factor, POT1, binds directly to the single-stranded portion of the telomeric DNA repeats [Baumann and Cech, 2001; Broccoli *et al*, 1997]. These proteins are thought to act as a scaffold for telomeric associated factors such as TIN2 and Tankyrase 1, which in turn regulate the activity of telomeric-binding proteins. TRF1 principally serves as a regulator of telomere length, whereas TRF2 appears to be the key factor in telomere protection (reviewed [de Lange, 2002]). Opening or uncapping of the T-loop permits access for telomerase and DNA polymerase during DNA replication. Concomitantly, the uncapping of the loop also exposes the end of the telomere to degradation [Teixeira *et al*, 2004].

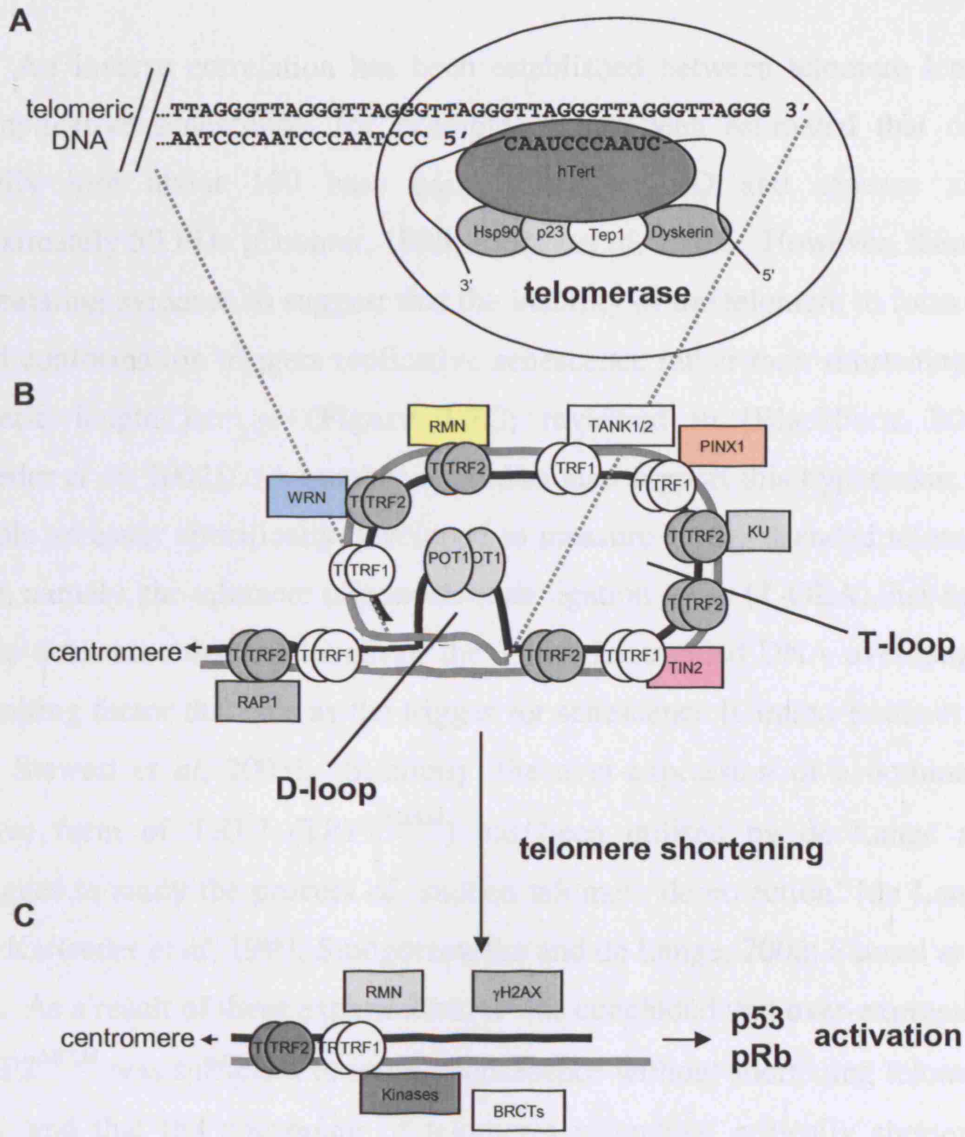

Figure 1.7: Regulation of Telomere Structure

Schematic diagram of the human telomere and the signalling pathways involved in the induction of telomere-dependent cellular senescence. **A:** Telomeres are maintained by the activity of telomerase, a multicomponent ribonucleoprotein complex; **B:** A number of cellular proteins are known to associate with the telomere; for example TRF1 [Kim *et al*, 1999], TRF2 [Stansel *et al*, 2001], TIN2 [Kim *et al*, 2004], TANK1/2 [Kaminker *et al*, 2001; Smith *et al*, 1998], KU [Hsu *et al*, 1999; Hsu *et al*, 2000; Song *et al*, 2000] and WRN [Opresko *et al*, 2002]. These factors are involved in regulating the formation of the T-loop; **C:** Upon critical telomere shortening, the formation of the T-loop structure is impaired and DNA damage signalling components are recruited to the telomere and the p53 and pRb pathways are activated.

1.3.6.5 Telomere Length and Structure

An inverse correlation has been established between telomere length and replicative senescence; for example, it has been estimated that cells typically lose about 100 base pairs (bps) per PD and senesce after approximately 50 PDs [Counter, 1996; Harley *et al*, 1990]. However, there is accumulating evidence to suggest that the inability of the telomere to form the closed conformation triggers replicative senescence rather than shortening of telomeric length *per se* (**Figure 1.7C**; reviewed in [Blackburn, 2001; Karlseder *et al*, 2002]). A number of studies also support this hypothesis; for example an assay specifically developed to measure single-stranded telomere length, namely, the telomere oligonucleotide ligation assay (T-OLA), has been used to determine that the length of the 3' single-stranded DNA overhang is the limiting factor that acts as the trigger for senescence [Cimino-Reale *et al*, 2001; Stewart *et al*, 2003]. Similarly, the over-expression of a dominant-negative form of TRF2 ($TRF2^{\Delta B\Delta M}$) has been utilised by de Lange and colleagues to study the process of 'sudden telomere deprotection' [de Lange, 2002; Karlseder *et al*, 1999; Smogorzewska and de Lange, 2002; Stansel *et al*, 2001]. As a result of these experiments, it was concluded that over-expression of $TRF2^{\Delta B\Delta M}$ was sufficient to induce senescence without shortening telomere length, and that the uncapping of telomeres resembled critically shortened telomeres that were subject to ERCC1/XPF end-nuclease activity [Zhu *et al*, 2003].

Using a novel biochemical technique designed for the quantitation of the absolute length of single stranded telomeric overhangs, Chai and colleagues [Chai *et al*, 2005] determined that normal HDFs maintain their telomeric overhangs at senescence. Since this technique measures the absolute lengths of individual telomeres, rather than the relative measurement that is obtained using the T-OLA technique [Cimino-Reale *et al*, 2001], the possibility that a few critically shortened telomeres induce senescence cannot

be ruled out, a hypothesis similarly supported by Baird and colleagues [Baird *et al*, 2003].

1.3.6.6 Downstream Signalling

Regardless of the exact initiation event, the generation of critically shortened telomeres leads to the induction of a p53-dependent DNA damage response [d'Adda di Fagagna *et al*, 2003; Gire *et al*, 2004; Herbig *et al*, 2004; Sedelnikova *et al*, 2004; Stewart *et al*, 2003; Zou *et al*, 2004]; for example, the accumulation of phosphorylated H2AX and a number of DNA damage proteins such as BCR1, MDE1, MRE11, Nijmegen breakage syndrome 1, Rad50 and 53BP1 ([d'Adda di Fagagna *et al*, 2003; Gire *et al*, 2004; Herbig *et al*, 2004; Sedelnikova *et al*, 2004; Takai *et al*, 2003; Zou *et al*, 2004]; reviewed in [Shay and Wright, 2004]), and active forms of ATR and ATM, Chk2 and Chk1 have all be detected in senescent cells [d'Adda di Fagagna *et al*, 2003; Herbig *et al*, 2004]. The net result is that p53 is modified at the post-translational level ([Atadja *et al*, 1995; Vaziri *et al*, 1997]; reviewed in [Itahana *et al*, 2001]) which leads to the transcriptional activation of *p21* ([Noda *et al*, 1994]; reviewed in [Itahana *et al*, 2001]). In addition to p53 activation, the pRb pathway may also be activated to induce the irreversible growth arrest [Itahana *et al*, 2001; Shay and Wright, 2001; Smogorzewska and de Lange, 2002; von Zglinicki *et al*, 2001].

It is also possible that genes located in close proximity to the telomere may be subject to higher order levels of gene regulation; the telomere position effect hypothesis proposes that as telomeres shorten, the heterochromatic region of the telomere spreads to neighbouring DNA sequences, thereby mediating stable transcriptional repression of these genes. As a consequence, the transcriptional changes resulting from this process induce replicative senescence. Whilst there is much evidence to suggest that telomere position effect occurs in yeast by a mechanism that depends both on telomere length and on the distance from the gene [Gottschling *et al*, 1990; Kyrion *et al*, 1993;

Renauld *et al*, 1993], there is little evidence to support this hypothesis in humans (reviewed in [Baur *et al*, 2001; Koering *et al*, 2002; Shay and Wright, 2000]).

1.3.7 Telomere-Independent Senescence

In addition to telomeric attrition, senescence can also be induced by a variety of stimuli in a telomere-independent manner, for example, by UV and IR [Di Leonardo *et al*, 1994; Medrano *et al*, 1995; Toussaint *et al*, 2000], oxidative stress [Dumont *et al*, 2000; von Zglinicki *et al*, 1995] and treatment with HDAC inhibitors [Ogryzko *et al*, 1996]. The induction of senescence by these telomere-independent mechanisms is referred to as stress or aberrant signalling-induced senescence (STASIS; [Drayton and Peters, 2002]) or stress-induced premature senescence (SIPS). Similar to telomere-dependent senescence, cells that undergo STASIS exhibit a decrease in bromo-deoxyuridine (BrdU) incorporation, acquire an enlarged, flattened morphology, exhibit SA acid-β-galactosidase activity [Chen *et al*, 2001; Suzuki *et al*, 2001] and up regulation of $p16^{INK4a}$. This form of senescence is commonly detected in MEFs; these cells have very long telomeres (40-60 kb) relative to humans (5-15 kb), therefore, they are unlikely to acquire critically shortened telomeres (reviewed in [Melk, 2003; Melk and Halloran, 2001]).

The signalling components that induce premature senescence are less well understood than replicative senecence, yet Ras activation has been shown to be associated with this process. Ras is a small guanine triphosphate (GTP) -binding protein that, upon mitogen stimulation, results in an increase in the active, GTP-bound state and transduces mitogenic signals from tyrosine-kinase receptors. A point mutation that maintains Ras in the GTP-bound state and transforms immortalised cells [Katz and McCormick, 1997] occurs in many human cancers [Barbacid, 1987] and is known as oncogenic Ras, H-Ras or $H\text{-}Ras^{V12}$. Co-expression of LT with oncogenic Ras is sufficient to transform REFs [Hirakawa and Ruley, 1988; Michalovitz *et al*, 1987] and, in

addition to small T antigen, can also transform primary HDFs [Hahn *et al*, 2002]. In contrast, expression of oncogenic Ras in primary cells such as primary REFs [Newbold and Overell, 1983] and pre-senescent HDFs [Serrano *et al*, 1997] is sufficient to induce premature senescence that is phenotypically indistinguishable from replicative senescence. Unlike replicative senescence, however, oncogenic Ras-induced premature senescence occurs rapidly and within a period of a few days [Serrano *et al*, 1997].

Ras signalling is mediated by MAPK signalling pathways that are known to be involved in many biological processes including development, proliferation, differentiation and apoptosis [Chang and Karin, 2001]. In oncogenic Ras-induced premature senescence, the ERK MAPK pathway is activated [Lin *et al*, 1998; Zhu *et al*, 1998] and, upon prolonged activation, p38 activation occurs and mediates the induction of premature senescence [Wang *et al*, 2002]. In HDFs, it has been shown that the effector molecule of this pathway is Ets2, a transcription factor that can activate the $p16^{INK4a}$ gene promoter [Ohtani *et al*, 2001]. These data indicate that the ability of oncogenic Ras to function as a promoter of cell proliferation, cell cycle arrest or terminal differentiation is context-dependent [Frame and Balmain, 2000].

1.3.8 Telomere-Dependent verus Telomere-Independent Senescence

In conclusion, the p53 and pRb pathways appear to be activated under different contexts; for example, dysfunctional telomeres are likely to be recognised as DNA damage signals and are detected by p53 [Bond *et al*, 1996], whereas $p16^{INK4a}$ is activated by strong physiological stimuli or stress, such as oncogenic Ras activity.

There is also evidence to suggest that there is a synergistic link between replicative senescence and premature senescence; for example, telomeres are particularly susceptible to oxidative DNA damage and shorten 5-10 times faster under chronic hyperoxia than normal conditions [Vaziri *et al*, 1997; von Zglinicki *et al*, 1995]. These findings indicate that stress exerts

a major influence upon the rate of telomere shortening and this may explain inconsistencies that have been observed in the replicative potential of some cells (reviewed in [Rubin, 2002]). Zglinicki and colleagues [von Zglinicki *et al*, 2003] even suggest that replicative senescence of serially passaged primary HDFs in the absence of stress is likely to be an extremely rare event. Accordingly, one model for senescence induction proposes that cells differ in their ability to express high levels of $p16^{INK4a}$ in response to stress and that only the cells that continue to grow, undergo replicative senescence via telomere shortening [Herbig *et al*, 2004]. In support of this model, $p16^{INK4a}$-deficient HDFs from melanoma-prone individuals show above-average lifespan [Brookes *et al*, 2004]. It has also been suggested that SIPS and replicative senescence share common pathways to lead to a permanent growth arrest; for example, p38 functions as a senescence-executing molecule and is activated in response to both telomeric- and non-telomeric- senescence-inducing stimuli [Iwasa *et al*, 2003].

1.3.9 Acquisition of Limitless Proliferative Potential

MEFs frequently undergo spontaneous immortalisation and inactivation of the p53 pathway appears to be very important in this process; for example, inactivation of the p53 pathway in is sufficient to bypass telomerase-induced cell cycle arrest [Harvey *et al*, 1993; Kamijo *et al*, 1997] (reviewed in [Lowe and Sherr, 2003; Sharpless, 2005]). Furthermore, under low oxygen conditions, MEFs behave as immortal cells as no secondary event is required to achieve immortalisation [Parrinello *et al*, 2003]. Unlike the p53 pathway, determining whether inactivation of the pRb pathway is sufficient to bypass senescence has been technically difficult due to functional redundancy exhibited by the three Rb family members; for example, pRb-null MEFs undergo senescence [Carneiro *et al*, 2003; Dannenberg *et al*, 2000; Sage *et al*, 2000], whereas pRb-, p107- and p130- null MEFs (triple knockout [TKO] MEFs) do not undergo senescence [Dannenberg *et al*, 2000; Sage *et al*, 2000].

Yet, recent evidence obtained from a conditional knockout mouse that mimics acute loss of pRb activity indicates that senescent MEFs can re-enter the cell cycle, divide and proliferate after acute loss of pRb, even in cells wt for p107 and p130 [Sage *et al*, 2003]. This indicates that care must be taken in both the design and interpretation of experimental data derived from knockout studies.

In contrast to MEFs, spontaneous immortalisation of REFs is less frequent, even though REFs exhibit long telomeres like MEFs. Furthermore, immortalisation does not appear to be so p53-dependent; for example, N-terminal fragments of LT that cannot bind to p53 retain the ability to immortalise REFs, although they are not as effective as wt LT. Similarly, both E7 and E1A, two viral oncoproteins that do not directly bind to or inactivate the p53 protein, are also both capable of immortalising REFs [Powell *et al*, 1999]. However, the possibility that these reagents indirectly abrogate p53 activity by inactivating downstream components of this pathway cannot be excluded. Similarly, the importance of the pRb pathway in mediating the induction of senescence is less clear in the rat; expression of a LT mutant defective in pRb-binding, but not p107 and p130, namely K1 [Srinivasan *et al*, 1997], suggested that pRb inactivation was not important to immortalise REFS [Powell *et al*, 1999]. However, there was some evidence to suggest that p130 activity was important in this process.

Unlike rodent cells however, human cells rarely become immortalised after the introduction of oncogenes; for example inhibition of either the p53 or pRb pathways is sufficient to extend the lifespan of HDFs i*n vitro* but it is insufficient to overcome eventual telomere-directed growth arrest [Sage *et al*, 2000; Smogorzewska and de Lange, 2002; Wei *et al*, 2003]. These findings have been used to describe senescence and immortalisation in two discrete stages, namely mortality stages I and II (M1 and M2, respectively). M1 results from the acquisition of shortened telomeres by replicative senescence ([Harley *et al*, 1990]; reviewed in [Campisi *et al*, 2001; Shay and Wright, 2001]). Inactivation of p53 or pRb is sufficient to bypass M1 and permit an extension of lifespan. However, as the telomeres continue to shorten, the cells

eventually exhibit critically shorted telomeres so that chromosomal abnormalities and extensive cell death become evident. This phenotype is described as M2 or crisis [Harley *et al*, 1990; Wright *et al*, 1989]; for example, sequestration of both p53 and pRb by LT or a combination of E6 and E7 enables cells to extend their lifespan by an additional 20-30 PDs before the cells eventually exhibit crisis [Bond *et al*, 1996; Hahn *et al*, 2002; Shay *et al*, 1991; Wei *et al*, 2001; Wei *et al*, 2003; Wright *et al*, 1989].

Escape from M2 results in immortalisation, however this event is rare and occurs at a rate of approximately 1 in 10 million in human cells [Wright and Shay, 1992]. These findings suggest that senescence is a complex and multicomponent process that requires multiple genetic alterations to be overcome and involves the activation of dominant oncogenes and the repression of growth suppressor genes.

In some cell types, namely retinal pigment epithelial cells and foreskin HDFs, reconstitution of telomerase activity by reactivation of hTERT appears to be sufficient to bypass replicative senescence [Bodnar *et al*, 1998; Kiyono *et al*, 1998; Yang *et al*, 1999]. Furthermore, transient ectopic expression of *TERT* results in elongation of telomeres and a greatly extended lifespan, thereby demonstrating that it is the length of the telomere rather that the telomerase itself that is responsible for the proliferative limits [Steinert *et al*, 2000]. However, other investigators have determined that the minimal requirements for immortalisation are the expression of LT and hTERT [O'Hare *et al*, 2001]. Similarly, expression of HPV E6, E7 and hTERT has also been shown to be sufficient [Kiyono *et al*, 1998; Klingelhutz *et al*, 1996], and, in this instance, it is worth noting that E6 can transcriptionally activate *TERT* in some cells [Veldman *et al*, 2001]. These experiments highlight the importance of inactivating both the p53 and pRb pathways in addition to reconstituting functional telomerase activity. The fact that some cell types can be immortalised by ectopic expression of hTERT alone can be accommodated in this hypothesis by presuming that $p16^{INK4a}$ is already inactivated in these cells [Dickson *et al*, 2000; Tsutsui *et al*, 2002; Jiang *et al*, 1999]; for example,

stochastic events have been shown to affect the ability of hTERT to immortalise human endothelial cells [Freedman and Folkman, 2005].

1.3.10 Senescence and Ageing

Ageing refers to the increase in tissue degeneration over time that culminates in the increased likelihood of organismal death [Medawar, 1952]. Senescence was originally linked to ageing by virtue of the fact that there is an inverse correlation between finite mitotic potential and age [Rohme, 1981]. It was proposed that the accumulation of senescent cells *in vivo* disrupts both tissue integrity and the homeostatic mechanisms that maintain a constant number of cells in a tissue by depleting progenitor cell populations. However, as it will be described below, determining whether senescence is a cause or a consequence of ageing remains contentious.

1.3.10.1 Evidence Supporting the Hypothesis that Senescence is Causal to Ageing

Telomeric dysfunction has provided much of the supportive evidence to associate senescence with organismal aging (reviewed in [Campisi *et al*, 2001; Shay and Wright, 2001]); for example, homozygous telomerase knockout mice exhibit sterility after several generations due to failure of both the female and male germ cell lineages [Blasco *et al*, 1997], and late generation mice exhibit abnormalities associated with premature aging [Rudolph *et al*, 1999] that has been attributed to the fact that the long telomeres exhibited in the mice only become critically shortened after many replication events over many generations.

In humans, evidence to link senescence with organismal ageing has mainly been obtained by measuring differences in the number of serial sub-cultivations that may be made from cells derived from different aged individuals [Hayflick, 1974; Schneider and Mitsui, 1976], genetic

backgrounds and species. Similarly, it has been shown that old stem cells exhibit a decline in function, relative to younger stem cells, when subjected to stress [Van Zant and Liang, 2003]. Moreover, there is some evidence based upon telomere shortening rates to suggest that adult stem cells exhibit a finite lifespan ([Allsopp *et al*, 2003; Harrison and Astle, 1982; Yui *et al*, 1998]; reviewed in [Allsopp and Weissman, 2002]), whereas ES cells exhibit an infinite life span [Verfaillie, 2002]. *In vivo* evidence also indicates that senescent cells in ageing human skin [Dimri *et al*, 1995] and liver [Paradis *et al*, 2001], in addition to sites of age-related pathology such as hyperplastic prostate [Choi *et al*, 2000] and atherosclerotic lesions [Vasile *et al*, 2001].

In addition to these observations, a number of human syndromes that exhibit premature ageing phenotypes have been described. These include Werner Syndrome (WS), Hutchinson-Gilford Progeria Syndrome (HGPS) and Dyskeratosis Congenita [Chang *et al*, 2004; Davis *et al*, 2003; DeBusk, 1972; Mitchell *et al*, 1999; Vasile *et al*, 2001].

1.3.10.2 WS

WS is an autosomal recessive human premature ageing disorder associated with the loss of function of the *WRN* gene [Yu *et al*, 1996]. The *WRN* gene encodes a member of the RecQ helicase family, namely WRN, that exhibits a unique activity amongst RecQ family members in that it exhibits 3' to 5' exonuclease activity [Huang *et al*, 1998] and becomes directed to DNA damage at S phase [Gray *et al*, 1998; Marciniak *et al*, 1998; Shiratori *et al*, 1999]. Therefore, the loss of WRN helicase activity is likely to trigger premature cell-cycle exit without involving telomeric loss and this has led to the hypothesis that WRN has a role in modulating the rate of telomere erosion; for example, HDFs derived from WS cells exhibit a reduced *in vitro* lifespan before entering replicative senescence [Martin *et al*, 1970].

1.3.10.3 HGPS

HGPS is a very rare dominantly inherited premature ageing syndrome that manifests in approximate 1 in every 8 million births [DeBusk, 1972] and results in death at a median age of 13 years. Both Eriksson and colleagues [Eriksson *et al*, 2003] and De Sandre-Giovannoli and colleagues [De Sandre-Giovannoli *et al*, 2003] determined that mutational truncation of the Lamin A protein is causal to HGPS [De Sandre-Giovannoli *et al*, 2003; Eriksson *et al*, 2003]. The *LMNA* gene encodes two splice variants, Lamin A and Lamin C, that are ubiquitously expressed in the inner nuclear membrane lamina. The first 566 aa are common to both splice variants, yet Lamin A has an additional 98 aa at the C-terminus that is not shared with Lamin C. The Lamin A/C proteins associate in the nuclear lamina and are thought to have a major role in nuclear structure. They are also able to associate with chromatin both directly and indirectly [Goldman *et al*, 2002], therefore, it is possible that the Lamin A/C proteins play a role in regulating gene expression and DNA synthesis; for example, Lamin A/C is known to interact with transcriptional regulators such as pRb [Markiewicz *et al*, 2002].

Disruption of Lamin A/C results in abnormal mitosis, chromosomal segregation and cell death and HDF cultures derived from HGPS patients appear to have a reduced rate of proliferation, altered expression levels of genes regulating the cell cycle and a slight increase in aneuploidy [Mukherjee and Costello, 1998]. This has raised the possibility that growth retardation and delayed maturation in some of the tissues in HGPS may arise as a result of a post-natal defect in cell proliferation.

1.3.10.4 Dyskeratosis CongenitalSyndrome

Dyskeratosis congenita syndrome is third example of a premature ageing syndrome. This autosomal dominant syndrome is associated with loss of function of either the telomerase RNA template gene or the telomere-

associated protein dyskerin [Mitchell *et al*, 1999; Vulliamy *et al*, 2001]. Cells derived from individuals presenting this syndrome are characterised by abnormally short telomeres, defects in epithelial and hematopoietic cell lineages, and hematopoietic malignancies.

1.3.10.5 Ageing and Calorific Restriction

Studies that involve caloric restriction also indirectly support the hypothesis that senescence is linked to ageing; for example, calorific restriction is known to extend lifespan in a variety of species, including rats, mice, fish, flies, worms and yeast. Similarly, a reduction in aging-associated pathology is evident in primates fed a calories restricted diet [Lane *et al*, 2001]. Moreover, it has been suggested that at least, in mice, $p16^{INK4a}$ and/or $p14^{ARF}$ are good candidates for *in vivo* biomarkers of ageing [Krishnamurthy *et al*, 2004; Melk *et al*, 2004] since age-associated increases in expression is attenuated in several tissues in response to calorific restriction.

1.3.10.6 Evidence Supporting the Hypothesis that Senescence is a Consequence of Ageing

A significant problem with associating senescence with ageing is that, as described previously, few biomarkers of senescence have been described to date. Therefore, it is difficult to measure ageing in qualitative and quantitative terms; for example, telomere length varies widely within between chromosomes within the same cell, between individuals and between different tissues [Castro *et al*, 1992; Dimri *et al*, 1995]. Furthermore, in contrast to some of the studies described above, no association of replicative lifespan *in vitro* and the age of the donor has been detected by other investigators [Cristofalo *et al*, 1998; Tesco *et al*, 1998]. Similarly, other than the observation that the ability to repair tissues is severely reduced in the elderly, there is little data to suggest that senescent cells can disrupt tissue integrity,

and there is conflicting data as to whether senescence-associated genes are truly differentially expressed *in vivo* [Mondello *et al*, 1999].

A second important issue is that cell death and irreversibly differentiated cells should not be considered detrimental to viability; for example terminally differentiated cells such as neurons have a fundamental role in normal physiological processes; moreover, the cells in *C. elegans* and *Drosophila* are all post-mitotic. Therefore, the genes that are critical for ageng in these organisms are survival genes. Conversely, an organ such as the heart, which commonly exhibits ageing, is mostly a post-mitotic tissue.

In conclusion, these findings indicate that the maintenance of telomeres has an important role in highly proliferative tissues, but may not necessarily be causal to the ageing process itself. It is more likely, however, that cellular stress resistance is more relevant to the ageing process as cells from progeroid syndrome patients are more susceptible to stress [Bridger and Kill, 2004; de Magalhaes *et al*, 2004].

1.3.11 Senescence and Tumorigenesis

Some of the components of the senescence pathway, namely p53, $p16^{INK4a}$, pRb and CDK4, are commonly mutated in cancers, therefore, and one hypothesis is that senescence represents a fundamental tumour-suppressive mechanism that negatively regulates cell growth under inappropriate conditions.

1.3.11.1 Senescence Bypass is a Prerequisite for Tumorigenesis

The bypass of senescence confers a potent growth advantage in that it generates a proliferative pool of cells that may undergo clonal evolution and malignant growth [Gray and Collins, 2000]. Indeed, the acquisition of a limitless proliferative potential is regarded as a prerequisite for tumorigenesis [Hanahan and Weinberg, 2000]. In support of this hypothesis, reactivation of

telomerase activity [Bodnar *et al*, 1996; Kim *et al*, 1994] or alternate lengthening of telomeres (ALT), a recombinational-based mechanism that maintains telomere length [Dunham *et al*, 2000; Reddel *et al*, 2001], has been detected in immortalised cells. Furthermore, reconstituted telomerase activity has been estimated to be present in approximately 90% of all human cancers [Newbold, 2002].

The ability to detect senescent cells *in vivo* has provided substantial supportive evidence to the hypothesis that the bypass of this process occurs during the very early stages of tumorigenesis [Braig *et al*, 2005; Chen *et al*, 2005; Collado *et al*, 2005; Michaloglou *et al*, 2005]. For example, the co-deletion of *PTEN* and *p53* is sufficient to bypass senescence and promote prostate cancer in mice, and this finding is supported by evidence from human cells [Chen *et al*, 2005]; it has also been shown that many benign naevi in melanoma are comprised of senescent cells. Moreover, senescence can be induced in lymphoma cells of mice treated with chemotherapeutic agents [Schmitt *et al*, 2002], as well as mice hepatocytes deficient in telomerase activity [Satyanarayana *et al*, 2003].

1.3.11.2 The Stem Cell Hypothesis of Tumorigenesis

It is possible that, rather than undergoing telomerase derepression; pre-existing telomerase-positive cells confer a potent growth advantage to promote tumorigenesis. Accordingly, the stem cell hypothesis of cancer development states that, despite the rarity of stem cells *in* vivo, they are more likely to become immortalised as they are able to divide over long periods of time; for example, the introduction of hTERT into adult human mesenchymal stem cells is sufficient to immortalise these cells and induce premalignant changes [Simonsen *et al*, 2002]. Additional studies have determined that stem cells are associated with the etiological origin of many different cancer types [Al-Hajj *et al*, 2003; Hemmati *et al*, 2003; Kim *et al*, 2005; Singh *et al*, 2003]. As a caveat, however, it remains possible that the stem-cell-like phenotype

that is exhibited in these cancers reflects cancerous cells that have evolved to acquire a non-differentiated state.

1.3.11.3 Senescent Cells Promote the Development of Tumorigenesis

A second, disparate model to link senescence with tumorigenesis has been described. In this model, senescent cells themselves promote the onset of tumorigenesis by their close proximity to cancer cells, possibly by the secretion of factors such as matrix metalloproteases and other secretory factors that promote malignant cell growth [Cunha and Matrisian, 2002; Hsu *et al*, 2002; Mueller and Fusenig, 2002; Tlsty, 2001; Tlsty and Hein, 2001]. There is some evidence to support this model; for example, senescence cells have been identified in premalignant lesions in the liver [Paradis *et al*, 2001], skin and breast [Krtolica *et al*, 2001], and senescent fibroblasts have been shown to promote the growth of tumour cells to a much greater extent than that exhibited by pre-senescent cells both *in vitro* as well as *in vivo* [Krtolica *et al*, 2001].

Consequently, a mathematical model has been developed to assess the relative contribution of these two disparate hypotheses to the induction of tumorigenesis [Wodarz, 2004]. Modelling tumorigenesis in this manner is dependent upon the relative contribution of parameters such as the duration of cell cycle arrest, the amount of cell death and the various costs derived from these outcomes. Consequently, it may be possible to model the spectrum of tumours that are likely to develop in different cellular contexts.

1.3.11.4 Senescence in the Context of Therapeutic Treatment

The high rate of cell proliferation exhibited by cancerous cells renders them more susceptible to apoptosis than most normal cells *in vivo*. Consequently, many chemotherapeutic strategies have been developed with the aim of targetting all proliferative cells for ablation by apoptosis. The

major disadvantage of this therapeutic rationale is the fact that it is highly toxic since normal cells that exhibit a high proliferative rate are also targetted in this manner; for example, blood and digestive cells. However, lowering the dosage of chemotherapeutic agents increases the risk of development of drug resistance and lowering effectiveness of the treatment.

It is possible that the efficacy of chemotherapeutic drugs is attributable to the induction of apoptosis and/or cellular senescence in cancer cells [Schmitt *et al*, 2002; te Poele *et al*, 2002], since the key signalling pathways involved in the induction of senescence are likely to remain functional in these cells ([Stampfer *et al*, 2003]; reviewed in [Duncan and Reddel, 1997]). Therefore, a novel therapeutic rationale has been proposed in order to specifically target cancer cells for the induction of senescence, rather than apoptosis [Chang *et al*, 2002; Rebbaa *et al*, 2003; Zheng *et al*, 2004]. The major advantage of this strategy is that, unlike the induction of apoptosis, it may enable lower doses of chemotherapeutic drugs to be used and, consequently, be less toxic; for example, mice bearing tumours that are susceptible to drug-induced senescence exhibit a better prognosis than mice bearing tumours with senescence defects [Schmitt *et al*, 2002]. However, this strategy does have its disadvantages; for example, the issue of drug resistance remains a significant concern since defects in the cellular senescence pathways may promote drug resistance *in vivo* [Chang *et al*, 2002; Schmitt *et al*, 2002; te Poele *et al*, 2002]. Moreover, the accumulation of senescence cells *in vivo* may promote tumorigenesis, as described previously ([Krtolica *et al*, 2001]; reviewed in [Campisi, 2005]). Nevertheless, the potential of this therapeutic treatment has been demonstrated; for example, a combined treatment of cells with pan caspase inhibitor (Q-VD-OPH) and doxorubicin was shown to greatly accelerate senescence and lead to the reversal of drug resistance in several tumour cell lines [Zheng *et al*, 2004].

These findings indicated that the induction of senescence is an important paradigm for chemotherapy treatment. The identification of novel senescence-associated genes may therefore reveal not only reveal novel

markers of this process but may also provide prognostic and/or diagnostic information.

1.4 EXPERIMENTAL TECHNIQUES TO IDENTIFY NOVEL SENESCENCE-ASSOCIATED GENES

Experiments using small DNA viral oncoproteins such as LT, E1A and E7 were the first to implicate the key cell cycle checkpoint proteins p53 and pRb with immortalisation. Experimental analysis has since been used to determine how these pathways function to induce cellular senescence; for example inactivation, knockout, modification and constitutive expression of cell cycle proteins such as $p16^{INK4a}$, pRb, the activating E2Fs 1-3, p53 and p21 have all been described.

However, as the signalling mechanisms linking pRb, p53 and senescence are poorly understood, the need to identify novel senescence-associated genes has increased. This has lead to the utilisation of differential screening methods, such as differential RNA screening and differential display; for example, el-Deiry and colleagues identified p21 by subtractive hybridisation approach [el-Deiry *et al*, 1993].

1.4.1 Microarray Analysis

Differential screening methods have since evolved into the use of microarrays. Microarray analysis is a technique that accurately measures differences in gene expression between any two RNA samples. Therefore, it is possible to analyse the expression of many genes to identify those that are significantly differential upon the induction of senescence. The development of microarray platforms over recent years has enabled this technique to become a readily available and feasible experimental approach to analyse biological processes such as senescence; for example, *CDKN2B*, *BHLHB2* and *TNFRSF10D* represent three genes whose expression was recently shown

to correlate with senescence induced by ERK *in vivo* [Collado *et al*, 2005]. Furthermore, microarray analysis may be utilised in a clinical setting to provide prognostic information; for example, microarray analysis of patients with B cell lymphomas enabled individuals to be categorised with respect to the appropriate form of treatment that should be utilised [Alizadeh *et al*, 2000].

1.4.1.1 Microarray Platform Technologies

Two different types of microarray platforms have been developed to perform gene expression profiling, namely oligonucleotide microarrays and complementary (cDNA) microarrays. These two platforms use different forms of sequence information for the hybridisation of samples derived from RNA, representative of different experimental conditions, and different measurement methodologies for the identification of differential hybridisation data. For example, affymetrix microarrays, an example of an oligonucleotide microarray platform, utilises absolute measurements of RNA hybridisation whereas cDNA microarrays utilise the competitive hybridisation of two cDNA samples such that differential hybridisation is measured in relative terms. Valid results may be obtained from either platform technology, however [Moreau *et al*, 2003].

The basis of microarray analysis is the high density positioning of DNA sequences on a solid support such that they may be used as probes for expression data. Typically, robotic printing is used to uniformly space the probes onto the slide and, in cDNA microarrays, the probes usually correspond to bacterial cDNA clones. There are many advantages to using a glass slide as the solid support. For example, the fluorescently labelled samples that are hybridised to the probes may be easily visualised, they are economical to produce, are resistant to high temperature and can be attached to the surface; for example, UV cross-linking of DNA to the surface of poly-L-lysine coated slides, or chemical cross-linking of DNA to the surface of

aldehyde coated slides; in this latter process, the double-stranded DNA is denatured, such that the strand that is not covalently attached to the slide is removed. These modifications aid in the stable spotting of probes to the array.

1.4.1.2 Analysis of Microarray Data

Samples that are hybridised to the array are scanned to create an image of the microarray data such that the fluorescence intensity of each spot can be determined in terms of spot detection and background measurement. As a result of these processes, a large number of data points are obtained and statistical analysis performed in order to extract significant information from the data whilst minimising the risk of identifying false-positive results. The ability to analyse the experimental data in this manner enables sophisticated statistical tools to be used to identify patterns in the expression data and to simplify the data set such that additional information may be obtained about its structure; for example, principle components analysis, hierarchical clustering and self-organising maps may all be utilised.

1.4.2 Functional Analysis of Senescence-Associated Genes

Gene expression profiling analysis has proven to be very successful in identifying many genes that are associated with the induction of senescence. However, functional validation of is critical. A few functional analysis techniques have been utilised to address this issue; for example, a retroviral expression screen was used to identify Dril1 as an effector of senescence that acts downstream of the $p19^{ARF}$ /p53 pathway in MEFs [Peeper *et al*, 2002]. *DRIL1* is the human ortholog of the mouse *Bright* and Drosophila *dead ringer* transcriptional regulators and is thought to interact with E2F1 to induce its activity, thereby inducing *CCNE1* expression and leading to immortalisation [Gregory *et al*, 1996; Herrscher *et al*, 1995]. However, it is technically difficult to identify novel, senescence-promoting genes using screening

methods such as these as tumour suppressor genes exhibit recessive phenotypes. This difficultly can be addressed by the utilisation of reverse genetic approaches such as Genetic Suppressor Element (GSE) screens. More recently, the development of RNA interference (RNAi) screening mechanisms has facilitated the use of this technique as a potent reverse genetic technique.

1.4.3 RNAi

RNAi is a biological process that was first identified in plants and *C. elegans* as a process that conferred post-translational gene silencing (PTGS) and co-suppression, respectively [Fire *et al*, 1998]. RNAi represents a highly conserved process of targetted gene silencing and/or down regulation mediated by double-stranded RNA, and the fact that it can be mediated by both endogenous and exogenous double-stranded RNAs has enabled this technique to be widely exploited in plants, *C. elegans* and *Drosophila.*

One hypothesis is that RNAi primarily evolved as a mechanism to protect against RNA viruses [Waterhouse *et al*, 2001] or transposable elements. However, RNAi may also have evolved to negatively regulate endogenous gene expression; for example small-temporal RNAs and miRNAs, that encodes short regulatory RNAs folded into double-stranded RNA-like hairpins [Bartel, 2004], have both been described. Typically, miRNAs base pair imperfectly with the 3'-untranslated region (UTR) of target mRNAs and inhibit protein accumulation and the level of miRNA mismatch with the target mRNA is thought to determine whether the mRNA is degraded or translationally inhibited. Bioinformatic searches have identified over 5300 putative miRNA regulated human genes [Lewis *et al*, 2005], in addition to over 200 different putative miRNA genes [Calin *et al*, 2004]. Despite the fact these miRNA genes represent only 1% of the genome, more than 50% are located within regions associated with amplification, deletion and translocation in cancer. Moreover, several studies have concluded that the

expression of specific miRNAs is associated with a number of different human cancers [He *et al*, 2005; Lu *et al*, 2005; O'Donnell *et al*, 2005].

Until recently, the technique had not been applicable to mammalian systems due to the induction of the interferon response by long double-stranded RNAs. However, the identification and effectiveness of short-interfering RNAs (siRNAs) in mediating RNAi, as described below, has successfully overcome this difficulty (summarised in **Figure 1.8**).

1.4.3.1 Mechanism of RNAi

Double-stranded RNA is first processed into an siRNA of approximately 22 nucleotides that possess 2-3 nucleotide overhangs at the 3' end by an Rnase-III type ribonuclease, namely Dicer [Bernstein *et al*, 2001; Elbashir *et al*, 2001; Zhang *et al*, 2002]. SiRNAs are then incorporated into a RNA-induced silencing complex (RISC), which contains members of the Argonaute (Ago) protein family [Hammond *et al*, 2001; Nykanen *et al*, 2001; Pham and Sontheimer, 2004]. The decision as to which strand is incorporated into the RISC complex appears to be determined by the sequence composition at the ends of the siRNA duplex; the incorporated strand is generally the one whose 5' terminus is at the thermodynamically less stable end of the duplex [Tomari *et al*, 2004]. Utilising its helicase activity, the RISC then unwinds the siRNA and the sequence of one of the single-stranded RNA species directs the RISC to homologous sequences in the host cell. RISC endonuclease activity subsequently targets the endogenous mRNA for degradation at the region homologous to the siRNA sequence [Elbashir *et al*, 2001; Meister *et al*, 2004; Rivas *et al*, 2005]. Alternatively, if there is a mismatch between the siRNA and target sequence (as in the case of miRNAs), translational inhibition results [Kim *et al*, 2004; Olsen and Ambros, 1999; Seggerson *et al*, 2002]. The guide siRNA remains associated with the complex, enabling it to carry out multiple rounds of RNA cleavage.

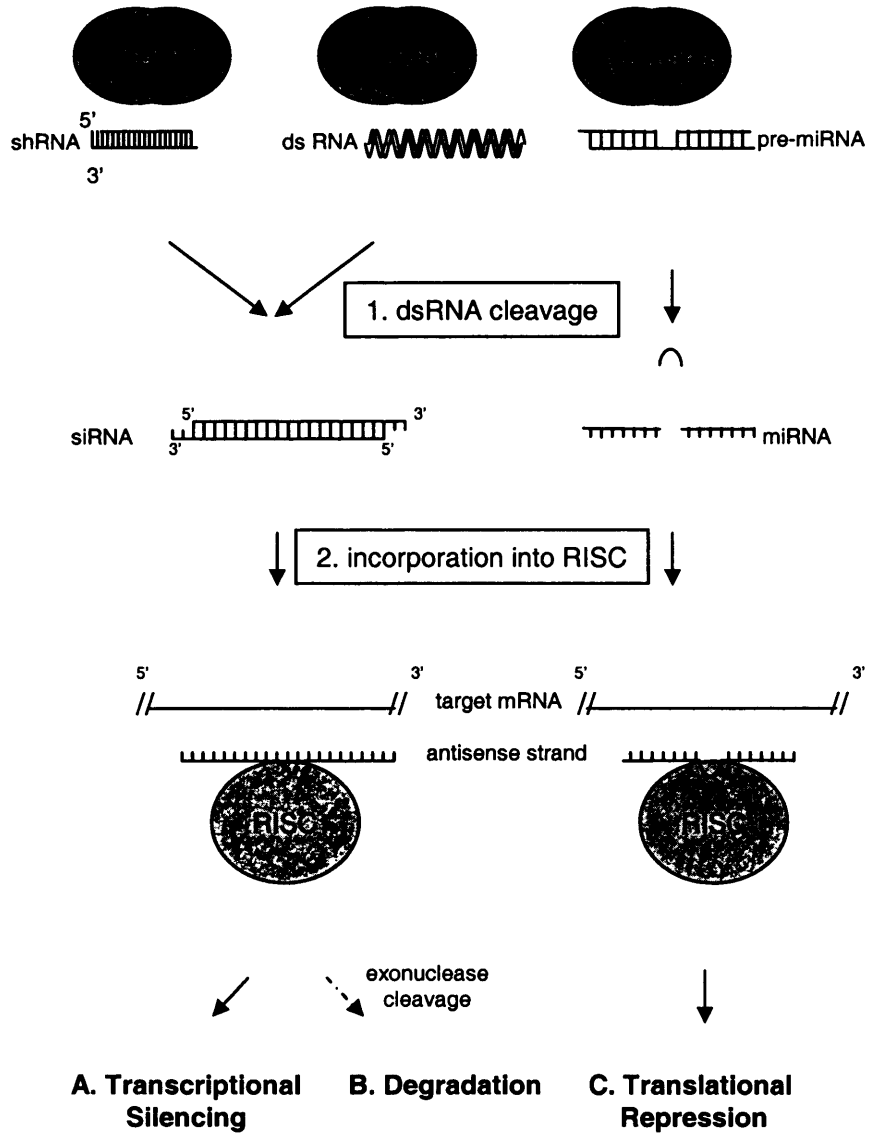

Figure 1.8: RNAi

Short-hairpin RNAs (shRNAs), longer double-stranded RNAs (dsRNAs) and micro-RNAs (miRNAs) represent three different types of RNA species that induce RNAi. As a result of these processes, the target mRNA is subject to transcriptional silencing (A), degradation (B) or translational repression (C), depending upon the type of RNA that induced the RNAi response.

1.4.3.2 RNA-Induced Transcriptional Silencing Complex

In a similar system to the RISC, the RNA-induced transcriptional silencing (RITS) complex mediates stable transcriptional silencing. In plants and *C. elegans*, stable and heritable suppression of gene expression has also been observed in the form of methylation of promoter regions of target genes. Similarly, in a mechanism known as transitive RNAi, the silencing signal has been described to move along the gene to result in alterations of chromatin structure [Kato *et al*, 2005]. Indeed, the activities of three PcG proteins, MES-3, -4 and –6, are thought to require RNAi machinery to mediate heterochromatin formation and this indicates that RISC may associate with a chromatin remodelling complex. This activity links RNAi to a higher order of gene regulation and genomic organisation and indicates that it has a profound role in evolution and development. Furthermore, RNAi mediated heterochromatin formation, also referred to as nuclear RNAi, appears to occur in most eukaryotes and controls heritable changes in gene expression (reviewed in [Wassenegger, 2005]).

1.4.3.3 Utilisation of RNAi as a Molecular Tool

There are many advantages in exploiting RNAi as a forward genetics research tool; for example, it may be utilised both *in vitro* and *in vivo* [Hemann *et al*, 2003; Paddison *et al*, 2002] and, unlike knockout animals, the suppression of gene expression is rapid.

Vector-based RNAi strategies that exploit the ability of miRNAs to form hairpin loop structures, namely short hairpin RNAs (shRNAs), have been developed. These systems use RNA polymerase III to drive expression from RNA gene promoters that are located within the 5' flanking region of the open reading frame (ORF), such as H1 or U6 promoters [Brummelkamp *et al*, 2002; Paddison *et al*, 2002]. The transcribed shRNAs are processed to form the siRNAs that subsequently enter the RISC complex to mediate knockdown

of the target gene. Consequently, a variety of plasmid-based delivery mechanisms of shRNA species may be utilised; for example, transient or stable transfection, or retroviral, lentiviral, or adenoviral infection. Furthermore, the silencing can be mediated under user-defined conditions; for example, constitutive, inducible, or tissue-specific silencing [Abbas-Terki *et al*, 2002; Brummelkamp *et al*, 2002; Chen *et al*, 2003; Czauderna *et al*, 2003; Dirac and Bernards, 2003; Paddison *et al*, 2002; Rubinson *et al*, 2003; van de Wetering *et al*, 2003; Wiznerowicz and Trono, 2003].

1.4.3.4 Effective RNAi Target Design

The overall potency of the silencing mediated by RNAi is dependent upon the target sequence that is utilised [Khvorova *et al*, 2003; Schwarz *et al*, 2003]. Whilst the significance of sequence in terms of silencing is not well understood, the accumulation of experimental data has indicated preferences or 'rules' for effective target design [Elbashir *et al*, 2002; Khvorova *et al*, 2003; Reynolds *et al*, 2004; Schwarz *et al*, 2003]; for example, the positioning of particular bases at particular positions in the siRNA also appears to be important, such as A at position 3, U at 10 and A at 19 of the sense strand [Khvorova *et al*, 2003]. Accordingly, in an attempt to design more effective siRNA species, a number of algorithms have been generated to incorporate these rules; for example, [Reynolds *et al*, 2004].

1.5 AIM OF THE RESEARCH

Due to the asynchronous nature of the growth arrest, senescence is a difficult process to study in serially sub-cultivated primary human cells. Consequently, a conditionally immortalised human mammary fibroblast cell line has been developed in the Jat laboratory by the retroviral transduction of early passage, adult interlobular mammary fibroblasts with a temperature sensitive (ts), non-DNA-binding mutant LT, namely U19tsA58, and hTERT

[O'Hare *et al*, 2001]. The principal advantage of utilising this model system that it enables cells undergoing cellular senescence in synchrony to be analysed. The HMF3A conditional growth arrest is critically dependent upon loss or inactivation of LT since, at the permissive temperature, 33.5℃, HMF3A cells grow normally whereas, at the non-permissive temperature, 39.5℃, HMF3A cells enter into an irreversible state of growth arrest within a period of between 5-7 days that is phenotypically indistinguishable from cellular senescence. In some systems, the sudden inactivation of a temperature sensitive mutant of LT induces significant cell death by apoptosis, which likely occurs as a response to the sudden release of a large amount of stable p53 [Yanai and Obinata, 1994]. However, in both the HMF3A system, and in an analogous system developed from REFs, no significant cell death occurs upon inactivation of the tsA58 temperature sensitive mutant of LT [Jat and Sharp, 1989; O'Hare *et al*, 2001].

The HMF3A system has been used in conjunction with microarrays, RNAi and *in silico* promoter analysis to promote the dissection of the transcriptional networks responsible for regulating cellular senescence [Hardy *et al*, 2005]. Changes in the transcriptome of HMF3A cells that occurred upon the induction of senescence were compared with the changes that occurred upon replicative senescece in primary human mammary fibroblasts. This analysis revealed that a number of genes such as *DUSP1*, *PHLDA1*, *NR4A3* and a novel splice variant of *STAC* were implicated in the induction of senescence, in addition to known p53 and E2F targets. RNAi followed by microarray analysis was used to functionally analyse the role of these candidate genes in senescence. *In silico* promoter analysis of all differential genes predicted that NF-κB and C/EBP transcription factors are activated upon senescence.

Our results [Hardy *et al*, 2005] suggested a putative signalling network for cellular senescence (summarized in **Figure 1.9**).

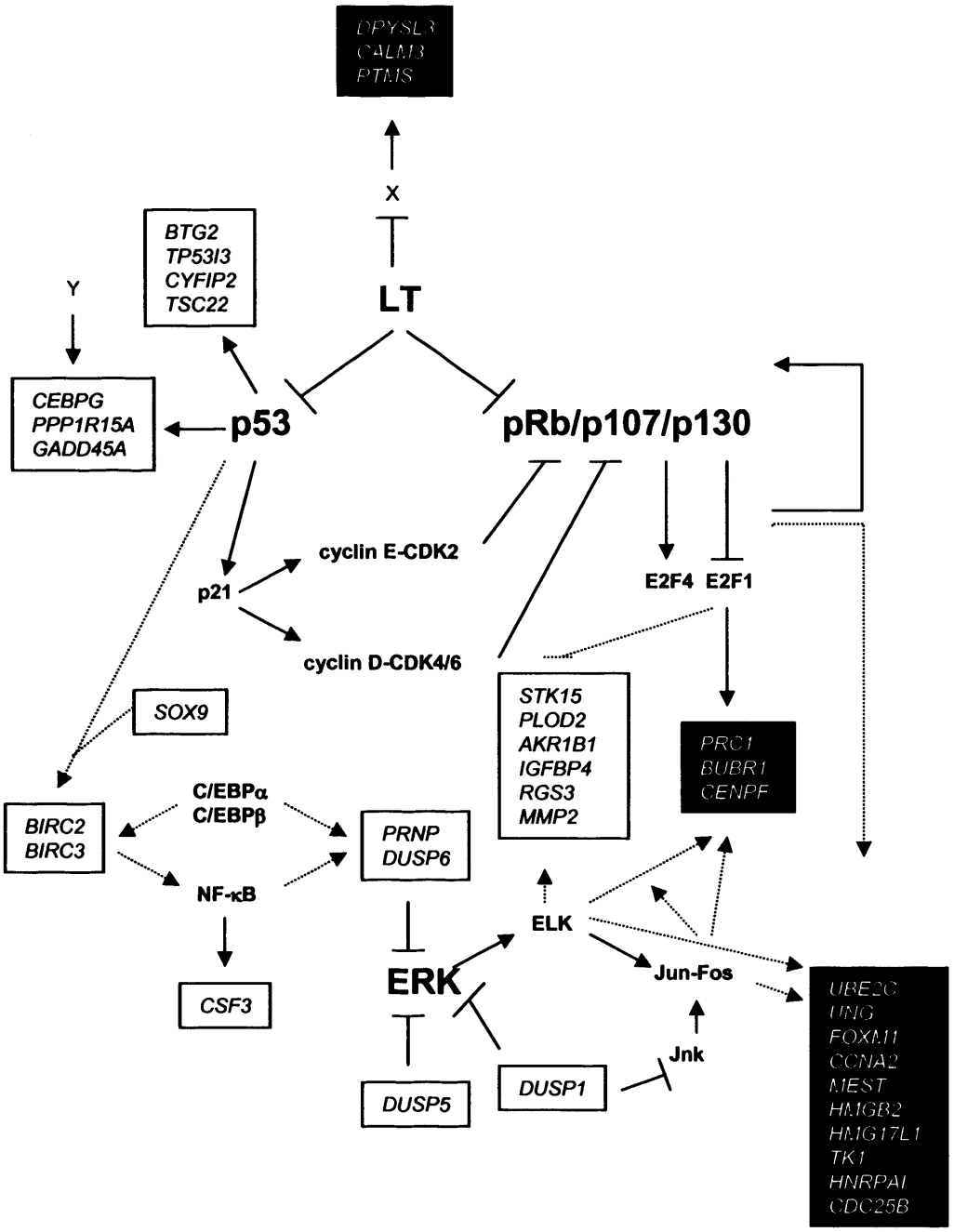

Figure 1.9: Transcriptional Networks Underlying Human Cellular Senescence

Microarray analysis, RNAi and in silico promoter analysis have been used to dissect the transcriptional networks regulating the induction of human cellular senescence (adapted from [Hardy *et al*, 2005]). Changes that occur in the transcriptome of HMF3A cells when they undergo senescence were compared with changes that occur upon replicative senescece in primary human mammary fibroblasts. Boxed genes indicate some of the genes identified by the microarray analysis. White boxes denote genes up-regulated upon senescence whereas black boxes denote genes down-regulated upon senescence.

Therefore, the aim of this thesis was to extend these findings and delineate the precise molecular basis of the induction of telomere-independent cellular senescence in the HMF3A system. To do this, a number of approaches were utilised, namely:

i. a genetic complementation assay to determine the relative importance of the p53 and pRb pathways in mediating the conditional HMF3A growth arrest;

ii. microarray analysis to identify novel genes critically involved in the induction of the conditional HMF3A growth arrest;

iii. functional analysis of the candidate genes identified by microarray analysis to assess their ability to bypass the conditional HMF3A growth arrest;

iv. and an RNAi screen to identify novel regulators of senescence in the HMF3A system.

It was anticipated that the genes identified in these independent experimental approaches would constitute novel putative markers of senescence and could also represent novel, direct targets for both cancer and anti-ageing therapies.

2. Materials and Methods

2.1 MAMMALIAN CELL CULTURE

2.1.1 Cell Media

Tissue culture media and cell culture reagents were purchased from Invitrogen. All cells were maintained in Dulbecco's Modified Eagle Medium (DMEM) supplemented with 2 millimolar (mM) glutamine, 100 units/ml penicillin, 100 μg/ml streptomycin and 10% volume per volume (v/v) heat inactivated foetal calf serum (FCS).

2.1.2 Cell Culture Conditions

All cell lines were maintained in a 5% CO_2 and 20% oxygen atmosphere. ϕ amphotropic, ϕ ecotropic and ψ_2 cell lines were maintained at 37°C. The HMF3A cell line and HMF3AEco^R cells were maintained at 33.5°C ±0.5°C, a temperature at which the cells proliferated continuously due to the functional activity of U19tsA58 LT. HMF3A temperature shift experiments were performed at 39.5°C ±0.5°C, a temperature at which U19tsA58 LT was inactivated and the cells became senescent within a period of 3-5 days [O'Hare *et al*, 2001].

2.1.3 Sub-Culturing of Cells

Cells were grown until a sub-confluent state was reached (approximately 80% confluence). Media was then removed and the monolayer of cells was washed once with 1x trypsin-ethylenediaminetetraacetic acid (EDTA; 0.25% [v/v] trypsin and 0.03%

[weight per volume [w/v]] EDTA). The monolayer was detached using 1x trypsin-EDTA (1 ml/T75 cm^2 flask) for 5 mins at 33.5°C and the trypsin-EDTA was inactivated by adding 10 ml of complete media. Cells were then plated at a defined ratio (e.g. 1 in 8 of the total cells), or counted using a haemocytometer and plated at the required density.

2.1.4 Preservation of Cells

Cells from a sub-confluent T75 cm^2 flask were trypsinised, resuspended in complete media and spun down at 1200 revolutions per minute (rpm) for 2 mins to remove any traces of trypsin. Cells were resuspended in FCS supplemented with 10% dimethyl sulphoxide (DMSO; BDH). 2x 1 ml aliquots were then transferred to cryotubes and frozen at -70°C wrapped in several layers of tissue for insulation. Tubes were transferred into liquid nitrogen (N_2) after 24 hrs.

2.1.5 Recovery of Frozen Cells

Cells were removed from liquid N_2 storage and thawed rapidly at 37°C. 9 ml of complete media was added to the cells in a 15 ml falcon tube and cells were pelleted at 1200 rpm for 2 mins to remove DMSO-containing media. The cell pellet was resuspended in 10 ml of complete media, transferred to a T25 cm^2 flask and incubated at the appropriate temperature in a 5% CO_2 and 20% oxygen atmosphere until sub-confluence was reached. Cells were then sub-cultured, as described above.

2.1.6 DNA Transfection of HMF3AEco^R Cells

Cells were plated at a density of $1x10^6$ cells/10 cm^2 plate the day prior to transfection. The following day, cells (at approximately 30% confluence)

were transfected with 10 μg of vector DNA using FuGENE 6 Transfection reagent (ROCHE), according to manufacturer's instructions.

Co-transfection of pEK-pm975 or pSG-13SE1A with a puromycin-resistance conferring vector was performed using 10 μg of the appropriate vector and 1μg of pBabepuro.

2.1.7 Selection of Stable HMF3AEco^R Transfectants

24 hrs post-transfection, fresh media was added to each plate. 48 hrs post-transfection, 2 μg/μl puromycin (Invitrogen) was added to each plate and the media was changed every 3-4 days by adding fresh puromycin each time.

2.1.8 Isolation of Clonal HMF3AEco^R Cell Lines

After transfection and selection with 2 μg/μl of puromycin, single clones were expanded into cell lines. Single clones were picked using sterile cloning cylinders (Sigma). Media was removed from each dish, and a cloning cylinder (diameter 0.25 cm) was applied around each selected clone by pressing it lightly against the Petri dish after the edge of the cloning cylinder had been dipped into sterile silicone grease. Then two drops of trypsin were added and the cells incubated at 37°C for 5 mins. The detached cells were then collected with a Pasteur pipette and the trypsin inactivated with complete medium. Cells were then plated into a T25 cm^2 flask and allowed to adhere and grow. When near confluence was reached, cells were sub-cultured, as described above.

2.1.9 Retroviral Infection of the HMF3A System

2.1.9.1 Packaging of Retroviral Constructs

ϕ amphotropic, ϕ ecotropic and ψ_2 retroviral packaging cells were plated at $0.5x10^6$ cells/10 cm^2 plate the day prior to transfection. Cells were transfected the following day (at approximately 30% confluence) with 10 μg of retroviral vector DNA and 12 μl of FuGENE 6 Transfection reagent (ROCHE), according to manufacturer's instructions. 24 hrs post-transfection, media was changed using 10 ml fresh media per plate. 48 hrs post-transfection, the retroviral supernatant was harvested, filtered through a 0.45 μm filter, and either used immediately or quickly frozen at -80°C. Frozen aliquots of retroviral supernatant were thawed rapidly at 37°C before use.

2.1.9.2 Retroviral Infection of the HMF3A System

Cells utilised for retroviral infection were seeded at $5x10^5$ cells/T75 cm^2 flask or $1x10^6$ cells/T180 cm^2 flask. The following day (at approximately 30% confluence), media was aspirated, and cells were infected with retroviral supernatant in the presence of 8 μg/ml polybrene. The volume of retroviral supernatant used for retroviral infection varied for each experiment. Cells were then incubated at 33.5°C for 24 hrs. The following day, media was replaced with 10 ml fresh media then, 4 days post-infection, antibiotic selection was added (2 μg/ml puromycin or 5 μg/ml blasticidin, where appropriate; Invitrogen), and media (including antibiotic) was changed every 3-4 days.

2.1.9.3 Titration of Transiently Produced Retroviruses

7 days post-antibiotic selection, media was removed from the flasks and cells were stained with methylene blue (2% [w/v] methylene blue and

50% ethanol in double-distilled [dd] H_20) at room temperature for 10-15 mins. Plates were then gently rinsed with water, and cell colonies counted.

2.2 BACTERIAL MANIPULATIONS

2.2.1 Bacterial Strains

The JS4 *Escherichia coli* strain (a kind gift from J. Sedivy, Brown University) was used for plasmid manipulation and preparation. JS4 is a *rec*A1 derivative of MC1061, and has the following genotype: F'*ara*D139, Δ(*ara*, *leu*)7697, Δ(*lac*)χ74, *gal*U, *gal*K, *hsd*R2 (rk^- mk^-), *mcr*A, *mcr*BC, *rps*L (Strr) *thi*, *rec*A1.

The TOP10 *Escherichia coli* strain (Invitrogen) was used for TOPO TA cloning (Invitrogen). TOP10 enables blue/white screening without isopropyl-beta-D-thiogalactopyranoside (IPTG) to be used to identify positively transformed clones and has the following genotype: F- *mcr*A Δ (*mrr-hsd*RMS-*mcr*BC) Φ80*lac*ZΔM15 Δ*lac*X74 *rec*A1 *ara*D139 Δ(*ara-leu*)7697 *gal*U *gal*K *rps*L (Str^R) *end*A1 *nup*G.

2.2.2 Media and Bacterial Growth

E. coli cells were grown in Luria Base (LB) Broth (25 g/L Luria Broth Base; Invitrogen). 15 g/L of agar (Oxoid) was added when LB agar plates were prepared. To make up the media, all the components were dissolved in ddH_2O and autoclaved for 20 mins at 121°C. When required, antibiotics were added: ampicillin or kanomycin (Sigma) were added to a final concentration of 50 μg/ml; chloramphenicol was added to a final concentration of 120 μg/ml.

2.2.3 Preparation of Competent Bacteria

5 ml of LB medium was inoculated with a single bacterial colony and incubated with shaking at 37°C overnight. The overnight culture was then diluted into 500 ml of LB and grown at 37°C with aeration for 2.0-2.5 hrs until the optical density (OD) reading at 600 nm (OD_{600}) reached 1.0-1.2 (mid-exponential phase). Bacteria were harvested by centrifugation at 2500 rpm for 20 mins, resuspended in 5 ml ice-cold 0.1 molar (M) calcium chloride ($CaCl_2$) and incubated on ice for 20 mins. Bacteria were then centrifuged again and resuspended in 5 ml of ice-cold 85:15 solution 0.1 M $CaCl_2$ and glycerol. 50 µl aliquots were frozen in pre-chilled 1.5 ml microfuge tubes using liquid N_2, and then stored at -70°C.

2.2.4 Bacterial Transformations

For JS4 cells, a single 50 µl aliquot of frozen competent bacteria was thawed on ice. 950 µl ice cold 0.1 M $CaCl_2$ was added; 100 µl of this mixture was then added to each DNA to be transformed. The DNA was incubated with the bacteria on ice for 30 mins followed by heat shock at 42°C for 90 seconds (sec). Transformations were returned to ice for 2 mins, after which 1 ml of LB medium was added and the transformations were incubated at 37°C with shaking for 30 mins. Cells were concentrated by centrifugation (2500 rpm for 10 mins) and resuspended in 100 µl LB medium. Transformations were then plated onto 10 cm^2 pre-warmed LB-agar plates containing 50 µg/ml final concentration ampicillin or kanomycin, or 120 µg/ml chloramphenicol, where appropriate. Plates were then incubated at 37°C overnight.

The same protocol was used for TOP10 transformations, except a heat shock at 42°C for 30 secs was used and 1 ml SOC medium was added to the cells immediated afterwards.

2.3 DNA MANIPULATION

2.3.1 Plasmids Used

PBabepuro-wtLT (containing full-length wt *LT* cDNA), pBabepuro-E7 (containing full-length cDNA encoding wt LT), pBabepuro (empty vector) and pRetroSuper (empty RNA interference vector) were kind gifts from O. Gjoerup (Dana-Farber Cancer Institute, Boston); pWZLpuroε-Eco^{R} (containing full-length cDNA encoding the murine ecotropic receptor) was a kind gift from J. Downward (CRUK, Lincoln's Inn Fields, London); pLPC-12SE1A (containing full-length cDNA encoding 12S E1A) was a kind gift from G. Hannon (Cold Spring Harbor Laboratory, New York); pBabepuro-DK (containing full-length cDNA encoding Cyclin D1-CDK4^{R24C} fusion construct) was a kind gift from J. Sedivy (Brown University, Rhode Island); pBabepuro-Bmi-1 (containing full-length cDNA encoding Bmi-1) was a kind gift from M. van Lohuizen (Netherlands Cancer Institute, Amsterdam); pRetroSuper-p14^{ARF} (vector allowing knockdown of p14^{ARF} expression via RNA interference) was a kind gift from R. Agami (Netherlands Cancer Institute, Amsterdam); pSK(-)-E1A (containing full-length cDNA encoding 13S E1A) was a kind gift from R. Ricciardi (University of Pennsylvania, Philidelphia); pEK-pm975 (containing the *Ad2 E1A* region with a point mutation that blocks splicing of *12S E1A*) was a kind gift from A. Berk (UCLA, Los Angeles); pSG-E1A13S (containing full-length cDNA encoding 13S E1A) was a kind gift from T. Kouzarides (Gurdon Institute, Cambridge); pHRCMV-LacZ (containing full-length cDNA encoding LacZ) was a kind gift from F. Savage (Cardiff Unversity, Cardiff); pLPCX was purchased from BDBiosciences; BAC contig RP3-447F3 (containing the *UBE2C* genomic sequence) and IMAGE clone 3345575 (containing full-length cDNA encoding UBE2C splice variant 1) were purchased from MRC GeneService.

2.3.2 Plasmid DNA Preparation

All plasmid preparations (both small scale and large scale preparations) were carried out using QIAGEN kits and following the manufacturer's instructions.

2.3.2.1 Small Scale Plasmid Preparation

Bacterial stocks were kept at -70°C in LB medium containing 15% glycerol. Liquid cultures of bacteria picked from single colonies were grown in a bacterial shaker (vigorous shaking) overnight at 37°C in 5 ml of LB medium with the appropriate antibiotic. 1.5 ml of culture was then transferred to a 1.5 ml microfuge tube and spun at 13000 rpm for 30 sec. The cell pellet was resuspended in 250 µl of solution P1 (50 mM Tris/hydrochloric acid [HCl], pH 8.0, 10 mM EDTA and 100 mg/ml RNAse A). 250 µl of solution P2 (200 mM sodium hydroxide [NaOH] and 1% sodium dodecyl sulphate [SDS]) was added and gently mixed by inverting the 1.5 ml microfuge tube 4-6 times. To the same 1.5 ml microfuge tube, 350 µl of solution N3 (3.0 M sodium acetate, pH 5.5) was added and immediately mixed by inverting the 1.5 ml microfuge tube 4-6 times. The mixture was then spun in a microfuge for 10 mins at 13000 rpm and the supernatant transferred to a QIAprep column. The column was centrifuged for 30 sec at 13000 rpm then the flow-through was discarded. The column was then washed with 0.5 ml of PB buffer (QIAprep Spin Miniprep kit, QIAGEN) and then 0.75 ml of PE buffer (QIAprep Spin Miniprep kit, QIAGEN). DNA was then eluted with 50 µl of ddH_20. All solutions used were from the QIAfilter Plasmid Mini kit, QIAGEN.

2.3.2.2 Large Scale Plasmid Preparation

200 ml of LB medium containing the appropriate antibiotic was inoculated with an overnight culture of bacteria and grown overnight at 37°C with vigorous shaking. Bacteria were harvested at 6100 rpm for 15 mins at 4°C using an SLA 1500 rotor and Sorvall RC5C centrifuge. The cell pellet was resuspended in 10 ml of resuspension buffer P1 (50 mM Tris-HCl pH 8.0, 10 mM EDTA and 100 μg/ml RNAse A, stored at 4°C). 10 ml of lysis buffer P2 (200 mM NaOH and 1% SDS) was added and, after a 5 mins incubation step at room temperature, 10 ml of ice-cold neutralisation buffer P3 (3mM potassium acetate pH 5.5) was added and the mixture was directly applied to a QIAfilter Cartridge. The QIAfilter Cartridge was incubated at room temperature for 10 mins before the cell lysate was filtered and directly applied to a previously equilibrated QIAGEN-tip 500 column (equilibration buffer QBT: 750 mM NaCl, 50 mM MOPS [3 – [N-morpholino] propanesulphonic acid] pH 7.0, 15% ethanol [v/v] and 0.15% Triton X-100) and allowed to enter the resin by gravity. The column was washed twice with 30 ml of wash buffer QC (1 M NaCl, 50 mM MOPS pH 7.0 and 15% ethanol). DNA was then eluted with 15 ml of elution buffer QF (1.25 M sodium chloride [NaCl], 50 mM Tris-HCl pH 8.5 and 15% ethanol) and precipitated in 10.5 ml of isopropanol at room temperature. Centrifugation was performed at 11000 rpm for 30 mins at 4°C using the SS34 rotor and Sorvall RC5C centrifuge. The DNA pellet was washed with 70% ethanol then centrifuged again at 11000 rpm for 5 mins. The supernatant was removed and the DNA pellet was air dried for 5 mins. DNA was resuspended in 200 μl ddH_2O in a 1.5 ml microfuge tube. All solutions used were from the QIAfilter Plasmid Maxi kit, QIAGEN.

2.3.3 DNA Quantification

To determine DNA concentration, the OD of the solution was measured at 260 nm (OD_{260}) using a BioRad spectrophotometer (Bio-Rad Smart Spec™ 3000 Spectrophotometer). DNA concentration was calculated using the relationship:

1 OD unit at 260 nm = 50 μg/ml DNA.

2.3.4 Restriction Digests

Restriction digests of DNA plasmids were performed using restriction enzymes from New England Biolabs, following the manufacturer's instructions. A 1 hr incubation time at 37°C was performed for all diagnostic restriction digests. A 3 hr incubation time was performed for all sub-cloning reactions, followed by an inactivation step at 70°C for 10 mins.

2.3.5 Dephosphorylation

1 unit of calf intestinal alkaline phosphatase (CIP; New England Biolabs) was added for every 1 μg of restriction-digested vector DNA used. Dephosphorylation was performed at 37°C for 30 mins before the reaction was incubated at 95°C for 10 mins to inactivate CIP. The DNA was then run on an agarose gel and purified, as described below.

2.3.6 DNA-Agarose Gel Electrophoresis

DNA fragments were loaded with 1x DNA loading buffer (2.5% Ficoll, 0.04% [w/v] bromophenol blue and 0.04% Xylene) and fractionated by electrophoresis on 1% (w/v) agarose (Invitrogen) gels, prepared in 1x TAE (40 mM Tris-acetate and 2 mM EDTA) with 1 μg/ml ethidium bromide

(BDH). Electrophoresis in 1x TAE was carried out in electrophoresis tanks and DNA fragments were separated at a constant voltage of 100 Volts (V) for a minimum of 20 mins. Samples were loaded alongside 5 µl 1kb+ DNA ladder (Invitrogen). Ethidium bromide stained DNA fragments were then visualised on a UVP (Dual intensity UV trans-illuminator), and an image was produced and printed with a Sony video graphic printer.

2.3.7 Extraction of DNA from Agarose Gels

DNA restriction fragments separated on agarose gels were viewed with a long wavelength UV emission transilluminator and the desired band was cut out using a scalpel and transferred to a 1.5 ml microfuge tube. DNA was then purified using the QIAquick Gel Extraction Kit (QIAGEN), according to the manufacturer's instructions. The gel slice was dissolved by adding 3 volumes of QG buffer (QIAquick spin kit, QIAGEN) then incubated at 50°C for 10 mins. The sample was then placed in a QIAquick spin column and centrifuged at 13000 rpm for 1 min, after which the DNA in the column was washed with 0.75 ml of PE buffer (QIAquick spin kit, QIAGEN). Traces of wash buffer were removed by centrifugation for 1 min. DNA was then eluted into a 1.5 ml microfuge tube by adding 50 µl of ddH_20 and centrifuging at 13000 rpm for 1 min.

2.3.8 Ligation

10 µl ligation reactions were performed using 1 µl of T4 DNA Ligase (New England Biolabs) and 1 µl 10x ligation buffer (500 mM Tris-HCl pH 7.5, 100 mM magnesium chloride [$MgCl_2$], 100 mM dithiothreitol [DTT], 10 mM ATP and 250 µg/ml bovine serum albumin [BSA]). The ratio of vector DNA:insert DNA was dependent on the sizes of the two DNA fragments. The

ligation mixture was incubated at 16°C overnight or at room temperature for 1 hr before transforming into competent *E. coli* cells.

2.3.9 DNA Sequencing

For sequencing, a 20 μl reaction containing 3.2 pmol of the primer, 500 ng plasmid DNA and 8 μl ABI dRhodamine was utilised. The sequencing reaction was performed by polymerase chain reaction (PCR) using an MJ Research Peltier Thermal Cycler. 25 cycles of 95°C for 30 sec, followed by 50°C for 15 sec and 60°C for 4 mins was used. After the final cycle, the sequencing reaction was cooled to 4°C, and then filtered using the DyeEx spin kit (QIAGEN), according to manufacturer's instructions. Samples were vacuum dried, run on a sequencing gel, then analysed by the Ludwig Institute for Cancer Research DNA sequencing facility.

For some of the miniprep DNA samples, DNA sequencing was outsourced to MWG Biotech.

2.3.10 Cloning of PCR Products

PCR products generated by amplification with SuperTaq (Ambion), or a combination of *Pfu* Turbo (Stratagene) and *Taq* (Promega) were directly cloned into pCR2.1-TOPO using the TA Cloning kit (Invitrogen), according to the manufacturer's instructions.

For SuperTaq (Ambion) cloning, 25 μl PCR reactions were set up using 1 unit of SuperTaq DNA polymerase (Ambion), 2.5 μl 10x reaction buffer (100 mM Tris-HCl [pH 9.0], 15 mM MgCl2, 500 ml potassium chloride [KCl], 1% Triton® X-100, and 0.1% [w/v] stabiliser; Ambion), 2 μl 25 mM $MgCl_2$, 1 μl of each primer (10 μM), 1 μl 10 mM dNTPs (Promega) and 100 ng template DNA.

For *Pfu* Turbo (Stratagene) cloning, 50 µl PCR reactions were set up using 1 unit of *Pfu* Turbo DNA polymerase (Stratagene), 5 µl 10x reaction buffer (100 mM KCl, 100 mM ammonium sulphate [$[NH_4]_2SO_4$], 200 mM Tris-HCl [pH 8.8], 20 mM magnesium sulphate [$MgSO_4$], 1% Triton® X-100 and 1 mg/ml nuclease free BSA; Stratagene), 1 µl of each primer (10 µM), 2 µl 10 mM dNTPs (Promega) and 100 ng template DNA.

For both PCR procedures, a 5 min, 95°C denaturation step was used before amplification. PCR amplification was performed by denaturing at 95°C for 30 sec, annealing at 55°C for 30 sec and extending at 72°C for 1 min, for a total of 22 cycles. A final 72°C extension step of 10 mins was used for SuperTaq (Ambion). For *Pfu* Turbo (Stratagene) cloning, 1 unit of *Taq* (Promega) was added at the end of the 22 cycles before a final extension step at 72°C for 10 mins was performed.

4 µl fresh PCR product was directly cloned into pCR2.1-TOPO by adding 1 µl salt solution (TA Cloning kit, Invitrogen) and 1 µl pCR2.1-TOPO (TA Cloning kit, Invitrogen). The reaction was mixed gently and incubated for 5 mins at room temperature before incubating on ice. The TOPO cloning reaction was transformed using TOP10 competent cells by adding 2 µl of TOPO cloning reaction to one vial of TOP10 competent cells. The DNA/cell mix was incubated for a further 10 mins on ice then cells were heat-shocked at 42°C for 30 sec before immediately transferring back onto ice. 250 µl of room temperature SOC medium (.5% yeast extract, 2% tryptone, 10mM NaCl, 2.5mM KCl, 10mM $MgCl_2$, 20mM $MgSO_4$, 20mM glucose) was added (TOPO TA Cloning kit, Invitrogen) and cells were shaken horizontally at 200 rpm at 37°C for 1 hr. 10 µl was then spread onto 10 cm^2 pre-warmed LB-agar plates containing 40 µl 40 mg/ml 5-bromo-4-chloro-3-indolyl-β-D-galactopyranoside (X-gal) and 50 µg/ml final concentration ampicillin or kanomycin, as appropriate. Plates were then incubated overnight at 37°C.

The sequences of all primers used for PCR cloning and sequencing can be found in **Supplementary Figure S1**.

2.3.10.1 Cloning of 12S and 13S E1A

For PCR amplification of 12S and 13S E1A, primers incorporating a 5' *Bgl* II restriction site and 3' *Not* I restriction were used: namely E1A 13S-F and E1A 13S-R. 25 μl PCR reactions were carried out using 100 ng plasmid DNA (pLPC-12SE1AORI or pSK[-]-13SE1A and SuperTaq DNA polymerase (Ambion). 2 μl of PCR product was cloned directly into pCR2.1-TOPO vector, and positive clones were sequenced using primers E1ASEQ-F, E1ASEQ-R (5'-3', M13F and M13R. One sequence-verified clone was *Eco*R I digested and gel purified then sub-cloned into *Eco*R I digested and gel purified pBabepuro.

2.3.10.2 Cloning of UBE2C

BAC contig RP3-447F3 (MRC GeneService) was *Bam*H I digested to isolate a 6722 bp *Bam*H I fragment containing the *UBE2C* gene (between bases 80233 and 86955 of the RP3-447F3 clone) and sub-cloned into *Bam*H I digested and gel purified pBluescriptSK(-). The 3' end was then PCR amplified using SuperTaq DNA polymerase (Ambion) and primers Ube2cAmp-F, that incorporated a *Cla* I restriction site directly downstream of the STOP codon, and Ube2cAmp-R, that spanned a unique *Eco*R I restriction site located in the *UBE2C* gene. The resultant PCR product was directly cloned into pCR2.1-TOPO then sequence verified using M13F and M13R primers.

The 3585 bp *Sal* I/*Eco*R I and 613 bp *Eco*R I/*Cla* I restriction digest fragments (derived from pBluescript-UBE2C and pCR2.1-UBE2C, respectively) were then sub-cloned into *Xho* I/*Cla* I digested and gel purified pLPCX vector in 1:1:1 molar ratio ligation.

2.3.10.3 Cloning of UBE2C#1

The *UBE2C#1* ORF was PCR amplified from IMAGE clone 3345575 (MRC GeneService) using a combination of *Pfu* Turbo (Stratagene) and *Taq* (Promega) DNA polymerases and M13F and Ube2c-ampR primers. The resultant PCR product was directly cloned into pCR2.1-TOPO (Invitrogen) and positive clones were sequence verified using primers UBE2C#1 SEQ-F, UBE2C#1 SEQ-R and M13R. One sequence-verified clone was sub-cloned as a gel purified *Eco*R I/*Cla* I restriction digest fragment into *Eco*R I/*Cla* I digested, gel purified pLPCX vector to generate pLPC-UBE2C#1.

2.3.10.4 Cloning of Myc-UBE2C#1

An N-terminal Myc-tag was cloned directly upstream of the *UBE2C#1* ORF by PCR amplification of pLPC-UBE2C#1 vector using a combination of *Pfu* Turbo and *Taq* DNA polymerases and primers Myc-UBE2C#1-F, that incorporated an *Eco*R I restriction site and Myc-tag sequence directly upstream of the *UBE2C#1* ORF, and Ube2c-ampR. The PCR product was directly cloned into pCR2.1-TOPO (Invitrogen) and positive clones were sequence verified, using the protocol described for UBE2C#1. One sequence-verified clone was sub-cloned as a gel purified, *Eco*R I/*Cla* I restriction digest fragment into *Eco*R I/*Cla* I digested and gel purified pLPCX vector to generate pLPC-Myc-UBE2C#1.

2.3.11 Design of ShRNA Constructs

ShRNA target sequences were designed using a search algorithm developed by Dharmacon (http://www.dharmacon.com/sidesign) and based upon the guidelines of Reynolds and colleagues [Reynolds *et al*, 2004]. The 5' UTR, ORF and 3' UTR regions of the gene of interest were used to search for a suitable shRNA target sequence.

2.3.12 Cloning of ShRNA Constructs

Target sequences were used to generate a pair of 64 mer shRNA oligos, based upon the templates designed by Oligoengine (**Supplementary Figure S2**). The two 64 mer shRNA oligos were resuspended to 3 mg/ml then 1 µl of each oligo was added to 48 µl Oligoengine Annealing Buffer (100 mM NaCl and 50 mM 4-[2-hydroxyethyl]-1-piperazineethanesulphonic acid [HEPES] pH 7.4), vortexed vigorously, and incubated at 95°C for 4 mins, followed by 70°C for 10 mins. Oligos were then annealed by cooling at room temperature for 1 hr, then at 4°C overnight. Oligos were phosphorylated by adding 2 µl to 1 µl T4 polynucleotide kinase (PNK; Promega), 1 µl 10x T4 PNK buffer (700 mM Tris-HCl [pH 7.6 at 25°C], 100 mM $MgCl_2$ and 50 mM DTT; Promega), and 1 µl 10 mM ATP (Promega). Samples were incubated at 37°C for 30 mins, followed by a 10 mins denaturation step at 70°C. 2 µl of phosphorylated oligos were ligated to 100 ng gel purified, *Hind* III/*Bgl* II digested pRetroSuper vector in a 10 µl reaction, using T4 DNA ligase (as described above). Ligated constructs were then transformed into JS4 competent cells and plated onto LB-agar plates containing 50 µg/ml final concentration ampicillin (as described above). Positive clones were prepped and digested using *Eco*R I and *Hind* III. Restriction digest products were resolved alongside 5 µl 1kb+ DNA ladder (Invitrogen) on a 3% agarose gel; 290 bp restriction digest products derived from positive clones were distinguished from 230 bp vector only restriction digest products upon the basis of size. Positive clones were then sequence verified using SuperRetroseq (see **Supplementary Figure S1**).

2.3.13 Recovery of ShRNA Inserts from Cells Expressing pSM2 Constructs

2.3.13.1 Genomic DNA Extraction

Genomic DNA was extracted from a near confluent T25 cm^2 culture using the QIAamp DNA Blood Mini kit (Qiagen). Media was removed from the culture and the cell monolayer was washed once with 1x trypsin-EDTA (0.25% [v/v] trypsin and 0.03% [w/v] EDTA). The monolayer was then detached, using 1x trypsin-EDTA (0.5 ml/T25 cm^2 flask) for 5 mins at 33.5°C), and the trypsin-EDTA was then inactivated by adding 1 ml of complete media. Cells were transferred to a 1.5 ml microfuge tube and centrifuged for 5 mins at 3000 rpm. The supernatant was discarded and the cell pellet was resuspended in 1x PBS (Phosphate Buffered Saline [without $CaCl_2$ or $MgCl_2$]) to a final volume of 200 µl, before 20 µl of QIAGEN Protease (QIAamp DNA Blood Mini Kit, Qiagen) was added. 200 µl Buffer AL (QIAamp DNA Blood Mini Kit, Qiagen) was then added and mixed by pulse-vortexing for 15 sec, followed at incubation at 56°C for 10 mins. The 1.5 ml microfuge tube was centrifuged briefly then 200 µl ethanol (96-100%) was added, followed by pulse-vortexing for 15 sec. The mixture was then applied to a QIAamp Spin Column (QIAamp DNA Blood Mini Kit, Qiagen) and centrifuged at 8000 rpm for 1 min. The QIAamp Spin Column was placed in a clean 2 ml collection tube then washed with 500 µl Buffer AW1 (QIAamp DNA Blood Mini Kit, Qiagen) and centrifuged at 8000 rpm for 1 min. The QIAamp Spin Column was placed in a clean 2 ml collection tube then washed with 500 µl Buffer AW2 (QIAamp DNA Blood Mini Kit, Qiagen) and centrifuged at 1300 rpm for 3 mins. The QIAamp Spin Column was then placed in a clean 1.5 ml microfuge tube and 200 µl Buffer AE (QIAamp DNA Blood Mini Kit, Qiagen) was added. Following incubation at room temperature for 1 min, the 1.5 ml microfuge tube was centrifuged at 8000 rpm for 1 min.

2.3.13.2 PCR Amplification of pSM2 Sequences from Genomic DNA

100 ng genomic DNA was used in a 25 µl PCR reaction that contained 0.5 µl of 6.6 µM primers SM2 F3 and 6.6 µM SM2 R3 (see **Supplementary Figure S1**), 0.25 µl AmpliTaq (Applied Biosystems), 2.5 µl 25 mM $MgCl_2$ (Applied Biosystems) and 0.625 µl 10 mM dNTPs (Promega). An initial denaturation step at 95°C for 10 mins was performed before PCR amplification. PCR amplification parameters were denaturation at 95°C for 30 sec; annealing at 67°C for 30 sec; extension at 72°C for 30 sec, and a final extension of 10 mins at 72°C after the last cycle. 40 cycles were used in total. A PCR reaction containing 100 ng pSM2 scrambled was used as the positive control for PCR amplification, and a PCR reaction that contained no template was used as the negative control to check for contamination of the reaction mixture. 5 µl of each PCR reaction was then resolved alongside 5 µl 1kb+ DNA ladder (Invitrogen) on a 3% agarose gel to check for the generation of 424 bp PCR products that could be visualised on a UVP.

2.3.13.3 Sequencing of ShRNA Inserts from the ShRNA Screen

4 µl of each PCR product was directly cloned into pCR2.1-TOPO vector (Invitrogen) using the TOPO TA Cloning Kit (Invitrogen), as described above. 2 µl of the cloning reaction was transformed onto LB-agar plates containing 50 µg/ml final concentration ampicillin and 40 µl of 40 mg/ml X-gal and incubated at 37°C overnight. Blue/white selection was used to identify positive clones that were picked and prepped using the QIAprep Spin Miniprep kit (QIAGEN), as described above. Positive clones were sequenced using M13R primer.

2.4 PROTEIN ANALYSIS

2.4.1 Preparation of Total Protein Extracts

HMF3A cultures grown in T75 cm^2 flasks were fed with fresh media the day prior to lysis and were harvested at no greater than 80% confluence on the day of lysis. For lysis, cells were washed twice with cold 1x PBS, and 0.5 ml of 1x radioimmunoprecipitation (RIPA) lysis buffer (150 mM NaCl, 1% Triton-X-100, 0.5% sodium deoxycholate, 0.1% SDS and 5 0mM Tris pH 8.0) was added to each T75 cm^2 flask. 2 µl of Protease Inhibitor Cocktail (2 mM 4-[2-aminoethyl] benzenesulphonyl fluoride [AEBSF], 1 mM EDTA, 130 µM Bestatin, 14 µM E-64, 1 µM Leupeptin and 0.3 µM Aprotinin; Sigma) was added per 1 ml of lysis buffer used. Cells were incubated on ice for 30 mins then scraped and transferred to a 1.5 ml microfuge tube. Lysates were passed three times through a 21-gauge needle to shear the DNA then centrifuged at 10000 rpm for 30 mins at 4°C. The supernatant from each lysis reaction was transferred to a fresh 1.5 ml microfuge tube, aliquoted then stored at -20°C.

2.4.2 Determination of Protein Concentration

Protein concentrations were determined using the Bio-Rad protein assay (Bio-Rad Laboratories), a protein assay based on the Bradford assay [Bradford, 1976]. The dye reagent was diluted 1:5 in PBS. A BSA standard curve was established with protein dilutions ranging from 1-15 µg/ml. 2 µl of each sample were mixed with 1 ml of freshly diluted dye and incubated at room temperature for 5 mins. OD_{595} was measured (Bio-Rad Smart Spec™ 3000 Spectrophotometer) and plotted against protein concentration of standards. The regression coefficient was calculated and the unknown sample concentrations determined.

2.4.3 Sodium-Dodecyl-Sulphate-Polyacrylamide-Gel-Electrophoresis

8% Sodium dodecyl sulphate-polyacrylamide gel electrophoresis (SDS-PAGE) gels were prepared from a 30% (w/v) acrylamide stock solution (containing a ratio of 29.2 acrylamide:0.8 N,N'-methylenebisacrylamide; Genomic Solutions) in 375 mM Tris-HCl pH 8.8 and 0.1% (w/v) SDS. Gels were polymerised by addition of ammonium persulphate (APS) (0.1% [w/v] final; Bio-Rad) and TEMED (N,N,N',N' tetraethylenemethyldiamine, 0.0006% [w/v] final; BDH Laboratory). For 10, 12 and 15% SDS-PAGE gels, quantities of the polymerising agents were adjusted accordingly.

30 μg of each cell lysate (unless otherwise stated) was heated at 90°C for 5 mins with 2x Laemmli sample buffer (8% SDS, 40% glycerol, 20% 2-mercaptoethanol, 0.008% bromophenol blue and 0.260 mM Tris-HCl, pH 6.8) and fractionated by SDS-PAGE. Electrophoresis was carried out at a constant voltage of 100-150 V during the day (or 40 V overnight) in running buffer (25 mM Tris, 190 mM Glycine, 0.1% [w/v] SDS). Proteins were stacked through 2 cm of stacking gel (5% polyacrylamide, 125 mM Tris-HCl pH 6.8 and 0.1% [w/v] SDS, polymerised by addition of APS and TEMED, as before). Proteins were fractionated alongside broad-range pre-stained SDS-PAGE standards (Bio-Rad Laboratories).

2.4.4 Western Blotting of SDS-PAGE

Following separation via SDS-PAGE, proteins were transferred to a nitrocellulose membrane, Hybond-c extra (Amersham Life Science) by electrophoretic transfer in a wet tank blotting system (Bio-Rad Laboratories Trans-Blot cell). The transfer was carried out in transfer buffer (25 mM Tris, 190 mM glycine and 20% [v/v] methanol) for 4 hrs at a constant voltage of 60 V at 4°C or, alternatively, overnight at a constant voltage of 20 V (4°C).

The nitrocellulose membrane was then blocked by incubation in 5% (w/v) skimmed milk powder (Marvel, Premier Brands) and 0.005% (v/v)

Tween-20 (BDH Laboratory) in 0.5x PBS (PBS/Marvel) at room temperature for 1 hr or overnight at 4°C. The filter was then incubated for 1 hr at room temperature, or overnight at 4°C with the primary antibody diluted in PBS/Marvel at the indicated dilutions (as described below). The filter was then washed three times (15 mins each at room temperature) in 0.05% (v/v) Tween 20 and 0.5x PBS (PBS/Tween) prior to incubation with horseradish peroxidase (HRP) conjugated secondary antibody (Amersham Life Sciences enhanced chemiluminescence [ECL™] western blotting analysis system) diluted 1:2000 in PBS/Tween for 1 hr. Following three further washes (15 mins each at room temperature) in PBS/Tween, the filters were developed in HRP detection reagents for 90 sec, according to manufacturer's instructions (ECL™, Amersham Pharmacia Biotech). The membrane was then wrapped with Saran-wrap and exposed to an auto-radiographic film for times varying from 10 sec to 2 hrs (Fujifilm Super RX X-ray film). Films were developed with an AGFA X-ray film processor.

2.4.5 Antibodies Used

Anti-Bmi-1 mouse monoclonal antibody (clone 1.T.21) was purchased from Abcam; anti-HPV16 E7 mouse monoclonal antibody (clone 8C9) was purchased from Zymed Laboratories Inc; anti-HPV16 E7 mouse monoclonal (clone ED17), anti-p21 mouse monoclonal (clone F3), anti-cyclin D1 mouse monoclonal (clone A12), anti-CDK4 rabbit polyclonal (clone H-22), anti-Myc mouse monoclonal (clone 9E10) and anti-Myc rabbit polyclonal antibodies (clone A-12) were purchased from Santa Cruz Biotechnology; anti-β Actin mouse monoclonal (clone AC-40) and anti-β-Tubulin mouse monoclonal antibodies (clone 2-28-33) were purchased from Sigma; anti-p21 mouse monoclonal antibody (clone SX118) was a kind gift from X. Lu (LICR, London); anti-E1A mouse monoclonal antibodies (clone M3 and M73) were a kind gift from E. Harlow (Massachusetts General Hospital Cancer Center, Charlestown); anti-$p16^{INK4a}$ mouse monoclonal antibody (clone JC8) was a

kind gift from G. Peters (CRUK, Lincoln's Inn Fields, London); anti-Ubch10 mouse monoclonal was a kind gift from F. Hofmann (Norvartis Pharma AG, Basel); and anti-AKR1B1 rabbit polyclonal (clone L3) was a kind gift from A. Martinez (Université Blaise Pascal Clermont II, France).

The antibodies were diluted for Western blot analysis as follows: p21 (F3) 1:500; p21 (SX118) 1:500; β-Actin (AC-40) 1:2000; β-Tubulin 1:2000; cyclin D1 (A12) 1:1000; Myc (9E10) 1:100; Myc (A-12) 1:1000; CDK4 (H-22) 1:100); Ubch10 1:1000; AKR1B1 1:1000; Bmi-1 (1.T.21) 1:2000; E7 (equal mixture of ED17 and 8C9) 1:100; and HRP-conjugated secondary antibodies 1:2000. Hybridoma tissue culture supernatant of anti-E1A mouse monoclonal antibody M73 was used at 1:50; hybridoma tissue culture supernatant of anti-E1A mouse monoclonal antibody M3 was used at 1:25; and hybridoma tissue culture supernatant of anti-$p16^{INK4a}$ mouse monoclonal antibody JC8 was used at 1:5.

2.5 RNA MANIPULATION

2.5.1 RNA Isolation

HMF3A cultures grown in T75 cm^2 flasks (or T180 cm^2 flasks if preparing RNA for microarray analysis) were fed with fresh media the day prior to RNA extraction and were harvested at no greater than 80% confluence on the day of RNA extraction. Media was removed and the cells were washed twice with 1x PBS. 2.5 ml of TRIzol (Life Technologies) was then added to each T75 cm^2 flask (5 ml of TRIzol for each T180 cm^2 flask) and cells were left to lyse for 5 mins at room temperature. Cell lysates were then passed several times through a 5 ml pipette, after which the samples were incubated for 5 mins at room temperature. 0.2 ml of chloroform (per 1 ml of TRIzol used) was then added, and the samples were vigorously shaken by hand for 15 sec, followed by a 5 mins incubation step at room temperature. Samples were then centrifuged at 11000 rpm for 15 mins at 4°C using a SS34 rotor and

Sorvall RC5C centrifuge. Following centrifugation, the aqueous phase of the mixture was transferred to a fresh tube and RNA was extracted with isopropyl alcohol (0.5 ml of isopropyl alcohol for each 1 ml of TRIzol used). Samples were incubated at room temperature for 10 mins then centrifuged at 10000 rpm for 10 mins at 4°C. Supernatant was removed and the pellet was washed once with ethanol diluted to 75% in DEPC (diethyl pyrocarbonate) treated H_20 (0.1% DEPC dissolved in ddH_20; 1 ml of ethanol for each 1 ml of TRIzol used). The RNA pellet was briefly air-dried then resuspended in 50-100 µl of DEPC treated H_20 and incubated at room temperature for at least 30 mins to ensure it was completely resuspended.

2.5.2 RNA Quantification

After RNA extraction, optical density of the solution was measured at 260nm (OD_{260}) using a Bio-Rad spectrophotometer (Bio-Rad Smart Spec™ 3000 Spectrophotometer). RNA concentration was calculated using the relationship:

1OD unit at 260 nm = 40 µg/ml RNA

2.5.3 Reverse Transcription (RT) of RNA

CDNA was reverse transcribed from equal amounts (2 µg) of total RNA using MoMuLV reverse transcriptase. The SuperScript™II kit (Invitrogen) was used, according to manufacturer's instructions. RNA was added to 0.5 µg of oligo dT primer (Promega) and 0.5 mM dNTPs (Promega) then denatured at 65°C for 10 mins followed by quick chilling on ice. 1 µl ribonuclease inhibitor (Promega) and 1 µl 0.1M DTT were then added to the mixture, together with 2 µl of 5x First-Strand Buffer (250 mM Tris-HCl [pH 8.3], 375 mM KCl and 15 mM $MgCl_2$), and incubated at 42°C for 2 mins. 200 units of MoMuLV reverse transcriptase enzyme was added and the reaction

was incubated at 42°C for 50 mins before heat inactivation at 70°C for 15 mins to denature the RNA-DNA duplex and inactivate the reverse transcriptase. The resultant cDNA was stored at -20°C.

2.5.4 Semi-Quantitative Reverse Transcription Polymerase Chain Reaction (RT-PCR)

For each gene studied, an optimal PCR cycle number was established that enabled the bands to be visible on a gel and did not result in saturation of the amplification procedure. The sequences of the primers used for PCR are given in **Supplementary Figure S3**, along with annealing temperatures and numbers of PCR cycles used.

All PCR reactions were carried out in a total volume of 25 µl and contained 10 µl of a 1:10 dilution of the cDNA generated by RT reaction, 1 µl of each oligonucletide primer (10 µM), 2.5 units *Taq* DNA polymerase (Promega), 2.5 µl 10x PCR buffer (10 mM Tris HCl pH 9, 50 mM KCl and 0.1% [w/v] Triton X-100; Promega), 1 µl 10 mM dNTPs (Promega) and 2 µl 25 mM $MgCl_2$ (Promega). The PCR reaction was performed in a PTC-200 Peltier Thermal cycler thermocycler. A 5 mins, 95°C denaturation step was used before amplification. Cycling conditions were denaturation at 95°C for 1 min, annealing at the specific temperature for each primer pair (**Supplementary Figure S3**) for 30 sec, extension at 72°C for 1 min, and a final extension of 5 mins at 72°C at the end of the last cycle. For each PCR reaction, a control amplification containing no cDNA was included to check for contamination of the reaction mixture. PCR products were resolved alongside 5 µl 1kb+ DNA ladder (Invitrogen) on 1-3% agarose gels, depending upon the size of the expected PCR product. Ethidium bromide stained DNA fragments were visualised on a UVP and images were reproduced and printed with a Sony video graphic printer.

2.5.5 Real-Time PCR

Quantitative real-time PCR analysis was performed using Assays-on-Demand Gene Expression Products (Applied Biosystems). Individual 20x Target Assay kits (containing gene-specific primers and TaqMan® MGB Probe; Applied Biosystems) were purchased for each gene: *AKR1B1*: Hs00739326_m1; *CDH13*: Hs00169908_m1; *p21*: Hs00355782_m1; *CKS2*: Hs00854958_g1; *CUL4B*: Hs00186086_m1; *FAP*: Hs00189476_m1; *GAPDH*: Hs99999905_m1; *NOL5A*: Hs00197340_m1; *PGK1*: Hs99999906_m1; *RNF11*: Hs00702517_s1; *UBE2C*: Hs00853610_g1.

CDNA amplification was carried out in a 20 µl reaction containing 1 µl 20x Target Assay Mix and 10 µl 2x TaqMan® Universal PCR Master Mix (containing AmpliTaq Gold DNA Polymerase, AmpErase UNG [uracil-N-glycosylase], dNTPs with dUTP, ROX passive reference dye, and optimised buffer components; Applied Biosystems). Reactions were performed in a MicroAmp® Optical 96-Well Reaction Plate (Applied Biosystems) covered with a MicroAmp® Optical Cap (Applied Biosystems). Real-time PCR quantitation was measured using the ABI Prism 7700 Sequence Detection System® (Applied Biosystems), according to the manufacturer's instructions. Before amplification, a 2 mins incubation step at 50°C was used to optimise UNG activity, followed by a 10 mins denaturation step at 95°C. Amplification parameters were: denaturation at 95°C for 15 sec, followed by a combined annealing and extension step at 60°C for 1 min. 40 cycles were used in total.

2.6 MICROARRAYS

2.6.1 Generation of FluorescentlyLabelled cDNA Targets

Microarrays were performed using the Sanger/LICR/CRUK Microarray Consortium protocol:

(http://www.sanger.ac.uk/Projects/Microarrays/). 25 µg of total RNA was used for each hybridisation reaction. 2.5 µl anchored oligo-dT_{17} (2 µg/µl) was added to the total RNA to a final volume of 12.9 µl. The RNA/oligo mixture was then heated to 70°C for 10 mins and quickly chilled on ice.

The RT was set up using 15.4 µl RNA/oligo mix; 6.0 µl 5x First Strand Buffer (250 mM Tris-HCl [pH 8.3], 375 mM KCl and 15 mM $MgCl_2$; Invitrogen); 3.0 µl 0.1 M DTT (Invitrogen); 0.6 µl dNTP mix (25 mM dATP, dTTP, dGTP and 10 mM dCTP; Promega); 3.0 µl 1 mM dCTP-Cy3 or dCTP-Cy5 (Amersham) and 400 units Superscript II (Invitrogen), in a total volume of 30 µl. The reaction was performed at 42°C for 2 hrs, after which, 1.5 µl of 1 M NaOH was added, then samples were incubated at 70°C for 20 mins to hydrolyse the RNA. The reaction was then neutralised by adding 1.5 µl of 1 M HCl. Unincorporated nucleotides and short oligomers were removed using AutoSeq™ G-50 columns (Amersham). Approximately 33 µl of cDNA was eluted and appeared faintly coloured pink or blue, depending on which Cy dye has been incorporated.

2.6.2 Competitive Hybridisation of Labelled cDNAs onto Microarrays

The two cDNA samples were combined then added to 8 µg polyA DNA (Sigma); 8 µg human C_0t1 DNA (Invitrogen); 0.7 µl 3 M sodium acetate pH 5.2 and 218 µl 100% ethanol, then precipitated at -70°C for 20 mins. CDNA was then pelleted, washed briefly in 70% ethanol, and dried thoroughly. The pellet was resuspended in 40 µl of hybridisation buffer (filter sterilised 5x SSC [3 M NaCl, 0.3 M sodium citrate, pH7.0], 6x Denhardt's solution [0.12% BSA, 0.12% Ficoll, 0.12% polyvinylpyrrolidone], 60 mM Tris-HCl pH 7.6, 0.12% sarkosyl [N-laurylsarcosine] and 48% formamide). 8 µl of ddH_20 was added to bring the final volume to 48 µl. The cDNA mixture was boiled at 100°C for 5 mins then left to cool to room temperature for 10 mins, after which the samples were centrifuged briefly to remove the

evaporated liquid from the lid of tube. Samples were then spotted onto the centre of a cover slip (25x60 mm; BDH) placed on a flat surface. The microarray slide, DNA side up, was then placed in a humid hybridisation chamber (2x7 cm 3MM paper moistened with 2 ml of 40% formamide and 2X SSC in a Petri dish sealed with autoclave tape) to prevent the buffer from evaporating during the hybridisation. Samples were then incubated at 47°C overnight.

After the hybridisation, microarray slides were removed from the humid chamber and quickly placed in slide rack submerged in 100-200 ml of room temperature wash solution 1 (2x SSC, filter sterilised). The cover slips were expected to slide off the array within 10-15 sec of being placed in the wash solution, at which point it could be carefully removed without scraping against the microarray slide. The slides were then washed at room temperature for 5mins with gentle shaking and then transferred into a slide rack containing wash solution 2 (0.1x SSC and 0.1% SDS, filter sterilised) at room temperature for 30 mins with gentle shaking. The last wash was repeated twice. Microarray slides were transferred to a slide rack containing wash solution 3 (0.1x SSC, filter sterilised) and washed at room temperature for 5mins with gentle shaking. Finally, the slides were centrifuged at 1000 rpm for 1 min to dry.

2.6.3 Microarray Image Acquisition

Laser scanning of the chips was performed after the hybridisation and post-hybridisation washes to achieve a quantitative evaluation of each individual complementary sequence present on the sample. To acquire images, a laser-based scanner (ScanArray 4000 Microarray Autoloader from Packard BioChip Technologies) was used. The pixel intensity of each spot was directly proportional to the number of dye molecules and, hence, the number of probes hybridised with the spotted PCR product. Scanning was performed at the two wavelengths compatible with efficient excitation for Cy3

and Cy5, and the two resultant images were acquired. Scanning was performed as soon as possible after the hybridisation/washing step, since fluorophore emission levels decreased with time once the slides had been dried.

3. Abrogation of the P53 and PRb Pathways in the HMF3A System

3.1 OBJECTIVES

There is much evidence to associate the activities of the p53 and pRb pathways with the induction of human cellular senescence; however, the downstream pathways that are critically involved in this process are poorly understood. Therefore, the aim of this chapter was to determine the relative functional importance of the p53 and pRb pathways in the induction of senescence and delineate the signalling pathways causal to this process.

The conditionally immortalised HMF3A system represented a potential system with which to address this aim, since the transcriptional changes that occurred upon the conditional HMF3A growth arrest directly correlated with the transcriptional changes that occurred upon replicative senescence [Hardy *et al*, 2005]. Moreover, it appeared that three pathways associated with the indication of replicative senescence, namely, the p53, pRb and ERK signalling pathways, were also important regulators of the conditional HMF3A growth arrest.

Genetic complementation of the HMF3A system represented a potential experimental strategy to dissect the pathways underlying the induction of telomere-independent cellular senescence in these cells; therefore, an HMF3A growth complementation assay was developed. Upon validation of both the sensitivity and specificity of this assay, components of the p53 and pRb pathways were functionally abrogated in the HMF3A system and assayed for their ability to complement the growth of these cells under the non-permissive conditions.

3.2 RESULTS

3.2.1 Reconstitution of Wt LT Activity in the HMF3A System

The conditionally immortalised phenotype of the HMF3A system is critically dependent upon the activity of U19tsA58 LT [Hardy *et al*, 2005; O'Hare *et al*, 2001]. Therefore, it was hypothesised that reconstitution of wt LT activity into these cells would be sufficient to overcome their growth conditionality (**Figure 3.1**).

To address this hypothesis, an experimental strategy that involved retroviral delivery of wt LT into the HMF3A system was considered suitable for two reasons: firstly, it represented a highly efficient way in which to infect the HMF3A cells and, secondly, it would enable wt LT to become integrated into the host genome, thereby maintaining stable, constitutive wt LT expression through successive cell divisions.

3.2.1.1 Constitutive Expression of Wt LT

The cDNA sequence encoding wt LT was cloned into a retroviral expression vector conferring blasticidin resistance, pWZLBlastε (**Figure 3.2A**). A β-galactosidase expressing construct, pWZLBlastε-LacZ, was similarly generated by subcloning the cDNA sequence encoding LacZ into the empty pWZLBlastε vector (**Figure 3.2B**). This construct served as a control vector that, unlike the empty vector itself, permitted stable expression of the blasticidin-resistance gene.

The resultant constructs, pWZLBlastε-wtLT and pWZLBlastε-LacZ, were used to generate recombinant retroviruses using a transient amphotropic retroviral packaging system, ϕ amphotropic; 10 μg of each construct was transfected into $5x10^5$ ϕ amphotropic cells using Fugene (Roche) and 48 hrs post-transfection, the retroviral supernatant was harvested.

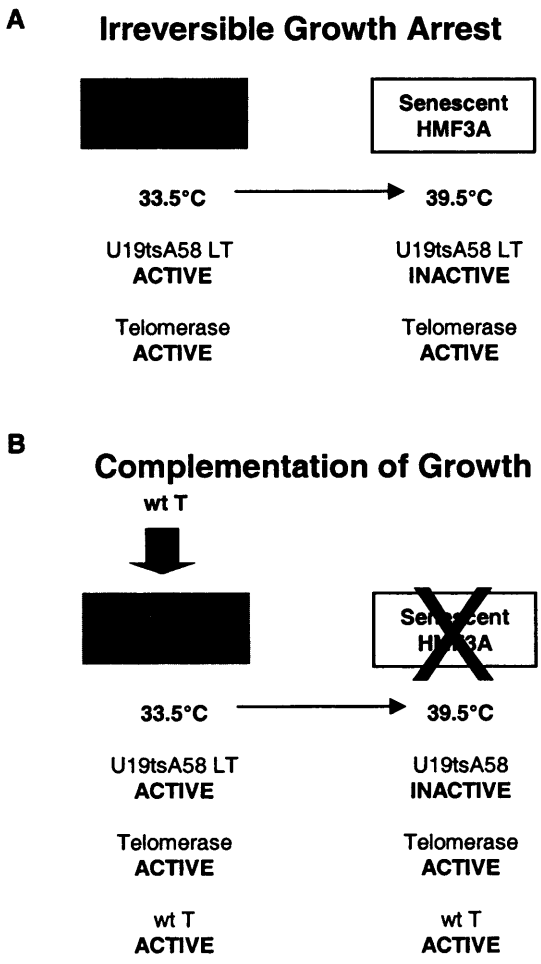

Figure 3.1: Model for Complementation of the Conditional HMF3A Growth Defect

A: HMF3A cells undergo an irreversible state of growth arrest when shifted from 33.5°C to 39.5°C within a period of 5-7 days [O'Hare *et al*, 2001]. The conditional growth of these cells is dependent upon the activity of a temperature-sensitive, DNA-binding mutant of LT (U19tsA58 LT); due to the thermolability of the temperature sensitive LT, the protein is functional at 33.5°C, but is inactivated upon shift to 39.5 °C; **B:** Reconstitution of wt LT activity was hypothesised to be sufficient to complement the conditional growth defect of HMF3A cells.

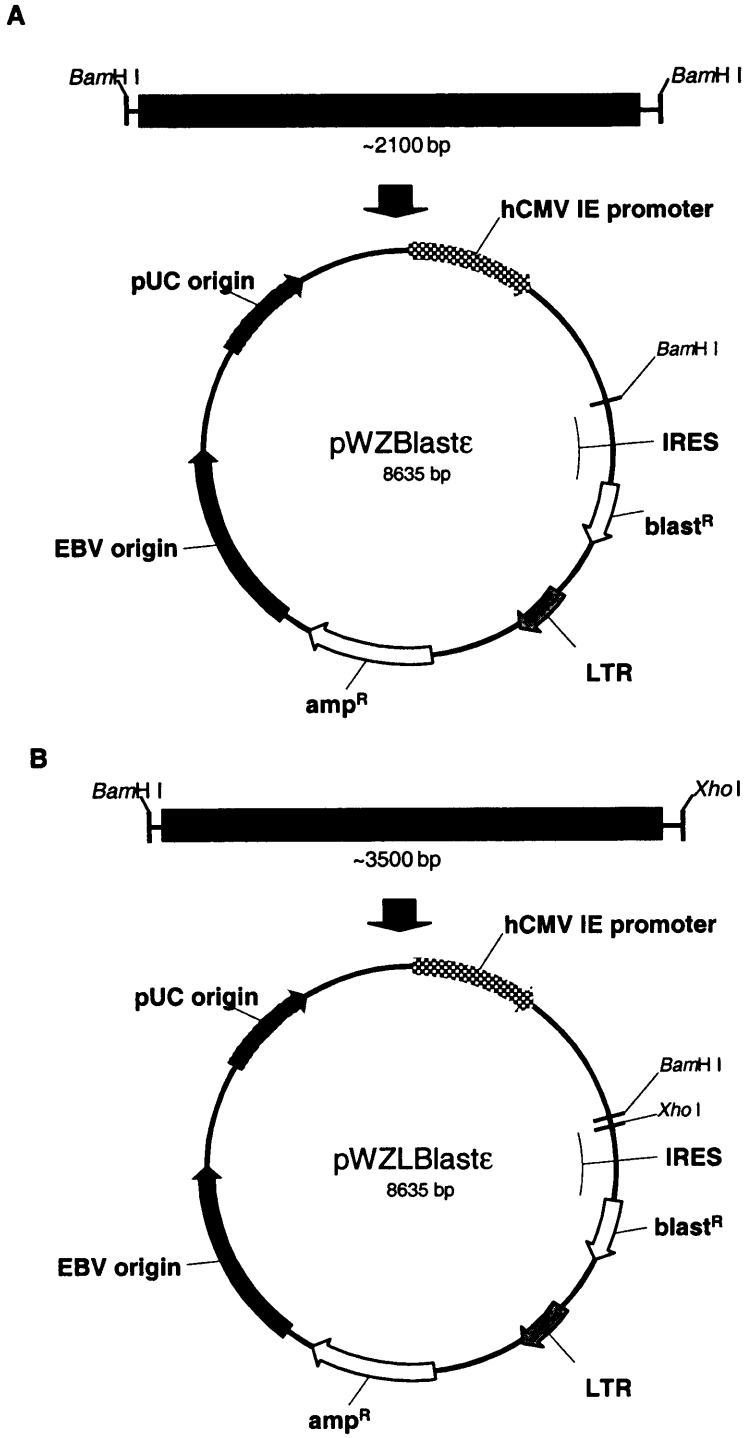

Figure 3.2: Construction of pWZLBlastε Retroviral Expression Constructs

A: Wt *LT* was sub-cloned from pBabepuro-wtLT into *Bam*H I digested pWZLBlastε as a *Bam*H I restriction fragment; **B:** *LacZ* was sub-cloned from pHRCMV-LacZ (gift from F. Savage) into *Bam*H I/*Xho* I digested pWZLBlastε as a *Bam*H I/*Xho* I restriction fragment. hCMV IE: human Cytomegalovirus Immediate Early promoter; IRES: Internal Ribosomal Entry Site; EBV: Epstein Barr Virus; amp^R: ampicillin resistance gene; $blast^R$: blasticidin resistance gene; LTR: Long Terminal Repeat.

The total viral harvest was then used to infect HMF3A cultures seeded at $5x10^5$ cells in duplicate T75 cm^2 flasks in the presence of 8 μg/ml polybrene. Following incubation at 33.5°C for 4 days, 5 μg/ml blasticidin was added to the culture medium and, after completion of 10 days of drug treatment, no viable cells remained in a non-infected culture, whereas blasticidin-resistant clones were observed in all infected HMF3A cultures. The resultant drug-resistant clones were incubated at 33.5°C in the presence of blasticidin for a further 7 days before they were trypsinised, pooled and replated as polyclonal cultures. Each culture was then expanded and used to seed duplicate cultures at $1x10^6$ cells per T75 cm^2 flask. One duplicate culture was then maintained at 33.5°C whereas selection was removed from the second duplicate culture, then shifted to 39.5°C for a further 7 days before RNA was extracted.

Semi-quantitative RT-PCR, using primers specific to the exogenous pWZL-derived wt *LT* transcript (WZL[F] and CMV LT3'), were used to analyse wt *LT* expression in these cultures. A PCR product of approximately 300 bp that corresponded to wt *LT* was generated from RNA derived from wt LT-infected HMF3A cells incubated at both 33.5°C (**Figure 3.3A**, lane 3) and 39.5°C for 7 days (**Figure 3.3A**, lane 4), but not from RNA derived from LacZ-infected HMF3A cells (**Figure 3.3A**, lanes 1 and 2, respectively). Semi-quantitative RT-PCR, using primers specific to *GAPDH* (GPDS and GPDA), was also performed as an internal control for experimental error since the level of *GAPDH* mRNA appeared to be unaltered upon the temperature shift. An 863 bp PCR product that corresponded to *GAPDH* was generated from all RNA samples analysed and exhibited approximately equal intensities under all conditions. This indicated that wt *LT* was stably expressed at both 33.5°C and 39.5°C in wt LT-infected HMF3A cultures, but not in LacZ-infected HMF3A cultures. However, the wt LT-infected HMF3A cells did not appear to be complemented for growth under non-permissive conditions as the culture did not expand when it was incubated at 39.5°C for 7 days, similar to the LacZ–infected culture (data not shown).

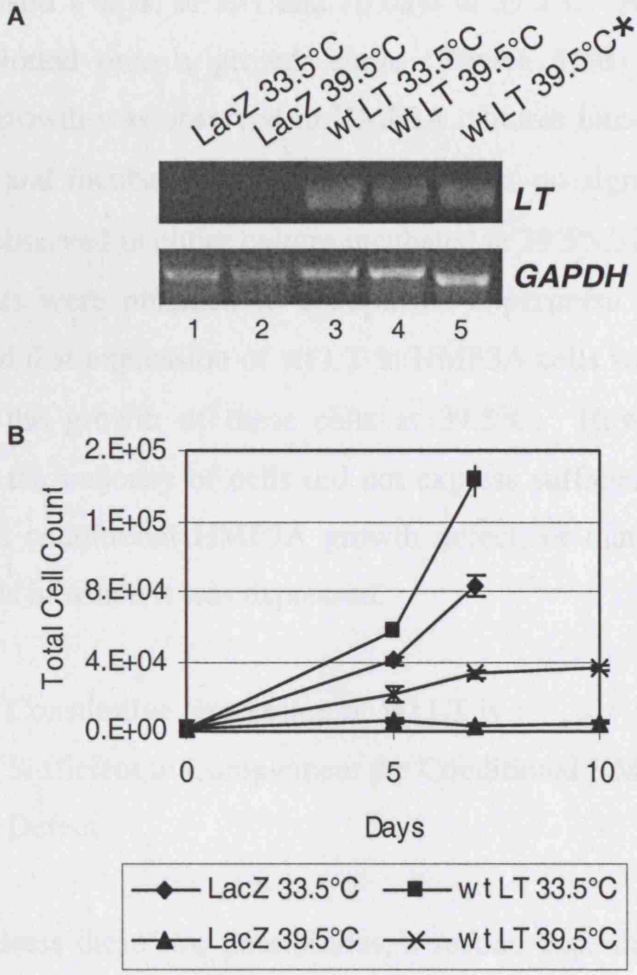

Figure 3.3: Growth Complementation in the HMF3A System

A: RT-PCR using wt LT-specific primers was used to analyse *wt LT* expression in HMF3A cells incubated at both 33.5°C and at 39.5°C for 7 days, in addition to HMF3A cells directly complemented for growth at 39.5°C by infection with wt LT (indicated by an asterisk). *GAPDH* was the loading control; **B:** Growth analysis of HMF3A cells that expressed either LacZ or wt LT. Cultures were incubated at 33.5°C for 7 days or 39.5°C for 10 days.

To verify this observation, LacZ- and wt LT- infected HMF3A cultures were seeded at 2000 cells in duplicate T25 cm^2 flasks and grown at either 33.5°C for 5 and 7 days, or 5, 7 and 10 days at 39.5°C. Average cell counts were then plotted onto a growth curve (**Figure 3.3B**) and, as a result, exponential growth was observed in HMF3A cultures infected with either wt LT or LacZ and incubated at 33.5°C. However, no significant increase in growth was observed in either culture incubated at 39.5°C, even after 10 days. Similar results were obtained in a duplicate experiment (data not shown). This indicated that expression of wt LT in HMF3A cells was not sufficient to complement the growth of these cells at 39.5°C. However, it was also possible that the majority of cells did not express sufficient wt T antigen to overcome the conditional HMF3A growth defect, or that wt LT could not rescue all cells in which it was expressed.

3.2.1.2 Constitutive Expression of Wt LT is Sufficient to Complement the Conditional HMF3A Growth Defect

To address these two possibilities, a second experimental approach to complement the conditional HMF3A growth arrest was investigated. This approach took advantage of the potent growth selection pressure that was exerted upon the HMF3A cells as they underwent an irreversible growth arrest. 10 μg of pWZLBlastε-wt LT and pWZLBlastε-LacZ retroviral expression constructs were packaged, using the ϕ amphotropic system, and the transiently produced virus was used to infect HMF3A cultures seeded at $5x10^5$ cells in duplicate T75 cm^2 flasks in the presence of 8 μg/ml polybrene. Following incubation of the cells at 33.5°C for 4 days, 5 μg/ml blasticidin was added to the culture medium and, after completion of 10 days of drug treatment, no viable cells remained in a non-infected culture, whereas blasticidin-resistant clones were observed in all infected HMF3A cultures.

Blasticidin was removed from the culture medium and drug-resistant clones were directly shifted to 39.5°C. Cultures were then incubated at 39.5°C for a further 14 days before examining for growth complementation activity. Significantly, multiple healthy, growing colonies were observed in the wt LT-infected HMF3A culture, yet no outgrowing colonies were observed in the LacZ-infected HMF3A culture. The wt LT-infected culture was trypsinised, replated and expanded under these conditions, then sub-cultivated for a minimum of 4 further passages, using a 1:5 split, to ensure that it could be continually propagated under these conditions. Having achieved this, the culture was considered complemented for growth. The same results were obtained in a duplicate experiment.

To confirm this observation, wt *LT* expression was analysed in the growth-complemented HMF3A culture, using semi-quantitative RT-PCR. Primers specific to the exogenous pWZL-derived wt *LT* transcript were used (WZL[F] and CMV-LT3') and a PCR product of approximately 300 bp, the same as that obtained from temperature-shifted wt LT-infected HMF3A cells, was generated from RNA extracted from growth complemented HMF3A cells (**Figure 3.3A**, lane 5). Interestingly, the intensity of the PCR product was not significantly different to that obtained by semi-quantitative RT-PCR of irreversibly arrested wt LT-infected HMF3A cells (**Figure 3.3A**, lane 4).

The findings from these experiments suggested that two different methods could be used to perform growth complementation analysis in the HMF3A system. In the first method, drug-resistant clones could be isolated at 33.5°C, pooled as a polyclonal population, then shifted to 39.5°C for a period of 7 days. In the second method, drug-resistant clones could be directly incubated at 39.5°C and assessed for their ability to grow under these conditions. The latter approach represented an unambiguous method with which to assess the growth complementation properties of exogenously expressed genes in the HMF3A system, whereas the former represented a less stringent procedure. However, the generation of polyclonal cell populations at

33.5°C had an inherent advantage in that it permitted the subsequent analysis of cultures incubated at 39.5°C when growth complementation did not occur.

3.2.2 Application of the HMF3A Complementation Assay

Having demonstrated that constitutive expression of wt LT was sufficient to complement the growth of HMF3A cells at 39.5°C, the possibility was raised that the HMF3A system could be used to dissect the signalling pathways critical for maintaining these cells in a growth competent-state under non-permissive conditions and to elucidate the genes required for this activity.

Previous studies using DNA tumour viruses indicated that pRb co-operated with p53 during senescence [Shay *et al*, 1991], however, it was not known whether these pathways functioned alone, in combination, or independently. Therefore, constitutive expression of a panel of LT mutants in the HMF3A system in the form of a complementation assay represented a suitable experimental regimen to address this issue.

The expression of LT mutants in the HMF3A system was complicated, however, by the fact that U19tsA58 LT was constitutively expressed in these cells and was readily detectable in its non-functional conformation under non-permissive conditions, as shown by Western blot analysis (data not shown). Consequently, the ability to detect expression of LT mutants in the HMF3A system at 39.5°C was obscured by the presence of U19tsA58 LT. This made it difficult to determine whether the inability of any given LT antigen mutant to complement the growth of HMF3A cells was due to the lack of physiological activity, or rather, the lack of stable expression. Therefore, alternative mechanisms to abrogate the pRb and p53 pathways were investigated.

3.2.3 *Development and Refinement of the HMF3A Complementation Assay*

Before utilising the HMF3A system for complementation analysis, an important refinement was made to the model system.

Retroviral transduction of HMF3A cells, like other human cells, necessitates the use of amphotropic retroviral packaging systems such as ϕ Amphotropic or LinX. However, transient packaging systems such as these are relatively inefficient with respect to their transduction efficiency; for example, retroviral titres ranging from between 1-10 colony forming units (cfu) per ml of retroviral supernatant for every 10 μg DNA packaged have been observed (unpublished observations). In contrast, ecotropic retroviruses, whose host range is restricted to murine or rat cell types, exhibit much greater transduction efficiency (unpublished observations). Therefore, it was hypothesised that engineering the HMF3A cells to become infectable with ecotropic retrovirues would increase their transduction efficiency. A second, more important aspect, was that ecotropic viruses would be safer to work with as they would not require the higher levels of containment needed for working with amphotropic viruses. This was due to the fact that ecotropic viruses, unlike amphotropic viruses, are unable to infect human cells.

3.2.3.1 Constitutive Expression of Eco^R

Human cells have previously been engineered to express the murine ecotropic receptor to enable them to become infected with ecotropic viruses (for example, [Berns *et al*, 2004]); therefore, the murine ecotropic receptor (Eco^R) utilised by Berns and colleagues (gift from J. Downward) was introduced into the HMF3A system. The Eco^R cDNA sequence was cloned into the pWZLBlastε vector (**Figure 3.4**).

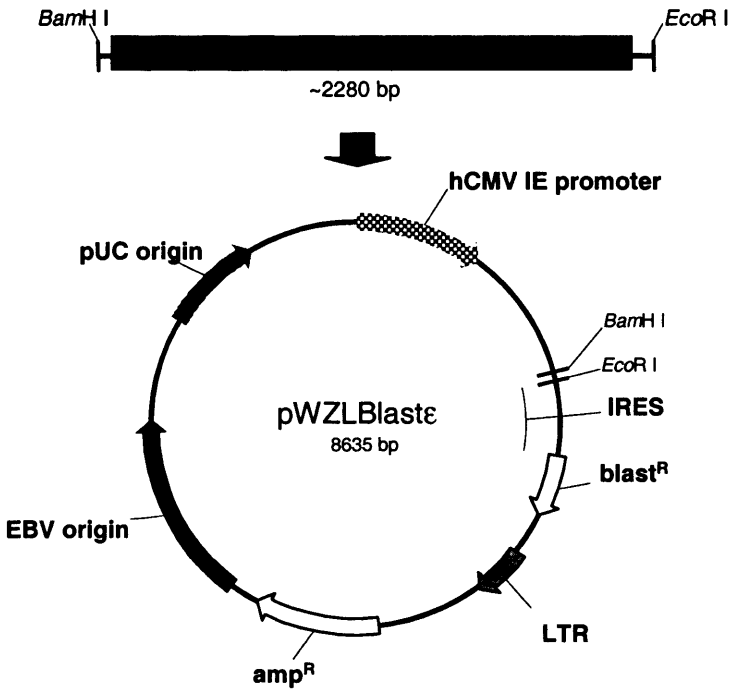

Figure 3.4: Construction of pWZLBlastε-Eco^R

Eco^R cDNA encoding the ORF of the murine ecotropic receptor was sub-cloned from pWZLneo-Eco^R into *Bam*H I/*Eco*R I digested pWZLBlastε as a *Bam*H I/*Eco*R I restriction fragment. hCMV IE: human Cytomegalovirus Immediate Early promoter; IRES: Internal Ribosomal Entry Site; EBV: Epstein Barr Virus; amp^R: ampicillin resistance gene; blast^R: blasticidin resistance gene; LTR: Long Terminal Repeat

10 μg of the resultant plasmid, pWZLBlastε-Eco^R, was packaged using the ϕ amphotropic system and used to infect HMF3A cultures seeded at 1x10^6 cells in duplicate T180 cm^2 flasks in the presence of 8 μg/ml polybrene. Following incubation at 33.5°C for 4 days, 5 μg/ml blasticidin was added to the culture medium and, after completion of 10 days of drug treatment, no viable cells remained in a non-infected culture, whereas blasticidin-resistant clones were observed in all infected HMF3A cultures. Drug-resistant clones were incubated at 33.5°C in the presence of blasticidin for a further 14 days before they were trypsinised, pooled and replated as polyclonal cultures.

All further experimental analyses described in this project utilised HMF3A cells engineered in this way (referred to as HMF3AEco^R cells), except where indicated. Stable expression of the ecotropic receptor was demonstrated by the generation of puromycin-resistant clones following infection of HMF3AEco^R cells with ecotropic retroviruses conferring puromycin drug resistance (see below).

It was imperative to demonstrate that the conditional growth phenotype of HMF3AEco^R cells was not compromised and, as it will be shown below, HMF3AEco^R cells retained the ability to enter into an irreversible growth arrest when incubated at 39.5°C for 7 days, similar to the parental HMF3A cell line. Furthermore, retroviral titres within the magnitude of 1x10^3 to 1x10^4 cfu/ml viral supernatant were observed as a result of this manipulation. This made it possible to simultaneously analyse many clonal expansion events in a heterogeneous population. Moreover, this provided greater confidence that the growth complementation observed in the HMF3A system was representative of a real phenomenon.

3.2.4 Abrogation of the P53 Pathway

To inactivate the p53 pathway, two different reagents were used; namely GSE p53 and p53 shRNA. GSE p53 is a dominant-negative peptide of p53 that was originally identified in a GSE screen. It corresponds to a

region in the oligomerisation domain of p53 (amino acids 273-368 in rat; **Figure 3.5A**; [Ossovskaya *et al*, 1996]) and functions as a dominant-negative peptide of p53 by promoting the accumulation of endogenous p53 protein into a functionally inactive form. However, the high level of sequence conservation exhibited in the oligomerisation domain between p53 and the p53 family members p63 and p73 (reviewed in [Levrero *et al*, 2000]), suggests that GSE p53 probably interacts with all three members of the p53 family. Therefore, RNAi represented a second, more specific method to abrogate p53 activity (**Figure 3.5B**).

3.2.4.1 Knockdown of P53 by ShRNA is Sufficient to Complement the Conditional HMF3A Growth Defect

The conditions for the HMF3A complementation assay were first refined using p53 RNAi. A p53 shRNA construct, pRetroSuper-p53, had previously been shown to efficiently knockdown p53 in HDFs [Berns *et al*, 2004]. Therefore, the same shRNA construct was reconstructed by cloning the p53 RNAi target sequence (depicted in **Figure 3.5B**) into the pRetroSuper retroviral expression vector, using the protocol described by Oligoengine. 10 μg of pRetroSuper-p53 and the empty pRetroSuper vector were then packaged, using the ϕ ecotropic system. 5% of the total retroviral supernatant harvest was used to infect HMF3AEco^R cultures seeded at $5x10^5$ cells in duplicate T75 cm^2 flasks in the presences of 8 μg/ml polybrene. Following incubation at 33.5°C for 4 days, 2 μg/ml puromycin was added to the culture medium and, after completion of 4 days of drug treatment, no viable cells remained in a non-infected culture, whereas multiple puromycin-resistant clones were observed in all infected cultures. One duplicate culture was then maintained under drug selection at the permissive temperature for a further 7 days before fixing and staining with 2% (w/v) methylene blue.

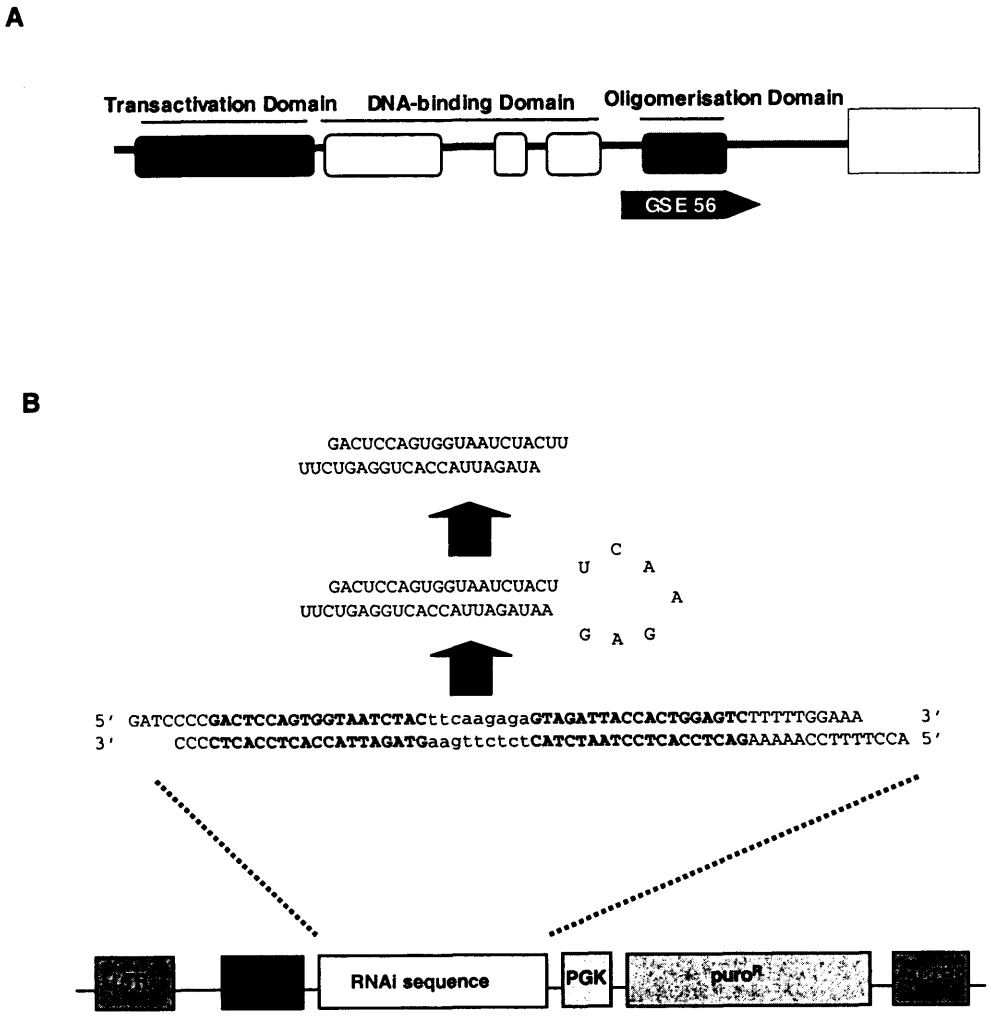

Figure 3.5: Abrogation of P53 Activity

A: Schematic diagram of the p53 protein to indicate the region of p53 that corresponds to the GSE p53 peptide; **B:** Schematic representation of shRNA-targetting of p53 by RNAi. In this method, a shRNA expression cassette is integrated into the HMF3A genome by retroviral infection. Consequently, the RNAi sequence is transcribed by RNA polymerase III into a shRNA that is then processed into a short double-stranded RNA species. This leads to the targetted degradation of endogenous *p53* mRNA. LTR: Long Terminal Repeat; ΔLTR: deleted Long Terminal Repeat; H1: H1 RNA Polymerase III promoter; puro^R: puromycin resistance gene; PGK: PGK promoter.

Selection was removed from the second duplicate culture, then shifted to 39.5°C for a further 14 days before fixing and staining with 2% (w/v) methylene blue (see **Figure 3.6A** for schematic representation of the experimental procedure).

The total number of colonies in the cultures incubated at 39.5°C for 7 days was approximately equal (between 10^3 to 10^4; **Figure 3.6B**). This indicated that the infectability of the retroviruses generated by transfection of pRetroSuper and pRetroSuper-p53 was comparable. However, whereas multiple colonies could be observed in the p53 shRNA-infected culture incubated at 39.5°C for 7 days, no outgrowing colonies could be observed in the control-infected culture incubated under the same conditions. This indicated that down-regulation of p53 by RNAi was sufficient to complement the growth of these cells under non-permissive conditions. It was also important to note the stringency of the conditional growth arrest; despite the increased efficiency of HMF3AEco^R retroviral transduction using the ϕ ecotropic system (within a magnitude of between 100- to 1000-fold relative to the original experimental regimen that utilised HMF3A cells and the ϕ amphotropic packaging system), little/no background reversion events were observed in the control culture incubated at 39.5°C. The same results were obtained in a duplicate experiment.

3.2.4.2 Abrogation of P53 is Sufficient to Complement the Conditional HMF3A Growth Defect

The growth complementation activity of shRNA p53 was then compared to GSE p53. 10 μg of pRetroSuper, pRetroSuper-p53, pLPCX and pLPC-GSEp53 retroviral expression constructs were packaged, using the ϕ amphotropic system and the transiently produced virus was used to infect HMF3A cultures seeded at $5x10^5$ cells in duplicate T75 cm^2 flasks in the presence of 8 μg/ml polybrene.

A

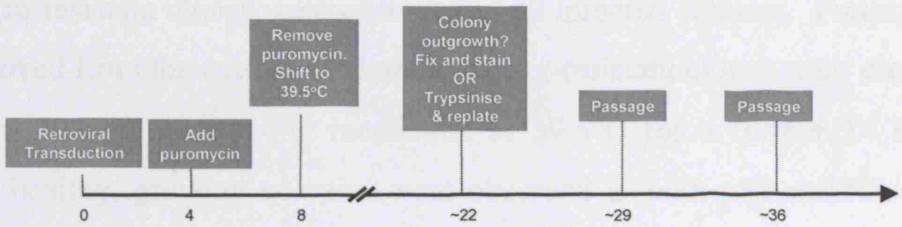

B

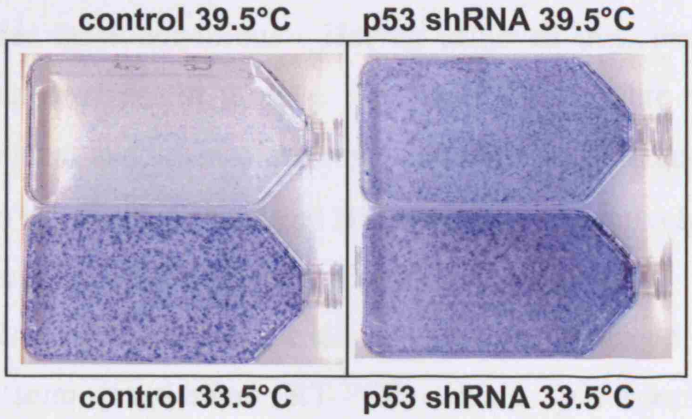

Figure 3.6: HMF3A Growth Complementation Assay

A: Schematic representation of the timescale of the HMF3A growth complementation assay utilising retroviral expression constructs confering puromycin resistance; **B:** Images of cultures analysed by the HMF3A complementation assay. To visualise outgrowing colonies, cultures were fixed and stained with 2% (w/v) methylene blue.

Following incubation at 33.5°C for 4 days, 2 μg/ml puromycin was added to the culture medium and after completion of 4 days of drug treatment, no viable cells remained in a non-infected culture, whereas multiple puromycin-resistant clones were observed in all infected cultures. Puromycin was removed from the culture medium and drug-resistant clones were directly shifted to 39.5°C. Following incubation at 39.5°C for a further 14 days, multiple healthy, growing colonies were observed in both p53 shRNA- and p53 GSE- infected HMF3A cultures, but not control-infected HMF3A cultures. The former cultures were trypsinised, pooled and replated as polyclonal populations. The cultures were then sub-cultivated for a minimum of 4 further passages, using a 1:5 split, to ensure that they could be continually propagated under these conditions. Having achieved this, they were both considered complemented for growth. The same results were obtained in a duplicate experiment and when ϕ ecotropic cells and HMF3AEco^R cells were substituted for ϕ amphotropic cells and HMF3A cells, respectively.

To determine whether p53 activity was abrogated under these conditions, RNA extracted from each growth-complemented culture was analysed by semi-quantitative RT-PCR, using *p21*-specific primers (CKDN1A-F and CDKN1A-R). *P21* expression was analysed, rather than *p53* expression, since the direct transcriptional activation of *p21* by p53 represented a more accurate read-out of p53 activity [el-Deiry *et al*, 1994]. A significant increase in the intensity of a 402 bp PCR product that corresponded to *p21* was observed from RNA extracted from the puro-infected HMF3A culture incubated at 39.5°C for 7 days (**Figure 3.7A**, lane 2), relative to the puro-infected HMF3A culture incubated at 33.5°C (**Figure 3.7A**, lane 1). However, a significant reduction was observed in the intensity of the PCR product derived from HMF3A cells complemented for growth at 39.5°C by expression of either p53 shRNA (**Figure 3.7A**, lane 3) or GSE p53 (**Figure 3.7A**, lane 4).

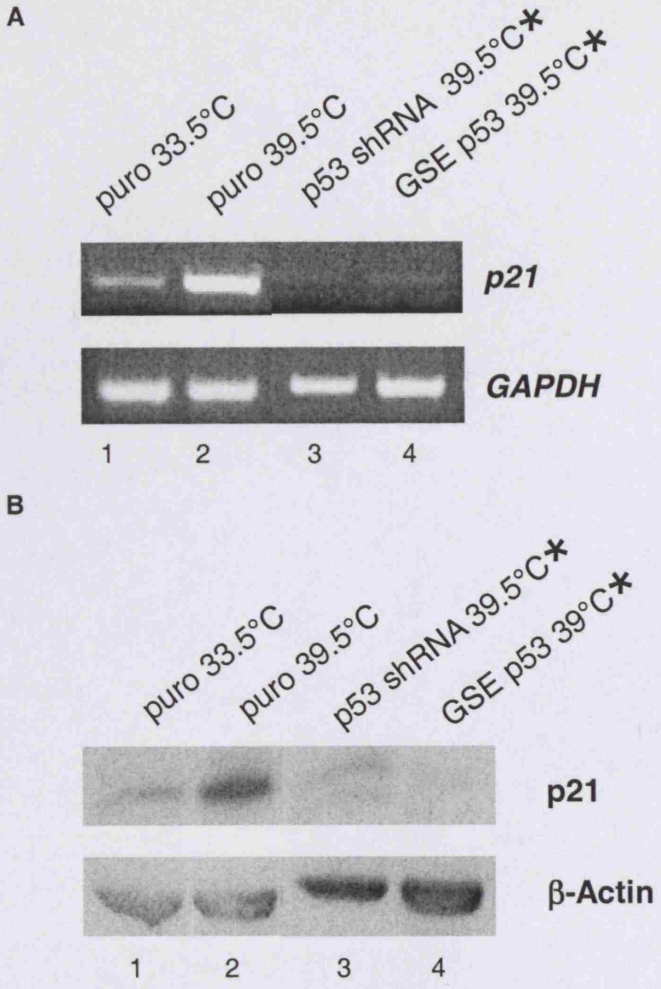

Figure 3.7: P53 Abrogation

A: Semi-quantitative RT-PCR using *p21*-specific primers was used to analyse p53 activity in HMF3A cultures incubated at both 33.5°C and at 39.5°C for 7 days, in addition to growth complemented HMF3A cells infected with either shRNA p53 or GSE p53 (indicated by an asterisk). *GAPDH* was the loading control; **B:** P21 Western blot analysis using sc-6246 p21 monoclonal antibody (Santa Cruz) for HMF3A cultures incubated at both 33.5°C and at 39.5°C for 7 days. β-Actin was the loading control.

Down-regulation of p21 was also analysed at the protein level. RIPA protein lysates were prepared from the same cultures, separated by 15% SDS-PAGE and analysed by Western blot, using sc6246 p21 monoclonal antibody (Santa Cruz). Similar to the semi-quantitative RT-PCR data, a significant increase in the intensity of a 21 kDa band that corresponded to p21 (as indicated in the literature [Yamamoto *et al*, 1998]) was observed in control-infected HMF3A cells grown at 39.5°C for 7 days (**Figure 3.7B**, lane 2), relative to control-infected HMF3A cells grown at 33.5°C (**Figure 3.7B**, lane 1). Conversely, a significant reduction was observed in the intensity of the 21 kDa band derived from growth complemented HMF3A cells infected with either the p53 shRNA construct (**Figure 3.7B**, lane 3), or GSE p53 (**Figure 3.7B**, lane 4), in comparison to puro-infected HMF3A cells at 39.5°C for 7 days (**Figure 3.7B**, lane 2). This indicated that p53 activity was abrogated in HMF3A cells that had bypassed the conditional growth defect.

3.2.5 Abrogation of the PRb Pathway

Similar to p53, abrogation of the pRb pathway is frequently observed in spontaneous human tumours, either by direct mutation of pRb itself, or by mutation of an upstream regulator (reviewed in [Hahn and Weinberg, 2002; Nevins, 2001; Ortega *et al*, 2002; Sellers and Kaelin, 1997; Sherr, 1996]). However, targetting pRb for inactivation is complicated by the problem of functional redundancy resulting from both the multiplicity of both Rb family members and potential pRb-binding partners. The viral oncoproteins adenovirus type 5 E1A and HPV type 16 E7 represent two reagents commonly used to inactivate this pathway, therefore, ectopic expression of E1A and E7 in the HMF3A system was investigated.

3.2.5.1 Constitutive Expression of Adenovirus Type 5 E1A

E1A functionally inactivates the pRb pathway by virtue of an LxCxE-binding motif that, similar to LT, confers the ability to bind to and inactivate the Rb family members (**Figure 3.8A**). An E1A retroviral expression construct, pLPC-12SE1AORI (gift from S. Lowe), was introduced into the HMF3A system and assessed for its ability to complement the conditional growth defect of these cells.

10 μg of pLPCX-12SE1AORI and pLPCX retroviral expression constructs were introduced into HMF3A cells and used to generated polyclonal populations at 33.5°C, using the protocol described for pRetroSuper-p53 and pLPC-GSEp53. One duplicate culture was then maintained under drug selection at 33.5°C, whereas selection was removed from the second duplicate culture, then shifted to 39.5°C for a further 7 days before RNA was extracted.

Semi-quantitative RT-PCR, using primers specific to *E1A* (E1A-F and E1A-R), was used to analyse *E1A* expression in these cultures. As a result, a 492 bp PCR product that corresponded to *E1A* was generated from RNA derived from E1A-infected HMF3A cells incubated at both 33.5°C (**Figure 3.8B**, lane 1) and 39.5°C for 7 days (**Figure 3.8B**, lane 2), but not from RNA extracted from puro-infected HMF3A cultures incubated at either 33.5°C (**Figure 3.8B**, lane 4) or 39.5°C for 7 days (**Figure 3.8B**, lane 5). This finding provided good evidence that *E1A* was stably expressed in E1A-infected HMF3A cultures under both permissive and non-permissive conditions.

E1A expression was also analysed at the protein level. RIPA protein lysates were derived from the same cultures, separated by 12% SDS-PAGE and analysed by Western blot using M73 monoclonal E1A antibody.

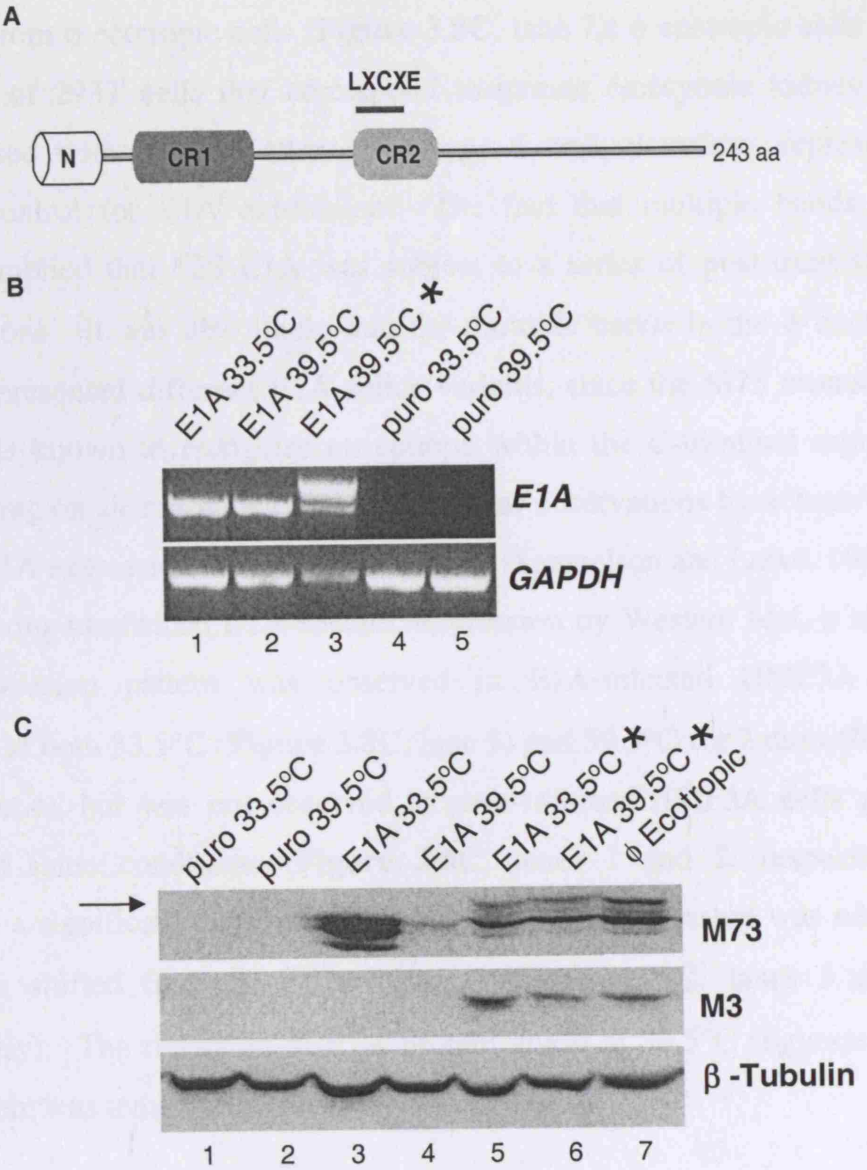

Figure 3.8: Adenovirus Type 5 E1A Expression

A: Schematic diagram of adenovirus type 5 E1A protein. N: N-terminal domain; CR1: Conserved Region 1; CR2: Conserved Region 2; LxCxE: Rb family binding motif; **B:** Semi-quantitative RT-PCR using *E1A*-specific primers was used to analyse E1A expression in HMF3A cultures incubated at both 33.5°C and at 39.5°C for 7 days, in addition to growth complemented HMF3A cells infected with E1A (indicated by an asterisk). *GAPDH* was the loading control; **C:** E1A Western blot analysis using M73 and M3 monoclonal antibodies, respectively, for HMF3A cultures incubated at both 33.5°C and at 39.5°C for 7 days, in addition to growth complemented HMF3A cells infected with E1A (indicated by an asterisk). ϕ ecotropic cell protein lysate was the positive control for E1A expression and β-Tubulin was the loading control.

A series of bands of approximately 45 kDa were observed from lysates prepared from ϕ ecotropic cells (**Figure 3.8C**, lane 7); ϕ ecotropic cells are a derivative of 293T cells that correspond to human embryonic kidney cells immortalised with sheared adenovirus type 5 and, therefore, represent a positive control for E1A expression. The fact that multiple bands were detected implied that 12S E1A was subject to a series of post-translational modifications. It was also likely that the multiple bands in the ϕ ecotropic sample represented different E1A splice variants, since the M73 monoclonal antibody is known to recognise an epitope within the C-terminal region of exon 2, a region shared with 13S E1A. Similar observations have been made in other E1A expression studies (for example, [Samuelson and Lowe, 1997]).

Having confirmed E1A-specific expression by Western blot, a similar E1A expression pattern was observed in E1A-infected HMF3A cells incubated at both 33.5°C (**Figure 3.8C**, lane 3) and 39.5°C for 7 days (**Figure 3.8C**, lane 4), but was not observed in puro-infected HMF3A cells grown under the same conditions (**Figure 3.8C**, lanes 1 and 2, respectively). However, a significant decrease in the level of E1A expression was noted in E1A cells shifted from 33.5°C to 39.5°C (**Figure 3.8C**, lanes 3 and 4, respectively). The reduction in E1A protein levels at 39.5°C suggested that E1A protein was temperature sensitive.

3.2.5.2 Constitutive Expression of Adenovirus Type 5 E1A is Sufficient to Complement the Conditional HMF3A Growth Defect

Despite the fact that E1A appeared to exhibit temperature sensitivity at 39.5°C, the fact that it remained detectable under these conditions signified that E1A could be tested in the HMF3A complementation assay. 10 μg of pLPC-12SE1AORI and pLPCX retroviral expression constructs were introduced into HMF3A cells and used to isolate puromycin-resistant clones, using the protocol described for pRetroSuper-p53 and pLPC-GSEp53.

Following incubation of puromycin-resistant clones at 39.5°C for 14 days, multiple healthy, growing colonies were observed in the E1A-infected HMF3A culture, but not the control-infected HMF3A culture. The former culture was trypsinised, pooled and replated as a polyclonal population, then sub-cultivated for a minimum of 4 further passages, using a 1:5 split, to ensure that it could be continually propagated under these conditions. Having achieved this, the culture was considered to be complemented for growth. The same result was obtained in a duplicate experiment and when ϕ ecotropic cells and HMF3AEco^R cells were substituted for ϕ amphotropic cells and HMF3A cells, respectively.

E1A expression was analysed in the growth complemented HMF3A culture, using semi-quantitative RT-PCR. Primers specific to *E1A* were used, as before, and, as a result, a 492 bp PCR product that corresponded to 12S *E1A* was generated from RNA extracted from growth complemented HMF3A cells (**Figure 3.8B**, lane 3), similar to that obtained from temperature-shifted E1A-infected HMF3A cells. This indicated that *E1A* was stably expressed in the growth-complemented HMF3A cells.

To further support this finding, E1A expression was also investigated at the protein level. RIPA protein lysates extracted from the same growth-complemented culture were analysed by Western blot, using M73 monoclonal E1A antibody. As a result, multiple bands of approximately 45 kDa that corresponded to E1A were again observed (**Figure 3.8C**, lane 6), indicating that, similar to the semi-quantitative RT-PCR data, E1A expression was also stable at the protein level.

The disparity of *E1A*-specific band sizes observed between temperature shifted E1A-infected HMF3A cultures and growth complemented E1A-infected cultures by RT-PCR will be discussed further in **Chapter 5**.

3.2.5.3 Constitutive Expression of HPV Type 16 E7

E7, like LT and E1A, possesses an LxCxE- binding motif that functionally inactivates Rb family members (**Figure 3.9A**). Therefore, an E7 retroviral expression construct, pBabepuro-E7 (gift from K. Munger), was introduced into the HMF3A system and assessed for its ability to complement the conditional growth defect of these cells.

10 μg of pBabepuro-E7 and pBabepuro retroviral expression constructs were introduced into HMF3A cells and used to generated polyclonal populations at 33.5°C, using the protocol described for pRetroSuper-p53 and pLPC-GSEp53. One duplicate culture was then maintained under drug selection at 33.5°C, whereas selection was removed from the second duplicate culture, then shifted to 39.5°C for a further 7 days before RNA was extracted.

Semi-quantitative RT-PCR, using primers specific to *E7* (E7-F and E7-R), was used to analyse *E7* expression in these cultures. As a result, a 203 bp PCR product that corresponded to *E7* was generated from RNA derived from E7-infected HMF3A cells incubated at both 33.5°C (**Figure 3.9B**, lane 3) and 39.5°C for 7 days (**Figure 3.9B**, lane 4), but not from RNA derived from puro-infected HMF3A cultures incubated at either 33.5°C (**Figure 3.9B**, lane 1) or at 39.5°C (**Figure 3.9B**, lane 2). This indicated that *E7* was stably expressed in E7-infected HMF3A cultures under both permissive and non-permissive conditions.

E7 expression was also analysed at the protein level. RIPA protein lysates prepared from the same cultures were separated by 15% SDS-PAGE and analysed by Western blot, using a mixture of 8C9 and ED17 E7 antibodies (Zymed and Upstate, respectively). As a positive control, lysates from CaSki, SiHa and RKO7.6 cells were used (gifts from K. Munger).

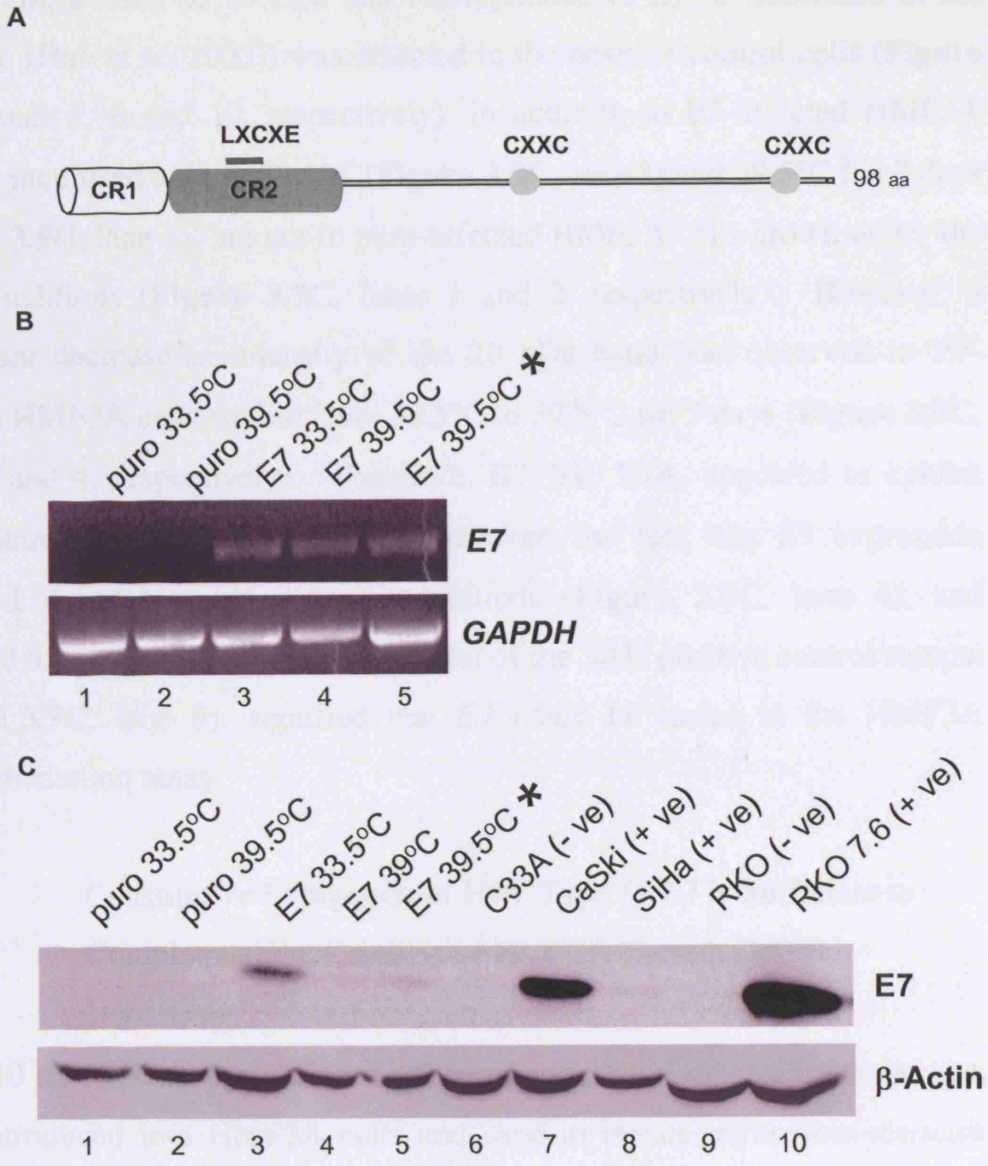

Figure 3.9: HPV Type 16 E7 Expression

A: Schematic diagram of HPV type 16 E7 protein. CR1: Conserved Region 1; CR2: Conserved Region 2; CXXC: zinc finger binding motif; LxCxE: Rb family binding motif; **B:** Semi-quantitative RT-PCR using *E7*-specific primers was used to analyse *E7* expression in HMF3A cultures incubated at both 33.5°C and at 39.5°C for 7 days, in addition to growth complemented HMF3A cells infected with E7 (indicated by an asterisk). *GAPDH* was the loading control; **C:** Western blot analysis of E7 using a mixture of 8C9 and ED17 E7 antibodies for HMF3A cultures incubated at both 33.5°C and at 39.5°C for 7 days, in addition to growth complemented HMF3A cells infected with E7 (indicated by an asterisk). CaSki, SiHa and RKO (+ ve) protein lysates (gift from K. Munger) were positive controls for E7 expression and β-Actin was the loading control.

As a result, a band of 18 kDa that corresponded to E7 (as indicated in the literature [Huh *et al*, 2005]) was detected in the positive control cells (**Figure 3.9C**, lanes 7, 8 and 10, respectively), in addition to E7-infected HMF3A samples incubated at both 33.5°C (**Figure 3.9C**, lane 3) and 39.5°C for 7 days (**Figure 3.9C**, lane 4), but not in puro-infected HMF3A cells grown under the same conditions (**Figure 3.9C**, lanes 1 and 2, respectively). However, a significant decrease in intensity of the 20 kDa band was observed in E7-infected HMF3A cells shifted from 33.5°C to 39.5°C for 7 days (**Figure 3.9C**, lanes 3 and 4, respectively). Therefore, E7, like E1A, appeared to exhibit temperature sensitivity at 39.5°C. However, the fact that E7 expression remained detectable under these conditions (**Figure 3.9C**, lane 4), and appeared to be of a similar intensity to that of the SiHa positive control sample (**Figure 3.9C**, lane 8), signified that E7 could be tested in the HMF3A complementation assay.

3.2.5.4 Constitutive Expression of HPV Type 16 E7 is Sufficient to Complement the Conditional HMF3A Growth Defect

10 μg of pBabepuro-E7 and pBabepuro retroviral expression constructs were introduced into HMF3A cells and used to isolate puromycin-resistant clones, using the protocol described for pRetroSuper-p53 and pLPC-GSEp53. Following incubation of the drug-resistant clones at 39.5°C for 14 days, multiple healthy, growing colonies were observed in the E7-infected HMF3A culture, but not the puro-infected HMF3A culture. The former culture was trypsinised, pooled and replated as a polyclonal population then sub-cultivated for a minimum of 4 further passages, using a 1:5 split, to ensure that it could be continually propagated under these conditions. Having achieved this, the culture was considered growth complemented. The same result was obtained in a duplicate experiment and when ϕ ecotropic cells and HMF3AEco^R cells were substituted for ϕ amphotropic cells and HMF3A cells, respectively.

Ecotopic *E7* expression was analysed in the growth complemented HMF3A cultures, using semi-quantitative RT-PCR. Primers specific to *E7* were used, as before, and, as a result, a 203 bp PCR product that corresponded to *E7* was generated from RNA derived from the growth complemented culture, similar to temperature-shifted E7-infected HMF3A cells (**Figure 3.9B**, lane 5).

Having demonstrated stable *E7* expression in growth complemented HMF3A cells at the RNA level, E7 expression was also investigated at the protein level. RIPA protein lysates were extracted from growth complemented cells then analysed by Western blot, using a mixture of 8C9 and ED17 E7 antibodies (Zymed and Upstate), as before. A weak band of approximately 20 kDa that corresponded to E7 was observed (**Figure 3.9C**, lane 6). This indicated that, similar to the semi-quantitative RT-PCR data, E7 expression was also stable at the protein level and was sufficient for growth complementation.

These findings indicated that constitutive expression of either E1A or E7 was sufficient to overcome the HMF3A conditional growth arrest at 39.5°C. By extension therefore, abrogation of the pRb pathway was sufficient to complement the HMF3A conditional growth defect. However, it was not possible to specifically attribute this activity to the inactivation of pRb, since both E1A and E7 could have utilised their multifunctional activity to abrogate multiple cellular pathways, in addition to the pRb pathway, to bypass this process.

3.2.5.5 Mutational Analysis of E7 Mutants

In an attempt to address this issue, a series of E7 mutants were obtained for analysis in the HMF3A complementation assay (gift from K. Muger). However, none of the mutants were able to complement the conditional HMF3A growth arrest (data not shown). Moreover, it was technically difficult to achieve high levels of E7 expression in the HMF3A system and

this was attributed to its short half-life [Reinstein *et al*, 2000]. Therefore, it was not possible to use the E7 mutants to delineate the key E7 functional activities required for growth complementation.

3.2.5.6 Constitutive Expression of a $P16^{INK4a}$-Insensitive Cyclin D1-$CDK4^{R24C}$ Fusion Construct (DK)

Since E7 mutants were unable to be utilised in the HMF3A system, an alternative method to specifically inactivate the pRb pathway was sought.

A $p16^{INK4a}$-insensitive cyclin D1-$CDK4^{R24C}$ fusion construct (DK) represented a reagent that has been utilised in a number of studies to specifically address this issue [Konstantinidis *et al*, 1998; Rao *et al*, 1999; Wei *et al*, 2003]. The R24C point mutation of CDK4 was originally identified in melanomas and renders CDK4 refractory to the two major negative regulators of CDK4, namely $p16^{INK4a}$ and $p15^{INK4b}$ [Wolfel *et al*, 1995]. Consequently, the R24C mutant of CDK4 has been utilised in numerous studies to constitutively phosphorylate pRb and mimic $p16^{INK4a}$ inactivation (for example, [Michaloglou *et al*, 2005]). However, the ability to coordinately express cyclin D1 and $CDK4^{R24C}$ as a fusion construct, namely DK, was considered advantageous as it permitted equal expression of the two components that function together to phosphorylate Rb family members. Therefore, pBabepuro-DK (gift from J. Sedivy) was introduced into the HMF3A system and assessed for its ability to complement the conditional growth defect of these cells.

10 μg of pBabepuro-DK and pBabepuro retroviral expression constructs were introduced into HMF3A cells and used to generated polyclonal populations at 33.5°C, using the protocol described for pRetroSuper-p53 and pLPC-GSEp53. One duplicate culture was then maintained under drug selection at 33.5°C, whereas selection was removed from the second duplicate culture, then shifted to 39.5°C for a further 7 days before RIPA protein lysates were prepared.

RIPA protein lysates were separated by 8% SDS-PAGE and analysed by Western blot analysis using sc-8396 monoclonal cyclin D1 antibody (Santa Cruz). Unfortunately, no positive control was available for this analysis, however two bands of approximately 67 kDa that could have corresponded to the fusion construct (as indicated in the literature [Rao *et al*, 1999]) were identified in DK-infected HMF3A cells incubated at 39.5°C for 7 days (**Figure 3.10**, lane 4), but not in puro-infected HMF3A cells (**Figure 3.10**, lanes 1 and 2, respectively). The slower migrating band observed in the DK-infected HMF3A cells incubated at 39.5°C for 7 days was also observed in the DK-infected HMF3A cells incubated at 33.5°C (**Figure 3.10**, lane 3). Furthermore, a band of approximately the same size was detected with a CDK4 rabbit polyclonal antibody in a duplicate Western blot (sc-601; Santa Cruz; data not shown). Therefore, it was likely that this band represented the DK fusion protein (indicated by an arrow).

3.2.5.7 Constitutive Expression of DK is Insufficient to Complement the Conditional HMF3A Growth Defect

Having demonstrated stable expression of DK in the HMF3A system under both permissive and non-permissive conditions, DK was tested in the HMF3A complementation assay.

10 μg of pBabepuro-DK, pBabepuro, pRetroSuper-p53 and pRetroSuper constructs were introduced into HMF3A cells and used to isolate puromycin-resistant clones, using the proctocol described for pRetroSuper-p53 and pLPC-GSEp53. Puromycin was removed from the culture medium and drug-resistant clones were directly shifted to 39.5°C. Following incubation at 39.5°C for a further 14 days, multiple healthy, growing colonies were observed in the positive control p53 shRNA-infected HMF3A culture, however, no outgrowing colonies were observed in the DK-infected culture, similar to the control-infected cultures.

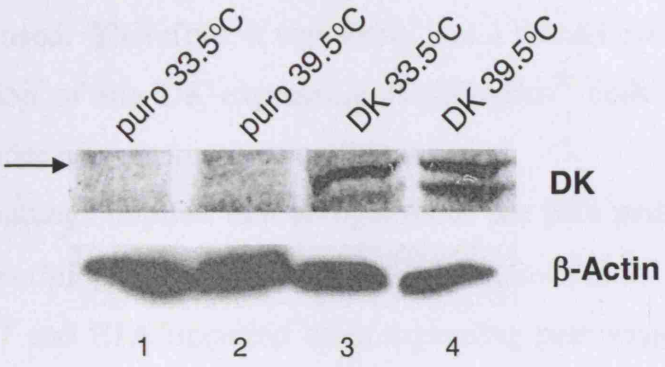

Figure 3.10: Constitutive Cyclin D1-CDK4^{R24C} (DK) Expression

Cyclin D1 Western blot using sc-8396 monoclonal antibody for HMF3A cultures incubated at both 33.5°C and at 39.5°C for 7 days. The arrow indicates the same band detected by the cyclin D1 antibody and the CDK4 antibody (data not shown). β-Actin was the loading control.

The same results were obtained in a duplicate experiment and when ϕ ecotropic cells and HMF3AEco^R cells were substituted for ϕ amphotropic cells and HMF3A cells, respectively. However in the latter experiments, a few outgrowing colonies were observed in DK-infected HMF3AEco^R cultures incubated under non-permissive conditions (approximately <5% of the total number of clones), but not in control-infected HMF3AEco^R cultures. This observation suggested that the ability of DK to complement growth was sufficiently inefficient to be undetectable when the amphotropic transduction procedure was used. Therefore, it was likely that a second event occurred in a minor population of the DK-expressing HMF3AEco^R cells to complement their growth under non-permissive conditions.

These findings implied that abrogation of the pRb pathway alone was insufficient to permit continued growth of HMF3A cells at 39.5°C. They also implied that E7 and E1A impaired other signalling pathways, in addition to the pRb pathway, to complement growth under non-permissive conditions.

3.2.5.8 Inactivation of the INK4A Locus

As described in **Chapter 1**, two splice variants are encoded by the *INK4A* locus; the cyclin-dependent kinase inhibitor p16^{INK4a} and p14^{ARF}. Both of these splice variants represent components of the pRb pathway; p16^{INK4a} negatively regulates pRb functional activity by inhibiting cyclin D-CDK4/6 complexes, whereas p14^{ARF} function downstreams of pRb to negatively regulate pRb effector signalling in an E2F-dependent process. Furthermore, p14^{ARF} acts as a link between the pRb and p53 pathways as it stabilises p53 by binding to the Mdm2 protein. Therefore, it was anticipated that abrogation of either, or even both, of these components would functionally inactivate the pRb pathway.

3.2.5.9 Knockdown of $P14^{ARF}$ by ShRNA

To analyse $p14^{ARF}$ activity, an shRNA construct that was used to efficiently knockdown $p14^{ARF}$ in HDFs [Berns *et al*, 2004], pSuperRetro-$p14^{ARF}$, was introduced into the HMF3A system (gift from R. Agami). However, instead of using the empty pRetroSuper vector as a control (as described in the pRetroSuper-p53 experiment), a functionally active control shRNA construct targetted against the *LAMIN A/C* housekeeping gene was used instead. This construct addressed the possibility that non-specific bystander effects of the RNAi process were causal to the growth complementation phenotype.

A region of the *LAMIN A/C* coding sequence known to confer efficient Lamin A/C knockdown (**Figure 4.5**; [Elbashir *et al*, 2001]) was incorporated into the pRetroSuper vector, using the protocol described by Oligoengine, and the resultant construct, pRetroSuper-LaminA/C, was introduced into HMF3A cells alongside pRetroSuper-$p14^{ARF}$.

10 μg of each shRNA construct was introduced into $HMF3AEco^{R}$ cells and used to generate polyclonal populations at 33.5°C, using the protocol described for pRetroSuper-p53 and pLPC-GSEp53. One duplicate culture was then maintained under drug selection at 33.5°C, whereas selection was removed from the second duplicate culture, then shifted to 39.5°C for a further 7 days before RNA was extracted.

Previous studies indicated that basal $p14^{ARF}$ expression levels were very low in some HDF strains (for example, [Wei *et al*, 2001]) therefore $p14^{ARF}$ expression was analysed at the RNA level by semi-quantitative RT-PCR. $P14^{ARF}$-specific primers (p14-F and p14-R) generated a 284 bp PCR product that corresponded to $p14^{ARF}$ in all RNA samples analysed (**Figure 3.11**).

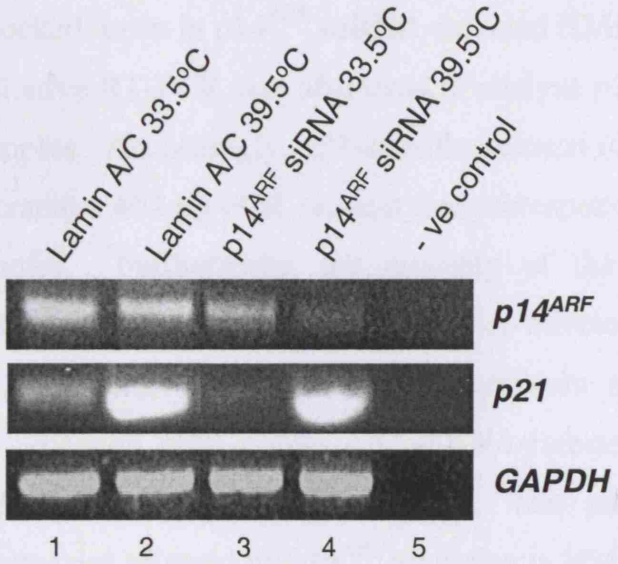

Figure 3.11: *P14*^{ARF} ShRNA Silencing

Semi-quantitative RT-PCR using *p14*^{ARF}- and *p21*- specific primers was used to analyse expression of *p14*^{ARF} and *p21*, respectively, in HMF3AEco^{R} cultures incubated at both 33.5°C and at 39.5°C for 7 days. *GAPDH* was the loading control.

However, the intensity of the PCR product generated from RNA derived from $p14^{ARF}$ shRNA-infected $HMF3AEco^R$ cells and incubated at either 33.5°C (**Figure 3.11**, lane 3) or 39.5°C for 7 days (**Figure 3.11**, lane 4) was significantly reduced, relative to Lamin A/C shRNA-infected $HMF3AEco^R$ cells (**Figure 3.11**, lanes 1 and 2, respectively). This indicated that the *$p14^{ARF}$* was effectively knocked down in $p14^{ARF}$ shRNA-infected $HMF3AEco^R$ cells.

Semi-quantitative RT-PCR was also used to analyse *p21* expression in the same RNA samples. Accordingly, *p21*-specific primers (CDKN1A-F and CDKN1A-R) generated a 402 bp PCR product that corresponded to *p21* in all of the RNA samples. Furthermore, the intensity of the PCR products generated from RNA derived from $p14^{ARF}$ shRNA-infected $HMF3AEco^R$ cultures (**Figure 3.11**, lanes 3 and 4, respectively) were not significantly different to those generated from Lamin A/C shRNA-infected $HMF3AEco^R$ cultures (**Figure 3.11**, lanes 1 and 2, respectively). This indicated that *p21* expression levels were not affected by $p14^{ARF}$ silencing in $HMF3AEco^R$ cells.

3.2.5.10 Knockdown of $P14^{ARF}$ by ShRNA is Insufficient to Complement the Conditional HMF3A Growth Defect

Having demonstrated the effectiveness of $p14^{ARF}$ knockdown mediated by RNAi, nonetheless, pRetroSuper-$p14^{ARF}$ was tested in the HMF3A complementation assay. 10 μg of pRetroSuper-$p14^{ARF}$, pRetroSuper-LaminA/C and pRetroSuper-p53 shRNA constructs were packaged, using the ϕ ecotropic system, and 5% of the total retroviral supernatant harvested was used to infect $HMF3AEco^R$ cultures seeded at $5x10^5$ cells in duplicate T75 cm^2 flasks, in the presence of 8 μg/ml polybrene, then used to isolate puromycin-resistant clones, using the protocol described for pRetroSuper-p53 and pLPC-GSEp53. Puromycin was removed from the culture medium and drug-resistant clones were directly shifted to 39.5°C. Following incubation at 39.5°C for a further 14 days, multiple healthy, growing colonies were

observed in the positive control p53 shRNA-infected HMF3AEco^{R} culture, however, no outgrowing colonies were observed in the p14^{ARF} shRNA-infected culture, similar to the Lamin A/C shRNA-infected culture. The same results were obtained in a duplicate experiment culture. This indicated that p14^{ARF} knockdown was insufficient to overcome the HMF3A conditional growth arrest.

3.2.5.11 Knockdown of P16^{INK4a} by ShRNA

Targetting p16^{INK4a} by RNAi, similar to p14^{ARF}, was technically difficult due to the limited region that could be used to specifically inactivate *p16^{INK4a}* mRNA, but not the alternatively spliced *p14^{ARF}* transcript (**Figure 3.12B**). However, p16^{INK4a} knockdown by shRNA was possible as it had previously been used to demonstrate that inactivation of p16^{INK4a} was insufficient to bypass the induction of senescence [Wei *et al*, 2003]. Moreover, p16^{INK4a} knockdown was insufficient to overcome the conditional growth arrest of BJ cells constitutively expressing hTERT and a temperature sensitive mutant of LT (BJ-TERT-tsLT cells; [Berns *et al*, 2004]). Therefore, the p16^{INK4a} shRNA construct utilised by Wei and colleagues, pRetroSuper-p16#2 (gift from U. Herbig), was used to silence p16^{INK4a} in the HMF3A system.

10 μg of pRetroSuper-p16#2 and pRetroSuper-LaminA/C shRNA constructs were introduced into HMF3AEco^{R} cells and used to generate polyclonal populations at 33.5°C, using the protocol described for pRetroSuper-p53 and pLPC-GSEp53. One duplicate culture was then maintained under drug selection at 33.5°C, whereas selection was removed from the second duplicate culture, then shifted to 39.5°C for a further 7 days before RIPA protein lysates were prepared.

RIPA lysates were separated by 12% SDS-PAGE then analysed by Western blot, using JC8 p16^{INK4a} monoclonal antibody (gift from G. Peters).

A

Name	Target Region	Target Sequence	Position in mRNA Sequence	G/C Content
P16#2	ORF	TAGTTACGGTCGGAGGCCG	338	63.16%
P16A	ORF	CCAACGCACCGAATAGTTA	325	47.37%

B

C

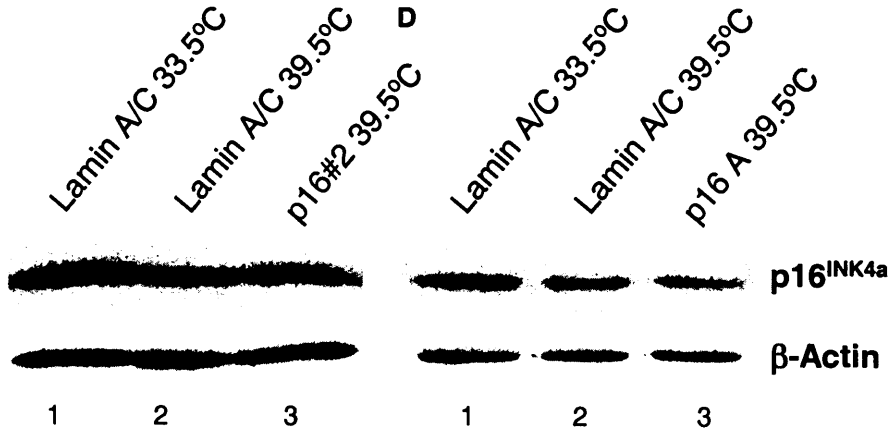

D

Figure 3.12: P16^{INK4a} ShRNA Silencing

A: P16^{INK4a} shRNA target sequences used in this study; **B:** Positions of the shRNA target sequences (indicated by black bars), and primer binding sites (indicated by black arrows) in *p16^{INK4a}* mRNA. The grey arrow indicates the ORF; **C:** P16^{INK4a} Western blot using JC8 monoclonal antibody for HMF3AEco^{R} cultures incubated at both 33.5°C and at 39.5°C for 7 days, including HMF3AEco^{R} cells infected with the p16#2 shRNA construct; **D:** P16^{INK4a} Western blot including HMF3AEco^{R} cells infected with the p16A shRNA construct. β-Actin was the loading control.

A 16 kDa band that corresponded to $p16^{INK4a}$ (as indicated in the literature [Parry *et al*, 1995]) was detected in Lamin A/C shRNA-infected HMF3AEco^R cultures incubated at both 33.5°C (**Figure 3.12C**, lane 1) and 39.5°C for 7 days (**Figure 3.12C**, lane 2). However, no significant reduction was observed in the intensity of the 16 kDa band in p16#2 shRNA-infected HMF3AEco^R cultures incubated at 39.5°C for 7 days (**Figure 3.12C**, lane 3). This indicated that the p16#2 shRNA construct was not effective in mediating $p16^{INK4a}$ knockdown in the HMF3A system. However, it was also possible that the heterogeneous nature of the HMF3AEco^R population expressing the shRNA construct masked a modest knockdown in $p16^{INK4a}$, in a similar manner to the activity of wt LT (**Section 3.2.1.1**). Indeed, Wei and colleagues [Wei *et al*, 2003] isolated individual p16#2 shRNA-infected clones in order to obtain significant knockdown of $p16^{INK4a}$. Therefore, it may be preferable to analyse individual $p16^{INK4a}$ shRNA-infected clones in the HMF3A system. It was also possible that the p16#2 shRNA target was inefficient in the HMF3A system due to an as yet unknown variable associated with the RNAi process; for example, the target sequence could have encompassed a known single nucleotide polymorphism (SNP) site. However, analysis of the p16#2 shRNA target sequence using the dbSNP at NCBI did not support this hypothesis.

In an attempt to obtain efficient $p16^{INK4a}$ knockdown, a second $p16^{INK4a}$ shRNA construct, namely pRetroSuper-p16A, was designed using the guidelines of Reynolds and colleagues [Reynolds *et al*, 2004] and generated using the Oligoengine protocol (**Figures 3.12A** and **B**). pRetroSuper-p16A was introduced into HMF3AEco^R cells, using the method described for pRetroSuper-p16#2. A small reduction in $p16^{INK4a}$ expression was observed in p16A shRNA-infected HMF3AEco^R cells incubated at 39.5°C for 7 days (**Figure 3.12D**, lane 3), relative to Lamin A/C shRNA-infected HMF3AEco^R cells incubated at 39.5°C for 7 days (**Figure 3.12D**, lane 2). However, the level of $p16^{INK4a}$ knockdown was not considered significant.

3.2.5.12 Constitutive Expression of Bmi-1

Since RNAi could not effectively knock down $p16^{INK4a}$ at the protein level, an alternative method to inactivate the *INK4A* locus was sought. Inactivation of the *INK4A* locus by constitutive expression of Bmi-1 represented one example. As described in **Chapter 1** (**Section 1.1.13**), Bmi-1 is a transcriptional repressor of the PcG family that promotes stable, epigenetic gene silencing though chromatin modifications mediated by histone methylation [van der Lugt *et al*, 1994]. Bmi-1 has been shown to be significantly down-regulated upon replicative senescence in primary HDFs, but not in quiescent HDFs, whereas its over-expression was sufficient to extend the replicative lifespan of some HDF strains [Itahana *et al*, 2003; Jacobs *et al*, 1999]. Therefore, a Bmi-1 retroviral expression construct, pBabepuro-Bmi-1 (gift from M. van Lohuizen) was introduced into $HMF3AEco^R$ cells and assessed for its ability to complement the conditional growth defect of these cells.

10 μg of pBabepuro-Bmi-1 and pBabepuro retroviral expression constructs were introduced into $HMF3AEco^R$ cells to generate polyclonal populations at 33.5°C, using the protocol described for pRetroSuper-p53 and pLPC-GSEp53. One duplicate culture was then maintained under drug selection at 33.5°C, whereas selection was removed from the second duplicate culture, then shifted to 39.5°C for a further 7 days before RNA was extracted.

Semi-quantitative RT-PCR, using primers specific to *BMI1* (Bmi-F and Bmi-R), was used to analyse global *BMI1* expression in these cultures. A significant increase in the intensity of a 378 bp PCR product that corresponded to *BMI1* was detected in RNA derived from Bmi-1 infected $HMF3AEco^R$ cells incubated at both 33.5°C (**Figure 3.13A**, lane 3) and 39.5°C for 7 days (**Figure 3.13A**, lane 4), relative to puro-infected $HMF3AEco^R$ cells (**Figure 3.13A**, lanes 1 and 2, respectively).

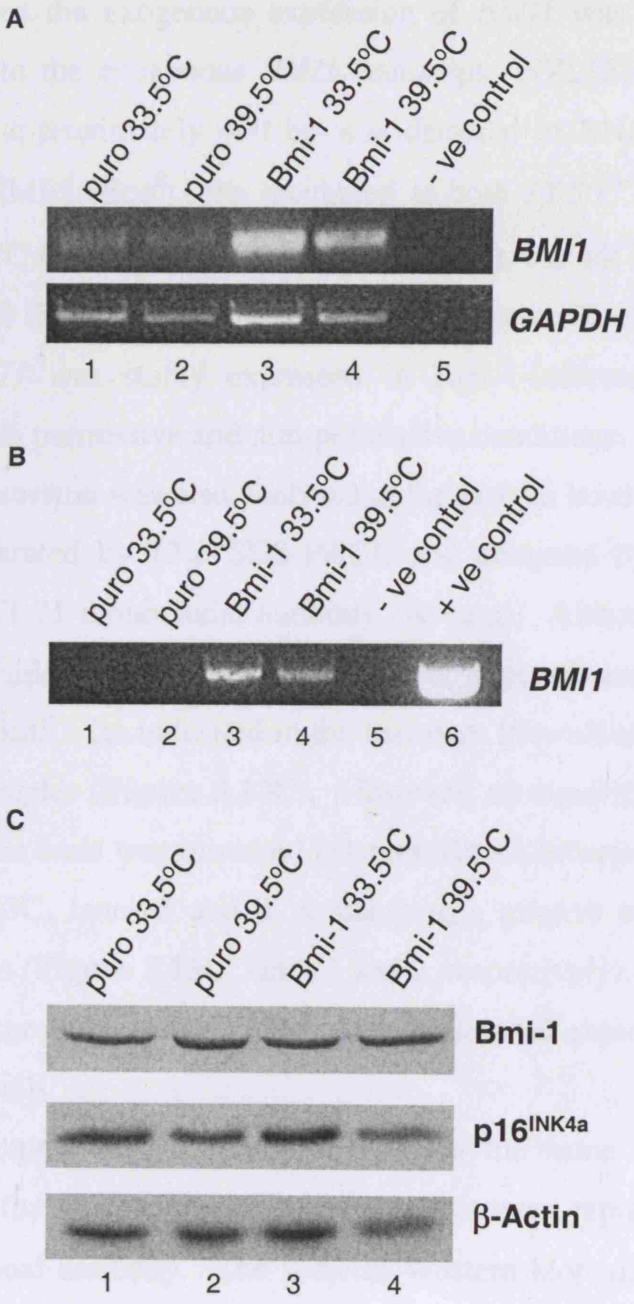

Figure 3.13: Constitutive Bmi-1 Expression

A: Semi-quantitative RT-PCR using *BMI1*-specific primers was used to analyse global *BMI1* expression levels in HMF3AEco^{R} cultures incubated at both 33.5°C and at 39.5°C for 7 days. *GAPDH* was the loading control; **B:** Semi-quantitative RT-PCR using primers specific to the exogenous *BMI1* transcript was used to analyse expression of exogenous *BMI1*. pBabepuro-Bmi-1 plasmid was the positive control for PCR; **C:** Bmi-1 and p16^{INK4a} Western blot analysis using 1.T.21 Bmi-1 monoclonal antibody and JC8 p16^{INK4a} monoclonal antibody, respectively, for HMF3AEco^{R} cultures incubated at both 33.5°C and at 39.5°C for 7 days. β-Actin was the loading control.

Furthermore, when the exogenous expression of *BMI1* was analysed using primers specific to the exogenous *BMI1* transcript (WZL[F] and Bmi-R), a PCR product of approximately 400 bp was detected in RNA derived from Bmi-1-infected HMF3AEco^R cells incubated at both 33.5°C (**Figure 3.13B**, lane 3) and 39.5°C for 7 days (**Figure 3.13B**, lane 4), but not in puro-infected HMF3AEco^R cells (**Figure 3.13B**, lanes 1 and 2, respectively). This indicated that ectopic *BMI1* was stably expressed in Bmi-1-infected HMF3AEco^R cultures under both permissive and non-permissive conditions.

Bmi-1 expression was also analysed at the protein level. RIPA protein lysates were separated by 12% SDS-PAGE and analysed by Western blot analysis, using 1.T.21 monoclonal antibody (Abcam). Although no positive control was available for this analysis, a band of approximately 40 kDa that corresponded to Bmi-1 (as indicated in the literature [Sewalt *et al*, 1998]) was detected in all samples (**Figure 3.13C**). However, no significant different in the intensity of this band was observed between Bmi-1-infected HMF3AEco^R cells (**Figure 3.13C**, lanes 3 and 4, respectively), relative to puro-infected HMF3AEco^R cells (**Figure 3.13C**, lanes 1 and 2, respectively). This indicated that exogenous expression of Bmi-1 did result in elevated expression of Bmi-1 in HMF3AEco^R cells.

P16^{INK4a} expression was also analysed in the same samples. The membrane used for Bmi-1 Western blot analysis was reprobed with JC8 p16^{INK4a} monoclonal antibody. The β-Actin Western blot indicated that the loading of the lysate derived from Bmi-1-infected HMF3AEco^R cells incubated at 39.5°C for 7 days (**Figure 3.13C**, lane 4) was lower than all other samples, yet no significant difference in the intensity of the 16 kDa band that corresponded to p16^{INK4a} was observed between Bmi-1-infected HMF3AEco^R cells (**Figure 3.13C**, lanes 3 and 4, respectively) and puro-infected HMF3AEco^R cells (**Figure 3.13C**, lanes 1 and 2, respectively). This indicated that ectopic expression of Bmi-1 did not affect the steady-state levels of p16^{INK4a} protein.

3.2.5.13 Constitutive Expression of Bmi-1 is Insufficient to Complement the Conditional HMF3A Growth Defect

Despite the discernable affect of Bmi-1 on $p16^{INK4a}$ expression, pBabepuro-Bmi-1 was tested in the HMF3A complementation assay. 10 μg of pBabepuro-Bmi-1, pBabepuro and pRetroSuper-p53 shRNA constructs were introduced into HMF3A cells, using the proctocol described for pRetroSuper-$p14^{ARF}$. Puromycin was removed from the culture medium and drug-resistant clones were directly shifted to 39.5°C. Following incubation at 39.5°C for a further 14 days, multiple healthy, growing colonies were observed in the positive control p53 shRNA-infected HMF3AEco^R culture, however, no outgrowing colonies were observed in the Bmi-1-infected culture, similar to the puro-infected culture. The same results were obtained in a duplicate experiment. This indicated that ectopic Bmi-1 expression was insufficient to overcome the HMF3A conditional growth arrest. This was not totally surprising since HMF3AEco^R cells incubated at 39.5°C already expressed Bmi-1 (**Figure 3.13C**, lane 2).

3.2.6 Abrogation of Downstream Targets of the P53 Pathway

The experiments described thus far indicated that abrogation of the p53 pathway was critical for the bypass of the HMF3A conditional growth arrest. In contrast, abrogation of the *INK4A* locus by ectopic expression of DK, Bmi-1 or $p14^{ARF}$ shRNA was insufficient to bypass the HMF3A conditional growth arrest. However, the fact that ectopic expression of either E1A or E7 was sufficient to complement the growth of these cells raised the possibility that these viral oncoproteins could also inactivate downstream components of the p53 pathway. To address this possibility, some of the known downstream targets of p53 were targetted for inactivation in the HMF3A system to assess their ability to bypass senescence in the HMF3A complementation assay.

3.2.6.1 Knockdown of P21 by ShRNA

P21 has been shown to be up-regulated upon replicative senescence in a number of cell types, for example, HDFs [Hardy *et al*, 2005], endothelial cells [Tang *et al*, 2002; Wagner *et al*, 2001], astrocytes [Evans *et al*, 2003] and prostate epithelial and uropithelial cells [Schwarze *et al*, 2001]. Furthermore, over-expression of p21 in HDFs was shown to induce premature senescence [McConnell *et al*, 1998] and SAHF [Chan *et al*, 2005], whereas knockdown of p21 by shRNA was sufficient to bypass the conditional growth arrest in an analogous conditionally immortalised HDF system, namely BJ-TERT-tsLT cells [Berns *et al*, 2004]. This indicated that p21 should be functionally analysed in the HMF3A system.

The p21 shRNA construct utilised by Berns and colleagues [Berns *et al*, 2004] was prepared by cloning the same p21 shRNA target sequence into the pRetroSuper vector (summarised in **Figures 3.14A** and **B**), using the Oligoengine protocol. The resultant construct, pRetroSuper-p21RB, was then introduced into HMF3A system.

10 μg of pRetroSuper-p21RB and pRetroSuper-LaminA/C were introduced into HMF3AEco^{R} cells and used to generate polyclonal populations at 33.5°C, using the protocol described for pRetroSuper-p14^{ARF}. One duplicate culture was then maintained under drug selection at 33.5°C, whereas selection was removed from the second duplicate culture, then shifted to 39.5°C for a further 7 days before RIPA protein lysates were prepared.

RIPA lysates, separated by 12% SDS-PAGE, were analysed by Western blot, using SX118 p21 monoclonal antibody (gift from X. Lu). A slight, but not significant, knockdown of p21 was observed in the p21 RB shRNA-infected HMF3AEco^{R} culture (**Figure 3.14**, lane 3).

A

Name	Target Region	Target Sequence	Position in mRNA Sequence	G/C Content
P21JD	ORF	CTTCGACTTTGTCACCGAG	244	52.63%
P21RB	ORF	GACCATGTGGACCTGTCAC	419	57.89%
P21A	ORF	CCAGCATGACAGATTTCTA	528	42.11%
P21B	3' UTR	AAACTAGGCGGTTGAATGA	775	42.11%
P21C	3' UTR	CACAGGCGGTTATGAAATT	979	42.11%
P21D	3' UTR	AACACCTCCTCATGTACAT	704	42.11%
P21E	ORF	CGACTGTGATGCGCTAATG	190	52.63%
P21F	3' UTR	GAATGAGAGGTTCCTAAGA	788	42.11%
P21G	3' UTR	CATTGCACTTTGATTAGCA	1734	36.84%

B

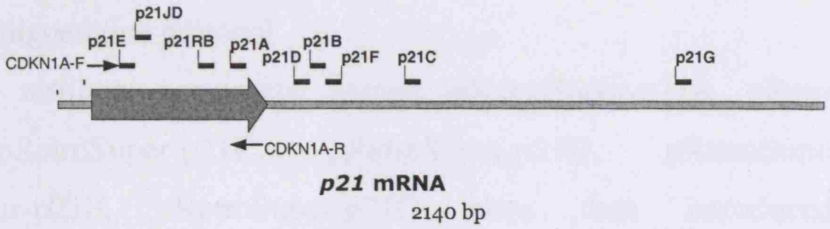

C

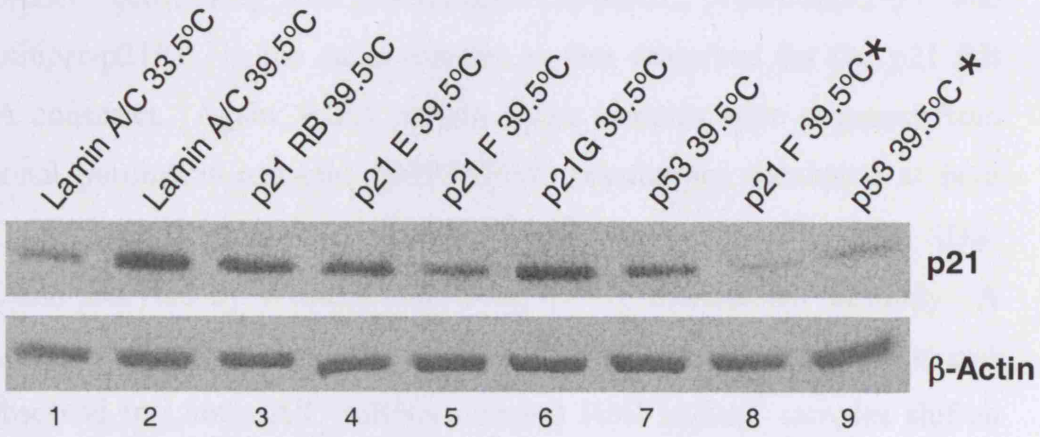

Figure 3.14: P21 ShRNA Silencing (I)

A: P21 shRNA target sequences used in this study; **B:** Positions of the shRNA target sequences (indicated by black bars), and primer binding sites (indicated by black arrows) in *p21* mRNA. The grey arrow indicates the ORF; **C:** P21 Western blot using SX118 p21 monoclonal antibody for HMF3AEco^{R} cultures incubated at both 33.5°C and at 39.5°C for 7 days, in addition to growth complemented HMF3AEco^{R} cells infected with p21- and p53- shRNA constructs, respectively (indicated by an asterisk). β-Actin was the loading control.

Therefore, a second p21 shRNA construct (p21 JD; gift from J. Downward; **Figures 3.14A** and **B**) was applied to the HMF3A system in the same manner as that described for the p21 RB shRNA construct. Again, however, no significant down-regulation of p21 was observed by Western blot analysis (data not shown).

In an attempt to obtain efficient knockdown of p21, a further 7 p21 shRNA constructs were designed using the criteria outlined by Reynolds and colleagues ([Reynolds *et al*, 2004]; **Figures 3.14A** and **B**) and generated, using the Oligoengine protocol.

The resultant constructs, namely pRetroSuper-p21A, pRetroSuper-p21B, pRetroSuper-p21C, pRetroSuper-p21D, pRetroSuper-p21E, pRetroSuper-p21F, pRetroSuper-p21G were then introduced into HMF3AEco^R cells, along with pRetroSuper-LaminA/C, pRetroSuper-p53 and pRetroSuper-p21RB, in the same manner as that described for the p21 RB shRNA construct. Again, RIPA protein lysate samples were prepared from polyclonal puromycin-resistant HMF3AEco^R populations incubated at both 33.5°C and 39.5°C for 7 days. Samples were then separated by 12% SDS-PAGE and analysed by Western blot, using SX118 monoclonal antibody. A significant increase in the intensity of a 21 kDa band that corresponded to p21 was observed in Lamin A/C shRNA-infected HMF3AEco^R samples shifted from 33.5°C (**Figure 3.14C**, lane 1) to 39.5°C for 7 days (**Figure 3.14C**, lane 2), similar to before. However, a significant reduction was observed in the intensity of the 21 kDa band derived from p21 F shRNA-infected HMF3AEco^R cells (**Figure 3.14C**, lane 5). Moreover, the reduction was similar to that achieved with the p53 shRNA construct (**Figure 3.14C**, lane 7). This indicated that the shRNA generated from pRetroSuper-p21F was effective at knocking down p21 in HMF3AEco^R cells.

3.2.6.2 Knockdown of P21 by ShRNA is Sufficient to Complement the Conditional HMF3A Growth Defect

Having demonstrating significant knockdown of p21 in HMF3AEco^R cells at 39.5°C, all p21 shRNA constructs were tested in the HMF3A complementation assay. 10 μg of pSuperRetro-LaminA/C, pRetroSuper-p21 constructs A-G, pSuperRetro-p21RB, pSuperRetro-p21JD and pRetroSuper-p53 were introduced into HMF3AEco^R cells, using the protocol described for pRetroSuper-p14^{ARF}. Puromycin was removed from the culture medium and drug-resistant clones were directly shifted to 39.5°C. Following incubation at 39.5°C for 14 days, multiple healthy, growing colonies were observed in both p21 F shRNA- and p53 shRNA- infected HMF3AEco^R cultures, but not in the Lamin A/C shRNA-infected HMF3AEco^R culture or any of the other p21 shRNA-infected HMF3AEco^R cultures. The former cultures were trypsinised, pooled and replated as polyclonal populations, then sub-cultivated for a minimum of 4 further passages, using a 1:5 split, to ensure that they could be continually propagated under these conditions. Having achieved this, both cultures were considered complemented for growth. The same results were obtained in a duplicate experiment. This indicated that of all the p21 shRNA constructs analysed in the HMF3A system, the only one that conferred HMF3A growth complementation was also the only one that significantly knocked-down p21 expression.

To analyse p21 expression in the growth complemented HMF3AEco^R cultures, RIPA protein lysates were extracted, separated by 12% SDS-PAGE, and analysed by Western blot, using SX118 monoclonal antibody. A significant reduction in the intensity of a 21 kDa band that corresponded to p21 was observed in p21 F shRNA-infected HMF3AEco^R cells incubated at 39.5°C for 7 days (**Figure 3.14C**, lane 8), relative to Lamin A/C shRNA-infected cells incubated at 39.5°C for 7 days (**Figure 3.14C**, lane 2). The reduction in the intensity of this band was similar to that exhibited in p53 shRNA-infected HMF3AEco^R cells (**Figure 3.14C**, lane 9). Moreover, the

level of p21 knockdown appeared to be significantly greater in both of the growth complemented cultures (**Figure 3.14C**, lanes 8 and 9, respectively), than their respective temperature shifted counterparts (**Figure 3.14C**, lanes 5 and 7, respectively).

To further verify this finding, Lamin A/C, p21 RB, p21 F and p53 shRNA constructs were retested in the HMF3A complementation assay. 1% or 5% of the total viral supernatant harvested from 10 μg transfection of pRetroSuper-LaminA/C, pRetroSuper-p21RB, pRetroSuper-p21F and pRetroSuper-p53 was used to infect duplicate HMF3AEco^R cultures seeded at $5x10^5$ cells in T75 cm^2 flasks. A 5-fold dilution of viral supernatant was used to determine whether there would be a proportional decrease in the number of growing clones that would be obtained with fewer viruses. Following the isolation of puromycin-resistant clones at 33.5°C, one culture was incubated for a further 7 days in 2 μg/ml puromycin at 33.5°C before fixing and staining with 2% (w/v) methylene blue. In contrast, puromycin was removed from duplicate cultures and drug-resistant clones were shifted to 39.5°C for 14 days before fixing and staining with 2% (w/v) methylene blue. Multiple colonies were observed from p21 F shRNA-infected cultures infected with 100μl of virus, similar to the positive control p53 shRNA-infected cultures (**Figure 3.15**). Moreover, there was a clear increase in the number of colonies when a 5-fold increase in virus quantity was used. However, no colonies were observed in HMF3AEco^R cultures infected with either the p21RB shRNA construct or the Lamin A/C control shRNA construct. This indicated that the p21 RB shRNA construct, like the Lamin A/C shRNA construct, had no effect upon the ability of HMF3AEco^R cells to bypass the conditional growth arrest. However, the fact that the p21F shRNA construct knocked-down p21 expression and was also sufficient to complement the growth of HMF3AEco^R cells indicated that p21 was involved in this process.

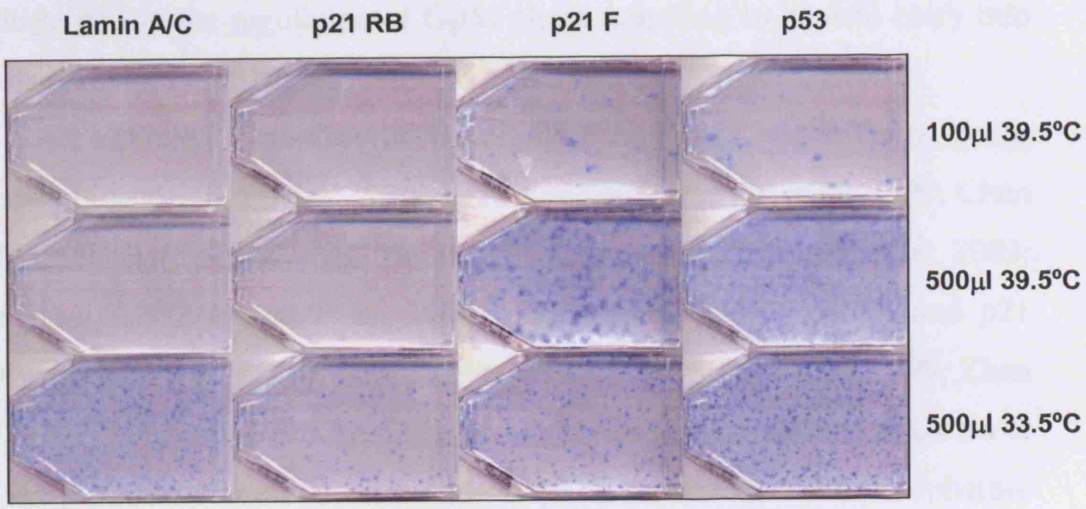

Figure 3.15: P21 ShRNA Silencing (II)

Analysis of Lamin A/C, p21 RB, p21 F and p53 shRNA expression constructs in the HMF3A complementation assay. Two dilutions of the retroviral supernatant were used, namely 100 µl and 500 µl. HMF3AEco^{R} cultures were either maintained at 33.5°C for 7 days (500 µl 33.5°C samples) or shifted to 39.5°C for 2 weeks directly post-drug-selection (500 µl 39.5°C and 100 µl 33.9°C samples), before fixing and staining with 2% (w/v) methylene blue.

3.2.6.3 Expression Analysis of Some of the Known P53 Targets

In addition to p21, a number of other p53 targets that are activated during G_1/S phase transition have been identified (**Figure 3.16A**). These include *GADD45A* and *BTG2*, two genes that were identified by microarray analysis as being significantly up-regulated upon the HMF3A temperature shift [Hardy *et al*, 2005]. There has also been increasing evidence to implicate p53 in the regulation of G_2/M phase transition to control entry into mitosis ([Taylor *et al*, 1999]; reviewed in [Taylor and Stark, 2001]).

Accordingly, a number of G_2/M phase transition p53 effector genes have been identified, namely, *SFN*, *RPRM* and *B99* [Carrier *et al*, 1999; Chan *et al*, 1999; Hermeking *et al*, 1997; Kastan *et al*, 1992; Monte *et al*, 2003; Ohki *et al*, 2000; Utrera *et al*, 1998]. SFN, GADD45A, RPRM and p21 inactivate Cdc2 [Ohki *et al*, 2000; Taylor *et al*, 2001; Wang *et al*, 1999; Zhan *et al*, 1999], whereas B99 associates with the microtubule networks [Utrera *et al*, 1998]. Other p53 effectors include Wip1, a serine-threonine phosphatase that positively regulates p53 activity [Bulavin *et al*, 2004], and PML [de Stanchina *et al*, 2004]. PML has previously been linked to senescence; ecotopic expression of PML IV was shown to be sufficient to induce cellular senescence in primary HDFs [Bischof *et al*, 2002] whereas knockdown of PML by RNAi impaired the induction of senescence of primary HDFs [de Stanchina *et al*, 2004; Ferbeyre *et al*, 2000; Pearson *et al*, 2000].

The lack of well-characterised antibodies to most of the genes described here meant that expression analysis in the HMF3A system was limited to the RNA level. Consequently, semi-quantitative RT-PCR, using primers specific to each of these known targets of p53, was used to analyse their expression profile, using RNA derived from HMF3AEco^R cells incubated at 33.5°C or at 39.5°C for 7 days. It should be noted that, due to the multiplicity of PML splice variants, the primers designed to analyse PML expression in the HMF3A system encompassed a region known to be present in the cDNA of all known variants.

A

Gene Symbol	Gene Name
B99	G-2 and S-phase expressed 1
BTG2	B-Cell translocation gene, 2
GADD45A	Growth arrest and DNA-damage-inducible α
PML	Promyelocytic Leukemia
RPRM	Reprimo
SFN	Stratifin
WIP1	Protein phosphatase 1D magnesium-dependent, δ isoform

B

Figure 3.16: Expression of Known Downstream Targets of P53

A: Table listing some known downstream targets of p53; **B:** Semi-quantitative RT-PCR using primers specific to each gene was used to analyse expression in HMF3AEco^{R} cells incubated at both 33.5°C and at 39.5°C for 7 days. *GAPDH* was the loading control.

Significant up-regulation in the intensity of 497, 378, 303, 352 and 233 bp PCR products, using primers specific to *BTG2* (BTG2-F and BTG2-R), *GADD45A* (GADD45A-F and GADD45A-R), *PML* (PML-F and PML-R), *RPRM* (RPRM-F and RPRM-R) and *SFN* (SFN-F and SFN-R), respectively, were observed upon the temperature shift of HMF3AEco^{R} cells from 33.5°C (**Figure 3.16B**, lane 1) to 39.5°C for 7 days (**Figure 3.16B**, lane 2). However, it was not known whether the senescence-associated PML splice variant (IV) was specifically down regulated in these cells as primers specific to this splice variant were not utilised. Furthermore, no significant change in the intensity of the 363 bp PCR product generated, using *WIP1* specific primers (WIP1-F and WIP1-R), was observed, whereas significant down-regulation in the intensity of the 373 bp PCR product generated, using the *B99* specific primers (B99-F and B99-R), was observed.

3.2.6.4 Knockdown of Some of the Known P53 Targets by ShRNA

To further investigate the functional activities of each of these genes in the HMF3A system, shRNA constructs were designed for PML, RPRM and SFN, using the guidelines of Reynolds and colleagues ([Reynolds *et al*, 2004]; **Figures 3.17A** and **B**) and generated using the pRetroSuper system, using the Oligoengine protocol. It should be noted that the 3 PML shRNA constructs were designed to target sequences present in the mRNA of all known *PML* splice variants, and that the BTG2 and GADD45A shRNA constructs were the same constructs utilised in our original analysis of the HMF3A system [Hardy *et al*, 2005]. RNAi was not used to functionally assess B99 for two reasons: firstly, the observation that it was significantly down-regulated upon the HMF3A temperature shift (**Figure 3.16B**) rendered it unlikely to mediate the conditional HMF3A growth arrest; secondly, B99 has been shown to negatively regulate p53 activity [Monte *et al*, 2003]. Therefore, it was possible that B99 knockdown would increase p53 expression and stabilisation.

A

Name	*Target Region*	*Target Sequence*	*Position in mRNA Sequence*	*G/C Content*
BTG2	ORF	CACCACTGGTTTCCCGAAA	225	52.63%
GADD45A	ORF	CGACATCAACATCCTGCGC	550	57.89%
PML#1	5' UTR	AAACCGAGAATCGAAACTA	112	36.84%
PML#2	ORF	CCGACTTCTGGTGCTTTGA	548	52.63%
PML#3	ORF	AGCATCTACTGCCGAGGAT	742	52.63%
RPRM	3'UTR	GGAAGAGTGACCTGTTAAA	969	42.11%
SFN#1	ORF	CTCTCAGTAGCCTATAAGA	201	42.11%
SFN#2	ORF	TGGACAGCCACCTCATCAA	379	52.63%
SFN#3	ORF	CGAGACAACCTGACACTGT	741	52.63%

B

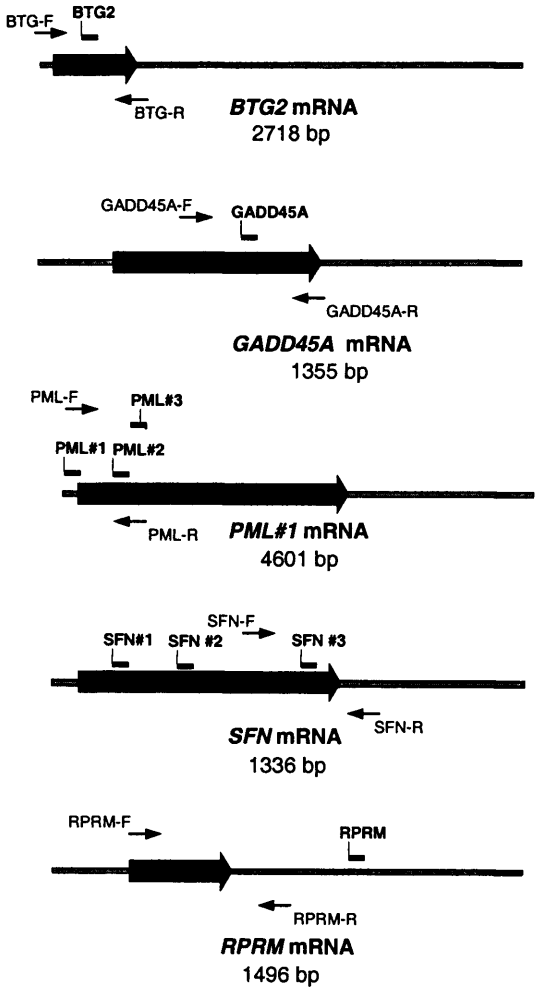

Figure 3.17: Design of ShRNA Constructs for Known P53 Targets

A: ShRNA target sequences used to knockdown known p53 targets; **B:** Positions of the shRNA target sequences (indicated by black bars), and primer binding sites (indicated by black arrows) in the corresponding mRNA sequences. A grey arrow indicates the ORF.

Note: 9 different *PML* splice variants have been described but for simplicity, only splice variant #1 is depicted. BTG2 and GADD45A shRNA targets were the same as those used in our previous study [Hardy *et al*, 2005].

The functional role of B99 should be addressed by ectopically expressing B99 in HMF3AEco^R cells.

The resultant constructs, pRetroSuper-BTG2, pRetroSuper-GADD45A, pRetroSuper-PML#1, pRetroSuper-PML#2, pRetroSuper-PML#3, pRetroSuper-RPRM, pRetroSuper-SFN#1, pRetroSuper-SFN#2 and pRetroSuper-SFN#3 were introduced into HMF3A cells along with pRetroSuper-Lamin A/C and pRetroSuper-p53. 10 μg of each shRNA construct was introduced into HMF3AEco^R cells and used to generate polyclonal populations at 33.5°C, using the protocol described for pRetroSuper-p14^{ARF}. One duplicate culture was then maintained under drug selection at 33.5°C, whereas selection was removed from the second duplicate culture, then shifted to 39.5°C for a further 7 days, before RNA was extracted; under these conditions, target gene expression was maximal, therefore, knockdown was more likely to be detectable.

The efficiency of RNAi knockdown mediated by each shRNA construct was then assessed by semi-quantitative RT-PCR, using the primers described above. A significant reduction in the intensity of each PCR product was observed from RNA derived from each shRNA-infected HMF3AEco^R culture, relative to the Lamin A/C-infected HMF3AEco^R culture, with the exception of *RPRM* (**Figure 3.18**, asterisked lanes).

3.2.6.5 Knockdown of Some of the Known P53 Targets by ShRNA is Insufficient to Complement the Conditional HMF3A Growth Defect

Having demonstrated efficient knockdown of *BTG2*, *GADD45A*, *PML* and *SFN* in the HMF3AEco^R system, the shRNA expression constructs were tested in the HMF3A complementation assay.

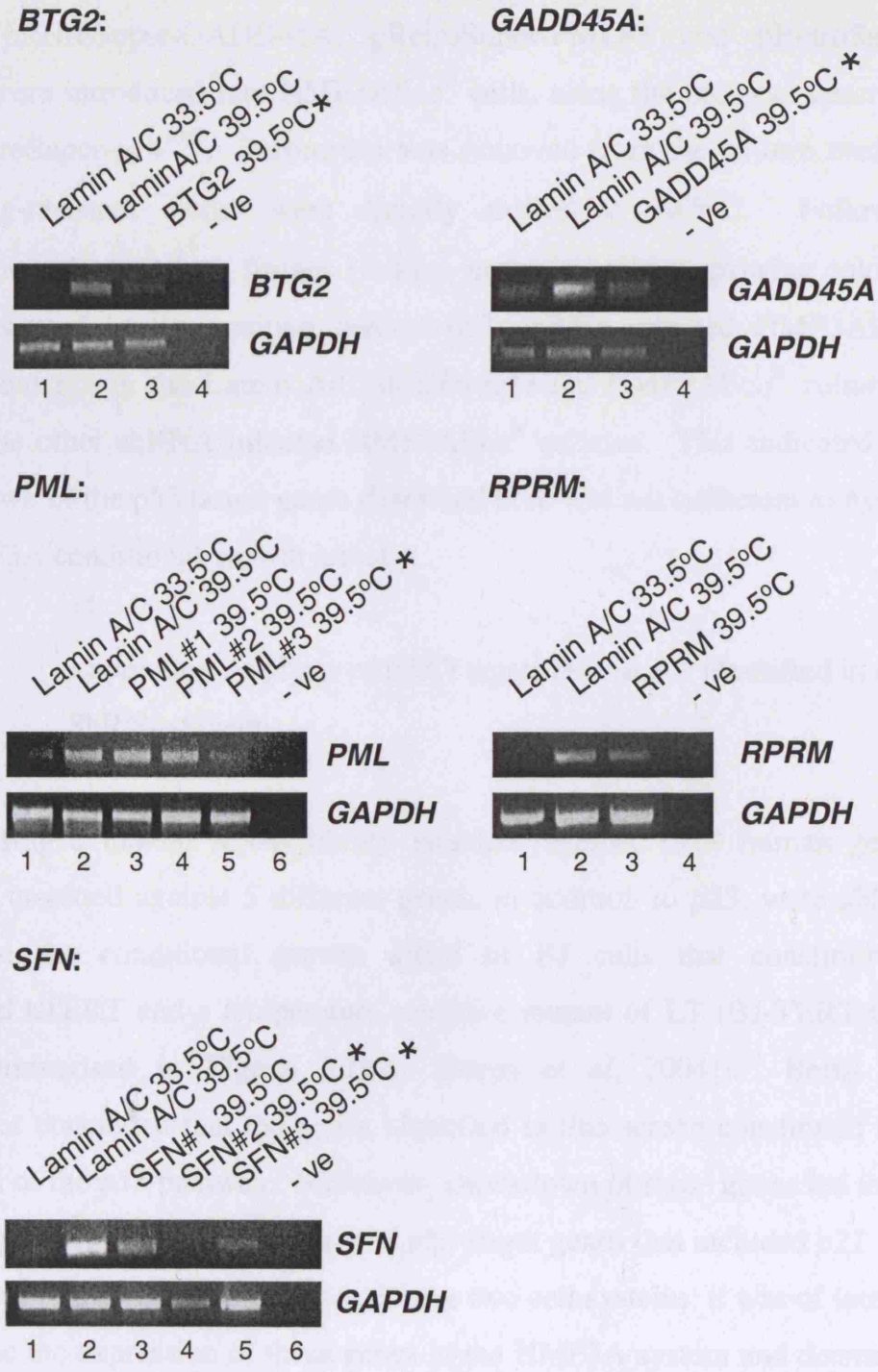

Figure 3.18: ShRNA-Targetting of Known P53 Targets

Semi-quantitative RT-PCR using primers specific to each of the known targets of p53 was used to analyse expression of each gene in HMF3AEco^{R} cultures incubated at both 33.5°C and at 39.5°C for 7 days (effective knockdown indicated by an asterisk). *GAPDH* was the loading control.

10 μg of pRetroSuper-LaminA/C, pRetroSuper-p53, pRetroSuper-BTG2, pRetroSuper-GADD45A, pRetroSuper-PML#3 and pRetroSuper-SFN#2 were introduced into HMF3AEco^R cells, using the protocol described for pRetroSuper-p14^{ARF}. Puromycin was removed from the culture medium and drug-resistant clones were directly shifted to 39.5°C. Following incubation at 39.5°C for a further 14 days, multiple healthy, growing colonies were observed in the positive control p53 shRNA-infected HMF3AEco^R culture, but not in the Lamin A/C shRNA-infected HMF3AEco^R culture or any of the other shRNA-infected HMF3AEco^R cultures. This indicated that knockdown of the p53 target genes described here was not sufficient to bypass the HMF3A conditional growth arrest.

3.2.6.6 Expression Analysis of P53 Targets Previously identified in a ShRNA Screen

Using a human RNAi library targetted against 7914 human genes, shRNAs targetted against 5 different genes, in addition to p53, were able to overcome the conditional growth arrest of BJ cells that constitutively expressed hTERT and a temperature sensitive mutant of LT (BJ-TERT-tsLT cells; summarised in **Figure 3.19A**; [Berns *et al*, 2004]). Berns and colleagues concluded that the genes identified in this screen constituted new members of the p53 pathway. Moreover, knockdown of these genes led to the down-regulation of a specific subset of p53 target genes that included *p21*.

Due to the analogous nature of these two cell systems, it was of interest to analyse the expression of these genes in the HMF3A system and determine if they were also responsible for the conditional growth arrest of HMF3AEco^R cells. Semi-quantitative RT-PCR, using primers specific to each of the candidate genes, was used to analyse their expression, using RNA derived from HMF3AEco^R cells incubated at both 33.5°C and 39.5°C for 7 days.

A

Gene Symbol	Gene Name
CCT2	T-complex protein 1, beta subunit
HDAC4	Histone deacetylase 4
HTATIP	Histone acetyl transferase TIP60
KIAA0828	Putative *S*-adenosyl-*L*-homocysteine hydrolase SAH3
RPS6KA6	Ribosomal S6 kinase 4, RSK4

B

Figure 3.19: Expression of Putative Downstream Targets of P53

A: Table listing putative downstream targets of p53, as identified in the shRNA screen by Berns and colleagues [Berns *et al*, 2004]; **B:** Semi-quantitative RT-PCR using primers specific to each candidate gene was used to analyse expression in HMF3AEco^{R} cultures incubated at both 33.5°C and at 33.5°C for 7 days. *GAPDH* was the loading control.

A small increase in the intensity of 385, 357, 263, 413 and 261 bp PCR products, using primers specific to *CCT2* (CCT2-F and CCT2-R), *HDAC4* (HDAC4-F and HDAC4-R), *HTATIP* (HTATIP-F and HTATIP-R), *KIAA0828* (KIAA0828-F and KIAA0828-R), and *RPS6KA6* (RPS6KA6-F and RPS6KA6-R), respectively, was observed from RNA derived from HMF3AEco^{R} cells incubated at 33.5°C (**Figure 3.19B**, lane 1), relative to HMF3AEco^{R} cells incubated at 39.5°C for 7 days (**Figure 3.19B**, lane 2).

3.2.6.7 Knockdown of HTATIP by ShRNA

To investigate the possibility that these candidate genes played a functional role in the HMF3A conditional growth arrest, RNAi was used to target a representative of this screen that was clearly upregulated, namely HTATIP.

The pRetroSuper-HTATIP shRNA construct described by Berns and colleagues (**Figures 3.20A** and **B**; [Berns *et al*, 2004]) was prepared, as previously described, and the resultant construct, pRetroSuper-HTATIP, was introduced into HMF3A cells along with pRetroSuper-LaminA/C and pRetroSuper-p53. 10 μg of each shRNA construct was then introduced into HMF3AEco^{R} cells and used to generate polyclonal populations at 33.5°C, using the protocol described for pRetroSuper-p14^{ARF}. One duplicate culture was maintained under drug selection at 33.5°C, whereas selection was removed from the second duplicate culture, then shifted to 39.5°C for a further 7 days before RNA was extracted.

Semi-quantitative RT-PCR analysis, using *HTATIP*-specific primers (HTATIP-F and HTATIP-R), was used to analyse the expression of *HTATIP* in these RNA samples.

A

Name	Target Region	Target Sequence	Position in mRNA Sequence	G/C Content
HTATIP	ORF	GTACGGCCGTAGTCTCAAG	14153	57.9%

B

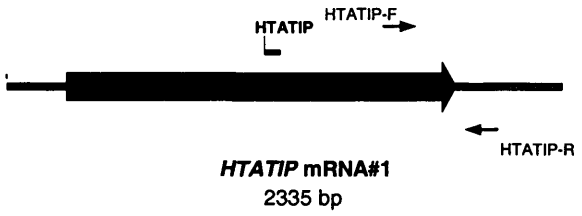

C

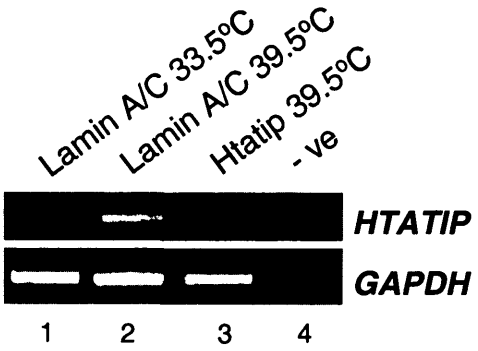

Figure 3.20: HTATIP ShRNA Silencing

A: ShRNA target sequence, as used by Berns and colleagues [Berns *et al*, 2004]; **B:** Position of the shRNA target sequence (indicated by a black bar), and primer binding sites (indicated by a black arrow) in *HTATIP* mRNA. A grey arrow indicates the ORF; **C:** Semi-quantitative RT-PCR using *HTATIP*-specific primers was used to analyse *HTATIP* expression in HMF3AEco^{R} cultures incubated at both 33.5°C and at 39.5°C for 7 days. *GAPDH* was the loading control.

A 263 bp PCR product that corresponded to *HTATIP* was observed from RNA derived from Lamin A/C shRNA-infected HMF3AEco^R cells incubated at 39.5°C for 7 days (**Figure 3.20C**, lane 2), but not from HTATIP shRNA-infected HMF3AEco^R cells incubated at 39.5°C for 7 days (**Figure 3.20C**, lane 3). This indicated that *HTATIP* mRNA was efficiently knocked-down in HTATIP shRNA-infected HMF3AEco^R cells.

3.2.6.8 Knockdown of HTATIP by ShRNA is Insufficient to Complement the Conditional HMF3A Growth Defect

Having demonstrated the effectiveness of HTATIP knockdown mediated by RNAi, pRetroSuper-HTATIP was tested in the HMF3A complementation assay.

10 μg of pRetroSuper-HTATIP, pRetroSuper-LaminA/C shRNA and pRetroSuper-p53 shRNA were introduced into HMF3AEco^R cells, using the protocol described for pRetroSuper-p14^{ARF}. Puromycin was removed from the culture medium and drug-resistant clones were directly shifted to 39.5°C. Following incubation at 39.5°C for a further 14 days, multiple healthy, growing colonies were observed in the positive control p53 shRNA-infected HMF3AEco^R culture, but not in the Lamin A/C shRNA-infected HMF3AEco^R culture or the HTATIP shRNA-infected HMF3AEco^R culture. A similar result was obtained in a duplicate experiment. This indicated that HTATIP knockdown alone was insufficient to overcome the conditional growth arrest of these cells. However, the activities of CCT2, HDAC4, KIAA828, and RPS6KA6 have yet to be analysed in this manner.

3.3 SUMMARY & DISCUSSION

Reconstitution of wt LT activity in HMF3A cells was sufficient to complement the conditional growth of these cells. This indicated that the HMF3A system could be used to dissect the pathways underlying the induction of telomere-independent cellular senescence by genetic complementation. An HMF3A complementation assay was developed and used to determine the relative functional activities of the p53 and pRb pathways in the loss of growth potential upon inactivation of LT. It was shown that the HMF3A conditional growth arrest could be complemented at the non-permissive temperature by ectopic expression of wt LT, E1A, E7, GSE p53 or an RNAi expression cassette directed against p53 or p21, but not by constitutive expression of DK or an RNAi expression cassette directed against $p14^{ARF}$, BTG2, GADD45A, HTATIP, PML or SFN (summarised in **Figure 3.23**). Therefore, it was concluded that abrogation of the p53 pathway, but not the pRb pathway, was sufficient to overcome the conditionality of these cells. However, the fact that ectopic expression of E1A or E7 was able to complement growth, unlike ectopic expression of DK or Bmi-1, suggested that these viral oncoproteins possessed functional activities, in addition to abrogation of pRb, that were necessary to permit the continued growth of these cells under non-permissive conditions.

3.3.1 Telomere-Independent Cellular Senescence is a P53-Dependent Process in the HMF3A System

The finding that p53 had a critical role in the induction of senescence in the HMF3A system was in accordance with other published studies of HDFs [Berns *et al*, 2004; Brown *et al*, 1997; Shay *et al*, 1991; Wei *et al*, 2001]. Moreover, it was in accordance with the observation that loss of p53 activity was sufficient to impair senescence and promote tumour progression in an *in vivo* model of prostate cancer [Chen *et al*, 2005].

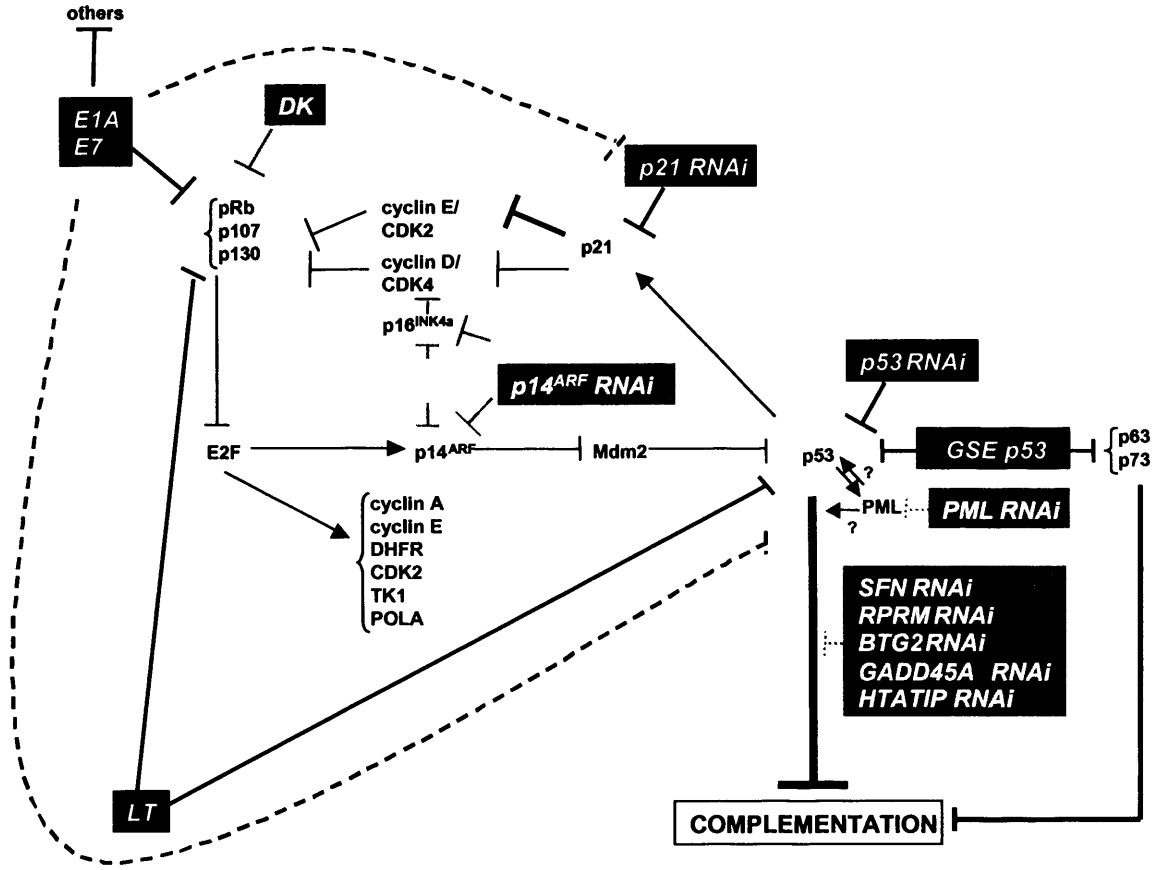

Figure 3.21: Summary of Inactivation of the P53 and PRb Pathways in the HMF3A System

Diagram to illustrate the p53 and pRb pathways and the methods used to inactivate components of these pathways in this study (denoted by coloured boxes). Reagents that were sufficient to complement the conditional growth arrest of HMF3A cells are denoted by black boxes whereas dark grey boxes denote reagents that were insufficient to complement the conditional HMF3A growth arrest. ShRNA targetting of $p16^{INK4a}$ was not successful, and is therefore denoted by a light grey box.

Inactivation of the p53 pathway has also been shown to be sufficient to bypass senescence in MEFs [Dirac and Bernards, 2003; Harvey *et al*, 1993]. Moreover, an analogous conditional fibroblast system in REFs, the tsa14 cell line, also suggested that inactivation of p53 was required to bypass the induction of an irreversible growth arrest; the tsa14 cell line was generated by infection of primary REFs with the thermolabile tsA58 LT, and LT mutants that lacked p53-binding activity were unable to overcome the irreversible growth arrest of these cells, unlike wt LT [Powell *et al*, 1999].

However, the results described here were not in agreement with studies that utilised a TRF2 inhibition model; de Lange and colleagues have used over-expression of a dominant-negative form of TRF2 ($TRF2^{\Delta B\Delta M}$) to study a process known as 'sudden telomere deprotection', where senescence occurs in the absence of telomere shortening ([Karlseder *et al*, 1999; Smogorzewska and de Lange, 2002; Stansel *et al*, 2001]; reviewed in [de Lange, 2002]). In addition to showing that wt LT expression was sufficient to bypass senescence induced in the TRF2 inhibition model, it was concluded that $p16^{INK4a}$ functioned in an additional fail-safe manner to p53 to induce senescence in the absence of a functional p53 pathway [Jacobs and de Lange, 2004; Smogorzewska and de Lange, 2002]. Therefore, the demonstration that abrogation of p53 activity alone was sufficient to complement the conditional HMF3A growth defect, was contradictory to the $TRF2^{\Delta B\Delta M}$ data that implied that both the p53 and pRb pathways must be inactivated.

The fact that the $TRF2^{\Delta B\Delta M}$ inhibition model represents a telomere-dependent system, unlike the HMF3A system, may help to reconcile the differences observed between these two systems. Moreover, the fact that different methods were used to measure the effects of p53 abrogation upon the induction of senescence may also be an important consideration.

To validate these findings, both hTERT and the p53 shRNA construct should be introduced directly into adult mammary fibroblasts and assessed for their ability to bypass the finite proliferative potential of these cells; it is hypothesised that hTERT and p53 inactivation will be sufficient to bypass this

process, in a similar manner to the combined activities of hTERT and LT [O'Hare *et al*, 2001].

As a caveat, however, it is possible that ectopic expression of hTERT and p53 may not be sufficient to bypass cellular senescence in this context, since there may be fundamental differences between immortalisation in primary cells, and maintenance of the immortal state (such as HMF3A cells grown under permissive conditions); for example, expression of an amino terminal LT mutant that retains p53-binding activity (*dl*1135), was sufficient to complement the growth of rat tsa14 cells, but was not able to immortalise REFS [Powell *et al*, 1999]. This indicated that LT functional activities, in addition to abrogation of p53, were required to initiate this process.

3.3.2 Inactivation of the PRb Pathway in the HMF3A System

Unlike p53, inactivation of the pRb pathway was technically difficult to achieve in the HMF3A system due to the existence of multiple pRb family members and the possibility that they exhibited functional redundancy. Consequently, a variety of reagents were used to determine the functional role of this pathway in the induction of the HMF3A growth arrest.

3.3.2.1 $P16^{INK4a}$ ShRNA-Targeting in the HMF3A System

ShRNA targeting was used to impair the negative regulatory activity of $p16^{INK4a}$, a CDKI that functions upstream of pRb. Unfortunately however, efficient $p16^{INK4a}$ knockdown could not be obtained by shRNA-targeting, even when two different shRNA constructs were utilised (namely p16A or p16#2). This finding was in contrast to those of others who have successfully achieved $p16^{INK4a}$ knockdown using identical, if not overlapping, target sequences for their $p16^{INK4a}$ shRNA constructs (for example, [Berns *et al*, 2004; Brookes *et al*, 2002; Bond *et al*, 2004; Narita *et al*; Wei *et al*, 2003]). As a result of

efficient $p16^{INK4a}$ knockdown, these studies concluded that downregulation of $p16^{INK4a}$ was not sufficient to prevent the induction of senescence.

The utilisation of alternative, more effective $p16^{INK4a}$ shRNA targets could have addressed this problem. However, the fact that only a limited region of the *INK4A* locus can be used to design shRNA constructs to specifically downregulate $p16^{INK4a}$, but not $p14^{ARF}$, renders this form of analysis unusable in the HMF3A system.

The reason for the discrepancy in $p16^{INK3a}$ knockdown efficiency in different HDF strains remains unclear. However it may reflect context-dependent activity since different HDF strains are known to exhibit different levels of intrinsic $p16^{INK4a}$ activity; for example, two commonly used HDF strains, WI-38 and BJ, differ greatly in their endogenous $p16^{INK4a}$ expression patterns [Itahana *et al*, 2003]. WI-38 cells express relatively high levels of $p16^{INK4a}$ in early passage, unlike BJ cells, and this has a profound effect upon the response of these two cells to abrogation of $p16^{INK4a}$ activity; for example WI-38 cells have been shown to senesce in response to telomere-dependent and -independent signals [Beausejour *et al*, 2003], whereas BJ cells have been shown to senesce only in response to telomere-dependent signals [Beausejour *et al*, 2003; de Magalhaes *et al*, 2002; Lorenz *et al*, 2001]. Consequently, the fact that $HMF3AEco^{R}$ cells readily expressed detectable levels of $p16^{INK4a}$ that did not subsequently rise upon incubation at the non-permissive temperature, and was tolerated without inducing premature senescence, indicate that HMF3A cells behave somewhat differently to WI-38 and BJ cells. Therefore, a possible explanation for the lack of growth complementation in the HMF3A system by $p16^{INK4a}$ silencing was that the level of $p16^{INK4a}$ knockdown obtained by pRetroSuper-p16#2 and pRetroSuper-p16A shRNA constructs was not sufficient to reduce $p16^{INK4a}$ levels below a threshold that was required to induce a physiological response, unlike the other HDF strains. Alternatively, the HMF3A cells may have been insensitive to $p16^{INK4a}$-negative regulation.

The different origins of the different fibroblast strains could explain this discrepancy; for example, HMF3A cells were originally derived from adult breast stromal fibroblasts, whereas WI-38 cells are derived from foetal lung fibroblasts, and BJ cells are derived from foreskin fibroblasts. Therefore, both the age and the tissue context of different cell lines derived from the same cell type may be important parameters for consideration when interpreting experimental data.

3.3.2.2 Bmi-1 Activity in the HMF3A System

The issue of context dependency may also be applicable to the analysis of Bmi-1 activity; it was hypothesised that ectopic Bmi-1 expression in the HMF3A system would reduce expression from the *INK4A* locus, as demonstrated in other HDF strains such as WI-38 HDFs [Itahana *et al*, 2003]. However, ectopic Bmi-1 expression had no effect upon $p16^{INK4a}$ expression in the HMF3A system. Therefore, this data supports the hypothesis that different HDF strains appear to exhibit differential activities in response to Bmi-1 abrogation [Itahana *et al*, 2003; Jacobs and de Lange, 2004].

One interpretation of this data is that endogenous $p16^{INK4a}$ activity precluded the functional activity of ecotopic *Bmi-1* expression in HMF3A cells and that $p16^{INK4a}$ negatively regulated Bmi-1 at the post-transcriptional level, perhaps by targetting Bmi-1 for degradation. In this model, active $p16^{INK4a}$ and $p14^{ARF}$ expression from the *INK4A* locus impaired the ability of Bmi-1 to target repressive PcG complexes to this locus, thereby inhibiting the induction of a heterochromatic process. Therefore, the epistatic ordering of events may be important in determining the effectiveness of exogenous Bmi-1 activity.

In support of this hypothesis, it is known that Bmi-1 functions during development to maintain cells in a replication-competent state until differentiation occurs. In this context, $p16^{INK4a}$ expression does not occur until after Bmi-1 activity is no longer required. Therefore, this process may

function as a putative tumour suppressive mechanism to limit the activity of Bmi-1 to actively dividing stem cells that do not express *p16^{INK4a}*. Indeed, the fact that endogenous *p16^{INK4a}* expression was readily detectable in the HMF3A system supports this hypothesis as it suggests that, in this context, exogenous Bmi-1 activity may not have been able to function as a transcriptional repressor. Again, the fact that HMF3A cells were originally derived from adult breast cells may be significant in terms of cell context. This may also help to explain why the introduction of Bmi-1 into other cellular systems was sufficient to impair p16^{INK4a} accumulation; simply put, *INK4A* activity must have been initially low in these settings.

3.3.2.3 Ectopic DK Expression in the HMF3A System

Since both p16^{INK4a} shRNA-targeting and constitutive Bmi-1 expression appeared to be functional inactivite in the HMF3A system, an alternative reagent was sought to specifically inactive the pRb pathway. Ectopic expression of a p16^{INK4a}-insensitive cyclin D1-Cdk4 construct, DK, represented one such reagent, yet expression of DK was unable to bypass the conditional HMF3A growth arrest. This finding was in accordance with other studies that have used HDFs to determine that DK activity is insufficient to bypass replicative senescence [Brookes *et al*, 2002; Wei *et al*, 2003]. Significantly, Wei and colleagues used the same DK construct, in addition to a functional p16^{INK4a} shRNA construct, to demonstrate that inactivation of p16^{INK4a} is insufficient to permit escape from replicative senescence. Moreover, ectopic expression of DK was also insufficient to bypass premature senescence induced by oncogenic Ras [Serrano *et al*; 1997; Wei *et al*, 2003]. These finding are also supported by evidence in MEFs [Krimpenfort *et al*, 2001; Sharpless *et al*, 2001].

3.3.2.4 Ectopic Expression of E1A and E7

In contrast to ectopic DK expression, however, introduction of E1A or E7 into the HMF3A complementation assay was sufficient to complement the growth of these cells. These findings are consistent with the demonstration that E1A expression is sufficient to bypass cellular senescence in primary IMR90 HDFs [Serrano *et al*, 1997; Narita *et al*, 2003].

The discrepancy between DK-, E1A- and E7-expressing HMF3A cells may be reconciled by the fact that these reagents do not function in the same physiological way to inactivate the pRb pathway. This hypothesis is consistent with that of Wei and colleagues [Wei *et al*, 2003] who used gene targeting of p53, p21 and pRb, in addition to ectopic expression of DK and $p16^{INK4a}$ RNAi, to conclude that p53, p21 and pRb acted in a linear genetic pathway (with pRb acting downstream of p53) to regulate entry into replicative senescence, and that $p16^{INK4a}$ formed a branch that entered at the level of pRb [Wei *et al*, 2003]. It should be noted that this model is also consistent with the senescence induction model proposed by Sharpless and DePinho [Sharpless and DePinho, 2005].

3.3.3 Possible Mechanisms by which E1A and E7 Bypass the Conditional HMF3A Growth Defect

It has yet to be demonstrated that the HMF3A system supports the Sharpless and DePinho senescence induction model, since the functional activity of the DK construct in the HMF3A system was not investigated; for example, the DK construct may not have been able to completely inactivate pRb activity to the same extent as E1A or E7 since the G_1 CDKIs could have functioned in a redundant manner ([Wei *et al*, 2003]. Therefore, it is

important that the phosphorylation status of pRb family members is analysed in DK-, E1A- and E7- expressing HMF3A cells.

It is also possible that E2F activity was not functionally equivalent in DK-, E1A- and E7-expressing HMF3AEco^R cells. For example, E2F may have been released from repressive pRb complexes in the presence of functional DK activity, but was not able to induce E2F-responsive genes due to the repressive chromatin organisation at E2F-taget gene promoters [Narita *et al*, 2003]. In contrast, E1A and E7 viral oncoproteins could have overridden the organisation of repressive chromatin structures to induce E2F-responsive genes, and this could have involved the activity of p300/CBP (reviewed in [Dimova and Dyson, 2005]). Consequently, CDK-independent regulation of E2F/pRb repressor complexes should also be addressed in these two settings; for example, ectopic expression of a p300-binding mutant of E1A could be used to assess the role of this protein in the induction of the conditional HMF3A growth arrest.

Similarly, it is possible that both E1A and E7, but not DK, could have targeted a number of other, additional cellular proteins, in addition to pRb and/or p300, to bypass senescence. The mechanism by which E1A and E7 could have achieved this is unknown, yet the observation that the HMF3A growth arrest was bypassed by inactivation of p53 and/or p21 suggested that inactivation of the p53 pathway was likely to be involved. This conclusion was in agreement with data derived from the immortalisation of REFs with a temperature sensitive mutant of p53 [Vousden *et al*, 1993]; Vousden and colleagues showed that both E1A and E7 were able to bypass the conditional growth arrest of these cells and they suggested that E1A and E7 were able to do so by modulating the activity of p53, without altering its conformation or stability. Quartin and colleagues also showed that activities mediated by the N-terminal region of LT could bypass the same conditional growth arrest [Quartin *et al*, 1994].

Neither E1A, nor E7, are known to bind directly to p53, yet there is evidence to suggest that they are both able to inactivate downstream

components of this pathway; for example, E7 has been shown to bind to and inactivate p21 [Helt *et al*, 2002]. However, there is no evidence of a similar interaction between p21 and E1A. However, p300/CBP, as described above, is a good candidate for this activity since it is involved in many transcriptional regulation processes by virtue of its endogenous HAT activity; for example LT, E1A and E7 have all been shown to interact with p300/CBP, and it has been implicated in the regulation of both p53 phosphorylation and acetylation status [Pearson *et al*, 2000; Pedeux *et al*, 2005; Webley *et al*, 2000].

Other possible candidates that may be affected by the activities of both E1A and E7 include p400 and PML. P400 is a SWI2/SNF1-related protein that functions as a negative regulator of *p21* transcription. It has been suggested that p400 functions in a p53-dependent process to negatively regulate the induction of premature senescence and it has also been shown to bind to E1A, as well as transcriptionally up-regulated by E1A [Chen *et al*, 2005; Fuchs *et al*, 2001]. PML promotes the formation of a complex between p53 and CBP and it has been shown that E7 may impair the ability of p53 to function as a transcriptional activator by either impairing the formation of this complex or recruiting it to a new substrate [Bischof *et al*, 2005; Massimi *et al*, 1997]. Furthermore, PML splice variant IV has been specifically associated with the induction of senescence [Bischof *et al*, 2005]. However, the observation that an effective shRNA targetted against all PML splice variants was insufficient to complement the growth defect of HMF3AEco^{R} cells indicated that this gene was unlikely to mediate the induction of senescence in these cells, at least, not by itself. To confirm this finding, RT-PCR should be performed using primers specific to PML splice variant IV.

3.3.3.1 Is Inactivation of the PRb Pathway Necessary, but Insufficient, to Bypass the Conditional HMF3A Growth Defect?

The ability of GSE p53 and shRNA constructs targeted against either p53 or p21 to bypass the conditional HMF3A growth defect indicate that

inactivation of the p53 pathway alone is critical for this process. However, the possibility that abrogation of the pRb pathway is also required to induce and/or maintain this process by acting downstream of p53 remains significant and should not be excluded. In this respect, Drayton and Peters [Drayton and Peters, 2002] have argued that there must be a potent selection pressure for the evolution of the $p16^{INK4a}$ pathway as it does not appear to play an obvious role in normal development. They also suggest that $p16^{INK4a}$ induction is likely to occur both *in vitro* (in response to stressful culture conditions) and *in vivo* during tumorigenesis. Moreover, there is much evidence to support the hypothesis that the pRb pathway is required to maintain a stable heterochromatic state upon the induction of senescence, such that it cannot be reversed by subsequent inactivation of p53 or pRb (reviewed in [Campisi, 2005]).

Therefore, the possibility that the pRb pathway must be inactivated to complement the HMF3A conditional growth defect needs further investigation; for example, if the pRb pathway is critically involved in the induction of the conditional HMF3A growth arrest, then ectopic expression of an E1A mutant defective for pRb-binding should not be sufficient to complement the growth of these cells.

3.3.4 Signalling Between the PRb and P53 Pathways in the HMF3A System does not Occur via $P14^{ARF}$

E2F has been shown to directly activate $p14^{ARF}$ in response to various oncogenic stimuli [Aslanian *et al*, 2004; Bates *et al*, 1998;DeGregori *et al*, 1997; Parisi *et al*, 2002; Zhu *et al*, 1999]. Since $p14^{ARF}$ also binds to Mdm2 and impairs the ability of Mdm2 to negatively regulate p53 activity, $p14^{ARF}$ provides a link between the pRb and p53 pathways [Dimri *et al*, 2000]. However, evidence from the HMF3A model system indicated that $p14^{ARF}$ did not act upstream of p53 to mediate bypass of the growth arrest as a functional

$p14^{ARF}$ shRNA construct was insufficient to complement the growth of these cells. Therefore, the link between the pRb and p53 pathways via E2F and $p14^{ARF}$ was probably not significant in the HMF3A system. Indeed, this conclusion is in accordance with the findings of both Brookes and colleagues [Brookes *et al*, 2002] and Wei and colleagues [Wei *et al*, 2001]. Wei and colleagues showed that in HDFs, Ras induced expression of both p21 and p16, but not $p14^{ARF}$; therefore, the induction of p21 appeared to be $p14^{ARF}$-independent. However, these findings were not in agreement with those of Dimri and colleagues [Dimri *et al*, 2000] who showed that HDFs deficient in $p14^{ARF}$ did not undergo senescence. The fact that $p14^{ARF}$ has been detected at very low levels in normal human cells may have precluded, to some extent, accurate analysis of $p14^{ARF}$ activity in these studies.

The HMF3A data was also in contrast to the substantial evidence linking the activity of $p19^{ARF}$ to the induction of senescence in mice; for example, the $p19^{ARF}$-p53 pathway has been shown to play a critical role in the induction of senescence in MEFs [Harvey *et al*, 1993; Kamijo *et al*, 1997] and a functional screen showed that down-regulation of $p19^{ARF}$ was sufficient to rescue premature senescence [Shvarts *et al*, 2002]. Conversely, enforced expression of $p19^{ARF}$ was sufficient to induce cell cycle arrest in MEFs [Quelle *et al*, 1995]. Therefore, the differential activities of $p14^{ARF}$ in humans and and $p19^{ARF}$ in mice may be species- and/or cell type- specific [Brookes *et al*, 2002].

It was also possible that, upon the HMF3A temperature shift, E2F activity was able to induce p53 activation in the absence of $p14^{ARF}$ induction, similar to the activation of E2F in response to DNA damage and apoptosis [Lindstrom and Wiman, 2003; Tolbert *et al*, 2002; Tsai *et al*, 2002]. Indeed, it has been shown that the cyclin A-binding domain of E2F1 can directly interact with and stabilise p53 in response to DNA damage [Hsieh *et al*, 2002; Nip *et al*, 2001; Rogoff *et al*, 2002]. Such possibilities require further investigation in the HMF3A cells.

3.3.5 *E2F Activity in the Induction of Telomere-Independent Cellular Senescence in the HMF3A System Remains Unresolved*

These observations highlight the importance of analysing E2F activity in the HMF3A system. E2F activity has been suggested to function as a key determinant of cell cycle progression (reviewed in [Dimova and Dyson, 2005]) and there is much evidence to link E2F activity to senescence; for example, knockdown of DP1 (a cognate binding partner of E2F) by RNAi was shown to be sufficient to induce premature senescence [Maehara *et al*, 2005], whereas over-expression of E2F target genes, such as cyclin E and c-Myc, was sufficient to overcome an Rb family-induced growth arrest [Alevizopoulos *et al*, 1997; Lukas *et al*, 1997]. However, it has also been shown that over-expression of E2F is sufficient to induce senescence in primary HDFs [Dimri *et al*, 2000]. Moreover, it has been suggested that E2F activity is critical to induce senescence; for example, a number of pRb variants that are defective for E2F-binding and transcriptional repression retained the ability to promote senescence *in vitro* [Sellers *et al*, 1998]. Therefore, it is likely that the growth promoting activity of E2F is context-dependent.

One possible method to investigate the activity of E2F in the HMF3A system would be to ectopically express the activating E2Fs 1-3; if DK, E1A and E7 are functionally equivalently in their ability to activate E2F, then ectopic expression of E2Fs 1-3 will be insufficient to complement the growth defect of HMF3AEco^{R} cells under non-permissive conditions. However, ectopic expression of E2F is not without its inherent problems; for example, over-expression of E2F may result in the titration of cellular factors (such as pocket proteins) away from E2F-responsive gene promoters. This, in turn, may result in E2F-target gene de-repression. Moreover, the multiplicity of E2F variants, binding partners and divergent activities exhibited by individual E2F family members will complicate the correct interpretation of experimental data, and these issues remain unresolved.

3.3.6 *Telomere-Independent Cellular Senescence is a P21-Dependent Process in the HMF3A System*

The fact that down-regulation of p21, like p53, by shRNA was sufficient to bypass the HMF3A conditional growth defect was in accordance other studies of HDFs [Berns *et al*, 2004; Brown *et al*, 1997; Wei *et al*, 2003]. Moreover, microarray analysis has shown that ectopic expression of *p21* in human fibrosarcoma cells is sufficient to induce changes that are known to occur in senescent cells, such as the up-regulation of *PAI-1* and other extracellular matrix components and secreted proteases [Chang *et al*, 2000], whereas down-regulation of a large number of genes involved in DNA replication, repair and mitosis by ectopic *p21* expression has also been described [Chang *et al*, 2000; Harvat *et al*, 1998].

In the HMF3A system, it was likely that p21 functioned in a p53-dependent process to induce the irreversible growth arrest, since p21 levels were significantly down-regulated in HMF3AEco^R cells complemented for growth at 39.5°C by the introduction of either p53 shRNA or GSE p53. However, the possibility that senescence occurred in a p53-independent process could not be excluded. Indeed, Chen and colleagues [Chen *et al*, 2005] used two immortalised human model systems that lacked functional p53 activity to demonstrate that the up-regulation of p21 in response to Chk2 induction was sufficient to induce senescence.

3.3.7 *Is P21 a Critical Mediator of Telomere-Independent Cellular Senescence in the HMF3A System?*

As described above, the HMF3A data suggested that p21 played an important role in the induction of an irreversible growth arrest. However, there appeared to be a fundamental difference between the HMF3A system and an analogous system developed by Berns and colleagues [Berns *et al*,

2004], since the shRNA p21 construct utilised in this study was not effective in the HMF3A system. The sequence targetted by the p21 RB shRNA construct did not encompass a known SNP (as indicated by analysis of the SNP database [dbSNP] at NCBI), and was reminiscent of the inactivity observed with the p16#2 shRNA construct. It was possible, therefore, that the relative inefficiency of the p21 RB and p16#2 shRNA constructs in the HMF3A system were indicative of an as yet unknown parameter that affected the efficiency of knockdown mediated by RNAi.

The design and utilisation of two independent functional shRNA constructs targetted against the same gene should have ruled out off-target RNAi effects. However, this was not achieved in the HMF3A system as only 1 functional p21 shRNA target was identified from 9 different constructs. Yet, the fact that the only effective p21 shRNA construct, namely pRetroSuper-p21F, targets the 3' UTR of *p21* provides an opportunity to conclusively demonstrate that p21F is a *bone fide* p21 shRNA construct, since constitutive expression of the wt *p21* ORF in HMF3AEco^R cells should not be targetted for degradation; therefore, reintroduction of the *p21* cDNA sequence into HMF3AEco^R cells complemented for growth under non-permissive conditions by p21F shRNA expression should be sufficient to irreversibly arrest the growth of these cells.

3.3.8 Inactivation of P21 Alone is Critical, but Insufficient, to Bypass the Conditional HMF3A Growth Defect

It is likely that p21 plays a critical role in the induction of telomere-independent cellular senescence in the HMF3A system, however, it is very unlikely that p21 activity alone is sufficient to mediate the irreversible growth arrest as there is much evidence to suggest that p21 is induced in normal cycling cells upon activation of G_1 phase checkpoint arrest, which is a reversible growth arrest [Khan and Wahl, 1998; Medema *et al*, 1998]. Therefore, signalling processes in addition to p21 activation, must occur for

senescence to be induced, rather than a transient G_1 phase growth arrest. Moreover, it is likely that the critical mediators of this process are downstream targets of p53, since abrogation of p53 in the HMF3A system was sufficient to complement the growth of these cells.

This hypothesis is supported by analysis of the HMF3A data; for example, inactivation of the pRb pathway by DK should have acted as a sink for p21 and functioned in a similar manner to the p21 shRNA construct, yet growth complementation was not observed. However, it could be argued that constitutive expression of DK construct in this setting did not constitute a physiologically accurate model of normal cell behaviour. Alternatively, *p21* and/or $p16^{INK4a}$ expression levels may have to be sufficiently inactivated to elicit a phenotypic response. Therefore, further experimental analysis is required to address this issue; one possible method would be to infect human mammary fibroblasts with hTERT and the p21 F shRNA construct and determine whether this is sufficient to bypass the replicative lifespan of these cells.

3.3.9 Models for P21-Dependent Induction of Telomere-Independent Cellular Senescence in the HMF3A System

Two putative models may explain how senescence is induced in the HMF3A system by p21 activity.

The first model proposes that the cellular context may be important in determining the physiological response to p21 activation and that a critical threshold of CDKI activity must be exceeded before p21 is able to activate critical downstream effectors of senescence (**Figure 3.22A**). P21 activity in this context may differ from its role in mediating a temporary growth arrest in normal cycling cells by virtue of the fact that cycling cells will not be exposed to the same milieu of CDKI activities as those about to undergo senescence. Moreover, p21 expression has been shown to peak in senescent cells [Noda *et al*, 1994].

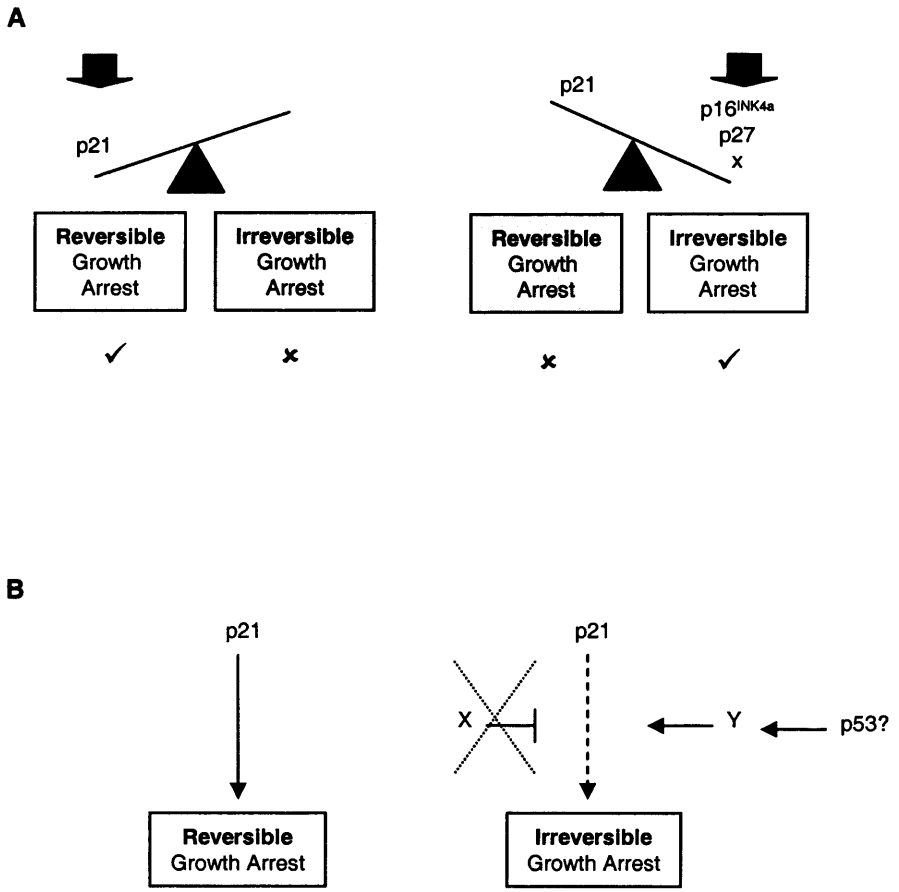

Figure 3.22: Modelling P21-Mediated Telomere-Independent Cellular Senescence

Two models for p21-mediated telomere-independent cellular senescence in the HMF3A system.

A: The first model hypothesises that the cellular context determines the physiological response to p21 activation. Under normal cell-cycling conditions, p21 activation induces a reversible growth arrest (left). However, upon the induction of senescence, the combined activities of p21 and additional negative growth regulators results in an irreversible growth arrest (right); **B:** The second model hypothesises that an as yet unknown factor (or factors) is (are) required for p21 to induce senescence. Again, under normal cell-cycling conditions, p21 activation induces a reversible growth arrest (left). However, upon the induction of senescence, an unknown factor (or factors) is (are) transcriptionally activated in order for p21 to mediate the irreversible growth arrest (right). Alternatively, a negative regulator (or negative regulators) of this process is (are) transcriptionally repressed.

There is also substantial evidence that p21 exhibits promiscuous activity as a CDKI. Therefore, it is possible that p21 targets unconventional cellular proteins for inactivation and/or modification to mediate this process. The cumulative effect would be the activation of genes critical for executing the induction of senescence.

This hypothesis is supported by the cell cycle model proposed by Sherr and McCormick [Sherr and McCormick, 2002]. Here, the authors described a model whereby the fluctuating expression levels of p21, p27, cyclin D and cyclin E form a complex and coordinated regulation of cell cycle progression and where p21 functions upstream of the pRb pathway; during G_0 (when cyclin D levels are low), p27 suppresses the activity of cyclin E-CDK2 [Blain *et al*, 1997; LaBaer *et al*, 1997; Soos *et al*, 1996]. However, up-regulation of cyclin D1 and association with CDK4 during late G_1 phase acts as a sink for p27 such that cyclin E-CDK2 is activated. In turn, cyclin E-CDK2 inactivates p27 in a negative feedback loop [Sheaff *et al*, 1997; Vlach *et al*, 1997], thereby activating cyclin D1-CDK4 and leading to the subsequent inactivation of pRb.

This model implies that low levels of p21 activity promote the formation of cyclin E- and cyclin D-associated complexes, rather than inactivates them [Alt *et al*, 2002; Blain *et al*, 1997; LaBaer *et al*, 1997; Muraoka *et al*, 2002] and that senescence is induced only when the up-regulation of p21 upsets this complex signalling balance.

This hypothesis is supported by the findings of Wei and colleagues, who concluded that as p21- or $p16^{INK4a}$ -deficient HDFs only exhibited a limited lifespan extension, the remaining CDKI activity was insufficient to inhibit all G_1 phase CDKs [Wei *et al*, 2003].

There is also increasing evidence to suggest that p21 possesses multiple activities, in addition to its role as a CDKI. Therefore, it is possible that these multiple activities are important to induce senescence; for example, there is evidence to suggest that p21 can regulate transcription as p21 contains a bipartite nuclear localisation signal (NLS) located between amino acids 140-

153 and can functionally co-operate with p300/CBP to enhance NF-κB target gene expression [Perkins *et al*, 1997]. P21 has also been shown to repress transcription when fused to GAL4 DNA-binding domain, independently of its ability to function as a CDKI [Delavaine and La Thangue, 1999] and has been shown to interact with several transcription factors involved in cell cycle control, such as E2F and c-Myc [Delavaine and La Thangue, 1999; Kitaura *et al*, 2000].

The HMF3A data does not support this hypothesis, however. For example, inactivation of the pRb pathway by DK should have acted as a sink for p21 and reduced the overall levels of CDKI activity in these cells, however, DK expression was insufficient to bypass the conditional HMF3A growth arrest. Moreover, $p16^{INK4a}$ expression was readily detectable in $HMF3AEco^{R}$ cells at both the permissive and non-permissive temperature; therefore, according to the model of senescence induction, $p16^{INK4a}$ should have been expressed at sufficient levels to promote the dissociation of p21 from cyclin D-Cdk4/6 complexes such that senescence would have been induced under both permissive and non-permissive conditions [McConnell *et al*, 1999; Mitra *et al*, 1999; Parry *et al*, 1999]. However, this observation could also be explained by the possibility that $p16^{INK4a}$ was functionally impaired in HMF3A cells; for example, by mutation.

These observations do not exclude the possibility, however, that p21 signalling via cyclin E-CDK2 and/or other, as yet unknown, targets may be more physiologically relevant to the induction of the conditional HMF3A growth arrest; for example, p27 may be redistributed upon the induction of the irreversible growth arrest. There is also some evidence that CDK2 activity may be critical in this process; for example, CDK2 has been shown to be down-regulated upon senescence in some HDF strains [Lucibello *et al*, 1993; Morisaki *et al*, 1999; Wyllie *et al*, 2003] and p53 has been shown to repress CDK2 both transcriptionally [Xie *et al*, 2003] and at the level of translation [Freedman and Folkman, 2005]. Therefore, p27 and cyclin E-CDK2 activity should be assessed in the HMF3A system.

The second model for p21-mediated induction of telomere-independent cellular senescence proposes that the functional activity of as yet uncharacterised protein(s) is (are) required to modify the cellular response to p21 activation. Alternatively (or in addition to this process), negative regulators must be inactivated (**Figure 3.22B**). It is likely that these modification factor(s) is (are) direct downstream targets of p53, as indicated by the analysis of p53 inactivation in the HMF3A system. It is also possible that these factors function by directly altering the functional activity of p21.

This second model is analogous to the p53 model of activity in the induction of a reversible growth arrest, senescence or apoptosis (reviewed in [Vousden and Lu, 2002]); for example, ING2 was identified as a member of a family of proteins that regulate p53 by modulating its acetylation status and was identified as a gene that specifically enhanced the senescence promoting activity of p53 [Pedeux *et al*, 2005]. In support of this hypothesis, a senescence rescue screen in MEFs identified Bcl6, a transcriptional repressor that is capable of sequestering p21 activity, as a positive hit [Shvarts *et al*, 2002]. It may, therefore, be of interest to assess the functionality of modifier genes such as these in the HMF3A system.

Both of these models may be reconciled, however, by the possibility that p21 stabilisation increases upon the induction of senescence. A recent study indicated that, despite the well documented transcriptional activation of p21 by p53, this did not necessarily result in an increase in stable p21 protein levels [Jascur *et al*, 2005]; Jascur and colleagues concluded that, for p21 protein levels to increase, both transcriptional activation and stabilisation of p21 by WISP39 and Hsp90 was required. Therefore, this finding suggests a model where the combination of novel factors is required to stabilise p21 such that p21 levels exceed a certain threshold to induce senescence.

Similarly, both of these models are consistent with the hypothesis that p21 activity is not required to maintain the senescence state; for example, *p21* expression levels have been shown to be transiently induced upon the induction of senescence, yet down-regulated in long-term senescent cells

[Stein and Dulic, 1998]. Therefore, by associating with as yet unknown cellular factors, p21 may activate downstream effectors to induce this process. Indeed, Zhang and colleagues have suggested that p21 activity may be required to induce permanent epigenetic changes but, once these are initiated, the permanent changes are sufficient to mediate stable transcriptional repression and, consequently, the senescent state [Zhang *et al*, 2005].

4. Identification of Novel Senescence-Associated Genes by Microarray Analysis

4.1 OBJECTIVES

The aim of this chapter was to identify novel genes and signalling pathways causal to the induction of cellular senescence. It was hypothesised that the activity of critical mediators of senescence would be abrogated in all cells that were able to bypass this process. Consequently, the generation of multiple growth-complemented HMF3A cultures, as described in **Chapter 3**, presented an opportunity to investigate this.

Gene expression profiling by cDNA microarray analysis was used to compare the transcriptome of irreversibly-arrested HMF3AEco^{R} cells incubated at the non-permissive temperature for 7 days, to HMF3A cells complemented for growth at the non-permissive temperature by expression of wt LT, E1A, E7, GSE p53 and p53 shRNA. Genes that exhibited significantly differential expression upon the induction of the irreversible growth arrest yet exhibited common expression profiles in all 5 conditions of growth complementation were used as a basis to identify putative genes involved in the induction of senescence.

Upon verification of the expression data by real-time PCR, the functional activity of each candidate gene was further analysed using the HMF3A complementation assay.

4.2 RESULTS & DISCUSSION

4.2.1 Rationale for Using Microarray Analysis

The Hanahan and Weinberg model of tumour development hypothesises that a limited, but essential set of alterations are required for the onset of tumorigenesis; namely, self-sufficiency in growth signals, insensitivity to anti-growth signals, evading apoptosis, limitless replicative potential, sustained angiogenesis, and tissue invasion and metastasis [Hanahan and Weinberg, 2000]. The authors state that most, if not all, cancers will have acquired these capabilities during their development; yet different genes may be inactivated in different ways, to achieve the same endpoint.

One of the acquired capabilities described by Hanahan and Weinberg is limitless replicative potential. Bypass of senescence may be considered one possible mechanism to acquire limitless replicative potential; therefore, HMF3A cells complemented for growth under non-permissive conditions represented an *in vitro* example of this. Consequently it was hypothesised that the critical effectors that induced the irreversible growth arrest in the HMF3A system would be inactivated in all growth complemented HMF3A cells, regardless of the precise molecular mechanism used to achieve growth complementation. Moreover, it was considered likely that these factors would be components of the p53 pathway, as indicated by the findings presented in **Chapter 3**.

HMF3A cultures complemented for growth under non-permissive conditions by expression of wt LT, E1A, E7, p53 shRNA and GSE p53 represented valuable resources with which to test this hypothesis and investigate the molecular basis of the downstream signalling pathways that induce senescence.

Many experimental techniques were applicable for this investigation, including those that assessed both gene and protein expression patterns; for example, gene expression profiling by microarray analysis or two-dimensional

difference gel electrophoresis (2D-DIGE), respectively. Experience of performing 2D-DIGE in the laboratory indicated that this technique was relatively insensitive at detecting significant changes in protein expression, unlike gene expression profiling. Furthermore, the rapid evolution in the development of microarray platform technologies over recent years and the unbiased nature of the analysis meant that gene expression profiling represented an attractive experimental regimen with which to assess the putative role of many novel genes in this process. Moreover, the complexity of human replicative senescence and the hypothesis that many genes are involved in the induction of this process has led to the application of this technique in numerous studies involving senescent HDFs (for example, [Cristofalo *et al*, 1998; Shelton *et al*, 1999]).

A major advantage in applying microarray analysis to the HMF3A system, unlike these other studies, however, was the rapid and synchronous nature of the conditional growth arrest. This meant that changes that occurred within the transcriptome during this process were likely to be directly relevant to the senescence response, as verified in our previous findings [Hardy *et al*, 2005].

4.2.2 Microarray Resources

To perform the microarray analysis, a 10K high-density human cDNA microarray developed by the LICR/CRUK microarray consortium (version Hver 1.3.1) was utilised. This microarray platform is representative of approximately 6000 unique human genes, as determined by the Human Genome Sequencing Project, and consists of 9932 gene-specific PCR products robotically spotted onto a glass slide by covalent linkage. Quantification of gene expression is calculated by measuring the intensity of Cy3- and Cy5-labelled cDNA samples competitively hybridised to the microarray slide, since the intensity of labelling is directly proportional to the relative abundance of mRNA (**Figure 4.1A**).

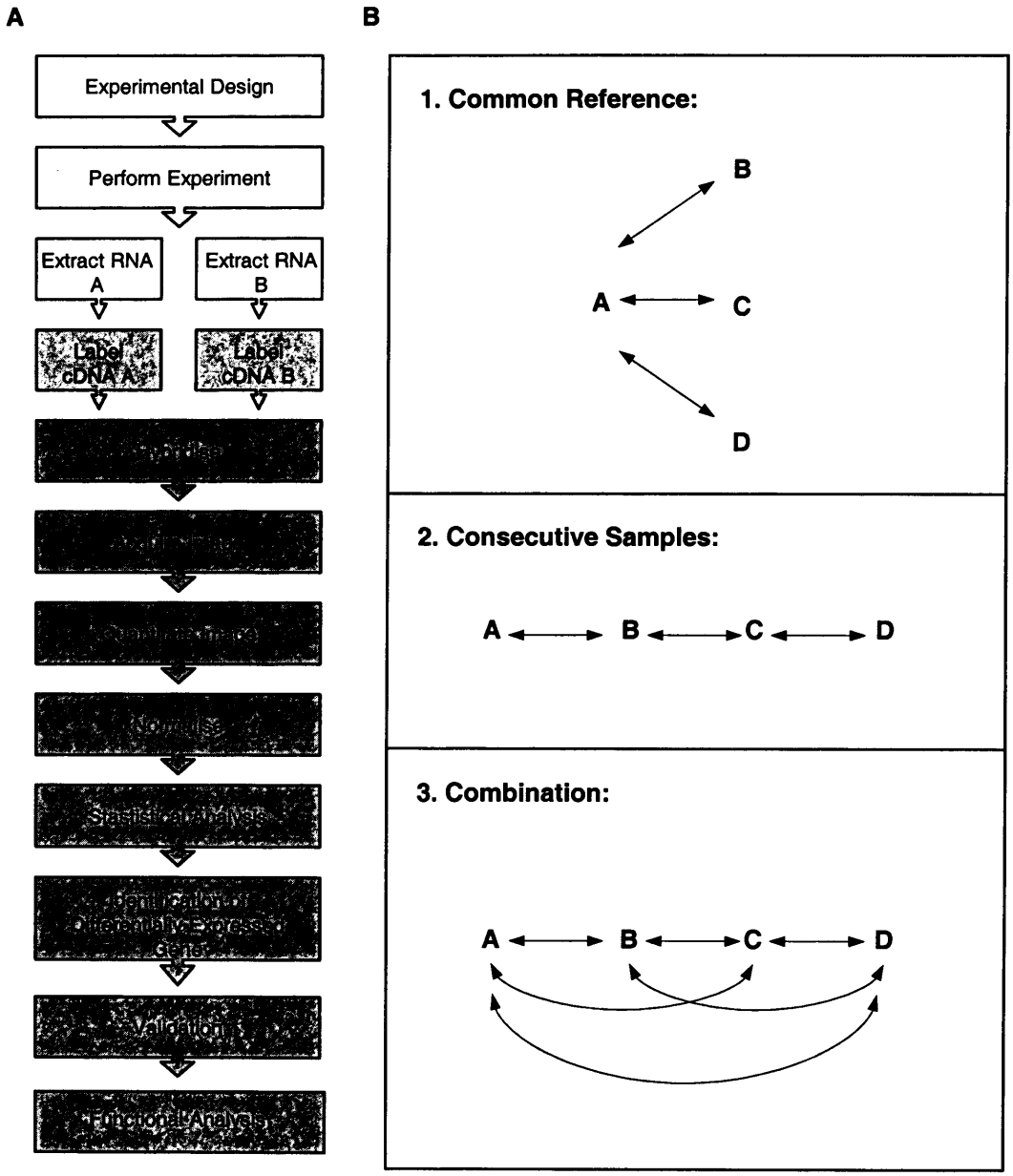

Figure 4.1: Microarray Experimental Design and Process

A: Flow chart depicting the microarray experimental process used in this study; **B:** Illustration of different possible micorarray experimental designs.

4.2.3 Microarray Experimental Design

It was important to utilise an appropriate experimental design to ensure the maximal amount of information was obtained from the microarray data (reviewed in [Larkin *et al*, 2005]). In this respect, possible designs included direct comparison, reference sample and loop configurations (**Figure 4.1B**). Since the aim of this experiment was to identify genes that exhibited significantly differential regulation upon the onset of the irreversible growth arrest, whilst simultaneously exhibiting significantly differential regulation in cultures that were complemented for growth under non-permissive conditions, a reference sample design, where RNA derived from HMF3A cells cultured at 33.5°C was used as the reference, was considered the most suitable as it enabled any two samples to be compared with equal efficiency (**Figure 4.2A**).

There were inherent disadvantages associated with the indirect nature of the comparisons used in this process, however; for example, technical variation was likely to have increased, greater quantities of RNA were required, and the number of microarrays required to be performed were also increased. Yet, the fact that neither the quantity of RNA derived from HMF3A cultures complemented for growth under non-permissive conditions, nor the availability of microarray slides was limiting argued that this form of experimental analysis was appropriate.

4.2.4 Sources of Variability

It was also important to address the issue of variability in the design of the microarray experiment in order to obtain biologically relevant and reproducible microarray data.

The clonal nature of the HMF3A system limited, to some extent, the experimental error that could have occurred as a result of biological variability.

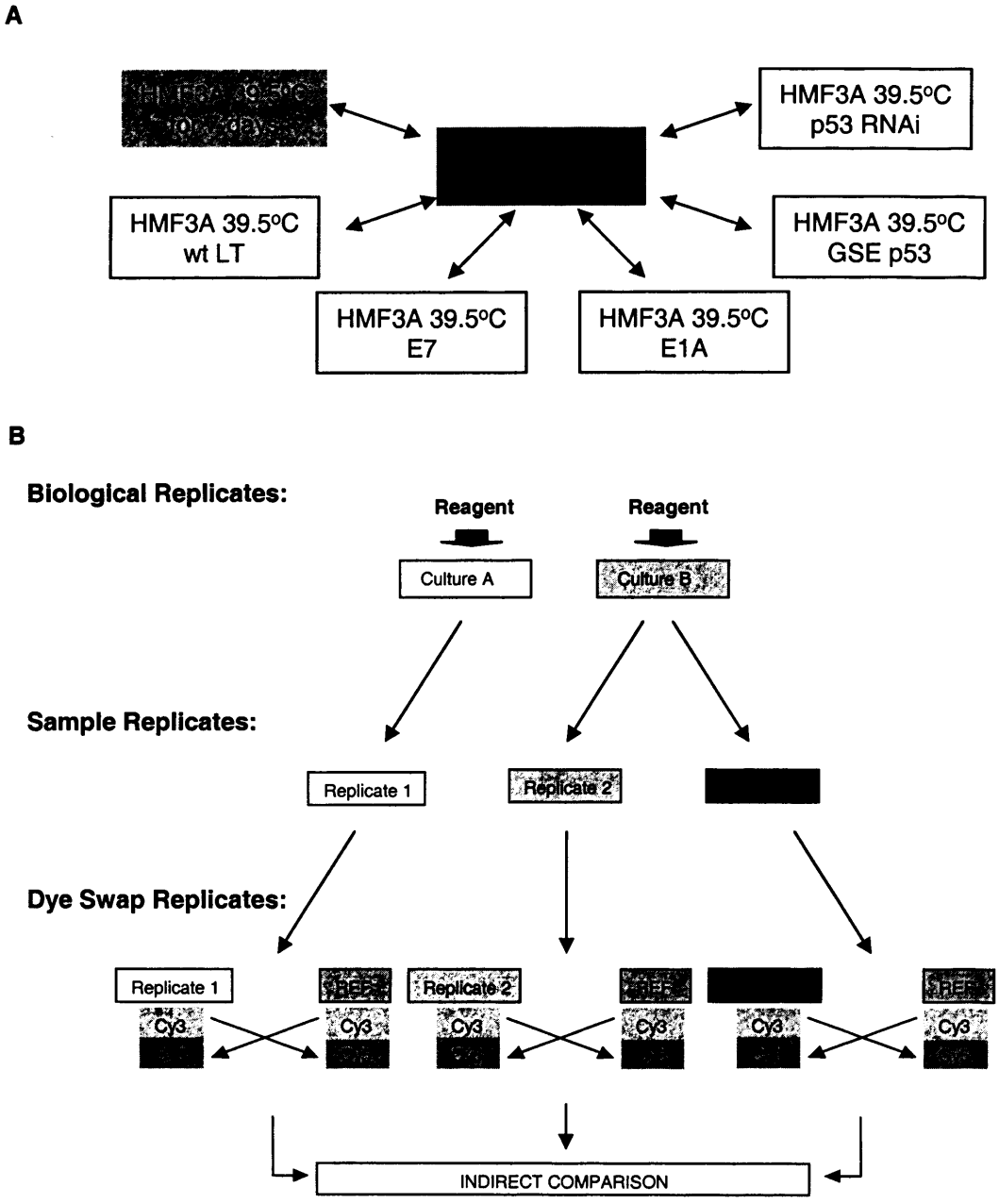

Figure 4.2: HMF3A Microarray Analysis

A: Reference sample experimental design used for the HMF3A microarray analysis. RNA derived from HMF3A cells growth at 33.5°C represents the reference sample; **B:** The strategy used to minimize the different sources of variability in this experiment.

However, to further minimise sources of technical variability, triplicate samples of each experimental condition were analysed, as suggested by Lee and colleagues [Lee *et al*, 2000]. Accordingly, triplicate RNA samples were extracted from two-independently generated HMF3A cultures complemented for growth under non-permissive conditions. Reciprocal-labelling experiments were utilised to address the issue of variability resulting from the use of two different dyes to label the cDNA samples; for example, differences may have occurred between the efficiency of dye labelling, hybridisation and detection (**Figure 4.2B**). Therefore, a total of 6 microarrays were performed for each experimental condition analysed in this study.

4.2.5 Microarray Procedure

To perform the microarray procedure, total RNA was derived from HMF3A cells incubated at 33.5°C and used to prepare the reference RNA sample. RNA was extracted from multiple HMF3A cultures using Trizol (Invitrogen), pooled, then subdivided into 50 μg aliquots, frozen and used once for each microarray experiment to ensure that it was not subject to multiple rounds of freeze-thaw cycles. RT was then performed, during which, two different labelling dyes, namely Cy3 and Cy5, were incorporated into the resultant cDNA products. For each microarray slide, cDNA representative of the reference sample and one of the condition variables was compared. Equal proportions of the cDNA samples were then mixed and used to perform a competitive hybridisation reaction to the microarray slide using the method developed and described by the Sanger/LICR/CRUK microarray consortium (see http://www.sanger.ac.uk/Projects/Microarrays/arraylab/methods.shtml; summarised in **Figure 4.1B**).

Since the relative intensity of fluorochrome activity for each microarray spot was directly proportional to the relative abundance of hybridised cDNA, the signal intensity of Cy3 and Cy5 probes for each spot was captured using a scanner. ScanArray software was used to measure the

intensity of fluorescence for each dye at their respective wavelengths and photomultiplier tube (PMT) gain settings were adjusted to balance the overall intensities between the two channels and to ensure that that the settings did not exceed saturation.

The resultant hybridisation data was then quantified using QuantArray software. The scanned microarray images were measured in terms of spot detection values and background values by employing a histogram method. Spots that appeared obscured, for example by dirt or air bubbles, were flagged during this process such that they were discarded during subsequent analysis steps (see later). The resultant data was then normalised using total intensity normalisation to balance the individual hybridisation intensities of the two channels. Using this method, it was assumed that the mean intensity of hybridisation across all spots did not change. The normalised data was then transformed using logarithmic base 2 of the Cy3:Cy5 ratio to enable up- and down-regulated genes to be represented on a linear scale. Locally weighted linear regression (LOWESS) was then performed as a final normalisation procedure to remove intensity-dependent effects that occurred with low-intensity spots displayed on the logarithmic base 2 scale [Yang *et al*, 2002]. Finally, the data was filtered by discarding the information provided by spots that were flagged in 3 or more of the 6 microarray slides. This procedure was designed to increase the confidence in subsequent statistical analyses.

As a result, the expression values that were obtained from this procedure were representative of the relative gene expression of samples grown at 39.5°C, compared to the reference sample grown at 33.5°C.

4.2.6 Statistical Analysis of Microarray Data

A statistical method that has been specifically designed to analyse microarray data, Significance Analysis of Microarrays (SAM; version 1.12; http://www-stat.stanford.edu/~tibs/SAM/; [Tusher *et al*, 2001]) was used to identify significantly differentially expressed genes from the expression

profile data generated in this study. SAM is a permutation-based method that measures the strength of the relationship between gene expression and the experimental condition by repeatedly scrambling the data sets between different experimental conditions so that *t*-test values for each gene permutation can be calculated. As a result, SAM calculates significant changes in gene expression in terms of a False-Discovery Rate (FDR or q-value), a value denoting error that reflects the probability that a gene is incorrectly identified as being significantly differentially expressed. As such, it should be stated that in this microarray study, a FDR of 5% or less was used, except where indicated.

One-class, two-class (unpaired) and multi-class SAM was used for these analyses; one-class SAM tested whether the mean gene expression of a condition differed from zero (ie exhibited a significant change in gene expression upon the temperature shift), two-class (unpaired) SAM was used to compare the expression profiles of two different conditions, and multi-class SAM was used to compare the expression profiles of more than two different conditions.

4.2.6.1 Global Transcriptional Changes that Occur Upon the HMF3A Temperature Shift

Initially, the microarray data was analysed using SAM to identify global transcriptional changes that occurred upon the temperature shift. One-class SAM was used to compare the expression profile of HMF3A cells shifted from the permissive to the non-permissive temperature for 7 days and, as a result, 246 and 404 genes were identified as being significantly up- or down-regulated upon the temperature shift, respectively (**Supplementary Figures S4** and **S5**).

4.2.6.2 Non-Specific Transcriptional Changes that Occur Upon the HMF3A Temperature Shift

To account for, and exclude, the non-specific transcriptional changes that occurred during the temperature shift, one-class SAM was used to identify genes that were significantly differentially expressed in HMF3A cells that expressed wt LT at 39.5°C, relative to HMF3A cells grown at 33.5°C. The basis of this comparison was the fact that both culture conditions exhibited wt LT activity; consequently, any statistically significant changes that were observed between these two samples were likely to represent non-specific temperature-sensitivity effects and/or leakiness of the conditional system.

It should be noted that a relatively stringent FDR value (≤ 2) was employed in an attempt to minimise the risk of discarding true-positives from the data set. This was a particularly important consideration as all consequent microarray data analyses described in this chapter disregarded the genes identified in this manner. Upon this basis, 77 and 144 genes were identified as being significantly up- or down- regulated upon the temperature shift, respectively (**Supplementary Figures S6** and **S7**). These genes included *p21* [Noda *et al*, 1994] and *SERPINE1* [West *et al*, 1996], two genes known to be up-regulated upon senescence (**Table 4.1**). However, these findings were in accordance with our previous findings [Hardy *et al*, 2005]; for example, *GSCN6*, *SSR4* and *TXNIP* similarly exhibited non-specific up-regulation in an analogous human mammary fibroblast cell line expressing wt LT and hTERT.

Clone ID	Gene	Score(d)	Numerator(r)	Denominator(s+s0)	q-value (%)
756630_A	*CDKN1A*	2.2247920	0.7506630	0.3374082	0.3529763
165952_B	*QSCN6*	1.6282249	0.4598973	0.2824532	1.7640331
666367_A	*SERPINE1*	2.8251800	0.5961055	0.2109974	0.3529763
136059_A	*SSR4*	1.8112815	0.3045188	0.1681234	0.5509293
152315_A	*SSR4*	1.6839477	0.3017661	0.1792016	1.2206217
298367_A	*TXNIP*	2.4705367	0.4718054	0.1909728	0.3529763
359721_A	*TXNIP*	2.4308885	0.5825555	0.2396471	0.3529763
299497_B	*TXNIP*	1.6750462	0.4901084	0.2925939	1.2206217

Table 4.1: Non-Specific Gene Expression Changes

A subset of the genes that exhibited significant, but non-specific, up-regulation in the HMF3A system upon temperature shift from 33.5°C to 39.5°C for 7 days. One-class SAM was used to identify statistically significant expression changes; Score (*d*): the *T*-statisc value; Numerator (*r*): the numerator of the *T*-statistic; Denominator (*s* + *s0*): the denominator of the *T*-statistic; q-value (%): the lowest FDR at which the gene is called significant.

4.2.6.3 Specific Transcriptional Changes that Occur Upon the HMF3A Temperature Shift

In an attempt to define the specific transcriptional changes that occurred upon the conditional HMF3A growth arrest, genes that exhibited non-specific expression changes upon the HMF3A temperature shift were subtracted from the gene sets that described the global expression changes that occurred upon the HMF3A temperature shift. Consequently, 177 and 298 genes were identified as being significantly up- or down- regulated, respectively (**Supplementary Figures S8** and **S9**), and these were inclusive of genes that were both causal and consequential to the HMF3A irreversible growth arrest.

Some of the genes identified, such as *IGFBP3*, have previously been shown to be induced upon senescence (**Table 4.2**; [Goldstein *et al*, 1993]). Many of the other up-regulated genes encoded metalloproteinases and collagenases and other extra-cellular matrix degrading enzymes that are involved in collagen turnover and are hallmarks of a senescent cell microenvironment, for example, *MTIB*, *MT1K*, *MT1X*, *MT1Y*, *MT3*, *TIMP3*, *CSPG2* and *FAP* [Millis *et al*, 1992;West *et al*, 1989]. Another large subset of up-regulated genes included those that encode for secreted factors, including *NRG1*, *FGF2*, *FGF7*, *VEGF*, *SCGF*, *CSF1*, *DAF*, *CD59* and *FTH1*.

It was also interesting to note that the majority of the transcriptional changes were representative of down-regulation events (**Table 4.3**) and included genes that had previously been identified as being significantly down regulated upon senescence, such as *CCNA2* [Stein *et al*, 1991] and *G22P1* [Salminen *et al*, 1997].

Clone ID	Gene	Score(d)	Numerator(r)	Denominator(s+s0)	q-value (%)
124554_A	*CSF1*	3.3358604	0.8115451	0.2432791	0.1147947
246147_A	*CSPG2*	3.9363946	0.8257784	0.2097804	0.1147947
310800_A	*DAF*	1.1575235	0.2629769	0.2271892	3.7008086
323181_A	*FAP*	1.3282128	0.2613827	0.1967928	0.6702531
665401_A	*FGF2*	3.2773093	0.9964529	0.3040460	0.1147947
365515_A	*FGF7*	2.1894704	0.4246861	0.1939675	0.1147947
1704018_B	*FTH1*	2.0329453	0.4566769	0.2246380	0.1147947
343563_A	*FTL*	1.5148032	0.2841200	0.1875623	0.1147947
196375_A	*IGFBP3*	5.2886789	1.3065807	0.2470524	0.1147947
266838_A	*IGFBP3*	5.2443098	1.2201963	0.2326705	0.1147947
356653_A	*IGFBP6*	3.7943612	0.8517660	0.2244821	0.1147947
299204_A	*IGFBP7*	4.9299530	1.1183687	0.2268518	0.1147947
232772_A	*MT1B*	3.5207820	0.7057613	0.2004558	0.1147947
66946_A	*MT1B*	2.9144909	0.7294288	0.2502766	0.1147947
202535_A	*MT1K*	3.8161016	0.7126796	0.1867559	0.1147947
240803_A	*MT1K*	3.6017229	0.7646988	0.2123147	0.1147947
202535_C	*MT1K*	3.4511303	0.7775184	0.2252939	0.1147947
274164_A	*MT1X*	3.4782330	0.7368786	0.2118543	0.1147947
293137_A	*MT1X*	3.4516814	0.6680150	0.1935332	0.1147947
111081_A	*MT1X*	3.3746754	0.7308715	0.2165754	0.1147947
297392_A	*MT1X*	3.2556901	0.7306515	0.2244229	0.1147947
2019011_A	*MT3*	1.7011090	0.4507703	0.2649861	0.1147947
269815_A	*NR4A3*	4.5272174	0.9919916	0.2191173	0.1147947
49439_B	*NRG1*	1.1728119	0.2443400	0.2083369	3.7008086
323346_C	*RGS3*	1.4890581	0.2883115	0.1936200	0.2114793
1627856_A	*SCGF*	1.9808436	0.4712348	0.2378960	0.1147947
249977_A	*TIMP3*	2.9730681	0.6266295	0.2107686	0.1147947
stSG89269	*TIMP3*	1.5941144	0.2856596	0.1791964	0.1147947
323783_B	*VEGF*	2.5578438	0.6839011	0.2673741	0.1147947

Table 4.2: Genes Specifically Up-Regulated Upon the HMF3A Temperature Shift

A subset of the genes that exhibited significant up-regulation in the HMF3A system upon temperature shift from 33.5°C to 39.5°C for 7 days. One-class SAM was used to identify statistically significant gene expression changes; Score (*d*): the *T*-statisc value; Numerator (*r*): the numerator of the *T*-statistic; Denominator (*s* + *s0*): the denominator of the *T*-statistic; q-value (%): the lowest FDR at which the gene is called significant.

Clone ID	Gene	Score(d)	Numerator(r)	Denominator(s+s0)	q-value (%)
427857_A	*CCNA2*	-2.7937249	-0.5285590	0.1891951	0.1147947
796474_A	*CDC2*	-2.8143519	-0.5435411	0.1931319	0.1147947
121716_D	*CDC25B*	-4.4466056	-0.6721728	0.1511654	0.1147947
785382_A	*CDC25B*	-1.9150084	-0.4941759	0.2580542	0.1147947
429755_A	*CDC25C*	-1.1228733	-0.1924010	0.1713470	2.5930212
264598_A	*CDK4*	-1.8793882	-0.3673538	0.1954646	0.1147947
124345_A	*CENPF*	-2.1270862	-0.3625689	0.1704533	0.1147947
784170_A	*CENPF*	-1.0270114	-0.2930007	0.2852945	3.7008086
358506_A	*COL16A1*	-1.2214940	-0.2766031	0.2264465	1.2451143
214997_A	*COL1A1*	-1.6035338	-0.3496424	0.2180449	0.1147947
298509_A	*COL1A1*	-2.8007483	-0.6628447	0.2366670	0.1147947
323321_A	*COL1A1*	-3.4062148	-0.7140276	0.2096249	0.1147947
359255_A	*COL5A2*	-3.8542479	-0.8593222	0.2229546	0.1147947
138991_A	*COL6A3*	-1.8211331	-0.3870435	0.2125289	0.1147947
127266_A	*FOXM1*	-2.2452769	-0.5462063	0.2432690	0.1147947
259115_A	*FOXM1*	-1.8793983	-0.3785349	0.2014128	0.1147947
stSG89294	*HMG17L1*	-2.9786371	-0.7344863	0.2465847	0.1147947
755378_A	*PRC1*	-4.0865420	-0.8077261	0.1976552	0.1147947
785707_A	*PRC1*	-4.8674222	-0.9673379	0.1987372	0.1147947
256425_A	*PSMB1*	-1.2507886	-0.2309135	0.1846143	0.6702531
1839895_A	*PSMB2*	-1.5141659	-0.2958663	0.1953989	0.1147947
290864_A	*PSMB2*	-1.4713791	-0.2776072	0.1886714	0.1147947
321823_A	*PSMB3*	-1.1479596	-0.2294990	0.1999191	1.8099168
321894_B	*PSMB3*	-1.3192227	-0.2326741	0.1763721	0.5408550
201275_A	*PSMB6*	-1.9554236	-0.3175377	0.1623882	0.1147947
30520_A	*PSMC3*	-1.7813368	-0.3736721	0.2097706	0.1147947
42744_A	*PSMC5*	-1.0978474	-0.2493394	0.2271166	2.5930212
43940_A	*PSMC5*	-1.6552036	-0.2682415	0.1620595	0.1147947
823598_A	*PSMD12*	-1.1280312	-0.2377652	0.2107789	2.5930212
298737_A	*PSMD8*	-1.2436315	-0.2174869	0.1748805	0.6702531
187848_B	*PSME3*	-1.6515298	-0.3102609	0.1878627	0.1147947
295286_A	*UBE2C*	-1.8672514	-0.3324552	0.1780452	0.1147947
758484_A	*UBE2C*	-1.1092758	-0.227078	0.2047083	2.5930212
769921_A	*UBE2C*	-1.0379475	-0.2476505	0.2385963	3.7008086

Table 4.3: Genes Specifically Down-Regulated Upon the HMF3A Temperature Shift

A subset of the genes that exhibited significant down-regulation in the HMF3A system upon temperature shift from 33.5°C to 39.5°C for 7 days. One-class SAM was used to identify statistically significant gene expression changes; Score (*d*): the *T*-statisc value; Numerator (*r*): the numerator of the *T*-statistic; Denominator (*s* + *s0*): the denominator of the *T*-statistic; q-value (%): the lowest FDR at which the gene is called significant.

Many of the other down-regulated genes including those that are required for cell cycle progression, cell proliferation and mitosis, were similarly identified in our original HMF3A microarray study [Hardy *et al*, 2005], such as *CDK4*, *CDC2*, *CDC25B*, *CDC25C*, *BUBR1*, *PRC1*, *FOXM1* and *UBE2C*. Down-regulation of a number of genes that encode proteosomal subunit components was also noted, namely *PSMB1*, *PSMB2*, *PSMB3*, *PSMB7*, *PSMB3*, *PSMB5*, *PSMB12*, *PSMB8*, *PSMB9*, *PSMB3*, and this finding was in accordance to that of Chondrogianni and colleagues [Chondrogianni *et al*, 2003] who identified a reduction in the expression level of catalytic subunits of the 20S proteosome and subunits of the 19S regulatory complex upon the induction of senescence.

4.2.6.4 Transcriptional Changes Associated with Wt LT Expression

Having identified the transcriptional changes that occurred upon the HMF3A conditional growth arrest, transcriptional changes that were causal to the growth-complementing activity of wt LT were investigated. Two-class (unpaired) SAM was used to compare the expression profiles of HMF3A cells irreversibly arrested at 39.5°C relative to HMF3A cells complemented for growth at 39.5°C by expression of wt LT. Genes that exhibited statistically significant differential expression were then subject to an additional filtering step whereby any gene that exhibited differential expression when the relative expression value did not cross the x-axis at y=1 was discarded. This filtration step was designed to remove genes that were significantly up-regulated upon the HMF3A temperature shift, when they already exhibited up-regulation at 39.5°C in growth complemented wt LT-infected HMF3A cells. In a reciprocal manner, genes that were significantly down-regulated upon the HMF3A temperature shift, when they already exhibited down-regulation at 39.5°C in growth complemented wt LT-infected HMF3A cells, were also removed from the data set, since they were unlikely to be causal to the HMF3A conditional growth arrest. As a result, 20 and 36 genes were

identified as exhibiting significant up- and down-regulation, relative to irreversibly arrested HMF3A cells incubated at 39.5°C, respectively (**Supplementary Figures S10** and **S11**).

Importantly, all the genes identified exhibited significantly differential gene expression patterns upon the HMF3A temperature shift. For example, *IGFBP3* exhibited significant up-regulation upon the HMF3A conditional growth arrest yet exhibited significant down-regulation in HMF3A cells complemented for growth at 39.5°C by expression of wt LT (**Table 4.4A**), whereas *PRC1* exhibited significant down-regulation upon the HMF3A conditional growth arrest yet exhibited significant up-regulation in HMF3A cells complemented for growth at 39.5°C by expression of wt LT. It was also important to note that multiple transcriptional changes were identified. This indicated that both the HMF3A system and the microarray experimental design utilised for this study were sensitive enough to identify putatively biologically relevant gene expression changes.

4.2.6.5 Transcriptional Changes Associated with E1A Expression

Expression changes that characterised the continued proliferation of HMF3A cells at 39.5°C by constitutive E1A expression were investigated. Two-class (unpaired) SAM was used to compare the expression profile of HMF3A cells that expressed E1A at 39.5°C against growth-arrested HMF3As incubated at 39.5°C for 7 days. Genes that exhibited statistically significant differential expression were again subject to filtering, using the protocol described for wt LT and, as a result, a total of 336 and 225 genes were identified as exhibiting significant up- or down- regulation upon the temperature shift, respectively. A comparison of these genes to those that were specifically up- or down- regulated upon the HMF3A temperature shift further refined the gene sets to 124 and 104 genes, respectively (**Supplementary Figures S12** and **S13**).

A

Clone ID	Gene	Score(d)	Numerator(r)	Denominator(s+s0)	Fold Change	q-value (%)
785707_A	*PRC1*	-4.3607106	-0.7210437	0.1653501	0.60537	0.7194245
755378_A	*PRC1*	-3.5751923	-0.5616180	0.1570875	0.67738	0.7194245
196375_A	*IGFBP3*	6.8838773	1.4755415	0.2143474	2.80723	0.7194245
266838_A	*IGFBP3*	6.2026905	1.3310898	0.2145988	2.51626	0.7194245

B

Clone ID	Gene	Score(d)	Numerator(r)	Denominator(s+s0)	Fold Change	q-value (%)
788174_A	*IFIT1*	1.6395911	0.8066453	0.4919796	2.04044	0.0855162
150355_A	*IFITM1*	5.0946173	1.5152118	0.2974143	2.89796	0.0447674
345996_A	*IFITM1*	4.8626472	1.5099362	0.3105173	2.86483	0.0447674
322180_A	*IFITM2*	4.8243066	1.4775783	0.3062779	2.82623	0.0447674
154387_A	*IFITM2*	4.6229761	1.4393208	0.3113407	2.75730	0.0447674
24033_A	*STAT1*	2.3260727	0.8259916	0.3551014	1.86327	0.0447674
26599_A	*STAT1*	2.1250257	0.9182531	0.4321139	2.02452	0.0447674

C

Clone ID	Gene	Score(d)	Numerator(r)	Denominator(s+s0)	Fold Change	q-value (%)
127266_A	*FOXM1*	-2.4772425	-0.5513849	0.2225801	0.69615	0.3354865
259115_A	*FOXM1*	-2.3025286	-0.3967856	0.1723260	0.76525	0.3354865

D

Clone ID	Gene	Score(d)	Numerator(r)	Denominator(s+s0)	Fold Change	q-value (%)
796005_A	*CDH11*	1.374288427	0.464172901	0.337755083	0.76127	4.6511628
31093_A	*CDH13*	2.149850567	0.700810265	0.325980920	0.63504	0.9900990
124554_A	*CSF1*	1.998821366	0.575213196	0.287776189	0.67075	0.9900990
380384_A	*CUL4B*	1.866286517	0.554936136	0.297347771	0.69289	0.9900990
665401_A	*FGF2*	2.199031680	0.731573136	0.332679671	0.59257	0.9900990
115383_A	*GADD45A*	1.335741341	0.432569435	0.323842215	0.75998	4.6511628
196375_A	*IGFBP3*	3.040091402	1.348404168	0.443540667	0.43981	0.9900990
266838_A	*IGFBP3*	3.023922350	1.289578756	0.426458952	0.45230	0.9900990
49439_B	*NRG1*	1.328744870	0.318083211	0.239386219	0.80020	4.6511628

Table 4.4: Gene Expression Changes in HMF3A Cultures Complemented For Growth under Non-Permissive Conditions

A subset of the genes that exhibited significant differential expression in the HMF3A system upon temperature shift from 33.5°C to 39.5°C for 7 days, but not in HMF3A cells complemented for growth under non-permissive conditions by expression of wt LT (**A**), E1A (**B**), E7 (**C**) or abrogation of p53 (**D**). In each case, two-class (unpaired) SAM was used to identify statistically significant gene expression changes; Score (*d*): the *T*-statisc value; Numerator (*r*): the numerator of the *T*-statistic; Denominator (*s* + *s0*): the denominator of the *T*-statistic; q-value (%): the lowest FDR at which the gene is called significant.

In accordance with the known functional activity of E1A, a number of genes associated with the induction of the interferon response were shown to be significantly down-regulated by E1A upon the temperature shift (**Table 4.4B**; reviewed in [Burgert *et al*, 2002]). It should also be noted that a relatively stringent FDR of ≤ 2 was employed in this analysis due to the extensive number of transcriptional changes that were identified. This finding may be attributable to the many known functions of E1A; for example, E1A-dependent reorganisation of the actin cytoskeleton has previously been described [Frisch, 1994] and acute morphological changes were indeed observed upon E1A expression in HMF3A cells (data not shown).

4.2.6.6 Transcriptional Changes Associated with E7 Expression

E7-mediated expression changes were investigated in the HMF3A system. Two-class (unpaired) SAM was used to compare the expression profile of HMF3A cells that expressed E7 at 39.5°C against growth-arrested HMF3A cells incubated at 39.5°C for 7 days. Genes that exhibited statistically significant differential expression were again subject to filtering, using the protocol described for wt LT and, as a result, a total of 49 and 70 genes were identified as being significantly up- or down- regulated by E7 expression. Again, a comparison of these genes to those that were specifically up- or down- regulated upon the HMF3A temperature shift further refined the gene sets to 32 and 50 genes, respectively (**Supplementary Figures S14** and **S15**).

One gene that exhibited significant up-regulation by E7, relative to irreversibly arrested HMF3A cells, was *FOXM1* (**Table 4.4C**). This finding was interesting since Foxm1 is known to bind to and interact with E7 [Luscher-Firzlaff *et al*, 1999]. In addition, it was evident that the number of expression changes exhibited by E7 activity was fewer when compared to E1A. This discrepancy could be explained by consideration of the known differences in functional activities of these two viral oncoproteins. For

example, E1A, unlike E7, is a known transcriptional activator [Geisberg *et al*, 1995].

4.2.6.7 Transcriptional Changes Associated with P53 Abrogation

GSE p53 and p53 shRNA were two different reagents that were used to inactivate p53 in the HMF3A system in **Chapter 3**. Therefore, it was of interest to determine how well the transcriptional changes that were induced in both the growth complemented cultures compared. Two-class (unpaired) SAM was used to compare the expression profile of HMF3A cells complemented for growth at 39.5°C by expression of GSE p53 and p53 shRNA. No statistically significant differential expression changes were observed between these two conditions, even when a less stringent FDR of ≤ 10 was used. Therefore, this finding provided good evidence that the abrogation of p53 activity by GSE p53 and shRNA acted via common effector pathways.

Having compared the two methods of p53 inactivation, specific expression changes that described the continued proliferation of HMF3As at 39.5°C by p53 abrogation were assessed using two-class (unpaired) SAM. The expression profile of HMF3A cells complemented for growth under non-permissive conditions by both GSE p53 and p53 shRNA was directly compared to irreversibly arrested HMF3A cells incubated at 39.5°C for 7 days. Genes that exhibited statistically significant differential expression were again subject to filtering, using the protocol described for wt LT and, as a result, 19 and 31 genes were identified as being up- or down- regulated upon p53 abrogation, respectively. A comparison of these genes to those specifically up- or down- regulated upon the HMF3A temperature shift further refined the gene sets to 18 and 27 genes, respectively (**Supplementary Figures S16** and **S17**).

Of the 27 down-regulated genes identified, 8 (30%) represented putative p53-responsive genes (namely, *CDH11*, *CDH13*, *CSF1*, *CUL4B*,

FGF2, *Gadd45a*, *IGFBP3* and *NRG1*; **Table 4.4D**), as identified by a bioinformatics based-approach [Hoh *et al*, 2002]. However, none of the up-regulated genes appeared to be representative of putative p53-responsive genes.

4.2.6.8 Common Transcriptional Changes Associated with HMF3A Growth Complementation

Having identified multiple gene sets of statistically significant transcriptional changes that occurred upon the complementation of HMF3A growth under non-permissive conditions, common expression changes that were exhibited under all conditions were investigated. The basis of this analysis was the assumption that the expression of critical regulators of senescence would be commonly abrogated in all growth-complemented conditions (ie cultures that expressed wt LT, E1A, E7, p53 GSE and p53 RNAi).

Multi-class SAM was used to compare the expression profiles of all growth complemented HMF3A cultures against irreversibly arrested HMF3A cultures. This form of experimental analysis was preferred to the simple overlapping of data sets as SAM provided additional information regarding the confidence of the overlap. Initial attempts to analyse the microarray data utilised information from HMF3A cultures complemented for growth with LT, E1A, E7 and p53 shRNA, but not GSE p53 due to the lack of availability of this data at that time. Genes that exhibited statistically significant differential expression were again subject to filtering, using the protocol described for wt LT and, as a result, 5 genes, namely *ATP5G2*, *ATP5I*, *CKS2*, *NOL5A* and *UBE2C*, were identified as being significantly down-regulated upon senescence, yet exhibited significantly increased expression in all cultures complemented for growth at 39.5°C (**Figure 4.5A**).

A

Clone ID	Gene	Score(d)	Numerator(r)	Denominator(s+s0)	Fold Change	q-value (%)
382331_A	*ATP5G2*	-2.865515682	-0.433929733	0.151431638	1.37998	0.3603575
755510_A	*ATP5I*	-2.271840499	-0.365128243	0.160719136	1.30220	2.8844264
221318_A	*CKS2*	-3.090247229	-0.502704879	0.162674648	1.44763	0.3603575
725454_A	*CKS2*	-2.735948054	-0.419617887	0.153372023	1.36361	0.3603575
296513_A	*NOL5A*	-3.295565446	-0.464827433	0.141046336	1.39886	0.3603575
295286_A	*UBE2C*	-3.751130773	-0.601802131	0.160432192	1.55494	0.3603575
758484_A	*UBE2C*	-3.500249057	-0.540025610	0.154282053	1.47480	0.3603575
769921_A	*UBE2C*	-2.682457026	-0.497357697	0.185411245	1.43343	0.6403649

B

Clone ID	Gene	Score(d)	Numerator(r)	Denominator(s+s0)	Fold Change	q-value (%)
221318_A	*CKS2*	-2.744558377	-0.458520987	0.167065489	1.40306	0.5847953
725454_A	*CKS2*	-2.704857173	-0.422081469	0.156045751	1.36385	0.5847953
295286_A	*UBE2C*	-3.693773726	-0.589610075	0.159622684	1.53673	0.5847953
758484_A	*UBE2C*	-3.145895410	-0.495551177	0.157523093	1.42892	0.5847953
769921_A	*UBE2C*	-2.581553763	-0.472130789	0.182886289	1.40354	1.0050251

Table 4.5: Genes Commonly Up-Regulated in HMF3A Cultures Complemented For Growth under Non-Permissive Conditions

A subset of the genes that exhibited significant down-regulation in the HMF3A system upon temperature shift from 33.5°C to 39.5°C for 7 days but not in any of the HMF3A cells complemented for growth under non-permissive conditions. **A:** Genes commonly regulated in HMF3A cultures complemented for growth under non-permissive conditions by expression of wt LT, E1A, E7 and p53 shRNA; **B:** The demonstration that GSE p53 could also complement the growth of HMF3A cells under non-permissive conditions enabled microarray data from this experimental condition to be incorporated into the statistical analysis. Multi-class SAM was used to identify statistically significant gene expression changes and putative p53 target genes are indicated (highlighted rows); Score (*d*): the *T*-statisc value; Numerator (*r*): the numerator of the *T*-statistic; Denominator (*s* + *s0*): the denominator of the *T*-statistic; q-value (%): the lowest FDR at which the gene is called significant.

Conversely, 6 genes, namely *AKR1B1*, *CDH13*, *CUL4B*, *DAF*, *DAP* and RNF11, exhibited significant transcriptional up-regulation upon senescence yet exhibited significantly reduced expression in all cultures complemented for growth (**Table 4.6A**).

Subsequent reanalysis of microarray expression data to incorporate information regarding gene expression derived from HMF3A cells complemented for growth with GSE p53 permitted the refinement of this experimental analysis and demonstrated that, with a larger experimental data set, there was more confidence in the differential expression data. Multi-class SAM of HMF3A cells irreversibly arrested for 7 days, compared to HMF3A cells complemented for growth under non-permissive conditions by expression of LT, E1A, E7, p53 shRNA and GSE p53, identified a number of significantly differentially expressed genes at a FDR of ≤ 5. Genes that exhibited statistically significant differential expression were again subject to filtering, using the protocol described for wt LT and, as a result, a refined gene list with respect to the above data set was revealed; namely 2 genes (*CKS2* and *UBE2C*) were significantly up-regulated (**Table 4.5B**) and 4 genes (*AKR1B1*, *CDH13*, *CUL4B* and *DAF*) were significantly down-regulated upon the bypass of senescence, respectively (**Table 4.6B**).

4.2.7 Validation of Microarray Data

The fact that considerable inconsistencies have been observed between different microarray studies in terms of the different platform technologies, methodologies, protocols and analyses [Bammler *et al*, 2005; Irizarry *et al*, 2005; Larkin *et al*, 2005], emphasised the need to independently verify the HMF3A microarray data. A number of techniques were available to facilitate this, including semi-quantitative RT-PCR, real-time PCR, northern blot and ribonuclease protection assay. In addition, *in silico* analysis of published data represented an indirect means with which to assess the validity of experimental data.

A

Clone ID	Gene	Score(d)	Numerator(r)	Denominator(s+s0)	Fold Change	q-value (%)
340619_A	*AKR1B1*	4.803840854	0.909342231	0.189294829	0.55581	0.3603575
340628_A	*AKR1B1*	4.680818459	0.882883414	0.188617316	0.56582	0.3603575
26025_A	*AKR1B1*	4.447809307	0.922877681	0.207490389	0.55168	0.3603575
31093_A	*CDH13*	3.732743405	0.840331145	0.225124273	0.58539	0.3603575
380384_A	*CUL4B*	4.632945922	0.573259280	0.123735370	0.67116	0.3603575
310800_A	*DAF*	2.971689465	0.340531460	0.114591872	0.78287	0.3603575
323181_A	*FAP*	3.621471349	0.559068332	0.154376020	0.68832	0.3603575
148753_A	*RNF11*	4.520430155	0.533605770	0.118043140	0.69436	0.3603575

B

Clone ID	Gene	Score(d)	Numerator(r)	Denominator(s+s0)	Fold Change	q-value (%)
340628_A	*AKR1B1*	4.854218512	0.877858439	0.180844442	0.56333	0.5847953
26025_A	*AKR1B1*	4.697942065	0.929308606	0.197811849	0.54424	0.5847953
340619_A	*AKR1B1*	4.598995915	0.873963048	0.190033447	0.56734	0.5847953
31093_A	*CDH13*	3.552860078	0.823013228	0.231648084	0.59297	0.5847953
380384_A	*CUL4B*	3.573417484	0.551925432	0.154453107	0.68777	0.5847953
310800_A	*DAF*	2.496148183	0.333022818	0.133414683	0.79103	0.5847953

Table 4.6: Genes Commonly Down-Regulated in HMF3A Cultures Complemented For Growth under Non-Permissive Conditions

A subset of the genes that exhibited both significant up-regulation in the HMF3A system upon the temperature shift from 33.5°C to 39.5°C for 7 days, but not in any of the HMF3A cells complemented for growth under non-permissive conditions. **A:** Genes commonly regulated in HMF3A cultures complemented for growth under non-permissive conditions by expression of wt LT, E1A, E7 and p53 shRNA; **B:** The demonstration that GSE p53 could also complement the growth of HMF3A cells under non-permissive conditions enabled microarray data from this experimental condition to be incorporated into the statistical analysis. In each case, multi-class SAM was used to identify statistically significant gene expression changes and putative p53 target genes are indicated (highlighted rows); Score (*d*): the *T*-statisc value; Numerator (*r*): the numerator of the *T*-statistic; Denominator (*s* + *s0*): the denominator of the *T*-statistic; q-value (%): the lowest FDR at which the gene is called significant.

Initially, correct clone annotation was assessed for each of the differentially expressed genes. The sequence of each microarray spot was analysed using Basic Local Alignment Search Tool (BLAST) and, as a result, correct clone sequence was obtained for each spot. This observation provided some reassurance that the genes identified as being significantly differential were unlikely to be due to artefactual effects resulting from functional redundancy. However, the possibility that one or more of the clonal spots were contaminated upon the microarray slide could not be addressed using this method.

Further validation of the microarray data was sought by assessment of expression changes at the protein level. This method has the advantage that it addresses the issue that changes at the transcriptional level may not necessary correspond to a concomitant change at the protein level. For example, in an ageing study, $p16^{INK4a}$ expression levels were shown to be higher in young versus old mice yet protein expression was not detected by immunohistochemistry or immunoprecipitation in some tissues [Krishnamurthy *et al*, 2004]. Unfortunately, however, well-characterised antibodies were not available for the majority of the candidate genes identified in this study.

4.2.8 Real-Time PCR Validation of Microarray Data

Real-time PCR was used as an alternative method to validate the microarray expression data for *AKR1B1*, *CDH13*, *CUL4B*, *CKS2* and *UBE2C*, since these genes exhibited common expression profiles in all cultures that were growth complemented. Therefore, these genes were considered to be strong candidates for mediating the irreversible growth arrest of HMF3A cells or, at least, markers of this process. The expression profiles of 3 additional genes that exhibited significantly differential expression in the 4-way overlap (ie wt LT/E1A/E7 and p53 RNAi), namely *NOL5A*, *FAP* and *RNF11*, were similarly analysed. However, it is important to note that the expression profile

of *DAF* was not analysed by real-time PCR due to the fact that statistical analysis of the HMF3A microarray data initially failed to identify this gene as a putative candidate gene. Furthermore, the fact that DAF is a secreted protein that functions in the complement cascade rendered this gene an unlikely candidate for mediating cell-autonomous induction of telomere-independent senescence.

Real-time PCR represents an accurate and reproducible method of cDNA quantification that measures the accumulation of PCR products during the log phase of the reaction. Quantification of target gene expression is calculated relative to the expression of endogenous housekeeping genes. Therefore, multiple endogenous control genes were utilised in this study to address the possibility that any individual housekeeping gene was not a suitable endogenous control. Semi-quantitative RT-PCR was used to confirm the suitability of *GAPDH* and *PGK1* as endogenous controls in the HMF3A system (data not shown). Conversely, *p21* was a suitable positive control as its expression is significantly up-regulated at the transcriptional level in HMF3A cells incubated at 39.5°C [Hardy *et al*, 2005].

4.2.8.1 Real-Time PCR Experimental Procedure

To perform real-time PCR analysis, 25 μg of RNA from each experimental condition was reverse-transcribed in a 100 μl reaction to generate cDNA at a concentration of 250 ng/μl. The quality of the cDNA was then assessed by semi-quantitative RT-PCR using 1 μl of cDNA as a template for PCR using *GAPDH* specific primers. Approximately equal intensities of each PCR product were observed as a result of this process, thereby indicating that each cDNA sample was of sufficient quality to be used for real-time PCR analysis (data not shown).

The standard curve method of cDNA quantification was used in the real-time PCR analysis in order to calculate the quantity of cDNA in each sample, relative to a calibrator sample. A standard sample of cDNA was

prepared by mixing 5 µl of cDNA derived from HMF3AEco^R cells incubated at 33.5°C and HMF3AEco^R cells incubated at 39.5°C for 7 days. This mix ensured that genes that were both up- and down-regulated upon the irreversible growth arrest were represented in the standard cDNA sample. CDNA samples were then diluted 1:250 and 1:25000, subdivided into 100 µl aliquots and frozen. In contrast, 1:500 dilutions were made from cDNA samples derived from each of the individual experimental sample conditions, subdivided into 100 µl aliquots and frozen. Diluted cDNA samples were thawed and used only once in each real-time PCR experiment.

The fact that the same stock of cDNA could be used to prepare multiple standard curves for real-time PCR analysis enabled separate real-time PCR experiments to be performed for each gene, namely, *GAPDH*, *PGK1*, *p21*, *AKR1B1*, *CDH13*, *CUL4B*, *FAP*, *RNF11*, *CKS2*, *NOL5A* and *UBE2C*. Real-time PCR was performed in a 96-well format in a series of 25 µl reactions, using a 6-carboxyfluorescein (6-FAM) labelled probe (TaqMan; Applied Biosystems) and Applied Biosystems Assays-on-Demand Gene Expression kits. Triplicate samples of the standard cDNA were used in a serial dilution of 4000, 2000, 1000, 400, 200, 80 and 40 pg, whereas 6 replicate samples consisting of 1000 pg cDNA were used for each of the HMF3A sample conditions analysed. Sample conditions consisted of HMF3AEco^R cells grown at 33.5°C, HMF3AEco^R cells irreversibly arrested at 39.5°C for 7 days and each of the HMF3A cells complemented for growth at 39.5°C by expression; ie wt LT, E1A, E7, GSE p53 and p53 shRNA, such that each condition was analysed in parallel. In each of these experiments, the cycle conditions recommended by the manufacturer were used for the PCR procedure.

Before analysing the real-time PCR data, two manual adjustments were made. Firstly, the baseline value was set at two cycles before the first observable amplification cycle. Secondly, the threshold value (ΔRn) was set at the point where all data points increased linearly in the exponential phase of

the logarithmic scale amplification plot. Quantification of the gene expression data was then performed using a series of calculations. Firstly, a standard curve for relative quantification was made for each of the two endogenous control genes, namely *GAPDH* and *PGK1*. The average values for each experimental replicate was used to plot a standard curve, unless a clear outlying value was observed, in which case this value was discarded from the calculation. Then, for each control standard curve, the relative quantity of each of the experimental samples was extrapolated. The value for HMF3AEco^R cells grown at 33.5°C was then designated the calibrator sample, such that the expression values for each of the experimental samples was calculated relative to this. The data was then normalised for each candidate gene by dividing the average expression value for each experimental condition by the corresponding average value of one of the endogenous control genes. In this manner, two normalised values of relative gene expression were obtained for each gene (**Supplementary Figure S18**).

The gene expression data for *p21* expression relative to *GAPDH* and *PGK1* was in accordance with the microarray array data since significant up-regulation was observed upon the irreversible arrest of HMF3AEco^R cells at 39.5°C, relative to cell grown at 33.5°C (compare **Figures 4.3A** and **4.3B**, respectively). Yet, significant *p21* down-regulation was observed in HMF3A cells complemented for growth with either p53 shRNA or GSE p53. This result thereby provided confidence that both microarray analysis and real-time PCR represented sensitive detection techniques for the identification of real and reproducible gene expression patterns.

Analysis of the gene expression data for each of the candidate genes, however, was somewhat variable (**Figures 4.3** and **4.4**). Expression data from genes *AKR1B1*, *CDH13* and *UBE2C* appeared to correlate with the microarray data (**Figures 4.3** and **4.4**), since a similar pattern of gene expression was observed with the microarray data. However, no concordance was observed with the remaining candidate genes (data not shown for *FAP*, *RNF11* or *NOL5A*).

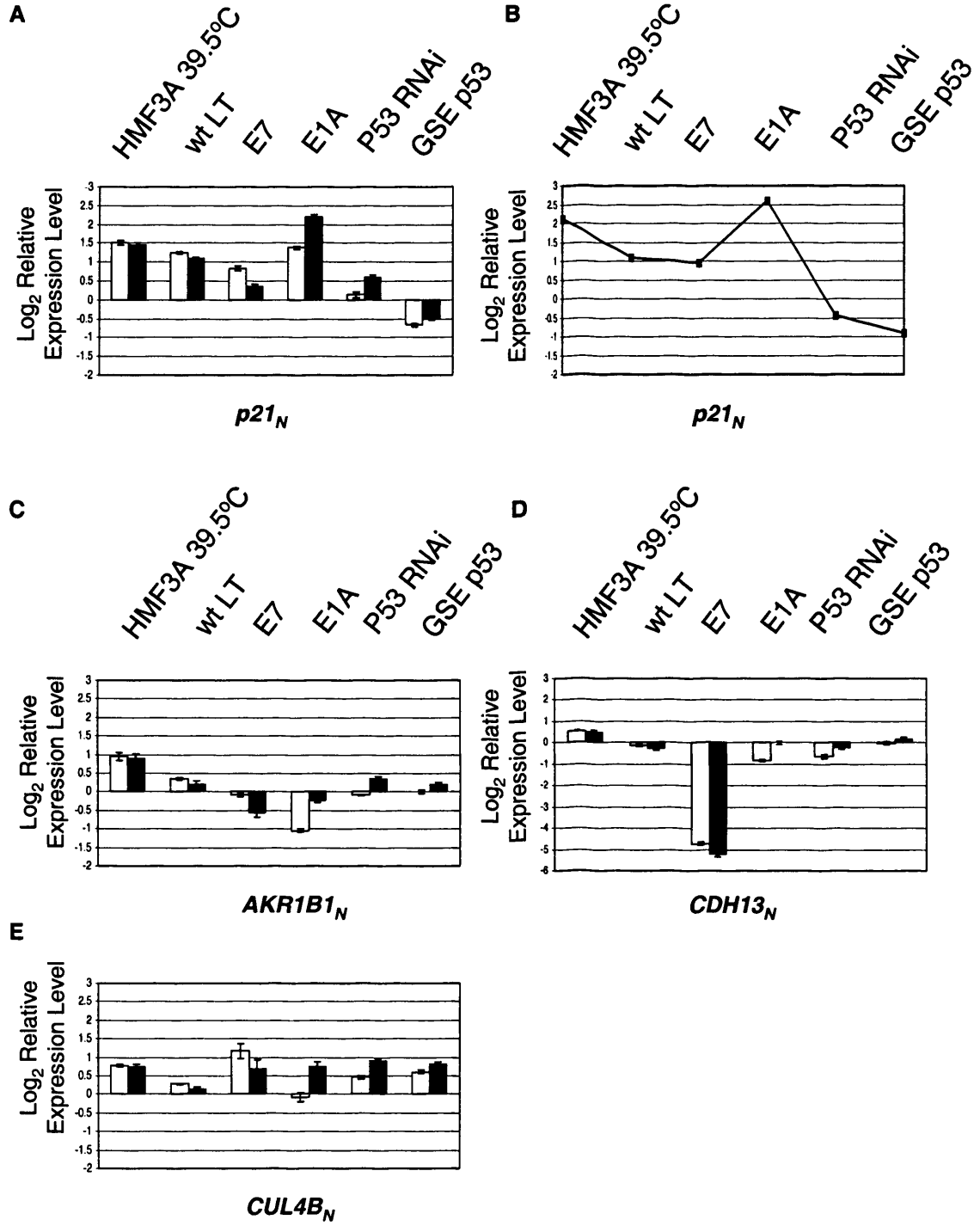

Figure 4.3: Real-Time PCR of Up-Regulated Microarray Candidate Genes

A: Real-time PCR analysis of *p21* expression in the HMF3A system; **B:** Microarray expression profile of *p21* in the HMF3A system; **C:** Real-time PCR analysis of *AKR1B1* expression; **D:** *CDH13* expression; **E:** and *CUL4B* expression. White bars indicate normalised expression values relative to *GAPDH*. Black bars indicate normalised expression values relative to *PGK1*.

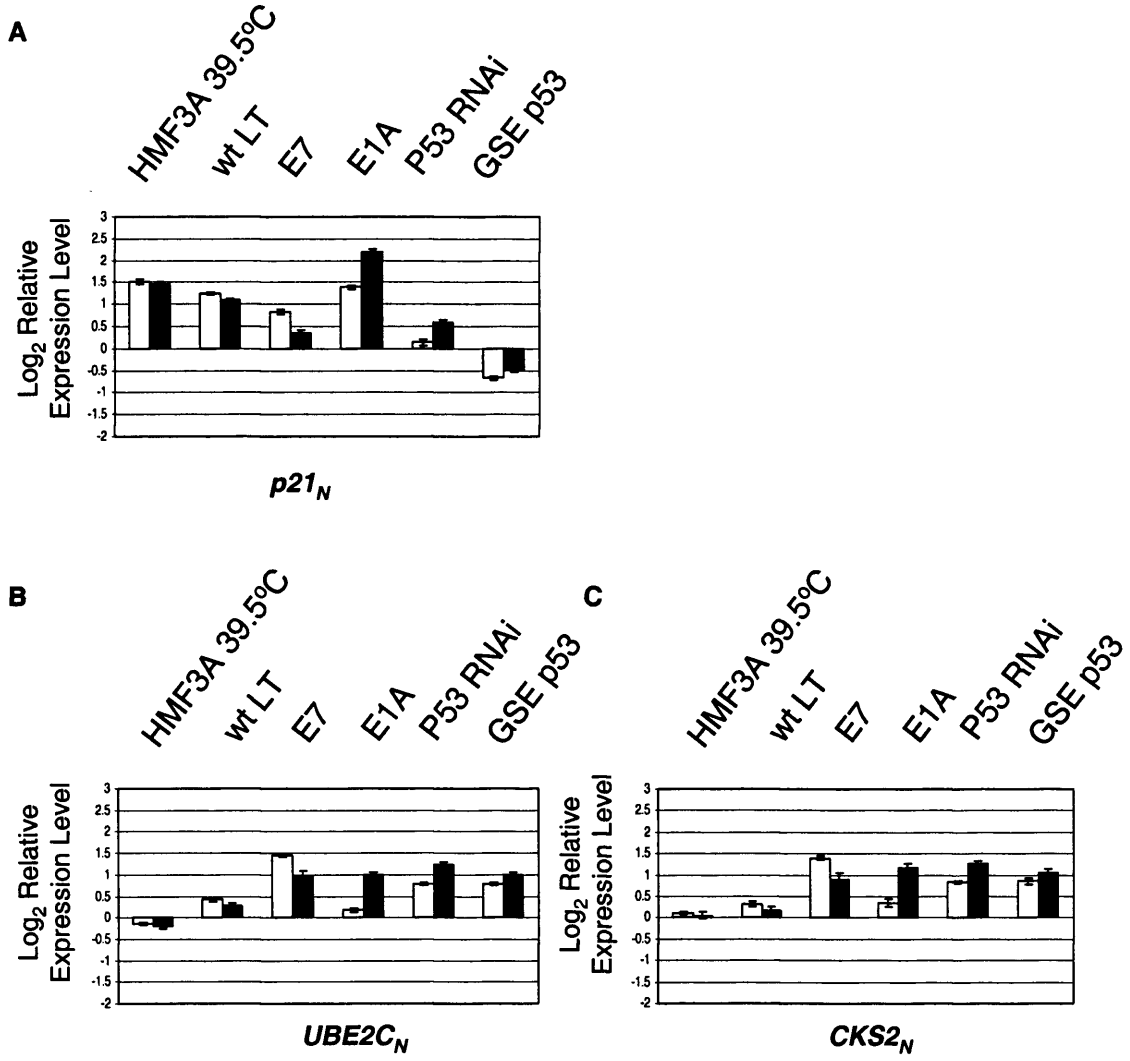

Figure 4.4: Real-Time PCR of Down-Regulated Microarray Candidate Genes

A Real-time PCR analysis of *p21* expression in the HMF3A system; **B:** *UBE2C* expression; **C:** and *CKS2* expression. White bars indicate normalised expression values relative to *GAPDH*. Black bars indicate normalised expression values relative to *PGK1*.

For example, microarray analysis indicated that *CUL4B* was significantly up-regulated upon the HMF3A conditional growth arrest, but was maintained at a low level in all growth-complemented cultures. However, real-time PCR indicated that it was maintained at a high level in all growth complemented cultures (**Figure 4.3E**). Furthermore, microarray analysis indicated that *CKS2* was significantly down-regulated upon the HMF3A conditional growth arrest, whereas real-time PCR indicated that there was no significant change in expression upon the temperature shift (**Figure 4.4C**).

4.2.9 Functional Analysis of Microarray Candidate Genes

Real-time PCR analysis confirmed the differential regulation of candidate genes *AKR1B1*, *CDH13* and *UBE2C*, as observed by cDNA microarray analysis, but not for *CUL4B*, *FAP*, *RAB1A*, *RNF11*, *CKS2*, or *NOL5A*. Therefore, it remained to be shown if/how these genes were causal to the induction of telomere-independent cellular senescence. Furthermore, additional experimental evidence was required to validate these data, as it was possible that translational regulation or decreased protein stability rendered the transcriptional changes meaningless.

In this respect, a major advantage of utilising the HMF3A system was the fact that testable predictions could be made and assessed using this model system. Consequently, each of the candidate genes described here was functionally analysed using the HMF3A complementation assay. For genes normally up-regulated upon senescence, ie *AKR1B1* and *CDH13*, RNAi silencing was used to suppress expression to determine whether HMF3AEco^R cells could maintain growth activity under non-permissive conditions. Conversely, constitutive expression was used to maintain expression of genes normally down-regulated upon senescence, ie *UBE2C*, and again, this activity was assessed by the ability of HMF3AEco^R cells to maintain growth at the non-permissive temperature.

4.2.10 Microarray Candidate Gene: AKR1B1

AKR1B1 encodes for aldo-keto reductase family 1, member B1 (AKR1B1), a member of the monomeric, NADPH-dependent aldo-keto reductase superfamily (AKR) [Jez *et al*, 1997], of which 13 are ubiquitously expressed in humans, AKR1B1 is highly expressed in the adrenal gland [Grimshaw and Mathur, 1989] and is known to catalyse the reduction of a number of aldehydes, including the aldehyde form of glucose that is reduced during the first step of the polyol pathway [Bohren *et al*, 1989]. AKR1B1 can also catalyse the reduction of a number of other aldehydes, including toxic aldehydes such as methylglyoxal [Vander Jagt *et al*, 1992] and lipid-derived aldehydes [Bucala, 1997; Ramana *et al*, 2000]. Consequently, it has been suggested that AKR1B1 primarily functions as an anti-oxidant agent [Rittner *et al*, 1999; Spycher *et al*, 1997]. However, little more is known about the physiological role of this enzyme.

With respect to tumourigenesis, there is some evidence to suggest that *AKR1B1* expression is down-regulated in malignant tumours of the adrenal cortex [Lefrancois-Martinez *et al*, 2004]. In contrast to the down-regulation of *AKR1B1* transcription observed in growth complemented HMF3A cells, however, one study presented evidence that both *AKR1B1* and *AKR1B10* are over-expressed by 29% and 54%, respectively, in some human liver cancers [Cao *et al*, 1998]. Therefore, there is little, and even contradictory, evidence to link the activity of AKR1B1 to cellular senescence. Yet, the fact that our original microarray analyses identified *AKR1B1* as a gene that was up-regulated upon replicative senescence in primary human fibroblasts [Hardy *et al*, 2005], argued that *AKR1B1* required functional assessment in the HMF3A system.

4.2.10.1. Expression Analysis of AKR1B1

The availability of an AKR1B1 rabbit polyclonal antibody (L3; gift from A. Martinez) enabled the transcriptional changes observed by both the microarray and real-time PCR analysis to be assessed at the protein level. RIPA protein lysates extracted from HMF3AEco^R cells incubated at 33.5°C and 39.5°C for 7 days were separated on 12% SDS-PAGE and analysed by Western blot analysis using the L3 antibody. A significant increase in the intensity of a band of approximately 37 kDa that corresponded to AKR1B1 (as indicated in the literature [Lefrancois-Martinez *et al*, 2004]), was observed in HMF3AEco^R cells incubated at 39.5°C for 7 days (**Figure 4.5A**, lane 2), relative to HMF3AEco^R cells incubated at 33.5°C (**Figure 4.5A**, lane 1). This indicated that AKR1B1 was up-regulated not only at the mRNA level, but also at the protein level upon the HMF3A temperature shift.

4.2.10.2. Knockdown of AKR1B1 by ShRNA

Having confirmed the up-regulation of AKR1B1 at the protein level upon the HMF3A temperature shift, the putative, positive regulatory role of AKR1B1 in telomere-independent cellular senescence was assessed by functional inactivation of AKR1B1 in the HMF3A complementation assay. Four shRNA targets were designed using the criteria outlined by Reynolds and colleagues (**Figures 4.5B** and **4.5C**, respectively; [Reynolds *et al*, 2004]). Multiple AKR1B1 shRNA constructs were generated to increase the likelihood of generating at least one functional shRNA construct. Target sequences that spanned both the ORF and 3'UTR were selected and constructs were generated using the Oligoengine protocol.

A

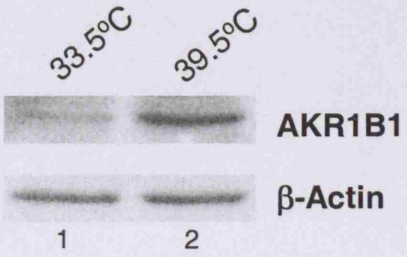

B

Name	Target Region	Target Sequence	Position in mRNA Sequence	G/C Content
AKR1B11#1	ORF	ACAAACCTGGCTTGAAGTA	589	42.11%
AKR1B1#2	ORF	TCACTCAGGAGAAGTTAAT	646	36.84%
AKR1B1#3	ORF	GTATAAGCCTGCAGTTAAC	605	42.11%
AKR1B1#4	3' UTR	TGTCTAGCTTGATGTTGGA	1158	42.11%
Lamin A/C	ORF	AACTGGACTTCCAGAAGAACA	820	42.86%

C

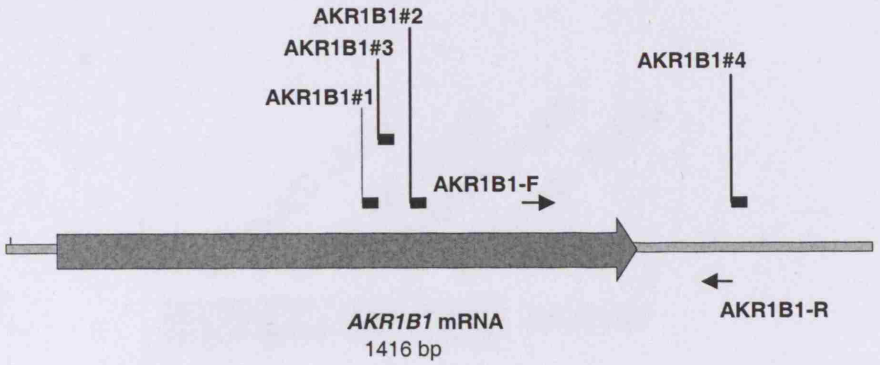

Figure 4.5: Functional Analysis of AKR1B1

A: Western blot analysis of AKR1B1 expression in the HMF3A system using L3 rabbit polyclonal anti-AKR1B1 (gift from A. Martinez). β-Actin was the loading control; **B:** AKR1B1 shRNA target sequences; **C:** Positions of shRNA target sequences (indicated by black bars) and primer binding sites (indicated by black arrows) in *AKR1B1* mRNA. A grey arrow indicates the ORF; **D:** Semi-quantitative RT-PCR using *AKR1B1*-specific primers demonstrated knockdown of *AKR1B1* in the HMF3A system at 39.5°C. *GAPDH* was the loading control; **E:** Western blot of AKR1B1 knockdown using L3 anti-AKR1B1 antibody. β-Actin was the loading control.

D

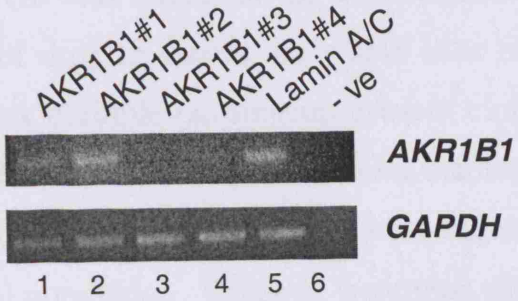
AKR1B1#1
AKR1B1#2
AKR1B1#3
AKR1B1#4
Lamin A/C -ve
AKR1B1
GAPDH
1 2 3 4 5 6

E


Lamin A/C 33.5°C
Lamin A/C 39.5°C
AKR1B1#3 39.5°C
AKR1B1#1 39.5°C
AKR1B1
β-Actin
1 2 3 4

To assess the effectiveness of AKR1B1 knockdown mediated by shRNA, 10 μg of the resultant shRNA constructs, namely, pRetroSuper-LaminA/C, pRetroSuper-AKR1B1#1, pRetroSuper-AKR1B1#2, pRetroSuper-AKR1B1#3 and pRetroSuper-AKR1B1#4, were packaged using the ϕ ecotropic system. 5% of the total retroviral supernatant harvest was used to infect HMF3AEco^R cultures seeded at 5x10^5 cells in duplicate T75 cm^2 flasks in the presence of 8 μg/ml polybrene. Following incubation at 33.5°C for 4 days, 2 μg/ml puromycin was added to the culture medium and upon the completion of 4 days of drug treatment, no viable cells remained in a non-infected culture, whereas multiple puromycin-resistant clones were observed in all infected HMF3AEco^R cultures. Cultures were maintained in puromycin for a further 3 days before drug-resistant clones were trypisinised, pooled and replated as a polyclonal population. Cultures were then shifted to 39.5°C for 7 days and RNA extracted, since, under these conditions, knockdown of *AKR1B1* was anticipated to be more readily detectable than at 33.5°C.

Semi-quantitative RT-PCR using *AKR1B1*-specific primers (AKR1B1-F and AKR1B1-R) generated a 349 bp PCR product that corresponded to *AKR1B1* in Lamin A/C shRNA-infected HMF3AEco^R cells (**Figure 4.5D**, lane 5). In contrast, however, a significant reduction in the intensity of the 349 bp PCR product was observed in HMF3AEco^R samples infected with shRNA constructs AKR1B1#3 (**Figure 4.5D**, lane 3) and AKR1B1#4 (**Figure 4.5D**, lane 4), and a partial knockdown was noted for AKR1B1#1 (**Figure 4.5D**, lane 1), but no reduction was detected for AKR1B1#2 (**Figure 4.5D**, lane 2). This indicated that efficient *AKR1B1* knockdown was mediated by shRNA constructs AKR1B1#3 and AKR1B1#4, and, to a lesser extent, by AKR1B1#1.

To validate this finding at the protein level, RIPA protein lysates were extracted from HMF3AEco^R cultures grown under the same conditions, separated on 12% SDS-PAGE and analysed by Western blot using the L3 rabbit polyclonal AKR1B1 antibody. In accordance with the semi-quantitative RT-PCR data, significant knockdown of the 37 kDa band that

corresponded to AKR1B1 was observed in HMF3AEco^R cells infected with AKR1B1#3 shRNA construct (**Figure 4.5E**, lane 3), relative to Lamin A/C control (**Figure 4.5E**, lane 2). A partial knockdown with the AKR1B1#1 shRNA construct was also noted (**Figure 4.5E**, lane 4).

4.2.10.3. Knockdown of AKR1B1 by ShRNA is Insufficient to Complement the Conditional HMF3A Growth Defect

Having identified a potent shRNA construct, Lamin A/C, AKR1B1#3 and p53 shRNA constructs were then tested in the HMF3A complementation assay. 10 μg of each shRNA construct was introduced into HMF3AEco^R cells, using the proctocol described above. Puromycin was removed from the culture medium and drug-resistant clones were directly shifted to 39.5°C. Puromycin-resistant HMF3AEco^R clones were incubated under non-permissive conditions for 14 days, following which, multiple healthy, growing colonies were observed in the positive control p53 shRNA-infected HMF3AEco^R culture. However, no outgrowing colonies were observed in AKR1B1#3 shRNA-infected HMF3AEco^R cultures or the Lamin A/C shRNA-infected HMF3AEco^R culture. The same result was obtained in a duplicate experiment. This indicated that abrogation of AKR1B1 activity alone was insufficient to bypass the irreversible growth arrest of HMF3AEco^R cells upon inactivation of U19tsA58 LT.

4.2.11 Microarray Candidate Gene: CDH13

CDH13 represented the second microarray candidate gene that was significantly up-regulated upon senescence in the HMF3A system. It encodes Cadherin 13 (CDH13), a member of the cadherin superfamily. Cadherins are cell surface glycoproteins consisting of an extracellular, transmembrane and intracellular portion, however, CDH13 represents a novel cadherin family member by virtue of the fact that it does not contain a transmembrane region

and instead utilises a glycosylphosphatidylinositol (GPI) anchor [Nagafuchi and Takeichi, 1988; Ranscht and Dours-Zimmermann, 1991].

The physiological role of CDH13 is not well understood, yet there is some evidence to suggest that it functions as a negative regulator of neuronal growth [Takeuchi *et al*, 2000]. Loss of cadherin expression has been described in the process of tumorigenesis in breast, lung, ovarian and bladder cancers and specifically, down-regulation of *CDH13* has been suggested to play a role in tumour cell invasion and metastasis [Behrens, 1993; Kawakami *et al*, 1999; Lee, 1996; Maruyama *et al*, 2001; Sato *et al*, 1998; Takeichi, 1993; Toyooka *et al*, 2001]. Indeed, in concordance with the down-regulation of *CDH13* in growth complemented HMF3A cultures, aberrant promoter methylation and *CDH13* gene deletion is commonly observed in breast, lung, pancreas, stomach, bladder and ovarian cancers [Lee, 1996; Maruyama *et al*, 2001; Mori *et al*, 1999; Sakai *et al*, 2004; Sato *et al*, 1998; Takeichi, 1993], and these epigenetic events are thought to occur early in tumorigenesis [Sakai *et al*, 2004]. There is also direct evidence to link the function of CDH13 to cell proliferation in keratinocytes [Mukoyama *et al*, 2005] and glioblastoma cells [Huang *et al*, 2003].

These findings were both in accordance with the pattern of *CDH13* expression displayed in the HMF3A microarray analysis. Therefore, *CDH13* was functionally analysed in the HMF3A system

4.2.11.1. Knockdown of CDH13 by ShRNA

Since no well-characterised antibodies have been raised against CDH13, it was not possible to verify up-regulation of CDH13 expression at the protein level. Consequently, verification of a positive regulatory role of CDH13 in the induction of senescence was assessed by shRNA analysis, similar to AKR1B1. Four shRNA targets were designed against *CDH13*, based upon the criteria outlined by Reynolds and colleagues (**Figure 4.6A**; [Reynolds *et al*, 2004]).

A

Name	Target Region	Target Sequence	Position in mRNA Sequence	G/C Content
CDH13#1	ORF	CAGGTTGGCTGAATATTAA	1653	36.84%
CDH13#2	ORF	AATCGCTGTTTATCAACTA	712	31.58%
CDH13#3	3' UTR	CTATCGAACTTCACAACTA	2324	36.84%
CDH13#4	3' UTR	TCACGCTGTTTGTTTCATA	3219	47.37%

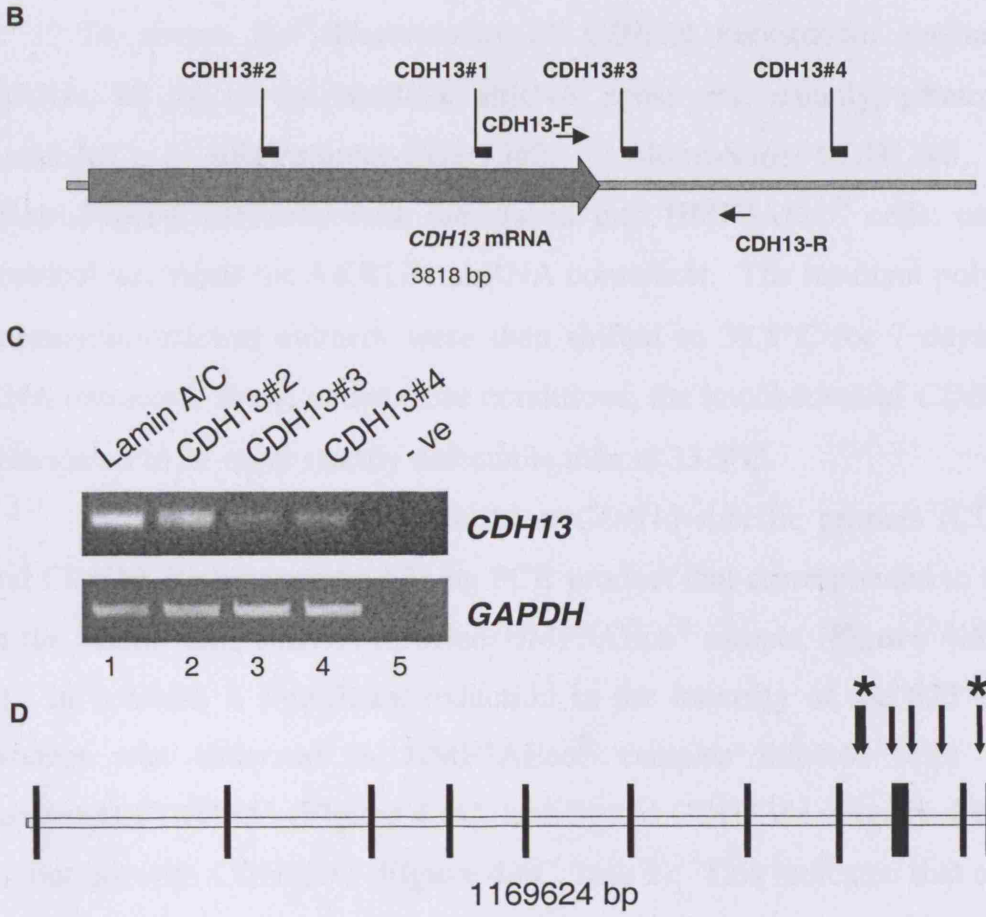

Figure 4.6: Functional Analysis of CDH13

A: CDH13 shRNA target sequences; **B:** Positions of shRNA target sequences (indicated by black bars) and primer binding sites (indicated by black arrows) in *CDH13* mRNA. A grey arrow indicates the ORF; **C:** Semi-quantitative RT-PCR using *CDH13*-specific primers demonstrated knockdown of *CDH13* in the HMF3A system at 39.5°C. *GAPDH* was the loading control; **D:** Genomic organisation of *CDH13* gene with exons (black lines) and consensus p53 binding sites (grey arrows) indicated. Consensus p53 sequences that exhibit a perfect match are indicated in black and asterisked.

Two of these constructs spanned regions in the ORF, whereas two other target sequences encompassed regions in the 3'UTR (**Figure 4.6B**). ShRNA constructs were generated using the Oligoengine protocol, however, it should be noted that due to technical difficulties, it was not possible to clone the CDH13 #1 shRNA construct.

To assess the effectiveness of *CDH13* knockdown mediated by shRNA, 10 μg of the resultant shRNA constructs, namely, pRetroSuper-LaminA/C, pRetroSuper-CDH13#2, pRetroSuper-CDH13#3, and pRetroSuper-CDH13#4, were introduced into HMF3AEco^R cells, using the protocol described for AKR1B1 shRNA constructs. The resultant polyclonal, puromycin-resistant cultures were then shifted to 39.5°C for 7 days before RNA extracted, since, under these conditions, the knockdown of *CDH13* was anticipated to be more readily detectable than at 33.5°C.

Semi-quantitative RT-PCR using *CDH13*-specific primers (CDH13-F and CDH13-R) generated a 623 bp PCR product that corresponded to *CDH13* in the Lamin A/C shRNA-infected HMF3AEco^R sample (**Figure 4.6C**, lane 1). In contrast, a significant reduction in the intensity of the 623 bp PCR product was observed in HMF3AEco^R samples infected with shRNA constructs CDH13#3 (**Figure 4.6C**, lane 3) and CDH13#4 (**Figure 4.6C**, lane 4), but not with CDH13#2 (**Figure 4.6C**, lane 2). This indicated that efficient *CDH13* knockdown was mediated by shRNA constructs CDH13#3 and CDH13#4, but not by CDH13#4.

4.2.11.2 Knockdown of CDH13 by ShRNA is Insufficient to Complement the Conditional HMF3A Growth Defect

Having identified two potent CDH13 shRNA constructs, Lamin A/C, CDH13#3, CDH13#4 and p53 shRNA constructs were tested in the HMF3A complementation assay, as described for AKR1B1 shRNA constructs. Puromycin-resistant HMF3AEco^R clones were incubated under non-permissive conditions for 14 days, following which, multiple healthy, growing

colonies were observed in the positive control p53 shRNA-infected HMF3AEco^R culture. However, no outgrowing colonies were observed in the CDH13#3 or CDH13#4 shRNA infected HMF3AEco^R cultures or the Lamin A/C shRNA-infected HMF3AEco^R culture. The same result was obtained in a duplicate experiment. This indicated that abrogation of CDH13 activity alone was insufficient to bypass the irreversible growth arrest of HMF3AEco^R cells upon inactivation of U19tsA58 LT.

4.2.12 Microarray Candidate Gene: UBE2C

In contrast to *AKR1B1* and *CDH13*, *UBE2C* was a candidate gene that exhibited significant down-regulation upon the HMF3A temperature shift.

UBE2C encodes Ubiquitin-conjugating enzyme E2C (UBE2C or Ubch10), a ubiquitin-conjugating enzyme that functions in the process of ubiquitin-mediated proteolysis. There is some *in silico* evidence to link UBE2C with the process of senescence; for example, UBE2C appears to be essential for the orderly progression of the cell cycle through G_1 to S phase by acting in a rate-limiting step for the ubiquitination, and subsequent degradation, of cell cycle regulated proteins such as cyclin A [Rape and Kirschner, 2004; Townsley *et al*, 1997]. Immunohistochemisty supports these findings since intense staining may be observed in cells undergoing mitosis and in normal cells present in the proliferative compartment of tissues [Wagner *et al*, 2004]. This has led to the suggestion that the activity of some E2 proteins, including UBE2C, may be involved in cell cycle progression and tumorigenesis [Okamoto *et al*, 2003].

In accordance with the microarray data, UBE2C over-expression in NIH3T3 cells leads to an increase in proliferative capacity [Okamoto *et al*, 2003]. Similarly, *UBE2C* expression levels are known to be highly elevated in different types of cancer, such as ovarian, metastatic prostatic adenocarcinomas, gastro-esophagus, lung, breast and thyroid [LaTulippe *et al*, 2002; Pallante *et al*, 2005; Wagner *et al*, 2004]. Furthermore, *UBE2C* is

located at a chromosomal region that is frequently associated with genomic amplification in many types of cancer, namely 20q13.1, and genomic amplification of the *UBE2C* locus has been described in some carcinomas [Wagner *et al*, 2004]. Accordingly, UBE2C was functionally analysed in the HMF3A system.

4.2.12.1 Expression Analysis of UBE2C

A monoclonal antibody raised against UBE2C (anti-UbcH10, gift from F. Hofmann) permitted the analysis of this protein in the HMF3A system. RIPA protein lysates were extracted from HMF3AEco^R cells incubated at 33.5°C and 39.5°C for 7 days, separated by 12% SDS-PAGE then analysed by Western blot analysis using anti-Ubch10. A significant reduction in a band of approximately 23 kDa that corresponded to UBE2C (as indicated in the literature [Wagner *et al*, 2004]) was observed in HMF3AEco^R cells incubated at 39.5°C for 7 days (**Figure 4.7,** lane 2), relative to HMF3AEco^R cells incubated at 33.5°C (**Figure 4.7**, lane 1). As it will be shown below, ectopic expression of UBE2C in HMF3AEco^R cells confirmed the identity of this 23 kDa band as UBE2C. This indicated that UBE2C was down-regulated upon the temperature shift not only at the mRNA level, but also at the protein level.

Abrogation of UBE2C activity either by RNAi or expression of a dominant negative peptide of UBE2C has previously been shown to be sufficient to reduce cell proliferation and promote cell cycle arrest [Pallante *et al*, 2005;Townsley *et al*, 1997;Wagner *et al*, 2004]. Therefore, it was hypothesised that constitutive expression of UBE2C in the HMF3AEco^R system may be sufficient to complement the growth of these cells under the non-permissive conditions. Ectopic expression of HMF3AEco^R cells was complicated, however, by the fact that 6 different splice variants of UBE2C have been described (**Figure 4.8A**).

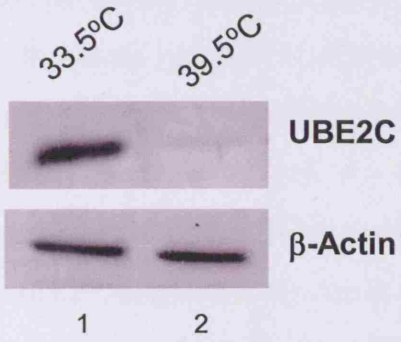

Figure 4.7: UBE2C Expression

Western blot analysis using anti-Ubch10 monoclonal antibody (gift from F. Hofmann) demonstrated a significant down-regulation of UBE2C in HMF3AEco^{R} cells upon the shift from 33.5°C to 39.5°C for 7 days. β-Actin was the loading control.

Furthermore, sequence analysis of the *UBE2C* clones utilised in the cDNA microarray analysis, namely 769921_A and 295286_A, indicated that these spots could not distinguish between splice variants 1,4 or 5. Therefore, it was necessary to determine which of these splice variants were differentially expressed at the mRNA level.

To address this problem, RNA was extracted from HMF3AEco^R cells incubated at both 33.5°C and 39.5°C for 7 days and analysed by semi-quantitative RT-PCR using primers specific to *UBE2C*. Two sets of primers (Splice-F and Ubch10com-R, and Splice-Fv2 and Ubch10com-R) were designed for this analysis in order to distinguish all known *UBE2C* splice variants (**Figure 4.8**). Analysis of the resultant PCR products revealed that splice variant #1 exhibited the most prominent differential expression upon the HMF3A temperature shift (**Figure 4.8C**, lanes 1 and 2). However, the fact that expression of splice variants #4 and #5 were also detected in HMF3AEco^R cells and also appeared to be differential upon the temperature shift (**Figure 4.8C**, lanes 4 and 5), indicated the constitutive expression of all *UBE2C* splice variants required assessment in the HMF3A complementation assay to conclusively assess the functional activity of UBE2C in these cells.

4.2.12.2 Constitutive Expression of UBE2C

It was decided that the entire *UBE2C* genomic region should be cloned into a retroviral expression vector in an attempt to functionally assess the role of all the UBE2C splice variants in the HMF3A system. It was anticipated that, upon transfection of this construct into a transient retroviral expression system, the activity of the transcription and splicing machinery would generate retroviruses that corresponded to each of the UBE2C splice variants. Thus, infection of HMF3AEco^R cells with a mixture of these viruses would generate clones expressing different UBE2C splice variants.

A

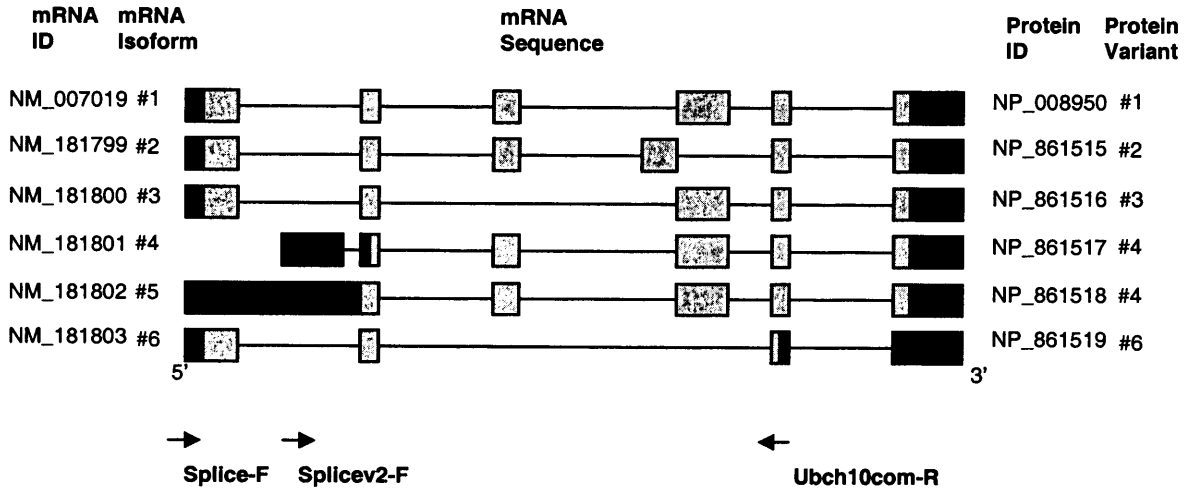

B

mRNA Isoform	*Splice-F + UbcH10com-R (bp)*	*Splicev2-F + Ubch10com-R (bp)*
1	**519**	**NA**
2	465	NA
3	432	NA
4	**NA**	**623**
5	**1159**	**769**
6	227	NA

Figure 4.8: Analysis of Endogenous *UBE2C* Expression

A: Diagram of PCR primers (indicated by black arrows) used to distinguish the known *UBE2C* splice variants by agarose gel electrophoresis. The 5' UTR is indicated in dark grey and the coding region is indicated in light grey; **B:** Table indicating the sizes of the PCR products expected from each splice variant; **C:** Semi-quantitative RT-PCR using primer combinations indicated. *GAPDH* was the loading control. Expression of *UBE2C* splice variants #1, #4 and #5 were detected using the method (as indicated). However, due to the relatively low intensity of the PCR products derived from splice variant #5, an asterisk indicates the positions of these PCR products.

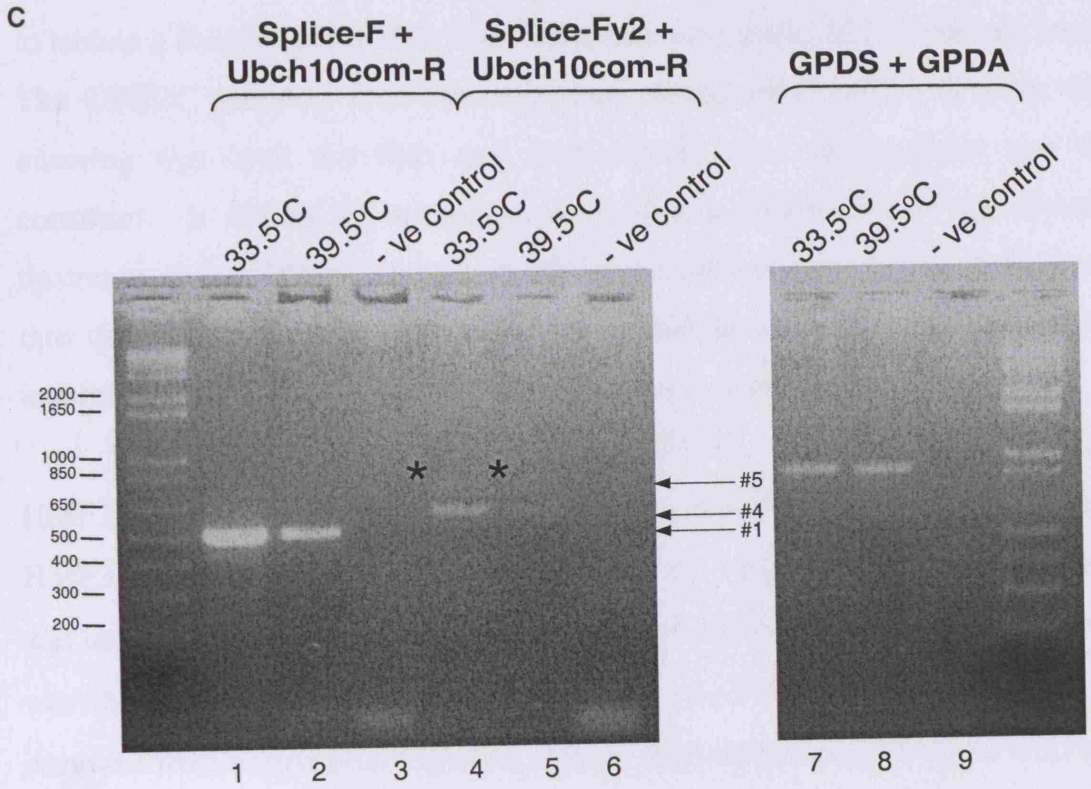
C
Splice-F + Ubch10com-R
Splice-Fv2 + Ubch10com-R
GPDS + GPDA
33.5°C
39.5°C
- ve control
33.5°C
39.5°C
- ve control
33.5°C
39.5°C
- ve control
2000
1650
1000
850
650
500
400
300
200
#5
#4
#1
1
2
3
4
5
6
7
8
9

Consequently, a polyclonal retroviral population would infect HMF3AEco^R cultures and multiple clones expressing different UBE2C splice variants would be generated.

To clone the genomic region of *UBE2C* into a retroviral expression vector, a BAC clone containing the *UBE2C* genomic sequence (RP3-447F3) was obtained from the MRC GeneService. *Bam*H I restriction digestion of the RP3-447F3 clone, followed by gel extraction on a 0.8% agarose gel, was used to isolate a *Bam*H I restriction fragment containing the *UBE2C* genomic locus. The *UBE2C* genomic sequence was then cloned into pLPCX (**Figure 4.9**) ensuring that both the start and stop codons were incorporated into the construct. It should be noted, however, that a region of 109 bp, directly upstream of the *UBE2C* initiator methionine codon in exon 1, was also cloned into the pLPCX vector. The sequence including the polyA signal was not incorporated into the resultant retroviral expression construct.

The resultant construct, pLPC-UBE2C, was used to infect HMF3AEco^R cells. 10 μg of pLPC-UBE2C and pLPCX were introduced into HMF3A cells, using the protocol described for AKR1B1 shRNA constructs, and used to generate polyclonal populations at 33.5°C. One duplicate culture was then maintained under drug selection at 33.5°C, whereas selection was removed from the second duplicate culture, then shifted to 39.5°C for a further 7 days before RIPA protein lysates were prepared.

RIPA cell lysates were separated by 12% SDS-PAGE and analysed by Western blot using anti-Ubch10. Similar to before, a significant decrease in a band of approximately 23 kDa that corresponded to UBE2C was observed in control cells at 39.5°C (**Figure 4.10**, lane 2), relative to control cells at 33.5°C (**Figure 4.10**, lane 1). However, the HMF3AEco^R culture that ectopically expressed UBE2C exhibited a signficant increase in the 23 kDa band (**Figure 4.10**, lane 3). This observation provided supportive evidence that this band was representative of UBE2C, rather than another, non-specific protein.

Figure 4.9: Generation of pLPC-UBE2C Retroviral Expression Construct

BAC contig RP3-447F3 (MRC GeneService) was *Bam*H I digested to isolate a 6722bp *Bam*H I fragment containing the *UBE2C* gene (between bases 80233 and 86955 of RP3-447F3 clone) and sub-cloned into *Bam*H I digested pBluescript SK(-). The 3' end of the *UBE2C* was PCR amplified using UBE2CAmp-F and UBE2CAmp-R primers (indicated by black arrows) using SuperTaq, cloned into pCR2.1 TA-cloning vector, and sequence verified. The UBE2CAmp-R primer incorporated a *Cla* I restriction site directly downstream of the STOP codon. The 3585bp *Sal* I/*Eco*R I and 613bp *Eco*R I/*Cla* I *UBE2C* restriction digest fragments, derived from pBluescript-UBE2C and pCR2.1-UBE2C, respectively, were then sub-cloned into *Xho* I/*Cla* I digested pLPCX vector in 1:1:1 ligation ratio. MoMuSV: Moloney Murine Sarcoma Virus; MoMuLV: Moloney Murine Leukemia Virus; LTR: Long Terminal Repeat; hCMV IE: human Cytomegalovirus Immediate Early promoter; puro^{R}: puromycin resistance gene; amp^{R}: ampicillin resistance gene.

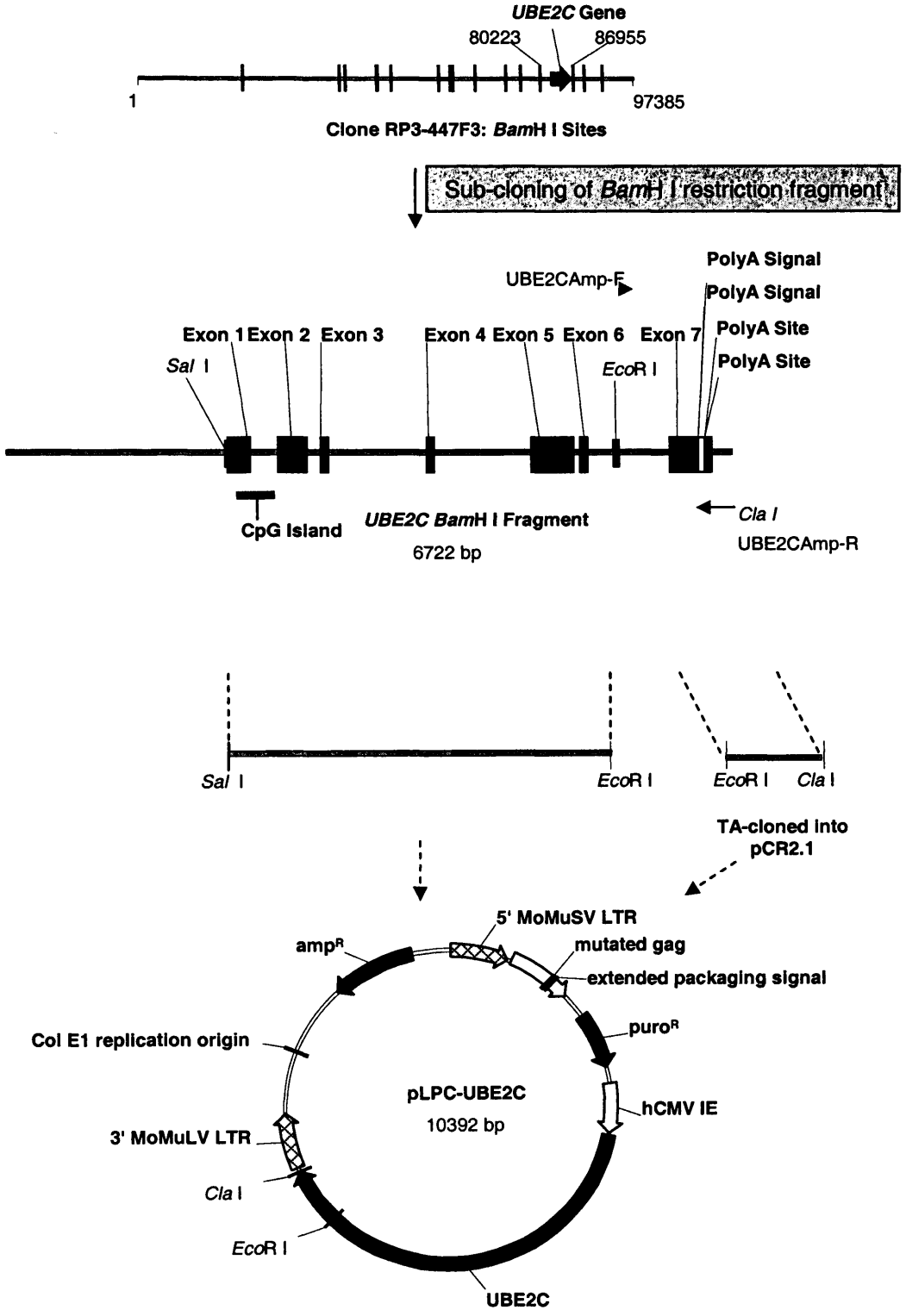
UBE2C Gene
80223
86955
1
97385
Clone RP3-447F3: BamH I Sites
Sub-cloning of BamH I restriction fragment
PolyA Signal
UBE2CAmp-F
PolyA Signal
Exon 1 Exon 2 Exon 3
Exon 4 Exon 5 Exon 6 Exon 7
PolyA Site
Sal I
EcoR I
PolyA Site
CpG Island
UBE2C BamH I Fragment
6722 bp
Cla I
UBE2CAmp-R
Sal I
EcoR I
EcoR I
Cla I
TA-cloned into
pCR2.1
5' MoMuSV LTR
ampR
mutated gag
extended packaging signal
puroR
Col E1 replication origin
pLPC-UBE2C
10392 bp
hCMV IE
3' MoMuLV LTR
Cla I
EcoR I
UBE2C

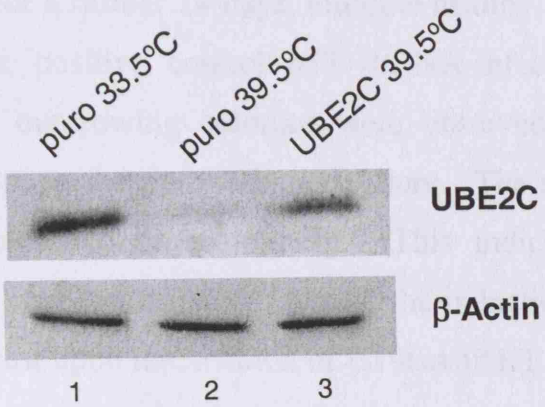

Figure 4.10: Constitutive Expression of UBE2C

Western blot analysis using the anti-Ubch10 monoclonal antibody indicated that UBE2C expression was elevated in HMF3AEco^{R} cells that constitutively expressed UBE2C at the non-permissive temperature. β-Actin was the loading control.

4.2.12.3 Constitutive Expression of UBE2C is Insufficient to Complement the Conditional HMF3A Growth Defect

Having demonstrated stable UBE2C expression in the HMF3A system under non-permissive conditions, pLPC-UBE2C, pLPCX and pRetroSuperp53 were then tested in the HMF3A complementation assay. 10 μg of each construct was introduced into HMF3AEco^R cells, using the protocol described for AKR1B1 shRNA constructs. Puromycin was removed from the culture medium and drug-resistant clones were directly shifted to 39.5°C. Following incubation at 39.5°C for a further 14 days, multiple healthy, growing colonies were observed in the positive control p53 shRNA-infected HMF3AEco^R culture, however, no outgrowing colonies were observed in the UBE2C-infected culture, similar to the puro-infected culture. The same results were obtained in a duplicate experiment culture. This indicated that ectopic UBE2C activity alone was insufficient to bypass the induction of the HMF3A irreversible growth arrest upon inactivation of U19tsA58 LT.

To determine whether the lack of complementation mediated by ectopic UBE2C expression in the HMF3A complementation assay was due to expression of an incorrect splice form, the identity of the exogenous *UBE2C* splice variant transcripts expressed in HMF3AEco^R cells was investigated. RNA was extracted from HMF3AEco^R puromycin-resistant polyclonal cultures infected with either *UBE2C* or control construct and incubated at both 33.5°C and 39.5°C for 7 days. Semi-quantitative RT-PCR, using two sets of primers (Splice-F and LNCXSEQ-R, and Splice-Fv2 and LNCXSEQ-R), was then used to distinguish all possible *UBE2C* splice variants (**Figure 4.11**). The reverse primer used was complementary to a sequence 3' to the multiple cloning site (MCS) of the pLPCX vector backbone, such that only exogenous *UBE2C* expression was detected. Accordingly, multiple PCR products specific to exogenous *UBE2C* were detected from HMF3AEco^R cells grown at both 33.5°C and 39.5°C for 7 days, namely #3, #4 and #5 (**Figure 4.11C**).

A

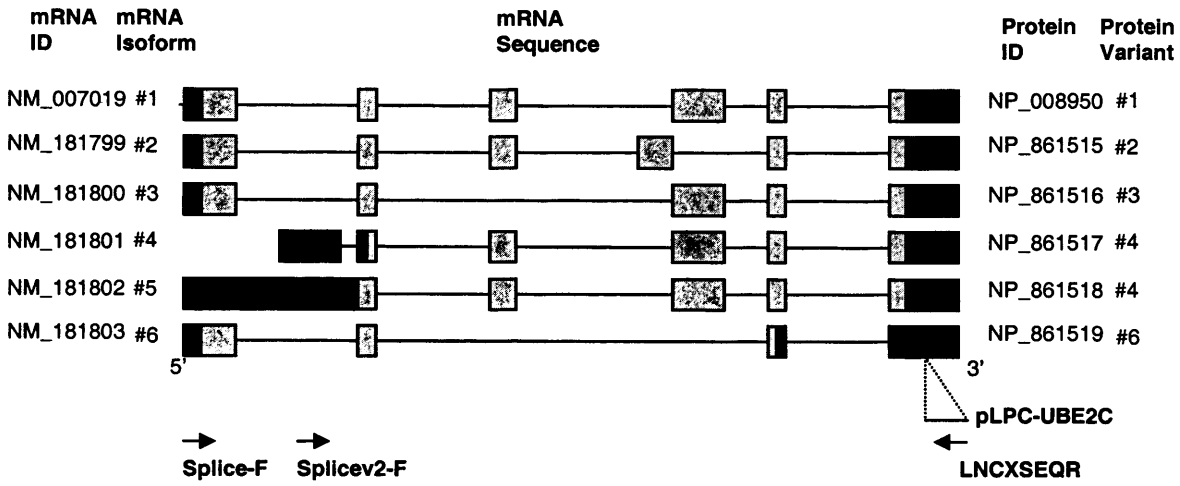

B

mRNA Isoform	*Splice-F + LNCXSEQR (bp)*	*Splicev2-F + LNCXSEQR (bp)*
1	719	NA
2	665	NA
3	632	NA
4	NA	823
5	1359	969
6	427	NA

Figure 4.11: Analysis of Exogenous *UBE2C* Expression

A: Diagram of PCR primers (indicated by black arrows) used to distinguish exogenous *UBE2C* splice variants by agarose gel electrophoresis. The 5' UTR is indicated in dark grey and the coding region is indicated in light grey; **B:** Table indicating the sizes of the PCR products expected from each splice variant; **C:** Semi-quantitative RT-PCR using primer combinations indicated. *GAPDH* was the loading control. Expression of *UBE2C* splice variants #3, #4 and #5 were detected using this method (as indicated).

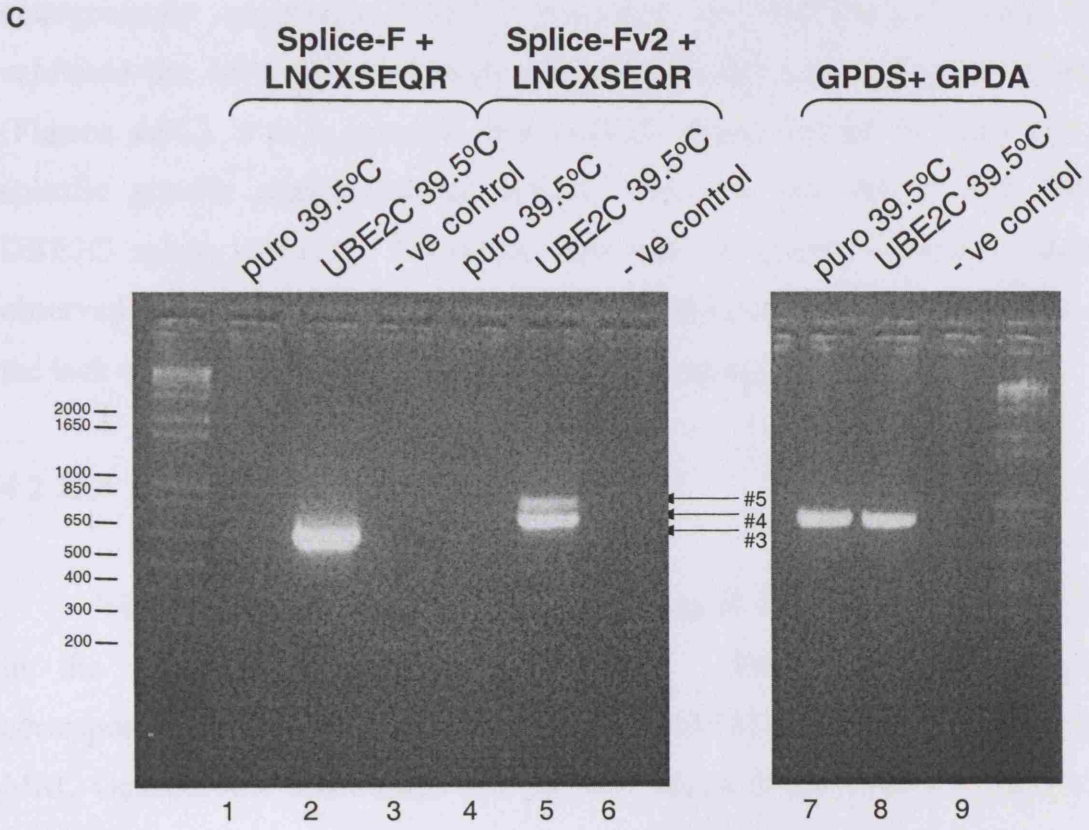
C
Splice-F + LNCXSEQR
Splice-Fv2 + LNCXSEQR
GPDS+ GPDA
puro 39.5°C
UBE2C 39.5°C
- ve control
puro 39.5°C
UBE2C 39.5°C
- ve control
puro 39.5°C
UBE2C 39.5°C
- ve control
2000
1650
1000
850
650
500
400
300
200
#5
#4
#3
1 2 3 4 5 6
7 8 9

However, the lack of detection of a 719 bp PCR product, using primers Splice-F and LNCXSEQ-R that corresponded to splice variant #1, indicated that this particular splice variant was not expressed under these conditions or, at least, expressed at too low a level to be detected by semi-quantitative RT-PCR.

Since this particular *UBE2C* splice variant was the most prominent endogenously expressed UBE2C transcript in HMF3AEco^R cells and exhibited the most differential down-regulation upon the temperature shift (**Figure 4.8C**), it was possible that UBE2C splice variant #1 conferred a specific growth complementing activity that was not shared with other UBE2C splice variants. Therefore, the lack of growth complementation observed in ectopically UBE2C infected HMF3AEco^R cells could be due to the lack of sufficient *UBE2C* splice variant #1 expression.

4.2.12.4 Constitutive Expression of UBE2C#1

To overcome this, constitutive expression of *UBE2C* splice variant #1 in the HMF3A system was undertaken. IMAGE clone 3345575, corresponding to *UBE2C* splice variant #1 (BC007656) was obtained from the MRC GeneService and cloned into pLPCX vector (**Figure 4.12**). Upon the generation of this construct, 10 μg of pLPC-UBE2C#1 and pLPCX was introduced into HMF3A cells, using the protocol described for AKR1B1 shRNA constructs, and used to generate polyclonal populations at 33.5°C. One duplicate culture was then maintained under drug selection at 33.5°C, whereas selection was removed from the second duplicate culture, then shifted to 39.5°C for a further 7 days before RNA was extracted.

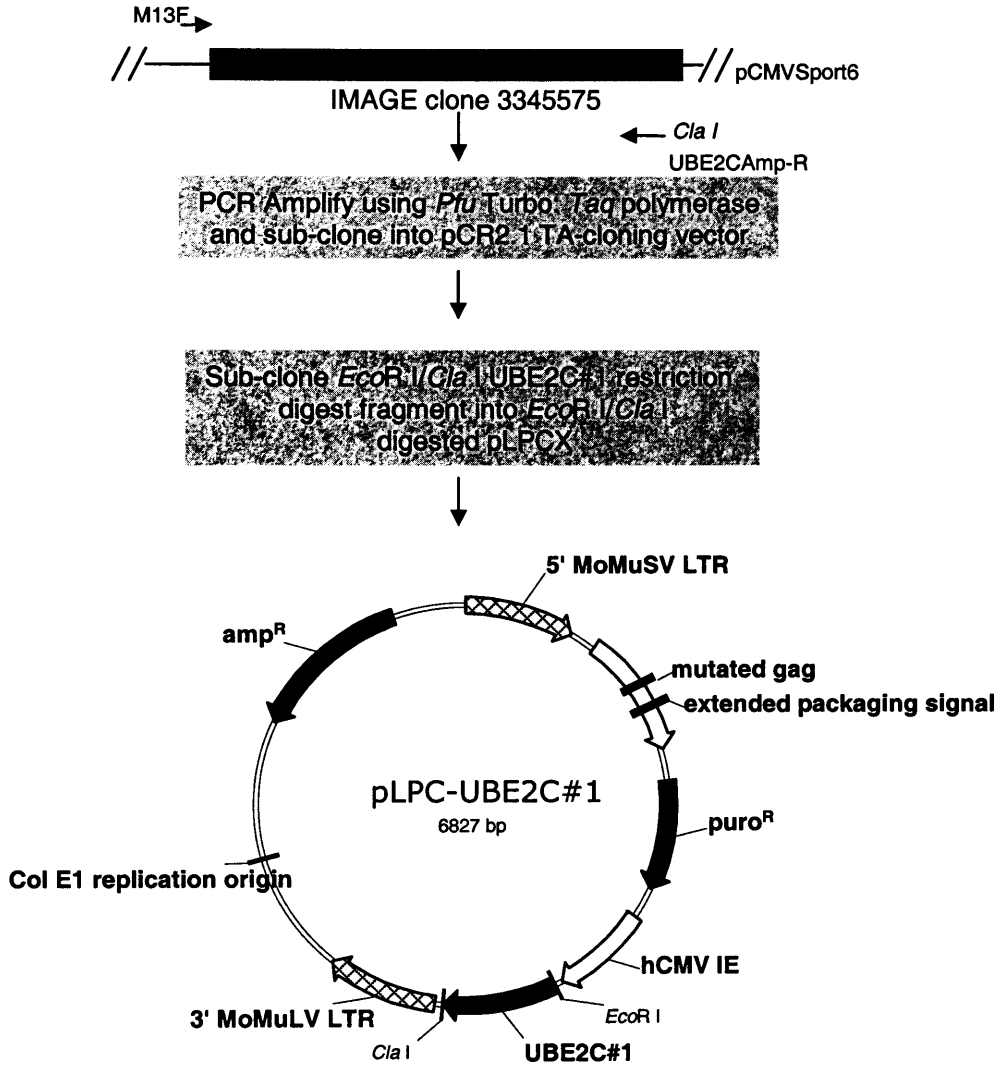

Figure 4.12: Generation of pLPC-UBE2C#1 Retroviral Expression Construct

The *UBE2C#1* ORF was PCR amplified from IMAGE clone 3345575 (MRC GeneService) using M13F and UBE2C-ampR primers (indicated by black arrows). The resultant sequence-verified PCR product was TOPO-cloned into pCR2.1 TA-cloning vector then sub-cloned as an *Eco*R I/*Cla* I restriction digest fragment into *Eco*R I/*Cla* I digested pLPCX to generate pLPC-UBE2C#1. MoMuSV: Moloney Murine Sarcoma Virus; MoMuLV: Moloney Murine Leukemia Virus; LTR: Long Terminal Repeat; hCMV IE: human Cytomegalovirus Immediate Early promoter; puro^R: puromycin resistance gene; amp^R: ampicillin resistance gene.

Semi-quantitative RT-PCR using primers specific to the exogenous *UBE2C* transcript (UBE2C-F and LNXCSEQ-R) generated a 521 bp PCR product that corresponded to the exogenous *UBE2C* splice variant #1 in UBE2C#1 infected HMF3AEco^R cells, at both 33.5°C and 39.5°C (**Figure 4.13A**, lanes 3 and 4, respectively), but not in control HMF3AEco^R cells (**Figure 4.13A**, lanes 1 and 2, respectively). This indicated that *UBE2C#1* was stably expressed at the mRNA level in HMF3AEco^R cells under both permissive and non-permissive conditions. RIPA protein lysates extracted from duplicate cultures incubated under the same conditions were analysed for UBE2C protein expression. Protein samples were separated by 12% SDS-PAGE and analysed by Western blot using anti-Ubch10 and, similar to before, a significant decrease in the intensity of a band of approximately 23 kDa that corresponded to UBE2C was observed in control HMF3AEco^R cells incubated at 33.5°C (**Figure 4.13B**, lane 1) and then shifted to 39.5°C for 7 days (**Figure 4.13B**, lane 2). However, a similar pattern of UBE2C expression was observed in UBE2C#1 infected HMF3AEco^R cells; a significant decrease in the intensity of the 23 kDa band was observed upon temperature shift to 39.5°C for 7 days (**Figure 4.13B**, lanes 3 and 4, respectively). This indicated that, unlike at the mRNA level, ectopic UBE2C#1 expression was not stable at the protein level at the non-permissive temperature.

4.2.12.5 Constitutive Expression of UBE2C#1 is Insufficient to Complement the Conditional HMF3A Growth Defect

At the same time as making the polyclonal UBE2C#1-expressing HMF3AEco^R cultures for RNA and protein analysis, the pLPC-UBE2C#1 retroviral expression construct was tested in the HMF3A complementation assay.

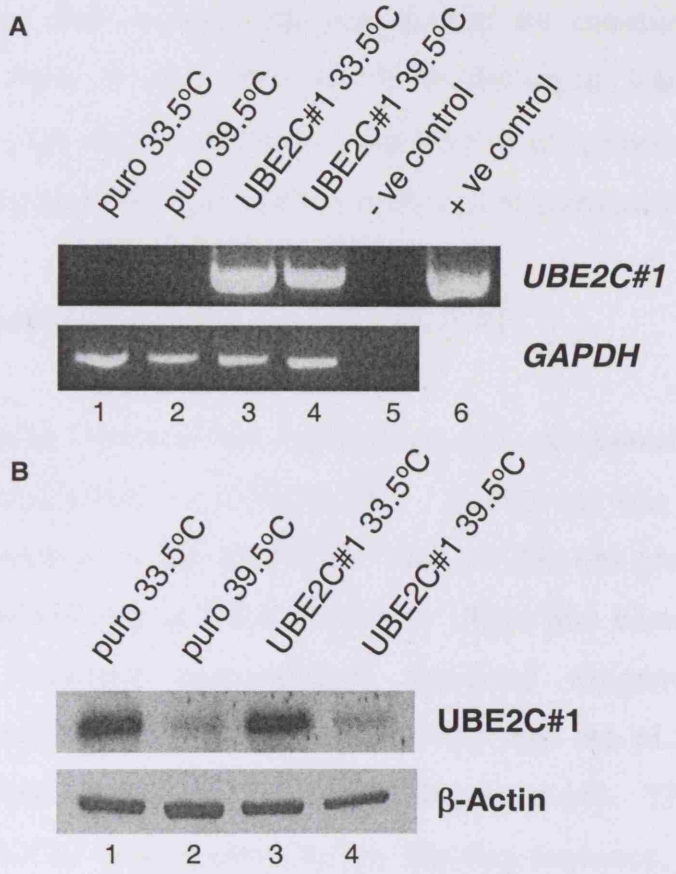

Figure 4.13: Constitutive Expression of UBE2C#1

A: Semi-quantitative RT-PCR using primers specific to the exogenous *UBE2C#1* transcript confirmed stable expression of *UBE2C#1* RNA at both permissive and non-permissive temperatures. pLPC-UBE2C#1 plasmid was the positive control for PCR and *GAPDH* was the loading control; **B:** Western blot analysis using the anti-Ubch0 monoclonal antibody indicated that there was no increase in UBE2C expression in UBE2C#1-infected HMF3AEco^{R} cells incubated at the non-permissive temperature for 7 days, relative to pLPCX-infected HMF3AEco^{R} cells incubated at the non-permissive temperature for 7 days. β-Actin was the loading control.

However, since exogenous UBE2C#1 expression could not be distinguished from the endogenous UBE2C splice variant #1 expression by Western blot analysis at 33.5°C and could not be detected at the protein level at 39.5°C, it was not surprising that it could not complement the conditional HMF3A growth defect. Also, it was not possible to determine whether lack of sufficient protein expression was due to instability of the protein at 39.5°C or whether the exogenous *UBE2C#1* mRNA could not be translated.

4.2.12.6 Constitutive Expression of Myc-UBE2C#1

To distinguish between the endogenous and exogenous proteins, an epitope tag was attached to the UBE2C ORF. A Myc-tag was chosen to be fused to the N-terminus of the *UBE2C#1* ORF, as this has previously been performed, yet did not impair UBE2C activity [Rape and Kirschner, 2004]. Moreover, this technical manipulation stabilised exogenous UBE2C expression. Accordingly, a Myc-tag was cloned into the pLPCUBE2C#1 construct to generate pLPCMyc- UBE2C#1, **Figure 4.14**). The ATG start codon of the *UBE2C#1* was replaced by the Myc-tag sequence, such that the *UBE2C#1* transcript read in-frame from the second codon onwards.

The resultant construct, pLPCMyc-UBE2C#1, in addition to pLPCX, was used to infect HMF3AEco^{R} cells. 10 μg of pLPCMyc-UBE2C#1 and pLPCX was introduced into HMF3A cells using the protocol described for AKR1B1 shRNA constructs and used to generate polyclonal populations at 33.5°C. One duplicate culture was then maintained under drug selection at 33.5°C, whereas selection was removed from the second duplicate culture, then shifted to 39.5°C for a further 7 days before RNA was extracted.

Figure 4.14: Generation of pLPC-Myc-UBE2C#1 Retroviral Expression Construct

An N-terminal Myc-tag was cloned directly upstream of the *UBE2C#1* ORF. In this process, PCR amplification of the *UBE2C#1* sequence in pLPC-UBE2C#1 vector was performed using a forward primer that incorporated an *Eco*R I restriction site and Myc-tag sequence directly upstream of the *UBE2C#1* ORF (indicated by black arrows). The resultant PCR product was TOPO-cloned into pCR2.1, sequence verified and sub-cloned as an *Eco*R I/*Cla* I restriction digest fragment into *Eco*R I/*Cla* I digested pLPCX vector to generate pLPC-Myc-UBE2C#1. MoMuSV: Moloney Murine Sarcoma Virus; MoMuLV: Moloney Murine Leukemia Virus; LTR: Long Terminal Repeat; hCMV IE: human Cytomegalovirus Immediate Early promoter; puro^{R}: puromycin resistance gene; amp^{R}: ampicillin resistance gene.

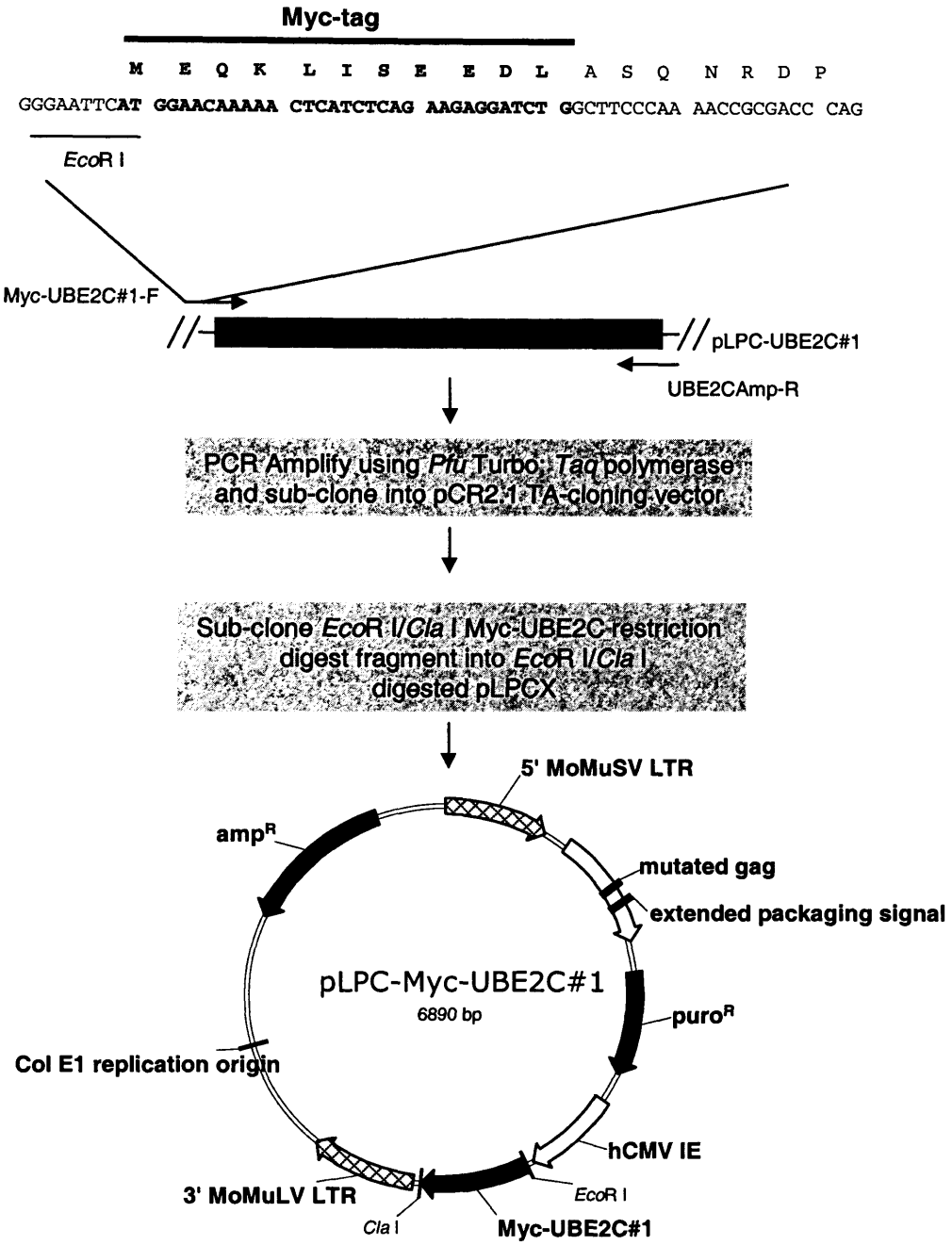
Myc-tag
M E Q K L I S E E D L A S Q N R D P
GGGAATTCAT GGAACAAAAA CTCATCTCAG AAGAGGATCT GGCTTCCCAA AACCGCGACC CAG
EcoR I
Myc-UBE2C#1-F
pLPC-UBE2C#1
UBE2CAmp-R
PCR Amplify using Pfu Turbo, Taq polymerase and sub-clone into pCR2.1 TA-cloning vector
Sub-clone EcoR I/Cla I Myc-UBE2C restriction digest fragment into EcoR I/Cla I digested pLPCX
5' MoMuSV LTR
amp^R
mutated gag
extended packaging signal
pLPC-Myc-UBE2C#1
6890 bp
puro^R
Col E1 replication origin
hCMV IE
3' MoMuLV LTR
EcoR I
Cla I
Myc-UBE2C#1

Semi-quantitative RT-PCR, using primers specific to the exogenous *UBE2C* transcript (N-myc UBE2C#1 and LNCXSEQ-R), generated a 659 bp PCR product that corresponded to the exogenous *Myc-UBE2C#1*, in Myc-UBE2C#1 infected HMF3AEco^R cells, at both 33.5°C (**Figure 4.15A**, lane 3) and 39.5°C for 7 days (**Figure 4.15A**, lane 4), but not in control HMF3AEco^R cells (**Figure 4.15A**, lanes 1 and 2, respectively). This observation implied that ectopic *Myc-UBE2C#1* was stably expressed at the transcriptional level in HMF3AEco^R cells under both permissive and non-permissive conditions.

Myc-UBE2C#1 expression was then analysed at the protein level. RIPA protein lysates were extracted from duplicate cultures incubated under the same conditions and then separated by 12% SDS-PAGE.

Western blot analysis was initially performed upon cell lysates derived from the same HMF3AEco^R cultures, using either the A14 rabbit polyclonal anti-c-Myc (Santa Cruz) or the 9E10 mouse monoclonal anti-c-Myc (Santa Cruz). Yet, Myc-UBE2C#1 expression could not be detected using either antibody (data not shown). The reasoning for this is unclear, but may indicate that the Myc epitope was masked in the Myc-UBE2C#1 construct. In contrast to the Myc Western blot data, Western blot analysis of the same lysates, using anti-Ubch10, identified a band of approximately 23 kDa that migrated slower than endogenous UBE2C in HMF3AEco^R cells infected with Myc-UBE2C#1 (**Figure 4.15B**, lane 5; indicated with arrow). The fact that this band exhibited retardation in mobility was attributed to the addition of the Myc tag to the UBE2C sequence. As a positive control, RIPA protein lysates derived from transient transfection of 10 μg pLPCMyc-UBE2C#1 and pLPCX into ϕ ecotropic cells were included in the Western blot analysis. A band exhibiting similar electrophoretic mobility was detected in ϕ ecotropic cell lysates transiently transfected with pLPCMyc-UBE2C#1 (**Figure 4.15B**, lane 2), but not pLPCX (**Figure 4.15B**, lane 1), thereby indicating that the identity of this band was Myc-UBE2C#1.

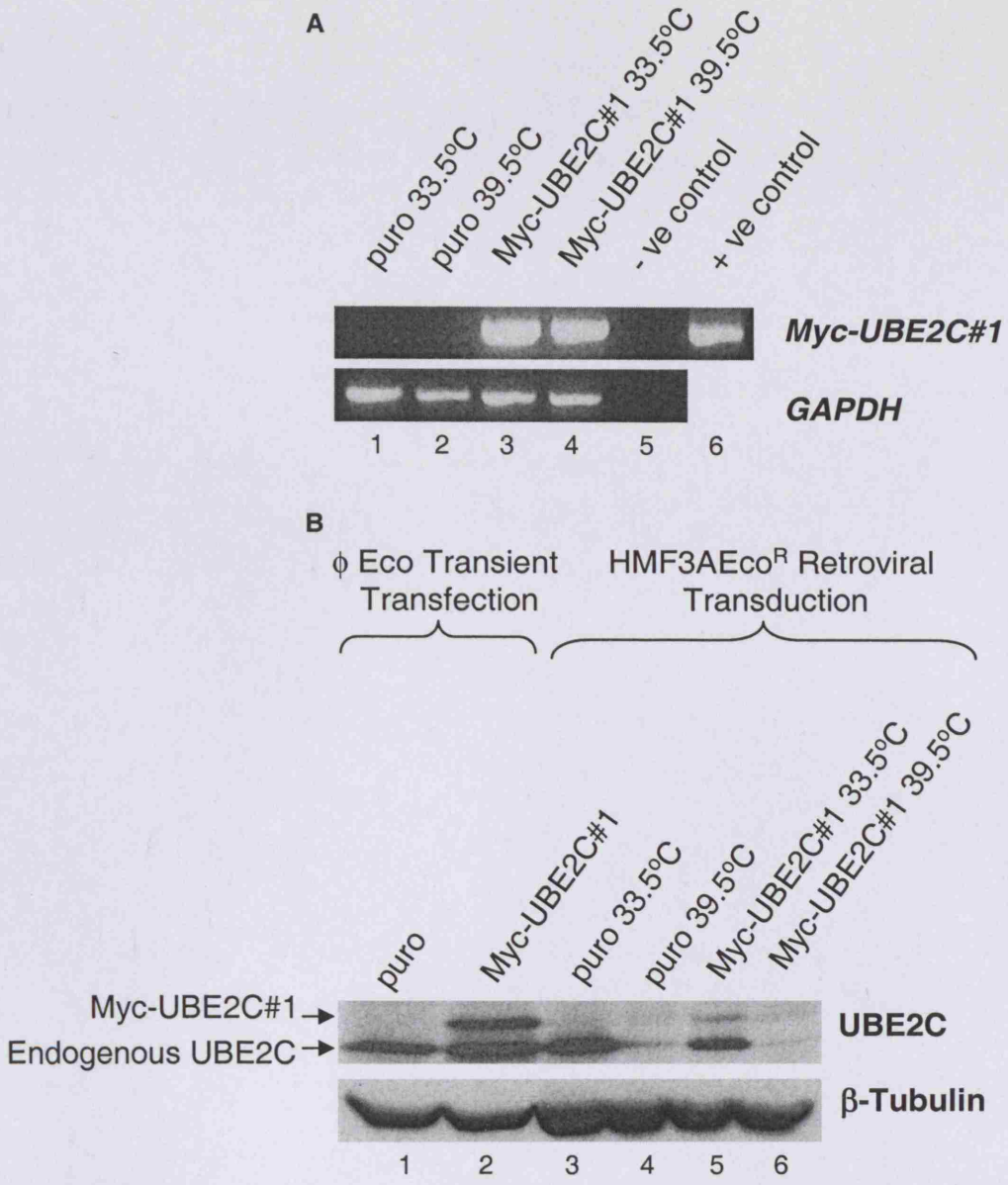

Figure 4.15: Constitutive Expression of Myc-UBE2C#1

A: Semi-quantitative RT-PCR using primers specific to the exogenous Myc-tagged *UBE2C* transcript demonstrated stable expression of *Myc-UBE2C#1* RNA at both 33.5°C and 39.5°C. pLPC-Myc-UBE2C#1 plasmid was the positive control for PCR and *GAPDH* was the loading control; **B:** Western Blot analysis using the anti-Ubch10 antibody indicated that Myc-UBE2C#1 expression could be distinguished from endogenous UBE2C expression using 12% SDS-PAGE since Myc-UBE2C migrated more slowly than endogenous UBE2C. Myc-UBE2C#1 expression was clearly detected at 33.5°C in Myc-UBE2C#1-infected HMF3AEco^R cells; however, it could not be detected at 39.5°C. Protein lysates derived from ϕ ecotropic cells transiently transfected with pLPC-Myc-UBE2C#1 was the positive control for Myc-UBE2C#1 expression and β-Tubulin was the loading control.

It should be noted, however, that a significant decrease in the intensity of this band was observed in Myc-UBE2C#1 infected HMF3AEco^R cells shifted from 33.5°C (**Figure 4.15B**, lane 5) to 39.5°C for 7 days (**Figure 4.15B**, lane 6).

4.2.12.7 Constitutive Expression of Myc-UBE2C#1 is Insufficient to Complement the Conditional HMF3A Growth Defect

Having detected exogenous Myc-UBE2C#1 expression in the HMF3A system, albeit at a low level, pLPCMyc-UBE2C#1, pLPCX and pRetroSuper-p53 were tested in the HMF3A complementation assay. 10 μg of each construct was introduced into HMF3AEco^R cells, using the protocol described for AKR1B1 shRNA constructs. Puromycin was removed from the culture medium and drug-resistant clones were directly shifted to 39.5°C. Following incubation at 39.5°C for a further 14 days, multiple healthy, growing colonies were observed in the positive control p53 shRNA-infected HMF3AEco^R culture, however, no outgrowing colonies were observed in the Myc-UBE2C#1-infected culture, similar to the puro-infected culture. The same results were obtained in a duplicate experiment culture. This indicated that ectopic UBE2C activity was insufficient to bypass the induction of the HMF3A irreversible growth arrest upon inactivation of U19tsA58 LT. However, since it was not possible to demonstrate significant expression of Myc-UBE2C#1 at 39.5°C, the capacity of UBE2C to complement the conditional HMF3A growth arrest remains to be determined.

4.3 SUMMARY

4.3.1 Microarray Analysis in the HMF3A System

In this chapter, gene expression profiling, using the Sanger/LICR/CRUK 10K human cDNA microarray, was used to investigate the signalling mechanisms involved in the induction of telomere-independent cellular senescence in the HMF3A system. As a result of this experimental approach, a number of known senescence-regulated genes were shown to exhibit significant changes in transcriptional activity upon the HMF3A conditional growth arrest. This indicated that both the experimental design and microarray analysis procedures used in this study appeared to be suitable for the identification of novel senescence-associated genes.

4.3.2 Identification of Candidate Genes by Microarray Analysis

Making the assumption that genes critically involved in mediating senescence would be commonly regulated in all HMF3A cultures complemented for growth at the non-permissive conditions, regardless of the reagent used to achieve complementation, 6 genes that fitted this profile were identified using SAM. These genes included *AKR1B1*, *CDH13*, *CUL4B* and *DAF* that were significantly up-regulated upon senescence, but were significantly down-regulated upon growth complementation. In contrast, *CKS2* and *UBE2C* were significantly down-regulated upon senescence, but were significantly up-regulated upon growth complementation.

4.3.3 Validation of Microarray Data by Real-Time PCR

Independent verification of the 10K cDNA microarray data by real-time PCR confirmed the differential expression profiles of three candidate genes identified in this study, namely *AKR1B1*, *CDH13* and *UBE2C*.

Furthermore, Western blot analysis validated the expression changes of both AKR1B1 and UBE2C at the protein level.

The fact that two of these three genes, namely *AKR1B1* and *UBE2C,* were shown to exhibit differential expression upon replicative senescence, as determined by microarray analysis of serially passaged primary human mammary fibroblasts [Hardy *et al*, 2005], provided further evidence that the genes identified in this study were intrinsically associated with the process of cellular senescence. Therefore, it is concluded that *AKR1B1*, *CDH13* and *UBE2C* represent novel markers of telomere-independent cellular senescence.

Microarray analysis has similarly been used to identify three genes whose expression correlates with *in vitro* oncogene-induced senescence, namely *CDKN2B*, *BHLHB2* and *TNFSF10D* [Collado *et al*, 2005]. However, it should be noted that of these three novel senescence-associated genes, only *BHLHB2* was represented on the 10K Sanger/LICR/CRUK microarray and it was not significantly differentially expressed upon the induction of the irreversible HMF3A growth arrest. This indicates that in the HMF3A system, at least, *BHLHB2* may not be a global marker of cellular senescence, as suggested by Collado and colleagues [Collado *et al*, 2005].

Real-time PCR data for *CKS2*, *CUL4B*, *FACL4*, *FAP*, *RAB1A* and *RANGAP1* was inconsistent with the microarray data. As no sequence information was supplied with the Assay-on-Demand kits, it was difficult to determine whether the lack of concordance observed was due to errors associated with the microarray procedure, or due to errors inherent to real-time PCR; for example, it was possible that individual splice variants were responsible for the differential expression observed by microarray analysis, yet were masked by real-time PCR by the expression of other, non-differential splice variants. Consequently, a real-time PCR experiment utilising specifically designed primers should address this issue.

The lack of concordance between different expression profiling techniques is not without precedent, however. For example, a cDNA microarray study that identified 17 differentially expressed genes, determined

that 4 of these genes did not correspond to the cDNA clones annotated in the microarrays, and that a further 5 genes could not be validated by northern blot analysis [Kothapalli *et al*, 2002]. Yet, this finding in itself is inconsistent with the findings of Larkin and colleagues [Larkin *et al*, 2005], who were able to validate differential expression data of approximate 90% of the genes identified by microarray analysis by real-time PCR. Therefore, the correlation between real-time PCR and microarray analysis data remains contentious.

4.3.4 Functional Analysis of Microarray Candidate Genes in the HMF3A System

The development of the HMF3A complementation assay, as described in **Chapter 3**, permitted functional analysis of the candidate genes identified in this study. Accordingly, RNAi was used to knockdown *AKR1B1* and *CDH13*, whereas constitutive expression was used to maintain *UBE2C* expression, and functional abrogation of candidate genes in conjunction with the HMF3A complementation assay represented a method with which to assess the ability of the candidate genes to complement growth under non-permissive conditions. Upon this basis, it was concluded that AKR1B1, CDH13 and UBE2C did not appear to be, by themselves, critical regulators of senescence.

However, the possibility that each of these genes do play an important role in senescence cannot be excluded. Indeed, there are two possible reasons to explain the lack of phenotypic activity observed for the microarray candidate genes in the HMF3A complementation assay.

Firstly, artefactual responses in the form of functional redundancy may have occurred as a result of compensatory gene activities and/or pathways, such that feedback mechanisms occurred to maintain steady-state expression of the targetted signalling pathways.

Secondly, technical manipulation of endogenous gene activity may not have equated to complete functional abrogation; for example, it was possible

that RNAi was not sufficiently efficient to knockdown target gene activity to bypass the effect of RNAi knockdown. Similarly, the converse was equally likely to be true for constitutive expression attempts. In this respect, it should be noted that a number of studies have shown that lower physiological levels of oncogenic Ras from a single copy allele activates the $p19^{ARF}$-p53 pathway in MEFS, but not to the same extent as over-expressing oncogenic Ras driven by a retroviral promoter [Guerra *et al*, 2003; Tuveson *et al*, 2004]. Accordingly, constitutive expression of UBE2C in $HMF3AEco^R$ cells under non-permissive conditions was not stable and was therefore not sufficient to mediate a physiological response, as indicated by Western blot analysis of Myc-UBE2C#1 expression in $HMF3AEco^R$ cells at 39.5°C.

To address this issue, constitutive Myc-UBE2C#1 expression should be attempted using an alternative experimental approach; for example, Myc-UBE2C#1 could be introduced into $HMF3AEco^R$ cells using a pWZL retroviral expression vector. The presence of an internal ribosomal entry site (IRES) directly downstream of the MCS in this vector system facilitates the concomitant translation of both the target gene and drug-resistance gene. If Myc-UBE2C#1 does not exhibit stable expression even under these conditions in $HMF3AEco^R$ cells at 39.5°C it may indicate that a mechanism of rapid UBE2C turnover specifically occurs at 39.5°C (discussed further in **Section 4.3.8**)

4.3.5 Alternative Methods to Functionally Validate Microarray Candidate Genes

To address these issues, alternative functional validation experimental methods should be considered. Examples include both reverse and combinatorial genetic approaches, as described below.

Reverse genetics approaches in the form of promoter analysis may be used to investigate critical, and, possibly, common mechanisms of transcriptional

regulation mediated by each of the candidate genes; for example, in our original HMF3A study [Hardy *et al*, 2005], we used *in silico* promoter analysis to analyse all differentially expressed genes in the HMF3A system to predict that NF-κB and C/EBP transcription factors were activated upon senescence. This prediction was subsequently confirmed by electrophoretic mobility shift assay. Therefore, a similar form of analysis could be applied to the candidate genes identified in this study.

An alternative reverse genetics approach would be to analyse the effect of p53 induction upon the HMF3A irreversible growth arrest, since inactivation of p53 was shown to be critical for maintaining growth of HMF3AEco^R cells (**Chapter 3**); for example, promoter binding sites occupied by p53 upon inactivation of LT by ChIP-chip analysis could be investigated. ChIP-chip analysis involves ChIP using an antibody targetted against the gene in question, followed by probing of an array in a procedure similar to microarray analysis. Since well-characterised p53 antibodies have been described, this experiment could easily be performed and would, therefore, enable p53 targets that are differentially occupied upon the growth arrest to be identified.

It is also important to consider senescence in an evolutionary context, since it may be argued that there is an immense selection pressure to lose senescence-promoting gene activity during the process of tumorigenesis and, as such, multiple pathways will have evolved to ensure that senescence ensues under appropriate physiological conditions. Assuming this hypothesis to be correct, it is likely that the functional abrogation of individual candidate genes in the HMF3A complementation assay may not be sufficient to generate a visible phenotype, since the action of other genes and/or pathways may mask this activity [Hartwell, 2004]. The exceptions to this hypothesis are p53 and p21, as shown in **Chapter 3**. Therefore, combinatorial genetics may be required to reveal functional interactions [Tong *et al*, 2004]. Such forms of experimental analysis are feasible in the HMF3A system, since combinatorial

siRNA constructs and/or retroviral expression constructs may be introduced into HMF3AEco^R cells under a variety of drug-selection conditions.

4.3.6 Alternative Methods to Analyse Growth Complementation in the HMF3A System

It is also important to consider the limitations of the microarray analysis used in this study.

Firstly, the 10K Sanger/LICR/CRUK cDNA microarray used in this study was restricted to the analysis of 6000 unique human genes, approximately 25% of the total 22 500 estimated number of unique human genes [International Human Genome Sequencing Consortium, 2004]. Therefore, this experiment was lacking with respect to complete genome coverage, an issue that can be addressed by the utilisation of genome wide affymetrix microarrays.

Secondly, the possibility that novel transcriptional regulation mechanisms played a significant role in the induction of senescence was not addressed. In this respect, miRNAs, rather than protein-encoding genes, have recently been identified as critical factors that regulate gene expression patterns [Lu *et al*, 2005]. Furthermore, the fact that two such miRNAs that function in this manner have been identified as regulators of *E2F1* transcription, directly links miRNA signalling to pathways associated with cell growth and proliferation [O'Donnell *et al*, 2005]. This indicates that differential miRNA expression upon HMF3A temperature shift should be investigated.

Thirdly, it is important to consider that microarray experiments restrict experimental analysis to changes that occur specifically at the transcriptional level. Consequently, the multiple facets of cell regulation that include post-transcriptional and post-translational mechanisms that regulate protein activity, including sub-cellular localisation, were not addressed in this analysis. Indeed, it is possible that post-transcriptional processes are

important in mediating such physiological responses; for example, *RAS* and *AKT*, two genes that may be involved in signalling the induction of senescence, are both known to be regulated at the level of translation [Rajasekhar *et al*, 2003]. Similarly, higher order methods of gene regulation may also be involved; for example, a study that compared the expression profile of senescent HDFs and human mammary epithelial cells did not identify common transcriptional changes, yet a correlation between chromosomal clustering of genes, whose expression is up-regulated, but not down-regulated upon senescence, was observed [Zhang *et al*, 2003]. It should be noted, however, that *AKR1B1*, *CDH13* and *UBE2C*, at least, do not exhibit chromosomal clustering in the human genome.

4.3.7 HMF3A Candidate Genes and their Association with P53

The finding that p53 has a critical role in the induction of senescence in the HMF3A system, as suggested in **Chapter 3**, indicated that the candidate genes identified by the microarray analysis were likely to represent downstream targets of p53. Indeed, in concordance with this finding, 4 of the 6 (67%) candidate genes identified in the 5-way overlap were representative of putative p53 effectors ([Hoh *et al*, 2002]; highlighted genes in **Figure 4.7** and **4.8**, respectively). For example, the p53 MH algorithm developed by Hoh and colleagues [Hoh *et al*, 2002] revealed multiple p53 consensus binding sites in *CDH13*, in addition to related cadherin family members, *CDH1, 2, 3, 4, 5, 6, 7, 9, 11, 12, 16, 17, 19* and *20* (**Figure 4.12D**). Specifically, 10 putative p53-responsive sites were identified towards the 3' end of the gene in a region spanning 175767 bases, including two sites that share 100% identity with the consensus sequence (asterisked). Therefore, this finding provided good evidence that *CDH13* is a direct transcriptional target of p53. However, experimental analysis is required to validate this observation. There is also evidence to link the function of CDH13 to cell proliferation in glioblastoma cells [Huang *et al*, 2003]; in this study, growth arrest was shown to be

dependent upon p21 expression. Further experimental analysis is required to validate this observation.

In contrast, however, neither *AKR1B1*, nor *UBE2C*, exhibited known p53 consensus binding sites, as indicated by the p53 MH algorithm [Hoh *et al*, 2002]. Yet the possibility that non-consensus p53 binding sites regulate gene transcriptional activity [Contente *et al*, 2002], or that p53 functions through a transcriptionally independent process [Chipuk and Green, 2003], cannot be excluded. It is interesting to note that *Seladin-1*, a gene similar to *AKR1B1* by virtue of the fact that it is a broadly expressed oxidoreductase, was identified in a GSE screen in Rat1 cells for genes that are involved in Ras-induced senescence [Wu *et al*, 2004]. There is some evidence to suggest that Seladin-1 can interact with p53, perhaps in response to cytonuclear localisation of Seladin-1 in response to reactive oxygen species (ROS), and inhibit p53 degradation in an Mdm2-dependent process. As oxidation of cholesterol produces ROS [Cutler *et al*, 2004], the authors suggest that Seladin-1 may act as a sensor and/or effector of oxidative stress. By extension, therefore, it is possible that AKR1B1 may be able to function in an analogous manner; a hypothesis that may be tested by applying AKR1B1 in the GSE screen, as described by Wu and colleagues [Wu *et al*, 2004].

4.3.8 Ubiquitin-Mediated Proteolysis and Senescence

It was also interesting to note that two of the candidate genes identified by microarray analysis, namely *UBE2C* and *CUL4B*, are implicated in the process of ubiquitin-mediated proteolysis. Moreover, UBE2C activity is linked to the regulation of cell cycle progression; UBE2C has been shown to undergo Anaphase-Promoting Complex (APC)-dependent degradation and function in an autoregulatory feedback loop to regulate both APC activity at G_2/M phase transition, and cyclin A degradation in early G_1 phase [Kramer *et al*, 2000; Rape and Kirschner, 2004; Sorensen *et al*, 2001]. In early G_1 phase, cyclin A is ubiqutinated by APC, however, upon APC-mediated degradation

of UBE2C in late G_1, cyclin A is stabilised. In turn, cyclin A binds to and phosphorylates Cdh1, thereby inactivating the APC. These activities are thought to be regulated by UBE2C as APC promotes the autoubiqutination and degradation of UBE2C. Moreover, it has been suggested that the availability of UBE2C is rate limiting for this process.

It was anticipated cloning a Myc-tag to the N-terminus of the *UBE2C#1* ORF would be sufficient to impair the ability of UBE2C to be degraded by ubiquitin-mediated proteolysis [Rape and Kirschner, 2004], and thereby stabilise UBE2C expression in the HMF3A system. This hypothesis was based upon the observation that UBE2C was shown to be autoubiquitinated by virtue of a destruction box motif located between amino acid residues 129-132 [Yamanaka *et al*, 2000]; it has been proposed that the ubiquitination machinery recognises the destruction box, since mutations within this motif stabilise UBE2C against targetted destruction [Lin *et al*, 2002]. However, Myc-UBE2C#1 expression in HMF3AEco^R cells at 39.5°C, unlike 33.5°C, was unstable. The reasoning for this is unclear, yet indicates that UBE2C stability, and therefore activity, may be involved in the induction of senescence.

Ubiquitin-mediated proteolysis is a rapid and specific process that facilitates the ordering of timely events and it is, therefore, a suitable mechanism with which to regulate the stability of critical regulators of cell proliferation in a cell cycle-dependent manner [Clarke, 2002; Pines and Lindon, 2005]; for example, proteolysis of most of the core components of the cell cycle machinery are controlled by two major classes of ubiquitin ligases, namely the Skp1/Cullin/F-box protein (SCF) and APC complexes [Peters, 2002]. Therefore, the findings from this microarray study indicate that the role of ubiquitin-mediated proteolysis in senescence, particularly the stability and functional activity of UBE2C, requires further investigation.

5. Identification of a Novel, Putative Role for 13S E1A in the Abrogation of Senescence

5.1 OBJECTIVES

HMF3A cells infected with a 12S E1A retrovirus and directly selected for growth at 39.5°C were able to complement the temperature sensitive growth defect of these cells (**Chapter 3**). In contrast however, HMF3A cells infected with the same 12S E1A retrovirus and maintained at the permissive temperature retained the conditional growth phenotype, since they entered into an irreversible growth arrest when they were shifted from 33.5°C to 39.5°C for 7 days.

RT-PCR analysis, using RNA derived from these two different culture conditions, revealed that HMF3A cells complemented for growth at 39.5°C contained an anomalous *E1A*-specific PCR product that was absent in HMF3A cultures infected with E1A and maintained at 33.5°C.

In this chapter, the possibility that this differential pattern of *E1A* expression was causal to the disparate HMF3A growth response was investigated.

5.2 RESULTS

5.2.1 Anomalies Associated with E1A Expression in the HMF3A System

In **Chapter 3**, expression of E1A in the HMF3A system was shown to be sufficient to bypass the conditional growth arrest of these cells (**Section 3.2.5.2**) and E1A expression was confirmed by both RT-PCR and Western blot analysis (**Figure 3.8**).

Analysis of the growth characteristics of E1A-infected HMF3A cells incubated at 33.5°C then shifted to 39.5°C indicated, however, that these cells entered into an irreversible growth arrest, identical to pLPCX-infected HMF3A cells. Therefore, growth analysis of E1A- and pLPCX-infected HMF3A cultures maintained at 33.5°C and shifted to 39.5°C for 10 days was performed to verify this. HMF3A cells were seeded at 2000 cells in duplicate T25 cm^2 flasks and incubated at either 33.5°C for 5 and 7 days, or at 39.5°C for 5, 7 and 10 days. Average cell counts were then determined. Exponential growth was observed for both E1A- and pLPCX-infected HMF3A cultures incubated at 33.5°C, however, no significant increase in growth was observed for either condition at 39.5°C, even after 10 days (**Figure 5.1A**). Similar results were obtained in a duplicate experiment (data not shown).

These findings were contradictory to those presented in **Section 3.2.5.2** as they suggested that E1A did not possess growth complementation activity in one experimental setting, yet did so under differential conditions. As such, the functional activity of E1A in the HMF3A system was investigated further.

Reanalysis of the RT-PCR data indicated that a PCR product that was larger and more prominent than the expected 492 bp *12S E1A* PCR product was detected in E1A-infected HMF3A cells that were complemented for growth at 39.5°C (**Figure 3.8B**, lane 3).

Figure 5.1: E1A Expression in the HMF3A System

A: Growth characteristics of HMF3A cells incubated at 33.5°C for 7 days or shifted from 33.5°C to 39.5°C for 10 days; **B:** RT-PCR analysis of two independently-generated, growth complemented HMF3A cultures infected with E1A and maintained at 39.5°C for a minimum of 4 passages. The two different PCR products identified are labelled as A and B (indicated by arrow); **C:** Known splice variants of *E1A* and location of primer binding sites used for the RT-PCR analysis. *GAPDH* was the loading control; **D:** Bar chart indicating the different *E1A* splice variants detected by TA-cloning of the RT-PCR products shown in **Figure 5.1B**. Some of these sequences did not align to any of the known *E1A* splice variants (labelled as other).

A

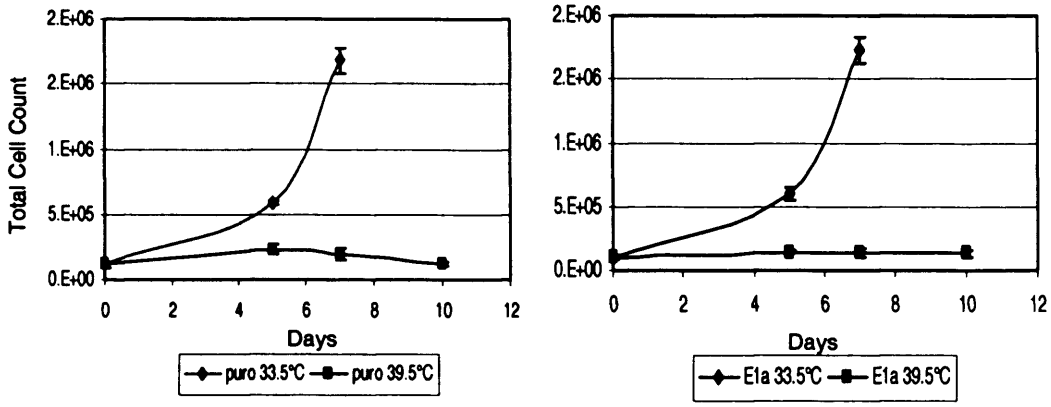
Total Cell Count
2.E+06
2.E+06
1.E+06
5.E+05
0.E+00
0
2
4
6
8
10
12
Days
puro 33.5℃
puro 39.5℃
E1a 33.5℃
E1a 39.5℃

B

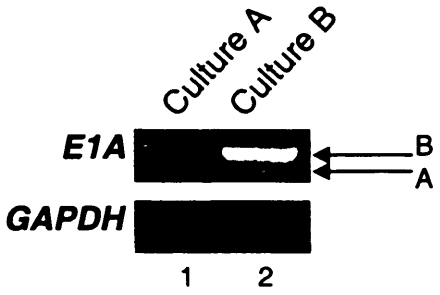
Culture A
Culture B
E1A
GAPDH
B
A
1
2

C

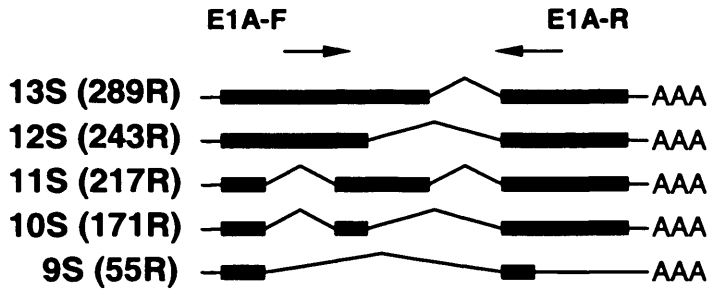
E1A-F
E1A-R
13S (289R)
12S (243R)
11S (217R)
10S (171R)
9S (55R)
AAA

D

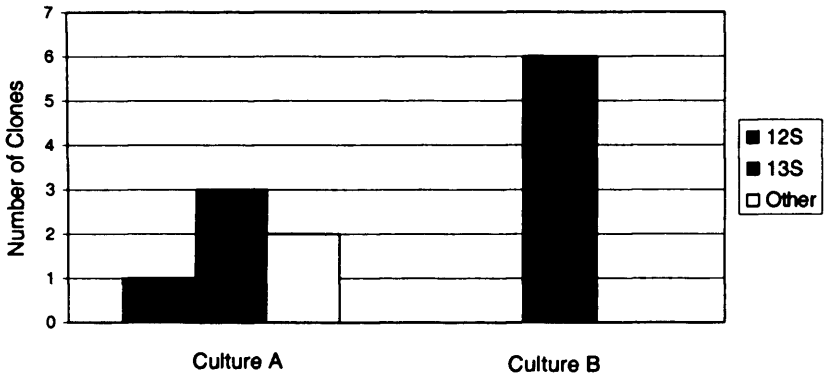
Number of Clones
7
6
5
4
3
2
1
0
Culture A
Culture B
12S
13S
Other

Significantly, this PCR product was not generated from RNA derived from E1A-infected HMF3A cells maintained at 33.5°C (**Figure 3.8B**, lane 1) or E1A-infected HMF3A cells shifted from 33.5°C to 39.5°C for 7 days (**Figure 3.8B**, lane 2). This finding was reproducible, since RT-PCR analysis of RNA derived from a second, independently generated, HMF3A culture directly complemented for growth at 39.5°C by infection with E1A was similarly able to generate two distinct PCR products (**Figure 5.1B**, lane 2).

5.2.2 Analysis of E1A Splice Variants Expressed in the HMF3A System

The Adenovirus *E1A* region is differentially processed to generate at least 5 different splice variants, namely *13S*, *12S*, *11S*, *10S* and *9S* (**Figure 5.1C**). The most abundant *E1A* mRNA species are the two largest variants, namely *12S* that encodes a 243 aa protein and *13S* that encodes a 289 aa protein. BLAST sequence alignment of the *E1A*-specific primers used in this study, E1A-F and E1A-R, indicated that they were capable of amplification of both *12S* and *13S E1A* splice variants. Furthermore, the resultant PCR products should be distinguishable upon the basis of size since the 492 bp *12S E1A*-specific PCR product differed from the 635 bp *13S E1A*-specific PCR product by 143 bp. Thus, it was likely that the smaller PCR product (indicated as PCR product A by an arrow in **Figure 5.1B**) corresponded to *12S E1A* mRNA, whereas the larger PCR product (indicated as PCR product B by an arrow in **Figure 5.1B**) was derived from *13S E1A* mRNA.

To confirm this possibility, cDNA derived from the two growth-complemented HMF3A cultures infected with E1A, was cloned into a TA-cloning vector (Invitrogen) and transformed using TOP10F cells. Blue/white screening was used to identify positive clones, of which, 6 were picked and prepped from each transformation plate. Sequence analysis of each of these clones, using the same *E1A*-specific primers, confirmed that *13S E1A* was present in the majority, if not all, bacterial clones analysed (**Figure 5.1D**). However, it should be noted that a few of the transcript sequences derived

from culture A did not align to any of the known *E1A* splice variants, unlike culture B. The reason for this is unclear, however it was possible that these transcripts were representative of novel *E1A* splice variants or artifacts resulting from the culmination of experimental procedures used to isolate the sequences.

5.2.3 Verification of 13S E1A Expression in Growth Complemented HMF3A Cells by Western Blot Analysis

Having shown that the larger PCR band was due to the *13S E1A* RNA, expression at the protein level was also investigated.

RIPA lysates were extracted from E1A- and pLPCX- infected HMF3A cells grown at both 33.5°C, and at 39.5°C for 7 days, in addition to growth-complemented E1A-infected HMF3A cells that had been serially sub-cultivated at 39.5°C for a minimum of 4 passages. RIPA lysates were also prepared from growth-complemented HMF3A cells shifted from 39.5°C to 33.5°C for 7 days. Samples separated by 12% SDS-PAGE were analysed by Western blot analysis using M73 monoclonal E1A antibody (as described in **Section 3.2.5.1**). Multiple bands of approximately 45 kDa, corresponding to E1A, were detected in the positive control for E1A expression, ϕ ecotropic cells (**Figure 3.8C**, lane 7). It was possible that the slowest migrating species identified by M73 (indicated by an arrow) was representative of the 289 aa 13S E1A protein, and, in accordance with this, a corresponding band was observed in E1A growth-complemented HMF3A cells (**Figure 3.8C,** lanes 5 and 6), but not in pLPCX-infected HMF3A cells incubated at both 33.5°C (**Figure 3.8C**, lane 1) and 39.5°C for 7 days (**Figure 3.8C**, lane 2) or E1A-infected HMF3A cells incubated at both 33.5°C (**Figure 3.8C**, lane 3) and 39.5°C for 7 days (**Figure 3.8C**, lane 4).

To confirm this finding, 13S E1A protein expression was analysed using a 13S-specific E1A monoclonal antibody, M3 (gift from E. Harlow).

This detected a band of approximately 45 kDa that corresponded to 13S E1A in the ϕ ecotropic positive control sample (**Figure 3.8C**, lane 7), and in the growth complemented E1A-infected HMF3A cells (**Figure 3.8C**, lanes 5 and 6). In contrast, however, no corresponding bands were detected in pLPCX-infected HMF3A cells incubated at both 33.5°C (**Figure 3.8**, lane 1) and 39.5°C for 7 days (**Figure 3.8**, lane 2), or in E1A-infected HMF3A cells incubated at both 33.5°C (**Figure 3.8C**, lane 4) and 39.5°C for 7 days (**Figure 3.8C**, lane 4). This indicated that the slowest migrating species detected with the M73 antibody was indeed the 289 aa 13S E1Aprotein.

5.2.4 Possible Sources of 13S E1A Contamination

It was difficult to reconcile the apparent paradoxical data described here; namely, 13S expression occurred upon the introduction of a DNA construct consisting only of a *12S* cDNA, since this observation implied the acquisition of a 138 bp sequence, specific to *13S*, in a cellular system that lacked endogenous *13S* expression.

Low level *13S* contamination of the pLPC-12SE1AORI construct utilised in this experiment represented a simple explanation for this observation, yet the plasmid preparation utilised for the retroviral packaging was amplified from a single bacterial clone. Moreover, sequence analysis of this plasmid preparation did not give any indication of contamination with a *13S E1A* plasmid construct. Indeed, this possibility was discounted by the fact that *13S* expression was undetectable in HMF3A cultures infected with E1A and grown under permissive conditions (**Figure 3.8A**, lane 1 and **Figure 3.8B**, lane 3). However, it could be argued that 13S expression did occur in cultures grown at 33.5°C, but was not detected due to selective outgrowth under these conditions; for example, 13S is known to be more pro-apoptotic than 12S. Alternatively, 13S, unlike 12S, could have exhibited significant cold-sensitivity. Yet, this possibility was rendered unlikely by the fact that 13S expression was readily observed, indeed elevated, in growth-

complemented E1A-infected HMF3A cultures that were shifted from 39.5°C to 33.5°C for 7 days (see **Figure 3.8C,** lanes 5 and 6).

An alternative explanation for the acquisition of 13S E1A expression in HMF3A cells was the possibility that *13S* cDNA was generated and packaged as a retrovirus as a consequence of a recombination event during production of virus particles after transient transfection of amphotropic retroviral packaging cells. ϕ amphotropic cells are a derivative of 293T cells and were originally developed by transformation of human embryonic kidney cells with sheared adeno 5 virus and, as such, express multiple *E1A* splice variants, including *13S E1A* (**Figure 3.8C**, lane 7). Alternatively, homologous recombination of the pLPC-12SE1AORI construct-derived sequences with integrated genomic *13S* sequences may have occurred during the transfection event. In any case, such recombinational events are likely to be rare and, therefore, signified that there was a very potent selection pressure for the retention of 13S expression in HMF3A cells at 39.5°C.

5.2.5 Structural and Functional Differences Between 12S and 13S E1A

Consideration of the functional activities of both 12S and 13S could give some indication as to how this phenotypic difference could have been mediated. In this respect, it was known that 12S and 13S differed by the internal inclusion of a 46 aa sequence that constituted the so-called conserved region 3 (CR3) 'unique region' in 13S. 12S represses the transcription of several viral promoters and a number of cellular genes involved in the control of cell growth and differentiation, whereas 13S functions as a potent transcriptional activator by virtue of the presence of the CR3 domain [Metcalf *et al*, 1994].

This suggested a possible model whereby transcriptional activation events mediated by 13S, but not 12S, were required to mediate senescence-bypass in the HMF3A system. Therefore, a testable hypothesis was that

constitutive expression of *13S* cDNA, but not *12S* cDNA, would be sufficient to permit continued HMF3A proliferation at 39.5°C.

5.2.6 Generation of 12S and 13S cDNA Retroviral Expression Constructs

To test the above hypothesis, separate 12S and 13S retroviral constructs were required. *12S* and *13S E1A* cDNA sequences, derived from pLPC-12SE1AORI and a *13S E1A* expression construct (gift from R. Ricciardi), respectively, were PCR-amplified, using primers that incorporated a *Bgl* II restriction site directly upstream of the common start codon and a *Not* I restriction site directly downstream of the common stop codon (**Figure 5.2**). The initial cloning strategy involving the directional cloning of the *Bgl* II/*Not* I digested *E1A* fragments into *Bgl* II/*Not* I digested pLPCX vector (BD Biosciences). However, due to technical difficulties encountered during this process, PCR products were cloned instead into a TA-cloning vector (Invitrogen), sequence verified, then sub-cloned into pBabepuro as *Eco*R I digested fragments.

5.2.7 Retroviral Expression of 12S and 13S E1A in the HMF3A System Using the Ψ_2 Retroviral Packaging System

As described in **Chapter 3**, the HMF3A system had been engineered to stably express the murine ecotropic receptor. This meant that the inherent problem of using an amphotropic E1A-expressing retroviral packaging cell line to assess the functional activities of 12S and 13S in HMF3AEco^R cells was circumvented; for example, one of a number of ecotropic retroviral packaging systems, such as TeFLY Mo or Ψ_2, could be utilised instead of the ϕ system.

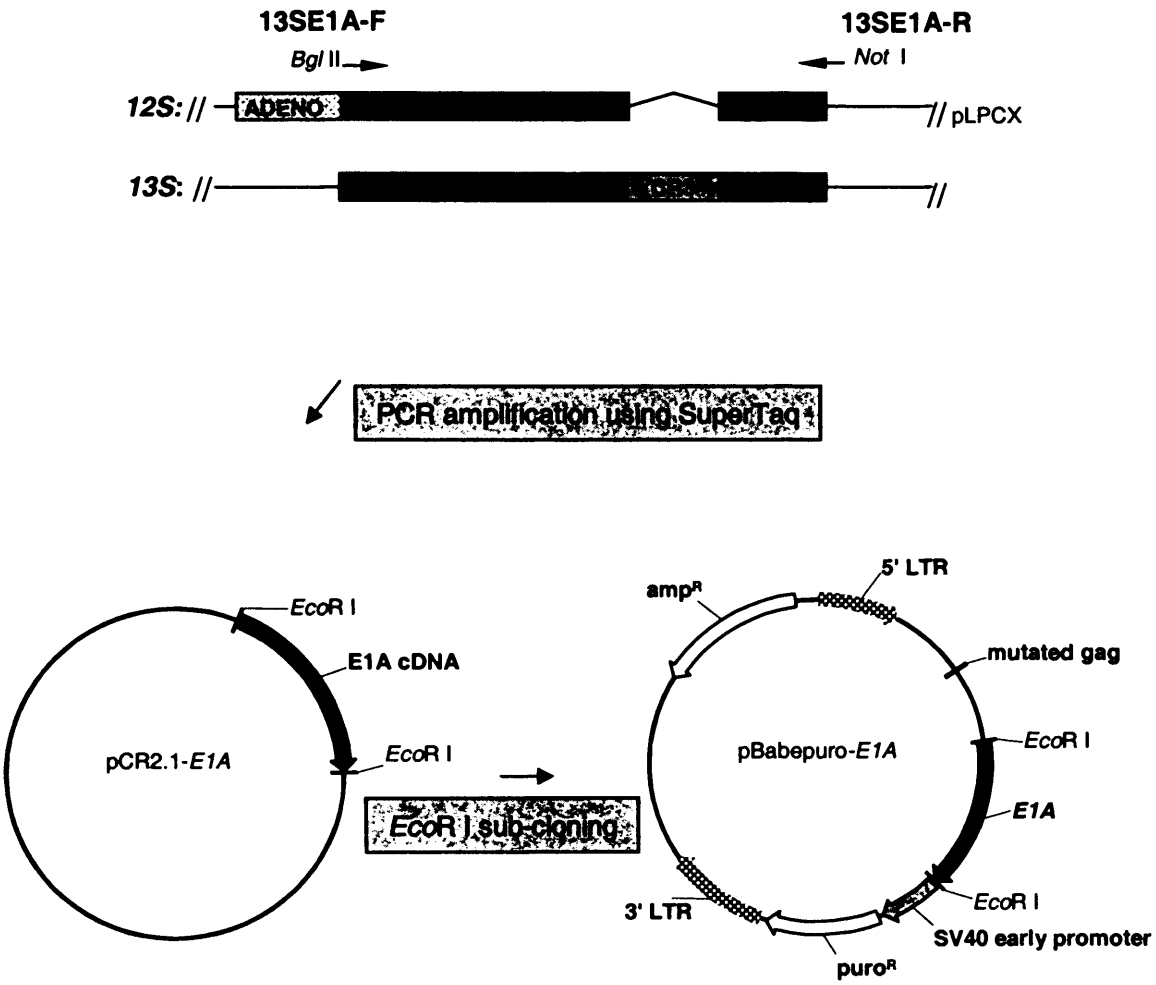

Figure 5.2: Generation of pBabepuro 12S and 13S E1A cDNA Retroviral Expression Constructs
12S and *13S* cDNA sequences were PCR-amplified using SuperTaq from pLPC-12SE1AORI and a wt 13S E1A expression construct (gift from R. Ricciardi) using common primers, then TA-cloned into pCR2.1-TOPO (Invitrogen). Sequence verified *12S* and *13S* were then sub-cloned into pBabepuro as *Eco*R I restriction digest fragments. CR3: Conserved Region 3; LTR: Long Terminal Repeat; puro^R: puromycin resistance gene; amp^R: ampicillin resistance gene.

5.2.7.1 Retroviral Expression of pBabepuro-Based Constructs

Retroviral delivery of the original pLPC-12SORIE1A, pBabepuro, pBabepuro-12S, pBabepuro-13S cDNA E1A-packaged constructs into HMF3AEco^R cells was performed using TeFLY Mo ecotropic retroviral packaging cells, a derivative of TE671 cells [Cosset *et al*, 1995]. 10 μg of each retroviral expression construct was packaged, using TeFLY Mo cells, and used to infect HMF3AEco^R cultures seeded at $5x10^5$ cells in duplicate T75 cm^2 cultures in the presence of 8 μg/ml polybrene. Following 4 days incubation at 33 C, 2 μg/ml puromycin was added to the culture medium. Unfortunately, the transfection efficiency of this procedure was extremely low, since only a few drug resistant colonies were observed upon completion of 4 days of drug treatment. Therefore, a NIH3T3-derived ecotropic retroviral packaging cell line, Ψ_2, was utilised for retroviral packaging instead [Mann *et al*, 1983]. Using the same protocol as described for TeFLY Mo infection, HMF3AEco^R cells were infected with pLPCX, pLPC-12SORIE1A, pBabepuro, pBabepuro-12SE1A and pBabepuro-13SE1A retroviral constructs. An increased level of transduction efficiency, relative to the TeFLY Mo system, was achieved using this method since >10 puromycin-resistant HMF3AEco^R clones were observed in each culture. The drug-resistant clones were trypsinised, pooled and replated then expanded under permissive conditions in the presence of puromycin before RNA was extracted.

Semi-quantitative RT-PCR using primers specific to *E1A* (E1A-F and E1A-R) were used to analyse *E1A* expression in each of these cultures. As a result, 492 bp and 635 bp PCR products that corresponded to *12S* and *13S E1A*, respectively, were generated from the positive control RNA sample of ϕ ecotropic cells (**Figure 5.3**, lane 5).

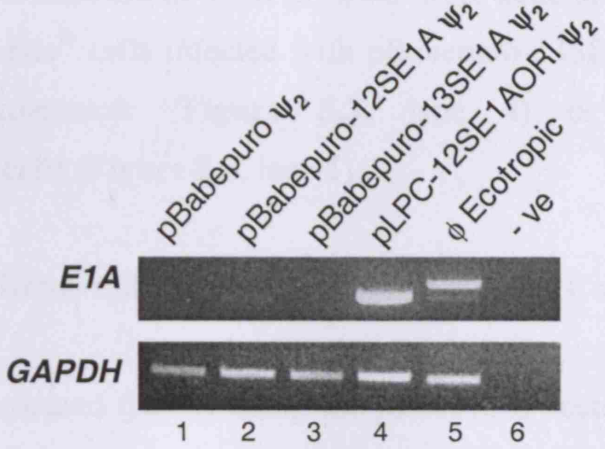

Figure 5.3: Expression of 12S and 13S E1A using pBabepuro-Based 12S and 13S Retroviral Expression Constructs

RT-PCR of 12S *E1A*- and 13S *E1A*- infected HMF3AEco^{R} cultures using E1A-F and E1A-R primers. RNA derived from HMF3AEco^{R} cells infected with retrovirally-packaged pLPC-12SE1AORI was the positive control for the transduction process whereas RNA derived from ecotropic cells was the positive control for PCR. *GAPDH* was the loading control.

In constrast, a 492 bp PCR product only that corresponded to *12S E1A* was generated from RNA derived from HMF3AEco^R cells infected with the pLPC-12SE1AORI derived-retroviral expression construct (**Figure 5.3**, lane 4). However, only a faint PCR product was generated from RNA derived from HMF3AEco^R cells infected with pBabepuro-12S (**Figure 5.3**, lane 3). This band was non-specific, as it was not observed in a duplicate experiment (data not shown). In contrast, no PCR products were generated from RNA derived from HMF3AEco^R cells infected with pBabepuro-13SE1A derived-retroviral expression constructs (**Figure 5.3**, lane 4) or pBabepuro-infected HMF3AEco^R cells (**Figure 5.3**, lane 1).

5.2.7.2 Retroviral Expression of pLPCX-Based Constructs

This indicated that by using the pBabepuro vector system, expression of *12S* and *13S* were too low to be detectable by RT-PCR. This could be attributed to the fact that constitutive gene expression was driven by the 5' LTR in the pBabepuro system, unlike the human cytomegalovirus immediate early promoter (hCMV IE) in the pLPCX system. Therefore, to overcome this problem, *12S* and *13S* sequences were sub-cloned from the pBabepuro vector backbone into pLPCX as *Eco*R I restriction fragments (**Figure 5.4**).

It should also be noted that the pLPC-12SE1AORI construct configuration that was utilised in the original E1A experiment contained a region of adenoviral genomic sequence, of unknown length, 5' to the *12S* start codon that may have facilitated relatively high levels of constitutive *12S* expression. Therefore, to recapitulate this configuration in a *13S* construct, the *13S* specific CR3 region of pBabepuro-13SE1A cDNA *E1A* was cloned into the pLPC-12SE1AORI construct. In this way, the 203 bp *Dra* III restriction fragment of *12S* was replaced with the 341 bp *Dra* III restriction fragment of *13S* (**Figure 5.5**).

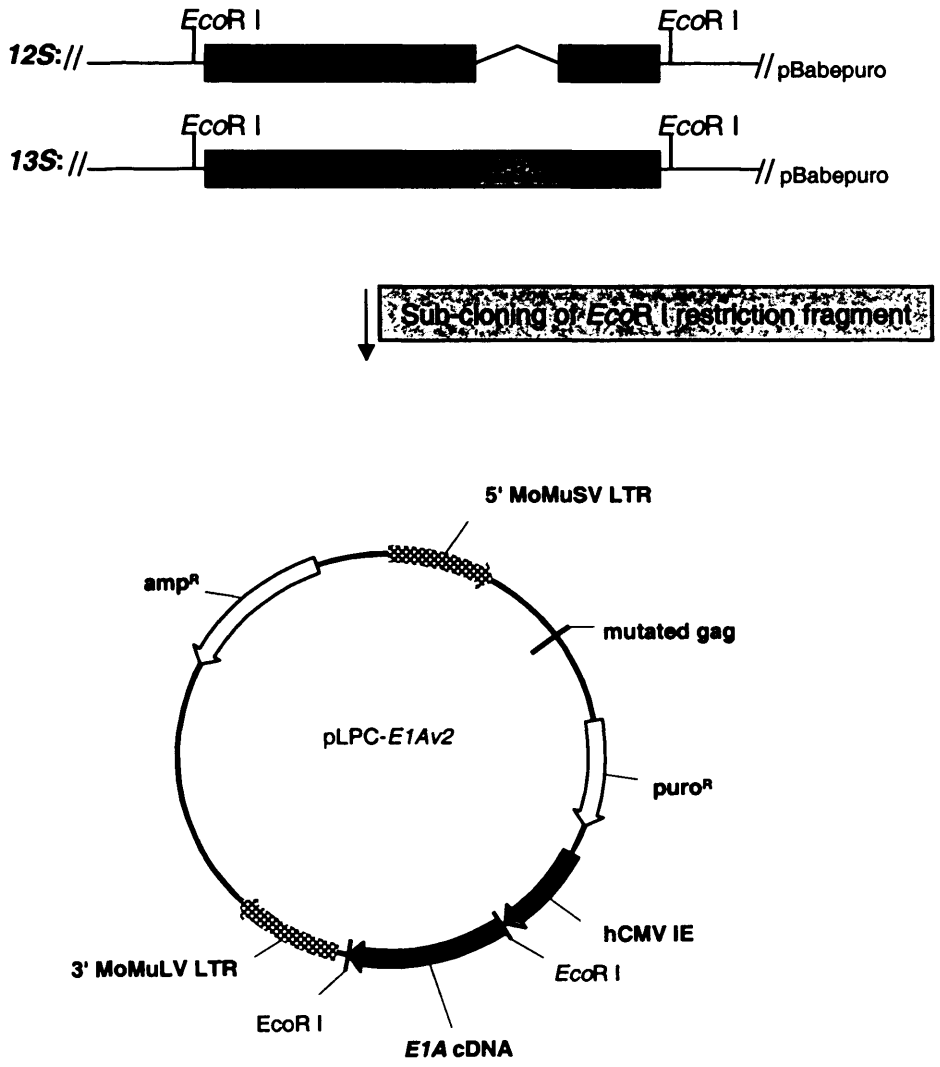

Figure 5.4: Generation of pLPC-E1Av2 12S and 13S Retroviral Expression Constructs

*Eco*R I restriction fragments of *12S* and *13S* E1A cDNA sequences from pBabepuro retroviral expression constructs were sub-cloned into *Eco*R I digested pLPCX vector. pLPC-12Sv2 and pLPC-13SE1Av2 were the resultant constructs. CR3: Conserved Region 3; MoMuSV: Moloney Murine Sarcoma Virus; MoMuLV: Moloney Murine Leukemia Virus; LTR: Long Terminal Repeat; hCMV IE: human Cytomegalovirus Immediate Early promoter; puro^R: puromycin resistance gene; amp^R: ampicillin resistance gene.

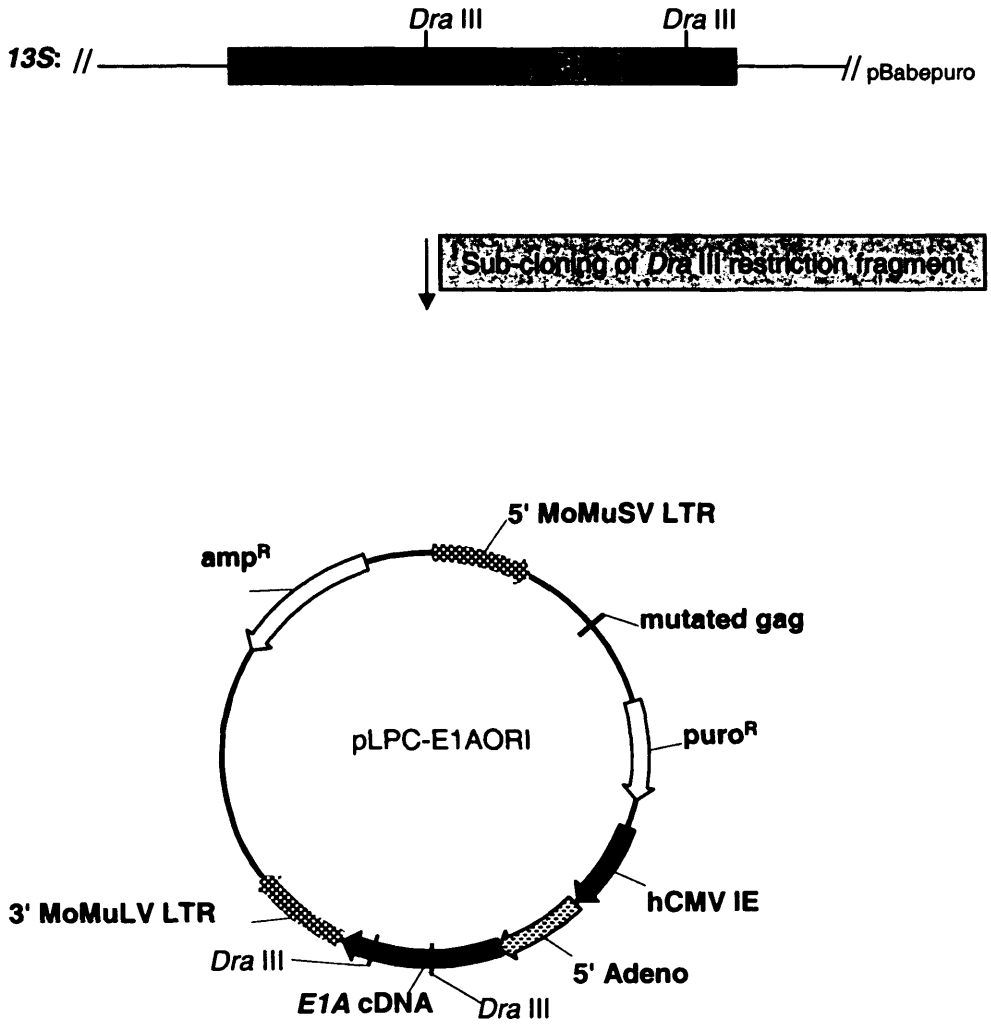

Figure 5.5: Generation of pLPC-13SE1AORI Retroviral Expression Construct

The pLPC-12SE1AORI construct configuration utilised in this experiment contained a region of the adenovirus sequence, of unknown length, 5' to the *12S* cDNA start codon. To recapitulate this configuration for a *13S* cDNA E1A construct, the 13S specific CR3 region was sub-cloned into the original configuration of pLPC-12SE1AORI construct by replacing the 203 bp *Dra* III restriction fragment of *12S* cDNA sequence with the 341 bp *Dra* III restriction fragment of *13S* cDNA sequence into *Dra* III digested pLPC-12SE1AORI construct. pLPC-13SORI was the resultant construct. CR3: Conserved Region 3; MoMuSV: Moloney Murine Sarcoma Virus; MoMuLV: Moloney Murine Leukemia Virus; LTR: Long Terminal Repeat; hCMV IE: human Cytomegalovirus Immediate Early promoter; puro^R: puromycin resistance gene; amp^R: ampicillin resistance gene.

10 μg of the resultant retroviral expression constructs, namely pLPCX, pLPC12SE1AORI, pLPC-13SE1AORI, pLPC-12SE1Av2 and pLPC-13SE1Av2, packaged using Ψ_2 ecotropic system, were used to infect HMF3AEco^R cells seeded at $5x10^5$ cells in duplicate T75 cm^2 flasks in the presence of 8 μg/ml polybrene. Following incubation at 33.5°C for 4 days, 2 μg/ml puromycin was added to the culture medium and, after completion of 4 days of drug treatment, no viable cells remained in a non-infected culture, whereas puromycin-resistant clones were observed in all infected HMF3A cultures. Cultures were maintained in puromycin-containing medium for a further 3 days before the drug-resistant colonies were trypsinised, pooled and replated as a polyclonal HMF3AEco^R population. Cultures were then expanded before RNA was extracted

Semi-quantitative RT-PCR using *E1A*-specific primers (E1A-F and E1A-R) was used to analyse *E1A* expression in these cultures. As a result, a 492 bp PCR product that corresponded to *12S E1A* was generated from RNA derived from pLPC-12SE1AORI-infected HMF3AEco^R cells (**Figure 5.6**, lane 2) and pLPC-12SE1Av2-infected HMF3AEco^R cells (**Figure 5.6**, lane 4). However, no 635 bp PCR product that corresponded to *13S E1A* was generated from RNA derived from pLPC-13SE1AORI-infected HMF3AEco^R cells (**Figure 5.6**, lane 3), or pLPC-13SE1Av2-infected HMF3AEco^R cells (**Figure 5.6**, lane 5), similar to pLPCX-infected HMF3AEco^R cells (**Figure 5.6**, lane 1), despite the fact that 635 bp PCR products were generated from the corresponding plasmids utilised in this experiment (**Figure 5.6**, lanes 3 and 5, respectively).

A more detailed analysis of the expression profiles of these cultures by RT-PCR was possible using a variety of *E1A*-specific primer combinations (**Figure 5.7A**). Accordingly, RT-PCR was performed, using the same RNA samples, and PCR products were obtained from 13S-infected HMF3AEco^R RNA samples (**Figure 5.7B**, lanes 3 and 5, respectively).

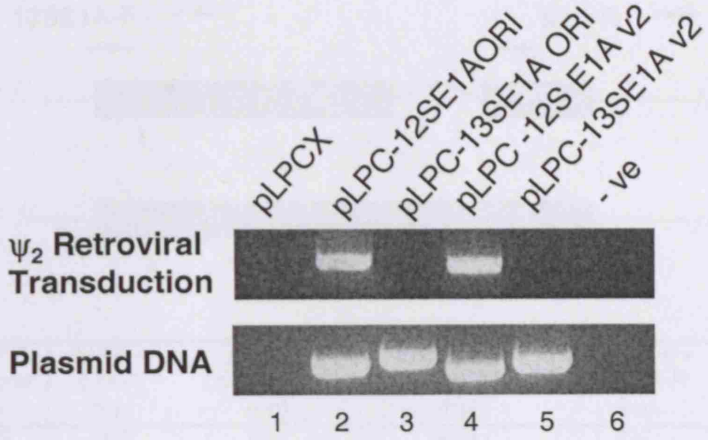

Figure 5.6: pLPC-Based 12S and 13S E1A Expression

RT-PCR of 12S and 13S E1A-infected HMF3AEco^{R} cells, in addition to PCR analysis of the corresponding plasmids used for retroviral delivery. *E1A*-specific primers E1A-F and E1A-R were used for both of these analyses.

A

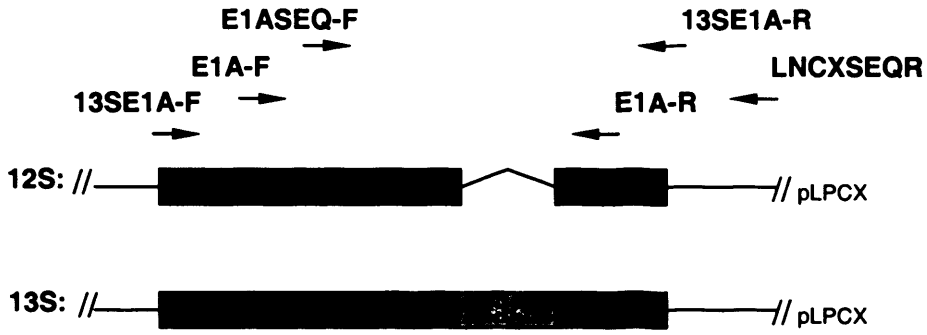

mRNA Isoform	*E1A-F + E1A-R (bp)*	*E1A-F + LNCXSEQ-R (bp)*	*13SE1A-F + LNCXSEQ-R (bp)*	*13SE1A-F + 13SE1A-R (bp)*	*E1ASEQ-F + LNCXSEQ-R (bp)*
12S	492	810	820	732	514
13S	630	948	958	870	652

Figure 5.7: ψ_2-Mediated Expression of 12S and 13S E1A

A: Diagram of *12S* and *13S E1A* mRNA transcripts with primer binding sites denoted and tabular listing of expected sizes of PCR product generated from various primer combinations; **B:** RT-PCR of RNA derived from 12S and 13S E1A-infected HMF3AEco^R cells, using the ψ_2 retroviral packaging system; **C:** RT-PCR of RNA derived from HMF3AEco^R populations transiently-transfected with the same pLPC-based 12S and 13S E1A retrovial expression constructs. *GAPDH* was the loading control.

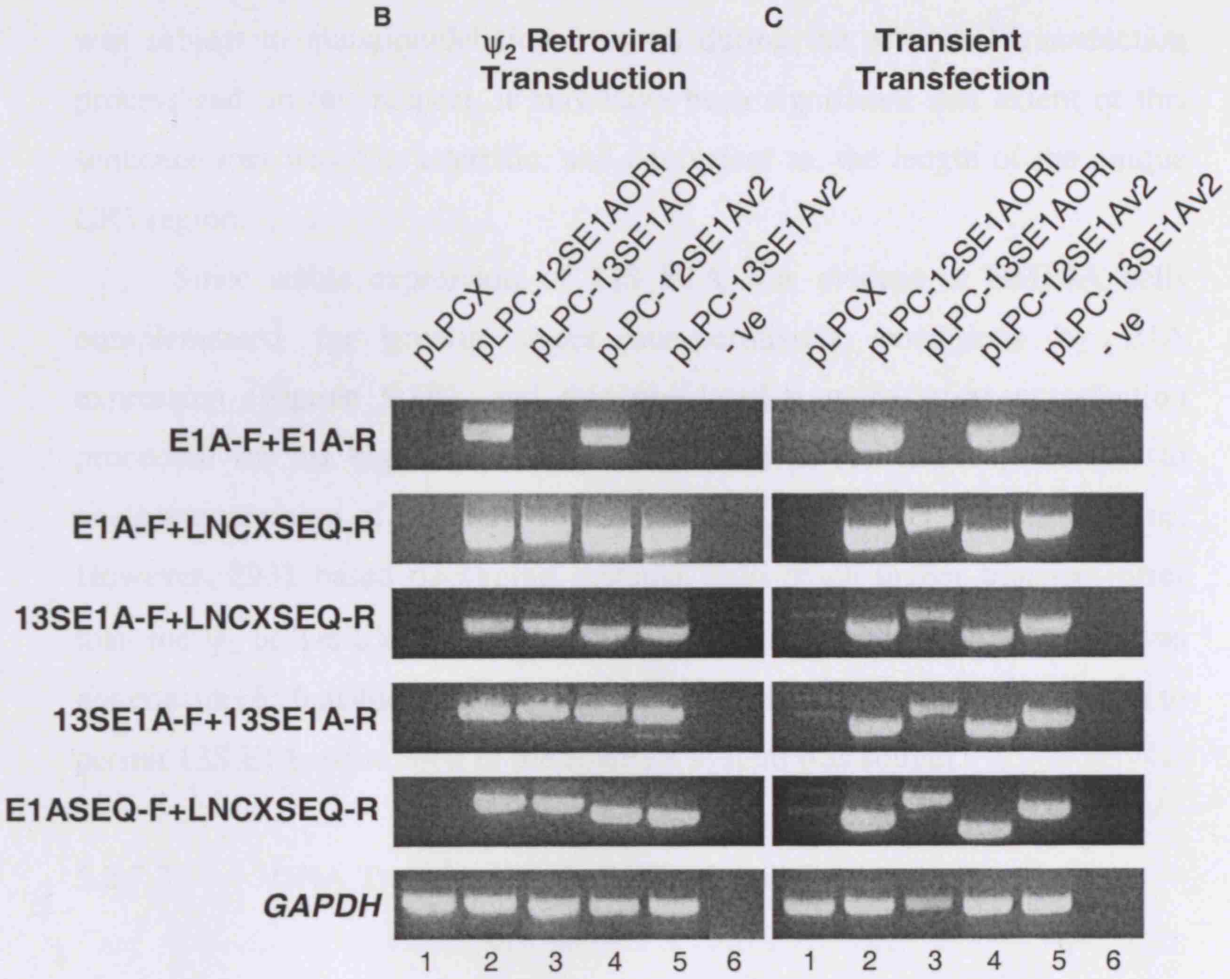
B
ψ2 Retroviral Transduction
C
Transient Transfection
pLPCX
pLPC-12SE1AORI
pLPC-13SE1AORI
pLPC-12SE1Av2
pLPC-13SE1Av2
- ve
E1A-F+E1A-R
E1A-F+LNCXSEQ-R
13SE1A-F+LNCXSEQ-R
13SE1A-F+13SE1A-R
E1ASEQ-F+LNCXSEQ-R
GAPDH
1 2 3 4 5 6 1 2 3 4 5 6

However, these PCR products exhibited the same agarose gel electrophoretic mobility as PCR products obtained from 12S-infected HMF3AEco^R RNA samples (**Figure 5.7B**, lanes 2 and 4, respectively), thereby indicating that *13S*-specific sequences were selectively lost in 13S-infected HMF3AEco^R cells, but not in 12S-infected. This observation implied that the 13S sequence was subject to mutation/deletion event(s) during the retroviral transduction process and, in this respect, it may have been significant that extent of this sequence loss was characteristic, and equivalent to, the length of the unique CR3 region.

Since stable expression of 13S E1A was evident in HMF3A cells complemented for growth under non-permissive conditions by E1A expression (**Figure 5.1B**), and this presented a more stringent selection procedure for the expression of 13S E1A, it was considered preferable to analyse expression of 13S E1A in HMF3AEco^R cells under these conditions. However, 293T-based packaging systems yield much higher transient titres than the ψ_2 or TeFLY Mo cells. Therefore, this experimental approach was not considered feasible. Consequently, an alternative experimental regimen to permit 13S E1A expression in the HMF3A system was sought.

5.2.7.3 DNA Transfection of pLPCX-Based Constructs

Direct DNA transfection represented a suitable experimental approach as it avoided the putative recombinational problems associated with retroviral delivery. A disadvantage of this process, however, was the relative inefficiency of direct DNA transfection relative to retroviral transduction. Nevertheless, 10 μg pLPCX, pLPC-12SE1AORI, pLPC-13SE1AORI, pLPC-12SE1Av2 and pLPC-13SE1Av2 were transfected using oligofectamine (Invitrogen) into HMF3AEco^R cultures seeded at 5x10^5 cells in duplicate T75 cm^2 flasks. 48 hrs post-transfection, 2 μg/ml puromycin was added to the culture medium and after completion of 4 days of drug treatment, no viable cells remained in a non-infected culture, whereas puromycin-resistant clones

were observed in all infected HMF3A cultures. Cultures were maintained in puromycin-containing medium for a further 3 days before the drug-resistant colonies were trypsinised, pooled and replated as a polyclonal HMF3AEco^R population. Cultures were expanded before RNA was extracted.

Semi-quantitative RT-PCR, using a combination of *E1A*-specific primers was used to analyse *E1A* expression in these cultures (**Figure 5.7C**). No PCR products were detected from RNA derived from 13S E1A-infected HMF3AEco^R cells when primers E1A-F and E1A-R were used (**Figure 5.7C**, lanes 3 and 5, respectively), in a similar manner to that observed by Ψ_2-mediated retroviral transduction of these constructs (**Figure 5.7B**, lanes 3 and 5, respectively). However, a different pattern of *13S* sequence loss was observed, relative to Ψ_2-mediated retroviral transduction samples, since the expected PCR products were generated for all other primer combinations (**Figure 5.7C**, lanes 3 and 5, respectively). As a result of this analysis, it appeared that the loss of *13S* sequence mediated by stable DNA transfection of HMF3AEco^R cells was inclusive of a region that spanned the binding site for the E1A-R primer. It was possible that this observation reflected a potent selection pressure for the loss of *13S* E1A-specific sequences and the fact that 13S is very pro-apoptotic.

5.2.8 Utilisation of Validated 13S E1A Mammalian Expression Constructs

The inability to stably express 13S in the HMF3A system was very surprising since both of the *12S* and *13S* cDNA expression constructs generated in this study were sequence verified, indicating that the presence of, as yet, unidentified mutations in the *13S*-specific constructs were unlikely. However, two bona fide 13S mammalian expression constructs that should have permitted expression of 13S in the HMF3A system, namely pSG-13SE1A and pEK-pm975 (gifts from T. Kouzarides and A. Berk, respectively), were introduced into HMF3AEco^R cells. The pSG-13SE1A vector utilises the SV40 promoter to drive 13S E1A expression, whereas pEK-

pm975 contains the Ad2 *E1A* region with a point mutation that blocks splicing of *12S E1A*.10 μg pLPCX, pLPC-12SE1AORI, pSG-13SE1A and pEK-pm975 were transiently transfected into HMF3AEco^R cultures seeded at 1x10^6 cells in duplicate 10 cm^2 plates using oligofectamine (Invitrogen) and RNA was extracted 48 hrs post-transfection.

Semi-quantitative RT-PCR, using *E1A*-specific primers (E1A-F and E1A-R), was used to analyse *E1A* expression in these cultures. 492 bp and 635 bp PCR products that corresponded to *12S* and *13S,* respectively, were generated from RNA derived from a positive control, namely ϕ ecotropic cells (**Figure 5.8A**, lane 5). Similarly, a 492 bp PCR product was generated from RNA derived from transient transfection of pLPC-12SE1AORI (**Figure 5.8A**, lane 2). Yet, in a similar manner to RNA extracted from pLPC-13SE1AORI- and pLPC-13SE1Av2-infected HMF3AEco^R cells, no PCR products were detected from RNA derived from the transient transfection of either pSG-13SE1A (**Figure 5.8A**, lane 3), or pEK-pm975 (**Figure 5.8A**, lane 4), similar to pLPCX (**Figure 5.8A**, lane 1). Yet, 635 bp PCR products that corresponded to *13S E1A* were generated from the corresponding plasmid constructs utilised in this experiment (**Figure 5.8B**, lanes 3 and 4, respectively). It should be noted a larger *13S* PCR product was generated from pEK-pm975 plasmid DNA, relative to pSG-13SE1A. This was due to the fact that pSG-13SE1A contains the cDNA sequence of *13S E1A*, whereas pEK-pm975 contains additional non-coding genomic DNA sequences from the Ad2 *E1A* region.

It was possible that the lack of detectable *13S E1A* expression occurred as a result of low transient-transfection efficiency. Therefore, stable 13S E1A expression was sought for one of these constructs, namely pEK-pm975. Due to the lack of a puromycin-resistance marker in pEK-pm975, 10 μg of this construct was co-transfected in a 10:1 ratio with pLPCX into HMF3AEco^R cultures seeded at 5x10^5 cells in duplicate 10 cm^2 dishes, alongside transfection of 10 μg of pLPCX alone.

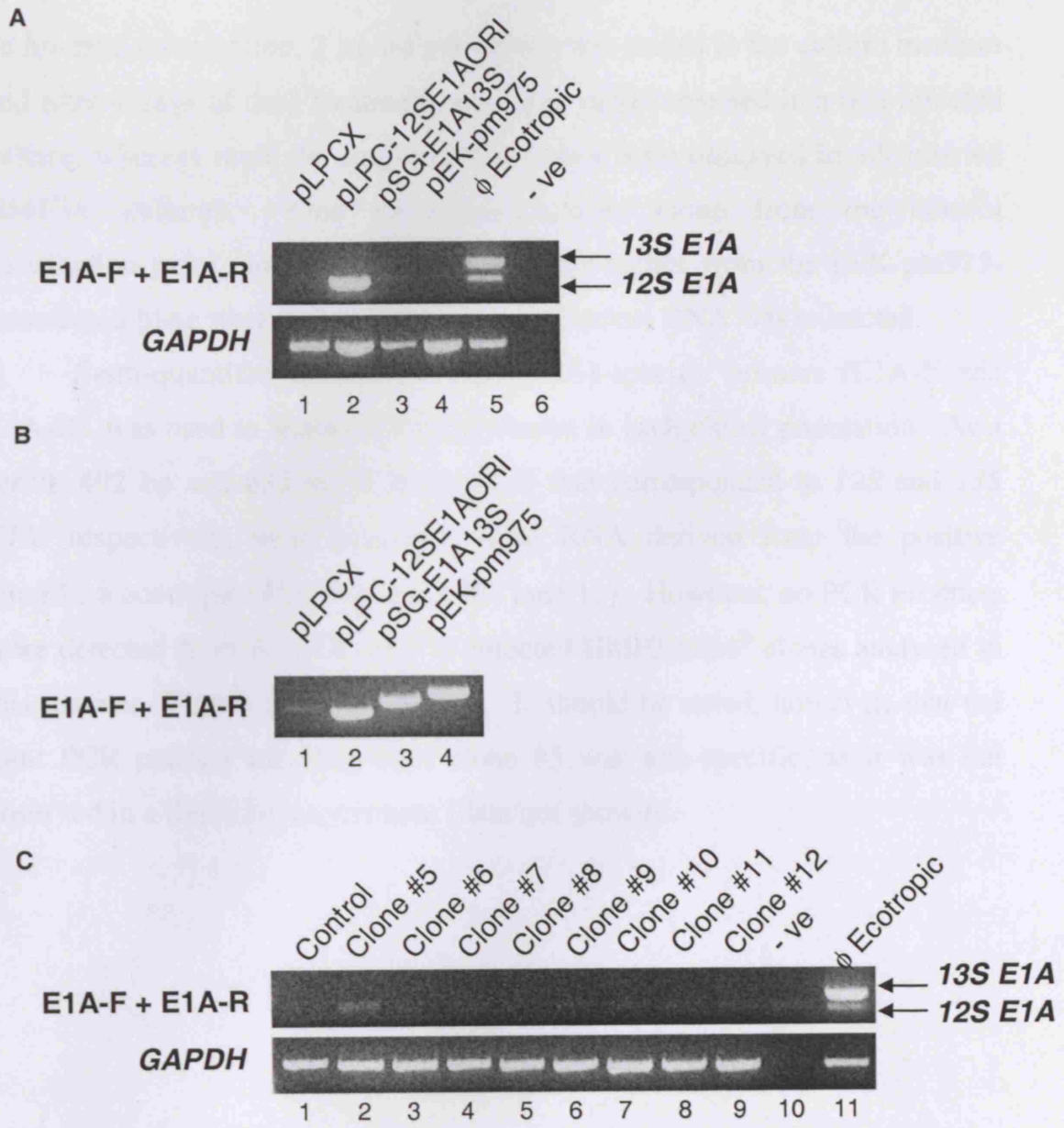

Figure 5.8: Expression of Alternative 13S E1A Mammalian Expression Constructs

A: RT-PCR of RNA derived from HMF3AEco^R cells transiently transfected with 12S and 13S E1A mammalian expression constructs. RNA derived from HMF3AEco^R cells infected with pLPC-12SE1AORI was the positive control for the transfection whereas RNA derived from ecotropic cells was the positive control for PCR. *GAPDH* was the loading control; **B:** PCR of the corresponding plasmids used for retroviral delivery; **C:** RT-PCR analysis of stable clones derived from pEK-pm975:pLPCX co-transfection. Again, RNA derived from ecotropic cells was the positive control for PCR and *GAPDH* was the loading control.

48 hrs post-transfection, 2 μg/ml puromycin was added to the culture medium and after 4 days of drug treatment, no viable cells remained in a non-infected culture, whereas multiple drug-resistant clones were observed in all infected HMF3A cultures. One puromycin-resistant clone from the control transfection plate, and 8 puromycin resistant clones from the pEK-pm975-transfected plate were isolated and expanded before RNA was extracted.

Semi-quantitative RT-PCR, using *E1A*-specific primers (E1A-F and E1A-R), was used to analyse *E1A* expression in each clonal population. As a result, 492 bp and 635 bp PCR products that corresponded to *12S* and *13S E1A*, respectively, were generated from RNA derived from the positive control, ϕ ecotropic cells (**Figure 5.8C**, lane 11). However, no PCR products were detected from the pEK-pm975-infected HMF3AEco^R clones analysed in this manner (**Figure 5.8C**, lanes 2-9). It should be noted, however, that the faint PCR product detected from clone #5 was non-specific, as it was not observed in a duplicate experiment (data not shown).

5.3 SUMMARY AND DISCUSSION

13S expression was detected in HMF3AEco^R cells complemented for growth at the non-permissive temperature following retroviral tranduction of a *12S* cDNA construct. In contrast, no 13S expression was detected in parallel cultures grown under permissive conditions, which resulted in the cells remaining conditional for growth. This suggested the intriguing possibility that 13S activity was required for the abrogation of the HMF3A growth defect and that 12S E1A expression was not sufficient to complement the growth of HMF3AEco^R cells.

5.3.1 Model for 13S E1A Expression in the HMF3A System

A potential source of generating 13S was through template switching of the pLPC-12SE1A cDNA-derived transcript and endogenous *13S* sequences within the ϕ amphotropic packaging cells during the process of virus production. Recombination between *E1A* splice variants was possible since ϕ cells contain lots of *E1A* mRNA transcripts and exhibited RT activity; RT is relatively error-prone [van Wamel and Berkhout, 1998] and promotes template switching. Significantly, template switching is influenced by a variety of factors, including the presence of specific sequences or secondary structures in the template sequence (reviewed in [Mikkelsen and Pedersen, 2000]).

The E1A expression data suggested a model for 12S and 13S recombination that could have occurred in ϕ cells. This model proposed that RT dissociated from pLPC-12SE1AORI-derived templates and re-associated with nearby *13S E1A* mRNA transcripts to generate replication-deficient retroviruses capable of conferring target cells with constitutive 13S expression activity. Such recombinational events were likely to be extremely rare, as evident by the lack of detectable *13S* expression in HMF3AEco^R cells infected with pLPC-12SE1A cDNA and cultivated under permissive conditions.

Therefore, the detectable and significant expression of 13S that was observed in growth complemented HMF3A cells was indicative of a potent selection pressure for the retention of 13S expression under non-permissive conditions, and this was all the more unexpected given the known pro-apoptotic activity of 13S, relative to 12S [Flinterman *et al*, 2005].

5.3.2 Lack of Verification of Putative 13S E1A Growth Complementation Activity in the HMF3A System

Independent expression of *12S* and *13S* transcripts in HMF3AEco^R cells and analysis of their growth-complementation abilities was considered to be the appropriate approach with which to validate this hypothesis. However, stable expression of *13S* in the absence of 293T-derived retroviral delivery could not be demonstrated in this project. It was possible that *13S E1A*-specific sequences promoted recombinational events in HMF3AEco^R cells in an as yet uncharacterised process, possibly involving the generation of a novel *E1A* splice variant. Alternatively, lack of expression of *13S E1A* may have resulted from a potent negative selection pressure, due to its proapoptotic activity. In this regard, it may be significant that *13S* expression could not be detected at 33.5°C in the original experiment. This indicated that 13S E1A expression in HMF3AEco^R cells was not causal to the growth complementation, but rather a bystander effect of this process. There was some evidence to negate this argument, however; increased 13S E1A expression was observed in growth-complemented cells that were shifted to the permissive temperature for several days (see **Figure 3.8**, lanes 5 and 6).

However, the inability to demonstrate stable *13S E1A* expression in HMF3AEco^R cells prevented the putative differential growth complementation activity of 13S E1A, relative to 12S E1A, to be investigated. Therefore, the putative activity of 13S E1A remains to be further investigated.

5.3.3 Model for 13S E1A-Mediated Senescence Bypass in the HMF3A System

12S and 13S E1A are known to possess disparate activities; 12S functions as a transcriptional repressor, whereas the presence of CR3 in 13S enables it to function as a potent transcriptional activator. The CR3 region of 13S consists of two functional domains, namely an N-terminal four-cysteine zinc finger domain and a C-terminal subdomain (**Figure 5.9**). The zinc finger component of this region confers potent transcriptional activational activity upon this splice variant. However, there is evidence that endogenous 13S E1A DNA-binding activity is, by itself, very weak [Chatterjee *et al*, 1988]. This observation indicated that the transcriptional activation activity of E1A was critically dependent upon direct interactions with components of the basal transcriptional machinery, such as TBP and TBP-associated factors such as the TBP-associated factor $TAF_{II}110$. In contrast, the C-terminal region is thought to bind to specific cellular transcription factors, such as TAFs, SP1, Jun, Oct4 and CBP, such that the juxtaposition of basal transcriptional complexes in close proximity to specific transcription factors promotes CR3-dependent transcriptional activation.

It is anticipated that the identification of cellular proteins that specifically interacted with 13S, such as transcription factors and/or coactivators, will reveal the mechanistic basis of the putative 13S E1A growth complementing activity. To this end, a panel of 13S CR3 point mutants and in-frame deletion mutants have been obtained with the aim being to analyse them in the HMF3A system in a growth complementation assay (**Figure 5.10**; gift from Rob Ricciardi).

Two likely candidates that are involved in mediating 13S functional activity include Sur2 and Notch. With respect to Sur2, the CR3 domain of 13S has been shown to exhibit *in vitro* binding activity.

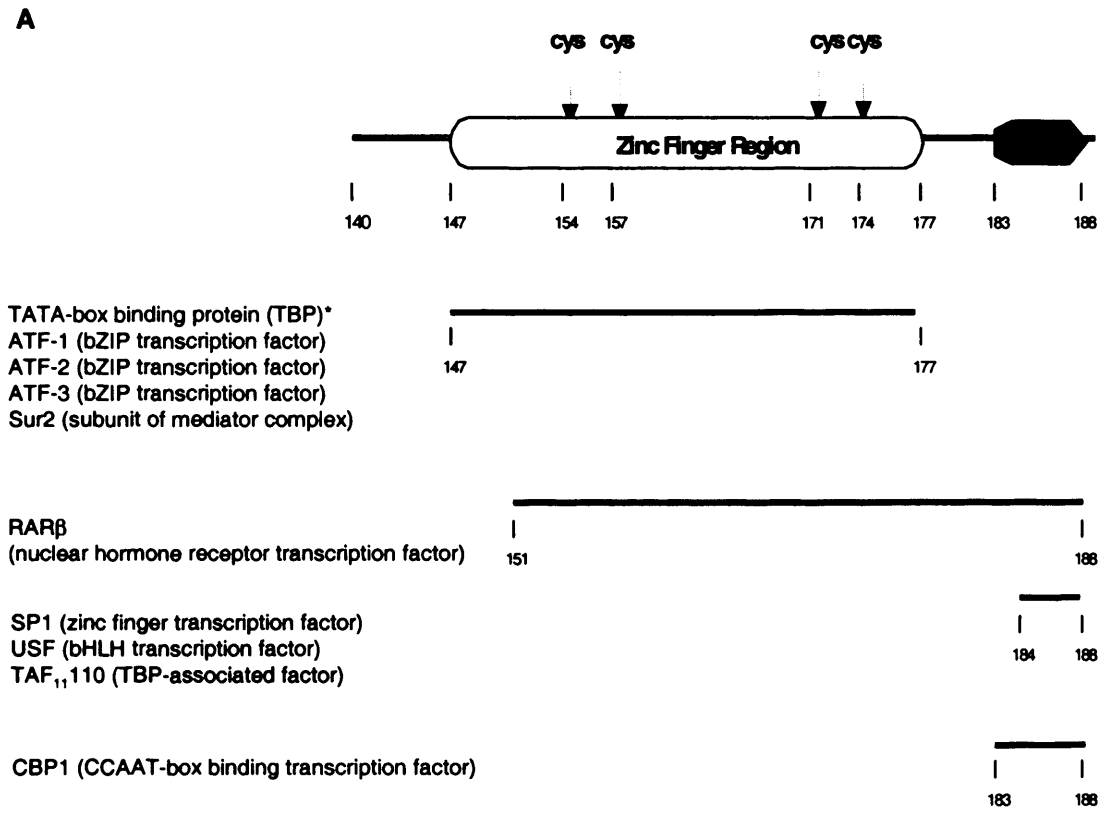

B

YY1*
TR*
P/CAF
Jun
BS69
Pax4
Oct4*
TAF_{II} 135
Taf_{II} 250

Figure 5.9: Cellular Proteins Known to Bind to the CR3 Region of 13S E1A

A: Known cellular interaction partners of E1A with binding regions denoted; **B:** Known, but unmapped interacting partners of E1A [Ansieau *et al*, 2001; Felzien *et al*, 1999; Folkers and van der Saag, 1995; Fujitani *et al*, 1999; Hateboer *et al*, 1995; Metcalf, 1996; Najafi *et al*, 2003; Wang and Berk, 2002].

Note: *Denotes additional N-terminal E1A binding activity

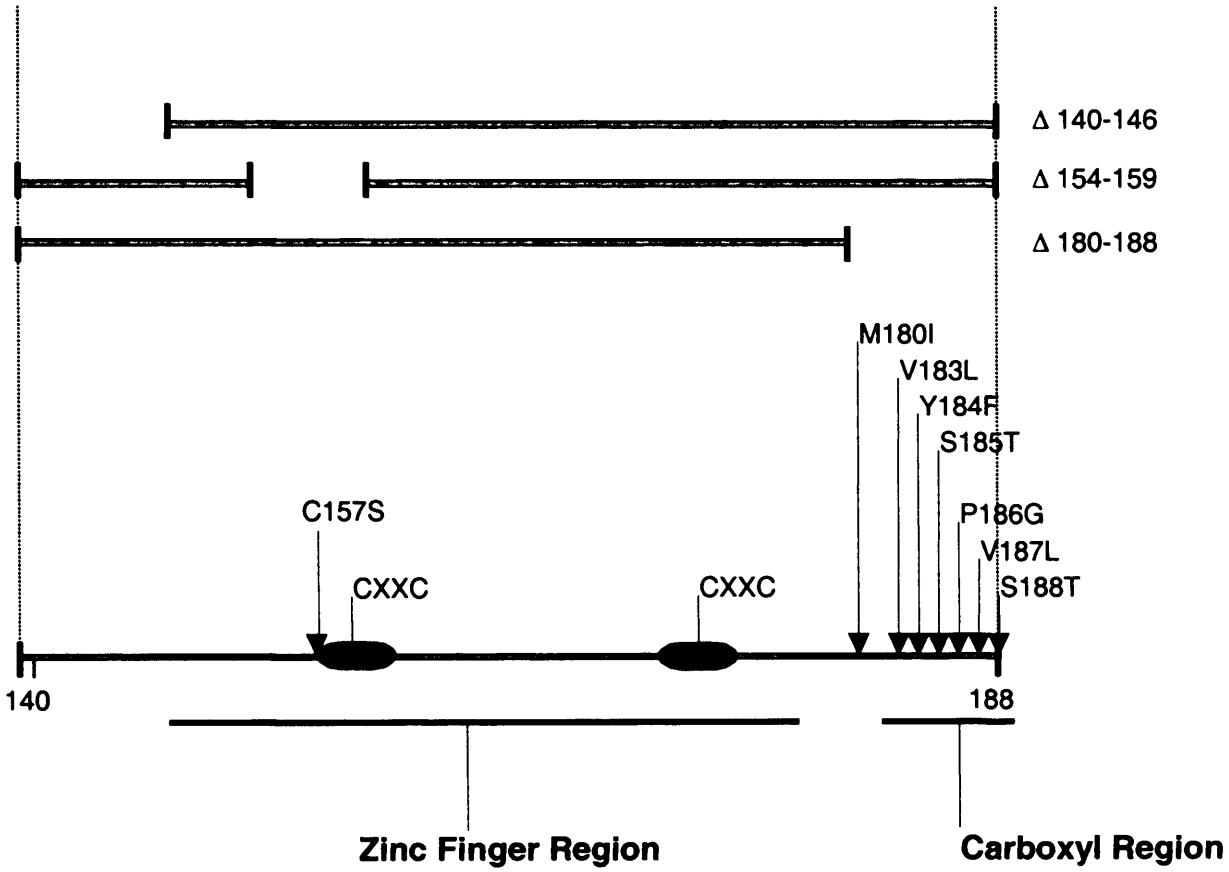

Figure 5.10: 13S E1A Mutants

Mutations located in 13S E1A Conserved Region 3 (CR3). The zinc finger domain spans amino acid residues 147-177 of the 13S E1A protein and the carboxyl region spans amino acid residues 180-188. Mutants that span the zinc finger domain and disrupt the formation of a zinc finger structure and are defective in TBP-binding. Consequently, these mutants are transactivation defective (namely D154-159 and C157S). The remaining point mutations that span the C-terminal domain are known to be transactivation negative, but sufficient in TBP-binding activity. Serines 185 and 188 are known phosphorylation sites of MAPK that may function in the regulation of transcriptional activation since phosphorylation at these sites may enhance the binding to cellular transcription factors [Whalen *et al*, 1997].

Sur2 is a subunit of the mammalian Mediator (of transcription) complex [Wang and Berk, 2002] and is thought to be required for high-level activation of mammalian activators [Boyer *et al*, 1999]. Consequently, the interaction of CR3 with Sur2 may facilitate synergistic transactivational activity from specific cellular promoters in combination with specific cellular transcription factors such as ELK-1. Alternatively, 13S E1A may modulate the transcriptional activation activity of CBF1 since co-immunoprecipitation analysis has indicated that CBF1 binds to 13S, but not 12S E1A. CBP1 is a major downstream transcriptional regulator of the developmentally important Notch pathway of gene regulation that controls many differentiation and proliferation processes, and it has been demonstrated that 13S, but not 12S, can mimic the intracellular activational domain of Notch ($Notch^{IC}$) by activating CBF1-responsive promoters, such as *CCND1* [Ansieau *et al*, 2001]. This activity is abrogated by mutations or deletions of the binding sites for CBF1. A retroviral expression vector containing Myc-tagged intracellular Notch construct has been obtained to investigate this possibility (gift from A. Capobianco).

Alternative strategies to elucidate the CR3-dependent critical function of 13S required for this activity include yeast two-hybrid screening for the identification of novel binding partners of the CR3 region, microarray analysis to compare the expression profile of 12S- and 13S- expressing cells, and a homology search of the CR3 sequence for the identification of putative cellular protein binding sites. The utilisation of multiple experimental approaches may provide good supportive evidence for 13S-specific functional activity in the process of telomere-independent cellular senescence.

5.3.4 Implication of Template Switching in the Interpretation of Experimental Data

The evidence presented here also has important ramifications for the interpretation of experimental data obtained from retroviral delivery of 12S

constructs via 293T-derived retroviral packaging systems; for example, Samuelson and Lowe [Samuelson and Lowe, 1997] utilised the pLPC-12SE1A cDNA construct in combination with the ϕ retroviral system to conclude that 12S induced p53 accumulation and chemosensitivity in MEFs. Yet, the possibility that this activity was specifically attributable to 13S was not addressed. Therefore, there is a possibility that the results from this and other studies may have been attributed to the incorrect E1A molecule (for example, [de Stanchina *et al*, 1998; Ferbeyre *et al*, 2000; Ryan *et al*, 2004]).

If this hypothesis is proved to be correct, such concerns may be readily and simply circumvented by the utilisation of non-E1A expressing retroviral packaging system such as Ψ_2.

6. RNAi Screen in the HMF3A System

6.1 OBJECTIVES

In **Chapter 3**, downstream effectors of the p53 pathway were targetted for inactivation in the HMF3A system in an attempt to identify critical mediators of the conditional growth arrest. However, an innate disadvantage of this experiment was the requirement of prior knowledge of the identity of these components; since the effectors and pathways that underlie the induction of cellular senescence are poorly understood, the application of this experimental procedure was somewhat limited. Consequently, an unbiased forward genetics approach was sought to investigate this process.

RNAi screening represented an attractive experimental regimen since retroviral shRNA libraries specifically designed for application into mammalian systems had recently been developed [Berns *et al*, 2004; Paddison *et al*, 2004]. These libraries shared common features in that they both permitted the simultaneous knockdown of many different genes in a cell population and enabled shRNA species that mediated significant changes in the particular phenotype under investigation to be identified.

This chapter details my use of a small fraction of one of the shRNA libraries, namely the CSHL shRNA library, utilised in conjunction with the HMF3A complementation assay, to identify novel genes associated with telomere-independent cellular senescence.

6.2 RESULTS

6.2.1 ShRNA Library

To perform the shRNA screen, pools 1-12 of release 1.3 of the pSM2 retroviral expression vector-based CSHL shRNA library were utilised (Open Biosystems; gift from A. Ashworth). Each pool consisted of approximately 170 different shRNA constructs targetted against 96 different genes, based upon a 96-well format (**Figure 6.1B**). Consequently, a total of 2050 shRNA constructs representative of 1152 genes were analysed in this screen.

6.2.2 Titration of Puromycin-Resistant Clones

Each shRNA pool was packaged to generate replication-deficient retroviruses. 10 μg of DNA from each pool, in addition to 10 μg of pRetroSuper-Lamin A/C, was packaged using the ϕ ecotropic system. 48 hrs post-infection, the retroviral supernatant was harvested and the titres measured; 1% of the total harvest from each shRNA pool was used to infect HMF3AEco^R cells seeded at 5x10^5 cells in a T75 cm^2 flask in the presence of 8 μg/ml polybrene. Following incubation at 33.5°C for 4 days, 2 μg/ml puromycin was added to the culture medium and after completion of 4 days of drug treatment, no viable cells remained in a non-infected culture, whereas multiple puromycin-resistant clones were observed in all infected cultures. Cultures were maintained under drug selection at 33.5°C for a further 7 days before fixing and staining with 2% (w/v) methylene blue and counting all visible colonies (**Figure 6.1A**). The number of infectious events varied considerably between each shRNA pool analysed but all were within a 10-fold range of each other; for example 36 colonies were observed in the HMF3AEco^R culture infected with retroviral supernatant derived from shRNA pool 1, whereas 283 colonies were observed in the HMF3AEco^R culture infected with retroviral supernatant derived from shRNA pool 12.

A

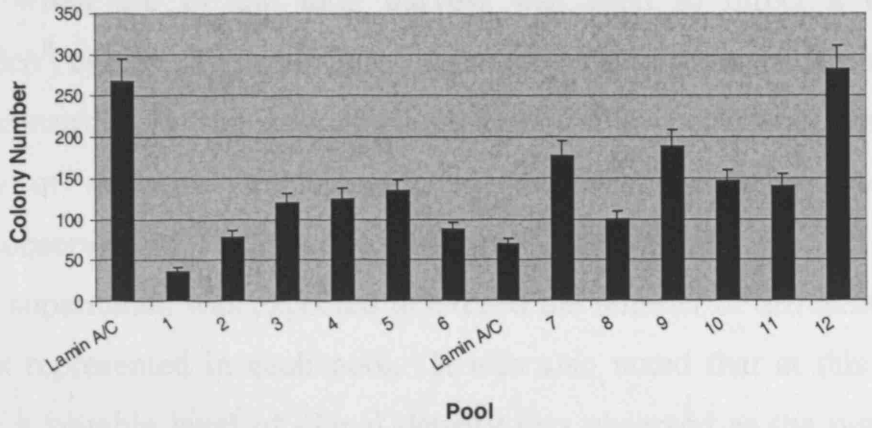

B

Pool	*Estimate of No of Puromycin-Resistant HMF3AEco^R Colonies Observed*	*No of Constructs Represented in the Pool*
Lamin A/C	1340	1
1	180	172
2	390	158
3	600	174
4	625	176
5	675	160
6	435	174
Lamin A/C	345	1
7	885	181
8	495	166
9	945	170
10	730	177
11	700	173
12	1415	169

Figure 6.1: Number of Puromycin-Resistant Colonies Obtained in the ShRNA Screen

A: Bar chart showing the number of puromycin-resistant colonies observed in HMF3AEco^R cultures infected with 1% of the total retroviral supernatant harvested from each pool; **B:** Table listing the estimated number of puromycin-resistant colonies observed in HMF3AEco^R cultures infected with 5% of the total retroviral supernatant harvested from each pool. The number of puromycin-resistant colonies observed in HMF3AEco^R cultures infected with 5% of the total retroviral supernatant is expected to exceed the number of different shRNA constructs represented in each pool.

The number of colonies observed in each culture was multiplied by a factor of 5 to calculate an estimate for the number of colonies that would be observed when 5% of the total harvest was used to infect a duplicate HMF3AEco^R culture (**Figure 6.1B**). Assuming equal representation of each shRNA construct in the retroviral supernatant of each pool and equal efficiency of retroviral transduction, the number of purmoycin-resistant colonies observed in HMF3AEco^R cultures infected with 5% of the total retroviral supernatant was expected to exceed the number of different shRNA constructs represented in each pool. It was also noted that at this level of infection, a suitable level of clonal density was observed as the puromycin-resistant colonies appeared to be well separated in each culture (data not shown).

6.2.3 ShRNA Screening Procedure

The shRNA screen itself was performed in two successive experiments; firstly with pools 1-6 then pools 7-12 and in parallel with the titration experiment described above. In both experiments, pRetroSuper-Lamin A/C was used as a negative control to assess the background rate of reversion and pRetroSuper-p53 was used as a positive control for growth complementation. 1% and 5% of the total retroviral supernatant generated from each shRNA pool was used to infect HMF3AEco^R cells seeded at $5x10^5$ cells in duplicate T75 cm^2 flasks (ie utilising 12% of the total harvest) in the presence of 8 μg/ml polybrene. The utilisation of two different dilutions of the retroviral supernatant served two purposes: firstly it addressed the possibility that at a higher clonal density, a higher level of background may be observed and secondly, it aided the identification of positive hits since an equivalent increase in the number of growth complementation events was expected across the two dilutions. Following incubation at 33.5°C for 4 days, 2 μg/ml puromycin was added to the culture medium and after completion of 4 days of drug treatment, no viable cells remained in a non-infected culture, whereas

multiple puromycin-resistant clones were observed in all infected cultures. Puromycin was removed from the culture medium and drug-resistant clones were directly shifted to 39.5°C. Following incubation at 39.5°C for 14 days, cultures were assessed for their ability to grow under these non-permissive conditions. Multiple growing colonies were observed in the p53 shRNA-infected HMF3AEco^R cultures, however, no such colonies were observed in any of the Lamin A/C shRNA-infected HMF3AEco^R cultures. A single growing colony was also observed in 1 of the 2 cultures infected with 5% of the viral supernatant generated from library pool 6. This culture was trypsinised, pooled and replated as a polyclonal population, then sub-cultivated for a minimum of 4 further passages, using a 1:5 split, to ensure that it was able to be continually propagated under these conditions. Having achieved this, the culture was considered complemented for growth. However, no other growing colonies were noted in any of the remaining cultures and to confirm this, each culture was fixed and stained with 2% (w/v) methylene blue.

6.2.4 Second Round Screening of the ShRNA Library

To support the possibility that the single colony was representative of a true positive hit, the screening procedure was repeated using the remaining freeze-thawed retroviral supernatant that was generated from pool 6 in the original experiment. Both the positive and negative control viral supernatants, namely p53 shRNA and Lamin A/C shRNA viral supernatants, were also included in this experiment. Using the protocol described for the first round of the shRNA screen, 15% of the total viral supernatant derived from pool 6 was used to infect 4 HMF3AEco^R cells seeded at $1x10^6$ cells in T180 cm^2 flasks (ie 60% of the total viral supernatant). Duplicate flasks were similarly infected with Lamin A/C- and p53- shRNA retroviral supernatants. Larger flasks were utilised in an attempt to recapitulate the same level of clonal density that was used in the original experiment.

Following incubation of puromycin-resistant clones at 39.5°C for 14 days, 4 growing colonies were observed in two of the HMF3AEco^R cultures infected with retroviral supernatant derived from shRNA pool 6; 1 colony was observed in one culture (A), and 3 colonies were observed in a second culture (B). No other colonies were observed in either of the 2 remaining cultures. Cultures A and B were each trypsinised, pooled and replated as a polyclonal population, then sub-cultivated for a minimum of 4 further passages, using a 1:5 split, to ensure that they were capable of being serially propagated under these conditions. Having achieved this, the cultures were considered complemented for growth. However, 2 growing colonies were also observed in 1 of the 2 Lamin A/C shRNA-infected HMF3AEco^R cultures. This finding indicated that the positive hits identified in cultures A and B, could have represented background reversion events. However, it should be noted that the number of infectious events was not equivalent between these cultures as many more drug-resistant clones were observed in the Lamin A/C shRNA-infected HMF3AEco^R cultures than in those infected with the retroviral supernatant derived from pool 6 of the shRNA library. Unfortunately, as the retroviral titres were not measured in a parallel experiment at 33.5°C, it was not possible to calculate the frequency of complementation relative to background. Nevertheless, the increase in the number of colonies growing at 39.5°C in cultures infected with retroviral supernatant derived from shRNA pool 6 correlated with an increase in the quantity of retroviral supernatant utilised in the experiment. This indicated that pool 6 potentially contained shRNA constructs that were able to complement the growth of HMF3AEco^R cells incubated at 39.5°C.

6.2.5 Identification of ShRNA Sequences

Two distinct methods of target shRNA sequence retrieval were possible. The first method utilised a DNA barcoding system that was simultaneously developed by both Berns and colleagues [Berns *et al*, 2004]

and Paddison and colleagues [Paddison *et al*, 2004]. In the CSHL library, each shRNA construct was labelled with a unique 60-nucleotide (nt) sequence such that each construct could be detected in a process analogous to microarray analysis. The second method involved the extraction of genomic DNA followed by PCR amplification using vector-specific primers that spanned the shRNA insert sequence and cloning into a TA-cloning vector. Sequencing of multiple colonies would allow determination of the identity of the functional shRNA species.

6.2.6 Extraction of Genomic DNA from Growth Complemented HMF3A Cultures

Since the level of background reversion in the HMF3A system was minimal and only one positive hit was identified in the first round of screening, the latter method of sequence retrieval was utilised. As a caveat, it should be noted that where more than one growing colony was observed in a mixed population, as observed in culture B in the second round of the screen, there was a risk that one colony may have outgrown the others, leading to potential loss of information. Therefore, care was taken to extract genomic DNA as soon as the trypsinised and replated culture had reached near-confluence. It should also be noted that genomic DNA harvested from these cultures were representative of a heterogeneous population of many different shRNAs species, therefore, the sequencing of multiple inserts was required to identify all shRNA target sequences. Nonetheless, a secondary growth complementation screen of HMF3A cells utilising the pure shRNA construct would validate these findings.

Genomic DNA was extracted from T25 cm^2 cultures of growth-complemented cells within one passage of their outgrowth as a polyclonal population. 100 ng of genomic DNA was then utilised as a template for PCR, using primers specific to the pSM2 vector (SM2 F3 and SM2 R3). 5 µl of each resultant PCR product was separated on a 3% agarose gel alongside a

positive control for PCR, namely 5 µl of the PCR product generated from the amplification of 100 ng of pSM2 scrambled control vector. A 424 bp PCR product that corresponded to the expected insert sequence was observed in all samples, but not in a negative control sample where water was substituted for template DNA (data not shown). 4 µl of each PCR product was then cloned directly in pCR2.1, using the TOPO cloning system (Invitrogen), and transformed, using TOPF10 competent cells. Blue/white selection was used to isolate 12 positive clones from each plate, from which, plasmid DNA was subsequently extracted and sequenced, using the M13R primer (**Figure 6.2A**).

6.2.7 Identification of Positive Hits From the ShRNA Screen

Sequence analysis revealed that a single shRNA target sequence representative of *RRM2* was identified from the first round of the screen. A single shRNA target sequence representative of a different gene, namely *TARBP1*, was identified from culture A of the second round of the shRNA screen. In contrast, a mixture of different shRNA target sequences were identified from culture B; 8 of the 12 clonal sequences were representative of *NEUROD2* whereas each of the 4 remaining sequences were representative of 3 different genes, namely *HTCD37*, *RPL31* and *STK39*, in addition to an unidentifiable gene. It was likely that the multiple genes identified in culture B reflected the polyclonal nature of this cell population. However, the fact that different shRNA target sequences were identified and did not correspond to the same gene, as determined by BLAST analysis, meant that it was possible that these targets represented false-positives derived from the screen. Yet, due to the non-saturating conditions used in this experiment, it was equally possible that these genes were representative of true positive hits.

A

No. of Clones	*Source Culture*	*ShRNA Target Sequence*	*Gene Target*	*No. shRNA Constructs Targeted in Screen*
11/11	**ORIGINAL**	**AGCTGTTTCTATGaCTTCCAAA**	***RRM2***	**2**
12/12	A	ACGGCAAATATTGTTATGGAAA	*TARBP1*	2
8/12	B	CGAGGCCAAGACAATTTGTAAC	*NEUROD2*	3
1/12	B	GTCTGGTATACTGTTCTCATAA	*HTCD37*	3
1/12	B	AGCACTCAAAGAGATTCGGAAA	*RRL31*	2
1/12	B	CTCTGTTAGATTGCTAACTATA	*STK39*	4
1/12	B	CGCCTCAAATTATTTATTTCTC	NA	NA

B

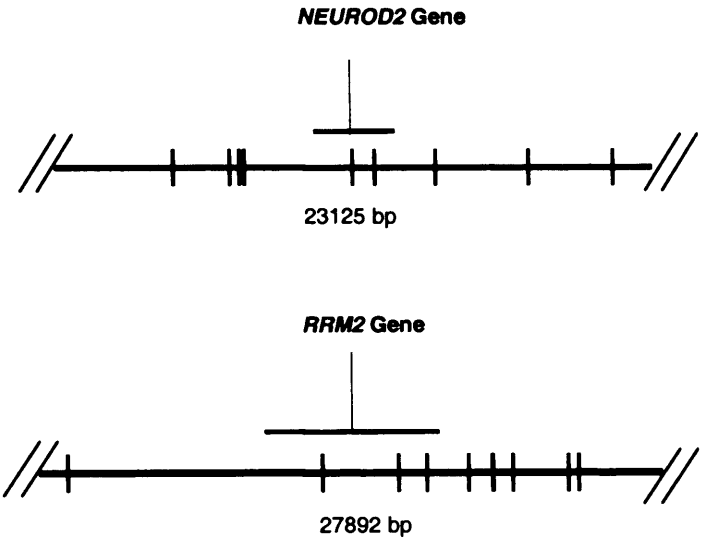

Figure 6.2: Candidate Genes Identified in the ShRNA Screen

A: Analysis of the shRNA target sequences derived from cultures exhibiting growth complementation under non-permissive conditions. Where a mismatch between the identified sequence and the validated gene sequence is observed, the sequence is shown in lower case. It should be noted that *RRM2* was not represented in Pool 6 of the shRNA library (highlighted row); **B:** *NEUROD2* and *RRM2* are putative transcriptional targets of p53; multiple p53 consensus binding-sites have been identified in their respective genomic loci (indicated by black bars). These loci are inclusive of 10 kb of sequence upstream and upstream of the ORF for each gene [Hoh *et al*, 2002].

6.3. SUMMARY & DISCUSSION

6.3.1 The HMF3A System Represents a Suitable Model for Utilisation in a RNAi Screen

The ability of cells to bypass senescence confers a potent selective growth advantage for tumorigenesis [Hanahan and Weinberg, 2000]. Therefore, telomere-independent cellular senescence represented a biological process that was suitable for analysis by RNAi screening. Concomitantly, there were many significant advantages to utilising the HMF3A model system in this form of experimental analysis. Firstly, the HMF3A system exhibited a very stringent conditional growth phenotype with little/no levels of background reversion (**Figure 3.6B**). Secondly, multiple positive controls, namely pRetroSuper-p53 and pRetroSuper-p21, had been identified as shRNA constructs that were sufficient to complement the growth of these cells under non-permissive conditions (**Figures 3.7** and **3.14**). This finding was important in two ways; firstly, it demonstrated that it was possible that individual shRNA constructs could generate true-positive hits in an RNAi screen; and, secondly, it facilitated the design of optimal screening conditions. The effectiveness of any screen is dependent upon its sensitivity; therefore, it was important to minimise the background levels of false-positive hits without losing information concerning the identity of all true positive hits. In this respect, the optimal conditions for performing an RNAi screen in the HMF3A system had been determined by the development of the HMF3A complementation assay (**Section 3.2.1.2**). Finally, HMF3AEco^R cells were readily infectable by virtue of their constitutive expression of the mouse ecotropic retrovirus receptor (**Section 3.2.3.1**). The aim of this technical manipulation was to achieve the high level of infection that was required for screen saturation.

Together, these suggested that the HMF3A system was suitable for the application in an *in vitro* RNAi screen with the aim of identifying novel genes that were causal to the bypass of telomere-independent senescence.

6.3.2 Positive Hits Identified in the HMF3A ShRNA Screen

Complementation of the HMF3A conditional growth defect by shRNA screening using pools 1-12 of release 1.3 of the pSM2-based CSHL shRNA library, identified *RRM2*, *NEUROD2* and *TARBP1* as positive hits. Therefore, these candidate genes represent putative mediators of the induction of telomere-independent cellular senescence.

The fact that *NEUROD2* was identified in this screen was particularly interesting since NeuroD2 is a basic helix-loop-helix (bHLH) transcription factor, a family of proteins that are thought to play an important role in the regulation of cell differentiation [Massari and Murre, 2000]. Indeed, BHLHB2, another bHLH transcription factor, was recently identified as a *de novo* marker of senescence [Collado *et al*, 2005]. Specifically, NeuroD2 functions as a positive regulator of neuronal differentiation [Farah *et al*, 2000; Mie *et al*, 2003], similar to NeuroD1. NeuroD1 is a NeuroD2-related bHLH transcription factor that has been shown to interact with pRb to promote NeuroD1-dependent gene activation [Batsche *et al*, 2005]. Since pRb is known to function as a positive regulator of differentiation in many cell types [Morris and Dyson, 2001], this observation suggests that pRb may also regulate NeuroD2 transcriptional activity. Therefore, this interaction may represent a mechanism by which NeuroD2 expression could mediate the induction of senescence.

The possible relationship of the two other genes identified in this study, namely *TARBP1* and *RRM2*, with the induction of senescence is less clear. TARBP1 has been shown to bind to a double-stranded RNA stem-loop structure generated by transcription of the TAR element from the HIV-1 long terminal repeat [Sheline *et al*, 1991; Wu *et al*, 1991] whereas RRM2 exhibits

ribonucleotide reductase activity in association with RRM1. Ribonucleotide reductase is required for the supply of deoxynucleotides for *de novo* synthesis of DNA and, as such, expression of the RRM2 is cell cycle regulated and peaks at S-G_2 phase where its activity is required to supply dNTPs for DNA replication [Bjorklund *et al*, 1993; Engstrom *et al*, 1985; Mann *et al*, 1988; Sun and Fuchs, 1992].

Interestingly, both *RRM2* and *NEUROD2* genes contain multiple p53 consensus binding sites, as identified using a bioinformatics approach [Hoh *et al*, 2002] (**Figure 6.2B**). Therefore, these genes are likely to represent direct downstream effectors of p53 and this hypothesis is in accordance with the model for the induction of senescence in the HMF3A system, as discussed in **Chapter 3**. The fact that *RRM2* expression was shown to be down-regulated in *p53*-null cells also provides indirect evidence that this gene is a target of p53 [Zhou *et al*, 2003], however, this requires further experimental validation. As a caveat, it should be noted that the microarray data analysis presented in **Chapter 4** did not reveal any significant up regulation of *RRM2* or *NEUROD2* in HMF3AEco^R cells upon the irreversible growth arrest. Unfortunately, however, none of the other genes identified in this experiment were represented in the SANGER/LICR/CRUK 10K cDNA microarray.

The possibility that NeuroD2, RRM2 and TARBP1 each potentially represent critical mediators of the induction of telomere-independent cellular senescence in the HMF3A system requires functional validation. Therefore, it is necessary to perform a secondary shRNA screen by reintroducing these specific shRNA constructs into HMF3AEco^R cells to confirm their growth complementation activities. Exhibition of this functional activity should also address the possibility that multiple shRNA constructs were expressed in the same cell and acted synergistically to complement the growth of these cells. Moreover, the utilisation of shRNAs targetted against different regions of the candidate genes should be used to address the possibility that the original shRNA constructs identified as positive hits in this screen functioned in a non-specific manner to bypass the conditional growth arrest; down regulation of

the target gene could easily be validated by semi-quantitative RT-PCR. Unfortunately, due to time constraints, it was not possible to apply pure plasmid preparations of these shRNA constructs to the HMF3A system and address these issues.

6.3.3 Saturation of the ShRNA Screening Procedure

It was evident that the shRNA screen described in this chapter was not performed under saturating conditions since the shRNA target sequences that gave a positive hit following 2 rounds of the shRNA screen were representative of one of a number of possible shRNA constructs targetted against each of the candidate genes (**Figure 6.2A**). This finding was in accordance with that of Westbrook and colleagues [Westbrook *et al*, 2005], who similarly voiced concerns over the lack of shRNA screen saturation.

To address this issue, a number of modifications to the shRNA screening procedure can be made; for example, the shRNA screen can be increased in scale by utilising greater quantities of retroviral supernatant representative of each shRNA pool in an attempt to increase the number of retroviral infections events. Indeed, the fact that only 1152 genes were analysed in this experiment rendered the screen lacking with respect to 22 500 estimated number of unique human genes [International Human Genome Sequencing Consortium, 2004].

It is likely that any increase in the number of infectious events in the HMF3AEco^R cells will lead to an increase in the number of background reversion events. Therefore, any improvement to the stringency of the conditional growth arrest would further minimize this risk. Constitutive expression of oncogenic Ras in HMF3AEco^R cells represents one example of a method that may be used to address this issue, since the conditionality of these cells appears to be increased in its presence (unpublished observations).

In terms of the shRNA library itself, several parameters could be modified. First, more effective shRNA targets could be utilised; since the

generation of shRNA libraries such as the CSHL shRNA library, rule-based designs of shRNA targets have been developed to incorporate a limited set of criteria (for example, [Reynolds *et al*, 2004]). However, as demonstrated by 8 of the 9 different p21 shRNA targets designed and generated in **Chapter 3** (**Figure 3.14**), these designs are not always effective in mediating effective knockdown of the target gene. It should also be noted that the CSHL shRNA library limited the design of shRNA targets to coding regions of genes. However, this ruling may have contributed to limit the effectiveness of knockdown as evidence presented in both **Chapters 3** and **4** (**Figures 3.14, 4.5** and **Figure 4.6**) indicated that shRNA targets designed against sequences in the 3' UTR are likely to confer an effective level of knockdown. The fact that multiple shRNA targets were utilised for each gene addressed this issue, yet analysis of the number of shRNA constructs designed for each gene in pools 1-12 used in the HMF3A shRNA screen revealed that 45% of genes (522) were targetted by only a single shRNA construct (**Figure 6.3**); assuming that effective knockdown occurred at a rate of 80% [Reynolds *et al*, 2004], the highest rate described so far, the expression levels of approximately 100 of these genes may not have been significantly altered in this screen.

The ability to achieve a sufficiently penetrable knockdown of the target gene in order to elicit an observable phenotype also appeared to vary in different cell types; for example, differential activities of the pRetroSuper-p21 RB shRNA construct was observed in the HMF3A system and in the study by Berns and colleagues ([Berns *et al*, 2004]; **Figure 3.14**) in a similar manner to the pRetroSuper-p16#2 construct utilised by Wei and colleagues ([Wei *et al*, 2003]; **Figure 3.12**). As suggested in **Chapter 3**, this observation may have been indicative of an, as yet, unknown parameter that affected the efficiency of knockdown mediated by RNAi.

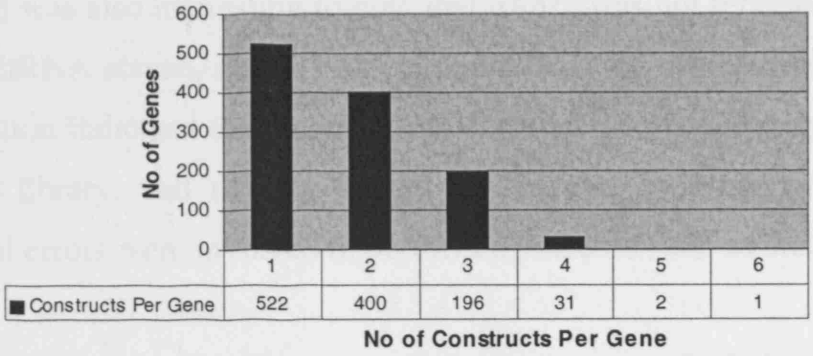

Figure 6.3: Effectiveness of the ShRNA Screen

Histogram showing the frequency of genes targetted by 1, 2, 3, 4, 5, or 6 shRNA targets in the shRNA screen.

There were also concerns regarding the quality of the plasmid preparations utilised in the shRNA screen. Recombination events between the LTR regions in the vector sequences that promoted the loss of hairpin sequences during the amplification of each of the plasmid pools in bacteria has been described in large-scale retroviral shRNA libraries [Downward, 2004]. Therefore, it was important that the library was prepared carefully such that the risk of recombination, and the concomitant risk of loss of information, was minimised. It was for this reason that the CHSL shRNA library was utilised in this screen as it had been shown to exhibit little recombination (gift from A. Ashworth).

It was also interesting to note that *RRM2* was not represented in pool 6 of the shRNA screen, nor any of the pools analysed in this experiment. This observation indicated that an error had occurred during the preparation of the shRNA library, and thereby served to illustrate that many variables and potential errors were involved in performing screens such as this.

6.3.4 Distinct Model Systems of Senescence and their Utilisation in ShRNA Screens

Prior to this experiment, an experiment describing an shRNA library that had been utilised to identify genes whose inhibition was sufficient to bypass human cellular senescence was published [Berns *et al*, 2004]. Here, the authors used a conditionally immortalised model human fibroblast system that was analogous to the HMF3A system, namely BJ-TERT-tsLT cells.

There is considerable evidence, based upon the differential phenotypes of these cells to suggest that the BJ-TERT-tsLT and HMF3AEco^R cells constitute distinct conditionally immortalised model systems. For example, the BJ-TERT-tsLT cells utilised by Berns and colleagues [Berns *et al*, 2004] had previously been shown to be capable of being immortalised by reconstitution of telomerase activity alone [Bodnar *et al*, 1998; Vaziri and Benchimol, 1998], unlike HMF3A cells that required the concomitant

expression of LT [O'Hare *et al*, 2001]. Furthermore, the two model systems exhibit significant differences in their patterns of growth complementation; for example, the expression of a shRNA targetted against p21, namely pRetroSuper-p21 RB, was sufficient to complement the growth of conditionally-immortalised BJ cells, but not HMF3AEco^R cells (**Figure 3.14**). Moreover, knockdown of one of the candidate genes identified in the shRNA screen performed by Berns and colleagues [Berns *et al*, 2004]; using the same shRNA construct (namely, pRetroSuper-HTATIP), was insufficient to complement the growth defect of HMF3AEco^R cells, despite the fact that effective knockdown of this gene was observed by semi-quantitative RT-PCR (**Figure 3.20**). It should also be noted that the other candidate genes identified by Berns and colleagues [Berns *et al*, 2004] did not exhibit significant changes upon the temperature shift, as indicated by semi-quantitative RT-PCR (**Figure 3.19B**). Therefore, it was unlikely that these candidate genes represented critical mediators of senescence in the HMF3A system, however, this evidence alone did not rule out this possibility.

The utilisation of a distinct shRNA library for screening the HMF3A system, namely the CSHL shRNA library rather than the CRUK/NKI shRNA library utilised by Berns and colleagues [Berns *et al*, 2004], was also possible. These libraries differ in many parameters, such as in the number and types of genes they target, the design of the shRNA targets and the level of knockdown efficiency that are achievable by their respective vector design.

In conclusion, there is significant evidence to support the view that the BJ and HMF3A conditionally immortalised models constitute distinct systems and that the different libraries could identify a different spectrum of putative positive hits. Therefore, these considerations supported the utilisation of the HMF3A system in an shRNA screening procedure that utilised the Hannon shRNA library.

7. Summary and Final Discussion

Cellular senescence is an irreversible program of cell cycle arrest that normal cells undergo both *in vitro* and *in vivo* in response to a variety of intrinsic and extrinsic stimuli. Senescence is associated with organismal ageing as it promotes the disruption of tissue renewal and repair processes as well as the depletion of progenitor cell populations. Senescence also represents an important tumour suppressive mechanism that limits the growth capacity of potentially cancerous cells. Bypass of senescence therefore represents a mechanism by which cells can overcome finite proliferative potential, one of the six proposed hallmarks of cancer cells [Hanahan and Weinberg, 2000].

In conjunction with hTERT, LT can immortalise many human cells including primary human fibroblasts. Consequently, the generation of a thermolabile mutant of LT, U19tsA58, led to the development of a conditionally immortalised human mammary fibroblast cell model, HMF3A [O'Hare *et al*, 2001]. HMF3A cells grow at 33.5°C, but undergo an irreversible growth arrest within 7 days upon temperature shift to 39.5°C. Since telomerase remains constitutively active in these cells at both 33.5°C and 39.5°C, the growth of HMF3A cells is entirely dependent upon LT activity.

Microarray analysis has determined that the transcriptional changes that occur upon the induction of the irreversible growth arrest in HMF3A cells directly correlate with the transcriptional changes that are induced upon replicative senescence in normal human mammary fibroblasts [Hardy *et al*, 2005]. Moreover, RNA interference and *in silico* analysis has indicated an important role for the p53, pRb and Erk signalling pathways in this process.

7.1 SUMMARY OF RESULTS

The aim of this thesis was to extend these initial findings [Hardy *et al*, 2005] in order to determine the precise molecular basis of the HMF3A conditional growth arrest and to identify novel genes associated with telomere-independent cellular senescence. A series of systematic experimental procedures were utilised to do this.

First, reconstitution of wt LT activity was shown to be sufficient to overcome the conditionality of HMF3A cells. This enabled a genetic complementation assay to be developed. Expression of shRNA constructs targetted against either p53 or p21, in addition to a dominant-negative peptide of p53 (GSE p53), was subsequently used in this assay to determine that inactivation of the p53 pathway was sufficient to bypass the induction of the conditional HMF3A growth arrest. In contrast, inactivation of the pRb pathway by expression of a $p16^{INK4a}$-insensitive cyclin D1-$CDK4^{R24C}$ fusion construct (DK) or an shRNA construct targetted against $p14^{ARF}$ was not sufficient. However, these findings appeared contradictory to the observation that constitutive expression of either E1A or E7 was sufficient to bypass the conditional HMF3A growth arrest. It was concluded that the p53 pathway, was critically involved in the induction of the conditional HMF3A growth arrest. However, inactivation of the pRb pathway by constitutive expression of the DK indicated that this pathway was not critically involved in the induction of the conditional HMF3A growth arrest. Moreover, it was possible that E1A and E7 targetted downstream effectors of the p53 pathway to bypass this process.

Transcriptional profiling, using the Sanger/LICR/CRUK 10K cDNA microarray, was used to identify *AKR1B1*, *CDH13* and *UBE2C* as three genes that were significantly differentially expressed upon the induction of the conditional HMF3A growth arrest, but not under 5 different conditions of HMF3A growth-complementation, namely expression of SV40 LT, E1A, E7, GSE p53 or RNAi of p53. Significantly, *AKR1B1* and *UBE2C* represent two

genes that were differentially expressed in primary HDFs upon replicative senescence [Hardy *et al*, 2005]. Moreover, sequence analysis indicated that at least one of these genes, *CDH13*, was a direct transcriptional target of p53 [Hoh *et al*, 2002]. Therefore, the HMF3A microarray data was in accordance with the HMF3A growth complementation data.

The development of a genetic complementation assay in the HMF3A system also enabled an RNA interference screen to be applied to this system. As a result, three putative critical regulators of senescence, namely, *NEUROD2*, *TARBP1* and *RRM2* were identified. Interestingly, it was possible that NeuroD2 interacted with pRb to bypass the conditional HMF3A growth arrest, since a NeuroD2-related protein had previously been shown to bind to pRb to promote neuronal differentiation.

Finally, a putative, novel functional activity of the 13S E1A splice variant that may have been critical for the continued growth of HMF3A cells under non-permissive conditions was detected. This finding was unexpected as a cDNA construct of *12S E1A* was utilised in the original experimental procedure. Therefore, in order to explain this observation, a model involving E1A recombination in the ϕ system was proposed.

7.2 FUTURE DIRECTIONS

It is essential that the senescence-associated activities of the candidate genes identified by these different experimental approaches are functionally validated. Firstly, ectopic expression or silencing by RNAi should be sufficient to complement the conditional growth of HMF3A cells. Upon confirmation of this activity, experimental analysis should be extended to primary human fibroblasts and other primary human cells; for example, ectopic expression or silencing should be sufficient to immortalise primary human cells in conjunction with hTERT alone. Moreover, the activities of each these genes may be impaired in different tumour types, therefore,

expression should be analysed in a variety of primary human tumours and cancer cell lines.

The fact that expression of a p21 shRNA construct was sufficient to bypass the conditional HMF3A growth arrest is particularly interesting and it will be important to determine how this activity differs from the ability of p21 to induce temporary cell cycle arrest. To facilitate this, two models have been proposed; the first model hypothesises that p21 functions synergistically with other negative regulators of the cell cycle to induce senescence. Therefore, the activity of CDKIs such as p27 should be analysed in the HMF3A system. The second model hypothesises that the activity of an as yet unknown factor is required for p21 to mediate the irreversible growth arrest; given the critical role of p53 in mediating the HMF3A growth arrest, it is likely that this factor is a transcriptional target of p53. Therefore, it will be important to determine the global transcriptional changes that are induced by p53 in the HMF3A system. ChIP-chip analysis represents one method that may be used to map the binding sites that are differentially occupied by p53 upon inactivation of LT in the HMF3A system. Furthermore, p53 target genes can be down-regulated by RNAi to functionally assess their growth complementation activities in the HMF3A system.

Microarray analysis and RNA interference represent two independent experimental techniques that were used to identify putative senescence-associated genes in the HMF3A system. *In silico* promoter analysis may help to determine whether the candidate genes identified from either of these experiments function by a common mechanism of transcriptional regulation. However, both of these methods were limiting with respect to total gene coverage and this should be addressed in future experiments; with respect to transcriptional profiling, whole genome microarrays have been developed and RNAi libraries can be improved by increasing the number of genes that are targetted and by improving target design. The RNAi screen should also be performed on a much larger scale, as there was substantial evidence to suggest that the HMF3A RNAi screen was performed under non-saturating conditions.

Furthermore, as there is increasing evidence to suggest that miRNAs play an important role in transcriptional regulation, the possibility that miRNAs are differentially expressed upon the HMF3A temperature shift should be investigated.

The activity of 13S E1A also remains to be functionally validated. If, as proposed, 13S E1A but not 12S is able to bypass the conditional HMF3A growth arrest, this will greatly narrow down the likely cellular mediators and pathways that are critically involved in this process; for example, CBF1 and Sur2 represent two candidate genes as they are both known to bind to the CR3 region of 13S E1A.

7.2.1 $P16^{INK4a}$ and $P14^{ARF}$ Expression Levels in the HMF3A System

Western blot analysis indicated that $p16^{INK4a}$ expression was readily detectable in HMF3A cultures grown under permissive conditions and was not significantly altered in cultures grown under non-permissive temperature for 7 days. Whilst $p16^{INK4a}$ protein levels were not quantified under these conditions (for example, by comparison with another fibroblast strain or between early and late passage cultures), the fact that $p16^{INK4a}$ was readily detectable in these cells, even under permissive conditions, appeared to contradict the expression data obtained from the serial cultivation of several other HDF strains; for example both TIG3 and FDF exhibit very low, if detectable, $p16^{INK4a}$ expression at early and mid passages [Brookes *et al*, 2004]. However, at later passages, $p16^{INK4a}$ expression rapidly accumulates and becomes readily detectable by Western blot.

In contrast, it should be noted that some other human fibroblast strains do not exhibit the same pattern of $p16^{INK4a}$ accumulation; for example early passage WI-38 HDFs contain a significant proportion of cells that express high levels of $p16^{INK4a}$ [Itahana *et al*, 2003]. Brookes and colleagues suggest that this contradiction may be explained by heterogeneity within each of the fibroblast strains; for example, the more homogeneous strains will switch on

$p16^{INK4a}$ expression at about the same point in their lifespan whereas the more heterogeneous strains will show a continually developing fraction of $p16^{INK4a}$-positive senescent cells. As discussed in **Chapter 3**, the different origins of the different fibroblast strains could also explain this discrepancy; for example, HMF3A cells were originally derived from adult breast stromal fibroblasts, whereas WI-38 cells were derived from foetal lung fibroblasts, and BJ cells were derived from foreskin fibroblasts. Therefore, both the age and the tissue context of different cell lines derived from the same cell type may be important parameters for consideration when interpreting experimental data.

Similar to $p16^{INK4a}$, semi-quantitative RT-PCR analysis of the alternatively spliced gene product encoded by the *INK4A* locus, $p14^{ARF}$, indicated that it too was unaltered upon the HMF3A temperature shift. Whilst this analysis was only performed at the transcriptional level, evidence from a number of human cell lines suggests that there is complete concordance between the presence of the $p14^{ARF}$ mRNA transcript and $p14^{ARF}$ protein [Stott *et al*, 1998]. Unlike $p16^{INK4a}$ however, the level of $p14^{ARF}$ expression detected in the HMF3A system appeared to be comparable to that exhibited by other HDF strains; for example, similar quantities of cDNA starting material and PCR cycle numbers were used by Wei and colleagues to show that $p14^{ARF}$ expression was not induced upon serial cultivation of LF1 HDFs to senescence [Wei *et al*, 2001]. Moreover, RNase protection analysis of both LF1 and WI-38 HDF strains was used to support this finding.

7.2.2 LT Expression in the HMF3A System May Affect $P16^{INK4a}$ and $P14^{ARF}$ Expression Levels

The fact that $p16^{INK4a}$ expression appeared to be elevated in the HMF3A system relative to some serially cultivated primary HDFs is consistent with the hypothesis that a negative feedback response to the abrogation of pRb function by LT occurs in LT-infected cells [Stott *et al*,

1998, Draetta, 1994]. In this model, pRb negatively regulates the expression of $p16^{INK4a}$, yet in LT-infected cells, the ability of LT to bind to and inactivate pRb results in the induction of *p16*^{INK4a} expression. Since $p16^{ARF}$ is inherently stable [Parry *et al*, 1995], $p16^{INK4a}$ protein levels become elevated in LT-infected cells to beyond those observed in primary cell counterparts.

Evidence to support this hypothesis has been obtained from some LT-infected HDF strains; for example, an approximately 50-fold increase in *p16*^{INK4a} mRNA levels has been detected in a LT-expressing derivative of WI-38 HDFs, namely VA13 cells, relative to their parental counterparts [Hara *et al*, 1996]. Moreover, a similar observation has been made in TIG-3 HDFs immortalised with a temperature-sensitive mutant of LT, namely SVts8 and SVts9-3 cell lines [Tsuyama *et al*, 1991; Hara *et al*, 1996].

With respect to $p14^{ARF}$ expression levels, the demonstration that $p14^{ARF}$ expression exhibits an inverse correlation with p53 status has also been interpreted by some as evidence of a negative feedback loop between $p14^{ARF}$ and p53 [Stott *et al*, 1998]. Stott and colleagues were able to demonstrate that SVts8 cells grown at the permissive temperature for LT function contained readily detectable levels of $p14^{ARF}$ protein. Moreover, a similar finding was obtained by the comparison of TIG-3 HDFs infected with HPV E6 with primary TIG-3 HDFs.

However, data from the HMF3A system does not support this hypothesis; in HMF3A cells grown at 33.5°C, *p14*^{ARF} expression levels were consistent with those observed in other primary HDF strains, despite the fact that p53 was functionally inactivated by LT under these conditions. Consequently, a negative feedback loop between $p14^{ARF}$ and p53 does not appear to operate in the HMF3A system.

7.2.3 Functional Inactivation of $P16^{INK4a}$ and $P14^{ARF}$ in LT-Expressing HDFs

The possibility that $p16^{INK4a}$ expression (and to a lesser extent, $p14^{ARF}$ expression) was significantly elevated in HMF3A cells has significant implications for the functional analysis of these proteins in this system; for example, downregulation of $p16^{INK4a}$ and/or $p14^{ARF}$ expression by RNAi or by transcriptional repression of the *INK4A* locus by ectopic Bmi-1 expression may not have been significant enough to reduce expression levels to below a particular threshold value, beyond which, a physiological response could have been observed.

However, there is some evidence to contradict this hypothesis since downregulation of both $p16^{INK4a}$ and $p14^{ARF}$ by RNAi has been reported by others within the same timeframe of assessment used in this study. For example, Jacobs and de Lange noted a significant knockdown of $p16^{INK4a}$ using a retroviral $p16^{INK4a}$ shRNA construct in IMR90 HDFs at approximately 8 days post puromycin drug-selection, as determined by immunohistochemistry analysis [Jacobs and de Lange, 2004]. Perhaps more significantly however, Bond and colleagues [Bond *et al*, 2004] successfully achieved siRNA knockdown of $p16^{INK4a}$ in a transformed thyroid epithelial cell line, HT-ori3, by transient transfection of a duplex siRNA construct that contained a target sequence that was almost overlapping to one of the shRNA sequences utilised in this study, namely p16A. Efficient knockdown of $p16^{INK4a}$ by this transient method was estimated to have occurred in over 99% of the cells within 48 hours, as shown by both immunocytochemistry and Western blot analysis. Whilst the efficiency of $p16^{INK4a}$ may be context-dependent and cell type specific, the authors chose to infect HT-ori3 cells prior to the infection of a strain of primary HDFs (HCA2) since these cells express high levels of $p16^{INK4a}$. Importantly, the HT-ori3 cell line, as used by Bond and colleagues, was generated by the introduction of SV40. Therefore, in an analogous manner to the HMF3A system, these cells express high levels

of $p16^{INK4a}$ [Bond *et al*, 2004]. Moreover, there is additional functional evidence that LT-expressing HDFs can obtain significant $p16^{INK4a}$ knockdown; using a model analogous to the HMF3A system, Berns and colleagues [Berns *et al*, 2004] demonstrated that $p16^{INK4a}$ knockdown was unable to bypass the conditional growth of BJ-TERT-tsLT cells (BJ cells that constitutively express hTERT and a temperature sensitive mutant of LT), using a protocol similar to that applied to the HMF3A system. Significantly, the $p16^{INK4a}$ shRNA construct used by Berns and colleagues was shown to be functional as it enhanced the ability of p53 knockdown to bypass the conditional growth arrest of these cells.

Whilst knockdown of $p14^{ARF}$ has not been analysed in other LT-infected cells, the same $p14^{ARF}$ shRNA construct used in this study was successfully utilised by Voorhoeve and Agami to downregulate $p14^{ARF}$ expression in HeLa cells at one week post-selection [Voorhoeve and Agami, 2003]. Moreover, semi-quantitative RT-PCR was used to demonstrate that this construct was able to significantly knockdown $p14^{ARF}$ expression levels by more than 10-fold in primary BJ HDF cells.

Similarly, whilst ectopic Bmi-1 expression has not been analysed in other LT-infected HDF strains, Jacobs and de Lange did observe a significant decrease in $p16^{INK4a}$ expression at 12 days post-selection. Again, the timing at which downregulation was observed is consistent with the analysis of $p16^{INK4a}$ and $p14^{ARF}$ expression in the HMF3A system [Jacobs and de Lange, 2004].

7.2.4 Implications for the Functional Analysis of Stable Proteins Inactivated by LT in the HMF3A System

Despite this evidence, the possibility that LT-mediated negative regulation of cellular proteins other than $p16^{INK4a}$ and $p14^{ARF}$ may have occurred in the HMF3A system cannot be discounted. This is a particularly important point to consider when determining the effectiveness of expression knockdown by RNAi; for example, whilst downregulation of PML, SRN,

BTG2 and GADD45A expression by shRNA was shown to be effective in the HMF3A system by semi-quantitative RT-PCR, the corresponding protein levels were not assessed. By extension therefore, it is possible that stable proteins may not be identified by functional screens, such as RNAi screens. Therefore, it may be important to consider the utilisation of alternative strategies to specifically target protein activity such as short peptide inhibitors or dominant-negative peptides (for example, GSEs).

7.2.5 Do the Microarray Candidate Genes Represent Markers of Senescence or Rather, Global Markers of Growth Arrest?

It is important to note that no controls were used in this microarray study to distinguish between HMF3A cells irreversibly arrested at 39.5°C for 7 days and reversibly arrested HMF3A cells grown at 33.5°C. Since both of these conditions represent non-growth states, it is possible that some of the candidate genes identified here represent general markers cell cycle arrest, rather than senescence *per se*. Indeed, some of the senescence-associated candidate genes identified in this study, namely AKR1B1, CDH13 and UBE2C, exhibit differential regulation in serum-starved, confluent HMF3A cells relative to proliferating HMF3A cells [Hardy *et al*, 2005]. This finding indicates that in the HMF3A system, common mechanisms of growth arrest may occur in response to both quiescence and senescence, despite the inherent differences in the reversibility of these two states.

However, the fact that quiescence and senescence represent two very different states of growth arrest indicates that specific signalling pathways are involved in the induction of each of these processes. In support of this hypothesis there is some evidence to suggest that quiescence and senescence do exhibit significant differences in their expression profiles; for example, DiPaolo and colleagues used 2D-DIGE analysis to show that dramatic changes occur between the protein expression profiles of senescent WI-38 HDFs and early passage WI-38 HDFs made quiescent by density-dependent

contact inhibition and serum starvation [DiPaolo *et al*, 1995]. Moreover, BJ HDFs cultivated to replicative senescence exhibit a different cell cycle distribution to that of early passage, quiescent BJ HDFs; Shelton and colleagues identified a substantial population of cells with G2 DNA content in quiescent cells whereas senescent cultures contained cells distributed in a distinct pattern of G1 and G2 phases of the cell cycle [Shelton *et al*, 1999]. Moreover, microarray analysis was used to identify a number of genes that were differentially expressed genes in senescent and quiescent cells; for example, MMP3, MMP11, CCL2 and IL15 [Shelton *et al*, 1999]. However, none of these genes appear to exhibit significantly differential expression upon the HMF3A temperature shift. Similarly, MYC, ID4 and MITF were identified in a small-scale microarray study of E-box-binding related genes that exhibit differential expression between senescent and quiescent WI-38 HDFs [Semov *et al*, 2002]). Again however, none of these genes were differentially expressed upon the HMF3A temperature shift.

In conclusion, the microarray candidate genes identified in this study represent markers of growth arrest and the inclusion of appropriate serum-starved/confluent controls in addition to the extension of the HMF3A microarray analysis to attain full genome coverage may be sufficient to identify genes that do exhibit truly differential expression between these two different growth arrest states.

7.3 FINAL REMARKS

The fact that senescent cells have been detected *in vivo* provides compelling evidence that cellular senescence represents a *bona fide* biological process [Braig *et al*, 2005; Chen *et al*, 2005; Collado *et al*, 2005; Michaloglou *et al*, 2005]. This has profound implications for the study of both organismal ageing and tumorigenesis; for example, the genes identified here may not only represent novel markers of senescence, but may also have prognostic and/or diagnostic value in the context of tumorigenic treatment. Moreover, as there

is accumulating evidence to suggest that the induction of senescence *in vivo* is critical to the efficacy of chemotherapeutic agents [Chang *et al*, 2002; Rebbaa *et al*, 2003; Zheng *et al*, 2004], elucidation of the pathways critical regulating the finite proliferative potential of normal human cells will be important for the development of novel chemotherapeutic agents.

8. References

Abbas-Terki, T., Blanco-Bose, W., Deglon, N., Pralong, W. & Aebischer, P. (2002) Lentiviral-mediated RNA interference, *Hum Gene Ther. 13*, 2197-201.

Adams, P. D. (2001) Regulation of the retinoblastoma tumor suppressor protein by cyclin/cdks, *Biochim Biophys Acta. 1471*, M123-33.

Afshari, C. A., Vojta, P. J., Annab, L. A., Futreal, P. A., Willard, T. B. & Barrett, J. C. (1993) Investigation of the role of G1/S cell cycle mediators in cellular senescence, *Exp Cell Res. 209*, 231-7.

Agarwal, M. L., Agarwal, A., Taylor, W. R. & Stark, G. R. (1995) p53 controls both the G2/M and the G1 cell cycle checkpoints and mediates reversible growth arrest in human fibroblasts, *Proc Natl Acad Sci U S A. 92*, 8493-7.

Alani, R. M. & Munger, K. (1998) Human papillomaviruses and associated malignancies, *J Clin Oncol. 16*, 330-7.

Alcalay, M., Tomassoni, L., *et al.* (1998) The promyelocytic leukemia gene product (PML) forms stable complexes with the retinoblastoma protein, *Mol Cell Biol. 18*, 1084-93.

Alcorta, D. A., Xiong, Y., Phelps, D., Hannon, G., Beach, D. & Barrett, J. C. (1996) Involvement of the cyclin-dependent kinase inhibitor p16 (INK4a) in replicative senescence of normal human fibroblasts, *Proc Natl Acad Sci U S A. 93*, 13742-7.

Alevizopoulos, K., Vlach, J., Hennecke, S. & Amati, B. (1997) Cyclin E and c-Myc promote cell proliferation in the presence of p16INK4a and of hypophosphorylated retinoblastoma family proteins, *Embo J. 16*, 5322-33.

Al-Hajj, M., Wicha, M. S., Benito-Hernandez, A., Morrison, S. J. & Clarke, M. F. (2003) Prospective identification of tumorigenic breast cancer cells, *Proc Natl Acad Sci U S A. 100*, 3983-8.

Ali, S. H. & DeCaprio, J. A. (2001) Cellular transformation by SV40 large T antigen: interaction with host proteins, *Semin Cancer Biol. 11*, 15-23.

Alizadeh, A. A., Eisen, M. B., *et al.* (2000) Distinct types of diffuse large B-cell lymphoma identified by gene expression profiling, *Nature. 403*, 503-11.

Allsopp, R. C., Morin, G. B., Horner, J. W., DePinho, R., Harley, C. B. & Weissman, I. L. (2003) Effect of TERT over-expression on the long-term transplantation capacity of hematopoietic stem cells, *Nat Med. 9*, 369-71.

Allsopp, R. C. & Weissman, I. L. (2002) Replicative senescence of hematopoietic stem cells during serial transplantation: does telomere shortening play a role?, *Oncogene. 21*, 3270-3.

Aloni-Grinstein, R., Schwartz, D. & Rotter, V. (1995) Accumulation of wild-type p53 protein upon gamma-irradiation induces a G2 arrest-dependent immunoglobulin kappa light chain gene expression, *Embo J. 14*, 1392-401.

Alt, J. R., Gladden, A. B. & Diehl, J. A. (2002) p21(Cip1) Promotes cyclin D1 nuclear accumulation via direct inhibition of nuclear export, *J Biol Chem. 277*, 8517-23.

Alvarez-Salas, L. M., Cullinan, A. E., Siwkowski, A., Hampel, A. & DiPaolo, J. A. (1998) Inhibition of HPV-16 E6/E7 immortalization of normal keratinocytes by hairpin ribozymes, *Proc Natl Acad Sci U S A. 95*, 1189-94.

Alwine, J. C., Reed, S. I. & Stark, G. R. (1977) Characterization of the autoregulation of simian virus 40 gene A, *J Virol. 24*, 22-7.

Androphy, E. J., Hubbert, N. L., Schiller, J. T. & Lowy, D. R. (1987) Identification of the HPV-16 E6 protein from transformed mouse cells and human cervical carcinoma cell lines, *Embo J. 6*, 989-92.

Ansieau, S., Strobl, L. J. & Leutz, A. (2001) Activation of the Notch-regulated transcription factor CBF1/RBP-Jkappa through the 13SE1A oncoprotein, *Genes Dev. 15*, 380-5.

Appella, E. & Anderson, C. W. (2001) Post-translational modifications and activation of p53 by genotoxic stresses, *Eur J Biochem. 268*, 2764-72.

Aslanian, A., Iaquinta, P. J., Verona, R. & Lees, J. A. (2004) Repression of the Arf tumor suppressor by E2F3 is required for normal cell cycle kinetics, *Genes Dev. 18*, 1413-22.

Atadja, P., Wong, H., Garkavtsev, I., Veillette, C. & Riabowol, K. (1995) Increased activity of p53 in senescing fibroblasts, *Proc Natl Acad Sci U S A. 92*, 8348-52.

Attardi, L. D., Lowe, S. W., Brugarolas, J. & Jacks, T. (1996) Transcriptional activation by p53, but not induction of the p21 gene, is essential for oncogene-mediated apoptosis, *Embo J. 15*, 3693-701.

Avantaggiati, M. L., Carbone, M., Graessmann, A., Nakatani, Y., Howard, B. & Levine, A. S. (1996) The SV40 large T antigen and adenovirus E1a oncoproteins interact with distinct isoforms of the transcriptional co-activator, p300, *Embo J. 15*, 2236-48.

Baird, D. M., Rowson, J., Wynford-Thomas, D. & Kipling, D. (2003) Extensive allelic variation and ultrashort telomeres in senescent human cells, *Nat Genet. 33*, 203-7.

Bammler, T., Beyer, R. P., *et al.* (2005) Standardizing global gene expression analysis between laboratories and across platforms, *Nat Methods. 2*, 351-6.

Bannister, A. J., Zegerman, P., Partridge, J. F., Miska, E. A., Thomas, J. O., Allshire, R. C. & Kouzarides, T. (2001) Selective recognition of methylated lysine 9 on histone H3 by the HP1 chromo domain, *Nature. 410*, 120-4.

Barbacid, M. (1987) ras genes, *Annu Rev Biochem. 56*, 779-827.

Barbeau, D., Charbonneau, R., Whalen, S. G., Bayley, S. T. & Branton, P. E. (1994) Functional interactions within adenovirus E1A protein complexes, *Oncogene. 9*, 359-73.

Barbosa, M. S., Edmonds, C., Fisher, C., Schiller, J. T., Lowy, D. R. & Vousden, K. H. (1990) The region of the HPV E7 oncoprotein homologous to adenovirus E1a and Sv40 large T antigen contains separate domains for Rb binding and casein kinase II phosphorylation, *Embo J. 9*, 153-60.

Barbosa, M. S., Lowy, D. R. & Schiller, J. T. (1989) Papillomavirus polypeptides E6 and E7 are zinc-binding proteins, *J Virol. 63*, 1404-7.

Bargou, R. C., Wagener, C., *et al.* (1996) Blocking the transcription factor E2F/DP by dominant-negative mutants in a normal breast epithelial cell line efficiently inhibits apoptosis and induces tumor growth in SCID mice, *J Exp Med. 183*, 1205-13.

Bartek, J., Bartkova, J. & Lukas, J. (1996) The retinoblastoma protein pathway and the restriction point, *Curr Opin Cell Biol. 8*, 805-14.

Bartel, D. P. (2004) MicroRNAs: genomics, biogenesis, mechanism, and function, *Cell. 116*, 281-97.

Bates, S., Phillips, A. C., Clark, P. A., Stott, F., Peters, G., Ludwig, R. L. & Vousden, K. H. (1998) p14ARF links the tumour suppressors RB and p53, *Nature. 395*, 124-5.

Batsche, E., Moschopoulos, P., Desroches, J., Bilodeau, S. & Drouin, J. (2005) Retinoblastoma and the related pocket protein p107 act as coactivators of NeuroD1 to enhance gene transcription, *J Biol Chem. 280*, 16088-95.

Baumann, P. & Cech, T. R. (2001) Pot1, the putative telomere end-binding protein in fission yeast and humans, *Science. 292*, 1171-5.

Baur, J. A., Zou, Y., Shay, J. W. & Wright, W. E. (2001) Telomere position effect in human cells, *Science. 292*, 2075-7.

Bea, S., Tort, F., *et al.* (2001) BMI-1 gene amplification and overexpression in hematological malignancies occur mainly in mantle cell lymphomas, *Cancer Res. 61*, 2409-12.

Beausejour, C. M., Krtolica, A., Galimi, F., Narita, M., Lowe, S. W., Yaswen, P. & Campisi, J. (2003) Reversal of human cellular senescence: roles of the p53 and p16 pathways, *Embo J. 22*, 4212-22.

Behrens, J. (1993) The role of cell adhesion molecules in cancer invasion and metastasis, *Breast Cancer Res Treat. 24*, 175-84.

Benanti, J. A. & Galloway, D. A. (2004) Normal human fibroblasts are resistant to RAS-induced senescence, *Mol Cell Biol. 24*, 2842-52.

Benevolenskaya, E. V., Murray, H. L., Branton, P., Young, R. A. & Kaelin, W. G., Jr. (2005) Binding of pRB to the PHD protein RBP2 promotes cellular differentiation, *Mol Cell. 18*, 623-35.

Bernardi, R., Scaglioni, P. P., Bergmann, S., Horn, H. F., Vousden, K. H. & Pandolfi, P. P. (2004) PML regulates p53 stability by sequestering Mdm2 to the nucleolus, *Nat Cell Biol. 6*, 665-72.

Berns, K., Hijmans, E. M., *et al.* (2004) A large-scale RNAi screen in human cells identifies new components of the p53 pathway, *Nature. 428*, 431-7.

Bernstein, E., Caudy, A. A., Hammond, S. M. & Hannon, G. J. (2001) Role for a bidentate ribonuclease in the initiation step of RNA interference, *Nature. 409*, 363-6.

Berry, D. E., Lu, Y., *et al.* (1996) Retinoblastoma protein inhibits IFN-gamma induced apoptosis, *Oncogene. 12*, 1809-19.

Bischof, O., Kirsh, O., Pearson, M., Itahana, K., Pelicci, P. G. & Dejean, A. (2002) Deconstructing PML-induced premature senescence, *Embo J. 21*, 3358-69.

Bischof, O., Nacerddine, K. & Dejean, A. (2005) Human papillomavirus oncoprotein E7 targets the promyelocytic leukemia protein and circumvents cellular senescence via the Rb and p53 tumor suppressor pathways, *Mol Cell Biol. 25*, 1013-24.

Bjorklund, S., Hjortsberg, K., Johansson, E. & Thelander, L. (1993) Structure and promoter characterization of the gene encoding the large subunit (R1 protein) of mouse ribonucleotide reductase, *Proc Natl Acad Sci U S A. 90*, 11322-6.

Blackburn, E. H. (2001) Switching and signaling at the telomere, *Cell. 106*, 661-73.

Blain, S. W., Montalvo, E. & Massague, J. (1997) Differential interaction of the cyclin-dependent kinase (Cdk) inhibitor p27Kip1 with cyclin A-Cdk2 and cyclin D2-Cdk4, *J Biol Chem. 272*, 25863-72.

Blasco, M. A., Lee, H. W., Hande, M. P., Samper, E., Lansdorp, P. M., DePinho, R. A. & Greider, C. W. (1997) Telomere shortening and tumor formation by mouse cells lacking telomerase RNA, *Cell. 91*, 25-34.

Bodnar, A. G., Kim, N. W., Effros, R. B. & Chiu, C. P. (1996) Mechanism of telomerase induction during T cell activation, *Exp Cell Res. 228*, 58-64.

Bodnar, A. G., Ouellette, M., *et al.* (1998) Extension of life-span by introduction of telomerase into normal human cells, *Science. 279*, 349-52.

Bohren, K. M., Bullock, B., Wermuth, B. & Gabbay, K. H. (1989) The aldo-keto reductase superfamily. cDNAs and deduced amino acid sequences of human aldehyde and aldose reductases, *J Biol Chem. 264*, 9547-51.

Bond, J., Haughton, M., Blaydes, J., Gire, V., Wynford-Thomas, D. & Wyllie, F. (1996) Evidence that transcriptional activation by p53 plays a direct role in the induction of cellular senescence, *Oncogene. 13*, 2097-104.

Bond, J., Jones, C., Haughton, M., DeMicco, C., Kipling, D. & Wynford-Thomas, D. (2004) Direct evidence from siRNA-directed "knock down" that p16(INK4a) is required for human fibroblast senescence and for limiting ras-induced epithelial cell proliferation, *Exp Cell Res. 292*, 151-6.

Bonetto, F., Fanciulli, M., *et al.* (1999) Interaction between the pRb2/p130 C-terminal domain and the N-terminal portion of cyclin D3, *J Cell Biochem. 75*, 698-709.

Boyer, S. N., Wazer, D. E. & Band, V. (1996) E7 protein of human papilloma virus-16 induces degradation of retinoblastoma protein through the ubiquitin-proteasome pathway, *Cancer Res. 56*, 4620-4.

Boyer, T. G., Martin, M. E., Lees, E., Ricciardi, R. P. & Berk, A. J. (1999) Mammalian Srb/Mediator complex is targeted by adenovirus E1A protein, *Nature. 399*, 276-9.

Bracken, A. P., Ciro, M., Cocito, A. & Helin, K. (2004) E2F target genes: unraveling the biology, *Trends Biochem Sci. 29*, 409-17.

Bradford, M. M. (1976) A rapid and sensitive method for the quantitation of microgram quantities of protein utilizing the principle of protein-dye binding, *Anal Biochem. 72*, 248-54.

Braig, M., Lee, S., *et al.* (2005) Oncogene-induced senescence as an initial barrier in lymphoma development, *Nature. 436*, 660-5.

Braithwaite, A. W., Cheetham, B. F., Li, P., Parish, C. R., Waldron-Stevens, L. K. & Bellett, A. J. (1983) Adenovirus-induced alterations of the cell growth cycle: a requirement for expression of E1A but not of E1B, *J Virol. 45*, 192-9.

Brehm, A., Miska, E. A., McCance, D. J., Reid, J. L., Bannister, A. J. & Kouzarides, T. (1998) Retinoblastoma protein recruits histone deacetylase to repress transcription, *Nature. 391*, 597-601.

Breiling, A., O'Neill, L. P., D'Eliseo, D., Turner, B. M. & Orlando, V. (2004) Epigenome changes in active and inactive polycomb-group-controlled regions, *EMBO Rep. 5*, 976-82.

Bridger, J. M. & Kill, I. R. (2004) Aging of Hutchinson-Gilford progeria syndrome fibroblasts is characterised by hyperproliferation and increased apoptosis, *Exp Gerontol. 39*, 717-24.

Broccoli, D., Smogorzewska, A., Chong, L. & de Lange, T. (1997) Human telomeres contain two distinct Myb-related proteins, TRF1 and TRF2, *Nat Genet. 17*, 231-5.

Brookes, S., Rowe, J., Gutierrez Del Arroyo, A., Bond, J. & Peters, G. (2004) Contribution of p16(INK4a) to replicative senescence of human fibroblasts, *Exp Cell Res. 298*, 549-59.

Brookes, S., Rowe, J., *et al.* (2002) INK4a-deficient human diploid fibroblasts are resistant to RAS-induced senescence, *Embo J. 21*, 2936-45.

Brown, D. R., Deb, S., Munoz, R. M., Subler, M. A. & Deb, S. P. (1993) The tumor suppressor p53 and the oncoprotein simian virus 40 T antigen bind to overlapping domains on the MDM2 protein, *Mol Cell Biol. 13*, 6849-57.

Brown, J. P., Wei, W. & Sedivy, J. M. (1997) Bypass of senescence after disruption of p21CIP1/WAF1 gene in normal diploid human fibroblasts, *Science. 277*, 831-4.

Brugarolas, J., Chandrasekaran, C., Gordon, J. I., Beach, D., Jacks, T. & Hannon, G. J. (1995) Radiation-induced cell cycle arrest compromised by p21 deficiency, *Nature. 377*, 552-7.

Brummelkamp, T. R., Bernards, R. & Agami, R. (2002) A system for stable expression of short interfering RNAs in mammalian cells, *Science. 296*, 550-3.

Bucala, R. (1997) Lipid and lipoprotein modification by advanced glycosylation end-products: role in atherosclerosis, *Exp Physiol. 82*, 327-37.

Buchkovich, K., Duffy, L. A. & Harlow, E. (1989) The retinoblastoma protein is phosphorylated during specific phases of the cell cycle, *Cell. 58*, 1097-105.

Bulavin, D. V., Phillips, C., *et al.* (2004) Inactivation of the Wip1 phosphatase inhibits mammary tumorigenesis through p38 MAPK-mediated activation of the p16(Ink4a)-p19(Arf) pathway, *Nat Genet. 36*, 343-50.

Bunn, C. L. & Tarrant, G. M. (1980) Limited lifespan in somatic cell hybrids and cybrids, *Exp Cell Res. 127*, 385-96.

Burgert, H. G., Ruzsics, Z., Obermeier, S., Hilgendorf, A., Windheim, M. & Elsing, A. (2002) Subversion of host defense mechanisms by adenoviruses, *Curr Top Microbiol Immunol. 269*, 273-318.

Burkhart, B. A., Alcorta, D. A., Chiao, C., Isaacs, J. S. & Barrett, J. C. (1999) Two posttranscriptional pathways that regulate p21(Cip1/Waf1/Sdi1) are identified by HPV16-E6 interaction and correlate with life span and cellular senescence, *Exp Cell Res. 247*, 168-75.

Calin, G. A., Sevignani, C., *et al.* (2004) Human microRNA genes are frequently located at fragile sites and genomic regions involved in cancers, *Proc Natl Acad Sci U S A. 101*, 2999-3004.

Cam, H. & Dynlacht, B. D. (2003) Emerging roles for E2F: beyond the G1/S transition and DNA replication, *Cancer Cell. 3*, 311-6.

Campisi, J. (2005) Senescent cells, tumor suppression, and organismal aging: good citizens, bad neighbors, *Cell. 120*, 513-22.

Campisi, J., Kim, S. H., Lim, C. S. & Rubio, M. (2001) Cellular senescence, cancer and aging: the telomere connection, *Exp Gerontol. 36*, 1619-37.

Cao, D., Fan, S. T. & Chung, S. S. (1998) Identification and characterization of a novel human aldose reductase-like gene, *J Biol Chem. 273*, 11429-35.

Caporossi, D. & Bacchetti, S. (1990) Definition of adenovirus type 5 functions involved in the induction of chromosomal aberrations in human cells, *J Gen Virol. 71*, 801-8.

Cardinali, M., Jakus, J., Shah, S., Ensley, J. F., Robbins, K. C. & Yeudall, W. A. (1998) p21(WAF1/Cip1) retards the growth of human squamous cell carcinomas in vivo, *Oral Oncol. 34*, 211-8.

Carneiro, C., Jiao, M. S., *et al.* (2003) p27 deficiency desensitizes Rb-/- cells to signals that trigger apoptosis during pituitary tumor development, *Oncogene. 22*, 361-9.

Carrier, F., Georgel, P. T., *et al.* (1999) Gadd45, a p53-responsive stress protein, modifies DNA accessibility on damaged chromatin, *Mol Cell Biol. 19*, 1673-85.

Carroll, R. B., Hager, L. & Dulbecco, R. (1974) Simian virus 40 T antigen binds to DNA, *Proc Natl Acad Sci U S A. 71*, 3754-7.

Carroll, R. B., Samad, A., Mann, A., Harper, J. & Anderson, C. W. (1988) RNA is covalently linked to SV40 large T antigen, *Oncogene. 2*, 437-44.

Cartwright, P., Muller, H., Wagener, C., Holm, K. & Helin, K. (1998) E2F-6: a novel member of the E2F family is an inhibitor of E2F-dependent transcription, *Oncogene. 17*, 611-23.

Castro, M., Pedrosa, D. & Osuna, J. I. (1992) Effect of a restricted diet on the in vitro glucose-induced insulin release of aging rats, *Experientia. 48*, 996-8.

Chai, W., Shay, J. W. & Wright, W. E. (2005) Human telomeres maintain their overhang length at senescence, *Mol Cell Biol. 25*, 2158-68.

Chan, H. M., Krstic-Demonacos, M., Smith, L., Demonacos, C. & La Thangue, N. B. (2001) Acetylation control of the retinoblastoma tumour-suppressor protein, *Nat Cell Biol. 3*, 667-74.

Chan, S. W. & Blackburn, E. H. (2002) New ways not to make ends meet: telomerase, DNA damage proteins and heterochromatin, *Oncogene. 21*, 553-63.

Chan, T. A., Hermeking, H., Lengauer, C., Kinzler, K. W. & Vogelstein, B. (1999) 14-3-3Sigma is required to prevent mitotic catastrophe after DNA damage, *Nature. 401*, 616-20.

Chang, B. D., Swift, M. E., Shen, M., Fang, J., Broude, E. V. & Roninson, I. B. (2002) Molecular determinants of terminal growth arrest induced in tumor cells by a chemotherapeutic agent, *Proc Natl Acad Sci U S A. 99*, 389-94.

Chang, B. D., Watanabe, K., Broude, E. V., Fang, J., Poole, J. C., Kalinichenko, T. V. & Roninson, I. B. (2000) Effects of p21Waf1/Cip1/Sdi1 on cellular gene expression: implications for carcinogenesis, senescence, and age-related diseases, *Proc Natl Acad Sci U S A. 97*, 4291-6.

Chang, L. & Karin, M. (2001) Mammalian MAP kinase signalling cascades, *Nature. 410*, 37-40.

Chang, S., Multani, A. S., *et al.* (2004) Essential role of limiting telomeres in the pathogenesis of Werner syndrome, *Nat Genet. 36*, 877-82.

Chang, T. H., Ray, F. A., Thompson, D. A. & Schlegel, R. (1997) Disregulation of mitotic checkpoints and regulatory proteins following acute expression of SV40 large T antigen in diploid human cells, *Oncogene. 14*, 2383-93.

Chatterjee, P. K., Bruner, M., Flint, S. J. & Harter, M. L. (1988) DNA-binding properties of an adenovirus 289R E1A protein, *Embo J. 7*, 835-41.

Chen, J., Jackson, P. K., Kirschner, M. W. & Dutta, A. (1995) Separate domains of p21 involved in the inhibition of Cdk kinase and PCNA, *Nature. 374*, 386-8.

Chen, Q., Hung, F. C., Fromm, L. & Overbeek, P. A. (2000) Induction of cell cycle entry and cell death in postmitotic lens fiber cells by overexpression of E2F1 or E2F2, *Invest Ophthalmol Vis Sci. 41*, 4223-31.

Chen, Q. M., Prowse, K. R., Tu, V. C., Purdom, S. & Linskens, M. H. (2001) Uncoupling the senescent phenotype from telomere shortening in hydrogen peroxide-treated fibroblasts, *Exp Cell Res. 265*, 294-303.

Chen, T. T. & Wang, J. Y. (2000) Establishment of irreversible growth arrest in myogenic differentiation requires the RB LXCXE-binding function, *Mol Cell Biol. 20*, 5571-80.

Chen, Y. C., Song, C. & Luo, C. Q. (2003) Short hairpin RNAs induced RNA interference in human cells, *Ai Zheng. 22*, 566-70.

Chen, Z., Trotman, L. C., *et al.* (2005) Crucial role of p53-dependent cellular senescence in suppression of Pten-deficient tumorigenesis, *Nature. 436*, 725-30.

Chin, L., Pomerantz, J., *et al.* (1997) Cooperative effects of INK4a and ras in melanoma susceptibility in vivo, *Genes Dev. 11*, 2822-34.

Chipuk, J. E. & Green, D. R. (2003) p53's believe it or not: lessons on transcription-independent death, *J Clin Immunol. 23*, 355-61.

Choi, J., Shendrik, I., *et al.* (2000) Expression of senescence-associated beta-galactosidase in enlarged prostates from men with benign prostatic hyperplasia, *Urology. 56*, 160-6.

Chondrogianni, N., Stratford, F. L., Trougakos, I. P., Friguet, B., Rivett, A. J. & Gonos, E. S. (2003) Central role of the proteasome in senescence and survival of human fibroblasts: induction of a senescence-like phenotype upon its inhibition and resistance to stress upon its activation, *J Biol Chem. 278*, 28026-37.

Cimino-Reale, G., Pascale, E., Battiloro, E., Starace, G., Verna, R. & D'Ambrosio, E. (2001) The length of telomeric G-rich strand 3'-overhang measured by oligonucleotide ligation assay, *Nucleic Acids Res. 29*, E35.

Clarke, D. J. (2002) Proteolysis and the cell cycle, *Cell Cycle. 1*, 233-4.

Classon, M. & Dyson, N. (2001) p107 and p130: versatile proteins with interesting pockets, *Exp Cell Res. 264*, 135-47.

Classon, M. & Harlow, E. (2002) The retinoblastoma tumour suppressor in development and cancer, *Nat Rev Cancer. 2*, 910-7.

Claudio, P. P., De Luca, A., *et al.* (1996) Functional analysis of pRb2/p130 interaction with cyclins, *Cancer Res. 56*, 2003-8.

Cleveland, J. L. & Sherr, C. J. (2004) Antagonism of Myc functions by Arf, *Cancer Cell. 6*, 309-11.

Cobrinik, D. (1996) Regulatory interactions among E2Fs and cell cycle control proteins, *Curr Top Microbiol Immunol. 208*, 31-61.

Cobrinik, D., Dowdy, S. F., Hinds, P. W., Mittnacht, S. & Weinberg, R. A. (1992) The retinoblastoma protein and the regulation of cell cycling, *Trends Biochem Sci. 17*, 312-5.

Collado, M., Gil, J., *et al.* (2005) Tumour biology: senescence in premalignant tumours, *Nature. 436*, 642.

Condorelli, G. & Giordano, A. (1997) Synergistic role of E1A-binding proteins and tissue-specific transcription factors in differentiation, *J Cell Biochem. 67*, 423-31.

Condorelli, G. L., Testa, U., *et al.* (1995) Modulation of retinoblastoma gene in normal adult hematopoiesis: peak expression and functional role in advanced erythroid differentiation, *Proc Natl Acad Sci U S A. 92*, 4808-12.

Contente, A., Dittmer, A., Koch, M. C., Roth, J. & Dobbelstein, M. (2002) A polymorphic microsatellite that mediates induction of PIG3 by p53, *Nat Genet. 30*, 315-20.

Conzen, S. D. & Cole, C. N. (1995) The three transforming regions of SV40 T antigen are required for immortalization of primary mouse embryo fibroblasts, *Oncogene. 11*, 2295-302.

Cosset, F. L., Takeuchi, Y., Battini, J. L., Weiss, R. A. & Collins, M. K. (1995) High-titer packaging cells producing recombinant retroviruses resistant to human serum, *J Virol. 69*, 7430-6.

Counter, C. M. (1996) The roles of telomeres and telomerase in cell life span, *Mutat Res. 366*, 45-63.

Cox, L. S. (1997) Multiple pathways control cell growth and transformation: overlapping and independent activities of p53 and p21Cip1/WAF1/Sdi1, *J Pathol. 183*, 134-40.

Cristofalo, V. J., Allen, R. G., Pignolo, R. J., Martin, B. G. & Beck, J. C. (1998) Relationship between donor age and the replicative lifespan of human cells in culture: a reevaluation, *Proc Natl Acad Sci U S A. 95*, 10614-9.

Cristofalo, V. J., Doggett, D. L., Brooks-Frederich, K. M. & Phillips, P. D. (1989) Growth factors as probes of cell aging, *Exp Gerontol. 24*, 367-74.

Cristofalo, V. J., Volker, C., Francis, M. K. & Tresini, M. (1998) Age-dependent modifications of gene expression in human fibroblasts, *Crit Rev Eukaryot Gene Expr. 8*, 43-80.

Cunha, G. R. & Matrisian, L. M. (2002) It's not my fault, blame it on my microenvironment, *Differentiation. 70*, 469-72.

Cutler, R. G., Kelly, J., *et al.* (2004) Involvement of oxidative stress-induced abnormalities in ceramide and cholesterol metabolism in brain aging and Alzheimer's disease, *Proc Natl Acad Sci U S A. 101*, 2070-5.

Czauderna, F., Santel, A., *et al.* (2003) Inducible shRNA expression for application in a prostate cancer mouse model, *Nucleic Acids Res. 31*, e127.

d'Adda di Fagagna, F., Reaper, P. M., *et al.* (2003) A DNA damage checkpoint response in telomere-initiated senescence, *Nature. 426*, 194-8.

Dahiya, A., Gavin, M. R., Luo, R. X. & Dean, D. C. (2000) Role of the LXCXE binding site in Rb function, *Mol Cell Biol. 20*, 6799-805.

Dalal, S., Gao, Q., Androphy, E. J. & Band, V. (1996) Mutational analysis of human papillomavirus type 16 E6 demonstrates that p53 degradation is necessary for immortalization of mammary epithelial cells, *J Virol. 70*, 683-8.

Dannenberg, J. H., van Rossum, A., Schuijff, L. & te Riele, H. (2000) Ablation of the retinoblastoma gene family deregulates G(1) control causing immortalization and increased cell turnover under growth-restricting conditions, *Genes Dev. 14*, 3051-64.

Davies, R., Hicks, R., Crook, T., Morris, J. & Vousden, K. (1993) Human papillomavirus type 16 E7 associates with a histone H1 kinase and with p107 through sequences necessary for transformation, *J Virol. 67*, 2521-8.

Davis, T., Singhrao, S. K., *et al.* (2003) Telomere-based proliferative lifespan barriers in Werner-syndrome fibroblasts involve both p53-dependent and p53-independent mechanisms, *J Cell Sci. 116*, 1349-57.

de Bruin, A., Maiti, B., Jakoi, L., Timmers, C., Buerki, R. & Leone, G. (2003) Identification and characterization of E2F7, a novel mammalian E2F family member capable of blocking cellular proliferation, *J Biol Chem. 278*, 42041-9.

de Bruin, A., Wu, L., *et al.* (2003) Rb function in extraembryonic lineages suppresses apoptosis in the CNS of Rb-deficient mice, *Proc Natl Acad Sci U S A. 100*, 6546-51.

de Lange, T. (2002) Protection of mammalian telomeres, *Oncogene. 21*, 532-40.

de Lange, T. & Petrini, J. H. (2000) A new connection at human telomeres: association of the Mre11 complex with TRF2, *Cold Spring Harb Symp Quant Biol. 65*, 265-73.

de Magalhaes, J. P., Chainiaux, F., Remacle, J. & Toussaint, O. (2002) Stress-induced premature senescence in BJ and hTERT-BJ1 human foreskin fibroblasts, *FEBS Lett. 523*, 157-62.

de Magalhaes, J. P., Migeot, V., Mainfroid, V., de Longueville, F., Remacle, J. & Toussaint, O. (2004) No increase in senescence-associated beta-galactosidase activity in Werner syndrome fibroblasts after exposure to H2O2, *Ann N Y Acad Sci. 1019*, 375-8.

De Sandre-Giovannoli, A., Bernard, R., *et al.* (2003) Lamin a truncation in Hutchinson-Gilford progeria, *Science. 300*, 2055.

de Stanchina, E., McCurrach, M. E., *et al.* (1998) E1A signaling to p53 involves the p19(ARF) tumor suppressor, *Genes Dev. 12*, 2434-42.

de Stanchina, E., Querido, E., Narita, M., Davuluri, R. V., Pandolfi, P. P., Ferbeyre, G. & Lowe, S. W. (2004) PML is a direct p53 target that modulates p53 effector functions, *Mol Cell. 13*, 523-35.

Debbas, M. & White, E. (1993) Wild-type p53 mediates apoptosis by E1A, which is inhibited by E1B, *Genes Dev. 7*, 546-54.

DeBusk, F. L. (1972) The Hutchinson-Gilford progeria syndrome. Report of 4 cases and review of the literature, *J Pediatr. 80*, 697-724.

DeCaprio, J. A., Ludlow, J. W., *et al.* (1988) SV40 large tumor antigen forms a specific complex with the product of the retinoblastoma susceptibility gene, *Cell. 54*, 275-83.

DeCaprio, J. A., Ludlow, J. W., *et al.* (1989) The product of the retinoblastoma susceptibility gene has properties of a cell cycle regulatory element, *Cell. 58*, 1085-95.

DeGregori, J. (2002) The genetics of the E2F family of transcription factors: shared functions and unique roles, *Biochim Biophys Acta. 1602*, 131-50.

DeGregori, J., Leone, G., Miron, A., Jakoi, L. & Nevins, J. R. (1997) Distinct roles for E2F proteins in cell growth control and apoptosis, *Proc Natl Acad Sci U S A. 94*, 7245-50.

Delavaine, L. & La Thangue, N. B. (1999) Control of E2F activity by p21Waf1/Cip1, *Oncogene. 18*, 5381-92.

Deng, C., Zhang, P., Harper, J. W., Elledge, S. J. & Leder, P. (1995) Mice lacking p21CIP1/WAF1 undergo normal development, but are defective in G1 checkpoint control, *Cell. 82*, 675-84.

Deppert, W., Haug, M. & Steinmayer, T. (1987) Modulation of p53 protein expression during cellular transformation with simian virus 40, *Mol Cell Biol. 7*, 4453-63.

Di Leonardo, A., Linke, S. P., Clarkin, K. & Wahl, G. M. (1994) DNA damage triggers a prolonged p53-dependent G1 arrest and long-term induction of Cip1 in normal human fibroblasts, *Genes Dev. 8*, 2540-51.

Dimova, D. K. & Dyson, N. J. (2005) The E2F transcriptional network: old acquaintances with new faces, *Oncogene. 24*, 2810-26.

Dimova, D. K., Stevaux, O., Frolov, M. V. & Dyson, N. J. (2003) Cell cycle-dependent and cell cycle-independent control of transcription by the Drosophila E2F/RB pathway, *Genes Dev. 17*, 2308-20.

Dimri, G. P., Itahana, K., Acosta, M. & Campisi, J. (2000) Regulation of a senescence checkpoint response by the E2F1 transcription factor and p14(ARF) tumor suppressor, *Mol Cell Biol. 20*, 273-85.

Dimri, G. P., Lee, X., *et al.* (1995) A biomarker that identifies senescent human cells in culture and in aging skin in vivo, *Proc Natl Acad Sci U S A. 92*, 9363-7.

Dimri, G. P., Testori, A., Acosta, M. & Campisi, J. (1996) Replicative senescence, aging and growth-regulatory transcription factors, *Biol Signals. 5*, 154-62.

DiPaolo, B. R., Pignolo, R. J. & Cristofalo, V. J. (1995) Identification of proteins differentially expressed in quiescent and proliferatively senescent fibroblast cultures, *Exp Cell Res. 1*, 178-85.

Dirac, A. M. & Bernards, R. (2003) Reversal of senescence in mouse fibroblasts through lentiviral suppression of p53, *J Biol Chem. 278*, 11731-4.

Donehower, L. A., Harvey, M., Slagle, B. L., McArthur, M. J., Montgomery, C. A., Jr., Butel, J. S. & Bradley, A. (1992) Mice deficient for p53 are developmentally normal but susceptible to spontaneous tumours, *Nature. 356*, 215-21.

Dorsman, J. C., Hagmeyer, B. M., Veenstra, J., Elfferich, P., Nabben, N., Zantema, A. & van der Eb, A. J. (1995) The N-terminal region of the adenovirus type 5 E1A proteins can repress expression of cellular genes via two distinct but overlapping domains, *J Virol. 69*, 2962-7.

Downward, J. (2004) Use of RNA interference libraries to investigate oncogenic signalling in mammalian cells, *Oncogene. 23*, 8376-83.

Draetta, G. F. (1994) Mammalian G1 cyclins, *Curr Opin Cell Biol. 6,* 842-6.

Drayton, S. & Peters, G. (2002) Immortalisation and transformation revisited, *Curr Opin Genet Dev. 12*, 98-104.

Duensing, S., Duensing, A., Crum, C. P. & Munger, K. (2001) Human papillomavirus type 16 E7 oncoprotein-induced abnormal centrosome synthesis is an early event in the evolving malignant phenotype, *Cancer Res. 61*, 2356-60.

Duensing, S. & Munger, K. (2002) Human papillomaviruses and centrosome duplication errors: modeling the origins of genomic instability, *Oncogene. 21*, 6241-8.

Duensing, S. & Munger, K. (2003) Human papillomavirus type 16 E7 oncoprotein can induce abnormal centrosome duplication through a mechanism independent of inactivation of retinoblastoma protein family members, *J Virol. 77*, 12331-5.

Dulic, V., Drullinger, L. F., Lees, E., Reed, S. I. & Stein, G. H. (1993) Altered regulation of G1 cyclins in senescent human diploid fibroblasts: accumulation of inactive cyclin E-Cdk2 and cyclin D1-Cdk2 complexes, *Proc Natl Acad Sci U S A. 90*, 11034-8.

Dulic, V., Lees, E. & Reed, S. I. (1992) Association of human cyclin E with a periodic G1-S phase protein kinase, *Science. 257*, 1958-61.

Dumaz, N. & Meek, D. W. (1999) Serine15 phosphorylation stimulates p53 transactivation but does not directly influence interaction with HDM2, *Embo J. 18*, 7002-10.

Dumont, P., Burton, M., *et al.* (2000) Induction of replicative senescence biomarkers by sublethal oxidative stresses in normal human fibroblast, *Free Radic Biol Med. 28*, 361-73.

Dunaief, J. L., Strober, B. E., *et al.* (1994) The retinoblastoma protein and BRG1 form a complex and cooperate to induce cell cycle arrest, *Cell. 79*, 119-30.

Duncan, E. L. & Reddel, R. R. (1997) Genetic changes associated with immortalization. A review, *Biochemistry (Mosc). 62*, 1263-74.

Dunham, M. A., Neumann, A. A., Fasching, C. L. & Reddel, R. R. (2000) Telomere maintenance by recombination in human cells, *Nat Genet. 26*, 447-50.

Dyson, N. (1998) The regulation of E2F by pRB-family proteins, *Genes Dev. 12*, 2245-62.

Dyson, N., Buchkovich, K., Whyte, P. & Harlow, E. (1989) The cellular 107K protein that binds to adenovirus E1A also associates with the large T antigens of SV40 and JC virus, *Cell. 58*, 249-55.

Dyson, N., Guida, P., Munger, K. & Harlow, E. (1992) Homologous sequences in adenovirus E1A and human papillomavirus E7 proteins mediate interaction with the same set of cellular proteins, *J Virol. 66*, 6893-902.

Eckner, R., Ludlow, J. W., *et al.* (1996) Association of p300 and CBP with simian virus 40 large T antigen, *Mol Cell Biol. 16*, 3454-64.

Egan, C., Bayley, S. T. & Branton, P. E. (1989) Binding of the Rb1 protein to E1A products is required for adenovirus transformation, *Oncogene. 4*, 383-8.

Elbashir, S. M., Harborth, J., Weber, K. & Tuschl, T. (2002) Analysis of gene function in somatic mammalian cells using small interfering RNAs, *Methods. 26*, 199-213.

Elbashir, S. M., Lendeckel, W. & Tuschl, T. (2001) RNA interference is mediated by 21- and 22-nucleotide RNAs, *Genes Dev. 15*, 188-200.

el-Deiry, W. S., Harper, J. W., *et al.* (1994) WAF1/CIP1 is induced in p53-mediated G1 arrest and apoptosis, *Cancer Res. 54*, 1169-74.

el-Deiry, W. S., Kern, S. E., Pietenpol, J. A., Kinzler, K. W. & Vogelstein, B. (1992) Definition of a consensus binding site for p53, *Nat Genet. 1*, 45-9.

el-Deiry, W. S., Tokino, T., *et al.* (1993) WAF1, a potential mediator of p53 tumor suppression, *Cell. 75*, 817-25.

Elledge, S. J. (1996) Cell cycle checkpoints: preventing an identity crisis, *Science. 274*, 1664-72.

Engstrom, Y., Eriksson, S., Jildevik, I., Skog, S., Thelander, L. & Tribukait, B. (1985) Cell cycle-dependent expression of mammalian ribonucleotide reductase. Differential regulation of the two subunits, *J Biol Chem. 260*, 9114-6.

Enoch, T. & Norbury, C. (1995) Cellular responses to DNA damage: cell-cycle checkpoints, apoptosis and the roles of p53 and ATM, *Trends Biochem Sci. 20*, 426-30.

Eriksson, M., Brown, W. T., *et al.* (2003) Recurrent de novo point mutations in lamin A cause Hutchinson-Gilford progeria syndrome, *Nature. 423*, 293-8.

Esteller, M., Gonzalez, S., *et al.* (2001) K-ras and p16 aberrations confer poor prognosis in human colorectal cancer, *J Clin Oncol. 19*, 299-304.

Esteller, M., Tortola, S., Toyota, M., Capella, G., Peinado, M. A., Baylin, S. B. & Herman, J. G. (2000) Hypermethylation-associated inactivation of p14(ARF) is independent of p16(INK4a) methylation and p53 mutational status, *Cancer Res. 60*, 129-33.

Evans, R. J., Wyllie, F. S., Wynford-Thomas, D., Kipling, D. & Jones, C. J. (2003) A P53-dependent, telomere-independent proliferative life span barrier in human astrocytes consistent with the molecular genetics of glioma development, *Cancer Res. 63*, 4854-61.

Evans, T., Rosenthal, E. T., Youngblom, J., Distel, D. & Hunt, T. (1983) Cyclin: a protein specified by maternal mRNA in sea urchin eggs that is destroyed at each cleavage division, *Cell. 33*, 389-96.

Ewen, M. E., Ludlow, J. W., *et al.* (1989) An N-terminal transformation-governing sequence of SV40 large T antigen contributes to the binding of both p110Rb and a second cellular protein, p120, *Cell. 58*, 257-67.

Farah, M. H., Olson, J. M., Sucic, H. B., Hume, R. I., Tapscott, S. J. & Turner, D. L. (2000) Generation of neurons by transient expression of neural bHLH proteins in mammalian cells, *Development. 127*, 693-702.

Felzien, L. K., Farrell, S., Betts, J. C., Mosavin, R. & Nabel, G. J. (1999) Specificity of cyclin E-Cdk2, TFIIB, and E1A interactions with a common domain of the p300 coactivator, *Mol Cell Biol. 19*, 4241-6.

Ferbeyre, G., de Stanchina, E., Querido, E., Baptiste, N., Prives, C. & Lowe, S. W. (2000) PML is induced by oncogenic ras and promotes premature senescence, *Genes Dev. 14*, 2015-27.

Filippova, M., Song, H., Connolly, J. L., Dermody, T. S. & Duerksen-Hughes, P. J. (2002) The human papillomavirus 16 E6 protein binds to tumor necrosis factor (TNF) R1 and protects cells from TNF-induced apoptosis, *J Biol Chem. 277*, 21730-9.

Fire, A., Xu, S., Montgomery, M. K., Kostas, S. A., Driver, S. E. & Mello, C. C. (1998) Potent and specific genetic interference by double-stranded RNA in Caenorhabditis elegans, *Nature. 391*, 806-11.

Flemington, E. K., Speck, S. H. & Kaelin, W. G., Jr. (1993) E2F-1-mediated transactivation is inhibited by complex formation with the retinoblastoma susceptibility gene product, *Proc Natl Acad Sci U S A. 90*, 6914-8.

Flinterman, M., Guelen, L., *et al.* (2005) E1A activates transcription of p73 and Noxa to induce apoptosis, *J Biol Chem. 280*, 5945-59.

Flores, E. R., Tsai, K. Y., Crowley, D., Sengupta, S., Yang, A., McKeon, F. & Jacks, T. (2002) p63 and p73 are required for p53-dependent apoptosis in response to DNA damage, *Nature. 416*, 560-4.

Flores-Rozas, H., Kelman, Z., *et al.* (1994) Cdk-interacting protein 1 directly binds with proliferating cell nuclear antigen and inhibits DNA replication catalyzed by the DNA polymerase delta holoenzyme, *Proc Natl Acad Sci U S A. 91*, 8655-9.

Folkers, G. E. & van der Saag, P. T. (1995) Adenovirus E1A functions as a cofactor for retinoic acid receptor beta (RAR beta) through direct interaction with RAR beta, *Mol Cell Biol. 15*, 5868-78.

Foster, S. A., Demers, G. W., Etscheid, B. G. & Galloway, D. A. (1994) The ability of human papillomavirus E6 proteins to target p53 for degradation in vivo correlates with their ability to abrogate actinomycin D-induced growth arrest, *J Virol. 68*, 5698-705.

Frame, S. & Balmain, A. (2000) Integration of positive and negative growth signals during ras pathway activation in vivo, *Curr Opin Genet Dev. 10*, 106-13.

Franklin, D. S., Godfrey, V. L., O'Brien, D. A., Deng, C. & Xiong, Y. (2000) Functional collaboration between different cyclin-dependent kinase inhibitors suppresses tumor growth with distinct tissue specificity, *Mol Cell Biol. 20*, 6147-58.

Freedman, D. A. & Folkman, J. (2005) CDK2 translational down-regulation during endothelial senescence, *Exp Cell Res. 307*, 118-30.

Freeman, D. J., Li, A. G., *et al.* (2003) PTEN tumor suppressor regulates p53 protein levels and activity through phosphatase-dependent and -independent mechanisms, *Cancer Cell. 3*, 117-30.

Frisch, S. M. (1994) E1a induces the expression of epithelial characteristics, *J Cell Biol. 127*, 1085-96.

Frolov, M. V. & Dyson, N. J. (2004) Molecular mechanisms of E2F-dependent activation and pRB-mediated repression, *J Cell Sci. 117*, 2173-81.

Fuchs, M., Gerber, J., *et al.* (2001) The p400 complex is an essential E1A transformation target, *Cell. 106*, 297-307.

Fujitani, Y., Kajimoto, Y., *et al.* (1999) Identification of a portable repression domain and an E1A-responsive activation domain in Pax4: a possible role of Pax4 as a transcriptional repressor in the pancreas, *Mol Cell Biol. 19*, 8281-91.

Gage, J. R., Meyers, C. & Wettstein, F. O. (1990) The E7 proteins of the nononcogenic human papillomavirus type 6b (HPV-6b) and of the oncogenic HPV-16 differ in retinoblastoma protein binding and other properties, *J Virol. 64*, 723-30.

Garcia-Cao, I., Garcia-Cao, M., *et al.* (2002) "Super p53" mice exhibit enhanced DNA damage response, are tumor resistant and age normally, *Embo J. 21*, 6225-35.

Gartel, A. L. & Tyner, A. L. (1998) The growth-regulatory role of p21 (WAF1/CIP1), *Prog Mol Subcell Biol. 20*, 43-71.

Gary, R. K. & Kindell, S. M. (2005) Quantitative assay of senescence-associated beta-galactosidase activity in mammalian cell extracts, *Anal Biochem. 343*, 329-34.

Gaubatz, S., Lindeman, G. J., Ishida, S., Jakoi, L., Nevins, J. R., Livingston, D. M. & Rempel, R. E. (2000) E2F4 and E2F5 play an essential role in pocket protein-mediated G1 control, *Mol Cell. 6*, 729-35.

Gaubatz, S., Wood, J. G. & Livingston, D. M. (1998) Unusual proliferation arrest and transcriptional control properties of a newly discovered E2F family member, E2F-6, *Proc Natl Acad Sci U S A. 95*, 9190-5.

Geisberg, J. V., Chen, J. L. & Ricciardi, R. P. (1995) Subregions of the adenovirus E1A transactivation domain target multiple components of the TFIID complex, *Mol Cell Biol. 15*, 6283-90.

Gershon, H. & Gershon, D. (2000) Paradigms in aging research: a critical review and assessment, *Mech Ageing Dev. 117*, 21-8.

Gewin, L. & Galloway, D. A. (2001) E box-dependent activation of telomerase by human papillomavirus type 16 E6 does not require induction of c-myc, *J Virol. 75*, 7198-201.

Gil, J., Bernard, D., Martinez, D. & Beach, D. (2004) Polycomb CBX7 has a unifying role in cellular lifespan, *Nat Cell Biol. 6*, 67-72.

Gilinger, G. & Alwine, J. C. (1993) Transcriptional activation by simian virus 40 large T antigen: requirements for simple promoter structures containing either TATA or initiator elements with variable upstream factor binding sites, *J Virol. 67*, 6682-8.

Gillison, M. L., Koch, W. M., *et al.* (2000) Evidence for a causal association between human papillomavirus and a subset of head and neck cancers, *J Natl Cancer Inst. 92*, 709-20.

Ginsberg, D., Mechta, F., Yaniv, M. & Oren, M. (1991) Wild-type p53 can down-modulate the activity of various promoters, *Proc Natl Acad Sci U S A. 88*, 9979-83.

Gire, V., Roux, P., Wynford-Thomas, D., Brondello, J. M. & Dulic, V. (2004) DNA damage checkpoint kinase Chk2 triggers replicative senescence, *Embo J. 23*, 2554-63.

Gire, V. & Wynford-Thomas, D. (1998) Reinitiation of DNA synthesis and cell division in senescent human fibroblasts by microinjection of anti-p53 antibodies, *Mol Cell Biol. 18*, 1611-21.

Gisselsson, D. (2003) Chromosome instability in cancer: how, when, and why?, *Adv Cancer Res. 87*, 1-29.

Goi, K., Takagi, M., *et al.* (1997) DNA damage-associated dysregulation of the cell cycle and apoptosis control in cells with germ-line p53 mutation, *Cancer Res. 57*, 1895-902.

Goldman, R. D., Gruenbaum, Y., Moir, R. D., Shumaker, D. K. & Spann, T. P. (2002) Nuclear lamins: building blocks of nuclear architecture, *Genes Dev. 16*, 533-47.

Goldstein, S., Moerman, E. J. & Baxter, R. C. (1993) Accumulation of insulin-like growth factor binding protein-3 in conditioned medium of human fibroblasts increases with chronologic age of donor and senescence in vitro, *J Cell Physiol. 156*, 294-302.

Goodman, R. H. & Smolik, S. (2000) CBP/p300 in cell growth, transformation, and development, *Genes Dev. 14*, 1553-77.

Gottschling, D. E., Aparicio, O. M., Billington, B. L. & Zakian, V. A. (1990) Position effect at S. cerevisiae telomeres: reversible repression of Pol II transcription, *Cell. 63*, 751-62.

Gray, J. W. & Collins, C. (2000) Genome changes and gene expression in human solid tumors, *Carcinogenesis. 21*, 443-52.

Gray, M. D., Wang, L., Youssoufian, H., Martin, G. M. & Oshima, J. (1998) Werner helicase is localized to transcriptionally active nucleoli of cycling cells, *Exp Cell Res. 242*, 487-94.

Greenfield, I., Nickerson, J., Penman, S. & Stanley, M. (1991) Human papillomavirus 16 E7 protein is associated with the nuclear matrix, *Proc Natl Acad Sci U S A. 88*, 11217-21.

Gregory, S. L., Kortschak, R. D., Kalionis, B. & Saint, R. (1996) Characterization of the dead ringer gene identifies a novel, highly conserved family of sequence-specific DNA-binding proteins, *Mol Cell Biol. 16*, 792-9.

Griffith, J. D., Comeau, L., Rosenfield, S., Stansel, R. M., Bianchi, A., Moss, H. & de Lange, T. (1999) Mammalian telomeres end in a large duplex loop, *Cell. 97*, 503-14.

Griffith, J. D., Lee, S. & Wang, Y. H. (1997) Visualizing nucleic acids and their complexes using electron microscopy, *Curr Opin Struct Biol. 7*, 362-6.

Grimshaw, C. E. & Mathur, E. J. (1989) Immunoquantitation of aldose reductase in human tissues, *Anal Biochem. 176*, 66-71.

Grossman, S. R., Mora, R. & Laimins, L. A. (1989) Intracellular localization and DNA-binding properties of human papillomavirus type 18 E6 protein expressed with a baculovirus vector, *J Virol. 63*, 366-74.

Grossman, S. R., Perez, M., *et al.* (1998) p300/MDM2 complexes participate in MDM2-mediated p53 degradation, *Mol Cell. 2*, 405-15.

Gruda, M. C., Zabolotny, J. M., Xiao, J. H., Davidson, I. & Alwine, J. C. (1993) Transcriptional activation by simian virus 40 large T antigen: interactions with multiple components of the transcription complex, *Mol Cell Biol. 13*, 961-9.

Gruis, N. A., Sandkuijl, L. A., van der Velden, P. A., Bergman, W. & Frants, R. R. (1995) CDKN2 explains part of the clinical phenotype in Dutch familial atypical multiple-mole melanoma (FAMMM) syndrome families, *Melanoma Res. 5*, 169-77.

Gu, W., Schneider, J. W., Condorelli, G., Kaushal, S., Mahdavi, V. & Nadal-Ginard, B. (1993) Interaction of myogenic factors and the retinoblastoma protein mediates muscle cell commitment and differentiation, *Cell. 72*, 309-24.

Guccione, E., Massimi, P., Bernat, A. & Banks, L. (2002) Comparative analysis of the intracellular location of the high- and low-risk human papillomavirus oncoproteins, *Virology. 293*, 20-5.

Guerra, C., Mijimolle, N., *et al.* (2003) Tumor induction by an endogenous K-ras oncogene is highly dependent on cellular context, *Cancer Cell. 4*, 111-20.

Haas-Kogan, D. A., Kogan, S. C., Levi, D., Dazin, P., T'Ang, A., Fung, Y. K. & Israel, M. A. (1995) Inhibition of apoptosis by the retinoblastoma gene product, *Embo J. 14*, 461-72.

Hahn, W. C., Dessain, S. K., *et al.* (2002) Enumeration of the simian virus 40 early region elements necessary for human cell transformation, *Mol Cell Biol. 22*, 2111-23.

Hahn, W. C. & Weinberg, R. A. (2002) Modelling the molecular circuitry of cancer, *Nat Rev Cancer. 2*, 331-41.

Hammond, S. M., Boettcher, S., Caudy, A. A., Kobayashi, R. & Hannon, G. J. (2001) Argonaute2, a link between genetic and biochemical analyses of RNAi, *Science. 293*, 1146-50.

Han, J., Sabbatini, P., Perez, D., Rao, L., Modha, D. & White, E. (1996) The E1B 19K protein blocks apoptosis by interacting with and inhibiting the p53-inducible and death-promoting Bax protein, *Genes Dev. 10*, 461-77.

Hanahan, D. & Weinberg, R. A. (2000) The hallmarks of cancer, *Cell. 100*, 57-70.

Hannon, G. J., Demetrick, D. & Beach, D. (1993) Isolation of the Rb-related p130 through its interaction with CDK2 and cyclins, *Genes Dev. 7*, 2378-91.

Hansen, U., Tenen, D. G., Livingston, D. M. & Sharp, P. A. (1981) T antigen repression of SV40 early transcription from two promoters, *Cell. 27*, 603-13.

Hara, E., Smith, R., Parry, D., Tahara, H., Stone, S. & Peters, G. (1996) Regulation of p16CDKN2 expression and its implications for cell immortalization and senescence, *Mol Cell Biol. 16*, 859-67.

Hardy, K., Mansfield, L., *et al.* (2005) Transcriptional networks and cellular senescence in human mammary fibroblasts, *Mol Biol Cell. 16*, 943-53.

Harley, C. B. (1991) Telomere loss: mitotic clock or genetic time bomb?, *Mutat Res. 256*, 271-82.

Harley, C. B., Futcher, A. B. & Greider, C. W. (1990) Telomeres shorten during ageing of human fibroblasts, *Nature. 345*, 458-60.

Harlow, E., Whyte, P., Franza, B. R., Jr. & Schley, C. (1986) Association of adenovirus early-region 1A proteins with cellular polypeptides, *Mol Cell Biol. 6*, 1579-89.

Harper, J. W., Adami, G. R., Wei, N., Keyomarsi, K. & Elledge, S. J. (1993) The p21 Cdk-interacting protein Cip1 is a potent inhibitor of G1 cyclin-dependent kinases, *Cell. 75*, 805-16.

Harris, S. L. & Levine, A. J. (2005) The p53 pathway: positive and negative feedback loops, *Oncogene. 24*, 2899-908.

Harrison, D. E. & Astle, C. M. (1982) Loss of stem cell repopulating ability upon transplantation. Effects of donor age, cell number, and transplantation procedure, *J Exp Med. 156*, 1767-79.

Hartwell, L. (2004) Genetics. Robust interactions, *Science. 303*, 774-5.

Hartwell, L. H. & Kastan, M. B. (1994) Cell cycle control and cancer, *Science. 266*, 1821-8.

Hartwell, L. H. & Weinert, T. A. (1989) Checkpoints: controls that ensure the order of cell cycle events, *Science. 246*, 629-34.

Harvat, B. L., Wang, A., Seth, P. & Jetten, A. M. (1998) Up-regulation of p27Kipl, p21WAFl/Cipl and p16Ink4a is associated with, but not sufficient for, induction of squamous differentiation, *J Cell Sci. 111*, 1185-96.

Harvey, M., McArthur, M. J., Montgomery, C. A., Jr., Butel, J. S., Bradley, A. & Donehower, L. A. (1993) Spontaneous and carcinogen-induced tumorigenesis in p53-deficient mice, *Nat Genet. 5*, 225-9.

Hateboer, G., Gennissen, A., Ramos, Y. F., Kerkhoven, R. M., Sonntag-Buck, V., Stunnenberg, H. G. & Bernards, R. (1995) BS69, a novel adenovirus E1A-associated protein that inhibits E1A transactivation, *Embo J. 14*, 3159-69.

Haupt, Y., Maya, R., Kazaz, A. & Oren, M. (1997) Mdm2 promotes the rapid degradation of p53, *Nature. 387*, 296-9.

Hayflick, L. (1974) The longevity of cultured human cells, *J Am Geriatr Soc. 22*, 1-12.

Hayflick, L. & Moorhead, P. S. (1961) The serial cultivation of human diploid cell strains, *Exp Cell Res. 25*, 585-621.

He, L., Thomson, J. M., *et al.* (2005) A microRNA polycistron as a potential human oncogene, *Nature. 435*, 828-33.

He, S., Cook, B. L., *et al.* (2000) E2F is required to prevent inappropriate S-phase entry of mammalian cells, *Mol Cell Biol. 20*, 363-71.

Helin, K., Harlow, E. & Fattaey, A. (1993) Inhibition of E2F-1 transactivation by direct binding of the retinoblastoma protein, *Mol Cell Biol. 13*, 6501-8.

Helt, A. M., Funk, J. O. & Galloway, D. A. (2002) Inactivation of both the retinoblastoma tumor suppressor and p21 by the human papillomavirus type 16 E7 oncoprotein is necessary to inhibit cell cycle arrest in human epithelial cells, *J Virol. 76*, 10559-68.

Hemann, M. T., Fridman, J. S., *et al.* (2003) An epi-allelic series of p53 hypomorphs created by stable RNAi produces distinct tumor phenotypes in vivo, *Nat Genet. 33*, 396-400.

Hemmati, H. D., Nakano, I., Lazareff, J. A., Masterman-Smith, M., Geschwind, D. H., Bronner-Fraser, M. & Kornblum, H. I. (2003) Cancerous stem cells can arise from pediatric brain tumors, *Proc Natl Acad Sci U S A. 100*, 15178-83.

Henning, W., Rohaly, G., Kolzau, T., Knippschild, U., Maacke, H. & Deppert, W. (1997) MDM2 is a target of simian virus 40 in cellular transformation and during lytic infection, *J Virol. 71*, 7609-18.

Herbig, U., Jobling, W. A., Chen, B. P., Chen, D. J. & Sedivy, J. M. (2004) Telomere shortening triggers senescence of human cells through a pathway involving ATM, p53, and p21(CIP1), but not p16(INK4a), *Mol Cell. 14*, 501-13.

Hermeking, H., Lengauer, C., *et al.* (1997) 14-3-3 sigma is a p53-regulated inhibitor of G2/M progression, *Mol Cell. 1*, 3-11.

Herrera, R. E., Sah, V. P., Williams, B. O., Makela, T. P., Weinberg, R. A. & Jacks, T. (1996) Altered cell cycle kinetics, gene expression, and G1 restriction point regulation in Rb-deficient fibroblasts, *Mol Cell Biol. 16*, 2402-7.

Herrscher, R. F., Kaplan, M. H., Lelsz, D. L., Das, C., Scheuermann, R. & Tucker, P. W. (1995) The immunoglobulin heavy-chain matrix-associating regions are bound by Bright: a B cell-specific trans-activator that describes a new DNA-binding protein family, *Genes Dev. 9*, 3067-82.

Hiebert, S. W. (1993) Regions of the retinoblastoma gene product required for its interaction with the E2F transcription factor are necessary for E2 promoter repression and pRb-mediated growth suppression, *Mol Cell Biol. 13*, 3384-91.

Hilleman, M. R. (1998) Discovery of simian virus 40 (SV40) and its relationship to poliomyelitis virus vaccines, *Dev Biol Stand. 94*, 183-90.

Hirakawa, T. & Ruley, H. E. (1988) Rescue of cells from ras oncogene-induced growth arrest by a second, complementing, oncogene, *Proc Natl Acad Sci U S A. 85*, 1519-23.

Hirao, A., Kong, Y. Y., *et al.* (2000) DNA damage-induced activation of p53 by the checkpoint kinase Chk2, *Science. 287*, 1824-7.

Hoh, J., Jin, S., Parrado, T., Edington, J., Levine, A. J. & Ott, J. (2002) The p53MH algorithm and its application in detecting p53-responsive genes, *Proc Natl Acad Sci U S A. 99*, 8467-72.

Holland, E. A., Beaton, S. C., *et al.* (1995) Analysis of the p16 gene, CDKN2, in 17 Australian melanoma kindreds, *Oncogene. 11*, 2289-94.

Hollstein, M., Rice, K., *et al.* (1994) Database of p53 gene somatic mutations in human tumors and cell lines, *Nucleic Acids Res. 22*, 3551-5.

Honda, S., Hjelmeland, L. M. & Handa, J. T. (2001) The use of hyperoxia to induce chronic mild oxidative stress in RPE cells in vitro, *Mol Vis. 7*, 63-70.

Horikoshi, N., Usheva, A., Chen, J., Levine, A. J., Weinmann, R. & Shenk, T. (1995) Two domains of p53 interact with the TATA-binding protein, and the adenovirus 13S E1A protein disrupts the association, relieving p53-mediated transcriptional repression, *Mol Cell Biol. 15*, 227-34.

Hsieh, J. K., Yap, D., *et al.* (2002) Novel function of the cyclin A binding site of E2F in regulating p53-induced apoptosis in response to DNA damage, *Mol Cell Biol. 22*, 78-93.

Hsu, H. L., Gilley, D., Blackburn, E. H. & Chen, D. J. (1999) Ku is associated with the telomere in mammals, *Proc Natl Acad Sci U S A. 96*, 12454-8.

Hsu, H. L., Gilley, D., *et al.* (2000) Ku acts in a unique way at the mammalian telomere to prevent end joining, *Genes Dev. 14*, 2807-12.

Hsu, J. Y., Reimann, J. D., Sorensen, C. S., Lukas, J. & Jackson, P. K. (2002) E2F-dependent accumulation of hEmi1 regulates S phase entry by inhibiting APC(Cdh1), *Nat Cell Biol. 4*, 358-66.

Hsu, M. Y., Meier, F. & Herlyn, M. (2002) Melanoma development and progression: a conspiracy between tumor and host, *Differentiation. 70*, 522-36.

Hu, Q. J., Dyson, N. & Harlow, E. (1990) The regions of the retinoblastoma protein needed for binding to adenovirus E1A or SV40 large T antigen are common sites for mutations, *Embo J. 9*, 1147-55.

Huang, Q., Lau, S. S. & Monks, T. J. (1999) Induction of gadd153 mRNA by nutrient deprivation is overcome by glutamine, *Biochem J. 341*, 225-31.

Huang, S., Li, B., Gray, M. D., Oshima, J., Mian, I. S. & Campisi, J. (1998) The premature ageing syndrome protein, WRN, is a 3'-->5' exonuclease, *Nat Genet. 20*, 114-6.

Huang, S., Wang, N. P., Tseng, B. Y., Lee, W. H. & Lee, E. H. (1990) Two distinct and frequently mutated regions of retinoblastoma protein are required for binding to SV40 T antigen, *Embo J. 9*, 1815-22.

Huang, Z. Y., Wu, Y., Hedrick, N. & Gutmann, D. H. (2003) T-cadherin-mediated cell growth regulation involves G2 phase arrest and requires p21(CIP1/WAF1) expression, *Mol Cell Biol. 23*, 566-78.

Huggins, J. W., Chesnut, R. W., Durham, N. N. & Carraway, K. (1976) Molecular changes in cell surface membranes resulting from trypsinization of sarcoma 180 tumor cells, *Biochim Biophys Acta. 426*, 630-7.

Huh, K. W., DeMasi, J., Ogawa, H., Nakatani, Y., Howley, P. M. & Munger, K. (2005) Association of the human papillomavirus type 16 E7 oncoprotein with the 600-kDa retinoblastoma protein-associated factor, p600, *Proc Natl Acad Sci U S A. 102*, 11492-7.

Huibregtse, J. M., Scheffner, M. & Howley, P. M. (1991) A cellular protein mediates association of p53 with the E6 oncoprotein of human papillomavirus types 16 or 18, *Embo J. 10*, 4129-35.

Hurford, R. K., Jr., Cobrinik, D., Lee, M. H. & Dyson, N. (1997) pRB and p107/p130 are required for the regulated expression of different sets of E2F responsive genes, *Genes Dev. 11*, 1447-63.

Hussussian, C. J., Struewing, J. P., *et al.* (1994) Germline p16 mutations in familial melanoma, *Nat Genet. 8*, 15-21.

Ikeyama, S., Wang, X. T., *et al.* (2003) Expression of the pro-apoptotic gene gadd153/chop is elevated in liver with aging and sensitizes cells to oxidant injury, *J Biol Chem. 278*, 16726-31.

Ikram, Z., Norton, T. & Jat, P. S. (1994) The biological clock that measures the mitotic life-span of mouse embryo fibroblasts continues to function in the presence of simian virus 40 large tumor antigen, *Proc Natl Acad Sci U S A. 91*, 6448-52.

Inoue, K., Wen, R., Rehg, J. E., Adachi, M., Cleveland, J. L., Roussel, M. F. & Sherr, C. J. (2000) Disruption of the ARF transcriptional activator DMP1 facilitates cell immortalization, Ras transformation, and tumorigenesis, *Genes Dev. 14*, 1797-809.

Inoue, K., Zindy, F., Randle, D. H., Rehg, J. E. & Sherr, C. J. (2001) Dmp1 is haplo-insufficient for tumor suppression and modifies the frequencies of Arf and p53 mutations in Myc-induced lymphomas, *Genes Dev. 15*, 2934-9.

Irizarry, R. A., Warren, D., *et al.* (2005) Multiple-laboratory comparison of microarray platforms, *Nat Methods. 2*, 345-50.

Irwin, M. S. & Kaelin, W. G. (2001) p53 family update: p73 and p63 develop their own identities, *Cell Growth Differ. 12*, 337-49.

Itahana, K., Dimri, G. & Campisi, J. (2001) Regulation of cellular senescence by p53, *Eur J Biochem. 268*, 2784-91.

Itahana, K., Zou, Y., *et al.* (2003) Control of the replicative life span of human fibroblasts by p16 and the polycomb protein Bmi-1, *Mol Cell Biol. 23*, 389-401.

Iwasa, H., Han, J. & Ishikawa, F. (2003) Mitogen-activated protein kinase p38 defines the common senescence-signalling pathway, *Genes Cells. 8*, 131-44.

Jacks, T. (1996) Lessons from the p53 mutant mouse, *J Cancer Res Clin Oncol. 122*, 319-27.

Jackson, S., Harwood, C., Thomas, M., Banks, L. & Storey, A. (2000) Role of Bak in UV-induced apoptosis in skin cancer and abrogation by HPV E6 proteins, *Genes Dev. 14*, 3065-73.

Jacobs, J. J. & de Lange, T. (2004) Significant role for p16INK4a in p53-independent telomere-directed senescence, *Curr Biol. 14*, 2302-8.

Jacobs, J. J., Keblusek, P., *et al.* (2000) Senescence bypass screen identifies TBX2, which represses Cdkn2a (p19(ARF)) and is amplified in a subset of human breast cancers, *Nat Genet. 26*, 291-9.

Jacobs, J. J., Kieboom, K., Marino, S., DePinho, R. A. & van Lohuizen, M. (1999) The oncogene and Polycomb-group gene bmi-1 regulates cell proliferation and senescence through the ink4a locus, *Nature. 397*, 164-8.

Jascur, T., Brickner, H., *et al.* (2005) Regulation of p21(WAF1/CIP1) stability by WISp39, a Hsp90 binding TPR protein, *Mol Cell. 17*, 237-49.

Jat, P. S. & Sharp, P. A. (1989) Cell lines established by a temperature-sensitive simian virus 40 large-T-antigen gene are growth restricted at the nonpermissive temperature, *Mol Cell Biol. 9*, 1672-81.

Jez, J. M., Flynn, T. G. & Penning, T. M. (1997) A new nomenclature for the aldo-keto reductase superfamily, *Biochem Pharmacol. 54*, 639-47.

Jiang, H., Lin, J., *et al.* (1995) The melanoma differentiation-associated gene mda-6, which encodes the cyclin-dependent kinase inhibitor p21, is differentially expressed during growth, differentiation and progression in human melanoma cells, *Oncogene. 10*, 1855-64.

Jin, S. & Levine, A. J. (2001) The p53 functional circuit, *J Cell Sci. 114*, 4139-40.

Jost, C. A., Marin, M. C. & Kaelin, W. G., Jr. (1997) p73 is a simian [correction of human] p53-related protein that can induce apoptosis, *Nature. 389*, 191-4.

Kalderon, D., Roberts, B. L., Richardson, W. D. & Smith, A. E. (1984) A short amino acid sequence able to specify nuclear location, *Cell. 39*, 499-509.

Kamijo, T., van de Kamp, E., Chong, M. J., Zindy, F., Diehl, J. A., Sherr, C. J. & McKinnon, P. J. (1999) Loss of the ARF tumor suppressor reverses premature replicative arrest but not radiation hypersensitivity arising from disabled atm function, *Cancer Res. 59*, 2464-9.

Kamijo, T., Zindy, F., *et al.* (1997) Tumor suppression at the mouse INK4a locus mediated by the alternative reading frame product p19ARF, *Cell. 91*, 649-59.

Kaminker, P. G., Kim, S. H., *et al.* (2001) TANK2, a new TRF1-associated poly(ADP-ribose) polymerase, causes rapid induction of cell death upon overexpression, *J Biol Chem. 276*, 35891-9.

Kammer, C., Warthorst, U., Torrez-Martinez, N., Wheeler, C. M. & Pfister, H. (2000) Sequence analysis of the long control region of human papillomavirus type 16 variants and functional consequences for P97 promoter activity, *J Gen Virol. 81*, 1975-81.

Kanda, T., Watanabe, S., Zanma, S., Sato, H., Furuno, A. & Yoshiike, K. (1991) Human papillomavirus type 16 E6 proteins with glycine substitution for cysteine in the metal-binding motif, *Virology. 185*, 536-43.

Kao, C. C., Yew, P. R. & Berk, A. J. (1990) Domains required for in vitro association between the cellular p53 and the adenovirus 2 E1B 55K proteins, *Virology. 179*, 806-14.

Karlseder, J., Broccoli, D., Dai, Y., Hardy, S. & de Lange, T. (1999) p53- and ATM-dependent apoptosis induced by telomeres lacking TRF2, *Science. 283*, 1321-5.

Karlseder, J., Smogorzewska, A. & de Lange, T. (2002) Senescence induced by altered telomere state, not telomere loss, *Science. 295*, 2446-9.

Kastan, M. B., Zhan, Q., *et al.* (1992) A mammalian cell cycle checkpoint pathway utilizing p53 and GADD45 is defective in ataxia-telangiectasia, *Cell. 71*, 587-97.

Kato, H., Goto, D. B., Martienssen, R. A., Urano, T., Furukawa, K. & Murakami, Y. (2005) RNA polymerase II is required for RNAi-dependent heterochromatin assembly, *Science. 309*, 467-9.

Katz, M. E. & McCormick, F. (1997) Signal transduction from multiple Ras effectors, *Curr Opin Genet Dev. 7*, 75-9.

Kawakami, M., Staub, J., Cliby, W., Hartmann, L., Smith, D. I. & Shridhar, V. (1999) Involvement of H-cadherin (CDH13) on 16q in the region of frequent deletion in ovarian cancer, *Int J Oncol. 15*, 715-20.

Kelley, W. L. & Georgopoulos, C. (1997) The T/t common exon of simian virus 40, JC, and BK polyomavirus T antigens can functionally replace the J-domain of the Escherichia coli DnaJ molecular chaperone, *Proc Natl Acad Sci U S A. 94*, 3679-84.

Kennedy, B. K., Barbie, D. A., Classon, M., Dyson, N. & Harlow, E. (2000) Nuclear organization of DNA replication in primary mammalian cells, *Genes Dev. 14*, 2855-68.

Khan, S. H. & Wahl, G. M. (1998) p53 and pRb prevent rereplication in response to microtubule inhibitors by mediating a reversible G1 arrest, *Cancer Res. 58*, 396-401.

Khvorova, A., Reynolds, A. & Jayasena, S. D. (2003) Functional siRNAs and miRNAs exhibit strand bias, *Cell. 115*, 209-16.

Kim, C. F., Jackson, E. L., *et al.* (2005) Identification of bronchioalveolar stem cells in normal lung and lung cancer, *Cell. 121*, 823-35.

Kim, J., Krichevsky, A., Grad, Y., Hayes, G. D., Kosik, K. S., Church, G. M. & Ruvkun, G. (2004) Identification of many microRNAs that copurify with polyribosomes in mammalian neurons, *Proc Natl Acad Sci U S A. 101*, 360-5.

Kim, J. H., Yoon, S. Y., *et al.* (2004) Overexpression of Bmi-1 oncoprotein correlates with axillary lymph node metastases in invasive ductal breast cancer, *Breast. 13*, 383-8.

Kim, J. H., Yoon, S. Y., *et al.* (2004) The Bmi-1 oncoprotein is overexpressed in human colorectal cancer and correlates with the reduced p16INK4a/p14ARF proteins, *Cancer Lett. 203*, 217-24.

Kim, N. W., Piatyszek, M. A., *et al.* (1994) Specific association of human telomerase activity with immortal cells and cancer, *Science. 266*, 2011-5.

Kim, S. H., Beausejour, C., Davalos, A. R., Kaminker, P., Heo, S. J. & Campisi, J. (2004) TIN2 mediates functions of TRF2 at human telomeres, *J Biol Chem. 279*, 43799-804.

Kim, S. H., Kaminker, P. & Campisi, J. (1999) TIN2, a new regulator of telomere length in human cells, *Nat Genet. 23*, 405-12.

Kitaura, H., Shinshi, M., Uchikoshi, Y., Ono, T., Iguchi-Ariga, S. M. & Ariga, H. (2000) Reciprocal regulation via protein-protein interaction between c-Myc and p21(cip1/waf1/sdi1) in DNA replication and transcription, *J Biol Chem. 275*, 10477-83.

Kiyono, T., Foster, S. A., Koop, J. I., McDougall, J. K., Galloway, D. A. & Klingelhutz, A. J. (1998) Both Rb/p16INK4a inactivation and telomerase activity are required to immortalize human epithelial cells, *Nature. 396*, 84-8.

Klingelhutz, A. J., Foster, S. A. & McDougall, J. K. (1996) Telomerase activation by the E6 gene product of human papillomavirus type 16, *Nature. 380*, 79-82.

Knudsen, E. S. & Wang, J. Y. (1996) Differential regulation of retinoblastoma protein function by specific Cdk phosphorylation sites, *J Biol Chem. 271*, 8313-20.

Knudson, A. G., Jr. (1971) Mutation and cancer: statistical study of retinoblastoma, *Proc Natl Acad Sci U S A. 68*, 820-3.

Koering, C. E., Pollice, A., *et al.* (2002) Human telomeric position effect is determined by chromosomal context and telomeric chromatin integrity, *EMBO Rep. 3*, 1055-61.

Koff, A., Giordano, A., *et al.* (1992) Formation and activation of a cyclin E-cdk2 complex during the G1 phase of the human cell cycle, *Science. 257*, 1689-94.

Konstantinidis, A. K., Radhakrishnan, R., Gu, F., Rao, R. N. & Yeh, W. K. (1998) Purification, characterization, and kinetic mechanism of cyclin D1. CDK4, a major target for cell cycle regulation, *J Biol Chem. 273*, 26506-15.

Kothapalli, R., Yoder, S. J., *et al.* (2002) Microarray results: how accurate are they?, *BMC Bioinformatics. 23*, 22.

Kramer, E. R., Scheuringer, N., Podtelejnikov, A. V., Mann, M. & Peters, J. M. (2000) Mitotic regulation of the APC activator proteins CDC20 and CDH1, *Mol Biol Cell. 11*, 1555-69.

Krimpenfort, P., Quon, K. C., Mooi, W. J., Loonstra, A. & Berns, A. (2001) Loss of p16Ink4a confers susceptibility to metastatic melanoma in mice, *Nature. 413*, 83-6.

Krishnamurthy, J., Torrice, C., Ramsey, M. R., Kovalev, G. I., Al-Regaiey, K., Su, L. & Sharpless, N. E. (2004) Ink4a/Arf expression is a biomarker of aging, *J Clin Invest. 114*, 1299-307.

Krtolica, A., Parrinello, S., Lockett, S., Desprez, P. Y. & Campisi, J. (2001) Senescent fibroblasts promote epithelial cell growth and tumorigenesis: a link between cancer and aging, *Proc Natl Acad Sci U S A. 98*, 12072-7.

Kubbutat, M. H., Jones, S. N. & Vousden, K. H. (1997) Regulation of p53 stability by Mdm2, *Nature. 387*, 299-303.

Kulju, K. S. & Lehman, J. M. (1995) Increased p53 protein associated with aging in human diploid fibroblasts, *Exp Cell Res. 217*, 336-45.

Kumazaki, T., Robetorye, R. S., Robetorye, S. C. & Smith, J. R. (1991) Fibronectin expression increases during in vitro cellular senescence: correlation with increased cell area, *Exp Cell Res. 195*, 13-9.

Kurki, S., Peltonen, K., Latonen, L., Kiviharju, T. M., Ojala, P. M., Meek, D. & Laiho, M. (2004) Nucleolar protein NPM interacts with HDM2 and protects tumor suppressor protein p53 from HDM2-mediated degradation, *Cancer Cell. 5*, 465-75.

Kurz, D. J., Decary, S., Hong, Y. & Erusalimsky, J. D. (2000) Senescence-associated (beta)-galactosidase reflects an increase in lysosomal mass during replicative ageing of human endothelial cells, *J Cell Sci. 113*, 3613-22.

Kussie, P. H., Gorina, S., Marechal, V., Elenbaas, B., Moreau, J., Levine, A. J. & Pavletich, N. P. (1996) Structure of the MDM2 oncoprotein bound to the p53 tumor suppressor transactivation domain, *Science. 274*, 948-53.

Kyrion, G., Liu, K., Liu, C. & Lustig, A. J. (1993) RAP1 and telomere structure regulate telomere position effects in Saccharomyces cerevisiae, *Genes Dev. 7*, 1146-59.

LaBaer, J., Garrett, M. D., *et al.* (1997) New functional activities for the p21 family of CDK inhibitors, *Genes Dev. 11*, 847-62.

Lachner, M., O'Carroll, D., Rea, S., Mechtler, K. & Jenuwein, T. (2001) Methylation of histone H3 lysine 9 creates a binding site for HP1 proteins, *Nature. 410*, 116-20.

Lai, A., Kennedy, B. K., *et al.* (2001) RBP1 recruits the mSIN3-histone deacetylase complex to the pocket of retinoblastoma tumor suppressor family proteins found in limited discrete regions of the nucleus at growth arrest, *Mol Cell Biol. 21*, 2918-32.

Lambert, P. F., Kashanchi, F., Radonovich, M. F., Shiekhattar, R. & Brady, J. N. (1998) Phosphorylation of p53 serine 15 increases interaction with CBP, *J Biol Chem. 273*, 33048-53.

Lamberti, C., Morrissey, L. C., Grossman, S. R. & Androphy, E. J. (1990) Transcriptional activation by the papillomavirus E6 zinc finger oncoprotein, *Embo J. 9*, 1907-13.

Lane, D. P. (1992) Cancer. p53, guardian of the genome, *Nature. 358*, 15-6.

Lane, D. P. & Crawford, L. V. (1979) T antigen is bound to a host protein in SV40-transformed cells, *Nature. 278*, 261-3.

Lane, M. A., Black, A., Handy, A., Tilmont, E. M., Ingram, D. K. & Roth, G. S. (2001) Caloric restriction in primates, *Ann N Y Acad Sci. 928*, 287-95.

Larkin, J. E., Frank, B. C., Gavras, H., Sultana, R. & Quackenbush, J. (2005) Independence and reproducibility across microarray platforms, *Nat Methods. 2*, 337-44.

LaTulippe, E., Satagopan, J., Smith, A., Scher, H., Scardino, P., Reuter, V. & Gerald, W. L. (2002) Comprehensive gene expression analysis of prostate cancer reveals distinct transcriptional programs associated with metastatic disease, *Cancer Res. 62*, 4499-506.

Lee, E. Y., Chang, C. Y., *et al.* (1992) Mice deficient for Rb are nonviable and show defects in neurogenesis and haematopoiesis, *Nature. 359*, 288-94.

Lee, J. O., Russo, A. A. & Pavletich, N. P. (1998) Structure of the retinoblastoma tumour-suppressor pocket domain bound to a peptide from HPV E7, *Nature. 391*, 859-65.

Lee, M. L., Kuo, F. C., Whitmore, G. A. & Sklar, J. (2000) Importance of replication in microarray gene expression studies: statistical methods and evidence from repetitive cDNA hybridizations, *Proc Natl Acad Sci U S A. 97*, 9834-9.

Lee, S. W. (1996) H-cadherin, a novel cadherin with growth inhibitory functions and diminished expression in human breast cancer, *Nat Med. 2*, 776-82.

Lee, W. H., Shew, J. Y., *et al.* (1987) The retinoblastoma susceptibility gene encodes a nuclear phosphoprotein associated with DNA binding activity, *Nature. 329*, 642-5.

Lefrancois-Martinez, A. M., Bertherat, J., *et al.* (2004) Decreased expression of cyclic adenosine monophosphate-regulated aldose reductase (AKR1B1) is associated with malignancy in human sporadic adrenocortical tumors, *J Clin Endocrinol Metab. 89*, 3010-9.

Leng, X., Connell-Crowley, L., Goodrich, D. & Harper, J. W. (1997) S-Phase entry upon ectopic expression of G1 cyclin-dependent kinases in the absence of retinoblastoma protein phosphorylation, *Curr Biol. 7*, 709-12.

Leung, K. M., Po, L. S., Tsang, F. C., Siu, W. Y., Lau, A., Ho, H. T. & Poon, R. Y. (2002) The candidate tumor suppressor ING1b can stabilize p53 by disrupting the regulation of p53 by MDM2, *Cancer Res. 62*, 4890-3.

Levine, A. J. (1997) p53, the cellular gatekeeper for growth and division, *Cell. 88*, 323-31.

Levine, S. S., Weiss, A., Erdjument-Bromage, H., Shao, Z., Tempst, P. & Kingston, R. E. (2002) The core of the polycomb repressive complex is compositionally and functionally conserved in flies and humans, *Mol Cell Biol. 22*, 6070-8.

Levrero, M., De Laurenzi, V., Costanzo, A., Gong, J., Wang, J. Y. & Melino, G. (2000) The p53/p63/p73 family of transcription factors: overlapping and distinct functions, *J Cell Sci. 113*, 1661-70.

Lewis, B. P., Burge, C. B. & Bartel, D. P. (2005) Conserved seed pairing, often flanked by adenosines, indicates that thousands of human genes are microRNA targets, *Cell. 120*, 15-20.

Li, R., Waga, S., Hannon, G. J., Beach, D. & Stillman, B. (1994) Differential effects by the p21 CDK inhibitor on PCNA-dependent DNA replication and repair, *Nature. 371*, 534-7.

Lill, N. L., Grossman, S. R., Ginsberg, D., DeCaprio, J. & Livingston, D. M. (1997) Binding and modulation of p53 by p300/CBP coactivators, *Nature. 387*, 823-7.

Lill, N. L., Tevethia, M. J., Eckner, R., Livingston, D. M. & Modjtahedi, N. (1997) p300 family members associate with the carboxyl terminus of simian virus 40 large tumor antigen, *J Virol. 71*, 129-37.

Lin, A. W., Barradas, M., Stone, J. C., van Aelst, L., Serrano, M. & Lowe, S. W. (1998) Premature senescence involving p53 and p16 is activated in response to constitutive MEK/MAPK mitogenic signaling, *Genes Dev. 12*, 3008-19.

Lin, Y., Hwang, W. C. & Basavappa, R. (2002) Structural and functional analysis of the human mitotic-specific ubiquitin-conjugating enzyme, UbcH10, *J Biol Chem. 277*, 21913-21.

Lindstrom, M. S. & Wiman, K. G. (2003) Myc and E2F1 induce p53 through p14ARF-independent mechanisms in human fibroblasts, *Oncogene. 22*, 4993-5005.

Lingner, J. & Cech, T. R. (1998) Telomerase and chromosome end maintenance, *Curr Opin Genet Dev. 8*, 226-32.

Linzer, D. I. & Levine, A. J. (1979) Characterization of a 54K dalton cellular SV40 tumor antigen present in SV40-transformed cells and uninfected embryonal carcinoma cells, *Cell. 17*, 43-52.

Lipinski, M. M. & Jacks, T. (1999) The retinoblastoma gene family in differentiation and development, *Oncogene. 18*, 7873-82.

Liu, G., Parant, J. M., *et al.* (2004) Chromosome stability, in the absence of apoptosis, is critical for suppression of tumorigenesis in Trp53 mutant mice, *Nat Genet. 36*, 63-8.

Liu, L., Lassam, N. J., Slingerland, J. M., Bailey, D., Cole, D., Jenkins, R. & Hogg, D. (1995) Germline p16INK4A mutation and protein dysfunction in a family with inherited melanoma, *Oncogene. 11*, 405-12.

Lorenz, M., Saretzki, G., Sitte, N., Metzkow, S. & von Zglinicki, T. (2001) BJ fibroblasts display high antioxidant capacity and slow telomere shortening independent of hTERT transfection, *Free Radic Biol Med. 31*, 824-31.

Lowe, S. W. & Ruley, H. E. (1993) Stabilization of the p53 tumor suppressor is induced by adenovirus 5 E1A and accompanies apoptosis, *Genes Dev. 7*, 535-45.

Lowe, S. W. & Sherr, C. J. (2003) Tumor suppression by Ink4a-Arf: progress and puzzles, *Curr Opin Genet Dev. 13*, 77-83.

Lozano, G. & Zambetti, G. P. (2005) What have animal models taught us about the p53 pathway?, *J Pathol. 205*, 206-20.

Lu, J., Getz, G., *et al.* (2005) MicroRNA expression profiles classify human cancers, *Nature. 435*, 834-8.

Lu, X. (2005) p53: a heavily dictated dictator of life and death, *Curr Opin Genet Dev. 15*, 27-33.

Lucibello, F. C., Sewing, A., Brusselbach, S., Burger, C. & Muller, R. (1993) Deregulation of cyclins D1 and E and suppression of cdk2 and cdk4 in senescent human fibroblasts, *J Cell Sci. 105*, 123-33.

Ludlow, J. W., DeCaprio, J. A., Huang, C. M., Lee, W. H., Paucha, E. & Livingston, D. M. (1989) SV40 large T antigen binds preferentially to an underphosphorylated member of the retinoblastoma susceptibility gene product family, *Cell. 56*, 57-65.

Ludlow, J. W., Shon, J., Pipas, J. M., Livingston, D. M. & DeCaprio, J. A. (1990) The retinoblastoma susceptibility gene product undergoes cell cycle-dependent dephosphorylation and binding to and release from SV40 large T, *Cell. 60*, 387-96.

Luedde, T., Rodriguez, M. E., Tacke, F., Xiong, Y., Brenner, D. A. & Trautwein, C. (2003) p18(INK4c) collaborates with other CDK-inhibitory proteins in the regenerating liver, *Hepatology. 37*, 833-41.

Lukas, J., Herzinger, T., *et al.* (1997) Cyclin E-induced S phase without activation of the pRb/E2F pathway, *Genes Dev. 11*, 1479-92.

Lukas, J., Parry, D., *et al.* (1995) Retinoblastoma-protein-dependent cell-cycle inhibition by the tumour suppressor p16, *Nature. 375*, 503-6.

Lumpkin, C. K., Jr., McClung, J. K., Pereira-Smith, O. M. & Smith, J. R. (1986) Existence of high abundance antiproliferative mRNA's in senescent human diploid fibroblasts, *Science. 232*, 393-5.

Lundblad, V. (2000) DNA ends: maintenance of chromosome termini versus repair of double strand breaks, *Mutat Res. 451*, 227-40.

Luo, R. X., Postigo, A. A. & Dean, D. C. (1998) Rb interacts with histone deacetylase to repress transcription, *Cell. 92*, 463-73.

Luscher-Firzlaff, J. M., Westendorf, J. M., *et al.* (1999) Interaction of the fork head domain transcription factor MPP2 with the human papilloma virus 16 E7 protein: enhancement of transformation and transactivation, *Oncogene. 18*, 5620-30.

Maeda, T., Hobbs, R. M., *et al.* (2005) Role of the proto-oncogene Pokemon in cellular transformation and ARF repression, *Nature. 433*, 278-85.

Maehara, K., Yamakoshi, K., *et al.* (2005) Reduction of total E2F/DP activity induces senescence-like cell cycle arrest in cancer cells lacking functional pRB and p53, *J Cell Biol. 168*, 553-60.

Maione, R., Fimia, G. M., Holman, P., Schaffhausen, B. & Amati, P. (1994) Retinoblastoma antioncogene is involved in the inhibition of myogenesis by polyomavirus large T antigen, *Cell Growth Differ. 5*, 231-7.

Malkin, D., Li, F. P., *et al.* (1990) Germ line p53 mutations in a familial syndrome of breast cancer, sarcomas, and other neoplasms, *Science. 250*, 1233-8.

Mallon, R. G., Wojciechowicz, D. & Defendi, V. (1987) DNA-binding activity of papillomavirus proteins, *J Virol. 61*, 1655-60.

Mann, G. J., Musgrove, E. A., Fox, R. M. & Thelander, L. (1988) Ribonucleotide reductase M1 subunit in cellular proliferation, quiescence, and differentiation, *Cancer Res. 48*, 5151-6.

Mann, R., Mulligan, R. C. & Baltimore, D. (1983) Construction of a retrovirus packaging mutant and its use to produce helper-free defective retrovirus, *Cell. 33*, 153-9.

Mantovani, F. & Banks, L. (2001) The human papillomavirus E6 protein and its contribution to malignant progression, *Oncogene. 20*, 7874-87.

Marciniak, R. A., Lombard, D. B., Johnson, F. B. & Guarente, L. (1998) Nucleolar localization of the Werner syndrome protein in human cells, *Proc Natl Acad Sci U S A. 95*, 6887-92.

Markiewicz, E., Dechat, T., Foisner, R., Quinlan, R. A. & Hutchison, C. J. (2002) Lamin A/C binding protein LAP2alpha is required for nuclear anchorage of retinoblastoma protein, *Mol Biol Cell. 13*, 4401-13.

Martin, D. W., Subler, M. A., Munoz, R. M., Brown, D. R., Deb, S. P. & Deb, S. (1993) p53 and SV40 T antigen bind to the same region overlapping the conserved domain of the TATA-binding protein, *Biochem Biophys Res Commun. 195*, 428-34.

Martin, G. M., Sprague, C. A. & Epstein, C. J. (1970) Replicative life-span of cultivated human cells. Effects of donor's age, tissue, and genotype, *Lab Invest. 23*, 86-92.

Martin-Caballero, J., Flores, J. M., Garcia-Palencia, P. & Serrano, M. (2001) Tumor susceptibility of p21(Waf1/Cip1)-deficient mice, *Cancer Res. 61*, 6234-8.

Martinez, L. A., Chen, Y., Fischer, S. M. & Conti, C. J. (1999) Coordinated changes in cell cycle machinery occur during keratinocyte terminal differentiation, *Oncogene. 18*, 397-406.

Martin-Ruiz, C., Saretzki, G., *et al.* (2004) Stochastic variation in telomere shortening rate causes heterogeneity of human fibroblast replicative life span, *J Biol Chem. 279*, 17826-33.

Maruyama, R., Toyooka, S., *et al.* (2001) Aberrant promoter methylation profile of bladder cancer and its relationship to clinicopathological features, *Cancer Res. 61*, 8659-63.

Massari, M. E. & Murre, C. (2000) Helix-loop-helix proteins: regulators of transcription in eucaryotic organisms, *Mol Cell Biol. 20*, 429-40.

Massimi, P. & Banks, L. (2000) Differential phosphorylation of the HPV-16 E7 oncoprotein during the cell cycle, *Virology. 276*, 388-94.

Massimi, P., Pim, D. & Banks, L. (1997) Human papillomavirus type 16 E7 binds to the conserved carboxy-terminal region of the TATA box binding protein and this contributes to E7 transforming activity, *J Gen Virol. 78*, 2607-13.

Matsumura, T., Zerrudo, Z. & Hayflick, L. (1979) Senescent human diploid cells in culture: survival, DNA synthesis and morphology, *J Gerontol. 34*, 328-34.

Mayol, X., Grana, X., Baldi, A., Sang, N., Hu, Q. & Giordano, A. (1993) Cloning of a new member of the retinoblastoma gene family (pRb2) which binds to the E1A transforming domain, *Oncogene. 8*, 2561-6.

McConnell, B. B., Gregory, F. J., Stott, F. J., Hara, E. & Peters, G. (1999) Induced expression of p16(INK4a) inhibits both CDK4- and CDK2-associated kinase activity by reassortment of cyclin-CDK-inhibitor complexes, *Mol Cell Biol. 19*, 1981-9.

McConnell, B. B., Starborg, M., Brookes, S. & Peters, G. (1998) Inhibitors of cyclin-dependent kinases induce features of replicative senescence in early passage human diploid fibroblasts, *Curr Biol. 8*, 351-4.

McEachern, M. J., Krauskopf, A. & Blackburn, E. H. (2000) Telomeres and their control, *Annu Rev Genet. 34*, 331-358.

McKeehan, W. L. (1977) The effect of temperature during trypsin treatment on viability and multiplication potential of single normal human and chicken fibroblasts, *Cell Biol Int Rep. 1*, 335-43.

Medawar, P. B. (1952) *An Unsolved Problem in Biology*, London.

Medema, R. H., Klompmaker, R., Smits, V. A. & Rijksen, G. (1998) p21wafl can block cells at two points in the cell cycle, but does not interfere with processive DNA-replication or stress-activated kinases, *Oncogene. 16*, 431-41.

Medrano, E. E., Im, S., Yang, F. & Abdel-Malek, Z. A. (1995) Ultraviolet B light induces G1 arrest in human melanocytes by prolonged inhibition of retinoblastoma protein phosphorylation associated with long-term expression of the p21Waf-1/SDI-1/Cip-1 protein, *Cancer Res. 55*, 4047-52.

Medrano, E. E., Yang, F., *et al.* (1994) Terminal differentiation and senescence in the human melanocyte: repression of tyrosine-phosphorylation of the extracellular signal-regulated kinase 2 selectively defines the two phenotypes, *Mol Biol Cell. 5*, 497-509.

Meister, G., Landthaler, M., Dorsett, Y. & Tuschl, T. (2004) Sequence-specific inhibition of microRNA- and siRNA-induced RNA silencing, *Rna. 10*, 544-50.

Melk, A. (2003) Senescence of renal cells: molecular basis and clinical implications, *Nephrol Dial Transplant. 18*, 2474-8.

Melk, A. & Halloran, P. F. (2001) Cell senescence and its implications for nephrology, *J Am Soc Nephrol. 12*, 385-93.

Melk, A., Schmidt, B. M., Takeuchi, O., Sawitzki, B., Rayner, D. C. & Halloran, P. F. (2004) Expression of p16INK4a and other cell cycle regulator and senescence associated genes in aging human kidney, *Kidney Int. 65*, 510-20.

Mercer, W. E., Shields, M. T., Lin, D., Appella, E. & Ullrich, S. J. (1991) Growth suppression induced by wild-type p53 protein is accompanied by selective down-regulation of proliferating-cell nuclear antigen expression, *Proc Natl Acad Sci U S A. 88*, 1958-62.

Metcalf, J. P. (1996) Adenovirus E1A 13S gene product upregulates tumor necrosis factor gene, *Am J Physiol. 270*, L535-40.

Metcalf, J. P., Monick, M. M., Stinski, M. F. & Hunninghake, G. W. (1994) Adenovirus E1A 13S gene product up-regulates the cytomegalovirus major immediate early promoter, *Am J Respir Cell Mol Biol. 10*, 448-52.

Michaloglou, C., Vredeveld, L. C., *et al.* (2005) BRAFE600-associated senescence-like cell cycle arrest of human naevi, *Nature. 436*, 720-4.

Michalovitz, D., Fischer-Fantuzzi, L., Vesco, C., Pipas, J. M. & Oren, M. (1987) Activated Ha-ras can cooperate with defective simian virus 40 in the transformation of nonestablished rat embryo fibroblasts, *J Virol. 61*, 2648-54.

Mie, M., Endoh, T., Yanagida, Y., Kobatake, E. & Aizawa, M. (2003) Induction of neural differentiation by electrically stimulated gene expression of NeuroD2, *J Biotechnol. 100*, 231-8.

Mikkelsen, J. G. & Pedersen, F. S. (2000) Genetic reassortment and patch repair by recombination in retroviruses, *J Biomed Sci. 7*, 77-99.

Millis, A. J., McCue, H. M., Kumar, S. & Baglioni, C. (1992) Metalloproteinase and TIMP-1 gene expression during replicative senescence, *Exp Gerontol. 27*, 425-8.

Mills, A. A., Zheng, B., Wang, X. J., Vogel, H., Roop, D. R. & Bradley, A. (1999) p63 is a p53 homologue required for limb and epidermal morphogenesis, *Nature. 398*, 708-13.

Missero, C., Calautti, E., Eckner, R., Chin, J., Tsai, L. H., Livingston, D. M. & Dotto, G. P. (1995) Involvement of the cell-cycle inhibitor Cip1/WAF1 and the

E1A-associated p300 protein in terminal differentiation, *Proc Natl Acad Sci U S A. 92*, 5451-5.

Mitchell, J. R., Wood, E. & Collins, K. (1999) A telomerase component is defective in the human disease dyskeratosis congenita, *Nature. 402*, 551-5.

Mitchell, P. J., Wang, C. & Tjian, R. (1987) Positive and negative regulation of transcription in vitro: enhancer-binding protein AP-2 is inhibited by SV40 T antigen, *Cell. 50*, 847-61.

Mitra, J., Dai, C. Y., Somasundaram, K., El-Deiry, W. S., Satyamoorthy, K., Herlyn, M. & Enders, G. H. (1999) Induction of p21(WAF1/CIP1) and inhibition of Cdk2 mediated by the tumor suppressor p16(INK4a), *Mol Cell Biol. 19*, 3916-28.

Miyashita, T., Harigai, M., Hanada, M. & Reed, J. C. (1994) Identification of a p53-dependent negative response element in the bcl-2 gene, *Cancer Res. 54*, 3131-5.

Moberg, K. H., Tyndall, W. A. & Hall, D. J. (1992) Wild-type murine p53 represses transcription from the murine c-myc promoter in a human glial cell line, *J Cell Biochem. 49*, 208-15.

Momand, J., Wu, H. H. & Dasgupta, G. (2000) MDM2--master regulator of the p53 tumor suppressor protein, *Gene. 242*, 15-29.

Mondello, C., Petropoulou, C., Monti, D., Gonos, E. S., Franceschi, C. & Nuzzo, F. (1999) Telomere length in fibroblasts and blood cells from healthy centenarians, *Exp Cell Res. 248*, 234-42.

Monte, M., Benetti, R., Buscemi, G., Sandy, P., Del Sal, G. & Schneider, C. (2003) The cell cycle-regulated protein human GTSE-1 controls DNA damage-induced apoptosis by affecting p53 function, *J Biol Chem. 278*, 30356-64.

Moran, E. (1988) A region of SV40 large T antigen can substitute for a transforming domain of the adenovirus E1A products, *Nature. 334*, 168-70.

Moreau, Y., Aerts, S., De Moor, B., De Strooper, B. & Dabrowski, M. (2003) Comparison and meta-analysis of microarray data: from the bench to the computer desk, *Trends Genet. 19*, 570-7.

Morgan, D. O. (1997) Cyclin-dependent kinases: engines, clocks, and microprocessors, *Annu Rev Cell Dev Biol. 13*, 261-91.

Mori, Y., Matsunaga, M., *et al.* (1999) Chromosome band 16q24 is frequently deleted in human gastric cancer, *Br J Cancer. 80*, 556-62.

Morisaki, H., Ando, A., Nagata, Y., Pereira-Smith, O., Smith, J. R., Ikeda, K. & Nakanishi, M. (1999) Complex mechanisms underlying impaired activation of Cdk4 and Cdk2 in replicative senescence: roles of p16, p21, and cyclin D1, *Exp Cell Res. 253*, 503-10.

Morris, E. J. & Dyson, N. J. (2001) Retinoblastoma protein partners, *Adv Cancer Res. 82*, 1-54.

Mueller, M. M. & Fusenig, N. E. (2002) Tumor-stroma interactions directing phenotype and progression of epithelial skin tumor cells, *Differentiation. 70*, 486-97.

Muggleton-Harris, A. L. & DeSimone, D. W. (1980) Replicative potentials of various fusion products between WI-38 and SV40 transformed WI-38 cells and their components, *Somatic Cell Genet. 6*, 689-98.

Mukherjee, A. B. & Costello, C. (1998) Aneuploidy analysis in fibroblasts of human premature aging syndromes by FISH during in vitro cellular aging, *Mech Ageing Dev. 103*, 209-22.

Mukoyama, Y., Zhou, S., Miyachi, Y. & Matsuyoshi, N. (2005) T-cadherin negatively regulates the proliferation of cutaneous squamous carcinoma cells, *J Invest Dermatol. 124*, 833-8.

Muller, H., Bracken, A. P., *et al.* (2001) E2Fs regulate the expression of genes involved in differentiation, development, proliferation, and apoptosis, *Genes Dev. 15*, 267-85.

Mulligan, G. J., Wong, J. & Jacks, T. (1998) p130 is dispensable in peripheral T lymphocytes: evidence for functional compensation by p107 and pRB, *Mol Cell Biol. 18*, 206-20.

Munger, K., Werness, B. A., Dyson, N., Phelps, W. C., Harlow, E. & Howley, P. M. (1989) Complex formation of human papillomavirus E7 proteins with the retinoblastoma tumor suppressor gene product, *Embo J. 8*, 4099-105.

Munro, J., Stott, F. J., Vousden, K. H., Peters, G. & Parkinson, E. K. (1999) Role of the alternative INK4A proteins in human keratinocyte senescence: evidence for the specific inactivation of p16INK4A upon immortalization, *Cancer Res. 59*, 2516-21.

Muraoka, R. S., Lenferink, A. E., Law, B., Hamilton, E., Brantley, D. M., Roebuck, L. R. & Arteaga, C. L. (2002) ErbB2/Neu-induced, cyclin D1-dependent transformation is accelerated in p27-haploinsufficient mammary epithelial cells but impaired in p27-null cells, *Mol Cell Biol. 22*, 2204-19.

Murphy, M., Ahn, J., Walker, K. K., Hoffman, W. H., Evans, R. M., Levine, A. J. & George, D. L. (1999) Transcriptional repression by wild-type p53 utilizes histone deacetylases, mediated by interaction with mSin3a, *Genes Dev. 13*, 2490-501.

Murray, A. W. (2004) Recycling the cell cycle: cyclins revisited, *Cell. 116*, 221-34.

Nagafuchi, A. & Takeichi, M. (1988) Cell binding function of E-cadherin is regulated by the cytoplasmic domain, *Embo J. 7*, 3679-84.

Najafi, S. M., Li, Z., Makino, K., Shao, R. & Hung, M. C. (2003) The adenoviral E1A induces p21WAF1/CIP1 expression in cancer cells, *Biochem Biophys Res Commun. 305*, 1099-104.

Narita, M., Nunez, S., *et al.* (2003) Rb-mediated heterochromatin formation and silencing of E2F target genes during cellular senescence, *Cell. 113*, 703-16.

Ned, R., Allen, S. & Vande Pol, S. (1997) Transformation by bovine papillomavirus type 1 E6 is independent of transcriptional activation by E6, *J Virol. 71*, 4866-70.

Nelson, D. A., Krucher, N. A. & Ludlow, J. W. (1997) High molecular weight protein phosphatase type 1 dephosphorylates the retinoblastoma protein, *J Biol Chem. 272*, 4528-35.

Nevels, M., Rubenwolf, S., Spruss, T., Wolf, H. & Dobner, T. (1997) The adenovirus E4orf6 protein can promote E1A/E1B-induced focus formation by interfering with p53 tumor suppressor function, *Proc Natl Acad Sci U S A. 94*, 1206-11.

Nevins, J. R. (1998) Toward an understanding of the functional complexity of the E2F and retinoblastoma families, *Cell Growth Differ. 9*, 585-93.

Nevins, J. R. (2001) The Rb/E2F pathway and cancer, *Hum Mol Genet. 10*, 699-703.

Newbold, R. F. (2002) The significance of telomerase activation and cellular immortalization in human cancer, *Mutagenesis. 17*, 539-50.

Newbold, R. F. & Overell, R. W. (1983) Fibroblast immortality is a prerequisite for transformation by EJ c-Ha-ras oncogene, *Nature. 304*, 648-51.

Newbold, R. F., Overell, R. W. & Connell, J. R. (1982) Induction of immortality is an early event in malignant transformation of mammalian cells by carcinogens, *Nature. 299*, 633-5.

Nielsen, S. J., Schneider, R., *et al.* (2001) Rb targets histone H3 methylation and HP1 to promoters, *Nature. 412*, 561-5.

Nigg, E. A. (2001) Cell cycle regulation by protein kinases and phosphatases, *Ernst Schering Res Found Workshop*, 19-46.

Nilsson, I. & Hoffmann, I. (2000) Cell cycle regulation by the Cdc25 phosphatase family, *Prog Cell Cycle Res. 4*, 107-14.

Nip, J., Strom, D. K., Eischen, C. M., Cleveland, J. L., Zambetti, G. P. & Hiebert, S. W. (2001) E2F-1 induces the stabilization of p53 but blocks p53-mediated transactivation, *Oncogene. 20*, 910-20.

Noda, A., Ning, Y., Venable, S. F., Pereira-Smith, O. M. & Smith, J. R. (1994) Cloning of senescent cell-derived inhibitors of DNA synthesis using an expression screen, *Exp Cell Res. 211*, 90-8.

North, S. & Hainaut, P. (2000) p53 and cell-cycle control: a finger in every pie, *Pathol Biol (Paris). 48*, 255-70.

Nurse, P. (1994) Ordering S phase and M phase in the cell cycle, *Cell. 79*, 547-50.

Nurse, P. (1997) Regulation of the eukaryotic cell cycle, *Eur J Cancer. 33*, 1002-4.

Nykanen, A., Haley, B. & Zamore, P. D. (2001) ATP requirements and small interfering RNA structure in the RNA interference pathway, *Cell. 107*, 309-21.

O'Donnell, K. A., Wentzel, E. A., Zeller, K. I., Dang, C. V. & Mendell, J. T. (2005) c-Myc-regulated microRNAs modulate E2F1 expression, *Nature. 435*, 839-43.

Ogawa, H., Ishiguro, K., Gaubatz, S., Livingston, D. M. & Nakatani, Y. (2002) A complex with chromatin modifiers that occupies E2F- and Myc-responsive genes in G0 cells, *Science. 296*, 1132-6.

Ogryzko, V. V., Hirai, T. H., Russanova, V. R., Barbie, D. A. & Howard, B. H. (1996) Human fibroblast commitment to a senescence-like state in response to histone deacetylase inhibitors is cell cycle dependent, *Mol Cell Biol. 16*, 5210-8.

Oh, S. T., Kyo, S. & Laimins, L. A. (2001) Telomerase activation by human papillomavirus type 16 E6 protein: induction of human telomerase reverse transcriptase expression through Myc and GC-rich Sp1 binding sites, *J Virol. 75*, 5559-66.

O'Hare, M. J., Bond, J., *et al.* (2001) Conditional immortalization of freshly isolated human mammary fibroblasts and endothelial cells, *Proc Natl Acad Sci U S A. 98*, 646-51.

Ohki, R., Nemoto, J., Murasawa, H., Oda, E., Inazawa, J., Tanaka, N. & Taniguchi, T. (2000) Reprimo, a new candidate mediator of the p53-mediated cell cycle arrest at the G2 phase, *J Biol Chem. 275*, 22627-30.

Ohtani, N., Zebedee, Z., *et al.* (2001) Opposing effects of Ets and Id proteins on p16INK4a expression during cellular senescence, *Nature. 409*, 1067-70.

Okamoto, Y., Ozaki, T., Miyazaki, K., Aoyama, M., Miyazaki, M. & Nakagawara, A. (2003) UbcH10 is the cancer-related E2 ubiquitin-conjugating enzyme, *Cancer Res. 63*, 4167-73.

Olovnikov, A. M. (1973) A theory of marginotomy. The incomplete copying of template margin in enzymic synthesis of polynucleotides and biological significance of the phenomenon, *J Theor Biol. 41*, 181-90.

Olsen, P. H. & Ambros, V. (1999) The lin-4 regulatory RNA controls developmental timing in Caenorhabditis elegans by blocking LIN-14 protein synthesis after the initiation of translation, *Dev Biol. 216*, 671-80.

Opresko, P. L., von Kobbe, C., Laine, J. P., Harrigan, J., Hickson, I. D. & Bohr, V. A. (2002) Telomere-binding protein TRF2 binds to and stimulates the Werner and Bloom syndrome helicases, *J Biol Chem. 277*, 41110-9.

Oren, M., Maltzman, W. & Levine, A. J. (1981) Post-translational regulation of the 54K cellular tumor antigen in normal and transformed cells, *Mol Cell Biol. 1*, 101-10.

Ortega, S., Malumbres, M. & Barbacid, M. (2002) Cyclin D-dependent kinases, INK4 inhibitors and cancer, *Biochim Biophys Acta. 1602*, 73-87.

Osada, M., Ohba, M., *et al.* (1998) Cloning and functional analysis of human p51, which structurally and functionally resembles p53, *Nat Med. 4*, 839-43.

Ossovskaya, V. S., Mazo, I. A., *et al.* (1996) Use of genetic suppressor elements to dissect distinct biological effects of separate p53 domains, *Proc Natl Acad Sci U S A. 93*, 10309-14.

Otterson, G. A., Kratzke, R. A., Coxon, A., Kim, Y. W. & Kaye, F. J. (1994) Absence of p16INK4 protein is restricted to the subset of lung cancer lines that retains wildtype RB, *Oncogene. 9*, 3375-8.

Owen-Schaub, L. B., Zhang, W., *et al.* (1995) Wild-type human p53 and a temperature-sensitive mutant induce Fas/APO-1 expression, *Mol Cell Biol. 15*, 3032-40.

Paddison, P. J., Caudy, A. A., Bernstein, E., Hannon, G. J. & Conklin, D. S. (2002) Short hairpin RNAs (shRNAs) induce sequence-specific silencing in mammalian cells, *Genes Dev. 16*, 948-58.

Paddison, P. J., Silva, J. M., *et al.* (2004) A resource for large-scale RNA-interference-based screens in mammals, *Nature. 428*, 427-31.

Pallante, P., Berlingieri, M. T., *et al.* (2005) UbcH10 overexpression may represent a marker of anaplastic thyroid carcinomas, *Br J Cancer. 93*, 464-71.

Paradis, V., Youssef, N., Dargere, D., Ba, N., Bonvoust, F., Deschatrette, J. & Bedossa, P. (2001) Replicative senescence in normal liver, chronic hepatitis C, and hepatocellular carcinomas, *Hum Pathol. 32*, 327-32.

Pardee, A. B. (1974) A restriction point for control of normal animal cell proliferation, *Proc Natl Acad Sci U S A. 71*, 1286-90.

Parisi, T., Pollice, A., Di Cristofano, A., Calabro, V. & La Mantia, G. (2002) Transcriptional regulation of the human tumor suppressor p14(ARF) by E2F1, E2F2, E2F3, and Sp1-like factors, *Biochem Biophys Res Commun. 291*, 1138-45.

Park, I. K., Morrison, S. J. & Clarke, M. F. (2004) Bmi1, stem cells, and senescence regulation, *J Clin Invest. 113*, 175-9.

Parrinello, S., Samper, E., Krtolica, A., Goldstein, J., Melov, S. & Campisi, J. (2003) Oxygen sensitivity severely limits the replicative lifespan of murine fibroblasts, *Nat Cell Biol. 5*, 741-7.

Parry, D., Bates, S., Mann, D. J. & Peters, G. (1995) Lack of cyclin D-Cdk complexes in Rb-negative cells correlates with high levels of p16INK4/MTS1 tumour suppressor gene product, *Embo J. 14*, 503-11.

Parry, D., Mahony, D., Wills, K. & Lees, E. (1999) Cyclin D-CDK subunit arrangement is dependent on the availability of competing INK4 and p21 class inhibitors, *Mol Cell Biol. 19*, 1775-83.

Paulovich, A. G., Toczyski, D. P. & Hartwell, L. H. (1997) When checkpoints fail, *Cell. 88*, 315-21.

Pavel, S., Smit, N. P., *et al.* (2003) Homozygous germline mutation of CDKN2A/p16 and glucose-6-phosphate dehydrogenase deficiency in a multiple melanoma case, *Melanoma Res. 13*, 171-8.

Peacocke, M. & Campisi, J. (1991) Cellular senescence: a reflection of normal growth control, differentiation, or aging?, *J Cell Biochem. 45*, 147-55.

Pearson, M., Carbone, R., *et al.* (2000) PML regulates p53 acetylation and premature senescence induced by oncogenic Ras, *Nature. 406*, 207-10.

Pedeux, R., Sengupta, S., *et al.* (2005) ING2 regulates the onset of replicative senescence by induction of p300-dependent p53 acetylation, *Mol Cell Biol. 25*, 6639-48.

Peeper, D. S., Shvarts, A., Brummelkamp, T., Douma, S., Koh, E. Y., Daley, G. Q. & Bernards, R. (2002) A functional screen identifies hDRIL1 as an oncogene that rescues RAS-induced senescence, *Nat Cell Biol. 4*, 148-53.

Pereira-Smith, O. M. & Smith, J. R. (1983) Evidence for the recessive nature of cellular immortality, *Science. 221*, 964-6.

Pereira-Smith, O. M. & Smith, J. R. (1988) Genetic analysis of indefinite division in human cells: identification of four complementation groups, *Proc Natl Acad Sci U S A. 85*, 6042-6.

Perkins, N. D., Felzien, L. K., Betts, J. C., Leung, K., Beach, D. H. & Nabel, G. J. (1997) Regulation of NF-kappaB by cyclin-dependent kinases associated with the p300 coactivator, *Science. 275*, 523-7.

Perricaudet, M., le Moullec, J. M., Tiollais, P. & Pettersson, U. (1980) Structure of two adenovirus type 12 transforming polypeptides and their evolutionary implications, *Nature. 288*, 174-6.

Peters, J. M. (2002) The anaphase-promoting complex: proteolysis in mitosis and beyond, *Mol Cell. 9*, 931-43.

Pham, J. W. & Sontheimer, E. J. (2004) The Making of an siRNA, *Mol Cell. 15*, 163-4.

Phillips, A. C. & Vousden, K. H. (2001) E2F-1 induced apoptosis, *Apoptosis. 6*, 173-82.

Pines, J. (1994) Cell cycle. p21 inhibits cyclin shock, *Nature. 369*, 520-1.

Pines, J. & Lindon, C. (2005) Proteolysis: anytime, any place, anywhere?, *Nat Cell Biol. 7*, 731-5.

Pirrotta, V. (1998) Polycombing the genome: PcG, trxG, and chromatin silencing, *Cell. 93*, 333-6.

Polager, S., Kalma, Y., Berkovich, E. & Ginsberg, D. (2002) E2Fs up-regulate expression of genes involved in DNA replication, DNA repair and mitosis, *Oncogene. 21*, 437-46.

Pomerantz, J., Schreiber-Agus, N., *et al.* (1998) The Ink4a tumor suppressor gene product, p19Arf, interacts with MDM2 and neutralizes MDM2's inhibition of p53, *Cell. 92*, 713-23.

Poon, R. Y. & Hunter, T. (1998) Expression of a novel form of p21Cip1/Waf1 in UV-irradiated and transformed cells, *Oncogene. 16*, 1333-43.

Powell, A. J., Darmon, A. J., Gonos, E. S., Lam, E. W., Peden, K. W. & Jat, P. S. (1999) Different functions are required for initiation and maintenance of immortalization of rat embryo fibroblasts by SV40 large T antigen, *Oncogene. 18*, 7343-50.

Prives, C. (1998) Signaling to p53: breaking the MDM2-p53 circuit, *Cell. 95*, 5-8.

Qin, X. Q., Chittenden, T., Livingston, D. M. & Kaelin, W. G., Jr. (1992) Identification of a growth suppression domain within the retinoblastoma gene product, *Genes Dev. 6*, 953-64.

Qin, X. Q., Livingston, D. M., Ewen, M., Sellers, W. R., Arany, Z. & Kaelin, W. G., Jr. (1995) The transcription factor E2F-1 is a downstream target of RB action, *Mol Cell Biol. 15*, 742-55.

Quartin, R. S., Cole, C. N., Pipas, J. M. & Levine, A. J. (1994) The amino-terminal functions of the simian virus 40 large T antigen are required to overcome wild-type p53-mediated growth arrest of cells, *J Virol. 68*, 1334-41.

Quelle, D. E., Zindy, F., Ashmun, R. A. & Sherr, C. J. (1995) Alternative reading frames of the INK4a tumor suppressor gene encode two unrelated proteins capable of inducing cell cycle arrest, *Cell. 83*, 993-1000.

Querido, E., Marcellus, R. C., Lai, A., Charbonneau, R., Teodoro, J. G., Ketner, G. & Branton, P. E. (1997) Regulation of p53 levels by the E1B 55-kilodalton protein and E4orf6 in adenovirus-infected cells, *J Virol. 71*, 3788-98.

Ragimov, N., Krauskopf, A., Navot, N., Rotter, V., Oren, M. & Aloni, Y. (1993) Wild-type but not mutant p53 can repress transcription initiation in vitro by interfering with the binding of basal transcription factors to the TATA motif, *Oncogene. 8*, 1183-93.

Rajasekhar, V. K., Viale, A., Socci, N. D., Wiedmann, M., Hu, X. & Holland, E. C. (2003) Oncogenic Ras and Akt signaling contribute to glioblastoma formation by differential recruitment of existing mRNAs to polysomes, *Mol Cell. 12*, 889-901.

Ramana, K. V., Dixit, B. L., Srivastava, S., Balendiran, G. K., Srivastava, S. K. & Bhatnagar, A. (2000) Selective recognition of glutathiolated aldehydes by aldose reductase, *Biochemistry. 39*, 12172-80.

Ramirez, R. D., Wright, W. E., Shay, J. W. & Taylor, R. S. (1997) Telomerase activity concentrates in the mitotically active segments of human hair follicles, *J Invest Dermatol. 108*, 113-7.

Randerson-Moor, J. A., Harland, M., *et al.* (2001) A germline deletion of p14(ARF) but not CDKN2A in a melanoma-neural system tumour syndrome family, *Hum Mol Genet. 10*, 55-62.

Ranscht, B. & Dours-Zimmermann, M. T. (1991) T-cadherin, a novel cadherin cell adhesion molecule in the nervous system lacks the conserved cytoplasmic region, *Neuron. 7*, 391-402.

Rao, L., Debbas, M., Sabbatini, P., Hockenbery, D., Korsmeyer, S. & White, E. (1992) The adenovirus E1A proteins induce apoptosis, which is inhibited by the E1B 19-kDa and Bcl-2 proteins, *Proc Natl Acad Sci U S A. 89*, 7742-6.

Rao, R. N., Stamm, N. B., *et al.* (1999) Conditional transformation of rat embryo fibroblast cells by a cyclin D1-cdk4 fusion gene, *Oncogene. 18*, 6343-56.

Rape, M. & Kirschner, M. W. (2004) Autonomous regulation of the anaphase-promoting complex couples mitosis to S-phase entry, *Nature. 432*, 588-95.

Rapp, L. & Chen, J. J. (1998) The papillomavirus E6 proteins, *Biochim Biophys Acta. 1378*, F1-19.

Rayman, J. B., Takahashi, Y., *et al.* (2002) E2F mediates cell cycle-dependent transcriptional repression in vivo by recruitment of an HDAC1/mSin3B corepressor complex, *Genes Dev. 16*, 933-47.

Rebbaa, A., Zheng, X., Chou, P. M. & Mirkin, B. L. (2003) Caspase inhibition switches doxorubicin-induced apoptosis to senescence, *Oncogene. 22*, 2805-11.

Reddel, R. R. (2000) The role of senescence and immortalization in carcinogenesis, *Carcinogenesis. 21*, 477-84.

Reddel, R. R., Bryan, T. M., Colgin, L. M., Perrem, K. T. & Yeager, T. R. (2001) Alternative lengthening of telomeres in human cells, *Radiat Res. 155*, 194-200.

Reiners, J. J., Jr., Mathieu, P., Okafor, C., Putt, D. A. & Lash, L. H. (2000) Depletion of cellular glutathione by conditions used for the passaging of adherent cultured cells, *Toxicol Lett. 115*, 153-63.

Reinstein, E., Scheffner, M., Oren, M., Ciechanover, A. & Schwartz, A. (2000) Degradation of the E7 human papillomavirus oncoprotein by the ubiquitin-proteasome system: targeting via ubiquitination of the N-terminal residue, *Oncogene. 19*, 5944-50.

Ren, B., Cam, H., Takahashi, Y., Volkert, T., Terragni, J., Young, R. A. & Dynlacht, B. D. (2002) E2F integrates cell cycle progression with DNA repair, replication, and G(2)/M checkpoints, *Genes Dev. 16*, 245-56.

Renauld, H., Aparicio, O. M., Zierath, P. D., Billington, B. L., Chhablani, S. K. & Gottschling, D. E. (1993) Silent domains are assembled continuously from the telomere and are defined by promoter distance and strength, and by SIR3 dosage, *Genes Dev. 7*, 1133-45.

Reynolds, A., Leake, D., Boese, Q., Scaringe, S., Marshall, W. S. & Khvorova, A. (2004) Rational siRNA design for RNA interference, *Nat Biotechnol. 22*, 326-30.

Rheinwald, J. G., Hahn, W. C., *et al.* (2002) A two-stage, p16(INK4A)- and p53-dependent keratinocyte senescence mechanism that limits replicative potential independent of telomere status, *Mol Cell Biol. 22*, 5157-72.

Rice, P. W. & Cole, C. N. (1993) Efficient transcriptional activation of many simple modular promoters by simian virus 40 large T antigen, *J Virol. 67*, 6689-97.

Rittner, H. L., Hafner, V., Klimiuk, P. A., Szweda, L. I., Goronzy, J. J. & Weyand, C. M. (1999) Aldose reductase functions as a detoxification system for lipid peroxidation products in vasculitis, *J Clin Invest. 103*, 1007-13.

Rivas, F. V., Tolia, N. H., Song, J. J., Aragon, J. P., Liu, J., Hannon, G. J. & Joshua-Tor, L. (2005) Purified Argonaute2 and an siRNA form recombinant human RISC, *Nat Struct Mol Biol. 12*, 340-9.

Rizos, H., Puig, S., *et al.* (2001) A melanoma-associated germline mutation in exon 1beta inactivates p14ARF, *Oncogene. 20*, 5543-7.

Roberts, J. M. (1999) Evolving ideas about cyclins, *Cell. 98*, 129-32.

Rodemann, H. P., Peterson, H. P., Schwenke, K. & von Wangenheim, K. H. (1991) Terminal differentiation of human fibroblasts is induced by radiation, *Scanning Microsc. 5*, 1135-42; discussion 1142-3.

Rogoff, H. A., Pickering, M. T., Debatis, M. E., Jones, S. & Kowalik, T. F. (2002) E2F1 induces phosphorylation of p53 that is coincident with p53 accumulation and apoptosis, *Mol Cell Biol. 22*, 5308-18.

Rohme, D. (1981) Evidence for a relationship between longevity of mammalian species and life spans of normal fibroblasts in vitro and erythrocytes in vivo, *Proc Natl Acad Sci U S A. 78*, 5009-13.

Rubin, H. (2002) Promise and problems in relating cellular senescence in vitro to aging in vivo, *Arch Gerontol Geriatr. 34*, 275-86.

Rubinson, D. A., Dillon, C. P., *et al.* (2003) A lentivirus-based system to functionally silence genes in primary mammalian cells, stem cells and transgenic mice by RNA interference, *Nat Genet. 33*, 401-6.

Rudolph, K. L., Chang, S., Lee, H. W., Blasco, M., Gottlieb, G. J., Greider, C. & DePinho, R. A. (1999) Longevity, stress response, and cancer in aging telomerase-deficient mice, *Cell. 96*, 701-12.

Rushton, J. J., Jiang, D., Srinivasan, A., Pipas, J. M. & Robbins, P. D. (1997) Simian virus 40 T antigen can regulate p53-mediated transcription independent of binding p53, *J Virol. 71*, 5620-3.

Ryan, K. M., O'Prey, J. & Vousden, K. H. (2004) Loss of nuclear factor-kappaB is tumor promoting but does not substitute for loss of p53, *Cancer Res. 64*, 4415-8.

Sabbatini, P., Chiou, S. K., Rao, L. & White, E. (1995) Modulation of p53-mediated transcriptional repression and apoptosis by the adenovirus E1B 19K protein, *Mol Cell Biol. 15*, 1060-70.

Saffer, J. D., Jackson, S. P. & Thurston, S. J. (1990) SV40 stimulates expression of the transacting factor Sp1 at the mRNA level, *Genes Dev. 4*, 659-66.

Sage, J., Miller, A. L., Perez-Mancera, P. A., Wysocki, J. M. & Jacks, T. (2003) Acute mutation of retinoblastoma gene function is sufficient for cell cycle re-entry, *Nature. 424*, 223-8.

Sage, J., Mulligan, G. J., *et al.* (2000) Targeted disruption of the three Rb-related genes leads to loss of G(1) control and immortalization, *Genes Dev. 14*, 3037-50.

Saito, H., Hammond, A. T. & Moses, R. E. (1995) The effect of low oxygen tension on the in vitro-replicative life span of human diploid fibroblast cells and their transformed derivatives, *Exp Cell Res. 217*, 272-9.

Sakaguchi, K., Herrera, J. E., *et al.* (1998) DNA damage activates p53 through a phosphorylation-acetylation cascade, *Genes Dev. 12*, 2831-41.

Sakai, M., Hibi, K., Koshikawa, K., Inoue, S., Takeda, S., Kaneko, T. & Nakao, A. (2004) Frequent promoter methylation and gene silencing of CDH13 in pancreatic cancer, *Cancer Sci. 95*, 588-91.

Salminen, A., Helenius, M., Lahtinen, T., Korhonen, P., Tapiola, T., Soininen, H. & Solovyan, V. (1997) Down-regulation of Ku autoantigen, DNA-dependent protein kinase, and poly(ADP-ribose) polymerase during cellular senescence, *Biochem Biophys Res Commun. 238*, 712-6.

Samuelson, A. V. & Lowe, S. W. (1997) Selective induction of p53 and chemosensitivity in RB-deficient cells by E1A mutants unable to bind the RB-related proteins, *Proc Natl Acad Sci U S A. 94*, 12094-9.

Sato, F., Harpaz, N., *et al.* (2002) Hypermethylation of the p14(ARF) gene in ulcerative colitis-associated colorectal carcinogenesis, *Cancer Res. 62*, 1148-51.

Sato, M., Mori, Y., Sakurada, A., Fujimura, S. & Horii, A. (1998) The H-cadherin (CDH13) gene is inactivated in human lung cancer, *Hum Genet. 103*, 96-101.

Satyanarayana, A., Wiemann, S. U., *et al.* (2003) Telomere shortening impairs organ regeneration by inhibiting cell cycle re-entry of a subpopulation of cells, *Embo J. 22*, 4003-13.

Scheffner, M., Huibregtse, J. M., Vierstra, R. D. & Howley, P. M. (1993) The HPV-16 E6 and E6-AP complex functions as a ubiquitin-protein ligase in the ubiquitination of p53, *Cell. 75*, 495-505.

Scheffner, M., Knippers, R. & Stahl, H. (1989) RNA unwinding activity of SV40 large T antigen, *Cell. 57*, 955-63.

Scheffner, M., Takahashi, T., Huibregtse, J. M., Minna, J. D. & Howley, P. M. (1992) Interaction of the human papillomavirus type 16 E6 oncoprotein with wild-type and mutant human p53 proteins, *J Virol. 66*, 5100-5.

Schmitt, C. A., Fridman, J. S., Yang, M., Lee, S., Baranov, E., Hoffman, R. M. & Lowe, S. W. (2002) A senescence program controlled by p53 and p16INK4a contributes to the outcome of cancer therapy, *Cell. 109*, 335-46.

Schneider, E. L. & Mitsui, Y. (1976) The relationship between in vitro cellular aging and in vivo human age, *Proc Natl Acad Sci U S A. 73*, 3584-8.

Schwarz, D. S., Hutvagner, G., Du, T., Xu, Z., Aronin, N. & Zamore, P. D. (2003) Asymmetry in the assembly of the RNAi enzyme complex, *Cell. 115*, 199-208.

Schwarz, E., Freese, U. K., Gissmann, L., Mayer, W., Roggenbuck, B., Stremlau, A. & zur Hausen, H. (1985) Structure and transcription of human papillomavirus sequences in cervical carcinoma cells, *Nature. 314*, 111-4.

Schwarze, S. R., Shi, Y., Fu, V. X., Watson, P. A. & Jarrard, D. F. (2001) Role of cyclin-dependent kinase inhibitors in the growth arrest at senescence in human prostate epithelial and uroepithelial cells, *Oncogene. 20*, 8184-92.

Sedelnikova, O. A., Horikawa, I., Zimonjic, D. B., Popescu, N. C., Bonner, W. M. & Barrett, J. C. (2004) Senescing human cells and ageing mice accumulate DNA lesions with unrepairable double-strand breaks, *Nat Cell Biol. 6*, 168-70.

Seggerson, K., Tang, L. & Moss, E. G. (2002) Two genetic circuits repress the Caenorhabditis elegans heterochronic gene lin-28 after translation initiation, *Dev Biol. 243*, 215-25.

Sellers, W. R. & Kaelin, W. G., Jr. (1997) Role of the retinoblastoma protein in the pathogenesis of human cancer, *J Clin Oncol. 15*, 3301-12.

Sellers, W. R., Novitch, B. G., *et al.* (1998) Stable binding to E2F is not required for the retinoblastoma protein to activate transcription, promote differentiation, and suppress tumor cell growth, *Genes Dev. 12*, 95-106.

Semov, A., Marcotte, R., *et al.* (2002) Microarray analysis of E-box binding-related gene expression in young and replicatively senescent human fibroblasts, *Anal Biochem. 1*, 38-51.

Serrano, M., Hannon, G. J. & Beach, D. (1993) A new regulatory motif in cell-cycle control causing specific inhibition of cyclin D/CDK4, *Nature. 366*, 704-7.

Serrano, M., Lee, H., Chin, L., Cordon-Cardo, C., Beach, D. & DePinho, R. A. (1996) Role of the INK4a locus in tumor suppression and cell mortality, *Cell. 85*, 27-37.

Serrano, M., Lin, A. W., McCurrach, M. E., Beach, D. & Lowe, S. W. (1997) Oncogenic ras provokes premature cell senescence associated with accumulation of p53 and p16INK4a, *Cell. 88*, 593-602.

Seshadri, T. & Campisi, J. (1990) Repression of c-fos transcription and an altered genetic program in senescent human fibroblasts, *Science. 247*, 205-9.

Severino, J., Allen, R. G., Balin, S., Balin, A. & Cristofalo, V. J. (2000) Is beta-galactosidase staining a marker of senescence in vitro and in vivo?, *Exp Cell Res. 257*, 162-71.

Sewalt, R. G., Lachner, M., *et al.* (2002) Selective interactions between vertebrate polycomb homologs and the SUV39H1 histone lysine methyltransferase suggest that histone H3-K9 methylation contributes to chromosomal targeting of Polycomb group proteins, *Mol Cell Biol. 22*, 5539-53.

Sewalt, R. G., van der Vlag, J., *et al.* (1998) Characterization of interactions between the mammalian polycomb-group proteins Enx1/EZH2 and EED suggests

the existence of different mammalian polycomb-group protein complexes, *Mol Cell Biol. 18*, 3586-95.

Shan, B., Durfee, T. & Lee, W. H. (1996) Disruption of RB/E2F-1 interaction by single point mutations in E2F-1 enhances S-phase entry and apoptosis, *Proc Natl Acad Sci U S A. 93*, 679-84.

Shapiro, G. I., Edwards, C. D., Kobzik, L., Godleski, J., Richards, W., Sugarbaker, D. J. & Rollins, B. J. (1995) Reciprocal Rb inactivation and p16INK4 expression in primary lung cancers and cell lines, *Cancer Res. 55*, 505-9.

Sharpless, N. E. (2005) INK4a/ARF: a multifunctional tumor suppressor locus, *Mutat Res. 576*, 22-38.

Sharpless, N. E., Bardeesy, N., *et al.* (2001) Loss of p16Ink4a with retention of p19Arf predisposes mice to tumorigenesis, *Nature. 413*, 86-91.

Shay, J. W., Pereira-Smith, O. M. & Wright, W. E. (1991) A role for both RB and p53 in the regulation of human cellular senescence, *Exp Cell Res. 196*, 33-9.

Shay, J. W. & Wright, W. E. (2000) Hayflick, his limit, and cellular ageing, *Nat Rev Mol Cell Biol. 1*, 72-6.

Shay, J. W. & Wright, W. E. (2001) Ageing and cancer: the telomere and telomerase connection, *Novartis Found Symp. 235*, 116-25; discussion 125-9, 146-9.

Shay, J. W. & Wright, W. E. (2001) Telomeres and telomerase: implications for cancer and aging, *Radiat Res. 155*, 188-193.

Shay, J. W. & Wright, W. E. (2004) Telomeres are double-strand DNA breaks hidden from DNA damage responses, *Mol Cell. 14*, 420-1.

Sheaff, R. J., Groudine, M., Gordon, M., Roberts, J. M. & Clurman, B. E. (1997) Cyclin E-CDK2 is a regulator of p27Kip1, *Genes Dev. 11*, 1464-78.

Sheline, C. T., Milocco, L. H. & Jones, K. A. (1991) Two distinct nuclear transcription factors recognize loop and bulge residues of the HIV-1 TAR RNA hairpin, *Genes Dev. 5*, 2508-20.

Shelton, D. N., Chang, E., Whittier, P. S., Choi, D. & Funk, W. D. (1999) Microarray analysis of replicative senescence, *Curr Biol. 9*, 939-45.

Shen, Y. & Shenk, T. (1994) Relief of p53-mediated transcriptional repression by the adenovirus E1B 19-kDa protein or the cellular Bcl-2 protein, *Proc Natl Acad Sci U S A. 91*, 8940-4.

Sherr, C. J. (1996) Cancer cell cycles, *Science. 274*, 1672-7.

Sherr, C. J. (2001) The INK4a/ARF network in tumour suppression, *Nat Rev Mol Cell Biol. 2*, 731-7.

Sherr, C. J. & DePinho, R. A. (2000) Cellular senescence: mitotic clock or culture shock?, *Cell. 102*, 407-10.

Sherr, C. J. & McCormick, F. (2002) The RB and p53 pathways in cancer, *Cancer Cell. 2*, 103-12.

Sherr, C. J. & Roberts, J. M. (1999) CDK inhibitors: positive and negative regulators of G1-phase progression, *Genes Dev. 13*, 1501-12.

Sherr, C. J. & Weber, J. D. (2000) The ARF/p53 pathway, *Curr Opin Genet Dev. 10*, 94-9.

Shiio, Y., Yamamoto, T. & Yamaguchi, N. (1992) Negative regulation of Rb expression by the p53 gene product, *Proc Natl Acad Sci U S A. 89*, 5206-10.

Shiratori, M., Sakamoto, S., *et al.* (1999) Detection by epitope-defined monoclonal antibodies of Werner DNA helicases in the nucleoplasm and their upregulation by cell transformation and immortalization, *J Cell Biol. 144*, 1-9.

Shvarts, A., Brummelkamp, T. R., Scheeren, F., Koh, E., Daley, G. Q., Spits, H. & Bernards, R. (2002) A senescence rescue screen identifies BCL6 as an inhibitor of anti-proliferative p19(ARF)-p53 signaling, *Genes Dev. 16*, 681-6.

Simonsen, J. L., Rosada, C., *et al.* (2002) Telomerase expression extends the proliferative life-span and maintains the osteogenic potential of human bone marrow stromal cells, *Nat Biotechnol. 20*, 592-6.

Singh, S. K., Clarke, I. D., Terasaki, M., Bonn, V. E., Hawkins, C., Squire, J. & Dirks, P. B. (2003) Identification of a cancer stem cell in human brain tumors, *Cancer Res. 63*, 5821-8.

Slack, R. S., Skerjanc, I. S., Lach, B., Craig, J., Jardine, K. & McBurney, M. W. (1995) Cells differentiating into neuroectoderm undergo apoptosis in the absence of functional retinoblastoma family proteins, *J Cell Biol. 129*, 779-88.

Smith, J. R. & Pereira-Smith, O. M. (1996) Replicative senescence: implications for in vivo aging and tumor suppression, *Science. 273*, 63-7.

Smith, S., Giriat, I., Schmitt, A. & de Lange, T. (1998) Tankyrase, a poly(ADP-ribose) polymerase at human telomeres, *Science. 282*, 1484-7.

Smogorzewska, A. & de Lange, T. (2002) Different telomere damage signaling pathways in human and mouse cells, *Embo J. 21*, 4338-48.

Soengas, M. S., Alarcon, R. M., Yoshida, H., Giaccia, A. J., Hakem, R., Mak, T. W. & Lowe, S. W. (1999) Apaf-1 and caspase-9 in p53-dependent apoptosis and tumor inhibition, *Science. 284*, 156-9.

Song, K., Jung, D., Jung, Y., Lee, S. G. & Lee, I. (2000) Interaction of human Ku70 with TRF2, *FEBS Lett. 481*, 81-5.

Soos, T. J., Kiyokawa, H., *et al.* (1996) Formation of p27-CDK complexes during the human mitotic cell cycle, *Cell Growth Differ. 7*, 135-46.

Sorensen, C. S., Lukas, C., Kramer, E. R., Peters, J. M., Bartek, J. & Lukas, J. (2001) A conserved cyclin-binding domain determines functional interplay between anaphase-promoting complex-Cdh1 and cyclin A-Cdk2 during cell cycle progression, *Mol Cell Biol. 21*, 3692-703.

Soule, H. R. & Butel, J. S. (1979) Subcellular Localization of simian virus 40 large tumor antigen, *J Virol. 30*, 523-32.

Spycher, S. E., Tabataba-Vakili, S., O'Donnell, V. B., Palomba, L. & Azzi, A. (1997) Aldose reductase induction: a novel response to oxidative stress of smooth muscle cells, *Faseb J. 11*, 181-8.

Srinivasan, A., McClellan, A. J., *et al.* (1997) The amino-terminal transforming region of simian virus 40 large T and small t antigens functions as a J domain, *Mol Cell Biol. 17*, 4761-73.

Stampfer, M. R., Garbe, J., Nijjar, T., Wigington, D., Swisshelm, K. & Yaswen, P. (2003) Loss of p53 function accelerates acquisition of telomerase activity in indefinite lifespan human mammary epithelial cell lines, *Oncogene. 22*, 5238-51.

Stansel, R. M., de Lange, T. & Griffith, J. D. (2001) T-loop assembly in vitro involves binding of TRF2 near the 3' telomeric overhang, *Embo J. 20*, 5532-40.

Steegenga, W. T., Riteco, N., Jochemsen, A. G., Fallaux, F. J. & Bos, J. L. (1998) The large E1B protein together with the E4orf6 protein target p53 for active degradation in adenovirus infected cells, *Oncogene. 16*, 349-57.

Stein, G. H., Drullinger, L. F., Robetorye, R. S., Pereira-Smith, O. M. & Smith, J. R. (1991) Senescent cells fail to express cdc2, cycA, and cycB in response to mitogen stimulation, *Proc Natl Acad Sci U S A. 88*, 11012-6.

Stein, G. H., Drullinger, L. F., Soulard, A. & Dulic, V. (1999) Differential roles for cyclin-dependent kinase inhibitors p21 and p16 in the mechanisms of senescence and differentiation in human fibroblasts, *Mol Cell Biol. 19*, 2109-17.

Stein, G. H. & Dulic, V. (1998) Molecular mechanisms for the senescent cell cycle arrest, *J Investig Dermatol Symp Proc. 3*, 14-8.

Steinert, S., Shay, J. W. & Wright, W. E. (2000) Transient expression of human telomerase extends the life span of normal human fibroblasts, *Biochem Biophys Res Commun. 273*, 1095-8.

Stevaux, O. & Dyson, N. J. (2002) A revised picture of the E2F transcriptional network and RB function, *Curr Opin Cell Biol. 14*, 684-91.

Stewart, N., Hicks, G. G., Paraskevas, F. & Mowat, M. (1995) Evidence for a second cell cycle block at G2/M by p53, *Oncogene. 10*, 109-15.

Stewart, S. A., Ben-Porath, I., Carey, V. J., O'Connor, B. F., Hahn, W. C. & Weinberg, R. A. (2003) Erosion of the telomeric single-strand overhang at replicative senescence, *Nat Genet. 33*, 492-6.

Stiegler, P., Kasten, M. & Giordano, A. (1998) The RB family of cell cycle regulatory factors, *J Cell Biochem Suppl. 30-31*, 30-6.

Stott, F. J., Bates, S., *et al* (1998) The alternative product from the human CDKN2A locus, p14(ARF), participates in a regulatory feedback loop with p53 and MDM2, *EMBO J. 17*, 5001-14.

Sugawara, O., Oshimura, M., Koi, M., Annab, L. A. & Barrett, J. C. (1990) Induction of cellular senescence in immortalized cells by human chromosome 1, *Science. 247*, 707-10.

Sugrue, M. M., Shin, D. Y., Lee, S. W. & Aaronson, S. A. (1997) Wild-type p53 triggers a rapid senescence program in human tumor cells lacking functional p53, *Proc Natl Acad Sci U S A. 94*, 9648-53.

Sun, L. & Fuchs, J. A. (1992) Escherichia coli ribonucleotide reductase expression is cell cycle regulated, *Mol Biol Cell. 3*, 1095-105.

Suzuki, K., Mori, I., Nakayama, Y., Miyakoda, M., Kodama, S. & Watanabe, M. (2001) Radiation-induced senescence-like growth arrest requires TP53 function but not telomere shortening, *Radiat Res. 155*, 248-253.

Tahara, H., Sato, E., Noda, A. & Ide, T. (1995) Increase in expression level of p21sdi1/cip1/waf1 with increasing division age in both normal and SV40-transformed human fibroblasts, *Oncogene. 10*, 835-40.

Takahashi, Y., Rayman, J. B. & Dynlacht, B. D. (2000) Analysis of promoter binding by the E2F and pRB families in vivo: distinct E2F proteins mediate activation and repression, *Genes Dev. 14*, 804-16.

Takai, H., Smogorzewska, A. & de Lange, T. (2003) DNA damage foci at dysfunctional telomeres, *Curr Biol. 13*, 1549-56.

Takeichi, M. (1993) Cadherins in cancer: implications for invasion and metastasis, *Curr Opin Cell Biol. 5*, 806-11.

Takeuchi, T., Misaki, A., Liang, S. B., Tachibana, A., Hayashi, N., Sonobe, H. & Ohtsuki, Y. (2000) Expression of T-cadherin (CDH13, H-Cadherin) in human brain and its characteristics as a negative growth regulator of epidermal growth factor in neuroblastoma cells, *J Neurochem. 74*, 1489-97.

Tang, J., Gordon, G. M., Nickoloff, B. J. & Foreman, K. E. (2002) The helix-loop-helix protein id-1 delays onset of replicative senescence in human endothelial cells, *Lab Invest. 82*, 1073-9.

Taubert, S., Gorrini, C., *et al.* (2004) E2F-dependent histone acetylation and recruitment of the Tip60 acetyltransferase complex to chromatin in late G1, *Mol Cell Biol. 24*, 4546-56.

Taylor, W. R., DePrimo, S. E., Agarwal, A., Agarwal, M. L., Schonthal, A. H., Katula, K. S. & Stark, G. R. (1999) Mechanisms of G2 arrest in response to overexpression of p53, *Mol Biol Cell. 10*, 3607-22.

Taylor, W. R., Schonthal, A. H., Galante, J. & Stark, G. R. (2001) p130/E2F4 binds to and represses the cdc2 promoter in response to p53, *J Biol Chem. 276*, 1998-2006.

Taylor, W. R. & Stark, G. R. (2001) Regulation of the G2/M transition by p53, *Oncogene. 20*, 1803-15.

te Poele, R. H., Okorokov, A. L., Jardine, L., Cummings, J. & Joel, S. P. (2002) DNA damage is able to induce senescence in tumor cells in vitro and in vivo, *Cancer Res. 62*, 1876-83.

Teixeira, M. T., Arneric, M., Sperisen, P. & Lingner, J. (2004) Telomere length homeostasis is achieved via a switch between telomerase- extendible and -nonextendible states, *Cell. 117*, 323-35.

Tesco, G., Vergelli, M., *et al.* (1998) Growth properties and growth factor responsiveness in skin fibroblasts from centenarians, *Biochem Biophys Res Commun. 244*, 912-6.

Tessema, M., Lehmann, U. & Kreipe, H. (2004) Cell cycle and no end, *Virchows Arch. 444*, 313-23.

Thomas, D. M., Carty, S. A., Piscopo, D. M., Lee, J. S., Wang, W. F., Forrester, W. C. & Hinds, P. W. (2001) The retinoblastoma protein acts as a transcriptional coactivator required for osteogenic differentiation, *Mol Cell. 8*, 303-16.

Thomas, M., Pim, D. & Banks, L. (1999) The role of the E6-p53 interaction in the molecular pathogenesis of HPV, *Oncogene. 18*, 7690-700.

Tibbetts, R. S., Brumbaugh, K. M., *et al.* (1999) A role for ATR in the DNA damage-induced phosphorylation of p53, *Genes Dev. 13*, 152-7.

Tjian, R. & Robbins, A. (1979) Enzymatic activities associated with a purified simian virus 40 T antigen-related protein, *Proc Natl Acad Sci U S A. 76*, 610-4.

Tlsty, T. D. (2001) Stromal cells can contribute oncogenic signals, *Semin Cancer Biol. 11*, 97-104.

Tlsty, T. D. & Hein, P. W. (2001) Know thy neighbor: stromal cells can contribute oncogenic signals, *Curr Opin Genet Dev. 11*, 54-9.

Todd, C. & Reynolds, N. J. (1998) Up-regulation of p21WAF1 by phorbol ester and calcium in human keratinocytes through a protein kinase C-dependent pathway, *Am J Pathol. 153*, 39-45.

Tolbert, D., Lu, X., Yin, C., Tantama, M. & Van Dyke, T. (2002) p19(ARF) is dispensable for oncogenic stress-induced p53-mediated apoptosis and tumor suppression in vivo, *Mol Cell Biol. 22*, 370-7.

Tomari, Y., Matranga, C., Haley, B., Martinez, N. & Zamore, P. D. (2004) A protein sensor for siRNA asymmetry, *Science. 306*, 1377-80.

Tommerup, H., Dousmanis, A. & de Lange, T. (1994) Unusual chromatin in human telomeres, *Mol Cell Biol. 14*, 5777-85.

Tong, A. H., Lesage, G., *et al.* (2004) Global mapping of the yeast genetic interaction network, *Science. 303*, 808-13.

Toussaint, O., Medrano, E. E. & von Zglinicki, T. (2000) Cellular and molecular mechanisms of stress-induced premature senescence (SIPS) of human diploid fibroblasts and melanocytes, *Exp Gerontol. 35*, 927-45.

Townsley, F. M., Aristarkhov, A., Beck, S., Hershko, A. & Ruderman, J. V. (1997) Dominant-negative cyclin-selective ubiquitin carrier protein E2-C/UbcH10 blocks cells in metaphase, *Proc Natl Acad Sci U S A. 94*, 2362-7.

Toyooka, K. O., Toyooka, S., *et al.* (2001) Loss of expression and aberrant methylation of the CDH13 (H-cadherin) gene in breast and lung carcinomas, *Cancer Res. 61*, 4556-60.

Trentin, J. J., Yabe, Y. & Taylor, G. (1962) The quest for human cancer viruses, *Science. 137*, 835-41.

Trimarchi, J. M., Fairchild, B., Verona, R., Moberg, K., Andon, N. & Lees, J. A. (1998) E2F-6, a member of the E2F family that can behave as a transcriptional repressor, *Proc Natl Acad Sci U S A. 95*, 2850-5.

Trimarchi, J. M., Fairchild, B., Wen, J. & Lees, J. A. (2001) The E2F6 transcription factor is a component of the mammalian Bmi1-containing polycomb complex, *Proc Natl Acad Sci U S A. 98*, 1519-24.

Trimarchi, J. M. & Lees, J. A. (2002) Sibling rivalry in the E2F family, *Nat Rev Mol Cell Biol. 3*, 11-20.

Tsai, K. Y., MacPherson, D., Rubinson, D. A., Crowley, D. & Jacks, T. (2002) ARF is not required for apoptosis in Rb mutant mouse embryos, *Curr Biol. 12*, 159-63.

Tsuyama, N., Miura, M., *et al* (1991) SV40 T-antigen is required for maintenance of immortal growth in SV40-transformed human fibroblasts, *Cell Struct Function. 1*, 55-62.

Turenne, G. A., Paul, P., Laflair, L. & Price, B. D. (2001) Activation of p53 transcriptional activity requires ATM's kinase domain and multiple N-terminal serine residues of p53, *Oncogene. 20*, 5100-10.

Tusher, V. G., Tibshirani, R. & Chu, G. (2001) Significance analysis of microarrays applied to the ionizing radiation response, *Proc Natl Acad Sci U S A. 98*, 5116-21.

Tuveson, D. A., Shaw, A. T., *et al.* (2004) Endogenous oncogenic K-ras(G12D) stimulates proliferation and widespread neoplastic and developmental defects, *Cancer Cell. 5*, 375-87.

Tyner, S. D., Venkatachalam, S., *et al.* (2002) p53 mutant mice that display early ageing-associated phenotypes, *Nature. 415*, 45-53.

Urist, M. & Prives, C. (2002) p53 leans on its siblings, *Cancer Cell. 1*, 311-3.

Utrera, R., Collavin, L., Lazarevic, D., Delia, D. & Schneider, C. (1998) A novel p53-inducible gene coding for a microtubule-localized protein with G2-phase-specific expression, *Embo J. 17*, 5015-25.

van de Wetering, M., Oving, I., *et al.* (2003) Specific inhibition of gene expression using a stably integrated, inducible small-interfering-RNA vector, *EMBO Rep. 4*, 609-15.

van der Lugt, N. M., Domen, J., *et al.* (1994) Posterior transformation, neurological abnormalities, and severe hematopoietic defects in mice with a targeted deletion of the bmi-1 proto-oncogene, *Genes Dev. 8*, 757-69.

van Lohuizen, M., Frasch, M., Wientjens, E. & Berns, A. (1991) Sequence similarity between the mammalian bmi-1 proto-oncogene and the Drosophila regulatory genes Psc and Su(z)2, *Nature. 353*, 353-5.

van Wamel, J. L. & Berkhout, B. (1998) The first strand transfer during HIV-1 reverse transcription can occur either intramolecularly or intermolecularly, *Virology. 244*, 245-51.

Van Zant, G. & Liang, Y. (2003) The role of stem cells in aging, *Exp Hematol. 31*, 659-72.

Vander Jagt, D. L., Robinson, B., Taylor, K. K. & Hunsaker, L. A. (1992) Reduction of trioses by NADPH-dependent aldo-keto reductases. Aldose reductase, methylglyoxal, and diabetic complications, *J Biol Chem. 267*, 4364-9.

Vasile, E., Tomita, Y., Brown, L. F., Kocher, O. & Dvorak, H. F. (2001) Differential expression of thymosin beta-10 by early passage and senescent vascular endothelium is modulated by VPF/VEGF: evidence for senescent endothelial cells in vivo at sites of atherosclerosis, *Faseb J. 15*, 458-66.

Vaziri, H. & Benchimol, S. (1998) Reconstitution of telomerase activity in normal human cells leads to elongation of telomeres and extended replicative life span, *Curr Biol. 8*, 279-82.

Vaziri, H., West, M. D., *et al.* (1997) ATM-dependent telomere loss in aging human diploid fibroblasts and DNA damage lead to the post-translational activation of p53 protein involving poly(ADP-ribose) polymerase, *Embo J. 16*, 6018-33.

Veldman, T., Horikawa, I., Barrett, J. C. & Schlegel, R. (2001) Transcriptional activation of the telomerase hTERT gene by human papillomavirus type 16 E6 oncoprotein, *J Virol. 75*, 4467-72.

Verfaillie, C. M. (2002) Adult stem cells: assessing the case for pluripotency, *Trends Cell Biol. 12*, 502-8.

Vlach, J., Hennecke, S. & Amati, B. (1997) Phosphorylation-dependent degradation of the cyclin-dependent kinase inhibitor p27, *Embo J. 16*, 5334-44.

Vogelstein, B., Lane, D. & Levine, A. J. (2000) Surfing the p53 network, *Nature. 408*, 307-10.

Vojta, P. J., Futreal, P. A., Annab, L. A., Kato, H., Pereira-Smith, O. M. & Barrett, J. C. (1996) Evidence for two senescence loci on human chromosome 1, *Genes Chromosomes Cancer. 16*, 55-63.

von Zglinicki, T., Burkle, A. & Kirkwood, T. B. (2001) Stress, DNA damage and ageing -- an integrative approach, *Exp Gerontol. 36*, 1049-62.

von Zglinicki, T., Petrie, J. & Kirkwood, T. B. (2003) Telomere-driven replicative senescence is a stress response, *Nat Biotechnol. 21*, 229-30.

von Zglinicki, T., Saretzki, G., Docke, W. & Lotze, C. (1995) Mild hyperoxia shortens telomeres and inhibits proliferation of fibroblasts: a model for senescence?, *Exp Cell Res. 220*, 186-93.

Vonlanthen, S., Heighway, J., *et al.* (2001) The bmi-1 oncoprotein is differentially expressed in non-small cell lung cancer and correlates with INK4A-ARF locus expression, *Br J Cancer. 84*, 1372-6.

Voorhoeve, P. M. & Agami, R., (2003) The tumor-suppressive functions of the INK4A locus, *Cancer Cell. 4*, 311-9.

Vousden, K. H., Androphy, E. J., Schiller, J. T. & Lowy, D. R. (1989) Mutational analysis of bovine papillomavirus E6 gene, *J Virol. 63*, 2340-2.

Vousden, K. H. & Lu, X. (2002) Live or let die: the cell's response to p53, *Nat Rev Cancer. 2*, 594-604.

Vousden, K. H., Vojtesek, B., Fisher, C. & Lane, D. (1993) HPV-16 E7 or adenovirus E1A can overcome the growth arrest of cells immortalized with a temperature-sensitive p53, *Oncogene. 8*, 1697-702.

Vulliamy, T., Marrone, A., Goldman, F., Dearlove, A., Bessler, M., Mason, P. J. & Dokal, I. (2001) The RNA component of telomerase is mutated in autosomal dominant dyskeratosis congenita, *Nature. 413*, 432-5.

Waga, S., Hannon, G. J., Beach, D. & Stillman, B. (1994) The p21 inhibitor of cyclin-dependent kinases controls DNA replication by interaction with PCNA, *Nature. 369*, 574-8.

Wagner, K. W., Sapinoso, L. M., *et al.* (2004) Overexpression, genomic amplification and therapeutic potential of inhibiting the UbcH10 ubiquitin conjugase in human carcinomas of diverse anatomic origin, *Oncogene. 23*, 6621-9.

Wagner, M., Hampel, B., Bernhard, D., Hala, M., Zwerschke, W. & Jansen-Durr, P. (2001) Replicative senescence of human endothelial cells in vitro involves G1 arrest, polyploidization and senescence-associated apoptosis, *Exp Gerontol. 36*, 1327-47.

Waldman, T., Kinzler, K. W. & Vogelstein, B. (1995) p21 is necessary for the p53-mediated G1 arrest in human cancer cells, *Cancer Res. 55*, 5187-90.

Wang, G. & Berk, A. J. (2002) In vivo association of adenovirus large E1A protein with the human mediator complex in adenovirus-infected and -transformed cells, *J Virol. 76*, 9186-93.

Wang, H. G., Moran, E. & Yaciuk, P. (1995) E1A promotes association between p300 and pRB in multimeric complexes required for normal biological activity, *J Virol. 69*, 7917-24.

Wang, W., Chen, J. X., Liao, R., Deng, Q., Zhou, J. J., Huang, S. & Sun, P. (2002) Sequential activation of the MEK-extracellular signal-regulated kinase and MKK3/6-p38 mitogen-activated protein kinase pathways mediates oncogenic ras-induced premature senescence, *Mol Cell Biol. 22*, 3389-403.

Wang, X. W., Zhan, Q., *et al.* (1999) GADD45 induction of a G2/M cell cycle checkpoint, *Proc Natl Acad Sci U S A. 96*, 3706-11.

Warbrick, E. (1998) PCNA binding through a conserved motif, *Bioessays. 20*, 195-9.

Wassenegger, M. (2005) The role of the RNAi machinery in heterochromatin formation, *Cell. 122*, 13-6.

Waterhouse, P. M., Wang, M. B. & Lough, T. (2001) Gene silencing as an adaptive defence against viruses, *Nature. 411*, 834-42.

Weber, J. D., Taylor, L. J., Roussel, M. F., Sherr, C. J. & Bar-Sagi, D. (1999) Nucleolar Arf sequesters Mdm2 and activates p53, *Nat Cell Biol. 1*, 20-6.

Webley, K., Bond, J. A., Jones, C. J., Blaydes, J. P., Craig, A., Hupp, T. & Wynford-Thomas, D. (2000) Posttranslational modifications of p53 in replicative senescence overlapping but distinct from those induced by DNA damage, *Mol Cell Biol. 20*, 2803-8.

Wei, W., Hemmer, R. M. & Sedivy, J. M. (2001) Role of p14(ARF) in replicative and induced senescence of human fibroblasts, *Mol Cell Biol. 21*, 6748-57.

Wei, W., Herbig, U., Wei, S., Dutriaux, A. & Sedivy, J. M. (2003) Loss of retinoblastoma but not p16 function allows bypass of replicative senescence in human fibroblasts, *EMBO Rep. 4*, 1061-6.

Wei, W., Jobling, W. A., Chen, W., Hahn, W. C. & Sedivy, J. M. (2003) Abolition of cyclin-dependent kinase inhibitor p16Ink4a and p21Cip1/Waf1 functions permits Ras-induced anchorage-independent growth in telomerase-immortalized human fibroblasts, *Mol Cell Biol. 23*, 2859-70.

Weinberg, R. A. (1995) The retinoblastoma protein and cell cycle control, *Cell. 81*, 323-30.

Weinmann, A. S., Yan, P. S., Oberley, M. J., Huang, T. H. & Farnham, P. J. (2002) Isolating human transcription factor targets by coupling chromatin immunoprecipitation and CpG island microarray analysis, *Genes Dev. 16*, 235-44.

Wells, J., Boyd, K. E., Fry, C. J., Bartley, S. M. & Farnham, P. J. (2000) Target gene specificity of E2F and pocket protein family members in living cells, *Mol Cell Biol. 20*, 5797-807.

West, M. D., Pereira-Smith, O. M. & Smith, J. R. (1989) Replicative senescence of human skin fibroblasts correlates with a loss of regulation and overexpression of collagenase activity, *Exp Cell Res. 184*, 138-47.

West, M. D., Shay, J. W., Wright, W. E. & Linskens, M. H. (1996) Altered expression of plasminogen activator and plasminogen activator inhibitor during cellular senescence, *Exp Gerontol. 31*, 175-93.

Westbrook, T. F., Martin, E. S., *et al.* (2005) A genetic screen for candidate tumor suppressors identifies REST, *Cell. 121*, 837-48.

Whalen, S. G., Marcellus, R. C., Whalen, A., Ahn, N. G., Ricciardi, R. P. & Branton, P. E. (1997) Phosphorylation within the transactivation domain of adenovirus E1A protein by mitogen-activated protein kinase regulates expression of early region 4, *J Virol. 71*, 3545-53.

Whitaker, L. L., Su, H., Baskaran, R., Knudsen, E. S. & Wang, J. Y. (1998) Growth suppression by an E2F-binding-defective retinoblastoma protein (RB): contribution from the RB C pocket, *Mol Cell Biol. 18*, 4032-42.

White, E., Chiou, S. K., Rao, L., Sabbatini, P. & Lin, H. J. (1994) Control of p53-dependent apoptosis by E1B, Bcl-2, and Ha-ras proteins, *Cold Spring Harb Symp Quant Biol. 59*, 395-402.

White, E., Sabbatini, P., Debbas, M., Wold, W. S., Kusher, D. I. & Gooding, L. R. (1992) The 19-kilodalton adenovirus E1B transforming protein inhibits programmed cell death and prevents cytolysis by tumor necrosis factor alpha, *Mol Cell Biol. 12*, 2570-80.

Whyte, P., Buchkovich, K. J., Horowitz, J. M., Friend, S. H., Raybuck, M., Weinberg, R. A. & Harlow, E. (1988) Association between an oncogene and an anti-oncogene: the adenovirus E1A proteins bind to the retinoblastoma gene product, *Nature. 334*, 124-9.

Whyte, P., Williamson, N. M. & Harlow, E. (1989) Cellular targets for transformation by the adenovirus E1A proteins, *Cell. 56*, 67-75.

Williams, E. C. (1957) The commoner urologic problems of the aging, *South Med J. 50*, 235-6.

Wiznerowicz, M. & Trono, D. (2003) Conditional suppression of cellular genes: lentivirus vector-mediated drug-inducible RNA interference, *J Virol. 77*, 8957-61.

Wodarz, D. (2004) Checkpoint genes, ageing, and the development of cancer, *Oncogene. 23*, 7799-809.

Wolfel, T., Hauer, M., *et al.* (1995) A p16INK4a-insensitive CDK4 mutant targeted by cytolytic T lymphocytes in a human melanoma, *Science. 269*, 1281-4.

Woods, D. B. & Vousden, K. H. (2001) Regulation of p53 function, *Exp Cell Res. 264*, 56-66.

Wright, W. E., Pereira-Smith, O. M. & Shay, J. W. (1989) Reversible cellular senescence: implications for immortalization of normal human diploid fibroblasts, *Mol Cell Biol. 9*, 3088-92.

Wright, W. E. & Shay, J. W. (1992) The two-stage mechanism controlling cellular senescence and immortalization, *Exp Gerontol. 27*, 383-9.

Wright, W. E. & Shay, J. W. (2000) Telomere dynamics in cancer progression and prevention: fundamental differences in human and mouse telomere biology, *Nat Med. 6*, 849-51.

Wu, C., Miloslavskaya, I., Demontis, S., Maestro, R. & Galaktionov, K. (2004) Regulation of cellular response to oncogenic and oxidative stress by Seladin-1, *Nature. 432*, 640-5.

Wu, F., Garcia, J., Sigman, D. & Gaynor, R. (1991) tat regulates binding of the human immunodeficiency virus trans-activating region RNA loop-binding protein TRP-185, *Genes Dev. 5*, 2128-40.

Wu, G. S., Burns, T. F., *et al.* (1997) KILLER/DR5 is a DNA damage-inducible p53-regulated death receptor gene, *Nat Genet. 17*, 141-3.

Wu, L., Timmers, C., *et al.* (2001) The E2F1-3 transcription factors are essential for cellular proliferation, *Nature. 414*, 457-62.

Wyllie, F., Haughton, M., Bartek, J., Rowson, J. & Wynford-Thomas, D. (2003) Mutant p53 can delay growth arrest and loss of CDK2 activity in senescing human fibroblasts without reducing p21(WAF1) expression, *Exp Cell Res. 285*, 236-42.

Xiao, Z. X., Chen, J., Levine, A. J., Modjtahedi, N., Xing, J., Sellers, W. R. & Livingston, D. M. (1995) Interaction between the retinoblastoma protein and the oncoprotein MDM2, *Nature. 375*, 694-8.

Xie, R. L., Gupta, S., Miele, A., Shiffman, D., Stein, J. L., Stein, G. S. & van Wijnen, A. J. (2003) The tumor suppressor interferon regulatory factor 1 interferes with SP1 activation to repress the human CDK2 promoter, *J Biol Chem. 278*, 26589-96.

Xiong, Y., Hannon, G. J., Zhang, H., Casso, D., Kobayashi, R. & Beach, D. (1993) p21 is a universal inhibitor of cyclin kinases, *Nature. 366*, 701-4.

Yamamoto, M., Aoyagi, M., Akazawa, K., Tajima, S. & Yamamoto, K. (1998) Decrease in p53 protein in cultured cardinal ligament fibroblasts from patients with prolapsus uteri, *Cell Biol Int. 22*, 31-40.

Yamanaka, A., Hatakeyama, S., Kominami, K., Kitagawa, M., Matsumoto, M. & Nakayama, K. (2000) Cell cycle-dependent expression of mammalian E2-C regulated by the anaphase-promoting complex/cyclosome, *Mol Biol Cell. 11*, 2821-31.

Yanai, N. & Obinata, M. (1994) Apoptosis is induced at nonpermissive temperature by a transient increase in p53 in cell lines immortalized with temperature-sensitive SV40 large T-antigen gene, *Exp Cell Res. 211*, 296-300.

Yang, A., Kaghad, M., Caput, D. & McKeon, F. (2002) On the shoulders of giants: p63, p73 and the rise of p53, *Trends Genet. 18*, 90-5.

Yang, A., Kaghad, M., *et al.* (1998) p63, a p53 homolog at 3q27-29, encodes multiple products with transactivating, death-inducing, and dominant-negative activities, *Mol Cell. 2*, 305-16.

Yang, A., Schweitzer, R., *et al.* (1999) p63 is essential for regenerative proliferation in limb, craniofacial and epithelial development, *Nature. 398*, 714-8.

Yang, A., Walker, N., *et al.* (2000) p73-deficient mice have neurological, pheromonal and inflammatory defects but lack spontaneous tumours, *Nature. 404*, 99-103.

Yang, I. V., Chen, E., *et al.* (2002) Within the fold: assessing differential expression measures and reproducibility in microarray assays, *Genome Biol. 3*, research0062.

Yang, J., Chang, E., *et al.* (1999) Human endothelial cell life extension by telomerase expression, *J Biol Chem. 274*, 26141-8.

Yew, P. R. & Berk, A. J. (1992) Inhibition of p53 transactivation required for transformation by adenovirus early 1B protein, *Nature. 357*, 82-5.

Yew, P. R., Liu, X. & Berk, A. J. (1994) Adenovirus E1B oncoprotein tethers a transcriptional repression domain to p53, *Genes Dev. 8*, 190-202.

Yu, C. E., Oshima, J., *et al.* (1996) Positional cloning of the Werner's syndrome gene, *Science. 272*, 258-62.

Yui, J., Chiu, C. P. & Lansdorp, P. M. (1998) Telomerase activity in candidate stem cells from fetal liver and adult bone marrow, *Blood. 91*, 3255-62.

Zakut, R. & Givol, D. (1995) The tumor suppression function of p21Waf is contained in its N-terminal half ('half-WAF'), *Oncogene. 11*, 393-5.

Zalvide, J., Stubdal, H. & DeCaprio, J. A. (1998) The J domain of simian virus 40 large T antigen is required to functionally inactivate RB family proteins, *Mol Cell Biol. 18*, 1408-15.

Zhan, Q., Antinore, M. J., Wang, X. W., Carrier, F., Smith, M. L., Harris, C. C. & Fornace, A. J., Jr. (1999) Association with Cdc2 and inhibition of Cdc2/Cyclin B1 kinase activity by the p53-regulated protein Gadd45, *Oncogene. 18*, 2892-900.

Zhang, H., Kolb, F. A., Brondani, V., Billy, E. & Filipowicz, W. (2002) Human Dicer preferentially cleaves dsRNAs at their termini without a requirement for ATP, *Embo J. 21*, 5875-85.

Zhang, H., Pan, K. H. & Cohen, S. N. (2003) Senescence-specific gene expression fingerprints reveal cell-type-dependent physical clustering of up-regulated chromosomal loci, *Proc Natl Acad Sci U S A. 100*, 3251-6.

Zhang, H. S., Postigo, A. A. & Dean, D. C. (1999) Active transcriptional repression by the Rb-E2F complex mediates G1 arrest triggered by p16INK4a, TGFbeta, and contact inhibition, *Cell. 97*, 53-61.

Zhang, R., Poustovoitov, M. V., *et al.* (2005) Formation of MacroH2A-containing senescence-associated heterochromatin foci and senescence driven by ASF1a and HIRA, *Dev Cell. 8*, 19-30.

Zhang, Y., Fujita, N. & Tsuruo, T. (1999) Caspase-mediated cleavage of p21Waf1/Cip1 converts cancer cells from growth arrest to undergoing apoptosis, *Oncogene. 18*, 1131-8.

Zhang, Y., Xiong, Y. & Yarbrough, W. G. (1998) ARF promotes MDM2 degradation and stabilizes p53: ARF-INK4a locus deletion impairs both the Rb and p53 tumor suppression pathways, *Cell. 92*, 725-34.

Zheng, W., Wang, H., Xue, L., Zhang, Z. & Tong, T. (2004) Regulation of cellular senescence and p16(INK4a) expression by Id1 and E47 proteins in human diploid fibroblast, *J Biol Chem. 279*, 31524-32.

Zheng, X., Chou, P. M., Mirkin, B. L. & Rebbaa, A. (2004) Senescence-initiated reversal of drug resistance: specific role of cathepsin L, *Cancer Res. 64*, 1773-80.

Zhou, B., Liu, X., *et al.* (2003) The human ribonucleotide reductase subunit hRRM2 complements p53R2 in response to UV-induced DNA repair in cells with mutant p53, *Cancer Res. 63*, 6583-94.

Zhou, B. B. & Elledge, S. J. (2000) The DNA damage response: putting checkpoints in perspective, *Nature. 408*, 433-9.

Zhu, J., Woods, D., McMahon, M. & Bishop, J. M. (1998) Senescence of human fibroblasts induced by oncogenic Raf, *Genes Dev. 12*, 2997-3007.

Zhu, J. W., DeRyckere, D., Li, F. X., Wan, Y. Y. & DeGregori, J. (1999) A role for E2F1 in the induction of ARF, p53, and apoptosis during thymic negative selection, *Cell Growth Differ. 10*, 829-38.

Zhu, J. Y., Rice, P. W., Chamberlain, M. & Cole, C. N. (1991) Mapping the transcriptional transactivation function of simian virus 40 large T antigen, *J Virol. 65*, 2778-90.

Zhu, L., van den Heuvel, S., *et al.* (1993) Inhibition of cell proliferation by p107, a relative of the retinoblastoma protein, *Genes Dev. 7*, 1111-25.

Zhu, X. D., Niedernhofer, L., Kuster, B., Mann, M., Hoeijmakers, J. H. & de Lange, T. (2003) ERCC1/XPF removes the 3' overhang from uncapped telomeres and represses formation of telomeric DNA-containing double minute chromosomes, *Mol Cell. 12*, 1489-98.

Zindy, F., Soares, H., Herzog, K. H., Morgan, J., Sherr, C. J. & Roussel, M. F. (1997) Expression of INK4 inhibitors of cyclin D-dependent kinases during mouse brain development, *Cell Growth Differ. 8*, 1139-50.

Zindy, F., Williams, R. T., *et al.* (2003) Arf tumor suppressor promoter monitors latent oncogenic signals in vivo, *Proc Natl Acad Sci U S A. 100*, 15930-5.

Zou, Y., Sfeir, A., Gryaznov, S. M., Shay, J. W. & Wright, W. E. (2004) Does a sentinel or a subset of short telomeres determine replicative senescence?, *Mol Biol Cell. 15*, 3709-18.

Zuo, L., Weger, J., *et al.* (1996) Germline mutations in the p16INK4a binding domain of CDK4 in familial melanoma, *Nat Genet. 12*, 97-9.

zur Hausen, H. (2001) Cervical carcinoma and human papillomavirus: on the road to preventing a major human cancer, *J Natl Cancer Inst. 93*, 252-3.

Supplementary Information

Supplementary Figure S1: PCR Cloning Primer Sequences

Primer Name	*Sequence (5' to 3')*
E1A 13S-F	GGGGATCCATGAGACATATTATCTGCCACGGAG
E1A 13S-R	GGGGATCCTTATGGCCTGGGGCGTTTACAGC
E1ASEQ-F	GGAGCAGAGAGCCTTGGGTCC
E1ASEQ-R	GGACCCAAGGCTCTCTGCTCC
M13F	GTAAAACGACGGCCAG
M13R	CAGGAAACAGCTATGAC
Ube2cAmp-F	GTCCCTTGAACACACATGCTGCC
Ube2cAmp-R	CCACAGCTCAAGATAAAGAGTCCTATAC
UBE2C#1 SEQ-F	CCAGTGGCTACCCTTACAATGCG
UBE2C#1 SEQ-R	CGCATTGTAAGGGTAGCCACTGG
Myc-UBE2C#1-F	GGGAATTCATGGAACAAAAACTCATCTCAGAAGAGGATCTGGCTTCCCAAAACCGCGACCCAG
SuperRetroseq	ATGTGTTCTGGGAATCACC
SM2 F3	CTAGTCGACTAGGGATAACA
SM2 R3	CTGCGAAGTGATCTTCCGTC

Supplementary Figure S2: ShRNA Oligo Sequences

ShRNA Target	*Forward Oligo (5'-3')*	*Reverse Oligo (5'-3')*
P53	GATCCCCGACTCCAGTGGTAATCTACTTCAAGAGAGTAGATTACCACTGGAGTCTTTTTGGAAA	AGCTTTTCCAAAAAGACTCCAGTGGTAATCTACTCTCTTGAAGTAGATTACCACTGGAGTCGGG
HTATIP	GATCCCCGTACGGCCGTAGTCTCAAGTTCAAGAGACTTGAGACTACGGCCGTACTTTTTGGAAA	AGCTTTTCCAAAAAGTACGGCCGTAGTCTCAAGTCTCTTGAACTTGAGACTACGGCCGTACGGG
B99	GATCCCCATTTGACTTCGATCTTTCATTCAAGAGATGAAAGATCGAAGTCAAATTTTTTGGAAA	AGCTTTTCCAAAAAATTTGACTTCGATCTTTCATCTCTTGAATGAAAGATCGAAGTCAAATGGG
RRPM	GATCCCCGGAAGAGTGACCTGTTAAATTCAAGAGATTTAACAGGTCACTCTTCCTTTTTGGAAA	AGCTTTTCCAAAAAGGAAGAGTGACCTGTTAAATCTCTTGAATTTAACAGGTCACTCTTCCGGG
P16 A	GATCCCCCCAACGCACCGAATAGTTATTCAAGAGATAACTATTCGGTGCGTTGGTTTTTGGAAA	AGCTTTTCCAAAAACCAACGCACCGAATAGTTATCTCTTGAATAACTATTCGGTGCGTTGGGGG
PML 1	GATCCCCAAACCGAGAATCGAAACTATTCAAGAGATAGTTTCGATTCTCGGTTTTTTTTGGAAA	AGCTTTTCCAAAAAAAACCGAGAATCGAAACTATCTCTTGAATAGTTTCGATTCTCGGTTTGGG
PML 2	GATCCCCCCGACTTCTGGTGCTTTGATTCAAGAGATCAAAGCACCAGAAGTCGGTTTTTGGAAA	AGCTTTTCCAAAAACCGACTTCTGGTGCTTTGATCTCTTGAATCAAAGCACCAGAAGTCGGGGG
PML 3	GATCCCCAGCATCTACTGCCGAGGATTTCAAGAGAATCCTCGGCAGTAGATGCTTTTTTGGAAA	AGCTTTTCCAAAAAAGCATCTACTGCCGAGGATTCTCTTGAAATCCTCGGCAGTAGATGCTGGG
SFN 1	GATCCCCCTCTCAGTAGCCTATAAGATTCAAGAGATCTTATAGGCTACTGAGAGTTTTTGGAAA	AGCTTTTCCAAAAACTCTCAGTAGCCTATAAGATCTCTTGAATCTTATAGGCTACTGAGAGGGG
SFN 2	GATCCCCTGGACAGCCACCTCATCAATTCAAGAGATTGATGAGGTGGCTGTCCATTTTTGGAAA	AGCTTTTCCAAAAATGGACAGCCACCTCATCAATCTCTTGAATTGATGAGGTGGCTGTCCAGGG
SFN 3	GATCCCCCGAGACAACCTGACACTGTTTCAAGAGAACAGTGTCAGGTTGTCTCGTTTTTGGAAA	AGCTTTTCCAAAAACGAGACAACCTGACACTGTTCTCTTGAAACAGTGTCAGGTTGTCTCGGGG
CDH13#1	GATCCCCCAGGTTGGCTGAATATTAATTCAAGAGATTAATATTCAGCCAACCTGTTTTTGGAAA	AGCTTTTCCAAAAACAGGTTGGCTGAATATTAATCTCTTGAATTAATATTCAGCCAACCTGGGG
CDH13#2	GATCCCCAATCGCTGTTTATCAACTATTCAAGAGATAGTTGATAAACAGCGATTTTTTTGGAAA	AGCTTTTCCAAAAAAATCGCTGTTTATCAACTATCTCTTGAATAGTTGATAAACAGCGATTGGG
CDH13#3	GATCCCCCTATCGAACTTCACAACTATTCAAGAGATAGTTGTGAAGTTCGATAGTTTTTGGAAA	AGCTTTTCCAAAAACTATCGAACTTCACAACTATCTCTTGAATAGTTGTGAAGTTCGATAGGGG
CDH13#4	GATCCCCTCACGCTGTTTGTTTCATATTCAAGAGATATGAAACAAACAGCGTGATTTTTGGAAA	AGCTTTTCCAAAAATCACGCTGTTTGTTTCATATCTCTTGAATATGAAACAAACAGCGTGAGGG
CDH13#5	GATCCCCCCAGCAGGTTGGCTGAATATTCAAGAGATATTCAGCCAACCTGCTGGTTTTTGGAAA	AGCTTTTCCAAAAACCAGCAGGTTGGCTGAATATCTCTTGAATATTCAGCCAACCTGCTGGGGG
AKR1B1#1	GATCCCCACAAACCTGGCTTGAAGTATTCAAGAGATACTTCAAGCCAGGTTTGTTTTTTGGAAA	AGCTTTTCCAAAAAACAAACCTGGCTTGAAGTATCTCTTGAATACTTCAAGCCAGGTTTGTGGG
AKR1B1#2	GATCCCCTCACTCAGGAGAAGTTAATTTCAAGAGAATTAACTTCTCCTGAGTGATTTTTGGAAA	AGCTTTTCCAAAAATCACTCAGGAGAAGTTAATTCTCTTGAAATTAACTTCTCCTGAGTGAGGG
AKR1B1#3	GATCCCCGTATAAGCCTGCAGTTAACTTCAAGAGAGTTAACTGCAGGCTTATACTTTTTGGAAA	AGCTTTTCCAAAAAGTATAAGCCTGCAGTTAACTCTCTTGAAGTTAACTGCAGGCTTATACGGG
AKR1B1#4	GATCCCCTGTCTAGCTTGATGTTGGATTCAAGAGATCCAACATCAAGCTAGACATTTTTGGAAA	AGCTTTTCCAAAAATGTCTAGCTTGATGTTGGATCTCTTGAATCCAACATCAAGCTAGACAGGG
Lamin A/C	GATCCCCCTGGACTTCCAGAAGAACATTCAAGAGATGTTCTTCTGGAAGTCCAGTTTTTGGAAA	AGCTTTTCCAAAAACTGGACTTCCAGAAGAACATCTCTTGAATGTTCTTCTGGAAGTCCAGGGG
P21 RB	GATCCCCGACCATGTGGACCTGTCACTTCAAGAGAGTGACAGGTCCACATGGTCTTTTTGGAAA	AGCTTTTCCAAAAAGACCATGTGGACCTGTCACTCTCTTGAAGTGACAGGTCCACATGGTCGGG
P21 A	GATCCCCCCAGCATGACAGATTTCTATTCAAGAGATAGAAATCTGTCATGCTGGTTTTTGGAAA	AGCTTTTCCAAAAACCAGCATGACAGATTTCTATCTCTTGAATAGAAATCTGTCATGCTGGGGG
P21 B	GATCCCCAAACTAGGCGGTTGAATGATTCAAGAGATCATTCAACCGCCTAGTTTTTTTTGGAAA	AGCTTTTCCAAAAAAAACTAGGCGGTTGAATGATCTCTTGAATCATTCAACCGCCTAGTTTGGG
P21 C	GATCCCCCACAGGCGGTTATGAAATTTTCAAGAGAAATTTCATAACCGCCTGTGTTTTTGGAAA	AGCTTTTCCAAAAACACAGGCGGTTATGAAATTTCTCTTGAAAATTTCATAACCGCCTGTGGGG
P21 D	GATCCCCAACACCTCCTCATGTACATTTCAAGAGAATGTACATGAGGAGGTGTTTTTTTGGAAA	AGCTTTTCCAAAAAACACCTCCTCATGTACATTCTCTTGAAATGTACATGAGGAGGTGTTGGG
P21 E	GATCCCCCGACTGTGATGCGCTAATGTTCAAGAGACATTAGCGCATCACAGTCGTTTTTGGAAA	AGCTTTTCCAAAAACGACTGTGATGCGCTAATGTCTCTTGAACATTAGCGCATCACAGTCGGGG
P21 F	GATCCCCGAATGAGAGGTTCCTAAGATTCAAGAGATCTTAGGAACCTCTCATTCTTTTTGGAAA	AGCTTTTCCAAAAAGAATGAGAGGTTCCTAAGATCTCTTGAATCTTAGGAACCTCTCATTCGGG
P21 G	GATCCCCCATTGCACTTTGATTAGCATTCAAGAGATGCTAATCAAAGTGCAATGTTTTTGGAAA	AGCTTTTCCAAAAACATTGCACTTTGATTAGCATCTCTTGAATGCTAATCAAAGTGCAATGGGG
Gadd45A	GATCCCCCGACATCAACATCCTGCGCTTCAAGAGAGCGCAGGATGTTGATGTCGTTTTTGGAAA	AGCTTTTCCAAAAACGACATCAACATCCTGCGCTCTCTTGAAGCGCAGGATGTTGATGTCGGGG
BTG2	GATCCCCCACCACTGGTTTCCCGAAATTCAAGAGATTTCGGGAAACCAGTGGTGTTTTTGGAAA	AGCTTTTCCAAAAACACCACTGGTTTCCCGAAATCTCTTGAATTTCGGGAAACCAGTGGTGGGG

Supplementary Figure S3: RT-PCR Primer Sequences

cDNA	*Forward Primer*	*Forward Primer Sequence (5'-3')*	*Reverse Primer*	*Reverse Primer Sequence (5'-3')*	*Size of PCR product (bp)*	*T_A (°C)*	*No of PCR Cycles*
12S E1A	E1A-F	ATTATCTGCCACGGAGGTGT	E1A-R	GGATGCAGGCGCCATTTTA	492	50	30
13S E1A	E1A-F	ATTATCTGCCACGGAGGTGT	E1A-R	GGATGCAGGCGCCATTTTA	635	50	30
AKR1B1	AKR1B1-F	CCATGCAGAGGAACTTGGTGGTG	AKR1B1-R	GTGTCTAGCTTGATGTTGGATCTC	349	56	40
P14^{ARF}	P14-F	GTGCGTGGGTCCCAGTCTGCAG	P14-R	GCTGCTGCCCTAGACGCTGGC	284	62	32
B99	B99-F	CACTCCAGATGCTGCAAGCCAG	B99-R	CAGCCTCCCAAGTTCTAGGGTTAC	373	58	22
BMI1	BMI-F	GTGGAGGGTACTTCATTGATGCCAC	BMI-R	CTTTCCGATCCAATCTGTTCTGGTC	378	55	32
BMI1 (pBabepuro-Bmi-1)	WZL(F)	GGTCTAGGCGCCGGCCGGATCC	BMI-R	CTTTCCGATCCAATCTGTTCTGGTC	438	53	30
BTG2	BTG2-F	AGCGAGCAGAGGCTTAAGGT	BTG2-R	AGCACTTGGTTCTTGCAGGT	497	56	26
CCT2	CCT2-F	CTCATGCTGTGACACAGCTTGCC	CCT2-R	GTCCAAAGATCGACAGCACGTGG	385	56	21
CDH13	CDH13-F	GCTTAGCTTGTCTGTGAGAACTCC	CDH13-R	CTGCCTGGCTGGTTGTGGCAG	623	56	24
P21	CDKN1A-F	GGTCTGCCGCCGTTTTCGACC	CDKN1A-R	GGTCTGCCGCCGTTTTCGACC	402	56	25
E7	E7-F	AGCTCAGAGGAGGAGGATGA	E7-R	GGTTTCTGAGAACAGATGGG	203	50	30
GADD45A	GADD45A-F	GGAGGAAGTGCTCAGCAAAG	GADD45A-R	TCCCGGCAAAAACAAATAAG	378	56	28
GAPDH	GPDS	CGGAGTCAACGGATTTGGTCG	GPDA	TGGAGGAGTGGGTGTCGCTG	863	56	17
HDAC4	HDAC4-F	GACCCAATGCAAACGCTGTCCGTTC	HDAC4-R	CTGGGTGTCCCTGGGTGCTCC	357	60	28
HTATIP	HTATIP-F	GGAGAGGCCACAGATCACCATC	HTATIP-R	CACTGCAGTGGGCAGTGTCTGG	263	66	55
KIAA0828	KIAA0828-F	CTCAGGCTCTTGCCTTGATAGAG	KIAA0828-R	CCTCAGGGCAGTAACCACACTC	413	56	28
Myc-UBE2C#1	Myc-UBE2C#1	GGGAATTCATGGAACAAAAACTCATCTCAGAAGAGGATCTGGCTTCCCAAAACCGCGACCCAG	LNCXSEQ-R	ACCTACAGGTGGGGTCTTTCATTCCC	659	58	28
PML	PML-F	CTGCCAGCAATGCCAGGCGGAAG	PML-R	CACTGGTGTGCCTCGAAGCACTTG	303	60	23
RPRM	RPRM-F	GCTGCTGCACCCAGGCGTCC	RPRM-R	GACTCCGACAGGTTTGCTTCGC	352	56	30
RPS6KA6	RPS6KA6-F	GCTTCATATGGACCCACATCAGCG	PRS6KA6-R	CACCACAAATCTTACAGGCCAGTTC	261	58	25
SFN	SFN-F	CCAGACCACTTTCGACGAGGC	SFN-R	CCATACTAGTCCTCTCGGCAGG	233	56	30
SV40 LT (pWZLBlaste-wtLT)	WZL(F)	GGTCTAGGCGCCGGCCGGATCC	CMV-LT 3'	CCAGAAGCCTCCAAAGTCAGG	~300	50	30
UBE2C#1 (pLPC-UBE2C#1)	UBE2C-F	CTACAGCAGGAGCTGATGACCC	LNCXSEQ-R	ACCTACAGGTGGGGTCTTTCATTCCC	521	56	30
UBE2C#1	Splice-F	GCAGTCCTGCAGTTGCAGTCGTG	UbcH10com-R	GGCAGCATGTGTGTTCAAGGGAC	519	58	25
UBE2C#1 (pLPC-UBE2C)	Splice-F	GCAGTCCTGCAGTTGCAGTCGTG	LNCXSEQ-R	ACCTACAGGTGGGGTCTTTCATTCCC	719	58	25
UBE2C#2	Splice-F	GCAGTCCTGCAGTTGCAGTCGTG	UbcH10com-R	GGCAGCATGTGTGTTCAAGGGAC	465	58	25
UBE2C#2 (pLPC-UBE2C)	Splice-F	GCAGTCCTGCAGTTGCAGTCGTG	LNCXSEQ-R	ACCTACAGGTGGGGTCTTTCATTCCC	665	58	25
UBE2C#3	Splice-F	GCAGTCCTGCAGTTGCAGTCGTG	UbcH10com-R	GGCAGCATGTGTGTTCAAGGGAC	432	58	25
UBE2C#3 (pLPC-UBE2C)	Splicev2-F	GGACAGGCCAGGAGCTCAGAC	LNCXSEQ-R	ACCTACAGGTGGGGTCTTTCATTCCC	632	58	25
UBE2C#4 (pLPC-UBE2C)	Splice-F	GCAGTCCTGCAGTTGCAGTCGTG	LNCXSEQ-R	GGCAGCATGTGTGTTCAAGGGAC	623	58	25
UBE2C#4	Splicev2-F	GGACAGGCCAGGAGCTCAGAC	UbcH10com-R	GGCAGCATGTGTGTTCAAGGGAC	769	58	25
UBE2C#4 (pLPC-UBE2C)	Splicev2-F	GGACAGGCCAGGAGCTCAGAC	LNCXSEQ-R	ACCTACAGGTGGGGTCTTTCATTCCC	823	58	25
UBE2C#5	Splicev2-F	GGACAGGCCAGGAGCTCAGAC	UbcH10com-R	GGCAGCATGTGTGTTCAAGGGAC	1159	58	25
UBE2C#5 (pLPC-UBE2C)	Splicev2-F	GGACAGGCCAGGAGCTCAGAC	LNCXSEQ-R	ACCTACAGGTGGGGTCTTTCATTCCC	969	58	25
UBE2C#6	Splice-F	GCAGTCCTGCAGTTGCAGTCGTG	UbcH10com-R	GGCAGCATGTGTGTTCAAGGGAC	227	58	25
UBE2C#6 (pLPC-UBE2C)	Splice-F	GCAGTCCTGCAGTTGCAGTCGTG	LNCXSEQ-R	ACCTACAGGTGGGGTCTTTCATTCCC	427	58	25
WIP	WIP1-F	GGAGGATCCATGGCCAAGGGTG	WIP1-R	CCAGAATTGGACTCTTCTAATGTCC	363	56	26

Supplementary Figure S4: Genes Up-Regulated Upon the HMF3A Temperature Shift

Clone ID	Gene	Score(d)	Numerator(r)	Denominator(s+s0)	q-value (%)
200909_A	*ADAM10*	1.384938033	0.244997407	0.176901349	0.540855
774119_A	*ADD3*	1.655508247	0.336669443	0.203363193	0.1147947
113871_A	*AGTRAP*	1.224524109	0.248028365	0.202550822	1.8099168
43309_A	*AK3*	1.272735173	0.351129465	0.275885724	1.2451143
470700_A	*AK3*	1.215473834	0.243487018	0.200322714	2.5930212
340628_A	*AKR1B1*	1.405282425	0.214770394	0.152830769	0.2933343
26025_A	*AKR1B1*	1.20996483	0.240137441	0.198466464	2.5930212
340619_A	*AKR1B1*	1.162902434	0.188305382	0.161927068	3.7008086
293270_A	*AKR1C2*	2.940001576	0.570637035	0.194094126	0.1147947
214107_A	*ANPEP*	2.73124557	0.652080178	0.238748278	0.1147947
300484_A	*ANXA1*	2.641993493	0.570480261	0.215927958	0.1147947
288649_A	*ANXA1*	1.945306021	0.513043776	0.263734225	0.1147947
306948_A	*ANXA4*	1.361862908	0.253723434	0.186306149	0.540855
327315_A	*AOAH*	1.132935403	0.280373915	0.247475641	3.7008086
163572_A	*APLP1*	2.421129742	0.497991073	0.205685414	0.1147947
796143_A	*APLP1*	1.31101159	0.271168735	0.206839312	0.6702531
1323860_A	*APLP2*	1.298910694	0.228816897	0.176160607	1.2451143
201585_A	*ARHGDIB*	1.356756997	0.2821756	0.207977995	0.540855
470419_A	*ARPC1B*	1.235990743	0.257782059	0.208563098	1.8099168
269738_A	*ATP2C1*	1.374989945	0.281541913	0.204759252	0.540855
1704062_A	*ATP2C1*	1.297608631	0.267283629	0.205981698	1.2451143
341038_A	*ATP6IP2*	3.121291432	0.62121223	0.199024104	0.1147947
772283_A	*ATP6V0B*	1.60764584	0.316973953	0.19716653	0.1147947
726576_A	*ATP6V0B*	1.130021442	0.255715464	0.226292577	3.7008086
258656_A	*ATP6V0E*	3.220771721	0.586400035	0.182068177	0.1147947
32649_A	*ATP6V1E1*	1.703283074	0.307846725	0.180737265	0.1147947
809439_B	*ATP6V1G1*	2.224106966	0.438519921	0.19716674	0.1147947
146646_A	*ATP6V1G1*	2.036911201	0.367364903	0.180353911	0.1147947
37045_A	*ATP6V1G1*	1.996934524	0.372721704	0.186646933	0.1147947
36832_A	*ATP6V1G1*	1.975338025	0.369142938	0.186875832	0.1147947
299995_A	*ATP6V1G1*	1.833333955	0.370857131	0.202285639	0.1147947
150354_A	*B4GALT1*	1.775951463	0.290576984	0.163617638	0.1147947
327700_A	*B4GALT1*	1.498315515	0.271689449	0.181329931	0.2114793
738975_B	*B4GALT1*	1.359781124	0.293283986	0.215684702	0.540855
784585_A	*BCHE*	1.252328896	0.218230106	0.174259419	1.8099168
310484_A	*BDKRB1*	2.445039902	0.574808118	0.235091508	0.1147947
324760_A	*BDKRB1*	2.262214109	0.489592283	0.216421726	0.1147947
781783_A	*BET1*	1.770128029	0.333177328	0.188222164	0.1147947
203351_A	*BET1*	1.479535523	0.263175976	0.17787743	0.2114793
201890_A	*BIRC3*	1.707781201	0.327036068	0.191497639	0.1147947
129632_A	*BIRC3*	1.524916413	0.407856521	0.267461559	0.1147947
360543_A	*BLCAP*	1.232774767	0.232684558	0.188748638	1.8099168
32510_A	*BTG2*	1.69883619	0.336134507	0.197861636	0.1147947
246304_A	*BTG3*	1.546444208	0.241529574	0.156183826	0.1147947
324159_A	*C10orf7*	2.309118206	0.383471284	0.166068278	0.1147947
47238_A	*C1orf8*	3.330604553	0.611229913	0.183519209	0.1147947

49164_A	*C1orf8*	2.958107511	0.588436088	0.198923158	0.1147947
33683_A	*C1orf8*	2.517267444	0.542832114	0.215643401	0.1147947
310406_A	*C6orf48*	2.277003661	0.459514788	0.201806785	0.1147947
309431_A	*CA12*	1.598628244	0.35607914	0.222740428	0.1147947
324853_A	*CALU*	2.060168122	0.397708277	0.193046515	0.1147947
324963_A	*CALU*	1.870955921	0.397025333	0.212204536	0.1147947
149103_A	*CALU*	1.639448206	0.337555137	0.205895578	0.1147947
282740_A	*CASK*	1.282013849	0.239547504	0.186852508	1.2451143
302591_B	*CASP4CASP5*	2.151373827	0.42111701	0.195743299	0.1147947
32662_A	*CAT*	1.548507403	0.33547128	0.216641702	0.1147947
320383_A	*CD164*	1.159883709	0.230806905	0.198991419	3.7008086
262752_A	*CD44*	2.744938769	0.626597166	0.228273641	0.1147947
267352_A	*CD59*	3.827508523	0.755480025	0.19738167	0.1147947
309771_A	*CD59*	3.745578169	0.710300396	0.18963705	0.1147947
309770_A	*CD59*	3.337518681	0.651067169	0.195075213	0.1147947
174515_A	*CD81*	1.457306147	0.439587335	0.30164378	0.2114793
261971_B	*CD81*	1.411356177	0.42731448	0.302768704	0.2933343
796005_A	*CDH11*	3.855502457	0.786607875	0.204022143	0.1147947
31093_A	*CDH13*	1.80056153	0.383542243	0.213012572	0.1147947
144932_A	*CDK2AP1*	1.231417802	0.28874065	0.234478216	1.8099168
753658_A	*CDK2AP1*	1.12412543	0.260843864	0.232041601	3.7008086
756630_A	*CDKN1A*	6.14746285	1.473255175	0.239652554	0.1147947
145973_A	*CLN2*	2.715168223	0.557013429	0.205148773	0.1147947
196320_A	*CLU*	1.811714745	0.309043608	0.170580721	0.1147947
37500_B	*CPNE3*	1.340785286	0.256028796	0.19095436	0.6702531
233825_A	*CPO*	1.180107998	0.298293318	0.252767813	3.7008086
272142_A	*CREG*	1.421579306	0.236066256	0.166059154	0.2933343
147907_A	*CREG*	1.280187245	0.28223969	0.220467506	1.2451143
269238_A	*CRYAB*	1.155328036	0.213851575	0.185100307	3.7008086
124554_A	*CSF1*	3.335860432	0.8115451	0.243279093	0.1147947
1074540_A	*CSF3*	3.916495861	1.13636929	0.290149493	0.1147947
1667001_A	*CSF3*	2.950630576	0.893110644	0.302684671	0.1147947
246147_A	*CSPG2*	3.936394638	0.825778386	0.209780386	0.1147947
256841_A	*CSRP2*	1.463056031	0.250367448	0.171126357	0.2114793
261517_A	*CTSB*	3.382766976	0.639561163	0.189064505	0.1147947
38764_A	*CTSB*	2.941777549	0.575670616	0.195688017	0.1147947
252292_B	*CTSL*	3.45526484	0.57678133	0.166928255	0.1147947
380384_A	*CUL4B*	1.733712891	0.372942406	0.215111976	0.1147947
297845_A	*CYB5*	1.421575082	0.234811873	0.165177257	0.2933343
471099_A	*CYFIP2*	1.919064141	0.373372749	0.194559807	0.1147947
47475_A	*CYFIP2*	1.546390703	0.282206762	0.18249383	0.1147947
37129_A	*CYLD*	1.248651941	0.29523776	0.236445202	1.8099168
310800_A	*DAF*	1.157523533	0.26297688	0.22718923	3.7008086
24927_A	*DDB2*	1.408798275	0.295794791	0.209962488	0.2933343
753447_B	*DDB2*	1.232201825	0.231079684	0.187533957	1.8099168
42188_A	*DDR2*	1.199879711	0.283300623	0.23610752	2.5930212
309588_A	*DDT*	2.189522685	0.417413573	0.190641355	0.1147947
139028_A	*DDT*	1.91594934	0.377567949	0.197065727	0.1147947
stSG89545	*DDT*	1.28318437	0.243641173	0.189872304	1.2451143
142621_A	*DGKA*	1.217915356	0.216853451	0.178052974	2.5930212

366944_A	*DGKA*	1.203831416	0.21617531	0.179572743	2.5930212
51003_A	*DKK3*	3.809193306	0.625921413	0.164318627	0.1147947
44394_B	*DNAJA1*	1.817456036	0.318730835	0.175371964	0.1147947
789269_A	*DNAJB4*	1.972843058	0.377735954	0.191467817	0.1147947
302434_A	*DTR*	1.138065976	0.256195887	0.225115145	3.7008086
222589_A	*DUSP1*	4.307586082	1.02966454	0.239035163	0.1147947
146239_A	*DUSP1*	3.937111057	1.022682304	0.259754497	0.1147947
252443_A	*DUSP4*	2.369795543	0.494694304	0.208749782	0.1147947
270148_A	*DUSP4*	1.774234822	0.384712733	0.216833042	0.1147947
197479_A	*DUSP5*	2.502051217	0.508641923	0.203289972	0.1147947
33285_A	*DUSP5*	1.723044944	0.352871123	0.204795078	0.1147947
40851_A	*DUSP6*	2.304054145	0.491388876	0.21327141	0.1147947
301122_A	*ECM1*	2.706583454	0.684770169	0.253001683	0.1147947
124873_A	*ECM1*	2.250918331	0.66700557	0.296325975	0.1147947
128045_A	*EFEMP2*	1.778171276	0.403721833	0.227043277	0.1147947
23448_A	*EFEMP2*	1.445833975	0.328660874	0.227315777	0.2114793
287704_A	*EMP1*	2.094028883	0.350725914	0.167488575	0.1147947
323643_A	*EMP1*	1.747073773	0.314484793	0.180006591	0.1147947
322146_A	*EMP1*	1.277843944	0.267356485	0.209224676	1.2451143
323181_A	*FAP*	1.328212828	0.26138271	0.196792792	0.6702531
503931_B	*FBXL11*	9.009322801	2.419547575	0.268560427	0.1147947
665401_A	*FGF2*	3.277309328	0.996452886	0.304046029	0.1147947
365515_A	*FGF7*	2.189470419	0.424686082	0.19396749	0.1147947
44014_A	*FKBP1A*	1.765243536	0.358265191	0.202955107	0.1147947
1704018_B	*FTH1*	2.032945337	0.456676856	0.22463804	0.1147947
343563_A	*FTL*	1.514803232	0.284119973	0.187562296	0.1147947
149986_A	*FVT1*	1.387598819	0.277143788	0.199729046	0.540855
34415_A	*FVT1*	1.181339867	0.213298171	0.180556144	3.7008086
149319_A	*G1P2*	2.80241801	0.905501479	0.323114352	0.1147947
115383_A	*GADD45A*	2.243438795	0.500595568	0.223137608	0.1147947
310141_A	*GADD45A*	1.945750815	0.460050718	0.236438661	0.1147947
415112_A	*GADD45A*	1.438247119	0.319734415	0.222308399	0.2933343
174799_A	*GAMT*	1.236948817	0.25623244	0.207148781	1.8099168
33937_A	*GAS6*	3.174153204	0.750902986	0.236567972	0.1147947
42497_A	*GAS6*	2.7667813	0.723690594	0.261564076	0.1147947
306144_A	*GBA*	1.156455318	0.246397764	0.213062935	3.7008086
809588_C	*GGH*	1.652425151	0.322044503	0.194892036	0.1147947
809588_A	*GGH*	1.526364791	0.359190989	0.235324472	0.1147947
309079_A	*GJA1*	1.7496394	0.418601543	0.239250181	0.1147947
486844_A	*GJA1*	1.730395408	0.401683331	0.23213384	0.1147947
308993_A	*GJA1*	1.630740767	0.355803501	0.2181852	0.1147947
811671_A	*GLA*	1.211641369	0.223697644	0.184623643	2.5930212
132691_A	*GLRX*	2.455256475	0.485224823	0.19762694	0.1147947
324214_A	*GLRX*	2.236177807	0.417249518	0.186590492	0.1147947
195328_A	*GLRX*	1.623150716	0.359204461	0.221300744	0.1147947
323667_B	*GM2A*	1.270570704	0.243239939	0.191441482	1.2451143
50492_A	*GNAL*	1.376071077	0.317670111	0.230852982	0.540855
359224_A	*GNAS*	1.329306298	0.29933552	0.225181751	0.6702531
323165_A	*GNG11*	2.899885599	0.593409795	0.20463214	0.1147947
346926_A	*GPAA1*	1.358149157	0.264834645	0.19499673	0.540855

346135_A	*GPC1*	1.192145199	0.260102566	0.218180274	2.5930212
783646_A	*GPC1*	1.139013708	0.275889451	0.24221785	3.7008086
774491_A	*GPX1*	1.258217179	0.236755489	0.188167427	1.8099168
stSG89160	*HMOX1*	2.335743948	0.522001469	0.223484029	0.1147947
42724_A	*HPCAL1*	2.16035503	0.408695713	0.189179883	0.1147947
24772_A	*HPCAL1*	1.967639247	0.410667824	0.208710933	0.1147947
35091_A	*HSPA1L*	2.521746806	0.659511659	0.26152969	0.1147947
50615_A	*HSPA1L*	2.382611916	0.593510321	0.249100711	0.1147947
33800_A	*HSPA6HSPA7*	1.864508289	0.560195393	0.30045208	0.1147947
300131_B	*HSPB1*	3.259099605	0.829192399	0.254423767	0.1147947
128225_A	*HSPE1*	1.940063355	0.345028196	0.177843778	0.1147947
148057_A	*ID3*	1.743671316	0.370913733	0.212719983	0.1147947
249092_A	*IER3*	4.125113784	0.737565013	0.178798707	0.1147947
259649_A	*IER3*	3.816384477	0.697503046	0.182765403	0.1147947
788174_A	*IFIT1*	1.734059861	0.726378185	0.41888876	0.1147947
345996_A	*IFITM1*	1.754524606	0.421910034	0.240469716	0.1147947
150355_A	*IFITM1*	1.633038501	0.39390169	0.24120784	0.1147947
154387_A	*IFITM2*	1.525078108	0.383972356	0.251772256	0.1147947
322180_A	*IFITM2*	1.393072132	0.345515169	0.24802389	0.2933343
364516_A	*IFNGR1*	1.159971878	0.216983699	0.187059448	3.7008086
196375_A	*IGFBP3*	5.288678888	1.306580741	0.247052387	0.1147947
266838_A	*IGFBP3*	5.244309778	1.220196349	0.232670533	0.1147947
147469_B	*IGFBP4*	4.678401532	0.974899263	0.208382982	0.1147947
273587_A	*IGFBP4*	3.998095084	1.050763738	0.262816095	0.1147947
356653_A	*IGFBP6*	3.79436122	0.851766009	0.224482056	0.1147947
299204_A	*IGFBP7*	4.929952973	1.11836873	0.226851805	0.1147947
324655_B	*IL1B*	7.964922517	2.252648825	0.282821185	0.1147947
183087_A	*IL3RA*	1.130922964	0.223468743	0.197598555	3.7008086
811740_A	*ITGA2*	4.325616514	1.354119453	0.313046579	0.1147947
50182_A	*ITGA2*	2.094484818	0.369506883	0.176418983	0.1147947
251172_A	*ITGB5*	2.015040768	0.321967965	0.159782358	0.1147947
770859_A	*ITGB5*	1.165726513	0.247941839	0.212692974	3.7008086
153213_A	*JUNB*	1.189579084	0.229292345	0.192750821	2.5930212
344988_A	*KRTHA3A*	1.646978583	0.341055546	0.207079527	0.1147947
129532_A	*KYNU*	1.200479092	0.324962637	0.270694124	2.5930212
32609_A	*LAMA4*	2.988426099	0.516494461	0.172831599	0.1147947
726425_B	*LAMA4*	2.763503424	0.55251818	0.199933959	0.1147947
157819_A	*LAMB2*	2.532032148	0.476871704	0.188335564	0.1147947
324122_B	*LDHA*	8.028896635	2.624870275	0.326927895	0.1147947
321351_A	*LGMN*	1.436904385	0.24159453	0.168135425	0.2933343
stSG89454	*LIF*	1.34912493	0.234036799	0.173473037	0.6702531
244990_A	*LIPA*	2.11252307	0.413727036	0.195844979	0.1147947
49584_A	*LIPA*	1.658205932	0.421064849	0.25392796	0.1147947
723880_A	*LOXL1*	1.345868933	0.314113158	0.2333906	0.6702531
667364_A	*LOXL1*	1.250669747	0.284761094	0.227686881	1.8099168
297957_A	*LPXN*	1.936786007	0.346144751	0.178721217	0.1147947
36636_A	*LRP11*	1.568454939	0.271510331	0.173106874	0.1147947
783679_A	*LTBP1*	2.368387486	0.480810165	0.203011614	0.1147947
788591_A	*LTBP1*	2.235368385	0.596012691	0.266628398	0.1147947
230488_A	*LY6E*	1.44444465	0.288035193	0.199408952	0.2933343

809579_B	*LY6E*	1.214349873	0.312162516	0.257061431	2.5930212
1467480_A	*MAN2A1*	2.441484852	0.567376257	0.232389833	0.1147947
212497_A	*MAN2A1*	1.501235136	0.309111931	0.205905074	0.2114793
112207_A	*MANBA*	1.949171985	0.517521124	0.265508189	0.1147947
23356_B	*MAP1LC3B*	1.807853715	0.3664981	0.202725529	0.1147947
33826_A	*MAP2K1*	1.269227755	0.233265363	0.183785268	1.2451143
1659533_B	*MATN4*	1.17577224	0.346835106	0.294984942	3.7008086
50437_A	*MCL1*	1.485030602	0.357392318	0.240663268	0.2114793
267815_A	*MCP*	3.354105738	0.685348926	0.204331342	0.1147947
49200_A	*MGLL*	1.352159911	0.254568936	0.188268366	0.540855
200814_A	*MME*	3.850518386	0.886517704	0.230233339	0.1147947
785655_A	*MME*	3.237737371	0.887022103	0.273963574	0.1147947
241959_A	*MME*	3.189783035	0.831479348	0.260669562	0.1147947
342581_A	*MRC2*	1.425242019	0.317747989	0.222943181	0.2933343
232772_A	*MT1B*	3.520782005	0.705761345	0.200455849	0.1147947
66946_A	*MT1B*	2.914490933	0.729428811	0.250276576	0.1147947
202535_A	*MT1K*	3.816101628	0.712679591	0.186755925	0.1147947
240803_A	*MT1K*	3.601722929	0.764698793	0.212314719	0.1147947
202535_C	*MT1K*	3.451130278	0.777518448	0.225293856	0.1147947
274164_A	*MT1X*	3.478233041	0.736878633	0.211854302	0.1147947
293137_A	*MT1X*	3.451681448	0.668014968	0.193533203	0.1147947
111081_A	*MT1X*	3.37467539	0.730871508	0.216575351	0.1147947
297392_A	*MT1X*	3.255690072	0.730651496	0.224422927	0.1147947
2019011_A	*MT3*	1.701108999	0.450770278	0.264986122	0.1147947
26128_B	*MTCYB*	1.414063391	0.394262415	0.278815234	0.2933343
365623_A	*MTND4*	1.378145487	0.370033132	0.268500775	0.540855
149218_A	*MTND4*	1.327332367	0.351178383	0.264574565	0.6702531
201516_B	*MTND4*	1.258131213	0.320689865	0.254893816	1.8099168
789273_A	*NAB1*	1.36341585	0.245877605	0.180339406	0.540855
365534_A	*NBL1*	2.021990812	0.40610353	0.20084341	0.1147947
327407_B	*NDRG1*	2.722220002	0.615184139	0.225986194	0.1147947
124123_A	*NDUFB5*	1.147053354	0.236842199	0.206478799	3.7008086
39620_A	*NEDD4L*	1.381045339	0.281495682	0.20382798	0.540855
258822_A	*NGFRAP1*	2.612927945	0.461555165	0.176642898	0.1147947
347367_A	*NGFRAP1*	2.250189737	0.449254534	0.199651846	0.1147947
110423_A	*NINJ1*	2.123651045	0.507314104	0.238887695	0.1147947
147436_A	*NINJ1*	2.072167637	0.415878362	0.200697258	0.1147947
177016_A	*NOVA2*	1.37027218	0.249855431	0.182340001	0.540855
293109_B	*NP*	1.567377648	0.309235319	0.19729471	0.1147947
202988_A	*NPC1*	1.663118673	0.291274954	0.175137805	0.1147947
269815_A	*NR4A3*	4.527217429	0.991991646	0.219117297	0.1147947
1644118_A	*NR6A1*	1.598960723	0.292282016	0.182794994	0.1147947
49439_B	*NRG1*	1.172811911	0.244339996	0.208336899	3.7008086
269423_A	*OSBPL3*	1.305271519	0.244538529	0.187346866	0.6702531
139540_A	*OSBPL3*	1.19372792	0.206909898	0.173330869	2.5930212
772905_A	*P4HA1*	2.362404042	0.748989788	0.317045592	0.1147947
342410_A	*P4HA2*	6.745628577	1.2130375	0.179825718	0.1147947
188294_B	*P4HB*	3.025971506	0.570090295	0.188399096	0.1147947
140806_A	*PAM*	4.249113489	0.770093843	0.181236355	0.1147947
304879_A	*PAM*	3.153605654	0.641358445	0.203373064	0.1147947

470764_A	*PAM*	3.079869018	0.632469413	0.205355945	0.1147947
44675_A	*PAPSS1*	1.536727565	0.266474378	0.173403786	0.1147947
266830_A	*PCBD*	1.815187901	0.387185957	0.213303513	0.1147947
299912_A	*PCBD*	1.481922866	0.288394383	0.194608228	0.2114793
363151_A	*PEA15*	1.608637158	0.281958723	0.175278012	0.1147947
340619_B	*PEX6*	1.707533333	0.334891469	0.196125875	0.1147947
41929_A	*PICALM*	1.259019158	0.228582184	0.181555763	1.8099168
27749_A	*PKIA*	1.612768135	0.327652986	0.203161868	0.1147947
28009_C	*PKIA*	1.185799187	0.206029251	0.173747168	2.5930212
810017_A	*PLAT*	7.546881391	1.838379525	0.243594596	0.1147947
46749_A	*PLAT*	7.321109635	1.968082238	0.268822943	0.1147947
127982_A	*PLAT*	3.744963671	1.735059613	0.463304791	0.1147947
143356_A	*PLAU*	6.150382585	1.55352965	0.252590734	0.1147947
22790_B	*PLAUR*	3.482506688	0.723047776	0.207622796	0.1147947
322441_A	*PLAUR*	3.447348951	0.646905198	0.187652949	0.1147947
365623_B	*PLD3*	1.38072121	0.312228505	0.226134358	0.540855
310449_A	*PLOD2*	8.978984234	1.678274775	0.186911429	0.1147947
139570_A	*PLOD2*	6.637058613	1.628755388	0.245403195	0.1147947
153114_A	*PLXNB2*	2.197425746	0.534301013	0.243148609	0.1147947
34853_A	*POLD4*	2.2493383	0.419776738	0.186622323	0.1147947
38922_A	*PON2*	1.523308181	0.338315329	0.222092504	0.1147947
51565_A	*PON2*	1.290450878	0.22209141	0.17210373	1.2451143
161368_A	*PPIB*	1.309349829	0.270914254	0.206907465	0.6702531
249588_A	*PRDX6*	1.842438305	0.385282612	0.209115611	0.1147947
148568_A	*PRDX6*	1.760770099	0.376775861	0.213983564	0.1147947
21436_A	*PRDX6*	1.686966481	0.404404035	0.239722626	0.1147947
49691_A	*PRNP*	8.108825075	1.549904825	0.191138027	0.1147947
812048_A	*PRNP*	8.021120894	1.545826275	0.192719483	0.1147947
51689_A	*PRNP*	7.620378727	1.484939075	0.194864209	0.1147947
300659_A	*PROCR*	1.25132003	0.227169153	0.181543608	1.8099168
197712_A	*PSAP*	1.579994315	0.321181586	0.203280216	0.1147947
246780_A	*PSAP*	1.524001271	0.315495707	0.207018008	0.1147947
1187505_A	*PTGS2*	1.479052401	0.394139061	0.266480796	0.2114793
1651583_A	*PTGS2*	1.266610102	0.352909133	0.278624916	1.2451143
42739_A	*PTP4A1*	2.119166112	0.415121244	0.195888959	0.1147947
297596_A	*PTP4A1*	1.665941602	0.361427831	0.216951081	0.1147947
241705_A	*PYGL*	1.426535101	0.283999754	0.199083607	0.2933343
356742_A	*PYGL*	1.217874019	0.245221218	0.201351876	2.5930212
165952_B	*QSCN6*	1.864134742	0.58330179	0.312907526	0.1147947
266103_A	*RAB7*	1.896376662	0.356290021	0.187879354	0.1147947
37917_A	*RCN2*	1.145407934	0.220131417	0.192186042	3.7008086
145098_A	*RECK*	1.838657942	0.402259533	0.218778884	0.1147947
323346_C	*RGS3*	1.489058135	0.28831151	0.19362005	0.2114793
148753_A	*RNF11*	2.154846763	0.408014144	0.189347173	0.1147947
356665_A	*RRAD*	1.234261176	0.216220151	0.175181846	1.8099168
154080_A	*S100A11*	1.671393654	0.448923005	0.268592024	0.1147947
154167_A	*S100A11*	1.445753277	0.413336326	0.285896863	0.2114793
788143_A	*SAT*	4.622189824	1.137447168	0.246084045	0.1147947
1627856_A	*SCGF*	1.980843634	0.471234767	0.237895995	0.1147947
123586_A	*SDC1*	1.955850617	0.436727978	0.223293115	0.1147947

140046_A	*SEC22L1*	2.313704051	0.470394081	0.2033078	0.1147947
149724_A	*SEC22L1*	2.124401103	0.458646945	0.215894703	0.1147947
308748_A	*SERF2*	1.939299	0.389774879	0.200987511	0.1147947
212807_A	*SERF2*	1.817133814	0.412102525	0.226787109	0.1147947
198206_A	*SERPINB2*	8.050703606	1.6526033	0.205274394	0.1147947
194174_B	*SERPINB2*	7.895838725	1.72346855	0.218275551	0.1147947
323254_C	*SERPINB2*	7.789253689	1.755576338	0.225384409	0.1147947
1509935_A	*SERPINB7*	2.594958314	0.686706751	0.26463113	0.1147947
666367_A	*SERPINE1*	4.614612317	0.885334418	0.19185456	0.1147947
42669_A	*SGK*	1.239110572	0.27178862	0.2193417	1.8099168
48503_A	*SLC16A2*	2.014065801	0.371674758	0.184539531	0.1147947
24776_A	*SLC16A2*	1.249385187	0.284770715	0.227928679	1.8099168
725710_A	*SLC20A1*	2.770550223	0.509316769	0.183832354	0.1147947
135747_A	*SLC2A1*	1.664316532	0.268364743	0.161246216	0.1147947
240183_A	*SLC9A1*	1.376056197	0.277584711	0.201724836	0.540855
30272_A	*SLC9A1*	1.365240388	0.321888389	0.235774148	0.540855
180405_A	*SMPD1*	2.121697344	0.369093593	0.173961472	0.1147947
180046_A	*SMPD1*	1.730182112	0.332183401	0.191993316	0.1147947
153625_A	*SMTN*	1.852759965	0.351162235	0.189534663	0.1147947
stSG89478	*SMTN*	1.438851359	0.274296359	0.190635647	0.2933343
47107_A	*SNX3*	2.078182015	0.419168512	0.201699615	0.1147947
774477_A	*SRPX*	3.912970705	0.827488014	0.211473092	0.1147947
38048_A	*SRPX*	3.749733422	0.867286144	0.231292747	0.1147947
136059_A	*SSR4*	2.894683219	0.549298148	0.189761057	0.1147947
191550_A	*SSR4*	2.850412823	0.552459296	0.193817293	0.1147947
152315_A	*SSR4*	2.75330504	0.543787976	0.197503716	0.1147947
358184_A	*SSR4*	2.148011864	0.451995225	0.21042492	0.1147947
505118_B	*STAC*	2.539227829	0.462368876	0.182090347	0.1147947
503572_A	*STAC*	2.52018016	0.484160588	0.192113483	0.1147947
26599_A	*STAT1*	1.704238347	0.605785775	0.355458364	0.1147947
24033_A	*STAT1*	1.646393131	0.495201671	0.300779723	0.1147947
154007_A	*STC1*	3.757442759	0.985440511	0.262263612	0.1147947
153589_A	*STC1*	2.374780136	0.707330336	0.297850873	0.1147947
298134_A	*STOM*	2.117841654	0.383302671	0.180987408	0.1147947
417759_A	*TAF10*	1.128073748	0.230452984	0.204288934	3.7008086
665226_A	*TCTE1L*	1.260049135	0.289354681	0.229637617	1.8099168
52431_A	*TDE1*	1.134561071	0.196048461	0.172796746	3.7008086
346727_A	*TFPI*	1.484177778	0.357867067	0.241121429	0.2114793
360874_B	*TFPI2*	5.224806891	1.668137163	0.319272501	0.1147947
199945_A	*TGM2*	2.566041548	0.447095445	0.174235466	0.1147947
769686_A	*THY1*	1.352477302	0.339529376	0.251042569	0.540855
266325_A	*TIMP1*	10.91610607	2.314252763	0.212003506	0.1147947
270187_A	*TIMP1*	9.205273935	2.249471863	0.244367726	0.1147947
249977_A	*TIMP3*	2.973068087	0.626629495	0.210768632	0.1147947
stSG89269	*TIMP3*	1.594114385	0.285659568	0.179196406	0.1147947
770670_A	*TNFAIP3*	4.08095483	1.022831498	0.250635339	0.1147947
309943_A	*TNFAIP3*	3.66179442	0.925258211	0.252678907	0.1147947
714213_A	*TNFRSF6*	1.686535977	0.363172107	0.215336116	0.1147947
299745_B	*TNFRSF6*	1.627123567	0.331454343	0.203705699	0.1147947
33906_A	*TNRC5*	1.238023781	0.241363976	0.194959079	1.8099168

1573002_A	*TOMM34*	1.141594932	0.195620588	0.171357267	3.7008086
241195_A	*TPD52L2*	1.440198364	0.264781258	0.183850548	0.2933343
150829_A	*TXNDC4*	1.283266061	0.232476675	0.181160152	1.2451143
359721_A	*TXNIP*	5.327015086	1.184731896	0.222400702	0.1147947
299497_B	*TXNIP*	4.407601287	0.997413064	0.22629385	0.1147947
298367_A	*TXNIP*	3.353794236	0.667568731	0.199048804	0.1147947
38211_A	*UBCUBBC20orf109*	1.645188713	0.291965295	0.177466143	0.1147947
242008_B	*UBE2L6*	1.270305311	0.277200983	0.218216031	1.2451143
324168_A	*UCHL1*	2.085142163	0.359874056	0.172589698	0.1147947
323783_B	*VEGF*	2.557843758	0.683901121	0.26737408	0.1147947
109669_A	*VEGFC*	3.85389313	0.904155965	0.234608469	0.1147947
45138_A	*VEGFC*	3.582857263	0.777304058	0.216950886	0.1147947
32682_A	*VIM*	2.627069391	0.424428991	0.161559871	0.1147947
214542_A	*WFS1*	1.235162233	0.216121582	0.174974248	1.8099168
249193_A	*XPC*	1.382307111	0.275934073	0.1996185	0.540855
301777_A	*ZFP36L1*	2.438944985	0.448393523	0.18384733	0.1147947
321704_A	*ZFP36L1*	2.024609449	0.439541467	0.217099385	0.1147947
147834_A	*ZNF217*	1.237751785	0.249841411	0.20185098	1.8099168

Supplementary Figure S5: Genes Down-Regulated Upon the HMF3A Temperature Shift

Clone ID	Gene	Score(d)	Numerator(r)	Denominator(s+s0)	q-value (%)
274217_A	*AATF*	-1.101608267	-0.21840475	0.198259904	2.5930212
36393_A	*ACAT2*	-1.929007719	-0.351771374	0.182358718	0.1147947
21766_A	*ACINUS*	-1.1031446	-0.224598547	0.203598465	2.5930212
180078_A	*ACTR1A*	-1.454542009	-0.324984514	0.223427382	0.2114793
207605_A	*ACTR2*	-1.616380572	-0.352392636	0.218013407	0.1147947
40678_B	*ACTR2*	-1.416513108	-0.320101295	0.22597835	0.2114793
147706_A	*ACTR2*	-1.402314912	-0.326597148	0.232898577	0.2114793
233688_A	*ADAM12*	-2.910426368	-0.598210668	0.205540561	0.1147947
48505_A	*ADD1*	-1.1368611	-0.200582483	0.176435347	1.8099168
223345_A	*ADD1*	-1.065603956	-0.187510934	0.175966815	3.7008086
192725_A	*AKT1*	-1.152594263	-0.294289538	0.255327957	1.8099168
203165_A	*AMFR*	-1.041869056	-0.190185338	0.182542458	3.7008086
245779_A	*AP1G1*	-1.430554935	-0.240667366	0.168233571	0.2114793
46755_A	*APPBP1*	-1.42424615	-0.238781369	0.167654565	0.2114793
273010_A	*APPBP1*	-1.090299201	-0.211383503	0.193876601	2.5930212
269766_A	*ARHA*	-2.532591489	-0.450686093	0.177954516	0.1147947
51293_A	*ARHA*	-2.22631483	-0.400258626	0.179785276	0.1147947
51426_A	*ARHA*	-2.090936096	-0.407822116	0.195042841	0.1147947
179500_D	*ARHGAP1*	-1.11588671	-0.220874114	0.197935966	2.5930212
263793_A	*ARHGDIA*	-2.200611558	-0.521515831	0.236986773	0.1147947
51532_A	*ARL6IP*	-3.916674483	-0.747126533	0.19075533	0.1147947
26491_A	*ARL6IP*	-3.182329066	-0.6025089	0.189329541	0.1147947
51532_C	*ARL6IP*	-2.883481665	-0.55033678	0.190858429	0.1147947
25433_A	*ATP1B1*	-1.499174147	-0.259083719	0.172817627	0.1147947
302373_C	*ATP1B1*	-1.15728481	-0.291614532	0.251981647	1.8099168
310385_A	*ATP5B*	-2.219307663	-0.37944073	0.170972568	0.1147947
342879_B	*ATP5B*	-2.089612167	-0.358538251	0.171581242	0.1147947
34310_A	*ATP5F1*	-1.533353513	-0.29328513	0.191270393	0.1147947
46596_A	*ATP5F1*	-1.329908917	-0.254697982	0.191515358	0.540855
382331_A	*ATP5G2*	-1.624363956	-0.288120709	0.177374478	0.1147947
186287_A	*ATP5G2*	-1.12719091	-0.205584389	0.182386486	2.5930212
267284_A	*ATP5O*	-1.451362198	-0.236085806	0.162664982	0.2114793
142511_A	*ATP5O*	-1.363707455	-0.260069795	0.190707907	0.2933343
357613_A	*ATP5O*	-1.018300236	-0.19651867	0.192986963	3.7008086
789029_A	*B4GALT2*	-1.105715692	-0.254750815	0.2303945	2.5930212
300300_A	*B4GALT2*	-1.078897433	-0.244299134	0.226434067	2.5930212
141228_A	*BANF1*	-1.559650076	-0.290308526	0.186136962	0.1147947
46154_A	*BAP1*	-1.307141613	-0.218659234	0.167280448	0.540855
309883_A	*BAP1*	-1.064306299	-0.200203893	0.188107402	3.7008086
184082_A	*BAT1ATP6V1G2*	-3.198151832	-0.596922293	0.186646014	0.1147947
42638_A	*BAT2*	-1.218606315	-0.270044114	0.221600783	1.2451143
22479_A	*BAT2*	-1.021143491	-0.253249697	0.248005985	3.7008086
29256_A	*BAT3*	-1.378459134	-0.295000023	0.214007086	0.2933343
376055_A	*BAT3*	-1.045840083	-0.198348751	0.189654952	3.7008086
1860539_A	*BCAT1*	-2.467300852	-0.47283733	0.191641538	0.1147947
2009885_B	*BCAT1*	-1.731217265	-0.341151517	0.197058754	0.1147947

141318_A	*BGN*	-1.770450194	-0.400914666	0.226447864	0.1147947
563403_A	*BRRN1*	-1.273667214	-0.224471459	0.176240274	0.6702531
244767_A	*BRRN1*	-1.208391108	-0.21039688	0.17411323	1.2451143
194384_A	*BTF3*	-1.270170771	-0.230524607	0.181491034	0.6702531
416084_A	*BUB1B*	-2.093833398	-0.37798521	0.180523059	0.1147947
321627_A	*C1QBP*	-2.280474543	-0.44840381	0.196627413	0.1147947
50036_B	*C5orf13*	-3.651107474	-0.769273748	0.210696002	0.1147947
197515_A	*C7orf14*	-1.139441756	-0.267503363	0.234767035	1.8099168
666534_A	*CAD*	-1.285580155	-0.297025332	0.231043806	0.540855
38031_A	*CAD*	-1.224115331	-0.304490408	0.248743236	1.2451143
230884_A	*CALM2CALM1CALM3*	-1.386097425	-0.23087616	0.166565608	0.2933343
265613_B	*CALM2CALM1CALM3*	-1.199547072	-0.225855775	0.188284212	1.2451143
167080_A	*CALM3*	-1.454611707	-0.294783918	0.202654713	0.2114793
33672_A	*CALM3*	-1.199392855	-0.240308497	0.200358453	1.2451143
265569_A	*CAMKK2*	-1.016235047	-0.208177498	0.20485172	3.7008086
49560_A	*CAPN1*	-1.092612451	-0.233071448	0.213315753	2.5930212
32026_A	*CBARA1*	-2.985143883	-0.538078599	0.180252149	0.1147947
294207_A	*CBX1*	-1.293307831	-0.230093731	0.177911032	0.540855
300675_C	*CBX3*	-1.122300613	-0.214878564	0.191462574	2.5930212
427857_A	*CCNA2*	-2.793724859	-0.528559046	0.189195097	0.1147947
128963_A	*CCNI*	-1.46453684	-0.272211157	0.185868426	0.2114793
261680_A	*CCNI*	-1.381499428	-0.243754823	0.176442217	0.2933343
299705_A	*CCT2*	-1.67425664	-0.31148021	0.186040899	0.1147947
299176_B	*CCT2*	-1.339682944	-0.261810171	0.195426964	0.2933343
243343_A	*CCT2*	-1.066604266	-0.177711795	0.166614555	3.7008086
796474_A	*CDC2*	-2.814351939	-0.543541143	0.193131902	0.1147947
121716_D	*CDC25B*	-4.446605616	-0.672172829	0.15116538	0.1147947
785382_A	*CDC25B*	-1.915008421	-0.494175881	0.258054156	0.1147947
429755_A	*CDC25C*	-1.122873327	-0.192401027	0.171347046	2.5930212
stSG89407	*CDC42EP1*	-1.181108603	-0.228334625	0.193322294	1.2451143
753401_A	*CDH2*	-1.798731237	-0.301563753	0.167653592	0.1147947
23806_A	*CDH2*	-1.756060087	-0.275817883	0.157066313	0.1147947
264598_A	*CDK4*	-1.879388187	-0.367353793	0.195464564	0.1147947
364403_A	*CDKN2C*	-1.70822532	-0.428893901	0.251075719	0.1147947
121357_A	*CDKN3*	-1.326060401	-0.256520288	0.193445403	0.540855
124345_A	*CENPF*	-2.127086181	-0.362568906	0.170453322	0.1147947
784170_A	*CENPF*	-1.027011354	-0.293000688	0.285294497	3.7008086
724615_A	*CHC1*	-1.504769554	-0.268509025	0.178438635	0.1147947
327662_A	*CIRBP*	-2.661304475	-0.611259259	0.229684076	0.1147947
221318_A	*CKS2*	-1.088325055	-0.211834794	0.194642945	2.5930212
781690_A	*CLTC*	-1.905642554	-0.337375244	0.17704015	0.1147947
783875_A	*CLTC*	-1.771076418	-0.353081204	0.199359666	0.1147947
358506_A	*COL16A1*	-1.221494006	-0.276603056	0.226446511	1.2451143
323321_A	*COL1A1*	-3.406214772	-0.714027575	0.209624942	0.1147947
298509_A	*COL1A1*	-2.800748263	-0.662844685	0.236666998	0.1147947
214997_A	*COL1A1*	-1.60353379	-0.3496424	0.218044922	0.1147947
195273_A	*COL2A1*	-3.896091874	-0.890423566	0.228542754	0.1147947
229864_A	*COL2A1*	-2.379204187	-0.68725961	0.28886113	0.1147947
359255_A	*COL5A2*	-3.854247881	-0.859322228	0.222954583	0.1147947
138991_A	*COL6A3*	-1.821133103	-0.387043488	0.21252894	0.1147947

309817_A	*COPE*	-1.235951549	-0.237189413	0.191908342	0.6702531
267101_A	*COPS3*	-1.364570137	-0.24744425	0.181334944	0.2933343
178323_A	*COX4I1*	-1.034386774	-0.189208641	0.182918659	3.7008086
172265_A	*COX8*	-1.689387244	-0.325100071	0.192436679	0.1147947
322848_A	*COX8*	-1.446668547	-0.296225948	0.204764214	0.2114793
365740_A	*CPSF5*	-1.959780335	-0.387277704	0.197612812	0.1147947
753091_A	*CPSF5*	-1.234607166	-0.24588704	0.199162168	0.6702531
33690_A	*CPSF6*	-1.384031372	-0.283094919	0.204543715	0.2933343
264153_A	*CPSF6*	-1.226387071	-0.235133509	0.191728627	0.6702531
292806_A	*CSE1L*	-1.03020229	-0.197274614	0.191491143	3.7008086
292806_C	*CSE1L*	-1.012641295	-0.171565473	0.169423738	3.7008086
44477_B	*CTNND1*	-1.318050008	-0.232662311	0.176520094	0.540855
25588_A	*CUGBP1*	-1.297910399	-0.221408267	0.170588253	0.540855
141887_A	*CUGBP1*	-1.22910999	-0.261853673	0.21304332	0.6702531
324910_A	*CYR61*	-1.745317477	-0.357379121	0.204764535	0.1147947
310770_A	*DAG1*	-1.51408885	-0.331810653	0.219148733	0.1147947
375715_A	*DAZAP2*	-2.106807573	-0.391263158	0.185713761	0.1147947
25872_A	*DAZAP2*	-1.410973278	-0.312723506	0.221636732	0.2114793
33487_A	*DCTN2*	-1.19594153	-0.22553024	0.188579654	1.2451143
39341_A	*DCTN2*	-1.078485616	-0.216477496	0.200723582	2.5930212
121348_A	*DCTN3*	-1.255454626	-0.265621495	0.211573951	0.6702531
263741_A	*DDX17*	-1.043361138	-0.226436077	0.2170256	3.7008086
127925_A	*DDX18*	-1.129767754	-0.233521133	0.206698352	1.8099168
267325_A	*DDX38*	-1.371901338	-0.276196259	0.201323704	0.2933343
120090_B	*DDX38*	-1.134026678	-0.281731311	0.248434465	1.8099168
306186_A	*DDX5*	-2.146423066	-0.439247721	0.204641726	0.1147947
300363_A	*DDX9*	-1.652646543	-0.303365885	0.183563682	0.1147947
294421_A	*DDX9*	-1.4587021	-0.316486053	0.216964144	0.2114793
774194_A	*DEK*	-2.011148315	-0.400053443	0.198917922	0.1147947
301013_A	*DHFR*	-1.222344549	-0.254581909	0.208273444	1.2451143
152833_B	*DKC1*	-1.57974208	-0.336275139	0.212867115	0.1147947
502104_B	*DKC1*	-1.293415249	-0.259929058	0.200963347	0.540855
33578_A	*DLAT*	-1.528599593	-0.320688251	0.209792186	0.1147947
124303_A	*DLAT*	-1.344588569	-0.272932871	0.20298616	0.2933343
357373_A	*DLG7*	-1.660310962	-0.269347253	0.162226992	0.1147947
259596_A	*DLG7*	-1.459391096	-0.287737544	0.197162738	0.2114793
768241_A	*DNMT1*	-1.666633413	-0.293560428	0.176139771	0.1147947
206863_A	*DNMT1*	-1.19621015	-0.2208233	0.18460243	1.2451143
376522_A	*DPYSL3*	-4.517472614	-0.728853438	0.161340975	0.1147947
360263_A	*DPYSL3*	-3.412499349	-0.766381566	0.224580722	0.1147947
427768_A	*DSTN*	-1.526052167	-0.329512129	0.215924551	0.1147947
471871_A	*DTYMK*	-1.508559023	-0.266901435	0.176924755	0.1147947
784852_B	*DTYMK*	-1.086117418	-0.180654594	0.16633063	2.5930212
342323_A	*DUT*	-1.634061006	-0.275109183	0.168359187	0.1147947
730908_A	*DUT*	-1.556599733	-0.277000828	0.177952509	0.1147947
195924_A	*E2F4*	-1.365377482	-0.324660448	0.237780725	0.2933343
51776_A	*EBNA1BP2*	-2.020148734	-0.393318091	0.194697591	0.1147947
22918_A	*EBNA1BP2*	-1.330907376	-0.301018723	0.226175561	0.540855
33505_A	*EBP*	-1.569870322	-0.268565611	0.171075029	0.1147947
121153_A	*ECHS1*	-1.083407395	-0.207357357	0.191393707	2.5930212

136352_A	*EFEMP1*	-3.310454999	-0.580694739	0.175412364	0.1147947
33636_A	*EIF3S7*	-1.342426873	-0.246345077	0.18350726	0.2933343
204614_A	*EIF4A1*	-2.672236744	-0.460123498	0.172186652	0.1147947
37928_A	*EIF4A1*	-2.485915089	-0.417912015	0.168111943	0.1147947
25988_A	*EIF4G1*	-1.150433823	-0.32989691	0.286758702	1.8099168
774115_B	*EIF5*	-1.496594309	-0.265999268	0.177736388	0.1147947
345208_A	*ELAVL1*	-1.196621869	-0.249188973	0.208243706	1.2451143
309908_A	*EMD*	-1.768637747	-0.384310625	0.217291882	0.1147947
307996_B	*ENO1*	-1.799908889	-0.449396518	0.24967737	0.1147947
346468_B	*EPB41L2*	-1.308854095	-0.221641572	0.169340167	0.540855
358350_A	*EWSR1*	-2.814579739	-0.51029393	0.181303774	0.1147947
stSG89196	*EWSR1*	-1.2119471	-0.246871562	0.203698298	1.2451143
376635_A	*FBL*	-3.551044142	-0.594129201	0.167311128	0.1147947
784863_A	*FNBP3*	-1.840609359	-0.340706998	0.185105545	0.1147947
1677198_A	*FNBP4*	-1.277450729	-0.214926292	0.168246248	0.6702531
127266_A	*FOXM1*	-2.245276859	-0.546206319	0.243269028	0.1147947
259115_A	*FOXM1*	-1.879398314	-0.378534859	0.20141279	0.1147947
376180_A	*FPGS*	-1.232986206	-0.252778494	0.205013238	0.6702531
300482_B	*FUBP3*	-1.34978245	-0.272815238	0.202117933	0.2933343
stSG89133	*G22P1*	-2.629734425	-0.387191545	0.147235988	0.1147947
297780_A	*GBAS*	-1.52647105	-0.280922438	0.184033911	0.1147947
41510_A	*GCN1L1*	-1.094589557	-0.200658369	0.183318366	2.5930212
40567_A	*GCN1L1*	-1.027195393	-0.252099415	0.245424986	3.7008086
290841_A	*GNAI2*	-1.650310972	-0.363866136	0.220483377	0.1147947
263350_A	*GNAI2*	-1.589961129	-0.329301458	0.207112898	0.1147947
774750_A	*GNAI3*	-1.743422654	-0.353959658	0.203025731	0.1147947
265467_A	*GNB1*	-2.321636389	-0.370807649	0.159718227	0.1147947
249289_A	*GNB1*	-1.679346403	-0.305929376	0.182171692	0.1147947
308856_A	*GNB2*	-1.314453671	-0.338520609	0.257537117	0.540855
257586_A	*GNB2L1*	-2.332468616	-0.403297489	0.172905859	0.1147947
302555_A	*GNB2L1*	-1.895763849	-0.329957197	0.174049736	0.1147947
198132_A	*GNB2L1*	-1.633454771	-0.2663448	0.163056122	0.1147947
298453_A	*GPRK6*	-1.324576577	-0.26604159	0.20085029	0.540855
37324_B	*GRB2*	-1.183799229	-0.247201529	0.208820485	1.2451143
42058_A	*GRB2*	-1.085127943	-0.240946025	0.222043886	2.5930212
53322_B	*GTF3C1*	-1.234464381	-0.246132659	0.199384172	0.6702531
stSG89400	*GTSE1*	-2.748091123	-0.537345648	0.195534145	0.1147947
stSG89322	*H1F0*	-1.51041639	-0.259876778	0.172056381	0.1147947
122926_A	*H2AFZ*	-2.379288635	-0.494502624	0.207836332	0.1147947
22188_A	*H3F3BH3F3A*	-3.028883498	-0.640257171	0.211383888	0.1147947
186993_A	*H3F3BH3F3A*	-2.457518755	-0.4942257	0.2011076	0.1147947
298610_B	*H3F3BH3F3A*	-1.656941564	-0.328771481	0.198420685	0.1147947
754345_A	*HDAC1*	-1.246245015	-0.242644511	0.194700487	0.6702531
309924_A	*HDAC2*	-1.174466822	-0.214771354	0.18286711	1.2451143
813673_A	*HDGF*	-2.68186023	-0.585361218	0.218266862	0.1147947
787878_A	*HDLBP*	-1.221799627	-0.349866301	0.286353255	1.2451143
212656_A	*HELZ*	-1.115406527	-0.190995597	0.171234068	2.5930212
233606_B	*HIP2*	-1.294536508	-0.26827457	0.207236001	0.540855
stSG89294	*HMG17L1*	-2.978637086	-0.734486298	0.246584688	0.1147947
139221_A	*HMGB1*	-2.542283243	-0.558288045	0.21960104	0.1147947

124257_A	*HMGB2*	-5.120596625	-0.976238	0.190649268	0.1147947
267145_A	*HMGB2*	-4.517672133	-0.950753866	0.210452162	0.1147947
124836_A	*HMGB3*	-1.382476264	-0.303217831	0.219329503	0.2933343
298516_A	*HNRPA2B1*	-2.127770314	-0.524306858	0.246411398	0.1147947
321813_A	*HNRPAB*	-1.676417498	-0.293586624	0.175127392	0.1147947
35170_A	*HNRPC*	-1.564159636	-0.291982568	0.186670568	0.1147947
310781_A	*HNRPC*	-1.405787877	-0.282237351	0.200768093	0.2114793
345600_B	*HNRPC*	-1.017826482	-0.201647949	0.198116233	3.7008086
358457_A	*HNRPH1*	-2.435847343	-0.529400996	0.21733751	0.1147947
321590_A	*HNRPH3*	-1.030145139	-0.278872915	0.270712256	3.7008086
681973_A	*HNRPH3*	-1.012614769	-0.244082466	0.24104178	3.7008086
306373_C	*HNRPL*	-1.703457733	-0.332591591	0.195244992	0.1147947
296047_A	*HNRPM*	-2.308710011	-0.452555824	0.196021077	0.1147947
487501_A	*HNRPR*	-2.498226672	-0.496478709	0.198732451	0.1147947
784486_A	*HNRPU*	-2.407918681	-0.500964209	0.208048641	0.1147947
767828_A	*HPS1*	-1.176612892	-0.200666413	0.170545822	1.2451143
323621_A	*HRMT1L2*	-3.217584367	-0.664009935	0.206369083	0.1147947
200018_A	*HRMT1L2*	-3.091093497	-0.710047038	0.229707396	0.1147947
361171_A	*HTATIP*	-1.385371257	-0.259282285	0.187157257	0.2933343
51683_A	*IDH2*	-1.50004617	-0.294972668	0.196642392	0.1147947
713714_A	*IDH3B*	-1.469193534	-0.32270691	0.219649013	0.2114793
261971_A	*IGHDPCOLN3*	-1.743386154	-0.422740011	0.242482143	0.1147947
810831_A	*ILF2*	-1.165740307	-0.229792324	0.197121368	1.8099168
231139_B	*ILF3*	-3.014867045	-0.710908113	0.235800817	0.1147947
343368_A	*ILF3*	-2.855783385	-0.675759681	0.23662848	0.1147947
29607_A	*IMPDH2*	-2.474769402	-0.5307602	0.214468548	0.1147947
36485_A	*IMPDH2*	-2.351680184	-0.549612353	0.2337105	0.1147947
280626_B	*IQGAP1*	-1.274297277	-0.254728334	0.199897103	0.6702531
682172_A	*IREB2*	-1.114658691	-0.181356606	0.162701468	2.5930212
667376_A	*IREB2*	-1.077482912	-0.232225433	0.215525862	2.5930212
154015_A	*ITGAL*	-1.147151315	-0.202881396	0.1768567	1.8099168
271814_A	*ITGB4BP*	-1.9570155	-0.370541439	0.189340064	0.1147947
415761_A	*ITGB4BP*	-1.882793837	-0.35539911	0.188761564	0.1147947
810531_A	*ITPA*	-1.277974272	-0.283295605	0.221675515	0.6702531
190242_A	*KARS*	-1.483694085	-0.404263889	0.272471188	0.1147947
150722_A	*KHDRBS1*	-2.187679411	-0.455930911	0.208408466	0.1147947
40983_A	*KIF22*	-1.134469149	-0.332864936	0.293410303	1.8099168
212780_A	*KIF23*	-3.06029672	-0.619498028	0.202430707	0.1147947
327575_A	*KIFC1*	-1.593468131	-0.392063521	0.246044156	0.1147947
292933_A	*KIFC1*	-1.587454522	-0.269163136	0.169556439	0.1147947
127980_A	*KNTC1*	-1.586752991	-0.32477399	0.204678354	0.1147947
112136_A	*KNTC1*	-1.091659425	-0.189095067	0.173218004	2.5930212
21687_A	*KPNA3*	-1.10183866	-0.209319362	0.189972788	2.5930212
47696_A	*KPNA6*	-1.180910154	-0.316213094	0.267770663	1.2451143
307553_A	*KRAS2*	-1.10576374	-0.189681106	0.171538547	2.5930212
49630_A	*LAMP2*	-2.069272499	-0.362178548	0.175026995	0.1147947
44050_A	*LASP1*	-2.513527146	-0.536836703	0.213579035	0.1147947
795814_A	*LASP1*	-2.300827226	-0.428503288	0.186238794	0.1147947
307225_A	*LBR*	-1.416479103	-0.306969587	0.216713107	0.2114793
34461_A	*LGALS3*	-1.326206989	-0.231290836	0.174400254	0.540855

1304246_A	*LMNB1*	-1.20425948	-0.240469615	0.19968256	1.2451143
50031_A	*LMO4*	-1.022054884	-0.202191091	0.197828017	3.7008086
415554_A	*LRP8*	-1.18201612	-0.197105635	0.166753762	1.2451143
37830_B	*LYPLA1*	-1.062193157	-0.254174805	0.239292451	3.7008086
25773_A	*LYPLA1*	-1.020666408	-0.212661262	0.208355306	3.7008086
298904_A	*M11S1*	-1.151865859	-0.20405309	0.177150046	1.8099168
214636_A	*MADH5*	-1.135811149	-0.216060108	0.19022538	1.8099168
362634_A	*MAPK3*	-1.026191242	-0.229951559	0.224082559	3.7008086
447509_A	*MARCKS*	-1.485488715	-0.277253478	0.186641255	0.1147947
32555_B	*MAT2A*	-2.298518027	-0.374183266	0.16279327	0.1147947
42288_A	*MATR3*	-1.182913424	-0.232796971	0.19679967	1.2451143
365824_A	*MAZ*	-3.319265512	-0.775618194	0.233671633	0.1147947
713558_A	*MBD2*	-1.149447625	-0.280910867	0.244387705	1.8099168
366261_A	*MBD2*	-1.136345778	-0.266323455	0.234368323	1.8099168
199078_A	*MBD3*	-1.354844574	-0.303943295	0.224338128	0.2933343
263092_A	*MBNL1*	-1.711339535	-0.367747194	0.214888505	0.1147947
375917_A	*MCM2*	-1.70210821	-0.376563334	0.221233487	0.1147947
376607_A	*MCM5*	-2.560604179	-0.428073551	0.167176776	0.1147947
stSG89161	*MCM5*	-1.9955808	-0.423921569	0.21243017	0.1147947
1842548_A	*MDFI*	-1.577847232	-0.292321759	0.185266199	0.1147947
42363_A	*ME3*	-1.103155067	-0.225910002	0.204785355	2.5930212
42991_A	*MEIS2*	-2.1751063	-0.456940825	0.210077468	0.1147947
796122_A	*MELK*	-1.10941924	-0.244153646	0.220073384	2.5930212
327289_A	*MELK*	-1.092076318	-0.194250724	0.177872847	2.5930212
240795_A	*MKI67*	-4.236052516	-0.840978798	0.198528888	0.1147947
688005_A	*MKI67*	-2.670672759	-0.54625613	0.204538773	0.1147947
300634_A	*MMP2*	-1.201995119	-0.331789097	0.276031983	1.2451143
166947_A	*MMS19L*	-1.129388101	-0.183549247	0.162520968	1.8099168
324917_A	*MORF4L2*	-1.377996857	-0.248981965	0.180683986	0.2933343
359821_A	*MRPL28*	-1.240230596	-0.254995286	0.205603125	0.6702531
32938_A	*MRPL3*	-1.981364428	-0.406982083	0.205404961	0.1147947
591864_C	*MRPL3*	-1.409585838	-0.217418079	0.154242525	0.2114793
267781_A	*MSC*	-1.607944808	-0.282968259	0.175981326	0.1147947
1581142_A	*MSH5*	-1.147307057	-0.220785283	0.192437832	1.8099168
755699_A	*MYBL2*	-4.490209745	-0.941644225	0.209710521	0.1147947
728122_A	*MYL6*	-2.166220372	-0.396317898	0.182953638	0.1147947
327155_A	*MYL6*	-2.106224398	-0.328717391	0.156069501	0.1147947
147328_A	*NAPA*	-1.313898105	-0.240453418	0.18300766	0.540855
34607_A	*NDUFA9*	-2.061436429	-0.350491554	0.170022975	0.1147947
140205_A	*NDUFB7*	-1.144886724	-0.205276287	0.179298338	1.8099168
132618_A	*NDUFB7*	-1.089236238	-0.237911596	0.218420567	2.5930212
27542_A	*NDUFV1*	-1.367630905	-0.335280515	0.24515424	0.2933343
126868_A	*NFIC*	-1.281125929	-0.363998316	0.28412376	0.6702531
240186_A	*NFIC*	-1.207489682	-0.346011304	0.286554253	1.2451143
49705_A	*NID*	-1.473215613	-0.40916399	0.277735307	0.1147947
300041_B	*NME1*	-1.468302866	-0.283125401	0.192824933	0.2114793
146758_A	*NNMT*	-1.466173903	-0.290044692	0.197824208	0.2114793
296513_A	*NOL5A*	-1.511829501	-0.291638457	0.19290433	0.1147947
813387_A	*NQO1*	-1.257447548	-0.222176848	0.17668876	0.6702531
289570_A	*NSMAF*	-1.248557477	-0.207929625	0.166535885	0.6702531

365687_B	*NUMA1*	-1.506936899	-0.295511999	0.19610111	0.1147947
231749_A	*NUMA1*	-1.360969801	-0.357950286	0.263011189	0.2933343
27548_A	*NUP153*	-1.197667435	-0.249663614	0.208458213	1.2451143
130371_B	*NUP155*	-1.966707395	-0.414508999	0.210762923	0.1147947
281853_A	*NUP160*	-1.07870725	-0.193133849	0.179041949	2.5930212
1030933_A	*ODF2*	-1.153244846	-0.227107633	0.196929242	1.8099168
34628_A	*OGT*	-1.533529479	-0.298222541	0.194468085	0.1147947
28012_A	*OGT*	-1.153135154	-0.203297139	0.17629949	1.8099168
272955_A	*PAFAH1B1*	-1.223553371	-0.24075274	0.196765213	1.2451143
113280_A	*PAFAH1B3*	-1.189355934	-0.259054504	0.217810746	1.2451143
26467_B	*PAFAH1B3*	-1.158084959	-0.21710914	0.18747255	1.8099168
44839_A	*PAICS*	-2.461060018	-0.460883629	0.187270373	0.1147947
306418_A	*PAICS*	-2.268462137	-0.461739063	0.203547177	0.1147947
1406874_A	*PAWRPPP1R12A*	-1.588072864	-0.306403856	0.192940679	0.1147947
250248_A	*PCBP2*	-1.280300863	-0.284903018	0.222528177	0.6702531
343368_B	*PCM1*	-1.304849079	-0.266129941	0.203954576	0.540855
198513_A	*PCNT2*	-1.16643632	-0.257616452	0.220857708	1.8099168
39040_A	*PCOLCE*	-1.178543741	-0.237184635	0.201252297	1.2451143
44421_A	*PCTK1*	-1.115417718	-0.288505361	0.258652303	2.5930212
29687_A	*PEPD*	-1.148920229	-0.228848177	0.199185436	1.8099168
30292_A	*PEPD*	-1.033198996	-0.18143859	0.175608562	3.7008086
360258_A	*PES1*	-1.933159498	-0.389975346	0.201729524	0.1147947
360757_A	*PES1*	-1.647986236	-0.322002813	0.195391688	0.1147947
271324_A	*PIGA*	-1.338910745	-0.324403248	0.242288927	0.2933343
180425_A	*PIK4CA*	-1.448457886	-0.286629794	0.197886177	0.2114793
346679_A	*PITPN*	-1.428830886	-0.284208464	0.198909799	0.2114793
24659_A	*PLEKHC1*	-1.153399884	-0.218675409	0.189592016	1.8099168
211287_B	*PLP2*	-1.205603689	-0.249522958	0.206969306	1.2451143
268928_A	*PMSCL1*	-1.940608254	-0.381424538	0.196548962	0.1147947
813548_A	*PMSCL2*	-1.711263162	-0.323155233	0.188840174	0.1147947
300658_A	*PMSCL2*	-1.311025053	-0.247490306	0.188776183	0.540855
299083_A	*POLD2*	-1.208699084	-0.242964877	0.201013536	1.2451143
469884_A	*POLD2*	-1.094093309	-0.204312274	0.186741179	2.5930212
264589_A	*POLR2A*	-1.901962274	-0.339520949	0.178510874	0.1147947
246310_A	*POLR2A*	-1.295595846	-0.27161285	0.209643193	0.540855
50142_A	*POLR2B*	-1.058563121	-0.202144098	0.190960835	3.7008086
156418_B	*POLR2E*	-1.982600714	-0.432662624	0.218229833	0.1147947
122145_A	*POLR2G*	-1.497924093	-0.272594758	0.18198169	0.1147947
219635_A	*POLR2G*	-1.251547312	-0.26725497	0.213539646	0.6702531
132911_A	*PPP1CB*	-1.586499507	-0.390835096	0.246350594	0.1147947
248282_A	*PPP1CCPPP1CA*	-1.425315362	-0.332225646	0.23308922	0.2114793
257259_A	*PPP1CCPPP1CA*	-1.412858031	-0.33805675	0.239271563	0.2114793
756666_A	*PPP1CCPPP1CA*	-1.123448161	-0.208971385	0.186008925	2.5930212
130545_A	*PPP1R14B*	-1.21750015	-0.262470753	0.215581701	1.2451143
23534_A	*PPP2CA*	-1.420760257	-0.293953354	0.206898632	0.2114793
40199_A	*PPP2R1A*	-1.756721907	-0.340767276	0.193979067	0.1147947
770027_A	*PPP2R1A*	-1.356021025	-0.241050154	0.177762844	0.2933343
37822_A	*PPP2R4*	-1.323664749	-0.45080712	0.340574998	0.540855
32427_A	*PPP2R4*	-1.160140856	-0.243066988	0.209515066	1.8099168
772455_A	*PPP4C*	-1.164109344	-0.223386384	0.191894675	1.8099168

129385_A	*PPP4R1*	-2.148569691	-0.370799056	0.172579488	0.1147947
32370_A	*PPP4R1*	-1.652349059	-0.31497709	0.19062382	0.1147947
364351_A	*PPP5C*	-1.187577094	-0.236986832	0.199554903	1.2451143
785707_A	*PRC1*	-4.867422212	-0.967337929	0.198737214	0.1147947
755378_A	*PRC1*	-4.086541968	-0.807726116	0.197655162	0.1147947
294653_A	*PRCC*	-1.047606369	-0.209292584	0.199781702	3.7008086
320325_A	*PRDX1*	-2.226181756	-0.421995468	0.189560204	0.1147947
25993_A	*PRDX1*	-2.060299461	-0.380270923	0.184570704	0.1147947
38129_A	*PRKCL1*	-1.48475352	-0.401732894	0.270572111	0.1147947
786105_A	*PRKDC*	-2.919109241	-0.523989445	0.179503198	0.1147947
47060_A	*PRNPIP*	-1.17089131	-0.224126256	0.191415082	1.8099168
42520_A	*PRPF8*	-3.834345452	-0.674947118	0.176026685	0.1147947
1326947_A	*PRPF8*	-3.405869455	-0.621192921	0.18238894	0.1147947
229944_A	*PRPSAP1*	-1.030229471	-0.181245194	0.175927013	3.7008086
811998_A	*PSIP1PSIP2*	-1.415933761	-0.22939099	0.162006865	0.2114793
667598_C	*PSIP1PSIP2*	-1.100585197	-0.193596504	0.175903242	2.5930212
256425_A	*PSMB1*	-1.250788578	-0.230913466	0.184614306	0.6702531
1839895_A	*PSMB2*	-1.514165897	-0.295866279	0.195398853	0.1147947
290864_A	*PSMB2*	-1.471379132	-0.27760716	0.188671399	0.1147947
321894_B	*PSMB3*	-1.319222713	-0.232674117	0.176372128	0.540855
321823_A	*PSMB3*	-1.147959572	-0.229499048	0.199919103	1.8099168
201275_A	*PSMB6*	-1.955423613	-0.317537698	0.162388188	0.1147947
297763_A	*PSMB7*	-1.410265747	-0.24855948	0.176250101	0.2114793
30520_A	*PSMC3*	-1.78133676	-0.373672085	0.209770602	0.1147947
43940_A	*PSMC5*	-1.655203599	-0.26824147	0.162059501	0.1147947
42744_A	*PSMC5*	-1.097847383	-0.249339378	0.227116611	2.5930212
823598_A	*PSMD12*	-1.128031193	-0.2377652	0.210778923	2.5930212
298737_A	*PSMD8*	-1.24363147	-0.217486859	0.174880473	0.6702531
37951_A	*PSMD9*	-1.386509188	-0.232375325	0.167597393	0.2933343
270006_A	*PSMD9*	-1.096505618	-0.188679544	0.172073486	2.5930212
187848_B	*PSME3*	-1.651529814	-0.310260906	0.187862734	0.1147947
231021_A	*PTGS1*	-1.204404516	-0.345867681	0.287169034	1.2451143
490251_A	*PTMS*	-3.812515595	-0.746094286	0.195696061	0.1147947
490340_A	*PTMS*	-3.208300495	-0.732089944	0.228186214	0.1147947
306757_A	*PTP4A2*	-2.050485026	-0.350485834	0.170928258	0.1147947
307106_B	*PTP4A2*	-2.009746149	-0.3318985	0.165144489	0.1147947
591665_A	*PTP4A2*	-1.792478708	-0.33252419	0.185510817	0.1147947
489497_A	*PTP4A2*	-1.131380642	-0.233637457	0.2065065	1.8099168
2109679_A	*PTRF*	-1.701393719	-0.726726499	0.427135995	0.1147947
44344_A	*PWP2H*	-1.099420193	-0.22194504	0.201874626	2.5930212
362133_A	*PXF*	-1.286226402	-0.251865429	0.195817337	0.540855
324334_C	*PYGB*	-1.461187418	-0.290038893	0.198495339	0.2114793
47727_A	*PYGB*	-1.237111321	-0.229764692	0.185726772	0.6702531
323762_F	*PYGB*	-1.189886547	-0.227432822	0.191138241	1.2451143
810616_A	*QARS*	-1.203168662	-0.2335215	0.194088748	1.2451143
32396_A	*RAB1B*	-2.292883567	-0.509034606	0.222006304	0.1147947
768212_A	*RAB1B*	-1.588616884	-0.428184788	0.269533071	0.1147947
788776_A	*RAB5B*	-1.105730812	-0.268504554	0.242829946	2.5930212
32057_A	*RAB5C*	-1.338274353	-0.298105862	0.222753923	0.2933343
271796_A	*RALY*	-1.211565515	-0.252331101	0.208268639	1.2451143

49402_A	*RALY*	-1.210619028	-0.234968936	0.194089908	1.2451143
stSG89500	*RANBP1*	-1.641637805	-0.294626646	0.179471163	0.1147947
47920_A	*RBM14*	-1.410821914	-0.278125121	0.197136944	0.2114793
stSG89113	*RBX1*	-1.048235884	-0.183569509	0.175122329	3.7008086
342714_A	*RDX*	-1.83658153	-0.360033859	0.196034782	0.1147947
193081_A	*RDX*	-1.655808501	-0.382448007	0.230973573	0.1147947
135538_A	*REST*	-1.094288746	-0.186030349	0.170001153	2.5930212
233867_A	*RNU3IP2*	-1.113883354	-0.195724458	0.175713604	2.5930212
249295_B	*RPA1*	-1.809807677	-0.373550883	0.206403635	0.1147947
308501_A	*RPA1*	-1.728244966	-0.342127906	0.197962622	0.1147947
151400_A	*RPL11*	-1.966223007	-0.376601898	0.191535699	0.1147947
207054_A	*RPL11*	-1.878094559	-0.35780375	0.190514236	0.1147947
430180_A	*RPL12*	-1.758879558	-0.325645401	0.185143661	0.1147947
201233_A	*RPL12*	-1.528698995	-0.279680784	0.182953469	0.1147947
324765_A	*RPL15*	-1.326019561	-0.223301023	0.168399494	0.540855
132643_A	*RPL18*	-1.28794427	-0.263014651	0.204212757	0.540855
stSG89276	*RPL3*	-1.37953447	-0.249817236	0.181088071	0.2933343
727149_A	*RPS15A*	-1.161001096	-0.217112192	0.187004295	1.8099168
303048_A	*RPS6*	-1.47664813	-0.282680347	0.191433789	0.1147947
126873_A	*RPS6*	-1.263287496	-0.238505918	0.188797814	0.6702531
178015_A	*RPS6KA4*	-1.323065707	-0.303868194	0.229669768	0.540855
325115_A	*RPS6KB2*	-1.143155447	-0.21166016	0.185154311	1.8099168
380356_A	*RRM1*	-1.123165429	-0.206447931	0.183809015	2.5930212
417504_A	*RRM2*	-2.179231434	-0.40037963	0.183725154	0.1147947
270362_A	*RTN3*	-1.144472635	-0.187906403	0.164186017	1.8099168
364553_A	*S100A4*	-2.986155468	-0.639492121	0.21415232	0.1147947
123056_A	*SART1*	-1.26960971	-0.287614892	0.226538037	0.6702531
233194_A	*SATB1*	-1.080693935	-0.222810226	0.206173292	2.5930212
stSG89487	*SCARF2*	-1.2025569	-0.243583229	0.202554431	1.2451143
24761_A	*SEC13L1*	-1.501319705	-0.301010301	0.200497136	0.1147947
37267_A	*SEC13L1*	-1.304953629	-0.275998365	0.211500515	0.540855
40704_A	*SEC14L1*	-1.222616639	-0.223158226	0.182525101	1.2451143
34980_A	*SET*	-3.165688264	-0.627961611	0.198364955	0.1147947
40524_A	*SET*	-3.052623952	-0.651794965	0.213519574	0.1147947
1876913_A	*SF1*	-1.917196497	-0.389848203	0.203342851	0.1147947
279329_A	*SF1*	-1.080305102	-0.34426135	0.318670484	2.5930212
273490_A	*SF3A3*	-1.446716806	-0.309998193	0.214277039	0.2114793
366681_A	*SF3A3*	-1.3963147	-0.25216701	0.180594683	0.2933343
345042_A	*SF3B1*	-1.978661901	-0.356356179	0.180099581	0.1147947
785486_A	*SFRS10*	-3.36557485	-0.666626763	0.198072184	0.1147947
2106983_A	*SFRS10*	-1.689466895	-0.41355886	0.244786602	0.1147947
1523306_A	*SFRS10*	-1.618822066	-0.378071756	0.233547444	0.1147947
204755_A	*SFRS11*	-1.779223042	-0.339146904	0.190615171	0.1147947
669372_A	*SFRS11*	-1.772113221	-0.309151634	0.174453658	0.1147947
40597_A	*SFRS3*	-2.31306554	-0.451597541	0.195237676	0.1147947
209239_A	*SFRS4*	-1.268620597	-0.205989799	0.162373053	0.6702531
132274_A	*SFRS5*	-1.218963322	-0.23364645	0.191676358	1.2451143
324973_A	*SFRS7*	-1.325394796	-0.282110765	0.212850364	0.540855
1580875_A	*SFTPA1SFTPA2*	-1.58810362	-0.357119232	0.224871493	0.1147947
39798_A	*SHMT1*	-1.248061187	-0.237066274	0.189947638	0.6702531

51583_A	*SHMT2*	-1.147023681	-0.21784275	0.189920011	1.8099168
261682_A	*SIAT4C*	-1.962675129	-0.452709885	0.230659613	0.1147947
342861_A	*SKB1*	-1.157845485	-0.228681996	0.197506489	1.8099168
324787_A	*SLC12A3*	-2.143661331	-0.455149933	0.212323619	0.1147947
308868_A	*SLC12A3*	-1.019103726	-0.1839108	0.180463279	3.7008086
202325_A	*SLC17A1*	-1.043273657	-0.208617008	0.199963841	3.7008086
41815_B	*SLC19A1*	-1.058340057	-0.273138913	0.258082373	3.7008086
267717_A	*SLC25A3*	-2.600308922	-0.484393759	0.186283158	0.1147947
754505_A	*SLC25A3*	-1.597227318	-0.315774402	0.197701603	0.1147947
265111_A	*SLC25A4*	-2.680392881	-0.408193381	0.152288638	0.1147947
296111_A	*SLC25A4*	-2.589450425	-0.457676045	0.176746402	0.1147947
1160864_A	*SLC27A2*	-1.156268325	-0.27761754	0.240097851	1.8099168
31842_A	*SLC35B1*	-1.139758924	-0.199308262	0.174868788	1.8099168
323577_A	*SLC4A2*	-1.082882609	-0.226817556	0.209457197	2.5930212
37618_A	*SLC7A6*	-1.151334861	-0.212532056	0.184596214	1.8099168
121605_A	*SMARCB1*	-1.516169881	-0.34667136	0.228649418	0.1147947
293442_A	*SMARCB1*	-1.466185213	-0.304387825	0.207605303	0.2114793
34823_A	*SMARCC1*	-1.578574561	-0.354186295	0.224370963	0.1147947
797218_B	*SMARCD2*	-1.612289883	-0.32681706	0.20270366	0.1147947
361368_A	*SMC1L1*	-1.600794209	-0.28547072	0.17833068	0.1147947
32733_A	*SMC1L1*	-1.302804892	-0.224946024	0.172662864	0.540855
46800_A	*SMC1L1*	-1.182654715	-0.19709278	0.166652851	1.2451143
300169_A	*SMC4L1*	-2.65473978	-0.530837606	0.199958433	0.1147947
795562_B	*SMC4L1*	-1.90244766	-0.403310438	0.21199555	0.1147947
273154_A	*SMT3H2*	-2.001143796	-0.363421064	0.181606671	0.1147947
322829_C	*SMT3H2*	-1.962055587	-0.340275973	0.173428304	0.1147947
323440_C	*SMT3H2*	-1.956018873	-0.35584966	0.181925474	0.1147947
299343_A	*SMT3H2*	-1.135199062	-0.211627209	0.186422995	1.8099168
486544_A	*SNAPC3*	-2.850652674	-0.63249875	0.221878574	0.1147947
124261_A	*SNRP70*	-1.395286523	-0.318162456	0.22802661	0.2933343
321292_A	*SNRP70*	-1.239775979	-0.297334972	0.239829596	0.6702531
796412_B	*SNRP70*	-1.05448604	-0.219030667	0.207713198	3.7008086
193218_A	*SNRPA*	-1.42875819	-0.310049373	0.217006191	0.2114793
141818_A	*SNRPA*	-1.320818681	-0.214508494	0.162405709	0.540855
249460_A	*SNRPC*	-1.129949803	-0.212368244	0.187944848	1.8099168
47542_C	*SNRPD1*	-2.241815174	-0.37036673	0.165208414	0.1147947
263278_A	*SPARC*	-2.550448512	-0.557067863	0.218419568	0.1147947
33411_A	*SPTAN1*	-2.535402383	-0.41962381	0.165505804	0.1147947
771091_A	*SRRM2*	-1.72267771	-0.313673175	0.182084654	0.1147947
205931_A	*STK15STK6*	-1.909161416	-0.339644216	0.177902305	0.1147947
129865_A	*STK15STK6*	-1.410139778	-0.256108404	0.181619161	0.2114793
209066_A	*STK15STK6*	-1.360421778	-0.282366413	0.207557992	0.2933343
37799_B	*STK18*	-1.038367282	-0.183083883	0.176319002	3.7008086
23697_A	*STMN1*	-1.621613015	-0.313193881	0.193137252	0.1147947
40791_A	*STOML2*	-1.606085228	-0.387455648	0.241242271	0.1147947
271286_A	*SURF4*	-1.52165499	-0.411392388	0.270358518	0.1147947
201196_A	*TAF11*	-1.566959556	-0.292777875	0.186844564	0.1147947
188403_A	*TAGLN*	-1.098332673	-0.259765563	0.236509	2.5930212
138581_A	*TAGLN*	-1.061344138	-0.213842229	0.201482461	3.7008086
45544_A	*TAGLN2*	-2.992442664	-0.730727154	0.244190862	0.1147947

301377_A	*TCERG1*	-1.286439334	-0.284953649	0.221505703	0.540855
380714_B	*TCF4*	-1.127819034	-0.19351342	0.171581977	2.5930212
729951_A	*TCOF1*	-1.19005689	-0.255606824	0.214785382	1.2451143
1319048_A	*TERT*	-2.417550984	-0.635632046	0.262923947	0.1147947
1270592_A	*TERT*	-2.313116152	-0.612993366	0.265007603	0.1147947
147717_A	*TFAP2A*	-1.489777144	-0.311947718	0.209392203	0.1147947
786168_A	*TGFB1I1*	-1.547796211	-0.326006855	0.210626472	0.1147947
810615_A	*TGFB1I1*	-1.471510741	-0.272613921	0.185261251	0.1147947
281778_A	*TGFB2*	-1.15027201	-0.248752331	0.216255224	1.8099168
114858_A	*THOC2*	-1.073147352	-0.205536299	0.191526633	3.7008086
358027_A	*THOC4*	-1.356648698	-0.27224115	0.20067181	0.2933343
252456_A	*TIAL1*	-1.301160692	-0.262064877	0.201408541	0.540855
246300_A	*TIAL1*	-1.117729545	-0.18560549	0.166055814	2.5930212
279745_A	*TIAL1*	-1.108419223	-0.193153576	0.174260399	2.5930212
357005_A	*TIMM23*	-1.075461109	-0.218031317	0.20273287	2.5930212
195152_A	*TK1*	-3.172997258	-0.769021416	0.242364349	0.1147947
241667_A	*TM4SF4*	-1.075387403	-0.226080023	0.210231236	2.5930212
1334613_A	*TMPO*	-2.294235068	-0.473854131	0.206541229	0.1147947
1288333_B	*TMPO*	-1.744589037	-0.425305892	0.243785718	0.1147947
264573_A	*TOMM40*	-1.728169911	-0.349655003	0.202326751	0.1147947
299778_A	*TOMM70A*	-1.188125139	-0.207357987	0.174525377	1.2451143
28513_A	*TOP2B*	-1.123226488	-0.235146485	0.209349127	2.5930212
341328_A	*TPM1*	-2.520203496	-0.460320919	0.182652282	0.1147947
291808_B	*TRIM28*	-1.74941587	-0.402449044	0.230047669	0.1147947
37241_A	*TRIO*	-2.148021816	-0.48067488	0.223775604	0.1147947
429234_A	*TRIO*	-2.01829049	-0.427522473	0.211824054	0.1147947
487275_B	*TRIO*	-1.76077242	-0.38194628	0.216919731	0.1147947
40854_A	*TSN*	-1.478037193	-0.293945478	0.198875562	0.1147947
34563_A	*TSN*	-1.375238325	-0.253007399	0.183973493	0.2933343
191603_A	*TUBB*	-2.628033089	-0.491813474	0.187141279	0.1147947
27464_A	*TUBB*	-1.595559727	-0.392325166	0.245885603	0.1147947
146345_A	*TXK*	-1.280058766	-0.245366896	0.191684087	0.6702531
148421_A	*TXK*	-1.143966279	-0.244152769	0.213426544	1.8099168
295286_A	*UBE2C*	-1.867251363	-0.332455233	0.178045248	0.1147947
758484_A	*UBE2C*	-1.109275823	-0.227077979	0.20470831	2.5930212
769921_A	*UBE2C*	-1.03794749	-0.247650455	0.238596323	3.7008086
298367_B	*UBE2M*	-1.022779316	-0.190417614	0.186176637	3.7008086
25867_A	*UNC84B*	-3.824799341	-0.838300461	0.219175017	0.1147947
321390_A	*UNC84B*	-3.564084697	-0.813972034	0.228381787	0.1147947
stSG89333	*UNC84B*	-2.144825056	-0.504260848	0.235105817	0.1147947
300740_B	*UQCRC1*	-2.462720524	-0.429154424	0.174260303	0.1147947
366955_A	*UQCRC1*	-1.512069953	-0.337060695	0.222913427	0.1147947
362812_A	*UQCRC2*	-1.452616599	-0.295753988	0.203600859	0.2114793
362441_A	*UQCRC2*	-1.411872431	-0.263096919	0.186346098	0.2114793
363211_A	*USP1*	-1.476475095	-0.340292401	0.230476222	0.1147947
287850_B	*USP14*	-1.223015878	-0.192366166	0.157288364	1.2451143
49297_A	*USP5*	-1.532543692	-0.339122097	0.221280541	0.1147947
33252_A	*USP7*	-1.351458357	-0.268417851	0.198613482	0.2933343
41572_A	*USP7*	-1.318870441	-0.231747729	0.175716827	0.540855
1409032_B	*USP7*	-1.265130555	-0.276811921	0.218801072	0.6702531

42813_A	*VARS2VARS1*	-1.364905616	-0.28365819	0.207822568	0.2933343
753418_A	*VASP*	-1.552849465	-0.328487725	0.211538679	0.1147947
47167_A	*VAT1*	-1.515961516	-0.284918795	0.187945929	0.1147947
261613_A	*VAT1*	-1.297537987	-0.264798756	0.204077845	0.540855
136030_A	*VCP*	-1.295317022	-0.320348743	0.247313003	0.540855
32020_A	*VCP*	-1.160982971	-0.354248359	0.305127954	1.8099168
234856_A	*VHL*	-1.038984614	-0.193678719	0.186411537	3.7008086
755145_A	*VIL2*	-1.195880867	-0.198051283	0.165611215	1.2451143
291303_A	*WDR1*	-1.516777498	-0.259683506	0.171207383	0.1147947
259364_A	*XPO1*	-2.472907527	-0.446421604	0.180524989	0.1147947
321717_A	*XPO1*	-1.93168969	-0.380501554	0.196978612	0.1147947
133178_A	*YES1*	-1.013675067	-0.192595394	0.18999717	3.7008086
264358_A	*YWHAH*	-2.405282953	-0.348732601	0.144986103	0.1147947
1680781_A	*YWHAH*	-1.604388181	-0.259365848	0.161660283	0.1147947
37231_A	*YWHAQ*	-1.571592013	-0.319124308	0.203057985	0.1147947
310740_B	*YWHAZ*	-1.246510578	-0.233319858	0.187178402	0.6702531
249295_A	*ZFP91*	-1.988399868	-0.429303084	0.215903798	0.1147947
667379_A	*ZNF205*	-1.13213749	-0.229123419	0.202381266	1.8099168
137638_A	*ZNF22*	-1.118164285	-0.197904683	0.176990703	2.5930212
726332_A	*ZWINT*	-1.730363211	-0.316857688	0.183116288	0.1147947
144708_A	*ZYX*	-1.399340724	-0.309643356	0.221278028	0.2114793

Supplementary Figure S6: Non-Specific Genes Up-Regulated Upon the HMF3A Temperature Shift

Clone ID	Gene	Score(d)	Numerator(r)	Denominator(s+s0)	q-value (%)
470700_A	*AK3*	2.3587286	0.5508561	0.2335394	0.3529763
43309_A	*AK3*	1.7345337	0.5257097	0.3030842	0.5509293
163572_A	*APLP1*	1.8215194	0.5479984	0.3008469	0.3529763
258656_A	*ATP6V0E*	1.6213243	0.3005126	0.1853501	1.7640331
784585_A	*BCHE*	1.7688235	0.3926117	0.2219621	0.5509293
310484_A	*BDKRB1*	2.4061425	0.5282693	0.2195503	0.3529763
324760_A	*BDKRB1*	1.6561553	0.5186505	0.3131654	1.7534953
324159_A	*C10orf7*	3.7876869	0.5191627	0.1370659	0.3529763
266703_A	*C12orf8*	1.8327384	0.3155468	0.1721723	0.3529763
47238_A	*C1orf8*	1.6063752	0.3105069	0.1932966	1.7640331
37197_A	*C20orf3*	2.2214023	0.4340078	0.1953756	0.3529763
309431_A	*CA12*	2.4576987	0.7056769	0.2871291	0.3529763
324853_A	*CALU*	2.178999	0.3901828	0.1790652	0.3529763
302591_B	*CASP4CASP5*	1.9005403	0.3897277	0.2050615	0.3529763
262752_A	*CD44*	2.3433157	0.4708889	0.2009499	0.3529763
267352_A	*CD59*	1.7927519	0.3052191	0.1702518	0.5509293
756630_A	*CDKN1A*	2.224792	0.750663	0.3374082	0.3529763
196320_A	*CLU*	1.7657646	0.5674654	0.321371	0.5509293
1074540_A	*CSF3*	2.1087757	0.6520701	0.3092174	0.3529763
1667001_A	*CSF3*	2.095282	0.6304058	0.3008692	0.3529763
252292_B	*CTSL*	1.7014559	0.302721	0.1779188	1.2206217
47475_A	*CYFIP2*	1.7496183	0.2982696	0.170477	0.5509293
stSG89545	*DDT*	1.9147095	0.3052584	0.1594281	0.3529763
139028_A	*DDT*	1.9124817	0.3441679	0.1799588	0.3529763
309588_A	*DDT*	1.8657835	0.3380767	0.1811983	0.3529763
146239_A	*DUSP1*	1.6948492	0.2963443	0.1748499	1.2206217
503931_B	*FBXL11*	2.1585341	0.8535835	0.3954459	0.3529763
44014_A	*FKBP1A*	2.9566584	0.517032	0.1748704	0.3529763
124069_A	*FKBP1A*	2.4136697	0.4150378	0.171953	0.3529763
52422_A	*FKBP4*	2.5164144	0.4202543	0.1670052	0.3529763
149319_A	*G1P2*	2.1087235	0.6344013	0.3008461	0.3529763
42497_A	*GAS6*	1.7201811	0.3073595	0.1786786	1.2206217
359224_A	*GNAS*	2.2918628	0.3766271	0.1643323	0.3529763
300131_B	*HSPB1*	2.6770189	0.4073335	0.1521594	0.3529763
128225_A	*HSPE1*	1.8559588	0.398963	0.2149633	0.3529763
259649_A	*IER3*	2.2038771	0.3627301	0.1645873	0.3529763
37231_B	*IGF2R*	2.1103036	0.4435892	0.2102016	0.3529763
273587_A	*IGFBP4*	2.2889745	0.5661999	0.2473596	0.3529763
147469_B	*IGFBP4*	2.0129377	0.6271612	0.3115651	0.3529763
324655_B	*IL1B*	2.4309762	0.9811082	0.4035861	0.3529763
811740_A	*ITGA2*	2.6407001	0.9258457	0.3506062	0.3529763
726425_B	*LAMA4*	1.7604623	0.517566	0.2939944	0.5509293
324122_B	*LDHA*	3.1876319	1.0154469	0.3185584	0.3529763

1467480_A	*MAN2A1*	1.7384027	0.2866268	0.1648794	0.5509293
200814_A	*MME*	1.6787723	0.5776849	0.3441115	1.2206217
26128_B	*MTCYB*	2.4738463	0.5355724	0.2164938	0.3529763
365623_A	*MTND4*	2.363333	0.3958489	0.167496	0.3529763
149218_A	*MTND4*	1.9620968	0.4142661	0.2111344	0.3529763
357613_B	*MTND4*	1.8487815	0.4431438	0.2396951	0.3529763
327407_B	*NDRG1*	1.7541081	0.5835475	0.3326748	0.5509293
39620_A	*NEDD4L*	1.6589027	0.2950039	0.1778307	1.7534953
258822_A	*NGFRAP1*	1.7749726	0.2614871	0.1473189	0.5509293
772905_A	*P4HA1*	3.1343599	0.9923436	0.3166017	0.3529763
342410_A	*P4HA2*	1.8520819	0.6150949	0.33211	0.3529763
266830_A	*PCBD*	2.5006547	0.4550084	0.1819557	0.3529763
156275_C	*PCDHGA8*	2.5714389	0.5449246	0.2119143	0.3529763
46749_A	*PLAT*	2.1505981	0.5111492	0.2376777	0.3529763
127982_A	*PLAT*	1.6072462	0.4440711	0.2762932	1.7640331
143356_A	*PLAU*	3.0707271	1.1745229	0.3824902	0.3529763
322441_A	*PLAUR*	2.0410741	0.417215	0.2044095	0.3529763
22790_B	*PLAUR*	2.0054709	0.3932965	0.1961118	0.3529763
310449_A	*PLOD2*	4.7974165	1.3914904	0.2900499	0.3529763
139570_A	*PLOD2*	1.8022395	0.7295551	0.4048047	0.5509293
148568_A	*PRDX6*	2.7415244	0.3670537	0.1338867	0.3529763
249588_A	*PRDX6*	2.2619785	0.3640285	0.1609337	0.3529763
812048_A	*PRNP*	6.2615262	0.9700034	0.1549148	0.3529763
49691_A	*PRNP*	4.523	0.9602667	0.2123075	0.3529763
51689_A	*PRNP*	4.3189041	0.964157	0.2232411	0.3529763
1651583_A	*PTGS2*	1.9795985	0.5040754	0.2546352	0.3529763
165952_B	*QSCN6*	1.6282249	0.4598973	0.2824532	1.7640331
37917_A	*RCN2*	1.9762331	0.3258132	0.1648658	0.3529763
381901_A	*RPN2*	2.0471851	0.4572706	0.2233655	0.3529763
324860_A	*RPN2*	2.0282905	0.4560691	0.2248539	0.3529763
788143_A	*SAT*	2.2542179	0.4463127	0.19799	0.3529763
51474_A	*SCARB1*	1.6340095	0.2847005	0.1742343	1.7640331
149724_A	*SEC22L1*	1.6069779	0.2603114	0.1619882	1.7640331
212807_A	*SERF2*	2.2557343	0.4535136	0.2010492	0.3529763
308748_A	*SERF2*	1.7949215	0.3768924	0.2099771	0.5509293
323254_C	*SERPINB2*	2.7133879	0.7534217	0.2776683	0.3529763
194174_B	*SERPINB2*	2.5999844	0.7316374	0.2814007	0.3529763
198206_A	*SERPINB2*	1.9974653	0.6224429	0.3116164	0.3529763
1509935_A	*SERPINB7*	1.7420163	0.5270641	0.3025598	0.5509293
666367_A	*SERPINE1*	2.82518	0.5961055	0.2109974	0.3529763
40562_A	*SGCB*	1.7135934	0.3104143	0.1811482	1.2206217
stSG89478	*SMTN*	1.6105072	0.2246767	0.1395068	1.7640331
774477_A	*SRPX*	1.851854	0.5241864	0.2830603	0.3529763
38048_A	*SRPX*	1.7501661	0.4856033	0.2774613	0.5509293
136059_A	*SSR4*	1.8112815	0.3045188	0.1681234	0.5509293
152315_A	*SSR4*	1.6839477	0.3017661	0.1792016	1.2206217
505118_B	*STAC*	1.6059115	0.283925	0.1767999	1.7640331

153589_A	*STC1*	2.6288413	0.9222648	0.3508256	0.3529763
154007_A	*STC1*	1.8370868	0.6468595	0.3521116	0.3529763
360874_B	*TFPI2*	3.3095883	0.9922862	0.2998216	0.3529763
266325_A	*TIMP1*	3.7573731	0.9416184	0.2506055	0.3529763
270187_A	*TIMP1*	2.2438225	0.7819253	0.3484791	0.3529763
770670_A	*TNFAIP3*	2.4430875	0.4771788	0.1953179	0.3529763
309943_A	*TNFAIP3*	1.746147	0.4026221	0.2305774	0.5509293
298367_A	*TXNIP*	2.4705367	0.4718054	0.1909728	0.3529763
359721_A	*TXNIP*	2.4308885	0.5825555	0.2396471	0.3529763
299497_B	*TXNIP*	1.6750462	0.4901084	0.2925939	1.2206217
365647_A	*UBN1*	1.693682	0.3708102	0.2189373	1.2206217
324168_A	*UCHL1*	2.1073336	0.3825485	0.181532	0.3529763
45138_A	*VEGFC*	2.9156105	0.6259028	0.214673	0.3529763
109669_A	*VEGFC*	2.168232	0.5466174	0.2521028	0.3529763
301777_A	*ZFP36L1*	1.6887376	0.2506822	0.1484436	1.2206217

Supplementary Figure S7: Non-Specific Genes Down-Regulated Upon the HMF3A Temperature Shift

Clone ID	Gene	Score(d)	Numerator(r)	Denominator(s+s0)	q-value (%)
308682_A	*ABCF2*	-1.7384175	-0.3183925	0.1831507	0.5509293
180078_A	*ACTR1A*	-1.5361748	-0.2608252	0.1697888	1.7534953
147706_A	*ACTR2*	-1.8869616	-0.3141623	0.1664911	0.3529763
207605_A	*ACTR2*	-1.6509994	-0.2634752	0.1595853	1.2206217
40678_B	*ACTR2*	-2.613587	-0.3902735	0.1493249	0.3529763
321766_A	*ADAM9*	-1.4978077	-0.2896414	0.1933769	1.7640331
47709_A	*ALAS1*	-1.8851409	-0.2574153	0.1365496	0.3529763
37660_A	*APBB1*	-1.9319276	-0.2767496	0.1432505	0.3529763
stSG89122	*APOBEC3A*	-1.5420593	-0.2485517	0.1611817	1.7534953
110178_B	*APOBEC3CAPOBEC3B*	-1.8064608	-0.2743216	0.1518558	0.3529763
273010_A	*APPBP1*	-1.5855314	-0.2718726	0.171471	1.7534953
46755_A	*APPBP1*	-1.5561319	-0.252524	0.1622767	1.7534953
269766_A	*ARHA*	-1.8301259	-0.3563185	0.1946961	0.3529763
51293_A	*ARHA*	-2.1188452	-0.3418902	0.1613568	0.3529763
51426_A	*ARHA*	-2.1196845	-0.358387	0.1690757	0.3529763
179500_D	*ARHGAP1*	-1.96896	-0.2720103	0.1381492	0.3529763
180079_A	*ARHGAP1*	-1.5520605	-0.241068	0.1553213	1.7534953
263793_A	*ARHGDIA*	-1.7437503	-0.4374894	0.2508899	0.5509293
26071_A	*ASNA1*	-2.2134122	-0.3532888	0.1596128	0.3529763
stSG89390	*ATF4*	-1.8540245	-0.2804715	0.1512771	0.3529763
156800_A	*ATP5D*	-2.0787647	-0.3270015	0.1573057	0.3529763
267284_A	*ATP5O*	-1.5236537	-0.2191362	0.1438228	1.7640331
300300_A	*B4GALT2*	-1.9926832	-0.4597041	0.230696	0.3529763
789029_A	*B4GALT2*	-1.9448229	-0.4863689	0.2500839	0.3529763
1860539_A	*BCAT1*	-1.744663	-0.3485085	0.1997569	0.5509293
2009885_B	*BCAT1*	-1.8131007	-0.3016397	0.1663668	0.3529763
141318_A	*BGN*	-1.4853508	-0.3834051	0.2581243	1.7640331
359462_B	*C14orf31*	-2.0589473	-0.3898201	0.1893298	0.3529763
50036_B	*C5orf13*	-3.1088029	-0.6782539	0.2181721	0.3529763
49560_A	*CAPN1*	-1.7100883	-0.3243781	0.189685	0.5509293
267759_A	*CAV1*	-1.9725181	-0.2841136	0.144036	0.3529763
32026_A	*CBARA1*	-2.2666246	-0.2976119	0.1313018	0.3529763
stSG89407	*CDC42EP1*	-1.6942802	-0.3366789	0.198715	0.5509293
753401_A	*CDH2*	-2.3939595	-0.3530823	0.1474888	0.3529763
327662_A	*CIRBP*	-2.7598201	-0.6898901	0.2499765	0.3529763
195273_A	*COL2A1*	-1.8712616	-0.7282087	0.3891539	0.3529763
203403_A	*COTL1*	-1.4988529	-0.2986147	0.1992289	1.7640331
178323_A	*COX4I1*	-1.7622417	-0.264407	0.1500401	0.5509293
30098_A	*COX4I1*	-1.6429295	-0.329504	0.2005588	1.2206217
271009_A	*COX6C*	-1.5636505	-0.2537059	0.1622523	1.7534953
127187_A	*CRAT*	-1.7442309	-0.2945047	0.168845	0.5509293
147371_A	*CRSP8*	-1.7512905	-0.2456358	0.1402599	0.5509293
324910_A	*CYR61*	-2.0065388	-0.3250883	0.1620145	0.3529763

140417_A	*DAB2*	-2.9007662	-0.6635403	0.2287466	0.3529763
150645_A	*DAB2*	-3.2976498	-0.6412125	0.1944453	0.3529763
34795_A	*DAZAP2*	-1.6429855	-0.4185865	0.2547719	1.2206217
375715_A	*DAZAP2*	-1.7070097	-0.2961777	0.1735068	0.5509293
205645_A	*DCN*	-1.9911336	-0.5527489	0.2776051	0.3529763
296513_B	*DCN*	-1.7890879	-0.5454718	0.3048882	0.3529763
33487_A	*DCTN2*	-2.1186227	-0.2897814	0.1367782	0.3529763
39341_A	*DCTN2*	-1.5871932	-0.3229067	0.2034451	1.7534953
120090_B	*DDX38*	-1.5094562	-0.2797273	0.1853166	1.7640331
267325_A	*DDX38*	-1.5963511	-0.2305036	0.144394	1.2206217
152833_B	*DKC1*	-1.7694855	-0.308322	0.1742439	0.3529763
124303_A	*DLAT*	-1.6571906	-0.3445359	0.2079036	0.5509293
33578_A	*DLAT*	-1.6063124	-0.2891903	0.1800337	1.2206217
360263_A	*DPYSL3*	-2.5889025	-0.7078192	0.2734051	0.3529763
376522_A	*DPYSL3*	-2.0683368	-0.5619942	0.2717131	0.3529763
136352_A	*EFEMP1*	-2.6803705	-0.9314824	0.34752	0.3529763
stSG89374	*EIF3S6IP*	-1.7410296	-0.218992	0.125783	0.5509293
376635_A	*FBL*	-2.5368017	-0.4373921	0.1724187	0.3529763
50483_A	*FBLN5*	-1.6422314	-0.2809475	0.1710767	1.2206217
stSG89133	*G22P1*	-1.6635321	-0.2629685	0.1580784	0.5509293
297780_A	*GBAS*	-1.8691844	-0.2848358	0.1523851	0.3529763
122217_A	*GBE1*	-1.4942601	-0.2271936	0.1520442	1.7640331
263350_A	*GNAI2*	-1.5201238	-0.2851452	0.1875803	1.7640331
198132_A	*GNB2L1*	-2.1902451	-0.3473177	0.1585748	0.3529763
257586_A	*GNB2L1*	-2.1854418	-0.4037025	0.1847235	0.3529763
302555_A	*GNB2L1*	-1.9403466	-0.3449727	0.1777892	0.3529763
186993_A	*H3F3BH3F3A*	-1.8929225	-0.2858739	0.1510225	0.3529763
139221_A	*HMGB1*	-2.3266514	-0.4631052	0.1990436	0.3529763
321813_A	*HNRPAB*	-1.4854497	-0.2336499	0.1572924	1.7640331
296047_A	*HNRPM*	-1.5078867	-0.2296529	0.1523012	1.7640331
stSG89199	*HPS4*	-1.6969996	-0.2243534	0.1322059	0.5509293
200018_A	*HRMT1L2*	-2.3958393	-0.4295683	0.1792976	0.3529763
323621_A	*HRMT1L2*	-3.1222504	-0.4819219	0.1543508	0.3529763
231139_B	*ILF3*	-1.6892012	-0.3592787	0.2126915	0.5509293
190242_A	*KARS*	-1.7462069	-0.478038	0.2737579	0.5509293
50280_A	*KIFC3*	-1.7889342	-0.3034126	0.1696052	0.3529763
289615_A	*LAMP2*	-1.5422034	-0.3323626	0.2155115	1.7534953
49630_A	*LAMP2*	-1.6857969	-0.3246942	0.1926058	0.5509293
44050_A	*LASP1*	-2.0929502	-0.3470948	0.16584	0.3529763
795814_A	*LASP1*	-1.7244276	-0.2882083	0.1671327	0.5509293
29627_A	*LIG1*	-1.5952811	-0.2550651	0.1598872	1.2206217
306925_B	*LSS*	-1.5523892	-0.2544768	0.1639259	1.7534953
447509_A	*MARCKS*	-2.6560458	-0.4483987	0.1688219	0.3529763
713558_A	*MBD2*	-1.4843988	-0.2807838	0.1891566	1.7640331
263092_A	*MBNL1*	-1.754034	-0.3440506	0.1961482	0.5509293
376607_A	*MCM5*	-1.9303638	-0.2947769	0.1527053	0.3529763
42991_A	*MEIS2*	-1.5414255	-0.3340075	0.2166874	1.7534953

300634_A	*MMP2*	-2.2263278	-0.6680158	0.3000528	0.3529763
810449_A	*MMP2*	-2.7627893	-0.6477014	0.2344375	0.3529763
265376_A	*MSC*	-1.9909566	-0.4403864	0.2211934	0.3529763
267781_A	*MSC*	-1.7116548	-0.3080013	0.1799436	0.5509293
273455_A	*MTHFD2*	-1.9140235	-0.2916758	0.1523888	0.3529763
755699_A	*MYBL2*	-2.1389039	-0.5917866	0.2766775	0.3529763
147328_A	*NAPA*	-1.9828515	-0.322757	0.1627742	0.3529763
108852_A	*NDUFS8*	-1.8232553	-0.2592356	0.1421828	0.3529763
27542_A	*NDUFV1*	-1.6672734	-0.3050324	0.1829529	0.5509293
813387_A	*NQO1*	-1.8083928	-0.2838343	0.1569539	0.3529763
289570_A	*NSMAF*	-1.4950856	-0.2536958	0.1696865	1.7640331
272955_A	*PAFAH1B1*	-1.7975038	-0.2875751	0.1599858	0.3529763
113280_A	*PAFAH1B3*	-1.6842081	-0.4036431	0.2396634	0.5509293
39091_A	*PDGFRA*	-2.3826359	-0.5508938	0.2312119	0.3529763
52073_A	*PDGFRA*	-3.4890751	-0.4907961	0.1406665	0.3529763
29687_B	*PEPD*	-2.1644063	-0.3086663	0.1426102	0.3529763
360258_A	*PES1*	-1.6977512	-0.3023527	0.1780901	0.5509293
360757_A	*PES1*	-1.6899606	-0.348805	0.2063983	0.5509293
268928_A	*PMSCL1*	-1.6482396	-0.2814706	0.1707704	1.2206217
122145_A	*POLR2G*	-2.0057474	-0.2881902	0.1436822	0.3529763
132911_A	*PPP1CB*	-2.1752818	-0.3327619	0.1529741	0.3529763
264214_A	*PPP1CB*	-1.5401413	-0.2527877	0.1641328	1.7534953
32370_A	*PPP4R1*	-1.5256973	-0.2609085	0.1710093	1.7640331
38129_A	*PRKCL1*	-1.5653115	-0.459039	0.2932573	1.7534953
786105_A	*PRKDC*	-1.5611277	-0.2770902	0.1774936	1.7534953
47060_A	*PRNPIP*	-1.8786892	-0.2774049	0.1476587	0.3529763
1326947_A	*PRPF8*	-1.8509255	-0.3604052	0.1947162	0.3529763
42520_A	*PRPF8*	-1.8197517	-0.299862	0.1647818	0.3529763
26210_A	*PRPS1*	-1.5671233	-0.2230384	0.1423234	1.7534953
297763_A	*PSMB7*	-1.5110735	-0.2078924	0.1375792	1.7640331
270006_A	*PSMD9*	-1.772054	-0.2459936	0.1388183	0.3529763
151011_A	*PTGFR*	-1.5686515	-0.1971554	0.1256847	1.7534953
490251_A	*PTMS*	-2.4380562	-0.4567347	0.1873356	0.3529763
490340_A	*PTMS*	-1.7304338	-0.4439931	0.2565791	0.5509293
306757_A	*PTP4A2*	-1.6057296	-0.2217292	0.1380863	1.2206217
307106_B	*PTP4A2*	-1.7276489	-0.2278664	0.1318939	0.5509293
489497_A	*PTP4A2*	-1.7068943	-0.3071365	0.1799388	0.5509293
50574_E	*RAB31*	-2.0562093	-0.3382938	0.164523	0.3529763
32057_A	*RAB5C*	-1.5584617	-0.2939454	0.1886125	1.7534953
151400_A	*RPL11*	-1.5748727	-0.2533549	0.1608733	1.7534953
430180_A	*RPL12*	-1.9790667	-0.3793572	0.1916849	0.3529763
298560_A	*RPL15*	-1.7772052	-0.2588037	0.145624	0.3529763
stSG89276	*RPL3*	-1.6324598	-0.2564744	0.1571092	1.2206217
303048_A	*RPS6*	-1.4913104	-0.29387	0.1970548	1.7640331
178015_A	*RPS6KA4*	-1.6891879	-0.4714346	0.2790895	0.5509293
252256_A	*RSU1*	-1.7560196	-0.235418	0.1340634	0.5509293
364553_A	*S100A4*	-5.471465	-1.0666326	0.1949446	0.3529763

stSG89487	*SCARF2*	-2.2866621	-0.4435861	0.1939885	0.3529763
34980_A	*SET*	-2.0626681	-0.3880457	0.188128	0.3529763
40524_A	*SET*	-1.9767845	-0.3648298	0.1845572	0.3529763
366681_A	*SF3A3*	-1.599508	-0.2122264	0.1326823	1.2206217
785486_A	*SFRS10*	-1.6709315	-0.2507458	0.1500635	0.5509293
324973_A	*SFRS7*	-1.630515	-0.2226978	0.1365813	1.2206217
39798_A	*SHMT1*	-1.4863963	-0.2243008	0.1509024	1.7640331
51583_A	*SHMT2*	-1.8632985	-0.2603225	0.1397106	0.3529763
267717_A	*SLC25A3*	-1.5967838	-0.2986455	0.1870294	1.2206217
754505_A	*SLC25A3*	-1.6317555	-0.3329241	0.2040282	1.2206217
323577_A	*SLC4A2*	-2.5442212	-0.4973158	0.1954688	0.3529763
121605_A	*SMARCB1*	-2.2804755	-0.3913008	0.1715874	0.3529763
293442_A	*SMARCB1*	-1.5231753	-0.2817724	0.1849901	1.7640331
358207_A	*SMARCD3*	-1.6228552	-0.2947267	0.18161	1.2206217
486544_A	*SNAPC3*	-2.2124286	-0.423358	0.1913544	0.3529763
193218_A	*SNRPA*	-1.5530819	-0.2645441	0.1703349	1.7534953
263278_A	*SPARC*	-2.5087048	-0.7446092	0.2968102	0.3529763
784829_A	*SRP72*	-1.9700922	-0.3454336	0.1753388	0.3529763
452969_A	*TAF1B*	-1.5158993	-0.2315438	0.1527435	1.7640331
45544_A	*TAGLN2*	-2.4539141	-0.4456186	0.181595	0.3529763
305018_A	*TCEB2*	-1.5071631	-0.2052192	0.1361626	1.7640331
30302_A	*TCF4*	-1.5496152	-0.398563	0.2572012	1.7534953
380714_B	*TCF4*	-2.1432418	-0.2622472	0.1223601	0.3529763
1270592_A	*TERT*	-1.7544604	-0.5376001	0.3064191	0.5509293
1319048_A	*TERT*	-1.7434528	-0.5805375	0.3329815	0.5509293
147717_A	*TFAP2A*	-2.1365813	-0.5814918	0.2721599	0.3529763
786168_A	*TGFB1I1*	-1.6037803	-0.2875813	0.1793146	1.2206217
195152_A	*TK1*	-1.5415966	-0.3385437	0.2196059	1.7534953
264573_A	*TOMM40*	-1.6644278	-0.3365342	0.2021921	0.5509293
28513_A	*TOP2B*	-1.5242193	-0.2889091	0.1895456	1.7640331
341328_A	*TPM1*	-1.724492	-0.4647591	0.2695049	0.5509293
45573_B	*UBE1C*	-1.6869726	-0.2131724	0.1263639	0.5509293
143928_A	*VAMP3*	-2.0196339	-0.3056277	0.1513283	0.3529763
753418_A	*VASP*	-2.0675838	-0.345104	0.1669117	0.3529763
261613_A	*VAT1*	-1.9528211	-0.3482132	0.1783129	0.3529763
47167_A	*VAT1*	-2.0489554	-0.3536766	0.1726131	0.3529763
755145_A	*VIL2*	-1.6758463	-0.2417262	0.1442413	0.5509293
291303_A	*WDR1*	-1.7649182	-0.2542606	0.1440637	0.5509293
264358_A	*YWHAH*	-1.9144029	-0.3214137	0.1678924	0.3529763
37231_A	*YWHAQ*	-1.5077975	-0.2876121	0.1907498	1.7640331
310740_B	*YWHAZ*	-1.7871491	-0.3278681	0.1834587	0.3529763
249295_A	*ZFP91*	-1.8458132	-0.3256073	0.1764032	0.3529763
362910_A	*ZMPSTE24*	-1.5031642	-0.2345161	0.156015	1.7640331

Supplementary Figure S8: Genes Specifically Up-Regulated Upon the HMF3A Temperature Shift

Clone ID	Gene	Score(d)	Numerator(r)	Denominator(s+s0)	q-value (%)
200909_A	*ADAM10*	1.384938	0.2449974	0.1769013	0.540855
774119_A	*ADD3*	1.6555082	0.3366694	0.2033632	0.1147947
113871_A	*AGTRAP*	1.2245241	0.2480284	0.2025508	1.8099168
340628_A	*AKR1B1*	1.4052824	0.2147704	0.1528308	0.2933343
26025_A	*AKR1B1*	1.2099648	0.2401374	0.1984665	2.5930212
340619_A	*AKR1B1*	1.1629024	0.1883054	0.1619271	3.7008086
293270_A	*AKR1C2*	2.9400016	0.570637	0.1940941	0.1147947
214107_A	*ANPEP*	2.7312456	0.6520802	0.2387483	0.1147947
300484_A	*ANXA1*	2.6419935	0.5704803	0.215928	0.1147947
288649_A	*ANXA1*	1.945306	0.5130438	0.2637342	0.1147947
306948_A	*ANXA4*	1.3618629	0.2537234	0.1863061	0.540855
327315_A	*AOAH*	1.1329354	0.2803739	0.2474756	3.7008086
1323860_A	*APLP2*	1.2989107	0.2288169	0.1761606	1.2451143
201585_A	*ARHGDIB*	1.356757	0.2821756	0.207978	0.540855
470419_A	*ARPC1B*	1.2359907	0.2577821	0.2085631	1.8099168
269738_A	*ATP2C1*	1.3749899	0.2815419	0.2047593	0.540855
1704062_A	*ATP2C1*	1.2976086	0.2672836	0.2059817	1.2451143
341038_A	*ATP6IP2*	3.1212914	0.6212122	0.1990241	0.1147947
772283_A	*ATP6V0B*	1.6076458	0.316974	0.1971665	0.1147947
726576_A	*ATP6V0B*	1.1300214	0.2557155	0.2262926	3.7008086
32649_A	*ATP6V1E1*	1.7032831	0.3078467	0.1807373	0.1147947
809439_B	*ATP6V1G1*	2.224107	0.4385199	0.1971667	0.1147947
146646_A	*ATP6V1G1*	2.0369112	0.3673649	0.1803539	0.1147947
37045_A	*ATP6V1G1*	1.9969345	0.3727217	0.1866469	0.1147947
36832_A	*ATP6V1G1*	1.975338	0.3691429	0.1868758	0.1147947
299995_A	*ATP6V1G1*	1.833334	0.3708571	0.2022856	0.1147947
150354_A	*B4GALT1*	1.7759515	0.290577	0.1636176	0.1147947
327700_A	*B4GALT1*	1.4983155	0.2716894	0.1813299	0.2114793
738975_B	*B4GALT1*	1.3597811	0.293284	0.2156847	0.540855
781783_A	*BET1*	1.770128	0.3331773	0.1882222	0.1147947
203351_A	*BET1*	1.4795355	0.263176	0.1778774	0.2114793
201890_A	*BIRC3*	1.7077812	0.3270361	0.1914976	0.1147947
129632_A	*BIRC3*	1.5249164	0.4078565	0.2674616	0.1147947
360543_A	*BLCAP*	1.2327748	0.2326846	0.1887486	1.8099168
32510_A	*BTG2*	1.6988362	0.3361345	0.1978616	0.1147947
246304_A	*BTG3*	1.5464442	0.2415296	0.1561838	0.1147947
310406_A	*C6orf48*	2.2770037	0.4595148	0.2018068	0.1147947
282740_A	*CASK*	1.2820138	0.2395475	0.1868525	1.2451143
32662_A	*CAT*	1.5485074	0.3354713	0.2166417	0.1147947
320383_A	*CD164*	1.1598837	0.2308069	0.1989914	3.7008086
174515_A	*CD81*	1.4573061	0.4395873	0.3016438	0.2114793
261971_B	*CD81*	1.4113562	0.4273145	0.3027687	0.2933343
796005_A	*CDH11*	3.8555025	0.7866079	0.2040221	0.1147947
31093_A	*CDH13*	1.8005615	0.3835422	0.2130126	0.1147947
144932_A	*CDK2AP1*	1.2314178	0.2887407	0.2344782	1.8099168
753658_A	*CDK2AP1*	1.1241254	0.2608439	0.2320416	3.7008086
145973_A	*CLN2*	2.7151682	0.5570134	0.2051488	0.1147947

37500_B	*CPNE3*	1.3407853	0.2560288	0.1909544	0.6702531
233825_A	*CPO*	1.180108	0.2982933	0.2527678	3.7008086
272142_A	*CREG*	1.4215793	0.2360663	0.1660592	0.2933343
147907_A	*CREG*	1.2801872	0.2822397	0.2204675	1.2451143
269238_A	*CRYAB*	1.155328	0.2138516	0.1851003	3.7008086
124554_A	*CSF1*	3.3358604	0.8115451	0.2432791	0.1147947
246147_A	*CSPG2*	3.9363946	0.8257784	0.2097804	0.1147947
256841_A	*CSRP2*	1.463056	0.2503674	0.1711264	0.2114793
261517_A	*CTSB*	3.382767	0.6395612	0.1890645	0.1147947
38764_A	*CTSB*	2.9417775	0.5756706	0.195688	0.1147947
380384_A	*CUL4B*	1.7337129	0.3729424	0.215112	0.1147947
297845_A	*CYB5*	1.4215751	0.2348119	0.1651773	0.2933343
37129_A	*CYLD*	1.2486519	0.2952378	0.2364452	1.8099168
310800_A	*DAF*	1.1575235	0.2629769	0.2271892	3.7008086
24927_A	*DDB2*	1.4087983	0.2957948	0.2099625	0.2933343
753447_B	*DDB2*	1.2322018	0.2310797	0.187534	1.8099168
42188_A	*DDR2*	1.1998797	0.2833006	0.2361075	2.5930212
142621_A	*DGKA*	1.2179154	0.2168535	0.178053	2.5930212
366944_A	*DGKA*	1.2038314	0.2161753	0.1795727	2.5930212
51003_A	*DKK3*	3.8091933	0.6259214	0.1643186	0.1147947
44394_B	*DNAJA1*	1.817456	0.3187308	0.175372	0.1147947
789269_A	*DNAJB4*	1.9728431	0.377736	0.1914678	0.1147947
302434_A	*DTR*	1.138066	0.2561959	0.2251151	3.7008086
252443_A	*DUSP4*	2.3697955	0.4946943	0.2087498	0.1147947
270148_A	*DUSP4*	1.7742348	0.3847127	0.216833	0.1147947
197479_A	*DUSP5*	2.5020512	0.5086419	0.20329	0.1147947
33285_A	*DUSP5*	1.7230449	0.3528711	0.2047951	0.1147947
40851_A	*DUSP6*	2.3040541	0.4913889	0.2132714	0.1147947
301122_A	*ECM1*	2.7065835	0.6847702	0.2530017	0.1147947
124873_A	*ECM1*	2.2509183	0.6670056	0.296326	0.1147947
128045_A	*EFEMP2*	1.7781713	0.4037218	0.2270433	0.1147947
23448_A	*EFEMP2*	1.445834	0.3286609	0.2273158	0.2114793
287704_A	*EMP1*	2.0940289	0.3507259	0.1674886	0.1147947
323643_A	*EMP1*	1.7470738	0.3144848	0.1800066	0.1147947
322146_A	*EMP1*	1.2778439	0.2673565	0.2092247	1.2451143
323181_A	*FAP*	1.3282128	0.2613827	0.1967928	0.6702531
665401_A	*FGF2*	3.2773093	0.9964529	0.304046	0.1147947
365515_A	*FGF7*	2.1894704	0.4246861	0.1939675	0.1147947
1704018_B	*FTH1*	2.0329453	0.4566769	0.224638	0.1147947
343563_A	*FTL*	1.5148032	0.28412	0.1875623	0.1147947
149986_A	*FVT1*	1.3875988	0.2771438	0.199729	0.540855
34415_A	*FVT1*	1.1813399	0.2132982	0.1805561	3.7008086
115383_A	*GADD45A*	2.2434388	0.5005956	0.2231376	0.1147947
310141_A	*GADD45A*	1.9457508	0.4600507	0.2364387	0.1147947
415112_A	*GADD45A*	1.4382471	0.3197344	0.2223084	0.2933343
174799_A	*GAMT*	1.2369488	0.2562324	0.2071488	1.8099168
306144_A	*GBA*	1.1564553	0.2463978	0.2130629	3.7008086
809588_C	*GGH*	1.6524252	0.3220445	0.194892	0.1147947
809588_A	*GGH*	1.5263648	0.359191	0.2353245	0.1147947
309079_A	*GJA1*	1.7496394	0.4186015	0.2392502	0.1147947
486844_A	*GJA1*	1.7303954	0.4016833	0.2321338	0.1147947
308993_A	*GJA1*	1.6307408	0.3558035	0.2181852	0.1147947

811671_A	*GLA*	1.2116414	0.2236976	0.1846236	2.5930212
132691_A	*GLRX*	2.4552565	0.4852248	0.1976269	0.1147947
324214_A	*GLRX*	2.2361778	0.4172495	0.1865905	0.1147947
195328_A	*GLRX*	1.6231507	0.3592045	0.2213007	0.1147947
323667_B	*GM2A*	1.2705707	0.2432399	0.1914415	1.2451143
50492_A	*GNAL*	1.3760711	0.3176701	0.230853	0.540855
323165_A	*GNG11*	2.8998856	0.5934098	0.2046321	0.1147947
346926_A	*GPAA1*	1.3581492	0.2648346	0.1949967	0.540855
346135_A	*GPC1*	1.1921452	0.2601026	0.2181803	2.5930212
783646_A	*GPC1*	1.1390137	0.2758895	0.2422178	3.7008086
774491_A	*GPX1*	1.2582172	0.2367555	0.1881674	1.8099168
stSG89160	*HMOX1*	2.3357439	0.5220015	0.223484	0.1147947
42724_A	*HPCAL1*	2.160355	0.4086957	0.1891799	0.1147947
24772_A	*HPCAL1*	1.9676392	0.4106678	0.2087109	0.1147947
35091_A	*HSPA1L*	2.5217468	0.6595117	0.2615297	0.1147947
50615_A	*HSPA1L*	2.3826119	0.5935103	0.2491007	0.1147947
33800_A	*HSPA6HSPA7*	1.8645083	0.5601954	0.3004521	0.1147947
148057_A	*ID3*	1.7436713	0.3709137	0.21272	0.1147947
788174_A	*IFIT1*	1.7340599	0.7263782	0.4188888	0.1147947
345996_A	*IFITM1*	1.7545246	0.42191	0.2404697	0.1147947
150355_A	*IFITM1*	1.6330385	0.3939017	0.2412078	0.1147947
154387_A	*IFITM2*	1.5250781	0.3839724	0.2517723	0.1147947
322180_A	*IFITM2*	1.3930721	0.3455152	0.2480239	0.2933343
364516_A	*IFNGR1*	1.1599719	0.2169837	0.1870594	3.7008086
196375_A	*IGFBP3*	5.2886789	1.3065807	0.2470524	0.1147947
266838_A	*IGFBP3*	5.2443098	1.2201963	0.2326705	0.1147947
356653_A	*IGFBP6*	3.7943612	0.851766	0.2244821	0.1147947
299204_A	*IGFBP7*	4.929953	1.1183687	0.2268518	0.1147947
183087_A	*IL3RA*	1.130923	0.2234687	0.1975986	3.7008086
251172_A	*ITGB5*	2.0150408	0.321968	0.1597824	0.1147947
770859_A	*ITGB5*	1.1657265	0.2479418	0.212693	3.7008086
153213_A	*JUNB*	1.1895791	0.2292923	0.1927508	2.5930212
344988_A	*KRTHA3A*	1.6469786	0.3410555	0.2070795	0.1147947
129532_A	*KYNU*	1.2004791	0.3249626	0.2706941	2.5930212
157819_A	*LAMB2*	2.5320321	0.4768717	0.1883356	0.1147947
321351_A	*LGMN*	1.4369044	0.2415945	0.1681354	0.2933343
stSG89454	*LIF*	1.3491249	0.2340368	0.173473	0.6702531
244990_A	*LIPA*	2.1125231	0.413727	0.195845	0.1147947
49584_A	*LIPA*	1.6582059	0.4210648	0.253928	0.1147947
723880_A	*LOXL1*	1.3458689	0.3141132	0.2333906	0.6702531
667364_A	*LOXL1*	1.2506697	0.2847611	0.2276869	1.8099168
297957_A	*LPXN*	1.936786	0.3461448	0.1787212	0.1147947
36636_A	*LRP11*	1.5684549	0.2715103	0.1731069	0.1147947
783679_A	*LTBP1*	2.3683875	0.4808102	0.2030116	0.1147947
788591_A	*LTBP1*	2.2353684	0.5960127	0.2666284	0.1147947
230488_A	*LY6E*	1.4444447	0.2880352	0.199409	0.2933343
809579_B	*LY6E*	1.2143499	0.3121625	0.2570614	2.5930212
112207_A	*MANBA*	1.949172	0.5175211	0.2655082	0.1147947
23356_B	*MAP1LC3B*	1.8078537	0.3664981	0.2027255	0.1147947
33826_A	*MAP2K1*	1.2692278	0.2332654	0.1837853	1.2451143
1659533_B	*MATN4*	1.1757722	0.3468351	0.2949849	3.7008086
50437_A	*MCL1*	1.4850306	0.3573923	0.2406633	0.2114793

267815_A	*MCP*	3.3541057	0.6853489	0.2043313	0.1147947
49200_A	*MGLL*	1.3521599	0.2545689	0.1882684	0.540855
342581_A	*MRC2*	1.425242	0.317748	0.2229432	0.2933343
232772_A	*MT1B*	3.520782	0.7057613	0.2004558	0.1147947
66946_A	*MT1B*	2.9144909	0.7294288	0.2502766	0.1147947
202535_A	*MT1K*	3.8161016	0.7126796	0.1867559	0.1147947
240803_A	*MT1K*	3.6017229	0.7646988	0.2123147	0.1147947
202535_C	*MT1K*	3.4511303	0.7775184	0.2252939	0.1147947
274164_A	*MT1X*	3.478233	0.7368786	0.2118543	0.1147947
293137_A	*MT1X*	3.4516814	0.668015	0.1935332	0.1147947
111081_A	*MT1X*	3.3746754	0.7308715	0.2165754	0.1147947
297392_A	*MT1X*	3.2556901	0.7306515	0.2244229	0.1147947
2019011_A	*MT3*	1.701109	0.4507703	0.2649861	0.1147947
789273_A	*NAB1*	1.3634159	0.2458776	0.1803394	0.540855
365534_A	*NBL1*	2.0219908	0.4061035	0.2008434	0.1147947
124123_A	*NDUFB5*	1.1470534	0.2368422	0.2064788	3.7008086
110423_A	*NINJ1*	2.123651	0.5073141	0.2388877	0.1147947
147436_A	*NINJ1*	2.0721676	0.4158784	0.2006973	0.1147947
177016_A	*NOVA2*	1.3702722	0.2498554	0.18234	0.540855
293109_B	*NP*	1.5673776	0.3092353	0.1972947	0.1147947
202988_A	*NPC1*	1.6631187	0.291275	0.1751378	0.1147947
269815_A	*NR4A3*	4.5272174	0.9919916	0.2191173	0.1147947
1644118_A	*NR6A1*	1.5989607	0.292282	0.182795	0.1147947
49439_B	*NRG1*	1.1728119	0.24434	0.2083369	3.7008086
269423_A	*OSBPL3*	1.3052715	0.2445385	0.1873469	0.6702531
139540_A	*OSBPL3*	1.1937279	0.2069099	0.1733309	2.5930212
188294_B	*P4HB*	3.0259715	0.5700903	0.1883991	0.1147947
140806_A	*PAM*	4.2491135	0.7700938	0.1812364	0.1147947
304879_A	*PAM*	3.1536057	0.6413584	0.2033731	0.1147947
470764_A	*PAM*	3.079869	0.6324694	0.2053559	0.1147947
44675_A	*PAPSS1*	1.5367276	0.2664744	0.1734038	0.1147947
363151_A	*PEA15*	1.6086372	0.2819587	0.175278	0.1147947
340619_B	*PEX6*	1.7075333	0.3348915	0.1961259	0.1147947
41929_A	*PICALM*	1.2590192	0.2285822	0.1815558	1.8099168
27749_A	*PKIA*	1.6127681	0.327653	0.2031619	0.1147947
28009_C	*PKIA*	1.1857992	0.2060293	0.1737472	2.5930212
365623_B	*PLD3*	1.3807212	0.3122285	0.2261344	0.540855
153114_A	*PLXNB2*	2.1974257	0.534301	0.2431486	0.1147947
34853_A	*POLD4*	2.2493383	0.4197767	0.1866223	0.1147947
38922_A	*PON2*	1.5233082	0.3383153	0.2220925	0.1147947
51565_A	*PON2*	1.2904509	0.2220914	0.1721037	1.2451143
161368_A	*PPIB*	1.3093498	0.2709143	0.2069075	0.6702531
300659_A	*PROCR*	1.25132	0.2271692	0.1815436	1.8099168
197712_A	*PSAP*	1.5799943	0.3211816	0.2032802	0.1147947
246780_A	*PSAP*	1.5240013	0.3154957	0.207018	0.1147947
42739_A	*PTP4A1*	2.1191661	0.4151212	0.195889	0.1147947
297596_A	*PTP4A1*	1.6659416	0.3614278	0.2169511	0.1147947
241705_A	*PYGL*	1.4265351	0.2839998	0.1990836	0.2933343
356742_A	*PYGL*	1.217874	0.2452212	0.2013519	2.5930212
266103_A	*RAB7*	1.8963767	0.35629	0.1878794	0.1147947
145098_A	*RECK*	1.8386579	0.4022595	0.2187789	0.1147947
323346_C	*RGS3*	1.4890581	0.2883115	0.19362	0.2114793

148753_A	*RNF11*	2.1548468	0.4080141	0.1893472	0.1147947
356665_A	*RRAD*	1.2342612	0.2162202	0.1751818	1.8099168
154080_A	*S100A11*	1.6713937	0.448923	0.268592	0.1147947
154167_A	*S100A11*	1.4457533	0.4133363	0.2858969	0.2114793
1627856_A	*SCGF*	1.9808436	0.4712348	0.237896	0.1147947
123586_A	*SDC1*	1.9558506	0.436728	0.2232931	0.1147947
42669_A	*SGK*	1.2391106	0.2717886	0.2193417	1.8099168
48503_A	*SLC16A2*	2.0140658	0.3716748	0.1845395	0.1147947
24776_A	*SLC16A2*	1.2493852	0.2847707	0.2279287	1.8099168
725710_A	*SLC20A1*	2.7705502	0.5093168	0.1838324	0.1147947
135747_A	*SLC2A1*	1.6643165	0.2683647	0.1612462	0.1147947
240183_A	*SLC9A1*	1.3760562	0.2775847	0.2017248	0.540855
30272_A	*SLC9A1*	1.3652404	0.3218884	0.2357741	0.540855
180405_A	*SMPD1*	2.1216973	0.3690936	0.1739615	0.1147947
180046_A	*SMPD1*	1.7301821	0.3321834	0.1919933	0.1147947
47107_A	*SNX3*	2.078182	0.4191685	0.2016996	0.1147947
26599_A	*STAT1*	1.7042383	0.6057858	0.3554584	0.1147947
24033_A	*STAT1*	1.6463931	0.4952017	0.3007797	0.1147947
298134_A	*STOM*	2.1178417	0.3833027	0.1809874	0.1147947
417759_A	*TAF10*	1.1280737	0.230453	0.2042889	3.7008086
665226_A	*TCTE1L*	1.2600491	0.2893547	0.2296376	1.8099168
52431_A	*TDE1*	1.1345611	0.1960485	0.1727967	3.7008086
346727_A	*TFPI*	1.4841778	0.3578671	0.2411214	0.2114793
199945_A	*TGM2*	2.5660415	0.4470954	0.1742355	0.1147947
769686_A	*THY1*	1.3524773	0.3395294	0.2510426	0.540855
249977_A	*TIMP3*	2.9730681	0.6266295	0.2107686	0.1147947
stSG89269	*TIMP3*	1.5941144	0.2856596	0.1791964	0.1147947
714213_A	*TNFRSF6*	1.686536	0.3631721	0.2153361	0.1147947
299745_B	*TNFRSF6*	1.6271236	0.3314543	0.2037057	0.1147947
33906_A	*TNRC5*	1.2380238	0.241364	0.1949591	1.8099168
1573002_A	*TOMM34*	1.1415949	0.1956206	0.1713573	3.7008086
241195_A	*TPD52L2*	1.4401984	0.2647813	0.1838505	0.2933343
150829_A	*TXNDC4*	1.2832661	0.2324767	0.1811602	1.2451143
38211_A	*UBCUBBC20orf109*	1.6451887	0.2919653	0.1774661	0.1147947
242008_B	*UBE2L6*	1.2703053	0.277201	0.218216	1.2451143
323783_B	*VEGF*	2.5578438	0.6839011	0.2673741	0.1147947
32682_A	*VIM*	2.6270694	0.424429	0.1615599	0.1147947
214542_A	*WFS1*	1.2351622	0.2161216	0.1749742	1.8099168
249193_A	*XPC*	1.3823071	0.2759341	0.1996185	0.540855
147834_A	*ZNF217*	1.2377518	0.2498414	0.201851	1.8099168

Supplementary Figure S9: Genes Specifically Down-Regulated Upon the HMF3A Temperature Shift

Clone ID	Gene	Score(d)	Numerator(r)	Denominator(s+s0)	q-value (%)
274217_A	*AATF*	-1.1016083	-0.2184047	0.1982599	2.5930212
36393_A	*ACAT2*	-1.9290077	-0.3517714	0.1823587	0.1147947
21766_A	*ACINUS*	-1.1031446	-0.2245985	0.2035985	2.5930212
233688_A	*ADAM12*	-2.9104264	-0.5982107	0.2055406	0.1147947
223345_A	*ADD1*	-1.065604	-0.1875109	0.1759668	3.7008086
48505_A	*ADD1*	-1.1368611	-0.2005825	0.1764353	1.8099168
192725_A	*AKT1*	-1.1525943	-0.2942895	0.255328	1.8099168
203165_A	*AMFR*	-1.0418691	-0.1901853	0.1825425	3.7008086
245779_A	*AP1G1*	-1.4305549	-0.2406674	0.1682336	0.2114793
26491_A	*ARL6IP*	-3.1823291	-0.6025089	0.1893295	0.1147947
51532_A	*ARL6IP*	-3.9166745	-0.7471265	0.1907553	0.1147947
51532_C	*ARL6IP*	-2.8834817	-0.5503368	0.1908584	0.1147947
25433_A	*ATP1B1*	-1.4991741	-0.2590837	0.1728176	0.1147947
302373_C	*ATP1B1*	-1.1572848	-0.2916145	0.2519816	1.8099168
310385_A	*ATP5B*	-2.2193077	-0.3794407	0.1709726	0.1147947
342879_B	*ATP5B*	-2.0896122	-0.3585383	0.1715812	0.1147947
34310_A	*ATP5F1*	-1.5333535	-0.2932851	0.1912704	0.1147947
46596_A	*ATP5F1*	-1.3299089	-0.254698	0.1915154	0.540855
186287_A	*ATP5G2*	-1.1271909	-0.2055844	0.1823865	2.5930212
382331_A	*ATP5G2*	-1.624364	-0.2881207	0.1773745	0.1147947
141228_A	*BANF1*	-1.5596501	-0.2903085	0.186137	0.1147947
309883_A	*BAP1*	-1.0643063	-0.2002039	0.1881074	3.7008086
46154_A	*BAP1*	-1.3071416	-0.2186592	0.1672804	0.540855
184082_A	*BAT1ATP6V1G2*	-3.1981518	-0.5969223	0.186646	0.1147947
22479_A	*BAT2*	-1.0211435	-0.2532497	0.248006	3.7008086
42638_A	*BAT2*	-1.2186063	-0.2700441	0.2216008	1.2451143
376055_A	*BAT3*	-1.3164321	-0.2182771	0.1658096	4.3356148
244767_A	*BRRN1*	-1.2083911	-0.2103969	0.1741132	1.2451143
563403_A	*BRRN1*	-1.2736672	-0.2244715	0.1762403	0.6702531
194384_A	*BTF3*	-1.2701708	-0.2305246	0.181491	0.6702531
416084_A	*BUB1B*	-2.0938334	-0.3779852	0.1805231	0.1147947
321627_A	*C1QBP*	-2.2804745	-0.4484038	0.1966274	0.1147947
197515_A	*C7orf14*	-1.1394418	-0.2675034	0.234767	1.8099168
38031_A	*CAD*	-1.2241153	-0.3044904	0.2487432	1.2451143
666534_A	*CAD*	-1.2855802	-0.2970253	0.2310438	0.540855
230884_A	*CALM2CALM1CALM3*	-1.3860974	-0.2308762	0.1665656	0.2933343
265613_B	*CALM2CALM1CALM3*	-1.1995471	-0.2258558	0.1882842	1.2451143
167080_A	*CALM3*	-1.4546117	-0.2947839	0.2026547	0.2114793
33672_A	*CALM3*	-1.1993929	-0.2403085	0.2003585	1.2451143
265569_A	*CAMKK2*	-1.016235	-0.2081775	0.2048517	3.7008086
294207_A	*CBX1*	-1.2933078	-0.2300937	0.177911	0.540855
300675_C	*CBX3*	-1.1223006	-0.2148786	0.1914626	2.5930212
427857_A	*CCNA2*	-2.7937249	-0.528559	0.1891951	0.1147947
128963_A	*CCNI*	-1.4645368	-0.2722112	0.1858684	0.2114793
261680_A	*CCNI*	-1.3814994	-0.2437548	0.1764422	0.2933343
243343_A	*CCT2*	-1.0666043	-0.1777118	0.1666146	3.7008086
299176_B	*CCT2*	-1.3396829	-0.2618102	0.195427	0.2933343

299705_A	*CCT2*	-1.6742566	-0.3114802	0.1860409	0.1147947
796474_A	*CDC2*	-2.8143519	-0.5435411	0.1931319	0.1147947
121716_D	*CDC25B*	-4.4466056	-0.6721728	0.1511654	0.1147947
785382_A	*CDC25B*	-1.9150084	-0.4941759	0.2580542	0.1147947
429755_A	*CDC25C*	-1.1228733	-0.192401	0.171347	2.5930212
264598_A	*CDK4*	-1.8793882	-0.3673538	0.1954646	0.1147947
364403_A	*CDKN2C*	-1.7082253	-0.4288939	0.2510757	0.1147947
121357_A	*CDKN3*	-1.3260604	-0.2565203	0.1934454	0.540855
124345_A	*CENPF*	-2.1270862	-0.3625689	0.1704533	0.1147947
784170_A	*CENPF*	-1.0270114	-0.2930007	0.2852945	3.7008086
724615_A	*CHC1*	-1.5047696	-0.268509	0.1784386	0.1147947
221318_A	*CKS2*	-1.0883251	-0.2118348	0.1946429	2.5930212
781690_A	*CLTC*	-1.9056426	-0.3373752	0.1770402	0.1147947
783875_A	*CLTC*	-1.7710764	-0.3530812	0.1993597	0.1147947
358506_A	*COL16A1*	-1.221494	-0.2766031	0.2264465	1.2451143
214997_A	*COL1A1*	-1.6035338	-0.3496424	0.2180449	0.1147947
298509_A	*COL1A1*	-2.8007483	-0.6628447	0.236667	0.1147947
323321_A	*COL1A1*	-3.4062148	-0.7140276	0.2096249	0.1147947
359255_A	*COL5A2*	-3.8542479	-0.8593222	0.2229546	0.1147947
138991_A	*COL6A3*	-1.8211331	-0.3870435	0.2125289	0.1147947
309817_A	*COPE*	-1.2359515	-0.2371894	0.1919083	0.6702531
267101_A	*COPS3*	-1.3645701	-0.2474443	0.1813349	0.2933343
172265_A	*COX8*	-1.6893872	-0.3251001	0.1924367	0.1147947
322848_A	*COX8*	-1.4466685	-0.2962259	0.2047642	0.2114793
365740_A	*CPSF5*	-1.9597803	-0.3872777	0.1976128	0.1147947
753091_A	*CPSF5*	-1.2346072	-0.245887	0.1991622	0.6702531
264153_A	*CPSF6*	-1.2263871	-0.2351335	0.1917286	0.6702531
33690_A	*CPSF6*	-1.3840314	-0.2830949	0.2045437	0.2933343
292806_A	*CSE1L*	-1.0302023	-0.1972746	0.1914911	3.7008086
292806_C	*CSE1L*	-1.0126413	-0.1715655	0.1694237	3.7008086
44477_B	*CTNND1*	-1.31805	-0.2326623	0.1765201	0.540855
141887_A	*CUGBP1*	-1.22911	-0.2618537	0.2130433	0.6702531
25588_A	*CUGBP1*	-1.2979104	-0.2214083	0.1705883	0.540855
310770_A	*DAG1*	-1.5140889	-0.3318107	0.2191487	0.1147947
121348_A	*DCTN3*	-1.2554546	-0.2656215	0.211574	0.6702531
263741_A	*DDX17*	-1.0433611	-0.2264361	0.2170256	3.7008086
127925_A	*DDX18*	-1.1297678	-0.2335211	0.2066984	1.8099168
306186_A	*DDX5*	-2.1464231	-0.4392477	0.2046417	0.1147947
294421_A	*DDX9*	-1.4587021	-0.3164861	0.2169641	0.2114793
300363_A	*DDX9*	-1.6526465	-0.3033659	0.1835637	0.1147947
774194_A	*DEK*	-2.0111483	-0.4000534	0.1989179	0.1147947
301013_A	*DHFR*	-1.2223445	-0.2545819	0.2082734	1.2451143
259596_A	*DLG7*	-1.4593911	-0.2877375	0.1971627	0.2114793
357373_A	*DLG7*	-1.660311	-0.2693473	0.162227	0.1147947
206863_A	*DNMT1*	-1.1962102	-0.2208233	0.1846024	1.2451143
768241_A	*DNMT1*	-1.6666334	-0.2935604	0.1761398	0.1147947
427768_A	*DSTN*	-1.5260522	-0.3295121	0.2159246	0.1147947
471871_A	*DTYMK*	-1.508559	-0.2669014	0.1769248	0.1147947
784852_B	*DTYMK*	-1.0861174	-0.1806546	0.1663306	2.5930212
342323_A	*DUT*	-1.634061	-0.2751092	0.1683592	0.1147947
730908_A	*DUT*	-1.5565997	-0.2770008	0.1779525	0.1147947
195924_A	*E2F4*	-1.3653775	-0.3246604	0.2377807	0.2933343

22918_A	*EBNA1BP2*	-1.3309074	-0.3010187	0.2261756	0.540855
51776_A	*EBNA1BP2*	-2.0201487	-0.3933181	0.1946976	0.1147947
33505_A	*EBP*	-1.5698703	-0.2685656	0.171075	0.1147947
121153_A	*ECHS1*	-1.0834074	-0.2073574	0.1913937	2.5930212
33636_A	*EIF3S7*	-1.3424269	-0.2463451	0.1835073	0.2933343
204614_A	*EIF4A1*	-2.6722367	-0.4601235	0.1721867	0.1147947
37928_A	*EIF4A1*	-2.4859151	-0.417912	0.1681119	0.1147947
25988_A	*EIF4G1*	-1.1504338	-0.3298969	0.2867587	1.8099168
774115_B	*EIF5*	-1.4965943	-0.2659993	0.1777364	0.1147947
345208_A	*ELAVL1*	-1.1966219	-0.249189	0.2082437	1.2451143
309908_A	*EMD*	-1.7686377	-0.3843106	0.2172919	0.1147947
307996_B	*ENO1*	-1.7999089	-0.4493965	0.2496774	0.1147947
346468_B	*EPB41L2*	-1.3088541	-0.2216416	0.1693402	0.540855
358350_A	*EWSR1*	-2.8145797	-0.5102939	0.1813038	0.1147947
stSG89196	*EWSR1*	-1.2119471	-0.2468716	0.2036983	1.2451143
784863_A	*FNBP3*	-1.8406094	-0.340707	0.1851055	0.1147947
1677198_A	*FNBP4*	-1.2774507	-0.2149263	0.1682462	0.6702531
127266_A	*FOXM1*	-2.2452769	-0.5462063	0.243269	0.1147947
259115_A	*FOXM1*	-1.8793983	-0.3785349	0.2014128	0.1147947
376180_A	*FPGS*	-1.2329862	-0.2527785	0.2050132	0.6702531
300482_B	*FUBP3*	-1.3497824	-0.2728152	0.2021179	0.2933343
40567_A	*GCN1L1*	-1.0271954	-0.2520994	0.245425	3.7008086
41510_A	*GCN1L1*	-1.0945896	-0.2006584	0.1833184	2.5930212
774750_A	*GNAI3*	-1.7434227	-0.3539597	0.2030257	0.1147947
249289_A	*GNB1*	-1.6793464	-0.3059294	0.1821717	0.1147947
265467_A	*GNB1*	-2.3216364	-0.3708076	0.1597182	0.1147947
308856_A	*GNB2*	-1.3144537	-0.3385206	0.2575371	0.540855
298453_A	*GPRK6*	-1.3245766	-0.2660416	0.2008503	0.540855
37324_B	*GRB2*	-1.1837992	-0.2472015	0.2088205	1.2451143
42058_A	*GRB2*	-1.0851279	-0.240946	0.2220439	2.5930212
53322_B	*GTF3C1*	-1.2344644	-0.2461327	0.1993842	0.6702531
stSG89400	*GTSE1*	-2.7480911	-0.5373456	0.1955341	0.1147947
stSG89322	*H1F0*	-1.5104164	-0.2598768	0.1720564	0.1147947
122926_A	*H2AFZ*	-2.3792886	-0.4945026	0.2078363	0.1147947
754345_A	*HDAC1*	-1.246245	-0.2426445	0.1947005	0.6702531
309924_A	*HDAC2*	-1.1744668	-0.2147714	0.1828671	1.2451143
813673_A	*HDGF*	-2.6818602	-0.5853612	0.2182669	0.1147947
787878_A	*HDLBP*	-1.2217996	-0.3498663	0.2863533	1.2451143
212656_A	*HELZ*	-1.1154065	-0.1909956	0.1712341	2.5930212
233606_B	*HIP2*	-1.2945365	-0.2682746	0.207236	0.540855
stSG89294	*HMG17L1*	-2.9786371	-0.7344863	0.2465847	0.1147947
124257_A	*HMGB2*	-5.1205966	-0.976238	0.1906493	0.1147947
267145_A	*HMGB2*	-4.5176721	-0.9507539	0.2104522	0.1147947
124836_A	*HMGB3*	-1.3824763	-0.3032178	0.2193295	0.2933343
298516_A	*HNRPA2B1*	-2.1277703	-0.5243069	0.2464114	0.1147947
310781_A	*HNRPC*	-1.4057879	-0.2822374	0.2007681	0.2114793
345600_B	*HNRPC*	-1.0178265	-0.2016479	0.1981162	3.7008086
35170_A	*HNRPC*	-1.5641596	-0.2919826	0.1866706	0.1147947
358457_A	*HNRPH1*	-2.4358473	-0.529401	0.2173375	0.1147947
321590_A	*HNRPH3*	-1.0301451	-0.2788729	0.2707123	3.7008086
681973_A	*HNRPH3*	-1.0126148	-0.2440825	0.2410418	3.7008086
306373_C	*HNRPL*	-1.7034577	-0.3325916	0.195245	0.1147947

487501_A	*HNRPR*	-2.4982267	-0.4964787	0.1987325	0.1147947
784486_A	*HNRPU*	-2.4079187	-0.5009642	0.2080486	0.1147947
767828_A	*HPS1*	-1.1766129	-0.2006664	0.1705458	1.2451143
361171_A	*HTATIP*	-1.3853713	-0.2592823	0.1871573	0.2933343
51683_A	*IDH2*	-1.5000462	-0.2949727	0.1966424	0.1147947
713714_A	*IDH3B*	-1.4691935	-0.3227069	0.219649	0.2114793
261971_A	*IGHDPCOLN3*	-1.7433862	-0.42274	0.2424821	0.1147947
810831_A	*ILF2*	-1.1657403	-0.2297923	0.1971214	1.8099168
29607_A	*IMPDH2*	-2.4747694	-0.5307602	0.2144685	0.1147947
36485_A	*IMPDH2*	-2.3516802	-0.5496124	0.2337105	0.1147947
280626_B	*IQGAP1*	-1.2742973	-0.2547283	0.1998971	0.6702531
667376_A	*IREB2*	-1.0774829	-0.2322254	0.2155259	2.5930212
682172_A	*IREB2*	-1.1146587	-0.1813566	0.1627015	2.5930212
154015_A	*ITGAL*	-1.1471513	-0.2028814	0.1768567	1.8099168
271814_A	*ITGB4BP*	-1.9570155	-0.3705414	0.1893401	0.1147947
415761_A	*ITGB4BP*	-1.8827938	-0.3553991	0.1887616	0.1147947
810531_A	*ITPA*	-1.2779743	-0.2832956	0.2216755	0.6702531
150722_A	*KHDRBS1*	-2.1876794	-0.4559309	0.2084085	0.1147947
40983_A	*KIF22*	-1.1344691	-0.3328649	0.2934103	1.8099168
212780_A	*KIF23*	-3.0602967	-0.619498	0.2024307	0.1147947
292933_A	*KIFC1*	-1.5874545	-0.2691631	0.1695564	0.1147947
327575_A	*KIFC1*	-1.5934681	-0.3920635	0.2460442	0.1147947
112136_A	*KNTC1*	-1.0916594	-0.1890951	0.173218	2.5930212
127980_A	*KNTC1*	-1.586753	-0.324774	0.2046784	0.1147947
21687_A	*KPNA3*	-1.1018387	-0.2093194	0.1899728	2.5930212
47696_A	*KPNA6*	-1.1809102	-0.3162131	0.2677707	1.2451143
307553_A	*KRAS2*	-1.1057637	-0.1896811	0.1715385	2.5930212
307225_A	*LBR*	-1.4164791	-0.3069696	0.2167131	0.2114793
34461_A	*LGALS3*	-1.326207	-0.2312908	0.1744003	0.540855
1304246_A	*LMNB1*	-1.2042595	-0.2404696	0.1996826	1.2451143
50031_A	*LMO4*	-1.0220549	-0.2021911	0.197828	3.7008086
415554_A	*LRP8*	-1.1820161	-0.1971056	0.1667538	1.2451143
25773_A	*LYPLA1*	-1.0206664	-0.2126613	0.2083553	3.7008086
37830_B	*LYPLA1*	-1.0621932	-0.2541748	0.2392925	3.7008086
298904_A	*M11S1*	-1.1518659	-0.2040531	0.17715	1.8099168
214636_A	*MADH5*	-1.1358111	-0.2160601	0.1902254	1.8099168
362634_A	*MAPK3*	-1.0261912	-0.2299516	0.2240826	3.7008086
32555_B	*MAT2A*	-2.298518	-0.3741833	0.1627933	0.1147947
42288_A	*MATR3*	-1.1829134	-0.232797	0.1967997	1.2451143
365824_A	*MAZ*	-3.3192655	-0.7756182	0.2336716	0.1147947
199078_A	*MBD3*	-1.3548446	-0.3039433	0.2243381	0.2933343
375917_A	*MCM2*	-1.7021082	-0.3765633	0.2212335	0.1147947
1842548_A	*MDFI*	-1.5778472	-0.2923218	0.1852662	0.1147947
42363_A	*ME3*	-1.1031551	-0.22591	0.2047854	2.5930212
327289_A	*MELK*	-1.0920763	-0.1942507	0.1778728	2.5930212
796122_A	*MELK*	-1.1094192	-0.2441536	0.2200734	2.5930212
240795_A	*MKI67*	-4.2360525	-0.8409788	0.1985289	0.1147947
688005_A	*MKI67*	-2.6706728	-0.5462561	0.2045388	0.1147947
166947_A	*MMS19L*	-1.1293881	-0.1835492	0.162521	1.8099168
324917_A	*MORF4L2*	-1.3779969	-0.248982	0.180684	0.2933343
359821_A	*MRPL28*	-1.2402306	-0.2549953	0.2056031	0.6702531
32938_A	*MRPL3*	-1.9813644	-0.4069821	0.205405	0.1147947

591864_C	*MRPL3*	-1.4095858	-0.2174181	0.1542425	0.2114793
1581142_A	*MSH5*	-1.1473071	-0.2207853	0.1924378	1.8099168
327155_A	*MYL6*	-2.1062244	-0.3287174	0.1560695	0.1147947
728122_A	*MYL6*	-2.1662204	-0.3963179	0.1829536	0.1147947
34607_A	*NDUFA9*	-2.0614364	-0.3504916	0.170023	0.1147947
132618_A	*NDUFB7*	-1.0892362	-0.2379116	0.2184206	2.5930212
140205_A	*NDUFB7*	-1.1448867	-0.2052763	0.1792983	1.8099168
126868_A	*NFIC*	-1.2811259	-0.3639983	0.2841238	0.6702531
240186_A	*NFIC*	-1.2074897	-0.3460113	0.2865543	1.2451143
49705_A	*NID*	-1.4732156	-0.409164	0.2777353	0.1147947
300041_B	*NME1*	-1.4683029	-0.2831254	0.1928249	0.2114793
146758_A	*NNMT*	-1.4661739	-0.2900447	0.1978242	0.2114793
296513_A	*NOL5A*	-1.5118295	-0.2916385	0.1929043	0.1147947
231749_A	*NUMA1*	-1.3609698	-0.3579503	0.2630112	0.2933343
365687_B	*NUMA1*	-1.5069369	-0.295512	0.1961011	0.1147947
27548_A	*NUP153*	-1.1976674	-0.2496636	0.2084582	1.2451143
130371_B	*NUP155*	-1.9667074	-0.414509	0.2107629	0.1147947
281853_A	*NUP160*	-1.0787072	-0.1931338	0.1790419	2.5930212
1030933_A	*ODF2*	-1.1532448	-0.2271076	0.1969292	1.8099168
28012_A	*OGT*	-1.1531352	-0.2032971	0.1762995	1.8099168
34628_A	*OGT*	-1.5335295	-0.2982225	0.1944681	0.1147947
306418_A	*PAICS*	-2.2684621	-0.4617391	0.2035472	0.1147947
44839_A	*PAICS*	-2.46106	-0.4608836	0.1872704	0.1147947
1406874_A	*PAWRPPP1R12A*	-1.5880729	-0.3064039	0.1929407	0.1147947
250248_A	*PCBP2*	-1.2803009	-0.284903	0.2225282	0.6702531
343368_B	*PCM1*	-1.3048491	-0.2661299	0.2039546	0.540855
198513_A	*PCNT2*	-1.1664363	-0.2576165	0.2208577	1.8099168
39040_A	*PCOLCE*	-1.1785437	-0.2371846	0.2012523	1.2451143
44421_A	*PCTK1*	-1.1154177	-0.2885054	0.2586523	2.5930212
271324_A	*PIGA*	-1.3389107	-0.3244032	0.2422889	0.2933343
180425_A	*PIK4CA*	-1.4484579	-0.2866298	0.1978862	0.2114793
346679_A	*PITPN*	-1.4288309	-0.2842085	0.1989098	0.2114793
24659_A	*PLEKHC1*	-1.1533999	-0.2186754	0.189592	1.8099168
211287_B	*PLP2*	-1.2056037	-0.249523	0.2069693	1.2451143
300658_A	*PMSCL2*	-1.3110251	-0.2474903	0.1887762	0.540855
813548_A	*PMSCL2*	-1.7112632	-0.3231552	0.1888402	0.1147947
299083_A	*POLD2*	-1.2086991	-0.2429649	0.2010135	1.2451143
469884_A	*POLD2*	-1.0940933	-0.2043123	0.1867412	2.5930212
246310_A	*POLR2A*	-1.2955958	-0.2716129	0.2096432	0.540855
264589_A	*POLR2A*	-1.9019623	-0.3395209	0.1785109	0.1147947
50142_A	*POLR2B*	-1.0585631	-0.2021441	0.1909608	3.7008086
156418_B	*POLR2E*	-1.9826007	-0.4326626	0.2182298	0.1147947
248282_A	*PPP1CCPPP1CA*	-1.4253154	-0.3322256	0.2330892	0.2114793
257259_A	*PPP1CCPPP1CA*	-1.412858	-0.3380568	0.2392716	0.2114793
756666_A	*PPP1CCPPP1CA*	-1.1234482	-0.2089714	0.1860089	2.5930212
130545_A	*PPP1R14B*	-1.2175002	-0.2624708	0.2155817	1.2451143
23534_A	*PPP2CA*	-1.4207603	-0.2939534	0.2068986	0.2114793
40199_A	*PPP2R1A*	-1.7567219	-0.3407673	0.1939791	0.1147947
770027_A	*PPP2R1A*	-1.356021	-0.2410502	0.1777628	0.2933343
32427_A	*PPP2R4*	-1.1601409	-0.243067	0.2095151	1.8099168
37822_A	*PPP2R4*	-1.3236647	-0.4508071	0.340575	0.540855
772455_A	*PPP4C*	-1.1641093	-0.2233864	0.1918947	1.8099168

364351_A	*PPP5C*	-1.1875771	-0.2369868	0.1995549	1.2451143
755378_A	*PRC1*	-4.086542	-0.8077261	0.1976552	0.1147947
785707_A	*PRC1*	-4.8674222	-0.9673379	0.1987372	0.1147947
294653_A	*PRCC*	-1.0476064	-0.2092926	0.1997817	3.7008086
25993_A	*PRDX1*	-2.0602995	-0.3802709	0.1845707	0.1147947
320325_A	*PRDX1*	-2.2261818	-0.4219955	0.1895602	0.1147947
229944_A	*PRPSAP1*	-1.0302295	-0.1812452	0.175927	3.7008086
667598_C	*PSIP1PSIP2*	-1.1005852	-0.1935965	0.1759032	2.5930212
811998_A	*PSIP1PSIP2*	-1.4159338	-0.229391	0.1620069	0.2114793
256425_A	*PSMB1*	-1.2507886	-0.2309135	0.1846143	0.6702531
1839895_A	*PSMB2*	-1.5141659	-0.2958663	0.1953989	0.1147947
290864_A	*PSMB2*	-1.4713791	-0.2776072	0.1886714	0.1147947
321823_A	*PSMB3*	-1.1479596	-0.229499	0.1999191	1.8099168
321894_B	*PSMB3*	-1.3192227	-0.2326741	0.1763721	0.540855
201275_A	*PSMB6*	-1.9554236	-0.3175377	0.1623882	0.1147947
30520_A	*PSMC3*	-1.7813368	-0.3736721	0.2097706	0.1147947
42744_A	*PSMC5*	-1.0978474	-0.2493394	0.2271166	2.5930212
43940_A	*PSMC5*	-1.6552036	-0.2682415	0.1620595	0.1147947
823598_A	*PSMD12*	-1.1280312	-0.2377652	0.2107789	2.5930212
298737_A	*PSMD8*	-1.2436315	-0.2174869	0.1748805	0.6702531
187848_B	*PSME3*	-1.6515298	-0.3102609	0.1878627	0.1147947
231021_A	*PTGS1*	-1.2044045	-0.3458677	0.287169	1.2451143
2109679_A	*PTRF*	-1.7013937	-0.7267265	0.427136	0.1147947
44344_A	*PWP2H*	-1.0994202	-0.221945	0.2018746	2.5930212
362133_A	*PXF*	-1.2862264	-0.2518654	0.1958173	0.540855
323762_F	*PYGB*	-1.1898865	-0.2274328	0.1911382	1.2451143
324334_C	*PYGB*	-1.4611874	-0.2900389	0.1984953	0.2114793
47727_A	*PYGB*	-1.2371113	-0.2297647	0.1857268	0.6702531
810616_A	*QARS*	-1.2031687	-0.2335215	0.1940887	1.2451143
32396_A	*RAB1B*	-2.2928836	-0.5090346	0.2220063	0.1147947
768212_A	*RAB1B*	-1.5886169	-0.4281848	0.2695331	0.1147947
788776_A	*RAB5B*	-1.1057308	-0.2685046	0.2428299	2.5930212
271796_A	*RALY*	-1.2115655	-0.2523311	0.2082686	1.2451143
49402_A	*RALY*	-1.210619	-0.2349689	0.1940899	1.2451143
stSG89500	*RANBP1*	-1.6416378	-0.2946266	0.1794712	0.1147947
47920_A	*RBM14*	-1.4108219	-0.2781251	0.1971369	0.2114793
stSG89113	*RBX1*	-1.0482359	-0.1835695	0.1751223	3.7008086
193081_A	*RDX*	-1.6558085	-0.382448	0.2309736	0.1147947
342714_A	*RDX*	-1.8365815	-0.3600339	0.1960348	0.1147947
135538_A	*REST*	-1.0942887	-0.1860303	0.1700012	2.5930212
233867_A	*RNU3IP2*	-1.1138834	-0.1957245	0.1757136	2.5930212
249295_B	*RPA1*	-1.8098077	-0.3735509	0.2064036	0.1147947
308501_A	*RPA1*	-1.728245	-0.3421279	0.1979626	0.1147947
132643_A	*RPL18*	-1.2879443	-0.2630147	0.2042128	0.540855
727149_A	*RPS15A*	-1.1610011	-0.2171122	0.1870043	1.8099168
325115_A	*RPS6KB2*	-1.1431554	-0.2116602	0.1851543	1.8099168
380356_A	*RRM1*	-1.1231654	-0.2064479	0.183809	2.5930212
417504_A	*RRM2*	-2.1792314	-0.4003796	0.1837252	0.1147947
270362_A	*RTN3*	-1.1444726	-0.1879064	0.164186	1.8099168
123056_A	*SART1*	-1.2696097	-0.2876149	0.226538	0.6702531
233194_A	*SATB1*	-1.0806939	-0.2228102	0.2061733	2.5930212
24761_A	*SEC13L1*	-1.5013197	-0.3010103	0.2004971	0.1147947

37267_A	*SEC13L1*	-1.3049536	-0.2759984	0.2115005	0.540855
40704_A	*SEC14L1*	-1.2226166	-0.2231582	0.1825251	1.2451143
1876913_A	*SF1*	-1.9171965	-0.3898482	0.2033429	0.1147947
279329_A	*SF1*	-1.0803051	-0.3442614	0.3186705	2.5930212
345042_A	*SF3B1*	-1.9786619	-0.3563562	0.1800996	0.1147947
204755_A	*SFRS11*	-1.779223	-0.3391469	0.1906152	0.1147947
669372_A	*SFRS11*	-1.7721132	-0.3091516	0.1744537	0.1147947
40597_A	*SFRS3*	-2.3130655	-0.4515975	0.1952377	0.1147947
209239_A	*SFRS4*	-1.2686206	-0.2059898	0.1623731	0.6702531
132274_A	*SFRS5*	-1.2189633	-0.2336464	0.1916764	1.2451143
1580875_A	*SFTPA1SFTPA2*	-1.5881036	-0.3571192	0.2248715	0.1147947
261682_A	*SIAT4C*	-1.9626751	-0.4527099	0.2306596	0.1147947
342861_A	*SKB1*	-1.1578455	-0.228682	0.1975065	1.8099168
308868_A	*SLC12A3*	-1.0191037	-0.1839108	0.1804633	3.7008086
324787_A	*SLC12A3*	-2.1436613	-0.4551499	0.2123236	0.1147947
202325_A	*SLC17A1*	-1.0432737	-0.208617	0.1999638	3.7008086
41815_B	*SLC19A1*	-1.0583401	-0.2731389	0.2580824	3.7008086
265111_A	*SLC25A4*	-2.6803929	-0.4081934	0.1522886	0.1147947
296111_A	*SLC25A4*	-2.5894504	-0.457676	0.1767464	0.1147947
1160864_A	*SLC27A2*	-1.1562683	-0.2776175	0.2400979	1.8099168
31842_A	*SLC35B1*	-1.1397589	-0.1993083	0.1748688	1.8099168
37618_A	*SLC7A6*	-1.1513349	-0.2125321	0.1845962	1.8099168
34823_A	*SMARCC1*	-1.5785746	-0.3541863	0.224371	0.1147947
797218_B	*SMARCD2*	-1.3204951	-0.2120757	0.160603	4.3356148
32733_A	*SMC1L1*	-1.3028049	-0.224946	0.1726629	0.540855
361368_A	*SMC1L1*	-1.6007942	-0.2854707	0.1783307	0.1147947
46800_A	*SMC1L1*	-1.1826547	-0.1970928	0.1666529	1.2451143
300169_A	*SMC4L1*	-2.6547398	-0.5308376	0.1999584	0.1147947
795562_B	*SMC4L1*	-1.9024477	-0.4033104	0.2119955	0.1147947
273154_A	*SMT3H2*	-2.0011438	-0.3634211	0.1816067	0.1147947
299343_A	*SMT3H2*	-1.1351991	-0.2116272	0.186423	1.8099168
322829_C	*SMT3H2*	-1.9620556	-0.340276	0.1734283	0.1147947
323440_C	*SMT3H2*	-1.9560189	-0.3558497	0.1819255	0.1147947
124261_A	*SNRP70*	-1.3952865	-0.3181625	0.2280266	0.2933343
321292_A	*SNRP70*	-1.239776	-0.297335	0.2398296	0.6702531
796412_B	*SNRP70*	-1.054486	-0.2190307	0.2077132	3.7008086
249460_A	*SNRPC*	-1.1299498	-0.2123682	0.1879448	1.8099168
47542_C	*SNRPD1*	-2.2418152	-0.3703667	0.1652084	0.1147947
33411_A	*SPTAN1*	-2.5354024	-0.4196238	0.1655058	0.1147947
771091_A	*SRRM2*	-1.7226777	-0.3136732	0.1820847	0.1147947
129865_A	*STK15STK6*	-1.4101398	-0.2561084	0.1816192	0.2114793
205931_A	*STK15STK6*	-1.9091614	-0.3396442	0.1779023	0.1147947
209066_A	*STK15STK6*	-1.3604218	-0.2823664	0.207558	0.2933343
37799_B	*STK18*	-1.0383673	-0.1830839	0.176319	3.7008086
23697_A	*STMN1*	-1.621613	-0.3131939	0.1931373	0.1147947
40791_A	*STOML2*	-1.6060852	-0.3874556	0.2412423	0.1147947
271286_A	*SURF4*	-1.521655	-0.4113924	0.2703585	0.1147947
201196_A	*TAF11*	-1.5669596	-0.2927779	0.1868446	0.1147947
138581_A	*TAGLN*	-1.0613441	-0.2138422	0.2014825	3.7008086
188403_A	*TAGLN*	-1.0983327	-0.2597656	0.236509	2.5930212
301377_A	*TCERG1*	-1.2864393	-0.2849536	0.2215057	0.540855
729951_A	*TCOF1*	-1.1900569	-0.2556068	0.2147854	1.2451143

281778_A	*TGFB2*	-1.150272	-0.2487523	0.2162552	1.8099168
114858_A	*THOC2*	-1.0731474	-0.2055363	0.1915266	3.7008086
358027_A	*THOC4*	-1.3566487	-0.2722411	0.2006718	0.2933343
246300_A	*TIAL1*	-1.1177295	-0.1856055	0.1660558	2.5930212
252456_A	*TIAL1*	-1.3011607	-0.2620649	0.2014085	0.540855
279745_A	*TIAL1*	-1.1084192	-0.1931536	0.1742604	2.5930212
357005_A	*TIMM23*	-1.0754611	-0.2180313	0.2027329	2.5930212
241667_A	*TM4SF4*	-1.0753874	-0.22608	0.2102312	2.5930212
1288333_B	*TMPO*	-1.744589	-0.4253059	0.2437857	0.1147947
1334613_A	*TMPO*	-2.2942351	-0.4738541	0.2065412	0.1147947
299778_A	*TOMM70A*	-1.1881251	-0.207358	0.1745254	1.2451143
291808_B	*TRIM28*	-1.7494159	-0.402449	0.2300477	0.1147947
37241_A	*TRIO*	-2.1480218	-0.4806749	0.2237756	0.1147947
429234_A	*TRIO*	-2.0182905	-0.4275225	0.2118241	0.1147947
487275_B	*TRIO*	-1.7607724	-0.3819463	0.2169197	0.1147947
34563_A	*TSN*	-1.3752383	-0.2530074	0.1839735	0.2933343
40854_A	*TSN*	-1.4780372	-0.2939455	0.1988756	0.1147947
191603_A	*TUBB*	-2.6280331	-0.4918135	0.1871413	0.1147947
27464_A	*TUBB*	-1.5955597	-0.3923252	0.2458856	0.1147947
146345_A	*TXK*	-1.2800588	-0.2453669	0.1916841	0.6702531
148421_A	*TXK*	-1.1439663	-0.2441528	0.2134265	1.8099168
295286_A	*UBE2C*	-1.8672514	-0.3324552	0.1780452	0.1147947
758484_A	*UBE2C*	-1.1092758	-0.227078	0.2047083	2.5930212
769921_A	*UBE2C*	-1.0379475	-0.2476505	0.2385963	3.7008086
298367_B	*UBE2M*	-1.0227793	-0.1904176	0.1861766	3.7008086
25867_A	*UNC84B*	-3.8247993	-0.8383005	0.219175	0.1147947
321390_A	*UNC84B*	-3.5640847	-0.813972	0.2283818	0.1147947
stSG89333	*UNC84B*	-2.1448251	-0.5042608	0.2351058	0.1147947
300740_B	*UQCRC1*	-2.4627205	-0.4291544	0.1742603	0.1147947
366955_A	*UQCRC1*	-1.51207	-0.3370607	0.2229134	0.1147947
362441_A	*UQCRC2*	-1.4118724	-0.2630969	0.1863461	0.2114793
362812_A	*UQCRC2*	-1.4526166	-0.295754	0.2036009	0.2114793
363211_A	*USP1*	-1.4764751	-0.3402924	0.2304762	0.1147947
287850_B	*USP14*	-1.2230159	-0.1923662	0.1572884	1.2451143
49297_A	*USP5*	-1.5325437	-0.3391221	0.2212805	0.1147947
1409032_B	*USP7*	-1.2651306	-0.2768119	0.2188011	0.6702531
33252_A	*USP7*	-1.3514584	-0.2684179	0.1986135	0.2933343
41572_A	*USP7*	-1.3188704	-0.2317477	0.1757168	0.540855
42813_A	*VARS2VARS1*	-1.3649056	-0.2836582	0.2078226	0.2933343
136030_A	*VCP*	-1.295317	-0.3203487	0.247313	0.540855
32020_A	*VCP*	-1.160983	-0.3542484	0.305128	1.8099168
234856_A	*VHL*	-1.0389846	-0.1936787	0.1864115	3.7008086
259364_A	*XPO1*	-2.4729075	-0.4464216	0.180525	0.1147947
321717_A	*XPO1*	-1.9316897	-0.3805016	0.1969786	0.1147947
133178_A	*YES1*	-1.0136751	-0.1925954	0.1899972	3.7008086
667379_A	*ZNF205*	-1.1321375	-0.2291234	0.2023813	1.8099168
137638_A	*ZNF22*	-1.1181643	-0.1979047	0.1769907	2.5930212
726332_A	*ZWINT*	-1.7303632	-0.3168577	0.1831163	0.1147947
144708_A	*ZYX*	-1.3993407	-0.3096434	0.221278	0.2114793

Supplementary Figure S10: Genes Up-Regulated by Ectopic Wt LT Expression

Clone ID	Gene	Score(d)	Numerator(r)	Denominator(s+s0)	Fold Change	q-value (%)
51532_A	*ARL6IP*	-4.4008882	-0.6335446	0.1439584	0.64498	0.7194245
26491_A	*ARL6IP*	-3.8096849	-0.526123	0.1381015	0.69564	0.7194245
51532_C	*ARL6IP*	-3.1544331	-0.5125697	0.1624919	0.69721	0.7194245
184082_A	*BAT1ATP6V1G2*	-3.7595441	-0.4943758	0.1314989	0.71132	0.7194245
796474_A	*CDC2*	-3.3665713	-0.4809563	0.1428624	0.71797	0.7194245
121716_D	*CDC25B*	-5.8422323	-0.6459509	0.1105658	0.63676	0.7194245
307996_B	*ENO1*	-2.4196914	-0.5212856	0.2154347	0.70539	1.3245033
122926_A	*H2AFZ*	-2.6674496	-0.4490411	0.168341	0.73333	0.7194245
stSG89294	*HMG17L1*	-2.2679771	-0.4867439	0.2146159	0.72099	2.9761905
124257_A	*HMGB2*	-6.699857	-0.8523026	0.1272121	0.55683	0.7194245
267145_A	*HMGB2*	-4.983676	-0.8178785	0.1641115	0.56958	0.7194245
298516_A	*HNRPA2B1*	-2.1746377	-0.4265846	0.1961635	0.76023	2.9761905
35170_A	*HNRPC*	-2.8847038	-0.3829436	0.1327497	0.76831	0.7194245
321590_A	*HNRPH3*	-2.4586372	-0.5883885	0.2393149	0.67837	1.3245033
212780_A	*KIF23*	-2.6895739	-0.4371262	0.1625262	0.73866	0.7194245
240795_A	*MKI67*	-4.6194183	-0.7020761	0.1519837	0.61591	0.7194245
688005_A	*MKI67*	-2.6244092	-0.4207138	0.160308	0.74888	0.7194245
785707_A	*PRC1*	-4.3607106	-0.7210437	0.1653501	0.60537	0.7194245
755378_A	*PRC1*	-3.5751923	-0.561618	0.1570875	0.67738	0.7194245
296111_A	*SLC25A4*	-2.5209865	-0.4068916	0.1614017	0.74607	0.7194245
300169_A	*SMC4L1*	-3.7572947	-0.5953573	0.1584537	0.66208	0.7194245
795562_B	*SMC4L1*	-2.2903059	-0.4112201	0.1795481	0.75210	1.863354
205931_A	*STK15STK6*	-4.5719023	-0.6324243	0.1383285	0.64305	0.7194245
209066_A	*STK15STK6*	-2.8763227	-0.4833939	0.1680597	0.71651	0.7194245
295286_A	*UBE2C*	-3.5158761	-0.6408865	0.1822836	0.62992	0.7194245
758484_A	*UBE2C*	-3.0200646	-0.5310731	0.1758483	0.68975	0.7194245
25867_A	*UNC84B*	-2.4595149	-0.5338239	0.2170444	0.68286	1.3245033
321390_A	*UNC84B*	-2.218338	-0.4895155	0.2206677	0.70782	2.9761905

Supplementary Figure S11: Genes Down-Regulated by Ectopic Wt LT Expression

Clone ID	Gene	Score(d)	Numerator(r)	Denominator(s+s0)	Fold Change	q-value (%)
293270_A	*AKR1C2*	3.9125645	0.5535548	0.1414813	1.47137	0.7194245
300484_A	*ANXA1*	2.167422	0.4419203	0.2038921	1.34523	1.3245033
341038_A	*ATP6IP2*	2.5834237	0.4619885	0.178828	1.36672	0.7194245
738975_B	*B4GALT1*	2.3266036	0.460977	0.198133	1.36911	0.7194245
310406_A	*C6orf48*	2.5711411	0.397025	0.1544159	1.32116	0.7194245
796005_A	*CDH11*	4.7288636	0.7455682	0.1576633	1.68248	0.7194245
31093_A	*CDH13*	2.6366833	0.5051882	0.1915999	1.41056	0.7194245
124554_A	*CSF1*	2.5385261	0.5381675	0.212	1.46450	0.7194245
246147_A	*CSPG2*	3.0435187	0.5527057	0.1816009	1.46335	0.7194245
380384_A	*CUL4B*	3.6218698	0.586447	0.1619183	1.51452	0.7194245
51003_A	*DKK3*	3.2577884	0.5518954	0.169408	1.44307	0.7194245
252443_A	*DUSP4*	3.1112205	0.47533	0.1527793	1.40055	0.7194245
270148_A	*DUSP4*	2.3609712	0.3831838	0.1622992	1.31671	0.7194245
301122_A	*ECM1*	2.2203138	0.4689502	0.211209	1.40402	1.3245033
323181_A	*FAP*	3.0205156	0.4208646	0.1393353	1.34516	0.7194245
665401_A	*FGF2*	2.6446823	0.7235693	0.273594	1.71622	0.7194245
115383_A	*GADD45A*	2.2221349	0.5225684	0.235165	1.40326	1.3245033
310141_A	*GADD45A*	2.203071	0.504099	0.2288165	1.40542	1.3245033
486844_A	*GJA1*	2.3570016	0.469974	0.1993949	1.39295	0.7194245
309079_A	*GJA1*	2.1185164	0.4863631	0.2295772	1.39635	1.863354
308993_A	*GJA1*	1.9257525	0.3823578	0.1985498	1.30030	4
stSG89160	*HMOX1*	2.0506171	0.7025886	0.342623	1.50316	1.863354
196375_A	*IGFBP3*	6.8838773	1.4755415	0.2143474	2.80723	0.7194245
266838_A	*IGFBP3*	6.2026905	1.3310898	0.2145988	2.51626	0.7194245
299204_A	*IGFBP7*	6.324082	1.3119845	0.2074585	2.47895	0.7194245
244990_A	*LIPA*	2.9500551	0.4358448	0.1477413	1.35522	0.7194245
667364_A	*LOXL1*	1.883027	0.4329218	0.2299074	1.33351	4
297957_A	*LPXN*	3.5595874	0.45602	0.1281103	1.37172	0.7194245
23356_B	*MAP1LC3B*	2.4072893	0.3767228	0.1564925	1.30215	0.7194245
232772_A	*MT1B*	4.5937401	0.6545524	0.1424879	1.58299	0.7194245
66946_A	*MT1B*	2.6725641	0.5899638	0.2207482	1.51937	0.7194245
202535_A	*MT1K*	3.7857509	0.5135984	0.1356662	1.42938	0.7194245
202535_C	*MT1K*	3.4248012	0.6975005	0.2036616	1.62010	0.7194245
240803_A	*MT1K*	3.4038531	0.5693469	0.1672654	1.49118	0.7194245
274164_A	*MT1X*	3.5223338	0.5870232	0.1666575	1.50848	0.7194245
293137_A	*MT1X*	3.4033272	0.4734626	0.1391176	1.39281	0.7194245
297392_A	*MT1X*	3.3055921	0.6128023	0.1853835	1.53776	0.7194245
111081_A	*MT1X*	3.1689832	0.5483195	0.173027	1.47013	0.7194245
2019011_A	*MT3*	2.0052257	0.5024289	0.2505598	1.42565	2.9761905
269815_A	*NR4A3*	5.8383067	1.0264115	0.1758064	2.04747	0.7194245
41929_A	*PICALM*	3.4666057	0.4215429	0.121601	1.34270	0.7194245
148753_A	*RNF11*	2.8190212	0.4099965	0.1454393	1.32828	0.7194245
123586_A	*SDC1*	1.8609731	0.4211546	0.2263088	1.32437	4
42669_A	*SGK*	2.6065462	0.5261184	0.201845	1.43478	0.7194245

298134_A	*STOM*	3.1973823	0.4072736	0.1273772	1.32736	0.7194245
249977_A	*TIMP3*	3.7462532	0.8484397	0.2264769	1.75549	0.7194245

Supplementary Figure S12: Genes Significantly Up-Regulated by Ectopic E1A Expression

Clone ID	Gene	Score(d)	Numerator(r)	Denominator(s+s0)	Fold Change	q-value (%)
274217_A	*AATF*	-2.0944419	-0.5032843	0.2402952	0.70906	0.0447674
21766_A	*ACINUS*	-1.773303	-0.4444719	0.2506463	0.73823	0.0447674
51532_A	*ARL6IP*	-3.2567634	-0.800405	0.245767	0.57405	0.0447674
26491_A	*ARL6IP*	-2.958628	-0.6904016	0.233352	0.62138	0.0447674
51532_C	*ARL6IP*	-2.6082368	-0.632835	0.2426294	0.64548	0.0447674
310385_A	*ATP5B*	-2.5446505	-0.5351206	0.2102924	0.69061	0.0447674
342879_B	*ATP5B*	-2.3790919	-0.4997055	0.2100405	0.70798	0.0447674
34310_A	*ATP5F1*	-2.7012416	-0.617783	0.2287034	0.65473	0.0447674
46596_A	*ATP5F1*	-2.3684214	-0.5697493	0.2405608	0.67498	0.0447674
382331_A	*ATP5G2*	-4.1135871	-0.9168689	0.2228879	0.52979	0.0447674
186287_A	*ATP5G2*	-3.6842665	-0.845753	0.2295581	0.55687	0.0447674
141228_A	*BANF1*	-3.4322701	-0.788842	0.229831	0.57997	0.0447674
309883_A	*BAP1*	-2.7651034	-0.6122453	0.2214186	0.65737	0.0447674
184082_A	*BAT1ATP6V1G2*	-3.7677513	-0.8678301	0.230331	0.54906	0.0447674
42638_A	*BAT2*	-2.2741055	-0.7307316	0.321327	0.59388	0.0447674
22479_A	*BAT2*	-1.9589898	-0.6408683	0.3271422	0.64305	0.0447674
193222_A	*BRRN1*	-2.3139833	-0.5833944	0.2521169	0.67140	0.0447674
244767_A	*BRRN1*	-1.9555288	-0.4340828	0.2219772	0.73968	0.0447674
321627_A	*C1QBP*	-3.915848	-0.9388061	0.2397453	0.52394	0.0447674
197515_A	*C7orf14*	-1.4810995	-0.4169463	0.2815113	0.76007	0.1030115
666534_A	*CAD*	-2.2387151	-0.6240098	0.2787357	0.65690	0.0447674
38031_A	*CAD*	-1.6916934	-0.5238476	0.3096587	0.70546	0.0447674
265613_B	*CALM2*	-1.927662	-0.445981	0.2313585	0.73604	0.0447674
230884_A	*CALM2*	-1.7438094	-0.380752	0.218345	0.76637	0.0447674
299705_A	*CCT2*	-2.5170916	-0.5812566	0.2309239	0.66963	0.0447674
299176_B	*CCT2*	-2.3194215	-0.5464536	0.2355991	0.68818	0.0447674
796474_A	*CDC2*	-1.5400799	-0.4077983	0.2647903	0.74969	0.1030115
121716_D	*CDC25B*	-2.0509827	-0.4226015	0.2060483	0.74390	0.0447674
429755_A	*CDC25C*	-1.5061697	-0.377273	0.2504851	0.76246	0.1030115
364403_A	*CDKN2C*	-3.2363944	-0.9623052	0.2973387	0.52309	0.0447674
291057_A	*CDKN2C*	-2.5586396	-0.6909371	0.2700408	0.62863	0.0447674
221318_A	*CKS2*	-3.3418198	-0.9025758	0.2700851	0.53136	0.0447674
725454_A	*CKS2*	-3.2752123	-0.7898636	0.2411641	0.57716	0.0447674
267101_A	*COPS3*	-2.1418096	-0.4989932	0.2329774	0.70712	0.0447674
323062_A	*COPS3*	-1.6020903	-0.4182172	0.2610447	0.75166	0.0855162
172265_A	*COX8*	-3.4108117	-0.8121914	0.2381226	0.57097	0.0447674
322848_A	*COX8*	-2.9727603	-0.7525738	0.2531566	0.59630	0.0447674
141887_A	*CUGBP1*	-2.3472414	-0.5992492	0.2552994	0.66582	0.0447674
33177_A	*CUGBP1*	-1.754512	-0.5726257	0.3263732	0.65534	0.0447674
263741_A	*DDX17*	-2.0351703	-0.710399	0.3490612	0.58694	0.0447674
50574_C	*DDX17*	-1.9984212	-0.604269	0.3023732	0.64945	0.0447674
stSG89312	*DDX17*	-1.4033763	-0.4236332	0.3018672	0.73698	0.2009245
300363_A	*DDX9*	-2.607349	-0.5885505	0.2257276	0.66651	0.0447674
294421_A	*DDX9*	-2.1723745	-0.5766942	0.2654672	0.67609	0.0447674
301013_A	*DHFR*	-4.3997619	-1.0794058	0.2453328	0.47728	0.0447674
768241_A	*DNMT1*	-1.8481246	-0.4482103	0.2425217	0.72943	0.0447674
206863_A	*DNMT1*	-1.5434096	-0.4300552	0.2786397	0.73033	0.0855162

471871_A	*DTYMK*	-2.1203351	-0.505153	0.238242	0.70204	0.0447674
784852_B	*DTYMK*	-2.0542672	-0.4357992	0.2121434	0.73864	0.0447674
51776_A	*EBNA1BP2*	-1.7943614	-0.4169605	0.2323727	0.75288	0.0447674
33477_A	*EBP*	-3.711519	-0.7687685	0.2071304	0.58824	0.0447674
33505_A	*EBP*	-3.4197948	-0.8176815	0.2391025	0.56393	0.0447674
stSG89395	*EIF3S7*	-3.4808842	-0.8434271	0.2423026	0.55950	0.0447674
33636_A	*EIF3S7*	-2.793484	-0.6250245	0.2237437	0.64993	0.0447674
309908_A	*EMD*	-2.128764	-0.5839255	0.2743026	0.66999	0.0447674
stSG89196	*EWSR1*	-2.8358044	-0.71593	0.252461	0.61121	0.0447674
358350_A	*EWSR1*	-1.7104248	-0.4111541	0.2403813	0.74992	0.0447674
127266_A	*FOXM1*	-2.6341945	-0.7717288	0.2929658	0.59606	0.0447674
259115_A	*FOXM1*	-2.3739834	-0.5935935	0.2500411	0.66512	0.0447674
300482_B	*FUBP3*	-0.7855162	-0.4304612	0.5479979	0.53367	1.8933154
41510_A	*GCN1L1*	-2.7356987	-0.6721749	0.245705	0.62546	0.0447674
40567_A	*GCN1L1*	-2.3191412	-0.6879905	0.2966574	0.63169	0.0447674
40567_C	*GCN1L1*	-1.7959478	-0.5969961	0.3324128	0.67503	0.0447674
298453_A	*GPRK6*	-4.1072582	-1.0117572	0.246334	0.49836	0.0447674
53322_B	*GTF3C1*	-2.4249042	-0.5813298	0.2397331	0.67243	0.0447674
stSG89400	*GTSE1*	-3.1752029	-0.7742072	0.2438292	0.58605	0.0447674
122926_A	*H2AFZ*	-2.5704829	-0.6867461	0.2671662	0.62211	0.0447674
754345_A	*HDAC1*	-5.0809878	-1.204085	0.2369785	0.43564	0.0447674
309924_A	*HDAC2*	-2.3964538	-0.5377283	0.224385	0.69019	0.0447674
813673_A	*HDGF*	-2.3103423	-0.6284624	0.2720213	0.65121	0.0447674
124257_A	*HMGB2*	-4.7694799	-1.1024174	0.23114	0.46763	0.0447674
267145_A	*HMGB2*	-4.1755738	-1.0882545	0.2606239	0.47269	0.0447674
124836_A	*HMGB3*	-2.5997535	-0.6865574	0.2640856	0.62765	0.0447674
298516_A	*HNRPA2B1*	-2.3795756	-0.6909589	0.2903707	0.63436	0.0447674
310781_A	*HNRPC*	-3.0748989	-0.749427	0.2437241	0.59792	0.0447674
35170_A	*HNRPC*	-3.0330415	-0.7203666	0.2375064	0.60721	0.0447674
345600_B	*HNRPC*	-2.7757923	-0.6642285	0.2392933	0.63429	0.0447674
358457_A	*HNRPH1*	-2.8238294	-0.7307594	0.2587831	0.60955	0.0447674
681973_A	*HNRPH3*	-1.7504639	-0.5034985	0.2876372	0.71786	0.0447674
321590_A	*HNRPH3*	-1.385862	-0.4514274	0.3257376	0.75157	0.2009245
306373_C	*HNRPL*	-2.5646015	-0.8023027	0.3128372	0.55831	0.0447674
784486_A	*HNRPU*	-2.8195347	-0.7043808	0.2498216	0.61886	0.0447674
361171_A	*HTATIP*	-1.7069451	-0.3917679	0.229514	0.76418	0.0447674
713714_A	*IDH3B*	-2.5282895	-0.6917934	0.2736211	0.62276	0.0447674
810831_A	*ILF2*	-4.1026504	-0.9809702	0.2391065	0.50907	0.0447674
29607_A	*IMPDH2*	-1.3950978	-0.394556	0.282816	0.76039	0.2009245
36485_A	*IMPDH2*	-1.3308242	-0.3939453	0.296016	0.76669	0.2555954
356816_A	*ITPA*	-2.2966946	-0.5155413	0.224471	0.70211	0.0447674
810531_A	*ITPA*	-1.6036496	-0.4314779	0.26906	0.74907	0.0855162
150722_A	*KHDRBS1*	-2.3803909	-0.6616623	0.2779637	0.63025	0.0447674
40983_A	*KIF22*	-1.3450502	-0.4730954	0.3517307	0.74978	0.2555954
307225_A	*LBR*	-3.1150784	-0.8277701	0.2657301	0.56768	0.0447674
365824_A	*MAZ*	-3.9397518	-1.3913602	0.3531593	0.37206	0.0447674
199078_A	*MBD3*	-1.4303494	-0.4447722	0.3109536	0.72973	0.2009245
375917_A	*MCM2*	-2.755692	-0.7799704	0.2830398	0.58437	0.0447674
1842548_A	*MDFI*	-1.7692685	-0.3974232	0.2246257	0.76138	0.0447674
240795_A	*MKI67*	-1.5462145	-0.3963955	0.2563651	0.75977	0.0855162
359821_A	*MRPL28*	-3.4303797	-0.9053928	0.2639337	0.53482	0.0447674
327155_A	*MYL6*	-1.9307392	-0.4036433	0.2090615	0.75387	0.0447674

34607_A	*NDUFA9*	-1.9191174	-0.4651979	0.242402	0.71917	0.0447674
140205_A	*NDUFB7*	-2.5176415	-0.6109983	0.2426868	0.65172	0.0447674
132618_A	*NDUFB7*	-2.0483307	-0.568286	0.2774386	0.67747	0.0447674
300041_B	*NME1*	-2.0939524	-0.5292732	0.2527628	0.69182	0.0447674
296513_A	*NOL5A*	-3.1715254	-0.8492239	0.2677651	0.55127	0.0447674
130371_B	*NUP155*	-1.6952837	-0.4390537	0.2589854	0.74206	0.0447674
stSG89515	*PIK4CA*	-3.2984503	-0.7079551	0.2146326	0.61217	0.0447674
180425_A	*PIK4CA*	-2.050352	-0.4946457	0.2412492	0.71320	0.0447674
299083_A	*POLD2*	-2.3398649	-0.6072418	0.25952	0.65697	0.0447674
469884_A	*POLD2*	-1.9234282	-0.4575084	0.2378609	0.72845	0.0447674
264589_A	*POLR2A*	-2.4892883	-0.5950595	0.2390481	0.65967	0.0447674
246310_A	*POLR2A*	-2.4392394	-0.6149059	0.2520892	0.65828	0.0447674
756666_A	*PPP1CCPPP1CA*	-1.7064305	-0.395929	0.2320217	0.76115	0.0447674
248282_A	*PPP1CCPPP1CA*	-1.6391653	-0.4773794	0.2912332	0.72466	0.0447674
257259_A	*PPP1CCPPP1CA*	-1.626595	-0.4986392	0.306554	0.71270	0.0447674
770027_A	*PPP2R1A*	-2.8330454	-0.5969878	0.210723	0.66309	0.0447674
40199_A	*PPP2R1A*	-2.0704473	-0.5096179	0.2461391	0.70307	0.0447674
772455_A	*PPP4C*	-2.9432571	-0.7107832	0.2414955	0.61202	0.0447674
785707_A	*PRC1*	-5.3389197	-1.2520248	0.234509	0.42276	0.0447674
755378_A	*PRC1*	-4.9858299	-1.1710024	0.2348661	0.44688	0.0447674
294653_A	*PRCC*	-2.5959559	-0.6546096	0.2521651	0.63642	0.0447674
256425_A	*PSMB1*	-2.2632254	-0.565606	0.2499115	0.67327	0.0447674
290864_A	*PSMB2*	-1.6273153	-0.386117	0.2372724	0.76612	0.0447674
321894_B	*PSMB3*	-3.1421745	-0.7708013	0.2453083	0.58270	0.0447674
321823_A	*PSMB3*	-3.0052078	-0.7534232	0.2507059	0.59463	0.0447674
323662_C	*PSMB3*	-2.9317855	-0.783415	0.2672143	0.58380	0.0447674
241950_A	*PSMB3*	-2.6886423	-0.7416383	0.2758412	0.60005	0.0447674
201275_A	*PSMB6*	-3.1450573	-0.6811173	0.2165675	0.62197	0.0447674
30520_A	*PSMC3*	-2.0351836	-0.5111911	0.2511769	0.70704	0.0447674
43940_A	*PSMC5*	-1.9860478	-0.4013715	0.2020956	0.75695	0.0447674
187848_B	*PSME3*	-1.8779369	-0.4227403	0.2251089	0.74898	0.0447674
44344_A	*PWP2H*	-2.0103522	-0.5195857	0.2584551	0.69870	0.0447674
362133_A	*PXF*	-2.0002677	-0.5007423	0.2503376	0.70756	0.0447674
stSG89500	*RANBP1*	-2.4287753	-0.6382288	0.262778	0.63551	0.0447674
47920_A	*RBM14*	-2.8072306	-0.6544327	0.233124	0.63941	0.0447674
299582_A	*RBX1*	-1.8966846	-0.430473	0.2269608	0.74008	0.0447674
200144_A	*RBX1*	-1.6390221	-0.4004243	0.2443068	0.75660	0.0447674
233867_A	*RNU3IP2*	-2.0847519	-0.4632876	0.2222267	0.72514	0.0447674
249295_B	*RPA1*	-3.1801562	-0.7830915	0.2462431	0.58531	0.0447674
308501_A	*RPA1*	-2.5292972	-0.6058494	0.2395327	0.66036	0.0447674
132643_A	*RPL18*	-1.8423416	-0.4552763	0.2471183	0.73375	0.0447674
727149_A	*RPS15A*	-3.1186101	-0.7729675	0.2478564	0.58372	0.0447674
340492_A	*RPS15A*	-2.8451945	-0.6965451	0.2448146	0.61267	0.0447674
324712_A	*RPS6KB2*	-2.0529344	-0.504389	0.2456917	0.71007	0.0447674
40597_A	*SFRS3*	-1.7931764	-0.447643	0.2496369	0.73391	0.0447674
209239_A	*SFRS4*	-3.24838	-0.7021957	0.216168	0.61286	0.0447674
161738_A	*SFRS4*	-2.4642827	-0.7468715	0.3030787	0.60930	0.0447674
132274_A	*SFRS5*	-2.8359994	-0.7191931	0.2535942	0.60619	0.0447674
342861_A	*SKB1*	-2.866907	-0.7330271	0.2556857	0.60166	0.0447674
308868_A	*SLC12A3*	-2.0397268	-0.4828223	0.2367093	0.71415	0.0447674
296111_A	*SLC25A4*	-1.8619303	-0.5836633	0.3134722	0.64681	0.0447674
265111_A	*SLC25A4*	-1.4934662	-0.4795233	0.3210808	0.68831	0.1030115

1160864_A	*SLC27A2*	-2.2815787	-0.6481235	0.284068	0.65015	0.0447674
295714_A	*SLC35B1*	-1.7552614	-0.3988834	0.2272502	0.76187	0.0447674
31842_A	*SLC35B1*	-1.653869	-0.3881437	0.2346883	0.76148	0.0447674
34823_A	*SMARCC1*	-2.1113346	-0.5748938	0.2722893	0.67882	0.0447674
32733_A	*SMC1L1*	-4.6683232	-1.0356977	0.2218565	0.48725	0.0447674
46800_A	*SMC1L1*	-3.8712539	-0.8908347	0.2301153	0.53675	0.0447674
361368_A	*SMC1L1*	-3.8318668	-0.8740494	0.2281001	0.54531	0.0447674
323440_C	*SMT3H2*	-3.5067822	-0.8076569	0.2303128	0.57143	0.0447674
322829_C	*SMT3H2*	-3.4235461	-0.7557459	0.2207495	0.59188	0.0447674
273154_A	*SMT3H2*	-3.2608161	-0.8009275	0.2456218	0.57162	0.0447674
299343_A	*SMT3H2*	-2.6737973	-0.6024487	0.2253158	0.66078	0.0447674
321292_A	*SNRP70*	-3.2612339	-1.0431779	0.3198722	0.48544	0.0447674
796412_B	*SNRP70*	-2.9402386	-0.8217002	0.2794672	0.56407	0.0447674
124261_A	*SNRP70*	-1.3347511	-0.4217926	0.3160084	0.74051	0.2555954
249460_A	*SNRPC*	-3.9199886	-0.9154387	0.2335309	0.53118	0.0447674
47542_C	*SNRPD1*	-2.3275332	-0.5566814	0.2391723	0.67479	0.0447674
47542_A	*SNRPD1*	-1.4515297	-0.4088173	0.2816458	0.75520	0.2009245
771091_A	*SRRM2*	-2.8133012	-0.6176597	0.2195498	0.65358	0.0447674
205931_A	*STK15STK6*	-3.4547121	-0.7408481	0.2144457	0.59978	0.0447674
209066_A	*STK15STK6*	-2.3200875	-0.6025856	0.2597254	0.66141	0.0447674
129865_A	*STK15STK6*	-1.7854707	-0.423602	0.2372495	0.74433	0.0447674
40791_A	*STOML2*	-2.0315991	-0.5844731	0.2876912	0.67971	0.0447674
201196_A	*TAF11*	-3.2639209	-0.7787182	0.2385837	0.58294	0.0447674
729951_A	*TCOF1*	-2.8497404	-0.790053	0.2772368	0.57978	0.0447674
358027_A	*THOC4*	-2.271888	-0.6761691	0.2976243	0.61630	0.0447674
714104_A	*TRIM28*	-3.1491797	-0.8709387	0.2765605	0.54893	0.0447674
291808_B	*TRIM28*	-1.9731296	-0.6432025	0.3259809	0.63374	0.0447674
40854_A	*TSN*	-1.8659733	-0.4466351	0.2393577	0.73786	0.0447674
295286_A	*UBE2C*	-4.0032834	-0.9947758	0.24849	0.49865	0.0447674
758484_A	*UBE2C*	-3.638037	-0.9309697	0.2558989	0.52643	0.0447674
769921_A	*UBE2C*	-2.9741953	-0.8906028	0.2994433	0.54487	0.0447674
298367_B	*UBE2M*	-1.9230041	-0.5092525	0.2648213	0.69679	0.0447674
362812_A	*UQCRC2*	-2.0100635	-0.4983248	0.247915	0.71191	0.0447674
362441_A	*UQCRC2*	-1.876063	-0.4235746	0.2257785	0.74780	0.0447674
234856_A	*VHL*	-2.9464207	-0.6998245	0.2375168	0.61575	0.0447674
726332_A	*ZWINT*	-4.3268262	-0.9475144	0.218986	0.52023	0.0447674

Supplementary Figure S13: Genes Significantly Down-Regulated by Ectopic E1A Expression

Clone ID	Gene	Score(d)	Numerator(r)	Denominator(s+s0)	Fold Change	q-value (%)
200909_A	*ADAM10*	3.5064577	0.8988764	0.2563489	1.84728	0.0447674
340619_A	*AKR1B1*	6.7635659	1.4278494	0.211109	2.68533	0.0447674
340628_A	*AKR1B1*	6.5824247	1.4212168	0.2159108	2.66559	0.0447674
26025_A	*AKR1B1*	4.9271472	1.4440341	0.2930771	2.67797	0.0447674
293270_A	*AKR1C2*	3.4087787	0.842114	0.2470427	1.79421	0.0447674
214107_A	*ANPEP*	3.0603371	0.8752888	0.2860106	1.86288	0.0447674
300484_A	*ANXA1*	7.6804428	2.1194129	0.2759493	4.35730	0.0447674
288649_A	*ANXA1*	5.9202332	1.9434778	0.3282772	3.90937	0.0447674
201585_A	*ARHGDIB*	4.3408208	1.1571004	0.2665626	2.23405	0.0447674
470419_A	*ARPC1B*	2.5004554	0.7041242	0.2815984	1.62072	0.0447674
1704062_A	*ATP2C1*	1.8272557	0.452145	0.2474448	1.37785	0.0447674
269738_A	*ATP2C1*	1.7246571	0.4319568	0.2504595	1.35619	0.0447674
738975_B	*B4GALT1*	5.0922299	1.5231598	0.2991145	2.84895	0.0447674
327700_A	*B4GALT1*	4.9541228	1.3302358	0.2685109	2.48451	0.0447674
150354_A	*B4GALT1*	2.6434995	1.0555872	0.3993143	1.87810	0.0447674
129632_A	*BIRC3*	1.9835515	0.6381654	0.3217287	1.60175	0.0447674
201890_A	*BIRC3*	1.6309888	0.3954141	0.2424383	1.31698	0.1030115
32662_A	*CAT*	1.6953746	0.4358124	0.2570597	1.36659	0.0855162
292058_B	*CD164*	3.0321311	0.7705261	0.2541203	1.68415	0.0447674
375566_B	*CD164*	1.9613696	0.4832332	0.2463754	1.39420	0.0447674
320383_A	*CD164*	1.9526871	0.4593408	0.2352352	1.38398	0.0447674
174515_A	*CD81*	1.0556651	0.3800665	0.3600256	1.35481	1.436637
796005_A	*CDH11*	5.8560428	1.4842448	0.2534553	2.81032	0.0447674
31093_A	*CDH13*	3.6764242	1.3597543	0.3698578	2.42266	0.0447674
753658_A	*CDK2AP1*	2.1097456	0.5825003	0.2760998	1.51937	0.0447674
665157_A	*CDK2AP1*	2.0552897	0.5316871	0.2586921	1.46043	0.0447674
144932_A	*CDK2AP1*	1.8069924	0.4974377	0.2752849	1.43656	0.0447674
124554_A	*CSF1*	3.7593302	1.0991356	0.2923754	2.17931	0.0447674
246147_A	*CSPG2*	8.7844635	2.1917416	0.249502	4.60978	0.0447674
38764_A	*CTSB*	7.3339017	1.9753865	0.26935	3.90425	0.0447674
261517_A	*CTSB*	6.8557555	1.7608822	0.2568473	3.37282	0.0447674
380384_A	*CUL4B*	2.2759615	0.6036221	0.2652163	1.53046	0.0447674
310800_A	*DAF*	1.3943393	0.3777764	0.2709357	1.31594	0.3910714
265997_A	*DDR2*	4.5164777	1.4225901	0.3149778	2.65257	0.0447674
42188_A	*DDR2*	3.5813519	1.1391497	0.3180781	2.19793	0.0447674
51003_A	*DKK3*	8.1504899	2.4586938	0.3016621	5.31916	0.0447674
789269_A	*DNAJB4*	1.8089772	0.4595342	0.2540298	1.37161	0.0447674
252443_A	*DUSP4*	2.2969817	0.5930317	0.2581787	1.51614	0.0447674
270148_A	*DUSP4*	1.464997	0.3966623	0.2707598	1.32475	0.2555954
197479_A	*DUSP5*	1.9571458	0.4697426	0.2400141	1.39619	0.0447674
40851_A	*DUSP6*	2.5514283	0.6705036	0.2627954	1.60262	0.0447674
301122_A	*ECM1*	5.115467	1.6410357	0.3207988	3.14745	0.0447674
124873_A	*ECM1*	4.2656597	1.5999785	0.3750835	3.11065	0.0447674
23448_A	*EFEMP2*	5.0446982	1.8717751	0.3710381	3.51381	0.0447674
128045_A	*EFEMP2*	3.762204	1.493664	0.3970183	2.63058	0.0447674
322146_A	*EMP1*	4.8348549	1.4848214	0.3071077	2.75131	0.0447674
287704_A	*EMP1*	4.1091545	1.2687105	0.3087522	2.32354	0.0447674

323181_A	*FAP*	3.3843095	0.992255	0.2931928	1.96210	0.0447674
665401_A	*FGF2*	4.2100181	1.6033298	0.3808368	3.14245	0.0447674
365515_A	*FGF7*	2.0636142	0.4823704	0.2337503	1.40317	0.0447674
1704018_B	*FTH1*	4.3788413	1.2270734	0.2802279	2.35558	0.0447674
343563_A	*FTL*	6.7915609	1.6540111	0.2435392	3.14403	0.0447674
357775_A	*FTL*	5.9220358	1.5083243	0.2546969	2.83329	0.0447674
149986_A	*FVT1*	2.6690582	0.6615885	0.2478734	1.58719	0.0447674
34415_A	*FVT1*	2.1179224	0.5178739	0.2445197	1.42627	0.0447674
310141_A	*GADD45A*	1.3137943	0.3752142	0.2855958	1.31431	0.5999218
486844_A	*GJA1*	3.7213412	1.0305254	0.2769231	2.07292	0.0447674
309079_A	*GJA1*	3.6198605	1.1051005	0.3052881	2.16537	0.0447674
308993_A	*GJA1*	2.4594049	0.7340887	0.2984822	1.65485	0.0447674
132691_A	*GLRX*	1.8535917	0.4753032	0.2564228	1.38971	0.0447674
323165_A	*GNG11*	3.3273808	0.9012081	0.2708461	1.86493	0.0447674
346135_A	*GPC1*	4.4744247	1.2764792	0.2852834	2.42479	0.0447674
783646_A	*GPC1*	4.1553702	1.415568	0.3406599	2.64452	0.0447674
stSG89160	*HMOX1*	2.4159728	0.6575161	0.2721537	1.59316	0.0447674
42724_A	*HPCAL1*	1.7057283	0.4078871	0.2391278	1.32817	0.0855162
148057_A	*ID3*	3.0635782	0.8297973	0.2708589	1.78244	0.0447674
788174_A	*IFIT1*	1.6395911	0.8066453	0.4919796	2.04044	0.0855162
150355_A	*IFITM1*	5.0946173	1.5152118	0.2974143	2.89796	0.0447674
345996_A	*IFITM1*	4.8626472	1.5099362	0.3105173	2.86483	0.0447674
322180_A	*IFITM2*	4.8243066	1.4775783	0.3062779	2.82623	0.0447674
154387_A	*IFITM2*	4.6229761	1.4393208	0.3113407	2.75730	0.0447674
196375_A	*IGFBP3*	10.357705	3.7456105	0.3616255	13.13423	0.0447674
266838_A	*IGFBP3*	7.9215587	3.8874707	0.4907457	12.38073	0.0447674
356653_A	*IGFBP6*	8.2545472	2.3231704	0.2814413	5.03439	0.0447674
299204_A	*IGFBP7*	6.196164	1.8317475	0.2956261	3.56722	0.0447674
153213_A	*JUNB*	2.3258361	0.604543	0.259925	1.51436	0.0447674
322185_A	*JUNB*	1.8704858	0.4715641	0.2521078	1.39458	0.0447674
344988_A	*KRTHA3A*	1.8378575	0.4580464	0.2492284	1.38382	0.0447674
129532_A	*KYNU*	1.6961324	0.5762109	0.3397205	1.52421	0.0855162
252515_A	*KYNU*	1.1849694	0.4126385	0.3482272	1.39402	0.6554931
157819_A	*LAMB2*	2.9849366	0.7157149	0.2397756	1.64264	0.0447674
49584_A	*LIPA*	1.7736402	0.5432853	0.3063109	1.48619	0.0447674
723880_A	*LOXL1*	5.5328244	1.5406579	0.2784578	2.94990	0.0447674
667364_A	*LOXL1*	5.2483998	1.6803597	0.3201661	3.17023	0.0447674
297957_A	*LPXN*	5.5778645	1.34801	0.2416713	2.53545	0.0447674
788591_A	*LTBP1*	2.3749213	0.7790058	0.3280133	1.75271	0.0447674
783679_A	*LTBP1*	2.3023602	0.5920091	0.2571314	1.51141	0.0447674
23356_B	*MAP1LC3B*	1.7872409	0.4637719	0.2594904	1.38129	0.0447674
50437_A	*MCL1*	1.5894211	0.4737172	0.2980438	1.40603	0.1030115
267815_A	*MCP*	3.1903671	0.837758	0.2625898	1.78968	0.0447674
49200_A	*MGLL*	4.0642568	1.0964662	0.2697827	2.11717	0.0447674
342581_A	*MRC2*	2.0460791	0.5710493	0.2790945	1.49546	0.0447674
66946_A	*MT1B*	9.105992	2.943874	0.3232898	7.74620	0.0447674
232772_A	*MT1B*	7.2475774	3.0409854	0.4195865	7.29509	0.0447674
202535_A	*MT1K*	12.740273	3.0446864	0.2389813	8.24913	0.0447674
240803_A	*MT1K*	12.693564	3.4583851	0.2724519	11.01232	0.0447674
202535_C	*MT1K*	8.024378	2.7014841	0.3366596	6.36641	0.0447674
2019011_A	*MT3*	2.0298022	1.094409	0.5391703	1.87924	0.0447674
789273_A	*NAB1*	1.9482252	0.4561101	0.2341157	1.37031	0.0447674

306798_A	*NAB1*	1.4964261	0.3912681	0.2614683	1.31397	0.2009245
365534_A	*NBL1*	4.1483898	1.0227714	0.2465466	2.04111	0.0447674
132469_A	*NDUFB5*	1.6744906	0.4079132	0.2436043	1.32345	0.0855162
110423_A	*NINJ1*	2.0121864	0.5807887	0.2886357	1.51916	0.0447674
202988_A	*NPC1*	1.633	0.3904063	0.2390731	1.30462	0.1030115
269815_A	*NR4A3*	5.7877795	1.7188906	0.2969862	3.27936	0.0447674
49439_B	*NRG1*	1.813228	0.4760223	0.2625275	1.39604	0.0447674
188294_B	*P4HB*	4.5662116	1.1465072	0.251085	2.20701	0.0447674
140806_A	*PAM*	4.2727217	0.9745766	0.2280927	1.96597	0.0447674
470764_A	*PAM*	3.6060933	0.9293581	0.2577188	1.91109	0.0447674
304879_A	*PAM*	3.5667119	0.9271606	0.2599483	1.90392	0.0447674
363151_A	*PEA15*	3.3627395	0.7141627	0.2123753	1.64355	0.0447674
361256_A	*PEA15*	1.622623	0.478665	0.2949946	1.42353	0.1030115
41929_A	*PICALM*	3.578697	0.8319945	0.2324853	1.77954	0.0447674
41929_C	*PICALM*	1.8059181	0.4702178	0.2603761	1.38170	0.0447674
159527_A	*PLD3*	2.1803141	0.6868936	0.3150434	1.62082	0.0447674
153114_A	*PLXNB2*	1.3111857	0.4075402	0.310818	1.33762	0.5999218
38922_A	*PON2*	2.0302974	0.5388046	0.2653821	1.46886	0.0447674
51565_A	*PON2*	1.7578965	0.4036324	0.229611	1.31906	0.0447674
42739_A	*PTP4A1*	1.5547271	0.3946695	0.2538513	1.31399	0.2009245
297596_A	*PTP4A1*	1.4920446	0.4415777	0.2959547	1.35173	0.2009245
145098_A	*RECK*	1.8179721	0.5165126	0.2841147	1.43326	0.0447674
323346_C	*RGS3*	2.2207855	0.6242155	0.2810787	1.52202	0.0447674
427808_A	*RGS3*	1.8808639	0.5036654	0.2677841	1.41882	0.0447674
148753_A	*RNF11*	2.5844014	0.606672	0.2347437	1.52616	0.0447674
154080_A	*S100A11*	3.3734509	1.0851069	0.3216608	2.17726	0.0447674
154167_A	*S100A11*	2.9649356	1.0111107	0.3410228	2.08390	0.0447674
1627856_A	*SCGF*	1.4975049	0.4251009	0.2838728	1.36523	0.2009245
123586_A	*SDC1*	3.6485512	1.0130327	0.2776534	2.03475	0.0447674
42669_A	*SGK*	3.6032986	1.0368227	0.2877427	2.05324	0.0447674
48503_A	*SLC16A2*	3.0600853	0.8332731	0.2723039	1.76199	0.0447674
24776_A	*SLC16A2*	2.543373	0.7610567	0.2992313	1.69854	0.0447674
725710_A	*SLC20A1*	2.9650983	0.7463384	0.2517078	1.66902	0.0447674
135747_A	*SLC2A1*	3.0293726	0.609778	0.2012885	1.52548	0.0447674
30272_A	*SLC9A1*	2.4251254	0.6799572	0.2803802	1.62715	0.0447674
240183_A	*SLC9A1*	2.353754	0.5789352	0.2459625	1.50126	0.0447674
812227_A	*SLC9A1*	1.6329217	0.4498684	0.2754991	1.35756	0.1030115
180405_A	*SMPD1*	2.3878359	0.5863441	0.2455546	1.49111	0.0447674
180046_A	*SMPD1*	2.1417868	0.536658	0.2505656	1.44924	0.0447674
24033_A	*STAT1*	2.3260727	0.8259916	0.3551014	1.86327	0.0447674
26599_A	*STAT1*	2.1250257	0.9182531	0.4321139	2.02452	0.0447674
346727_A	*TFPI*	2.7102242	0.8708131	0.3213066	1.83117	0.0447674
199945_A	*TGM2*	2.0990586	0.4621069	0.2201496	1.37724	0.0447674
769686_A	*THY1*	6.7795076	2.1308395	0.3143059	4.42755	0.0447674
249977_A	*TIMP3*	3.3014458	0.897415	0.2718249	1.86563	0.0447674
stSG89269	*TIMP3*	2.0470191	0.5144418	0.2513127	1.41905	0.0447674
299745_B	*TNFRSF6*	1.7795421	0.4417968	0.2482643	1.36604	0.0447674
714213_A	*TNFRSF6*	1.7361055	0.44453	0.2560501	1.37439	0.0447674
24999_A	*TOMM34*	1.8594359	0.4583641	0.2465071	1.37218	0.0447674
192334_A	*TPD52L2*	2.3685133	0.6158395	0.260011	1.54292	0.0447674
241195_A	*TPD52L2*	2.2253767	0.5065601	0.2276289	1.42293	0.0447674
323783_B	*VEGF*	3.673047	1.3987534	0.3808155	2.59692	0.0447674

32682_A	*VIM*	2.7746936	0.7929988	0.2857969	1.69072	0.0447674
147834_A	*ZNF217*	1.5398092	0.3745707	0.2432579	1.30512	0.2009245

Supplementary Figure S14: Genes Significantly Up-Regulated by Ectopic E7 Expression

Clone ID	Gene	Score(d)	Numerator(r)	Denominator(s+s0)	Fold Change	q-value (%)
51532_A	*ARL6IP*	-3.0101178	-0.5782576	0.1921046	0.66734	0.3354865
51532_C	*ARL6IP*	-2.8760285	-0.4695853	0.1632756	0.72559	0.3354865
26491_A	*ARL6IP*	-2.8600576	-0.496034	0.173435	0.70996	0.3354865
184082_A	*BAT1ATP6V1G2*	-2.8282696	-0.4952007	0.1750896	0.70904	0.3354865
167080_A	*CALM3*	-2.1813787	-0.4164016	0.1908892	0.75112	0.3354865
121716_D	*CDC25B*	-5.1046793	-0.6327722	0.1239592	0.64458	0.3354865
785382_A	*CDC25B*	-1.8983157	-0.4788848	0.2522682	0.73049	1.6131478
364403_A	*CDKN2C*	-1.9679595	-0.4644879	0.2360252	0.73745	1.2169201
222163_A	*CKB*	-2.7647605	-0.6755212	0.2443326	0.60786	0.3354865
783875_A	*CLTC*	-2.1160831	-0.4535799	0.2143488	0.72425	0.3354865
138991_A	*COL6A3*	-1.9984336	-0.4995838	0.2499877	0.69541	0.7951466
322848_A	*COX8*	-3.1906801	-0.6115445	0.1916659	0.65686	0.3354865
172265_A	*COX8*	-2.8881908	-0.5476133	0.1896043	0.68246	0.3354865
471871_A	*DTYMK*	-3.4014426	-0.5750824	0.1690701	0.66951	0.3354865
784852_B	*DTYMK*	-2.722201	-0.4407214	0.1618989	0.73365	0.3354865
121153_A	*ECHS1*	-2.5354745	-0.4267694	0.1683193	0.74658	0.3354865
127266_A	*FOXM1*	-2.4772425	-0.5513849	0.2225801	0.69615	0.3354865
259115_A	*FOXM1*	-2.3025286	-0.3967856	0.172326	0.76525	0.3354865
stSG89400	*GTSE1*	-2.9412418	-0.4939346	0.167934	0.71390	0.3354865
122926_A	*H2AFZ*	-2.9579569	-0.5740718	0.1940771	0.67473	0.3354865
stSG89294	*HMG17L1*	-1.7191831	-0.4116424	0.2394407	0.76309	2.5262424
124257_A	*HMGB2*	-3.8473747	-0.7629792	0.1983116	0.58592	0.3354865
267145_A	*HMGB2*	-3.8234928	-0.7392445	0.1933427	0.60251	0.3354865
358457_A	*HNRPH1*	-2.1031004	-0.4264605	0.2027771	0.75018	0.3354865
487501_A	*HNRPR*	-2.1117866	-0.3847034	0.1821697	0.76856	0.3354865
212780_A	*KIF23*	-2.2981854	-0.420165	0.1828247	0.75095	0.3354865
365824_A	*MAZ*	-1.6056805	-0.4184657	0.2606158	0.74262	3.018439
240795_A	*MKI67*	-3.8486386	-0.7582294	0.1970124	0.59028	0.3354865
146758_A	*NNMT*	-3.7647278	-0.7014246	0.1863148	0.61576	0.3354865
139478_A	*NNMT*	-2.7238166	-0.5578902	0.2048193	0.67931	0.3354865
39040_A	*PCOLCE*	-2.4348843	-0.4209165	0.1728692	0.75251	0.3354865
127929_A	*PCOLCE*	-2.2524167	-0.4413902	0.1959629	0.74434	0.3354865
785707_A	*PRC1*	-4.2467425	-0.7354111	0.1731706	0.60424	0.3354865
755378_A	*PRC1*	-3.1736714	-0.5469797	0.1723492	0.68828	0.3354865
30520_A	*PSMC3*	-2.2957065	-0.4324444	0.1883709	0.74620	0.3354865
417504_A	*RRM2*	-4.4229998	-0.8452852	0.1911113	0.55271	0.3354865
308868_A	*SLC12A3*	-3.0592145	-0.4667096	0.1525586	0.72551	0.3354865
324787_A	*SLC12A3*	-2.061137	-0.3921221	0.1902455	0.76835	0.3354865
300169_A	*SMC4L1*	-2.2224801	-0.4108845	0.1848766	0.75470	0.3354865
205931_A	*STK15STK6*	-2.8041613	-0.4165472	0.1485461	0.75112	0.3354865
188403_A	*TAGLN*	-2.4106689	-0.5337663	0.2214183	0.69944	0.3354865
138581_A	*TAGLN*	-2.3710998	-0.436154	0.1839458	0.74186	0.3354865
191603_A	*TUBB*	-2.573751	-0.458975	0.1783292	0.72665	0.3354865

27464_A	*TUBB*	-1.9592416	-0.4776774	0.2438073	0.72841	1.2169201
726332_A	*ZWINT*	-2.8558635	-0.4852021	0.1698968	0.71404	0.3354865

Supplementary Figure S15: Genes Significantly Down-Regulated by Ectopic E7 Expression

Clone ID	Gene	Score(d)	Numerator(r)	Denominator(s+s0)	Fold Change	q-value (%)
200909_A	*ADAM10*	2.6106761	0.4410228	0.1689305	1.35406	0.3354865
26025_A	*AKR1B1*	4.5723109	0.923617	0.2020022	1.88750	0.3354865
340619_A	*AKR1B1*	6.057066	0.9691526	0.1600036	1.94838	0.3354865
340628_A	*AKR1B1*	4.9498886	0.904377	0.1827065	1.84663	0.3354865
1979334_A	*AKR1B10*	1.9378644	0.5140136	0.2652474	1.36652	0.7951466
293270_A	*AKR1C2*	3.1972272	0.5937084	0.1856948	1.50839	0.3354865
288649_A	*ANXA1*	1.7468052	0.4657631	0.2666371	1.40059	1.6131478
300484_A	*ANXA1*	2.4507257	0.5784333	0.2360253	1.48220	0.3354865
341038_A	*ATP6IP2*	3.9255039	0.6913796	0.176125	1.62361	0.3354865
146646_A	*ATP6V1G1*	2.5176389	0.4587428	0.1822115	1.36721	0.3354865
36832_A	*ATP6V1G1*	2.4650595	0.4400041	0.1784963	1.35473	0.3354865
37045_A	*ATP6V1G1*	2.5297606	0.4965203	0.1962717	1.40090	0.3354865
809439_B	*ATP6V1G1*	2.7878697	0.5290624	0.189773	1.44278	0.3354865
772208_A	*C1S*	2.4959965	0.4676648	0.187366	1.38439	0.3354865
292058_B	*CD164*	2.0830979	0.4082087	0.1959623	1.30626	0.3354865
174515_A	*CD81*	1.656916	0.4934032	0.2977841	1.46299	2.0109515
261971_B	*CD81*	1.8378303	0.5372027	0.2923027	1.51684	1.2169201
796005_A	*CDH11*	1.9924059	0.4691217	0.2354549	1.35999	0.3354865
31093_A	*CDH13*	2.6111187	0.6528811	0.2500388	1.54563	0.3354865
233825_A	*CPO*	1.4528985	0.3728481	0.2566236	1.30979	4.0368983
147907_A	*CREG*	1.7694555	0.4106727	0.2320899	1.32762	1.6131478
124554_A	*CSF1*	2.2853193	0.5066553	0.2217	1.44929	0.3354865
246147_A	*CSPG2*	3.0773139	0.8763911	0.2847909	1.76850	0.3354865
380384_A	*CUL4B*	2.4433526	0.4911967	0.2010339	1.41492	0.3354865
310800_A	*DAF*	1.6081947	0.384155	0.2388734	1.30455	2.5262424
51003_A	*DKK3*	2.6083135	0.4061879	0.1557282	1.32116	0.3354865
44394_B	*DNAJA1*	2.2211387	0.3920229	0.1764963	1.30588	0.3354865
789269_A	*DNAJB4*	2.2860346	0.398702	0.1744077	1.32071	0.3354865
270148_A	*DUSP4*	1.9453527	0.383633	0.1972049	1.31692	0.7951466
301122_A	*ECM1*	1.8777373	0.4612589	0.2456461	1.39645	0.7951466
323181_A	*FAP*	2.3295261	0.4186088	0.179697	1.34069	0.3354865
665401_A	*FGF2*	2.8472293	0.8728983	0.3065782	1.90290	0.3354865
1704018_B	*FTH1*	2.0533856	0.4234752	0.2062327	1.35479	0.3354865
343563_A	*FTL*	2.8415134	0.481293	0.1693791	1.39820	0.3354865
357775_A	*FTL*	2.3398056	0.4383362	0.1873387	1.35023	0.3354865
809588_C	*GGH*	2.0904607	0.3780275	0.1808345	1.30185	0.3354865
50492_A	*GNAL*	1.8792123	0.3943519	0.2098496	1.33359	0.7951466
42724_A	*HPCAL1*	2.519675	0.46963	0.1863852	1.38160	0.3354865
35091_A	*HSPA1L*	3.3306928	0.8792963	0.263998	1.86454	0.3354865
50615_A	*HSPA1L*	3.1488014	0.7766148	0.2466382	1.73290	0.3354865
33800_A	*HSPA6HSPA7*	2.8006104	0.8658757	0.3091739	1.87439	0.3354865
196375_A	*IGFBP3*	7.5422794	2.7370105	0.362889	6.15770	0.3354865
266838_A	*IGFBP3*	6.5563129	2.7033019	0.4123205	5.72661	0.3354865

356653_A	*IGFBP6*	2.3375396	0.6195498	0.2650436	1.50687	0.3354865
129532_A	*KYNU*	1.5474421	0.4033896	0.2606816	1.36459	3.018439
244990_A	*LIPA*	2.4899764	0.4307934	0.1730111	1.35407	0.3354865
49584_A	*LIPA*	1.873322	0.4572652	0.2440932	1.39837	0.7951466
112207_A	*MANBA*	1.4828735	0.4004321	0.2700379	1.34309	3.4014606
23356_B	*MAP1LC3B*	2.4208239	0.4641695	0.1917403	1.38273	0.3354865
1659533_B	*MATN4*	1.4468788	0.5130758	0.3546087	1.40987	4.0368983
267815_A	*MCP*	3.4201316	0.6945704	0.2030829	1.61736	0.3354865
30217_A	*NCKAP1*	2.5381664	0.4901013	0.1930927	1.38786	0.3354865
124123_A	*NDUFB5*	2.0847152	0.4136956	0.1984422	1.33531	0.3354865
140806_A	*PAM*	3.569043	0.551501	0.1545235	1.46930	0.3354865
304879_A	*PAM*	3.1164946	0.6169091	0.1979497	1.53419	0.3354865
470764_A	*PAM*	2.6058748	0.4725785	0.1813512	1.39779	0.3354865
363151_A	*PEA15*	2.1282813	0.4218472	0.1982103	1.32401	0.3354865
159527_A	*PLD3*	2.0641154	0.4698996	0.2276518	1.40944	0.3354865
365623_B	*PLD3*	1.9585018	0.4062388	0.2074233	1.34101	0.3354865
148753_A	*RNF11*	3.1417427	0.6219074	0.1979498	1.52893	0.3354865
725710_A	*SLC20A1*	2.3396326	0.3960175	0.1692648	1.31616	0.3354865
258898_B	*SLC6A8*	1.9211587	0.4231252	0.2202448	1.31385	0.7951466
47107_A	*SNX3*	2.0987949	0.3999465	0.1905601	1.32236	0.3354865
52431_A	*TDE1*	2.6431693	0.418927	0.1584942	1.33490	0.3354865
346727_A	*TFPI*	1.5781029	0.3962426	0.2510879	1.32178	2.5262424
249977_A	*TIMP3*	2.8732852	0.5941196	0.2067736	1.51192	0.3354865
1573002_A	*TOMM34*	2.7095253	0.426746	0.1574984	1.34222	0.3354865
186690_A	*TOMM34*	2.3045975	0.4005491	0.1738044	1.31990	0.3354865
24999_A	*TOMM34*	2.5693184	0.4614315	0.1795929	1.37584	0.3354865

Supplementary Figure S16: Genes Significantly Up-Regulated by p53 Abrogation

Clone ID	Gene	Score(d)	Numerator(r)	Denominator(s+s0)	Fold Change	q-value (%)
51532_A	*ARL6IP*	-2.398947306	-0.554406298	0.231103991	1.47009	0.990099
26491_A	*ARL6IP*	-1.814166432	-0.443753974	0.244604886	1.36750	0.990099
51532_C	*ARL6IP*	-1.738080742	-0.458522639	0.263809746	1.38975	1.6393443
184082_A	*BAT1ATP6V1G2*	-1.732701741	-0.380011991	0.219317602	1.30070	1.6393443
121716_D	*CDC25B*	-2.902496758	-0.662643548	0.228301219	1.59596	0.990099
785382_A	*CDC25B*	-1.596956406	-0.494589115	0.309707336	1.41173	3.4482759
298509_A	*COL1A1*	-1.979433376	-0.810807589	0.409616004	1.86708	0.990099
323321_A	*COL1A1*	-1.921751966	-0.728833028	0.379254472	1.75457	0.990099
359255_A	*COL5A2*	-1.784491958	-0.568267203	0.318447612	1.51531	0.990099
427768_A	*DSTN*	-1.637241884	-0.459768763	0.280819082	1.38997	1.6393443
346468_B	*EPB41L2*	-1.48633647	-0.348262843	0.234309559	1.28226	4.6511628
122926_A	*H2AFZ*	-1.540456677	-0.376065489	0.244125976	1.29703	3.4482759
267145_A	*HMGB2*	-1.870203856	-0.504937958	0.269990866	1.43072	0.990099
124257_A	*HMGB2*	-1.681318139	-0.489183225	0.290952208	1.43418	1.6393443
365824_A	*MAZ*	-1.502822155	-0.478182617	0.318189757	1.41930	4.6511628
240795_A	*MKI67*	-2.14562141	-0.526356093	0.245316387	1.44380	0.990099
728122_A	*MYL6*	-1.97926706	-0.445151998	0.224907496	1.36349	0.990099
327155_A	*MYL6*	-1.768086322	-0.406179248	0.229728177	1.33487	0.990099
146758_A	*NNMT*	-1.850076981	-0.542525569	0.293244862	1.48745	0.990099
785707_A	*PRC1*	-2.582067742	-0.639141549	0.247530899	1.56214	0.990099
755378_A	*PRC1*	-1.90706068	-0.488417213	0.256109949	1.41149	0.990099
2109679_A	*PTRF*	-1.485083742	-0.638766682	0.430121658	1.46132	4.6511628
205931_A	*STK15STK6*	-1.487356245	-0.401839944	0.27017061	1.34349	4.6511628
209066_A	*STK15STK6*	-1.4357486	-0.397585443	0.276918566	1.32918	4.6511628
191603_A	*TUBB*	-1.649104614	-0.362620197	0.219889141	1.28505	1.6393443
295286_A	*UBE2C*	-2.037965596	-0.53122677	0.260665229	1.46445	0.990099
758484_A	*UBE2C*	-1.506639937	-0.391759148	0.260021747	1.31933	4.6511628
769921_A	*UBE2C*	-1.466144626	-0.431853153	0.294550173	1.35583	4.6511628

Supplementary Figure S17: Genes Significantly Down-Regulated by p53 Abrogation

Clone ID	Gene	Score(d)	Numerator(r)	Denominator(s+s0)	Fold Change	q-value (%)
340628_A	*AKR1B1*	2.608445113	0.687899472	0.263720125	0.63332	0.990099
26025_A	*AKR1B1*	2.554426155	0.759630664	0.297378205	0.60599	0.990099
340619_A	*AKR1B1*	2.342342918	0.657604405	0.280746427	0.65036	0.990099
341038_A	*ATP6IP2*	1.380817834	0.422688898	0.306114889	0.76682	3.4482759
327700_A	*B4GALT1*	1.455181436	0.35363971	0.243021043	0.78791	3.4482759
738975_B	*B4GALT1*	1.447940573	0.434503136	0.300083542	0.75199	3.4482759
796005_A	*CDH11*	1.374288427	0.464172901	0.337755083	0.76127	4.6511628
31093_A	*CDH13*	2.149850567	0.700810265	0.32598092	0.63504	0.990099
124554_A	*CSF1*	1.998821366	0.575213196	0.287776189	0.67075	0.990099
246147_A	*CSPG2*	1.641193314	0.486951616	0.296705825	0.72840	0.990099
380384_A	*CUL4B*	1.866286517	0.554936136	0.297347771	0.69289	0.990099
24927_A	*DDB2*	1.431193779	0.373057214	0.260661567	0.77498	3.4482759
51003_A	*DKK3*	1.874556446	0.474347296	0.253045085	0.72919	0.990099
301122_A	*ECM1*	1.727817183	0.492085426	0.28480179	0.70771	0.990099
124873_A	*ECM1*	1.376390175	0.457515199	0.332402256	0.71771	3.4482759
665401_A	*FGF2*	2.19903168	0.731573136	0.332679671	0.59257	0.990099
115383_A	*GADD45A*	1.335741341	0.432569435	0.323842215	0.75998	4.6511628
196375_A	*IGFBP3*	3.040091402	1.348404168	0.443540667	0.43981	0.990099
266838_A	*IGFBP3*	3.02392235	1.289578756	0.426458952	0.45230	0.990099
49584_A	*LIPA*	1.639485645	0.44762985	0.273030661	0.72407	0.990099
244990_A	*LIPA*	1.388266714	0.378555648	0.272682219	0.77979	3.4482759
23356_B	*MAP1LC3B*	1.456134993	0.426598847	0.292966551	0.75760	3.4482759
267815_A	*MCP*	2.007116496	0.579510358	0.288727814	0.68138	0.990099
232772_A	*MT1B*	1.982356875	0.498026509	0.251229491	0.71127	0.990099
66946_A	*MT1B*	1.705490793	0.497310788	0.291593945	0.70795	0.990099
240803_A	*MT1K*	2.161884351	0.532933833	0.246513572	0.68973	0.990099
202535_C	*MT1K*	1.987213352	0.589409929	0.296601232	0.67316	0.990099
202535_A	*MT1K*	1.983942114	0.473392337	0.23861197	0.72319	0.990099
274164_A	*MT1X*	2.142435176	0.521772448	0.243541767	0.69497	0.990099
297392_A	*MT1X*	2.090542976	0.549164083	0.262689689	0.68249	0.990099
111081_A	*MT1X*	2.017253086	0.513368891	0.254489084	0.69976	0.990099
293137_A	*MT1X*	1.785174097	0.445109945	0.249336995	0.73848	0.990099
110423_A	*NINJ1*	1.471069508	0.462177533	0.314177903	0.73590	1.6393443
147436_A	*NINJ1*	1.377626676	0.378672307	0.274872949	0.77857	3.4482759
269815_A	*NR4A3*	2.26188395	0.745260349	0.329486554	0.61933	0.990099
49439_B	*NRG1*	1.32874487	0.318083211	0.239386219	0.80020	4.6511628
42739_A	*PTP4A1*	1.449939388	0.426063611	0.293849257	0.75917	3.4482759
148753_A	*RNF11*	1.618190853	0.409091689	0.252808059	0.75899	0.990099
123586_A	*SDC1*	1.784490426	0.53211587	0.298189255	0.69966	0.990099
725710_A	*SLC20A1*	1.341575178	0.359121406	0.267686382	0.79081	4.6511628
299745_B	*TNFRSF6*	1.419472645	0.342781147	0.241484856	0.78796	3.4482759

Supplementary Figure S18: **Raw Real-Time PCR Data**

		GAPDH Calibrator								*PGK1* Calibrator							
Candidate Gene	Culture	Total RNA of Target Gene (ng)	Standard Deviation of Target Gene	Total RNA of Calibrator Gene (ng)	Standard Deviation of Calibrator Gene	Expression Normalised to Calibrator Gene	Standard Deviation of Normalised Gene Expression	Relative Gene Expression	Standard Deviation of Relative Gene Expression	Total RNA of Target Gene (ng)	Standard Deviation of Target Gene	Total RNA of Calibrator Gene (ng)	Standard Deviation of Calibrator Gene	Expression Normalised to Calibrator Gene	Standard Deviation of Normalised Gene Expression	Relative Gene Expression	Standard Deviation of Relative Gene Expression
AKR1B1	HMF3AEco^N 33.5°C	2.006	0.222	2.991	0.047	0.671	0.075	1.000	0.112	2.006	0.222	2.363	0.146	0.849	0.106	1.000	0.127
	HMF3AEco^N 39.5°C	3.106	0.081	2.397	0.054	1.296	0.044	1.932	0.034	3.106	0.081	1.957	0.147	1.587	0.126	1.869	0.079
	Wt LT	2.892	0.150	3.406	0.067	0.849	0.047	1.266	0.056	2.892	0.150	2.974	0.359	0.973	0.126	1.146	0.131
	E1A	1.066	0.042	1.723	0.060	0.631	0.036	0.941	0.060	1.066	0.042	1.902	0.130	0.572	0.045	0.674	0.079
	E7	1.066	0.014	3.328	0.045	0.326	0.006	0.486	0.019	1.066	0.014	1.494	0.073	0.727	0.037	0.856	0.051
	RNAi p53	1.766	0.060	2.813	0.031	0.629	0.022	0.937	0.036	1.766	0.060	1.635	0.100	1.082	0.076	1.274	0.070
	GSE p53	1.641	0.092	2.444	0.018	0.672	0.038	1.001	0.057	1.641	0.092	1.687	0.139	0.973	0.097	1.146	0.100
CDH13	HMF3AEco^N 33.5°C	2.241	0.064	2.991	0.047	0.749	0.024	1.000	0.033	2.241	0.064	2.363	0.146	0.948	0.065	1.000	0.068
	HMF3AEco^N 39.5°C	2.623	0.051	2.397	0.054	1.094	0.032	1.460	0.030	2.623	0.051	1.957	0.147	1.340	0.104	1.413	0.078
	Wt LT	2.344	0.164	3.406	0.067	0.688	0.050	0.918	0.073	2.344	0.164	2.974	0.359	0.788	0.110	0.831	0.140
	E1A	0.048	0.000	1.723	0.060	0.028	0.001	0.038	0.046	0.048	0.000	1.902	0.130	0.025	0.002	0.027	0.089
	E7	1.425	0.121	3.328	0.045	0.428	0.037	0.571	0.086	1.425	0.121	1.494	0.073	0.954	0.093	1.005	0.096
	RNAi p53	1.343	0.075	2.813	0.031	0.476	0.027	0.637	0.057	1.343	0.075	1.635	0.100	0.822	0.066	0.866	0.063
	GSE p53	1.809	0.044	2.444	0.018	0.740	0.019	0.988	0.025	1.809	0.044	1.687	0.139	1.072	0.092	1.130	0.086
P21	HMF3AEco^N 33.5°C	1.380	0.075	2.991	0.047	0.462	0.026	1.000	0.057	1.380	0.075	2.363	0.146	0.584	0.033	1.000	0.057
	HMF3AEco^N 39.5°C	3.156	0.092	2.397	0.054	1.317	0.049	2.853	0.037	3.156	0.092	1.957	0.147	1.613	0.059	2.761	0.037
	Wt LT	3.711	0.226	3.406	0.067	1.090	0.070	2.361	0.084	3.711	0.226	2.974	0.359	1.248	0.080	2.137	0.084
	E1A	1.418	0.041	1.723	0.060	0.823	0.045	1.783	0.055	1.418	0.041	1.902	0.130	0.746	0.041	1.277	0.055
	E7	3.996	0.290	3.328	0.045	1.201	0.089	2.602	0.074	3.996	0.290	1.494	0.073	2.674	0.197	4.576	0.074
	RNAi p53	1.427	0.068	2.813	0.031	0.507	0.025	1.099	0.049	1.427	0.068	1.635	0.100	0.873	0.043	1.494	0.049
	GSE p53	0.707	0.057	2.444	0.018	0.289	0.023	0.627	0.061	0.707	0.057	1.687	0.139	0.419	0.034	0.717	0.061

Candidate Gene	Culture	GAPDH Calibrator								PGK1 Calibrator							
		Total RNA of Target Gene (ng)	Standard Deviation of Target Gene	Total RNA of Calibrator Gene (ng)	Standard Deviation of Calibrator Gene	Expression Normalized to Calibrator Gene	Standard Deviation of Normalized Gene Expression	Relative Gene Expression	Standard Deviation of Relative Gene Expression	Total RNA of Target Gene (ng)	Standard Deviation of Target Gene	Total RNA of Calibrator Gene (ng)	Standard Deviation of Calibrator Gene	Expression Normalized to Calibrator Gene	Standard Deviation of Normalized Gene Expression	Relative Gene Expression	Standard Deviation of Relative Gene Expression
CKS2	HMF3AEco^{N} 33.5°C	2.789	0.090	2.991	0.047	0.932	0.034	1.000	0.036	2.789	0.090	2.363	0.146	1.180	0.063	1.000	0.070
	HMF3AEco^{N} 39.5°C	2.403	0.122	2.397	0.054	1.002	0.056	1.075	0.056	2.403	0.122	1.957	0.147	1.228	0.111	1.040	0.091
	Wt LT	3.939	0.147	3.406	0.067	1.156	0.049	1.240	0.042	3.939	0.147	2.974	0.359	1.324	0.167	1.122	0.126
	E1A	4.215	0.295	1.723	0.080	2.446	0.206	2.623	0.084	4.215	0.295	1.902	0.130	2.216	0.217	1.878	0.096
	E7	3.949	0.118	3.328	0.045	1.187	0.039	1.273	0.033	3.949	0.118	1.494	0.073	2.643	0.152	2.239	0.057
	RNAi p53	4.675	0.355	2.813	0.031	1.662	0.126	1.783	0.077	4.675	0.355	1.635	0.100	2.860	0.279	2.424	0.096
	GSE p53	4.134	0.206	2.444	0.018	1.692	0.085	1.814	0.050	4.134	0.206	1.667	0.139	2.450	0.237	2.076	0.097
CUL4B	HMF3AEco^{N} 33.5°C	1.994	0.066	2.991	0.047	0.667	0.024	1.000	0.037	1.994	0.066	2.363	0.146	0.844	0.059	1.000	0.070
	HMF3AEco^{N} 39.5°C	2.748	0.041	2.397	0.054	1.146	0.031	1.719	0.027	2.748	0.041	1.957	0.147	1.404	0.106	1.664	0.077
	Wt LT	2.744	0.552	3.406	0.067	0.806	0.163	1.208	0.202	2.744	0.552	2.974	0.359	0.923	0.217	1.093	0.235
	E1A	2.577	0.277	1.723	0.080	1.495	0.175	2.242	0.117	2.577	0.277	1.902	0.130	1.355	0.173	1.606	0.126
	E7	2.102	0.060	3.328	0.045	0.632	0.026	0.947	0.041	2.102	0.060	1.494	0.073	1.407	0.067	1.667	0.062
	RNAi p53	2.576	0.129	2.813	0.031	0.916	0.047	1.374	0.051	2.576	0.129	1.635	0.100	1.576	0.125	1.868	0.079
	GSE p53	2.461	0.126	2.444	0.018	1.015	0.053	1.523	0.052	2.461	0.126	1.667	0.139	1.470	0.143	1.743	0.097
FAP	HMF3AEco^{N} 33.5°C	1.386	0.076	2.991	0.047	0.464	0.026	1.000	0.057	1.386	0.076	2.363	0.146	0.587	0.033	1.000	0.057
	HMF3AEco^{N} 39.5°C	1.412	0.062	2.397	0.054	0.589	0.022	1.271	0.037	1.412	0.062	1.957	0.147	0.721	0.027	1.230	0.037
	Wt LT	1.615	0.062	3.406	0.067	0.474	0.030	1.023	0.064	1.615	0.062	2.974	0.359	0.543	0.035	0.926	0.064
	E1A	0.019	0.000	1.723	0.080	0.011	0.001	0.024	0.055	0.019	0.000	1.902	0.130	0.010	0.001	0.017	0.055
	E7	1.120	0.061	3.328	0.045	0.337	0.025	0.726	0.074	1.120	0.061	1.494	0.073	0.750	0.055	1.278	0.074
	RNAi p53	1.457	0.094	2.813	0.031	0.518	0.025	1.117	0.049	1.457	0.094	1.635	0.100	0.891	0.044	1.519	0.049
	GSE p53	1.765	0.074	2.444	0.018	0.722	0.059	1.558	0.081	1.765	0.074	1.667	0.139	1.046	0.085	1.783	0.081

Candidate Gene	Culture	GAPDH Calibrator								PGK1 Calibrator							
		Total RNA of Target Gene (ng)	Standard Deviation of Target Gene	Total RNA of Calibrator Gene (ng)	Standard Deviation of Calibrator Gene	Expression Normalized to Calibrator Gene	Standard Deviation of Normalized Gene Expression	Relative Gene Expression	Standard Deviation of Relative Gene Expression	Total RNA of Target Gene (ng)	Standard Deviation of Target Gene	Total RNA of Calibrator Gene (ng)	Standard Deviation of Calibrator Gene	Expression Normalized to Calibrator Gene	Standard Deviation of Normalized Gene Expression	Relative Gene Expression	Standard Deviation of Relative Gene Expression
RNF11	HMF3AEco^{R} 33.5°C	2.812	0.062	2.991	0.047	0.940	0.025	1.000	0.027	2.812	0.062	2.363	0.146	1.190	0.076	1.000	0.066
	HMF3AEco^{R} 39.5°C	2.900	0.197	2.397	0.054	1.210	0.066	1.287	0.071	2.900	0.197	1.957	0.147	1.482	0.150	1.245	0.101
	Wt LT	3.920	0.046	3.406	0.067	1.151	0.027	1.224	0.023	3.920	0.046	2.974	0.359	1.318	0.160	1.106	0.121
	E1A	2.303	0.020	1.723	0.060	1.337	0.063	1.422	0.047	2.303	0.020	1.902	0.130	1.211	0.084	1.018	0.069
	E7	3.021	0.073	3.328	0.045	0.906	0.025	0.966	0.026	3.021	0.073	1.494	0.073	2.022	0.110	1.699	0.055
	RNAi p53	3.352	0.074	2.813	0.031	1.192	0.029	1.267	0.025	3.352	0.074	1.635	0.100	2.051	0.134	1.723	0.085
	GSE p53	3.178	0.096	2.444	0.018	1.301	0.041	1.383	0.032	3.178	0.096	1.687	0.139	1.884	0.166	1.583	0.066
UBE2C	HMF3AEco^{R} 33.5°C	2.466	0.091	2.991	0.047	0.825	0.033	1.000	0.040	2.466	0.091	2.363	0.146	1.043	0.075	1.000	0.072
	HMF3AEco^{R} 39.5°C	1.789	0.047	2.397	0.054	0.746	0.026	0.905	0.034	1.789	0.047	1.957	0.147	0.914	0.073	0.876	0.079
	Wt LT	3.738	0.020	3.406	0.067	1.097	0.022	1.331	0.020	3.738	0.020	2.974	0.359	1.257	0.152	1.205	0.121
	E1A	3.878	0.040	1.723	0.060	2.250	0.107	2.729	0.047	3.878	0.040	1.902	0.130	2.039	0.141	1.954	0.069
	E7	3.094	0.099	3.328	0.045	0.930	0.032	1.127	0.035	3.094	0.099	1.494	0.073	2.070	0.121	1.984	0.058
	RNAi p53	4.006	0.103	2.813	0.031	1.424	0.040	1.728	0.028	4.006	0.103	1.635	0.100	2.451	0.163	2.349	0.066
	GSE p53	3.494	0.035	2.444	0.018	1.430	0.018	1.734	0.013	3.494	0.035	1.687	0.139	2.071	0.172	1.985	0.063